COPY 3
BMR PUBLICATIONS COMPACTUS
(LENDING SECTION)
Copy 3



DEPARTMENT OF MINERAL RESOURCES
LIBRARY
CANBERRA A.C.T.

AGSO BULLETIN 243

Detailed Studies of the Mount Isa Inlier

Compiled and edited by
A.J. Stewart & D.H. Blake

AGSO
AUSTRALIAN GEOLOGICAL
SURVEY ORGANISATION

BMR
555(94)
BUL.45
COPY 3

Department of Primary Industries and Energy

Bureau of Mineral Resources
Geology and Geophysics
Minerals and Land Use Program

Bulletin 243

BUREAU OF MINERAL RESOURCES
LIBRARY
8 FEB 1993
CANBERRA, A.C.T.

Detailed Studies of the Mount Isa Inlier

A.J. Stewart & D.H. Blake

Editors

Australian Government Publishing Service
Canberra

© Commonwealth of Australia 1992
ISBN 0 644 25220 0
ISSN 0084-7089

This work is copyright. Apart from any use as permitted under the *Copyright Act 1968*, no part may be reproduced by any process without prior written permission from the Australian Government Publishing Service. Requests and inquiries concerning reproduction and rights should be addressed to the Manager, Commonwealth Information Services, Australian Government Publishing Service, GPO Box 84, Canberra ACT 2601.

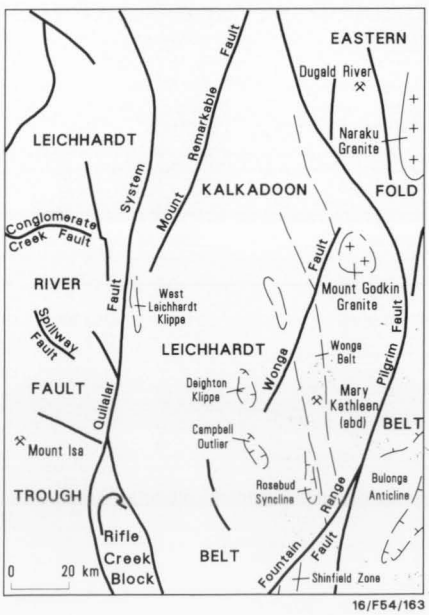
Copy editing: A.J. Stewart

Line drawings (BMR-authored papers only): H.Apps, J. Mifsud, N. Jeffery, N. Montgomery, Cartographic Services Unit

Desk-top publishing: J.A. Haldane, Bureau of Mineral Resources, Minerals and Land Use Program

Cover design: Saimonne Bissett

Cover: Central Mount Isa Inlier, Queensland. Landsat–5 Thematic Mapper false colour composite image of bands 1 (displayed as red), 4 (green) and 7 (blue). The Landsat scene (path aa, row 74) was acquired on 1 October 1986 and processed by L. Macias, Minerals and Land Use Program. Major geological features are outlined below:



Printed for AGPS by Union Offset Co. Pty Ltd, Canberra

Foreword

The Proterozoic Mount Isa Inlier of northwestern Queensland is one of Australia's most important producers of copper, zinc, lead, and silver, accounting for over 40% of Australia's export earnings of these metals. Hence, it has been a focus of geological mapping and exploration for many years. BMR's interest began in the early 1950's, and by 1958 the entire inlier had been mapped at the broad reconnaissance level (1:250 000 scale) by joint BMR-GSQ (Geological Survey of Queensland) parties (Carter & others, 1961). This work established a stratigraphic framework for the inlier, and provided the first insight into its extremely complex structure. A more detailed (1:100 000 scale) second stage of mapping, again by joint BMR-GSQ parties, began in 1969 and was largely completed by 1980. This work extensively revised the stratigraphic picture, and the timing of major igneous events was determined using U-Pb geochronology. Blake (1987) synthesised the mapping results and prepared a 1:500 000 map of the entire inlier.

The third BMR mapping stage began in 1983 and finished in 1989, and was concerned with detailed structural, petrological (both igneous and metamorphic), sedimentological, and geochronological studies by BMR and BMR-supported university workers. The results of this work are presented as separate papers in this bulletin and as a set of individual geological maps at various scales on which most of the papers are based; the individual maps are synthesised into a 1:250 000 scale transect map which accompanies this bulletin. The maps are listed in the Table of Contents, and the locations of the mapped areas are shown in Figure 1.

BMR is currently (1992) preparing a metallogenic analysis and Geographic Information System of the Mount Isa Inlier in ARC/INFO format (Wyborn & Gallagher, in preparation), which will incorporate the following digital datasets: the 1:500 000 scale geological map of Blake (1987); geochemical data; regional geophysical data; metallogenic data (Raymond & Fortowski, in press); and Landsat TM imagery.

References

BLAKE, D.H., 1987 - Geology of the Mount Isa Inlier and environs, Queensland and Northern Territory. *Bureau of Mineral Resources, Australia, Bulletin* 225, 83 pp.

CARTER, E.K., BROOKS, J.H., & WALKER, K.R., 1961 - The Precambrian mineral belt of northwestern Queensland. *Bureau of Mineral Resources, Australia, Bulletin* 51, 344 pp.

RAYMOND, O., & FORTOWSKI, D., in press 1992 - Mount Isa Inlier mineral deposit database, with explanatory notes. *Bureau of Mineral Resources, Australia, Record and Database.*

WYBORN, L.A.I., & GALLAGHER, R., in preparation - Mount Isa Inlier Geographic Information System. *Bureau of Mineral Resources, Australia.*

Alastair Stewart
Principal Research Scientist
Minerals and Land Use Program



Acknowledgements

We thank our colleagues for assistance during preparation of this Bulletin, especially E.J. Anderson, G.M. Bladon, M.A. Craig, G.W. D'Addario, B.R. Goleby, D.A. Harris, C.A. Heinrich, I.M. Hodgson, M.J. Jackson, R.W. Johnson, R.S. Needham, M. Nicoll, A.G.L. Paine, M.S. Rattenbury, N. Williams, P.R. Williams, and L.A.I. Wyborn. We especially thank J.A. Haldane, who desk-topped the entire Bulletin. A.L. Jaques, Chief of the Minerals and Land Use Program, provided resources and encouragement to complete this Bulletin. We also wish to thank the referees (listed below), several of whom reviewed more than one paper, and the staff of BMR's Cartographic Services Unit, namely H.E.J. Apps, N. Jeffery, J.M. Mifsud, and N.R. Montgomery for the text-figures in the BMR-authored papers, N. Jeffery for digitising the Mount Isa - Cloncurry map accompanying this bulletin, R.A. Swoboda for map colour design, R.P. Stephens for digitising and printing the 16 maps of the individual areas (Fig. 1) on which this Bulletin is based, and S.L. Bissett and L. McMahon for cover design. Lastly we thank most heartily D.M. Pillinger, who designed and drew all 22 sheets making up the 16 individual maps at the remarkable rate of one sheet per month.

Referees: J.H.C. Bain, D.H. Blake, R.S. Blewett, M.A. Etheridge, C.A. Heinrich, M.J. Jackson, R.J. Korsch, B. Krapez, S. Lonker, R.J.H. Loosveld, W. Nijman, C.W. Passchier, P.J. Pearson, M.S. Rattenbury, J. Reinhardt, R.D. Shaw, J.W. Sheraton, E.L. Simpson, A.J. Stewart, P.G. Stuart-Smith, I.P. Sweet, F. Vanderhor, P.R. Williams, K.H. Wolf, and L.A.I. Wyborn.

Contents

D.H. Blake & A.J. Stewart
Stratigraphic and tectonic framework, Mount Isa Inlier 1

R.J. Holcombe & A.J. Stewart
Note on deformation terminology 13

P. Wellman
Structure of the Mount Isa region inferred from gravity and magnetic anomalies 15

W. Nijman, J.H. van Lochem, H. Spliethoff, & J. Feijth
Deformation model and sedimentation patterns of the Proterozoic of the Paroo Range, Mount Isa Inlier, Queensland, Australia 29

W. Nijman, H.F. Mijnlieff, & G. Schalkwijk
The Hero Fan delta (Lower Mount Isa Group) and its structural control: deformation in the Hero/Western Fault Zone and Paroo Range compared, Proterozoic, Mount Isa Inlier, Queensland, Australia 75

A.J. Stewart
Geology of the Horse's Head structure, north of Mount Isa, and its bearing on the 'roof thrust + imbricate stack' hypothesis, Mount Isa Inlier, Queensland 111

J.H.C. Bain, C.A. Heinrich, & G.A.M. Henderson
Stratigraphy, structure, and metasomatism of the Haslingden Group, East Moondarra area, Mount Isa: a deformed and mineralised Proterozoic multistage rift-sag sequence 125

K.A. Connors, J.M. Proffett, G.S. Lister, R.J. Scott, N.H.S. Oliver, & D.J. Young
Geology of the Mount Novit Ranges, southwest of Mount Isa mine 137

D.H. Blake
Stratigraphy, folding, and faulting within the Quilalar Fault System, Mount Isa Inlier 161

D.H. Blake
The compressional Lake Mary Kathleen Fold and Thrust Zone, Mount Isa Inlier 181

P.R. Williams & D.H. Blake
Black Mountain – a strike-slip pull-apart structure in the Quilalar Fault System, Mount Isa Inlier 191

C.W. Passchier
Geology of the Myubee area, Mount Isa Inlier, Queensland 199

A.J. Stewart
Stratigraphy, extension, and contraction in the Ballara–Mount Frosty area, Mount Isa Inlier, Queensland 209

J. Reinhardt
The Corella Formation of the Rosebud Syncline (central Mount Isa Inlier): deposition, deformation, and metamorphism 229

R.J. Holcombe, P.J. Pearson, & N.H.S. Oliver
Structure of the Mary Kathleen Fold Belt 257

P.J. Pearson, R.J. Holcombe, & R.W. Page
Synkinematic emplacement of the Middle Proterozoic Wonga Batholith into a mid-crustal extensional shear zone, Mount Isa Inlier, Queensland, Australia 289

E.J. Hill, R.J.H. Loosveld, & R.W. Page
Structure and geochronology of the Tommy Creek Block, Mount Isa Inlier 329

R.J.H. Loosveld
Structural geology of the central Soldiers Cap Belt, Mount Isa Inlier, Australia 349

D.H. Blake & A.J. Stewart
The BMR 1983-1990 Mount Isa Project: results, some remaining problems, and bibliography 361

List of maps on which many of the above papers are based

A.J. Stewart - Geology of the Ballara-Mount Frosty Region, 1:25 000 (two sheets)

D.H. Blake - Geology of Black Mountain, Duchess, 1:5000

P.J.Pearson - Geology of the Breakfast Creek Area, 1:25 000

R.J.H. Loosveld - Structural Geology of the Central Soldiers Cap Group, 1:100 000

P.J. Pearson - Geology of the East Limb, Little Beauty Syncline, 1:15 000

G.A.M. Henderson & J.H.C. Bain - Geology of the Haslingden Group, East Moondarra Area, 1:35 000

D.H. Blake - Geology of the Lake Mary Kathleen Zone, 1:50 000

R.J. Holcombe - Geology of the Mary Kathleen Area, 1:25 000 (two sheets)

N.H.S. Oliver - Geology of the Mount Godkin Area, 1:25 000

K.A. Connors, J.M. Proffett, G.S. Lister, R.J. Scott, N.H.S. Oliver, & D.J. Young - Geology of the Mount Novit Area, 1:25 000 (two sheets)

C.W. Passchier - Geology of the Myubee Area, 1:25 000

W. Nijman - Geology of the Paroo Range - Hero/Western Fault Zone, 1:20 000 (two sheets)

D.H. Blake - Geology of the Rifle Creek Region, 1:50 000 (two sheets)

J. Reinhardt - Geology of the Rosebud Syncline, 1:25 000

E.J. Hill - Geology of the Tommy Creek Block, 1:25 000 (two sheets)

D.H. Blake - Geology of the West Leichhardt Klippe and the Gorge Creek Sector of the Quilalar Fault Zone, 1:50 000

D.H. Blake & A.J. Stewart - Geology of the Mount Isa - Cloncurry Transect, 1:250 000 (accompanies this Bulletin).

The locations of the maps are shown in Figure 1. Each sheet (except Geology of the Mount Isa – Cloncurry Transect) is available as a colour electrostatic plot on paper (AUD30), or in digital form on optical disc or Exabyte 8 mm tape (prices on application) both of which can be displayed on Intergraph Microstation software on computers that will run Unix. The digital data comprise a scanned raster image (.RLE format) of the black and white geological map, and an Intergraph vector design file containing the boundaries of coloured polygons. The coloured map and data are available from the Publication Sales Centre, Bureau of Mineral Resources, and an uncoloured Ozalar film or paper copy (AUD20) of the map is available from BMR Copy Service, both at GPO Box 378, Canberra, ACT, 2601, Australia. All orders to be prepaid to Collector of Public Monies.

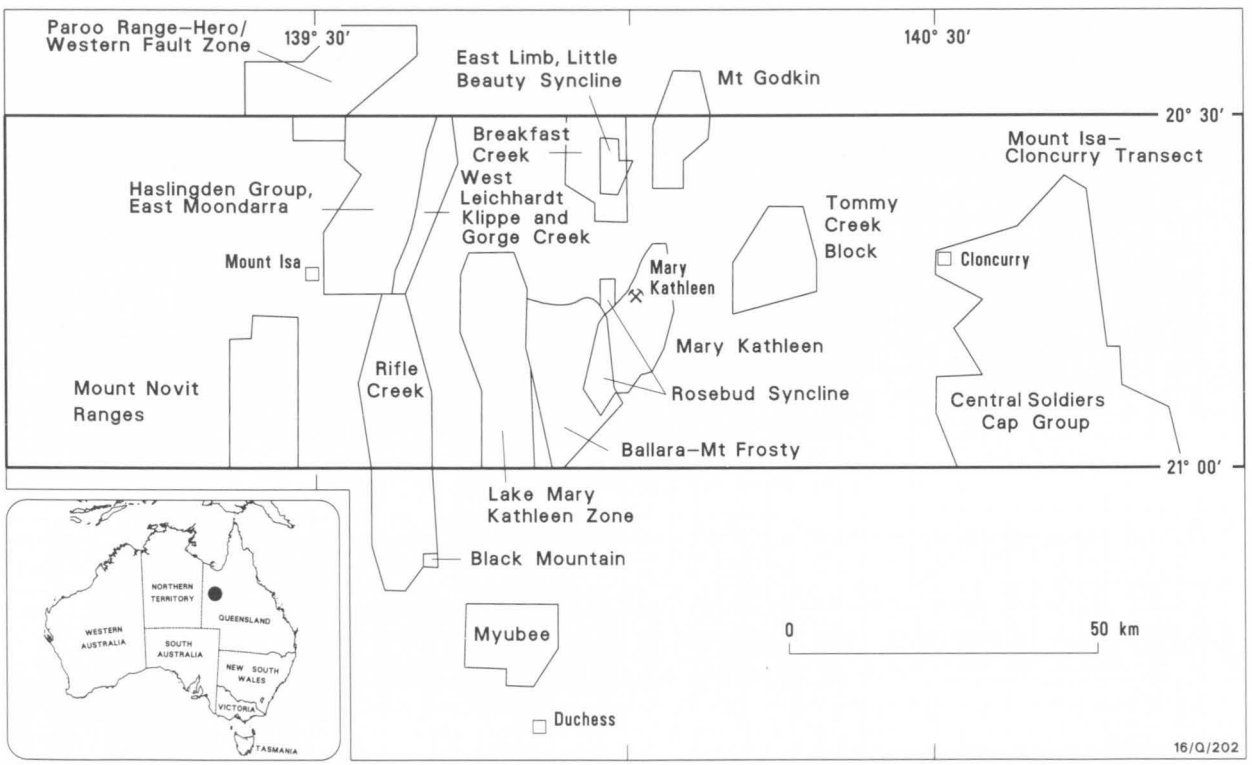


Fig. 1. Location of maps.

Stratigraphic and tectonic framework, Mount Isa Inlier

D.H.Blake [1] *& A.J.Stewart* [1]

This paper is based on the following map, which accompanies this bulletin:

Blake, D.H., & STEWART, A.J., 1992 - Geology of the Mount Isa - Cloncurry Transect 1:250 000 scale map. Bureau of Mineral Resources, Canberra.

Two major Proterozoic tectonostratigraphic cycles are evident in the Mount Isa Inlier, an earlier cycle represented by basement, which was deformed and metamorphosed during the Barramundi Orogeny (1900-1870 Ma), and a later cycle, represented by cover sequences 1-3, which was terminated by the Isan Orogeny (1620-1520 Ma). Cover sequence 1 (1870-1850 Ma) is mainly felsic volcanics, cover sequence 2 (1790-1720? Ma) is dominated by mixed shallow-water sediments and bimodal volcanics, and cover sequence 3 (1680-1625 Ma) contains mostly fine-grained clastic sediments and carbonates, with only minor volcanics.

Large granitic batholiths were emplaced at around 1860 Ma, 1800 Ma, 1740 Ma, 1670 Ma, and 1500 Ma. Abundant mafic dykes range in age from pre-1900 Ma to around 1100 Ma.

Extensional deformation during the second tectonostratigraphic cycle was terminated by the compressional Isan Orogeny, which consisted of two main phases, early thrusting and folding indicative of north-south shortening being followed by a dominating phase of upright folding resulting from east-west shortening. Subsequent transcurrent faulting subdivided the area into several meridional belts, each with its own distinctive stratigraphy. The late faults include those of the Pilgrim Fault Zone, separating the Eastern Fold Belt from the Kalkadoon-Leichhardt Belt, and the Quilalar Fault Zone, the boundary between the Kalkadoon-Leichhardt Belt and the Western Fold Belt.

[1] Bureau of Mineral Resources, GPO Box 378, Canberra, ACT, 2601.

Introduction

Two major Proterozoic tectonostratigraphic cycles have been recognised in the Mount Isa Inlier, separated by an orogenic event, the Barramundi Orogeny, at around 1870 Ma (Etheridge & others, 1987). The first cycle is represented by the relatively restricted basement sequence, and the second cycle by the three cover sequences of Blake (1987). The second cycle was terminated by region-wide deformation and metamorphism between about 1520 and 1620 Ma - the Isan Orogeny of Blake & others (1990). An intracratonic, rather than continental margin, setting is favoured for at least the second cycle (see Blake, 1987, for discussion).

The Mount Isa Inlier is subdivided by major north-striking strike-slip faults or fault zones into a series of meridional belts (Fig. 1), the Proterozoic stratigraphy in each of which differs, to a greater or lesser degree, from that in adjacent belts. The most significant stratigraphic differences are across the Pilgrim Fault (Fig. 1), where a probable displacement of several hundred kilometres is indicated, sufficient for the fault to be regarded as the boundary between two separate terranes (e.g., Blake & Stewart, in BMR, 1988). Other major faults with stratigraphic significance include the Mount Isa, Quilalar, and Wonga Belt Faults in the western terrane (BMR, 1988), and the Cloncurry 'Overthrust' in the eastern terrane. The major tectonic units proposed by Blake (1987) for the Mount Isa Inlier need to be modified to allow for the effects of these faults.

The Western Fold Belt is now taken to comprise only the Lawn Hill Platform and Leichhardt River Fault Trough, the boundary between which is a fault zone that includes the Mount Isa Fault. The boundary between the Western Fold Belt and the Kalkadoon-Leichhardt Belt is the Quilalar Fault Zone, which marks the eastern limit of the Leichhardt River Fault Trough. Hence the Ewen Block and Myally Shelf, previously part of the Western Fold Belt, are now regarded as part of the Kalkadoon-Leichhardt Belt. The Kalkadoon-Leichhardt Belt is taken to extend east across the Wonga Belt to the Pilgrim Fault Zone, and therefore includes the Mary Kathleen Zone, previously the most westerly zone of the Eastern Fold Belt. Consequently, the Eastern Fold Belt comprises only the Quamby-Malbon and Cloncurry-Selwyn Zones of Blake (1987).

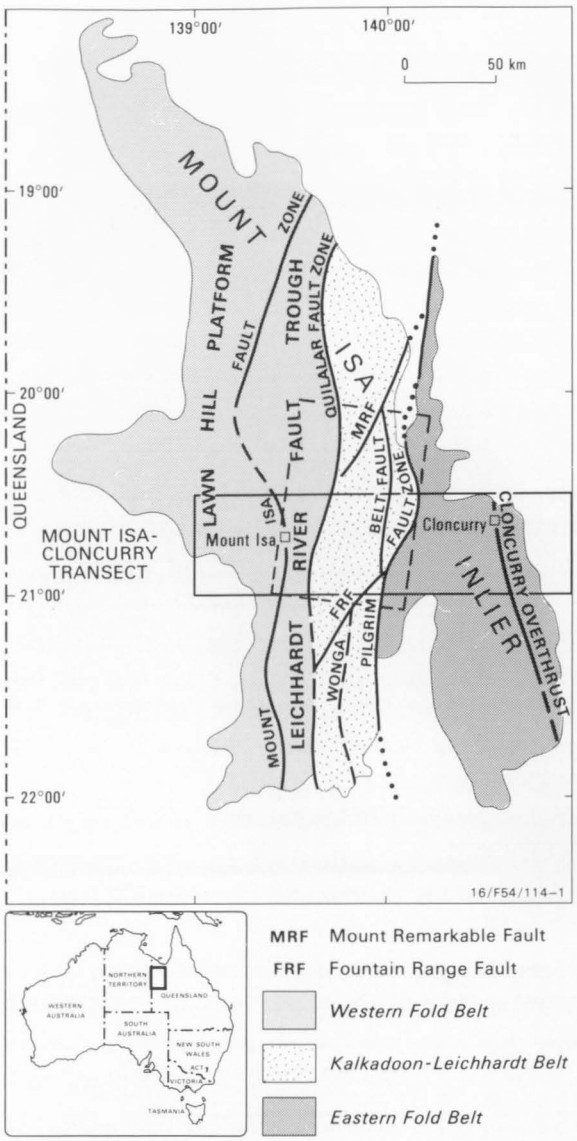


Fig. 1. Tectonic units of the Mount Isa Inlier. Solid rectangle shows locations of transect map, dashed rectangle shows locations of Landsat TM imagery on front cover of Bulletin.

In this paper, stratigraphic names in italics are of units that crop out within the Mount Isa-Cloncurry transect (Mount Isa, Mary Kathleen, Marraba, and Cloncurry 1:100 000 Sheets) and are shown on the accompanying map (Blake & Stewart, 1992).

Stratigraphy

Descriptions of the main, currently recognised, Proterozoic stratigraphic units in the Mount Isa Inlier are summarised in Table 1, which is based partly on Blake (1987) and partly on the more recent work described in this bulletin. Relationships are shown schematically in Figure 2.

The oldest rocks exposed, the **basement**, represent sedimentary, volcanic, and intrusive rocks which were highly deformed and metamorphosed during the 1900-1870 Ma Barramundi Orogeny. The main basement units are the *Yaringa Metamorphics* in the Western Fold Belt west of Mount Isa (Page & Williams, 1988), the *Kurbayia Migmatite* (Blake & Page, 1988a) in the eastern part of this belt and in the Kalkadoon-Leichhardt Belt, the Plum Mountain Gneiss in the Kalkadoon-Leichhardt Belt, and the Double Crossing Metamorphics in the Eastern Fold Belt. The basement units may be correlated with other early Proterozoic sequences in northern Australia, such as that of the Pine Creek Inlier (Needham & others (1988), the Murphy Metamorphics of the Murphy Inlier (Blake, 1987), and the Warramunga Group of the Tennant Creek Inlier (Blake & Page, 1988b).

The three cover sequences of the second tectonostratigraphic cycle in the Mount Isa Inlier are major stratigraphic packages, with preserved thicknesses of several kilometres, separated by regional unconformities attributed to basin subsidence and tectonism. Sedimentary and volcanic features indicate mainly fluvial to shallow-marine or lacustrine depositional environments.

TABLE 1. DESCRIPTIONS OF STRATIGRAPHIC UNITS, MOUNT ISA INLIER

Unit	Main rock types at lowest metamorphic grade (maximum thickness in metres)
Quamby Conglomerate	Conglomerate, lithic sandstone (300+)
COVER SEQUENCE 3	
Tommy Creek beds	Calcareous and pelitic metasediments, bimodal volcanics (1000+)
McNAMARA GROUP	Dolomite, siltstone; quartz sandstone and conglomerate at base (8500)
MOUNT ISA GROUP	Siltstone, shale - commonly dolomitic or pyritic; quartz sandstone and conglomerate at base (4500+)

Surprise Creek Formation	Sandstone, siltstone, shale (2000+)
Carters Bore Rhyolite	Porphyritic rhyolite, conglomerate (200+)
Fiery Creek Volcanics	Rhyolite, basalt, sandstone, conglomerate (250)
Bigie Formation	Lithic and feldspathic sandstone, conglomerate (600)
?COVER SEQUENCE 3	
Lady Clayre Dolomite	Dolomite, dolomitic siltstone (3000)
Coocerina Formation	Calcareous black shale, scapolitic siltstone (400)
Knapdale Quartzite	Sandstone (2000+)
COVER SEQUENCE 2 - west of Pilgrim Fault	
MOUNT ALBERT GROUP	
White Blow Formation	Pelitic and calcareous metasediments (1000)
Deighton Quartzite	Feldspathic, lithic and quartz sandstone (2700)
Corella Formation	Banded calc-silicate rocks, metapelite,metasiltstone, marble, felsic and mafic volcanics (1000+)
Ballara Quartzite	Quartz and feldspathic sandstone (1250)
Quilalar Formation	Quartz and feldspathic sandstone in lower part; calcareous and micaceous siltstone, greywacke, sandstone and dolomite in upper part (1500+)
Argylla Formation	Felsic volcanics (2000)
Magna Lynn Metabasalt	Metabasalt, sandstone (1500)
HASLINGDEN GROUP	
Myally Subgroup	Feldspathic and quartz sandstone (3700+)
Eastern Creek Volcanics	Metabasalt, sandstone (7200)
Mount Guide Quartzite	Greywacke, conglomerate in lower part; quartz sandstone in upper part (6000+)
Bottletree Formation	Greywacke, conglomerate, bimodal volcanics (3000)
COVER SEQUENCE 2 - east of Pilgrim fault	
MARY KATHLEEN GROUP	
Roxmere Quartzite	Feldspathic sandstone (2000+)
Corella beds	Banded and brecciated calc-silicate rocks (1000+)
Doherty Formation	Banded and brecciated calc-silicate rocks (1000+)
Marimo Slate	Carbonaceous slate and siltstone (2000)
Staveley Formation	Partly calcareous sandstone, siltstone, shale and mudstone (2000+)
Answer Slate	Partly carbonaceous slate and siltstone (1000+)
Kuridala Formation	Greywacke, siltstone, carbonaceous slate (1000+)
Overhang Jaspilite	Siltstone, chert, marble, jaspilite (1000)
SOLDIERS CAP GROUP	Greywacke, siltstone, sandstone, metabasalt (5000+)
MALBON GROUP	
Mitakoodi Quartzite	Quartz and feldspathic sandstone (3000)
Marraba Volcanics	Mafic volcanics, siltstone, sandstone (3500)
Argylla Formation	Felsic volcanics, sandstone (2000+)
COVER SEQUENCE 1	
Leichhardt Volcanics	Felsic volcanics (1000+)
Orient beds	Sandstone, siltstone, conglomerate,carbonates (1000+)
Candover Metamorphics	Siltstone, sandstone, bimodal volcanics (1000+)
BASEMENT	
Yaringa Metamorphics	Schist, gneiss, migmatite
Kurbayia Migmatite	Migmatite, gneiss, schist
Plum Mountain Gneiss	Quartzofeldspathic gneiss
Double Crossing Mets	Gneiss, schist, migmatite

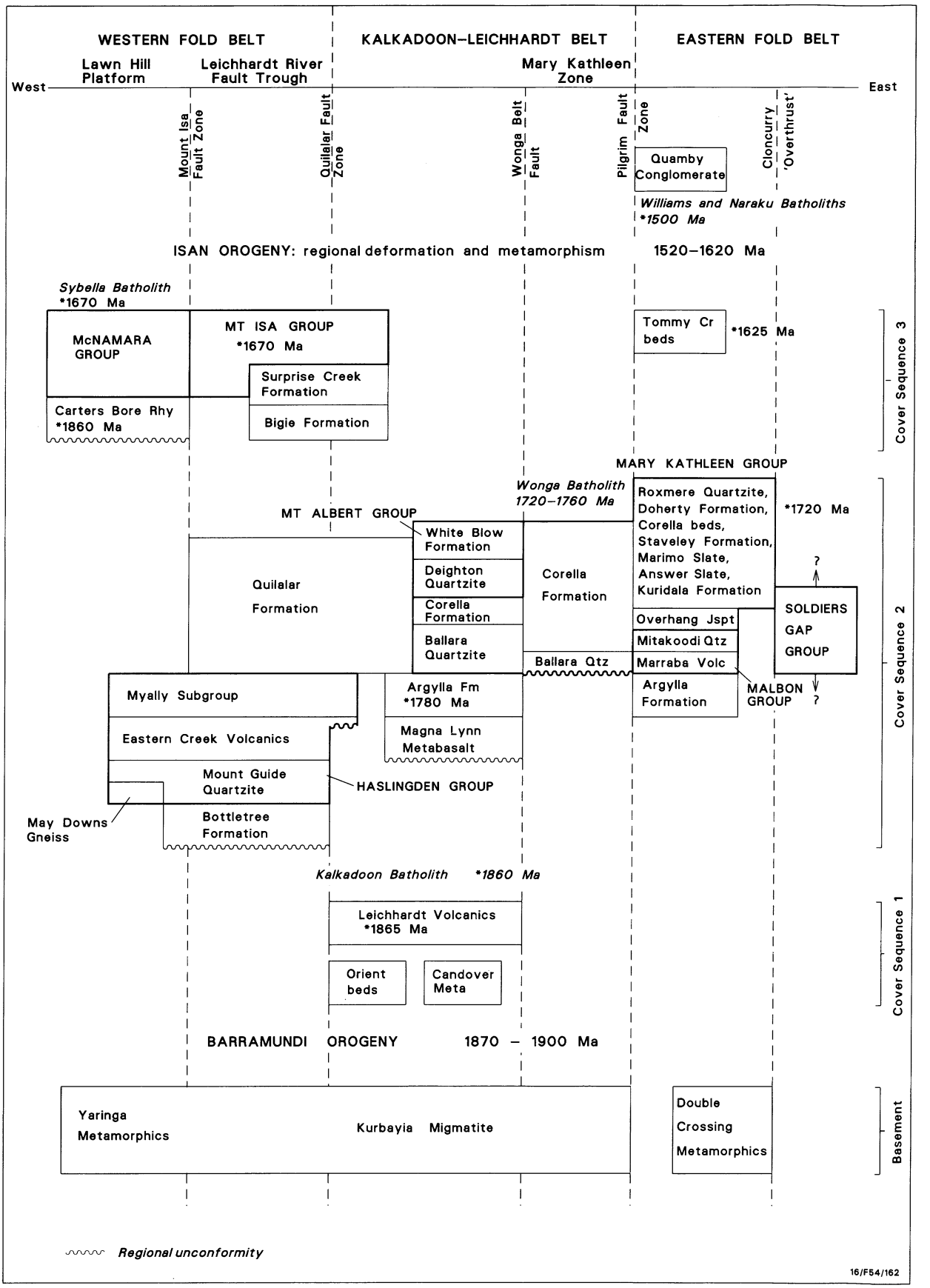


Fig. 2. Stratigraphic framework.

Cover sequence 1 is confined to the Kalkadoon-Leichhardt Belt. It consists mainly of the felsic *Leichhardt Volcanics*, but is taken to include the Candover Metamorphics of the Ewen Block and a newly named unit to the south, the *Orient beds* (Blake, this volume). The *Leichhardt Volcanics*, together with coeval granites of the Kalkadoon and Ewen Batholiths, range in age from about 1870 to 1850 Ma (e.g., Page, 1988), and are part of an Australia-wide 1880-1840 Ma felsic magmatic event (Wyborn, 1988). The *Leichhardt Volcanics* are considered to be related to the Barramundi Orogeny, rather than to subsequent basin formation, as they consist predominantly of subaerial pyroclastics, not basin-type sediments, and are only slightly younger than this orogeny. Possible correlatives include the Cliffdale Volcanics of the Murphy Inlier, and the Edith River and El Sherana Groups of the Pine Creek Inlier. In contrast to these volcanic units, the Candover Metamorphics and *Orient beds* are largely sedimentary, and may represent local basin infillings.

Cover sequence 2 ranges in age from about 1790 Ma, the age of the *Bottletree Formation* at the base of the Leichhardt River Fault Trough succession, to perhaps 1760 Ma or 1720 Ma. The *Bottletree Formation* lies unconformably on basement and *Kalkadoon Granite,* and consists of bimodal volcanics and clastic sediments, including conglomerate containing basement and granite clasts. It passes up into the *Haslingden Group,* which comprises the *Mount Guide Quartzite* and correlative Leander Quartzite at the base, basaltic lavas and subordinate sediments of the *Eastern Creek Volcanics* and correlatives in the middle part, and clastics of the *Myally Subgroup* at the top. The *Haslingden Group* reaches a thickness of at least 10 km in the Western Fold Belt, but is less than 1 km thick to the east, in the western part of the adjacent Kalkadoon-Leichhardt Belt, where the *Mount Guide Quartzite, Bottletree Formation,* and most of the *Eastern Creek Volcanics* are absent. Clastics and carbonates of the succeeding *Quilalar Formation* appear to be conformable on the *Haslingden Group;* they extend eastwards from the Leichhardt River Fault Trough across to the eastern side of the Kalkadoon-Leichhardt Belt, where they are assigned to the *Ballara Quartzite* and *Corella Formation.* The *Corella Formation* is overlain by the *Mount Albert Group,* comprising the *Deighton Quartzite* and *White Blow Formation.* This group was tentatively regarded as part of cover sequence 3 by Blake (1987), but is now known to lie conformably, rather than unconformably, on Corella Formation (Stewart, 1989 and this volume), and hence belongs to cover sequence 2.

Recent sedimentological studies in the Western Fold Belt and Kalkadoon-Leichhardt Belt indicate that the Bottletree-Quilalar package represents two extensional rift-sag cycles of basin formation (Eriksson & others, 1992). The earlier cycle is represented by the *Bottletree Formation* and lower *Mount Guide Quartzite* (rift phase) and the upper *Mount Guide Quartzite* (sag phase, 20-25 Ma time-span - Eriksson & Simpson, 1990; Simpson & Eriksson, 1991), and the later cycle by the *Eastern Creek Volcanics* and *Myally Subgroup* (rift phase), and the *Quilalar Formation* (sag phase). The earlier rift-sag cycle is restricted to the Leichhardt River Fault Trough, whereas the later cycle extends eastwards from the Leichhardt River Fault Trough, across the Kalkadoon-Leichhardt Belt, to the Pilgrim Fault Zone.

In the eastern part of the Kalkadoon-Leichhardt Belt, the *Ballara Quartzite* and overlying *Corella Formation,* correlatives of the *Quilalar Formation,* crop out on both sides of a north-south trending highly deformed zone known as the Wonga Belt. East of this belt, in the Mary Kathleen Zone of Blake (1987), they lie unconformably on basement *Kurbayia Migmatite* (Blake, in press) and include significant amounts of basaltic volcanics. To the west, in contrast, they are conformable to disconformable on probable Haslingden Group equivalents - the 1780 Ma old *Argylla Formation* (mainly felsic volcanics and feldspathic sandstone) and the underlying *Magna Lynn Metabasalt* - and do not contain basalt. The cover sequence 2 units on both sides of the Wonga Belt are intruded by, and hence are older than, 1760-1720 Ma granites of the Wonga Batholith.

In the Eastern Fold Belt, most of the stratigraphic units exposed are assigned to cover sequence 2. The oldest rocks seen in the western part of this belt are felsic volcanics and clastics mapped as *Argylla Formation.* These pass up into the *Marraba Volcanics* (basalt and clastics) and *Mitakoodi Quartzite* (mainly sandstone) of the *Malbon Group,* conformably overlying which are the *Overhang Jaspilite* and Answer Slate of the *Mary Kathleen Group.* Stratigraphic relationships between the last two formations and other units assigned to the *Mary Kathleen Group* in the Eastern Fold Belt - *Marimo Slate, Corella beds* (Ryburn & others, 1988; previously mapped as Corella Formation), *Staveley Formation, Roxmere Quartzite* (previously assigned to the Mount Albert Group), Kuridala Formation, Agate Downs Siltstone, and Doherty Formation - are uncertain because of faulting complexities. The *Mary Kathleen Group* consists predominantly of metasediments, which include evaporites, carbonates,

calc-silicate rocks, and black slate. Its relationship to turbiditic sediments and mafic volcanics of the *Soldiers Cap Group* (Llewllyn Creek Formation, Mount Norna Quartzite, and Toole Creek Volcanics) to the east has yet to be resolved satisfactorily. The *Soldiers Cap Group* may be correlated with the Kuridala Formation and Answer Slate of the *Mary Kathleen Group* (e.g., Blake, 1987), although Beardsmore & others (1988) have proposed that the Soldiers Cap Group, Kuridala Formation, and conformably underlying quartzofeldspathic rocks represent a rift sequence, named by them the Maronan Supergroup, that predates cover sequence 2. This proposal has been disputed by Loosveld (1989), who favours the view of Blake (1987). Unfortunately there is no direct geochronological evidence available to support or negate either interpretation.

U-Pb zircon ages have been obtained by Page (1983a) for felsic volcanics in two of the cover sequence 2 units in the Eastern Fold Belt: 1766+23/-19 Ma (*Argylla Formation*) and 1720 ± 7 Ma (Doherty Formation of the Mary Kathleen Group).

Cover sequence 2 may have no correlatives in other parts of northern Australia. It is younger than the Hatches Creek Group of the Tennant Creek Inlier, dated at about 1800-1820 Ma (Blake & Page, 1988b; Page, personal communication, 1991), and except perhaps for part of the sequence in the Eastern Fold Belt, is older than the Tawallah Group of the McArthur Basin (e.g., Plumb & others, 1990).

Cover sequence 3 is largely confined to the Western Fold Belt and western part of the Kalkadoon-Leichhardt Belt, where it overlies cover sequence 2 disconformably and locally with angular unconformity. The oldest units of the sequence are the *Carters Bore Rhyolite* in the west, dated at 1678 Ma by Page (1978), and the possibly correlative clastic *Bigie Formation* and bimodal Fiery Creek Volcanics to the east and north. These rift-type units are overlain by sag-phase sediments of the *Surprise Creek Formation* and *Mount Isa Group* (east of the Mount Isa Fault zone) and *McNamara Group* (to west). The *Mount Isa Group* and correlative *McNamara Group* consist of basal sandstone and conglomerate passing up into several thousand metres of mainly siltstone, shale, and carbonate. A tuff bed in the Urquhart Shale of the *Mount Isa Group* has been dated at 1670 +20/-17 Ma (Page, 1981), although recent ion microprobe results indicate a more precise age of about 1650 Ma (R.W Page, BMR, unpublished data, 1992). The two groups correlate with the McArthur Group of the McArthur Basin.

The isotopic dating indicates a time gap of about 70 Ma between deposition of cover sequences 2 and 3 in the Western Fold Belt. Hence cover sequence 3 here is unlikely to have been associated with the same basin-forming events as those relating to cover sequence 2.

The cover sequence 3 units of the Western Fold Belt extend eastwards into the western part of the Kalkadoon-Leichhardt Belt, but are not known farther east. However, some possible cover sequence 3 units are exposed within fault-bounded blocks in the Eastern Fold Belt. These are the Knapdale Quartzite, Coocerina Formation, Lady Clayre Dolomite, and probably the part mapped as Corella Formation that contains the Dugald River Shale Member, all of which crop out in the vicinity of the Dugald River Pb-Zn prospect, and the *Tommy Creek beds* between Cloncurry and Mary Kathleen. The Dugald River Pb-Zn deposit has a Pb-isotope composition (Gulson, 1985) very close to that for the Mount Isa Pb-Zn deposit, giving a model age of 1540 Ma according to the calibration scheme of (Cumming & Richards, 1975). The U-Pb zircon age of about 1650 Ma for the Mount Isa Group suggests that the Dugald River sequence may also be of this age, i.e., 1650 Ma. Other units in the Eastern Fold Belt could also be of this vintage, and a collaborative study between BMR, CSIRO, and industry is being conducted (1992) to better document the age of these sequences.

The *Tommy Creek beds*, previously mapped as part of the Corella Formation, include felsic volcanics dated at 1626 Ma (Hill & others, this volume) and hence are appreciably younger than the *Mount Isa Group*.

Deposition of cover sequence 3 was terminated by the Isan Orogeny, a period of major deformation and high temperature/low pressure metamorphism which lasted from about 1620 Ma to about 1520 Ma. This orogeny postdates the Sybella Batholith of the Western Fold Belt, emplaced at around 1670 Ma, and was closely followed, at around 1500 Ma, by intrusion of granite plutons (Naraku and Williams Batholiths) in the Eastern Fold Belt.

Some time later in the Proterozoic, coarse clastics of the *Quamby Conglomerate* were deposited in the Eastern Fold Belt. This formation, the youngest of Proterozoic age exposed in the Mount Isa Inlier, crops out in two narrow fault-bounded areas close to the Pilgrim Fault Zone. It is folded, but not metamorphosed.

Igneous activity

The Mount Isa Inlier has a long history of igneous activity, starting sometime before the 1870 Ma-old Barramundi Orogeny and probably ending at around 1100 Ma with the

emplacement of dolerite dykes. Throughout this period the magmatism was predominantly bimodal, resulting in abundant felsic and mafic igneous rocks, but very few of intermediate composition (e.g., Blake, 1987).

Pre-1870 Ma

Metamorphosed felsic and subordinate mafic igneous rocks are present in the basement *Kurbayia Migmatite* (Blake & Page, 1988a) and Plum Mountain Gneiss, in the southern half of the Kalkadoon-Leichhardt Belt. They include metarhyolite, some of which has contorted flow-banding evident, metadacite, and banded gneissic 'tuff', representing extrusives; homogeneous to streaky and xenolithic felsic gneiss that is probably intrusive; and amphibolite of either extrusive or intrusive origin. Meta-igneous rocks have also been identified in the Double Crossing Metamorphics of the Eastern Fold Belt and the Saint Ronans Metamorphics of the Western Fold Belt.

1870-1840 Ma

Extrusion of the *Leichhardt Volcanics* of cover sequence 1 and emplacement of the Kalkadoon and Ewen Batholiths took place between about 1870 and 1840 Ma. These units belong to the Kalkadoon-Leichhardt magmatic suite of Wyborn (1988).

The *Leichhardt Volcanics* consist predominantly of subaerial felsic ignimbritic deposits, but also include some rhyolite lava and rare bedded tuff. Isotopic dating by Page (e.g., 1988) indicates a range in age from around 1870 Ma in the south to 1850 Ma in the north. The volcanics are intruded by granites of the Kalkadoon Batholith, dated at around 1860 Ma, and Ewen Batholith, dated at close to 1840 Ma. Some volcanics are also present in the two other cover sequence 1 units, the Candover Metamorphics and *Orient beds.*

Kalkadoon Granite, which makes up most of the Kalkadoon Batholith, crops out in the eastern part of the Western Fold Belt, where it is overlain by the *Bottletree Formation* of cover sequence 2, and much more extensively in the Kalkadoon- Leichhardt Belt. The Ewen Batholith, which may be 10-20 Ma younger than the Kalkadoon Batholith, is restricted to the Ewen Block in the north of the Kalkadoon-Leichhardt Belt.

The occurrence of mafic dykes forming net-veined complexes with *Kalkadoon Granite* (e.g., Blake, 1981) indicates that the extensive felsic magmatism of the period was probably accompanied by local minor mafic magmatism.

1840-1790 Ma

The *Leichhardt Volcanics* of cover sequence 1 and the comagmatic Kalkadoon and Ewen Batholiths are intruded by swarms of metamorphosed mafic dykes. Many, if not most of these dykes postdate granite and predate the *Magna Lynn Metabasalt* of cover sequence 2, hence were probably intruded after 1840 Ma but before 1790 Ma ago.

Two granites were emplaced between 1840 and 1790 Ma in the Western Fold Belt west of the Mount Isa Fault Zone: the Yeldham Granite, dated at about 1820 Ma, in the north, and the *Big Toby Granite,* dated at about 1800 Ma, in the south (Wyborn & others, 1988).

1790-1760 Ma

Widespread igneous activity, both extrusive and intrusive, took place during deposition of cover sequence 2 in the Western Fold Belt and Kalkadoon-Leichhardt Belt. Comparable magmatism in the Eastern Fold Belt may be of similar age, but could be somewhat younger. The oldest cover sequence 2 unit in the Leichhardt River Fault Trough, the *Bottletree Formation*, includes both felsic volcanics, which have been dated at about 1790 Ma (Page, 1983a), and mafic volcanics. Voluminous mafic volcanism is represented by the *Eastern Creek Volcanics* of the overlying *Haslingden Group* and by probable correlatives in the southwest. This mafic volcanism locally persisted into Myally Subgroup time. Most of the innumerable mafic dykes within the Leichhardt River Fault Trough were probably intruded during this period, many of them being possible feeders for basalt lava flows.

In the Kalkadoon-Leichhardt Belt to the east, bimodal volcanism of similar age is represented by the *Magna Lynn Metabasalt* and overlying felsic volcanics, dated at 1783 Ma, of the *Argylla Formation.* The *Corella Formation* higher in the sequence also contains some mafic and felsic volcanics, but almost all of them east of the Wonga Belt; west of this belt, it is intruded by large mafic sills of possibly comparable age.

1760-1720 Ma

Granites of the Wonga Batholith were emplaced in the eastern part of the Kalkadoon-Leichhardt Belt during this period, intruding *Corella Formation* of cover sequence 2 and older units. They include *Wonga Granite* dated at 1760-1740 Ma and *Burstall Granite* dated at 1745 and 1726 Ma (Page, 1983b, 1988; Pearson & others, this volume). Rhyolite dykes spatially associated with *Burstall Granite* are dated at 1737 ± 15 Ma (Page, 1983b). A body of *Wonga Granite* previously dated at 1670 Ma (Page,

1978) is now known to be about 1720 Ma old (Pearson & others, this volume).

The *Lunch Creek Gabbro,* which intrudes the *Corella Formation* east of Mary Kathleen and forms net-veined complexes with *Burstall Granite*, has been dated at about 1740 Ma (Page, 1983b). Other mafic intrusions forming net-veined complexes with granites of the Wonga Batholith to the north and south (e.g., Blake, 1981) are likely to be of comparable age. Possible correlatives are mafic sills in the *Corella Formation* of the Kalkadoon-Leichhardt Belt and in the *Myally Subgroup* of the Western Fold Belt.

The cover sequence 2 volcanism in the Eastern Fold Belt may be younger than that to the west, and possibly took place between 1760 and 1720 Ma, rather than before 1760 Ma. The felsic volcanics of the *Argylla Formation* here are similar in chemistry to the 1783 Ma-old Argylla volcanics to the west, but the only sample dated has given an imprecise zircon age of 1766 Ma, and rhyolite in the Doherty Formation of the Mary Kathleen Group south of Cloncurry has been dated at 1720 Ma (Page, 1983a). Argylla-type felsic volcanics and/or high-level sills, together with mafic lavas, are present in the overlying *Marraba Volcanics* and *Mitakoodi Quartzite* of the *Malbon Group*. Mafic volcanics and sills and other minor intrusions of possibly broadly similar age occur in the *Soldiers Cap Group* (mainly Toole Creek Volcanics), and locally in the Mary Kathleen Group (Kuridala, Staveley, and Doherty Formations).

1680-1620 Ma

Minor volcanism during deposition of cover sequence 3 in the western part of the Mount Isa Inlier is represented by the *Carters Bore Rhyolite,* Fiery Creek Volcanics, and tuff beds in the *Mount Isa* and *McNamara Groups.* The *Carters Bore Rhyolite*, a unit of felsic porphyry and local conglomerate exposed at the base of cover sequence 3 west of Mount Isa, has been dated at 1678 ± 1 Ma (Page, 1978). The Fiery Creek Volcanics, exposed to the north, consist mainly of felsic and mafic extrusives showing intense potassic and hematitic alteration; this unit has yet to be isotopically dated, but is thought to be a probable correlative of the *Carters Bore Rhyolite,* as it occupies a similar stratigraphic position.

Several fine-grained tuff beds, typically highly potassic like the Fiery Creek Volcanics, occur in the *Mount Isa* and *McNamara Groups.* Zircon crystals from one of these beds indicate an age of about 1670 Ma for the *Mount Isa Group* (Page, 1981).

In the Eastern Fold Belt, bimodal volcanism accompanied sedimentation in the Tommy Creek area at around 1625 Ma (Hill & others, this volume).

The large Sybella Batholith in the Western Fold Belt west of the Mount Isa Fault was emplaced at around 1670 Ma (Page & Bell, 1986). This 1670 Ma age is geochronologically indistinguishable from that of the tuff bed in the Mount Isa Group.

Other intrusions which may have been emplaced between 1680 and 1620 Ma include dolerite bodies forming net-veined complexes with *Sybella Granite,* and also foliated granites intruding cover sequence 2 in the Eastern Fold Belt – a large pluton mapped as Naraku Granite west and north of Quamby, and the Maramungee Granite and related granites of the Williams Batholith south of Cloncurry.

1620-1540 Ma

This was the period of the Isan Orogeny (Blake & others, 1990), when cover sequence 3 and older rocks of the Mount Isa Inlier were complexly deformed and regionally metamorphosed to greenschist and amphibolite facies - the last such event recognised in the inlier.

Although no volcanic rocks of this age are known, there are some intrusions that appear to have been emplaced during the Isan Orogeny. One of these is a mafic dyke cutting the West Leichhardt Klippe in the Kalkadoon-Leichhardt Belt (Blake, this volume) – it postdates Isan structures, but is metamorphosed. Another example may be the bimodal Myubee Igneous Complex in the Kalkadoon-Leichhardt Belt southeast of Mount Isa; this intrusive complex postdates early folding in the *Corella Formation,* but is deformed and metamorphosed (Passchier, 1991). Other intrusions which appear to cut early Isan structures but are metamorphosed include, in the Eastern Fold Belt, mafic dykes cutting *Mitakoodi Quartzite* and older units in the Duck Creek Anticline, and mafic dykes within the *Soldiers Cap Group* to the east.

1540-1450 Ma

The main granites of the Williams and Naraku Batholiths in the Eastern Fold Belt cut Isan structures and are neither deformed nor metamorphosed to any significant extent, hence they postdate the Isan Orogeny. Isotopic dating shows that these granites crystallised around 1500 Ma ago (e.g., Page, 1988). Minor amounts of mafic magma were also intruded at this time, in places forming net-veined complexes with granite (Blake, 1981, 1987). The *Mount Philp Breccia* bodies, which intrude Corella Formation in the eastern part of the Kalkadoon-Leichhardt Belt, may be

of similar age, as they clearly postdate the strong deformation evident in the adjacent rocks (Blake & others, 1982), and show igneous rather than metamorphic textures.

~1100 Ma

The youngest igneous rocks in the Mount Isa Inlier are unmetamorphosed dolerite dykes. These include the Lakeview Dolerite, which has been dated near Mary Kathleen at 1116 ± 12 Ma (Rb-Sr; Page, 1983b). The Lakeview Dolerite and other unmetamorphosed dolerite dykes in the Kalkadoon-Leichhardt Belt and Western Fold Belt generally trend between northeast and north, whereas those in the Eastern Fold Belt trend about east-west.

Deformation events

Stratigraphy, igneous intrusions, and structural features indicate that the Mount Isa Inlier has a complex Proterozoic history of deformation, dominated at different periods by extension, shortening, and transcurrent faulting.

Barramundi Orogeny, at around 1870 Ma

The earliest known deformation is recorded in basement units, including the *Yaringa Metamorphics* and *Kurbayia Migmatite.* These units were tightly folded and in places partially melted to form migmatite, before the onset of Leichhardt volcanism of cover sequence 1. This early shortening is attributed to the Barramundi Orogeny, a widespread event in northern Australia dated at around 1870 Ma (e.g., Page, 1988). Barramundi structures in the Kalkadoon-Leichhardt Belt appear to be mainly upright and north-trending (Blake, in press), like the main phase of the much younger Isan Orogeny, implying east-west compression.

Extension associated with cover sequences 1 and 2, 1870-1760 Ma

The Barramundi compressional deformation was followed by extension leading to basin formation and deposition of cover sequence 2. Extension in the Western Fold Belt and Kalkadoon-Leichhardt Belt was accompanied by felsic volcanism and plutonism between 1870 and 1840 Ma (Kalkadoon-Leichhardt suite), intrusion of dyke swarms between 1840 and 1790 Ma, granite emplacement at 1820 Ma (Yeldham Granite) and 1800 Ma (*Big Toby Granite*), and probably two phases of rifting and thermal subsidence between 1790 and 1760 Ma (Bottletree-Quilalar sequence).

Extension between 1760 and 1700 Ma

Extensional structures postdating cover sequence 2 have been reported by several workers (e.g., Passchier, 1986, 1991; Passchier & Williams, 1989; Oliver & others, 1991; Stewart, 1989, this volume; Holcombe & others, this volume; Pearson & others, this volume) in the eastern part of the Kalkadoon-Leichhardt Belt. The extension took place before the Isan Orogeny, and is presumed to have been coeval with emplacement of spatially associated granites of the Wonga Batholith, and hence to be older than 1700 Ma. Extension of possibly similar age has been documented in the western part of the Eastern Fold Belt (Passchier & Williams, 1989).

Extension associated with cover sequence 3, 1700-1660 Ma

Cover sequence 3 in the western part of the Mount Isa Inlier consists of basal rift-type deposits succeeded by typical thermal subsidence (sag-phase) sediments, implying deposition in an extensional basin. Emplacement of the Weberra Granite at 1700 Ma north of Mount Isa, and of the Sybella Batholith at 1670 Ma west of Mount Isa, may be related to this extension, as may some of the extensional structures in the eastern part of the Kalkadoon-Leichhardt Belt.

Isan Orogeny, 1620-1520 Ma

This orogeny is generally thought to consist of two main phases, an early phase of thrusting and folding resulting from north-south compression – D_1 of Bell (1983) – and a later phase of east-west compression, D_2, which resulted in the formation of the major north-trending upright folds characteristic of much of the Mount Isa Inlier (papers in this volume). D_1 has been dated at around 1620 Ma and D_2 at around 1550 Ma (e.g., Page & Bell, 1986). Regional metamorphism in general peaked during D_2. The copper mineralisation at the Mount Isa mine probably took place during the waning stages of the metamorphism (e.g., Perkins, 1984).

Extension at around 1500 Ma

The large granite plutons of the Williams and Naraku Batholiths were emplaced in the Eastern Fold Belt at around 1500 Ma, shortly after the Isan Orogeny, implying crustal extension at that time.

Subsequent transcurrent faulting

The main faults mapped in the Mount Isa Inlier cut, and hence postdate, Isan folds. They have displacements ranging up to many kilometres, but do not mark abrupt

changes in metamorphic grade, and so appear to have had predominantly horizontal displacements. Although mainly of Proterozoic age, some of the major faults were active during the Phanerozoic, and all have probably been reactivated several times. Examples include the Pilgrim, Quilalar, and Mount Isa Faults and their offshoots.

References

BEARDSMORE, T.J., NEWBERY, S.P., & LAING, W.P., 1988 - The Maronan Supergroup - an inferred early volcanosedimentary rift sequence in the Mount Isa Inlier, and its implications for ensialic rifting in the Middle Proterozoic of northwest Queensland. *Precambrian Research* 40/41, 487-507.

BELL, T.H., 1983 - Thrusting and duplex formation at Mount Isa, Queensland, Australia. *Nature* 304, 493-497.

BLAKE, D.H., 1981, Intrusive felsic-mafic net-veined complexes in north Queensland. *BMR Journal of Australian Geology & Geophysics* 6, 95-99.

BLAKE, D.H., 1987 - Geology of the Mount Isa Inlier and environs, Queensland and Northern Territory. *Bureau of Mineral Resources, Australia, Bulletin* 225, 83 pp.

BLAKE, D.H., in press - Documentation and significance of a major unconformity in the Wonga Belt of the Mount Isa Inlier, northwest Queensland. *Australian Journal of Earth Sciences.*

BLAKE, D.H., this volume - Stratigraphy, folding, and thrusting within the Quilalar Fault System, Mount Isa Inlier. *In* STEWART, A.J. & BLAKE, D.H. (Editors), Detailed Studies of the Mount Isa Inlier. *Bureau of Mineral Resources, Australia, Bulletin* 243.

BLAKE, D.H., & PAGE, R.W., 1988a - Early Proterozoic migmatitic basement in the Kalkadoon-Leichhardt Belt of the Mount Isa Inlier, northwest Queensland. *BMR Journal of Australian Geology & Geophysics* 10, 323-328.

BLAKE, D.H., & PAGE, R.W., 1988b - The Proterozoic Davenport province, central Australia: regional geology and geochronology. *Precambrian Research* 40/41, 329-340.

BLAKE, D.H., & STEWART, A.J., 1992 - Geology of the Mount Isa - Cloncurry Transect 1:250 000 scale map. *Bureau of Mineral Resources, Canberra, Australia.*

BLAKE, D.H., BULTITUDE, R.J., & DONCHAK, P.J.T., 1982 - Proterozoic intrusive breccias near Duchess, northwestern Queensland. *BMR Journal of Australian Geology & Geophysics* 7, 135-140.

BLAKE, D.H., ETHERIDGE, M.A, PAGE, R.W., STEWART, A.J., WILLIAMS, P.R., & WYBORN, L.A.I., 1990 - Mount Isa Inlier - regional geology and mineralisation. *In:* HUGHES, F.E. (Editor), Geology of the Mineral Deposits of Australia and Papua New Guinea. *Australasian Institute of Mining and Metallurgy, Monograph* 14, 915-925.

BMR, 1988 - Block and possible terrane boundaries in the Mount Isa Inlier. *BMR Research Newsletter* 9, 2-3.

CUMMING, G.L., & RICHARDS, J.R., 1975 - Ore lead isotope ratios in a continuously changing earth. *Earth and Planetary Science Letters* 28, 155-171.

ERIKSSON, K.A., & SIMPSON, E.L., 1990 - Recognition of high- frequency sea-level fluctuations in Proterozoic siliciclastic tidal deposits, Mount Isa, Australia. *Geology* 18, 474-477.

ERIKSSON, K.A., SIMPSON, E.L., & JACKSON, M.J., 1992 - Stratigraphic evolution of a Proterozoic synrift to post- rift basin: constraints on nature of lithospheric extension in the Mount Isa Inlier, Australia. *In* STEEL, R., & FROSTIAK, L., (Editors), Tectonics and Sedimentation. *International Association of Sedimentologists, Special Publication.*

ETHERIDGE, M.A., RUTLAND, R.W.D., & WYBORN, L.A.I., 1987 - Orogenesis and tectonic process in the Early to Middle Proterozoic of northern Australia. *American Geophysical Union, Geodynamic Series* 17, 131-147.

GULSON, B.L., 1985 - Shale-hosted lead-zinc deposits in northern Australia: lead isotope variations. *Economic Geology* 80, 2001-2012.

HILL, E.J., LOOSVELD, R.J.H, & OLIVER, N.H.S., this volume - Structure and geochronology of the Tommy Creek Block, Mount Isa Inlier. *In:* STEWART, A.J., & BLAKE, D.H. (Editors), Detailed Studies of the Mount Isa Inlier. *Bureau of Mineral Resources, Australia, Bulletin* 243.

HOLCOMBE, R.J., PEARSON, P.J., & OLIVER, N.H.S., this volume - Structure of the Mary Kathleen Fold Belt. *In* STEWART, A.J. & BLAKE, D.H. (Editors), Detailed Studies of the Mount Isa Inlier. *Bureau of Mineral Resources, Australia, Bulletin* 243.

LOOSVELD, R.J.H., 1989 - The intra-cratonic evolution of the central eastern Mount Isa Inlier, northwest Queensland, Australia. *Precambrian Research* 44, 243-276.

NEEDHAM, R.S., STUART-SMITH, P.G., & PAGE, R.W., 1988 - Tectonic evolution of the Pine Creek Inlier, Northern Territory. *Precambrian Research* 40/41, 543-564.

OLIVER, N.H.S., HOLCOMBE, R.J., HILL, E.J., & PEARSON, P.J., 1991 - Tectono-metamorphic evolution of the Mary Kathleen Fold Belt, northwest Queensland: a reflection of mantle plume processes? *Australian Journal of Earth Sciences* 38, 425-455.

PAGE, R.W., 1978 - Response of U-Pb zircon and Rb-Sr total rock and mineral systems to low-grade regional metamorphism in Proterozoic igneous rocks, Mount Isa, Australia. *Journal of the Geological Society of Australia* 25, 141-164.

PAGE, R.W., 1981 - Depositional ages of the stratiform base metal deposits at Mount Isa and McArthur River, Australia, based on U-Pb zircon dating of concordant tuff horizons. *Economic Geology* 76, 648-658.

PAGE, R.W., 1983a - Timing of superposed volcanism in the Proterozoic Mount Isa Inlier, Australia. *Precambrian Research* 21, 223-245.

PAGE, R.W., 1983b - Chronology of magmatism, skarn formation and uranium mineralization, Mary Kathleen, Queensland, Australia. *Economic Geology* 78, 838-853.

PAGE, R.W., 1988. Geochronology of Early to Middle Proterozoic fold belts in northern Australia: a review. *Precambrian Research* 40/41, 1-19.

PAGE, R.W., & BELL, T.H., 1986 - Isotopic and structural responses of granite to successive deformation and metamorphism. *Journal of Geology* 94, 365-379.

PAGE, R.W., & WILLIAMS, I.S., 1988 - Age of the Barramundi Orogeny in northern Australia by means of ion microprobe and conventional U-Pb zircon studies. *Precambrian Research* 40/41, 21-36.

PASSCHIER, C.W., 1986 - Evidence for early extensional tectonics in the Proterozoic Mount Isa inlier, Australia. *Geology* 14, 1008-1011.

PASSCHIER, C.W., 1991 - Deformation in the Revenue granite pluton, Mount Isa Inlier, Australia. *Geologie en Mijnbouw* 70, 275-285.

PASSCHIER, C.W., this volume - Geology of the Myubee area, Mount Isa Inlier, Queensland. *In:* STEWART, A.J., & BLAKE, D.H. (Editors), Detailed Studies of the Mount Isa Inlier. *Bureau of Mineral Resources, Australia, Bulletin* 243.

PASSCHIER, C.W., & WILLIAMS, P.W., 1989 - Proterozoic extensional deformation in the Mount Isa inlier, Queensland, Australia. *Geological Magazine* 126, 43-53.

PEARSON, P.J., HOLCOMBE, R.J., & PAGE, R.W., this volume - Synkinematic emplacement of the Middle Proterozoic Wonga Batholith into a mid-crustal extensional shear zone, Mount Isa Inlier, Queensland, Australia. *In* STEWART, A.J. & BLAKE, D.H. (Editors), Detailed Studies of the Mount Isa Inlier. *Bureau of Mineral Resources, Australia, Bulletin* 243.

PERKINS, W.G., 1984 - Mount Isa silica dolomite and copper orebodies: the result of a syntectonic hydrothermal alteration system. *Economic Geology* 79, 610-637.

PLUMB, K.A., AHMAD, M., & WYGRALAK, A.S., 1990 - Mid-Proterozoic basins of the North Australian Craton - regional geology and mineralisation. *In* HUGHES, F.E. (Editor), Geology of the Mineral Deposits of Australia and Papua New Guinea. *Australasian Institute of Mining and Metallurgy, Monograph* 14, 881-902.

RYBURN, R.J., WILSON, I.H., GRIMES, K.G., & HILL, R.M., 1988 - Cloncurry, Queensland. *Bureau of Mineral Resources, Australia, 1:100 000 Geological Map Commentary.*

SIMPSON, E.L., & ERIKSSON, K.A., 1991 - Depositional facies and controls on parasequence development in siliciclastic tidal deposits from the Lower Proterozoic, upper Mount Guide Quartzite, Mount Isa Inlier, Australia. *Canadian Society of Petroleum Geologists, Memoir* 16, 371-387.

STEWART, A.J., 1989 - Extensional faulting as the explanation for the Deighton 'Klippe' and other Mount Albert Group outliers, Mount Isa Inlier, northwestern Queensland. *Australian Journal of Earth Sciences* 36, 405-421.

STEWART, A.J., this volume - Stratigraphy, extension, and contraction in the Ballara-Mount Frosty area, Mount Isa Inlier. *In:* STEWART, A.J., & BLAKE, D.H. (Editors), Detailed Studies of the Mount Isa Inlier. *Bureau of Mineral Resources, Australia, Bulletin* 243.

WYBORN, L.A.I., 1988 - Petrology, geochemistry and origin of a major Australian 1880-1840 Ma felsic volcano-plutonic suite: a model for intracontinental felsic magma generation. *Precambrian Research* 40/41, 37-60.

WYBORN, L.A.I., PAGE, R.W., & McCULLOCH, M.T., 1988 - Petrology, geochronology and isotope geochemistry of the post- 1830 Ma granites of the Mount Isa Inlier: mechanisms for the generation of Proterozoic anorogenic granites. *Precambrian Research*, 40/41, 509-541.

Note on deformation terminology

R. J. Holcombe [1] *& A. J. Stewart* [2]

[1] Department of Earth Sciences, University of Queensland, Qld, 4072.

[2] Bureau of Mineral Resources, GPO Box 378, Canberra, ACT, 2601.

The D_1, D_2, D_3 terminology of Bell (1983) referred initially to a first, second, and third episode of structures and fabrics in the Lake Moondarra area, where Winsor (1983) had made a detailed structural analysis of overprinting cleavages and folds. 'D' in this sense referred to generations of observed structures in that small area, and was used in the same way as the commonly used 'F' terminology of structural geology. Bell extended the D nomenclature to the northern half of the Leichhardt River Fault Trough, and applied it both to generations of observed structures, e.g., 'D_1 synclines', 'D_2 hinge', and to the broader deformation events that produced the structures, e.g., 'emplaced pre D_2', 'postdates D_3'. These terms are convenient to use, and have gained widespread use throughout the Mount Isa Inlier. But their interchangeable use is an over-simplification. It leads to the erroneous impression that there is a one-to-one correlation between observed generations of overprinting structures and crustal deformation events; i.e., all 'D_1 structures' (for example) formed at the same time during the same D_1 orogenic event all over the inlier. Certainly, some structures, such as the north-trending upright folds, appear to be widespread and correlatable from one area to another, and moreover they seem to be related to the middle stages of a crustal contraction event at about 1550 Ma (Page & Bell, 1986). We do not know, however, whether the folding stage was reached synchronously in all areas, or whether it occurred as simply one step in a sequence of steps controlled by the occurrence of the previous step, or by the attainment of certain physical conditions controlled by position in the crust during contractional uplift. For example, a number of studies report a generation of thrust faults earlier than the folding (Bell, 1983; Loosveld & Schreurs, 1987; Stewart, this volume; Hill & others, this volume). Are they independent crustal contraction events, D_1 and D_2, or are they two expressions (F_1, F_2?) of a single crustal event, D_2, in which strain rate or crustal position locally generated brittle contractional structures before ductile folding? There are many ways in which local fabrics may be related to each other, and to the crustal deformation regime. Structures or fabrics are local in definition, and may be present in one area but not in another. A crustal-scale deformation event may be represented by one fabric in one area, but by multiple fabric generations in another, controlled perhaps by the presence or absence of local heterogeneities. It is important to try and use the local fabrics to interpret crustal events, but to go directly to an orogeny-based nomenclature to annotate local structures is scientifically dangerous.

Notwithstanding, we recognize that the D nomenclature for orogenic events and fabric elements is firmly entrenched in Mount Isa geology, and its simplicity ensures that this somewhat unsatisfactory practice will probably continue. To avoid the problem of D_1 in one area (for example) not being contemporaneous with D_1 in another, most of the papers in this volume use a superscript letter after the D to denote the particular area concerned, as follows:

D^A — East Moondarra area (Bain & others, this volume)

D^F — Ballara-Mount Frosty area (Stewart, this volume b)

D^H — Horse's Head (Stewart, this volume a)

D^K — Mary Kathleen area (Holcombe & others, this volume)

D^M — Myubee area (Passchier, this volume)

D^N — Mount Novit area (Connors & others, this volume)

D^P — Paroo Range area (Nijman & others, this volume a), Hero/Western Fault Zone (Nijman & others, this volume b)

D^S — Soldiers Cap Belt (Loosveld, this volume)

D^T — Tommy Creek Block (Hill & others, this volume)

D^W — Wonga Belt (Pearson & others, this volume)

Thus, a first-generation fold in the Mary Kathleen area is a $D^K{}_1$ fold, and is not necessarily the same age as a first-generation fold in the Paroo Range area, which is denoted as a $D^P{}_1$ fold. The superscript is not usually added to F, S, and L symbols for fold axis, foliation, and lineation

(respectively), as these clearly refer to fabric elements only in the particular area being described. Where authors have been sure that the structures in their areas correlate directly with the D_1, D_2, and D_3 nomenclature of Bell (1983), they have not used a superscript.

References

BELL, T.H., 1983 - Thrusting and duplex formation at Mount Isa, Queensland, Australia. *Nature* 304, 493-497.

HILL, E.J., LOOSVELD, R.J.H., & PAGE, R.W., this volume - Structure and geochronology of the Tommy Creek Block, Mount Isa Inlier. *In*: STEWART, A.J., & BLAKE, D.H. (Editors), Detailed Studies of the Mount Isa Inlier. *Bureau of Mineral Resources, Australia, Bulletin* 243.

LOOSVELD, R.J.H., & SCHREURS, G., 1987 - Discovery of thrust klippen, northwest of Mary Kathleen, Mt Isa Inlier, Australia. *Australian Journal of Earth Sciences* 34, 387- 402.

PAGE, R.W., & BELL, T.H., 1986 - Isotopic and structural responses of granite to successive deformations and metamorphism. *Journal of Geology* 94, 365-379.

STEWART, A.J., this volume - Stratigraphy, extension, and contraction in the Ballara-Mount Frosty area, Mount Isa Inlier, Queensland. *In:* STEWART, A.J., & BLAKE, D.H. (Editors), Detailed Studies of the Mount Isa Inlier. *Bureau of Mineral Resources, Australia, Bulletin* 243.

WINSOR, C.N., 1983 - Syntectonic vein and fibre growth associated with multiple slaty cleavage development in the Lake Moondarra area, Mount Isa, Australia. *Tectonophysics* 92, 195-210.

Structure of the Mount Isa region inferred from gravity and magnetic anomalies

Peter Wellman [1]

Most of the Mount Isa region lies within the Mount Isa Geophysical Domain, 800 km long and 150 to 250 km wide. This domain is inferred to have formed later than crust to the east and west, and earlier than the Tasman Orogenic System to the south, and the crust to the north. Within this domain most major features are parallel with the domain's arcuate north-northeast to north-northwest-trending margins. The domain can be subdivided using geophysical anomalies into six zones that extend the length of the domain. The zone boundaries are broadly consistent with the boundaries of the major geological blocks of Blake & Stewart, and are fault zones that bound the extent of stratigraphic units and batholiths. There are changes in rocks and structures within some zones, in particular at a 20° bend in the domain at 21.5-22°S. Magnetic anomalies indicate two major and widespread faulting sets in the Mount Isa Domain and the surrounding crust: a northwest-striking set of normal faults in the northern third of the region, and a northeast-striking set of dextral faults with displacements of about 3 km in the central part.

[1]Bureau of Mineral Resources, G.P.O. Box 378, Canberra, ACT, 2601.

Introduction

The geology of the Mount Isa Inlier has been extensively studied over a long period; the results to 1983 are summarised by Blake (1987). Results of subsequent structural and other work are presented in this bulletin. The major geological tectonic divisions of the inlier broadly correlate with long-wavelength geophysical anomalies. These anomalies show that the inlier is near the centre of an elongate geophysical domain – the Mount Isa Domain – and that the tectonic divisions of the inlier can be traced along most of the length of this domain. This paper describes the relation between the mapped structure of the inlier and the structures in the whole domain, and discusses the relation of the Mount Isa Domain with the surrounding region: from 17° to 25°S and from 138° to 142°30'E (Fig. 1). Although mineral exploration companies have gained further understanding by analysis of detailed magnetic and gamma-ray radiometric surveys of the inlier, there have been relatively few studies using the regional geophysical data to relate the Proterozoic rocks of the Mount Isa Inlier to the Proterozoic rocks of the surrounding area.

Geophysical features which give unity to the Mount Isa Domain are the subparallel arcuate trends in gravity and magnetic anomalies, and the relative high in regional gravity anomaly. At the boundaries of the domain there is a change in the upper-crustal density and magnetisation, and a change in trend direction; boundaries of the Domain are narrower in the east and west than in the south.

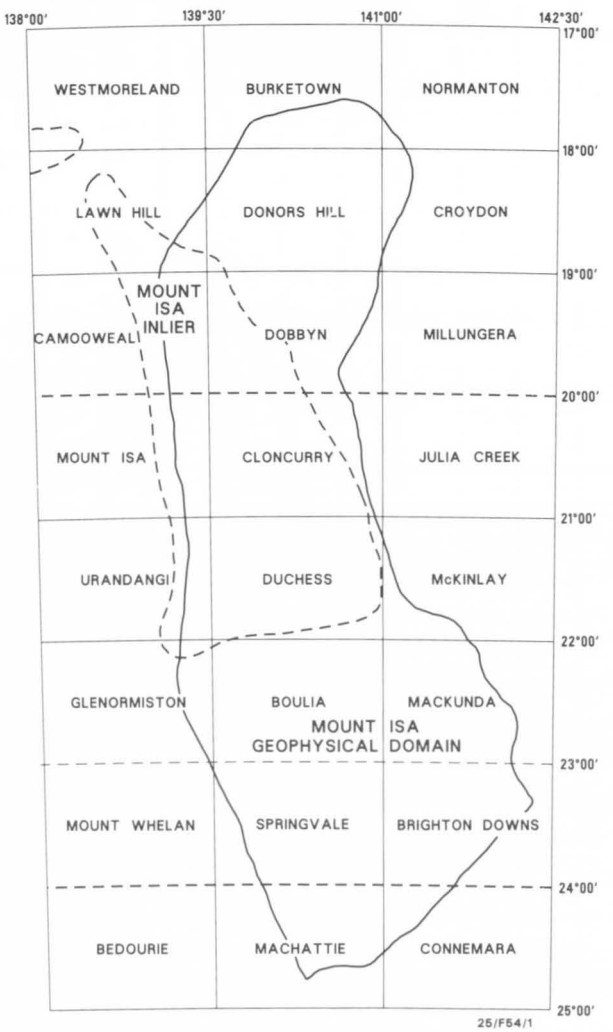


Fig. 1. Location of Mount Isa Geophysical Domain and Mount Isa Inlier. Names refer to 1:250 000 sheet areas.

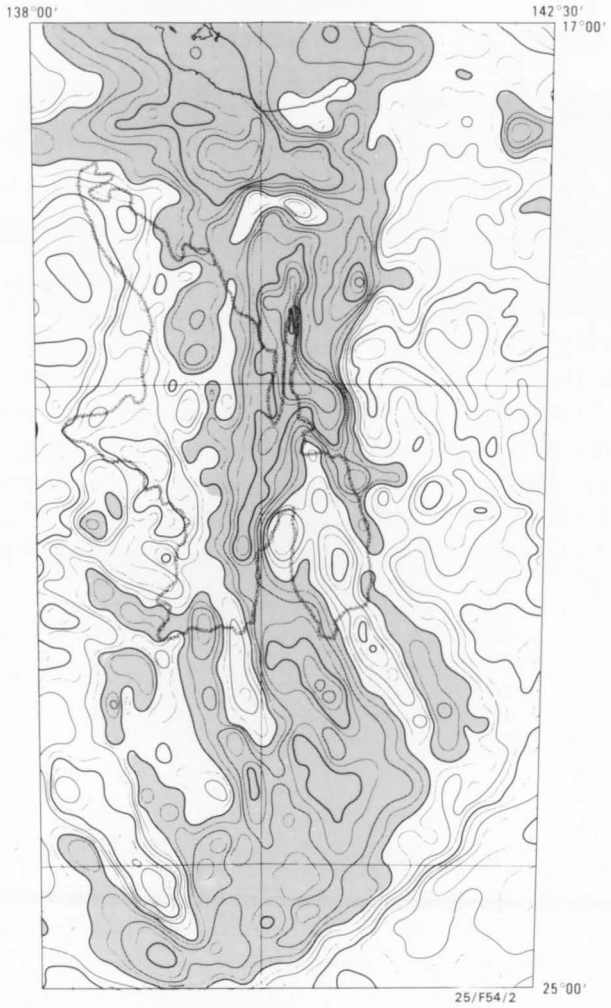


Fig. 2. Bouguer gravity anomalies. Contour interval 20 $\mu m.s^{-2}$.

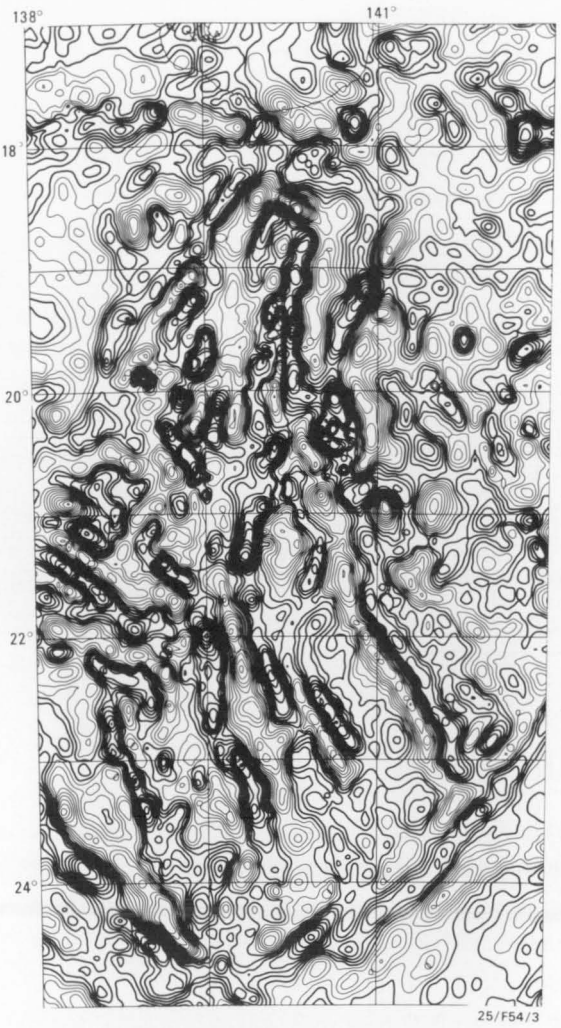


Fig. 3. Residual gravity anomalies. Contour interval 20 $\mu m.s^{-2}$. The regional used was 24 minute wavelength.

Gravity and magnetic data

Gravity surveys in the Mount Isa region were carried out by BMR from 1959 to 1966 (Gibb, 1967; Shirley & Zadoroznyj, 1974). In these surveys helicopters were used to establish stations on a grid with an 11 km spacing. Anomaly accuracy (s.d.) at the stations is about 12 $\mu m.s^{-2}$ (Barlow, 1977). Subsequently BMR carried out a survey in 1975 consisting of numerous short traverses covering the eastern part of the CLONCURRY 1:250 000 Sheet area (Mutton & Almond, 1979), and another survey in 1986 consisting of two 375 km-long east-west traverses across the Mount Isa region through Boulia and Duchess. All these data have been integrated, and are available from BMR's 1:1 000 000 Bouguer anomaly maps, and as data on computer tape. This paper uses Bouguer anomalies (Fig. 2), and also residual anomalies (Fig. 3) calculated by subtracting a regional of 24-minute wavelength from the Bouguer anomalies. Figure 4 is an interpretation of the residual gravity anomaly.

Aeromagnetic surveys in the Mount Isa region differ in quality as a result of a gradual tightening of survey specifications with time. About one quarter of BRIGHTON DOWNS was flown in 1957 as a private company survey with 8-16 km flight-line spacing, the three southernmost 1:250 000 sheets were flown in 1963 under the Petroleum Search Subsidy Act with an 8 km flight-line spacing, 11.75 sheets were flown by BMR at 3 km flight-line spacing, and nine sheets were flown by BMR at 1.5 km flight-line spacing. Two small areas have been over-flown by BMR at a closer spacing; the Prospector 1:100 000 sheet area in CLONCURRY at 0.5 km flight-line spacing, and an area in GLENORMISTON with 1 km flight-line spacing. The BMR data are available as 1:250 000 maps of flight-line systems, observed profiles and contours, and as computer tapes of either observed profiles or a grid. All data are available as 1:1 000 000 scale contour maps.

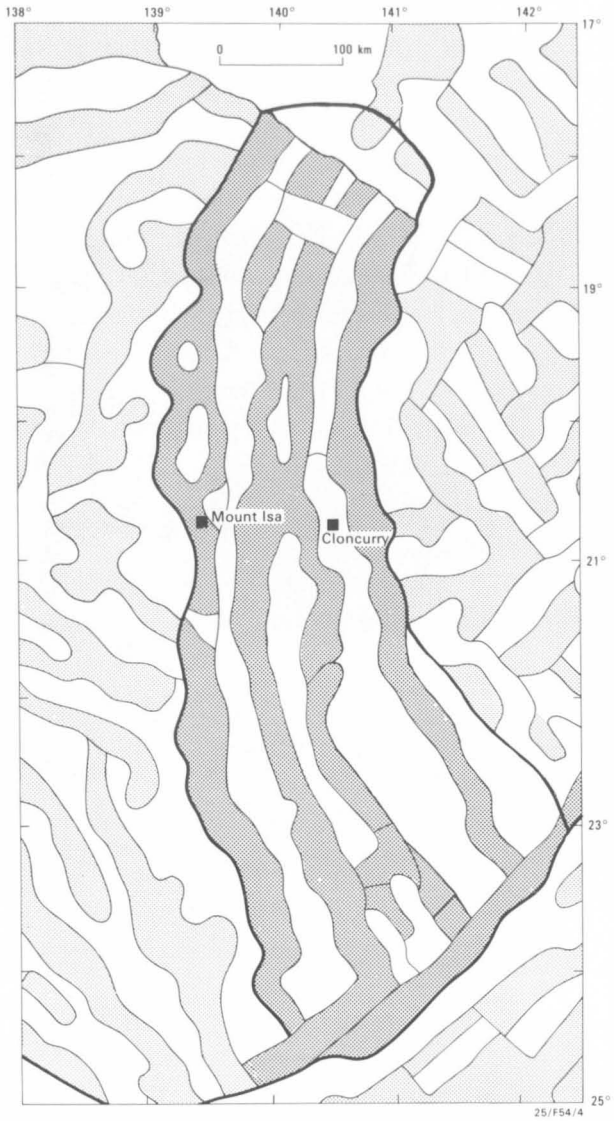


Fig. 4. Interpretation of residual gravity anomalies. Stippled areas are residual gravity anomaly highs. Thick lines give the subsurface extent of the Mount Isa Domain and the Tasman Orogenic Zone (after Wellman, 1986).

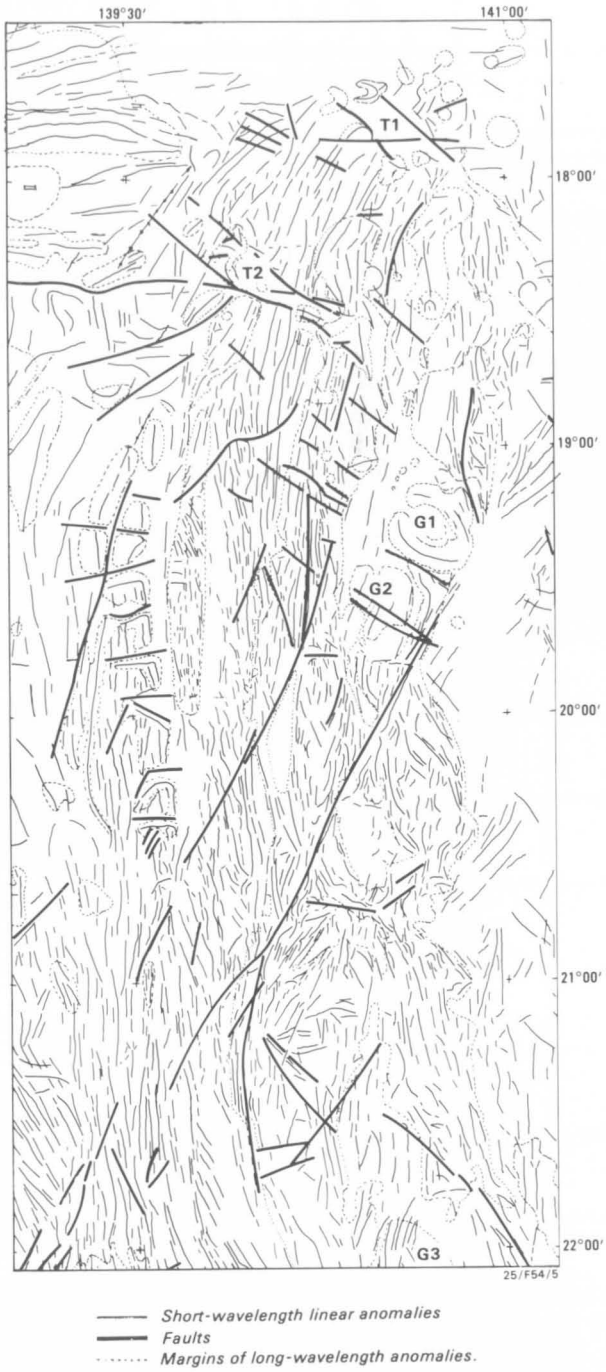


Fig. 5. Short-wavelength magnetic anomalies. Straight lines, short-wavelength linear anomalies; wavy lines, faults; dotted lines, margins of long-wavelength anomalies.

For convenience, the magnetic anomalies are considered in this paper to consist of two components – one with a 40 to 100 km wavelength, called the long-wavelength component, and the other with wavelengths less than 40 km, the short-wavelength component. I am not in a position to produce good figures of the aeromagnetic data for this paper, so the only figure is of interpreted trends of short-wavelength anomalies for the central part of the region (Fig. 5). Interpretation of the short-wavelength anomalies used computer-produced images of Geoimage (1989). Physical property measurements on rocks from throughout the Mount Isa Inlier are reported by Hone & others (1987), and for the Mount Isa mine area by Clark (1980) and Young (1984).

Interpretation of gravity and magnetic anomalies

Previous regional geophysical studies of the Mount Isa area include modelling of the crustal thickness from the regional gravity anomalies by Wellman (1976a) and Shirley (1979), and interpretations of the upper crustal structure from gravity and magnetics by Wellman (1976b, 1986, 1988), Tucker & others (1979), Hone & others

(1982), Gunn (1983), and Murray & others (1989). Interpretations of regional geophysical data were reviewed by Dooley (1980). Interpretations of partial and whole sheet areas include Tucker (1975) and Mutton & Almond (1979) for CLONCURRY, Hone (1984) for DUCHESS and part of URANDANGI, Young (1984) for part of MOUNT ISA, and Young (1986) for most of GLENORMISTON.

The interpretation that follows is based on the concept that the Mount Isa Geophysical Domain (hereafter called Mount Isa Domain; Fig. 1) represents a segment of Middle Proterozoic upper crust, 150 to 300 km wide and 800 km long, which has a very different geological history from that of the surrounding area.

This paper is concerned only with the Early to Middle Proterozoic rocks in the area of Figure 1. The cover rocks of Palaeozoic age in this area are non-magnetic, gently dipping, and generally less than 1 km thick (GSA, 1971; Tucker & others, 1979), and those of Late Proterozoic (Adelaidean) age, west and south of Mount Isa Inlier, are generally less than 2 km, although locally up to 10 km thick (Tucker & others, 1979).

Margins of the Mount Isa Domain

The Mount Isa Domain is defined from gravity and magnetic anomalies using the following three interpretation methods which have been found useful in mapping major basement units (provinces, cratons, and fold belts) elsewhere (Gibb & Thomas, 1976; Klasner & King, 1986; Rivers & others, 1989).

1. At the boundary of many geophysical domains there is an abrupt change in the dominant trend of the geological structures and geophysical anomalies; the domain with younger structures has trends parallel to the boundary and the adjacent domain with older structures has its trends truncated at the boundary. These domains are hereafter referred to as older and younger. This truncation of gravity and magnetic trends is found on some margins of the Mount Isa Domain (Figs. 4, 5). On the central part of the western margin, the northerly-trending Mount Isa structures truncate the northwesterly trends that are continuous with Arunta Block structures. This margin is inferred to continue southwards along strike, where both sets of trends are north-northwest and subparallel for about 300 km. At the northwestern margin the Mount Isa structures trend north-northeast, truncating east-west trends of the Murphy Tectonic Ridge and South Nicholson Basin to the west, but with an overlap zone where both trends are present. The northeastern boundary is where the Mount Isa structures are well defined and north to north-northeast trending, and there Mount Isa structures give way to poorly defined adjacent structures, trending west, northwest, and north. In the central part of the eastern margin, between 19° and 20.5°S, there is an abrupt change, consistent with the Mount Isa Domain having been thrust eastwards over non-magnetic upper crust. On the southeast margin there are well defined north-northwest to northerly Mount Isa structures, whereas basement trends outside the Domain are generally poorly defined. At the southern margin there is the clearest discontinuity, with northeast trends of the Tasman Orogenic System, of likely Early Palaeozoic age, truncating north-northwest trends of the Mount Isa Domain.

The northern margin of the Mount Isa Domain is relatively poorly defined, mainly because the Domain becomes progressively more dislocated northwards, as discussed below; it is taken to be at about 17.5°S, at the northern extent of trends, and of gravity and magnetic highs, of the Domain.

2. Along domain boundaries elsewhere there are long-wavelength geophysical anomalies caused by a combination of two causes:

- Domains having different history, and hence differing in mean thickness and physical properties of the crustal layers.

- The presence of rock bodies formed by boundary processes adjacent to and parallel to the boundary. Commonly the margin of the younger craton coincides with gravity and magnetic highs. In the Mount Isa Domain, there are gravity and magnetic highs on the eastern and western margins consistent with the edge of this domain being denser and more magnetic than adjacent older crust. Correlation of these gravity and magnetic anomalies with geology shows that the physical property contrast is at least partly in the upper crust. Similarly, the southern margin of the Mount Isa Domain is a gravity and magnetic high relative to the other side of the boundary, consistent with the Mount Isa Domain crust being denser and more magnetic than the edge of the Tasman Domain.

Overall, the Mount Isa Domain differs from the surrounding domains by being a relative high on both Bouguer (Fig. 2) and free-air anomaly maps (Wellman & Murray, 1979). This can be explained by two models

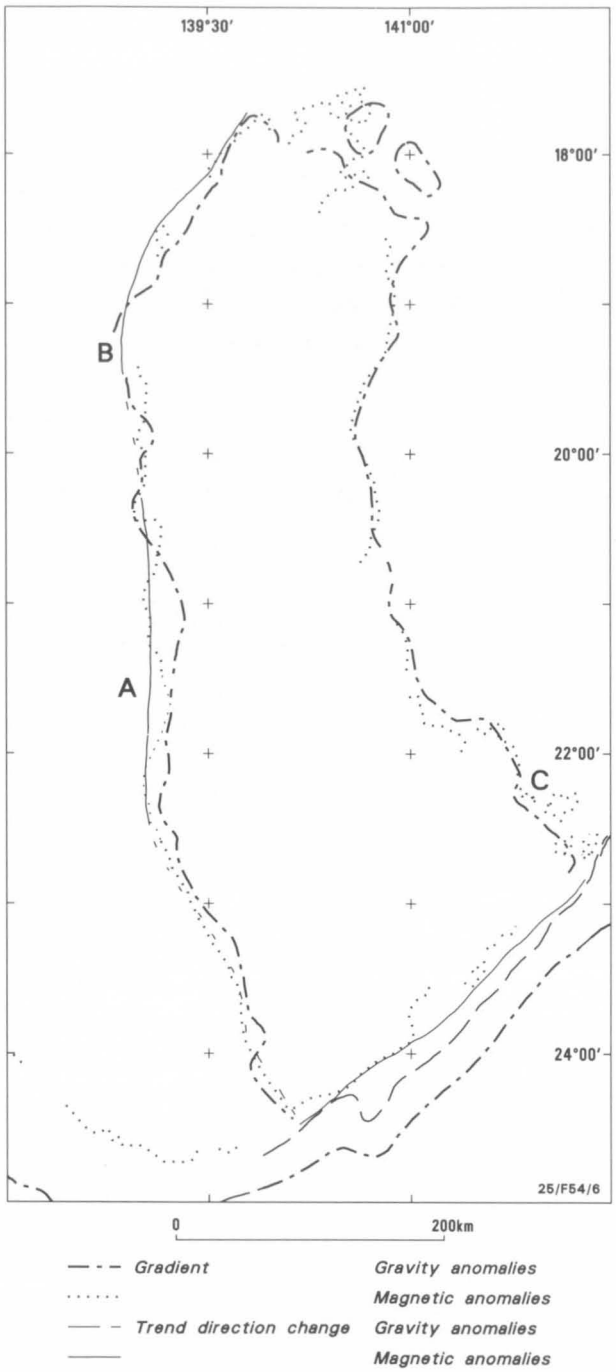


Fig. 6. Estimates of the extent of Mount Isa Geophysical Domain.

- The Mount Isa Domain crust is of relatively high density, with areas of 3 x 3° being in regional isostatic equilibrium, so the gravity high over the Mount Isa Domain is due to higher-density crust being closer to the surface than the deeper isostatic compensation (Wellman, 1976b).

- The Mount Isa Domain is a region of thin crust, with 3 x 3° areas not being in isostatic equilibrium, so that the gravity high is due to denser mantle being relatively close to the surface (Shirley, 1979).

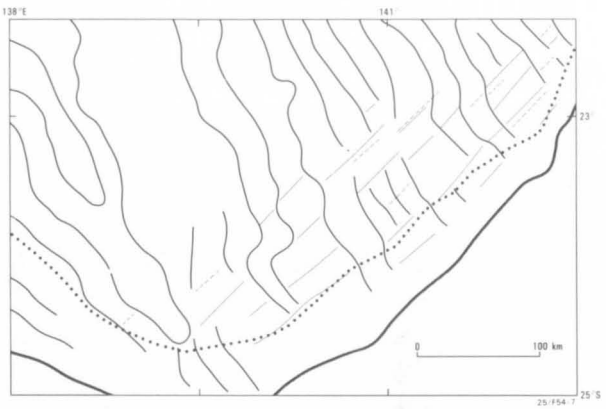


Fig. 7. Crustal reworking at the southern end of the Mount Isa and Arunta Geophysical Domains. The thickest line gives the boundary between Proterozoic and Phanerozoic crust as defined by the major gravity gradient. Other gravity gradients are marked by medium thickness lines, terminations of gravity anomalies by thin continuous lines, terminations of magnetic anomalies by thin broken lines, and the southern margin of positive magnetic anomalies by a dotted line (from Wellman, 1988).

The first model is preferred, because, in spite of the very high lithospheric strength estimates derived by correlating topography and gravity (Wellman, 1979; Zuber & others, 1989), gravity anomaly modelling indicates that compensation is complete within a radius of 200 km (Wellman, 1978).

3. At the boundaries between some major domains, the older domain has a marginal band of major reworking (Klasner & King, 1986; Beeson & others, 1988; Wellman, 1988; Rivers & others, 1989) that can be recognised both in geology and geophysics. On gravity and magnetic maps, older structures become less well-defined, there are offsets and fractures parallel to the domain boundary, and surface and average crustal magnetisation decrease. Along the eastern and western margins of the Mount Isa Domain these features are not prominent (Figs. 3, 6). However, a reworked zone is well developed along the southern margin of the Mount Isa Domain (Fig. 7 Wellman, 1986, 1988). The domain boundary here is taken to be the major southwest-trending gravity gradient, indicating a change in mean crustal density. Northwest-trending structures of the Mount Isa Domain become increasingly deformed towards this boundary. Offsets of northwest structures to the southwest, and the presence of southwest fractures, some of which are associated with the offsets, begin to be recognisable about 120 km northwest from the boundary.

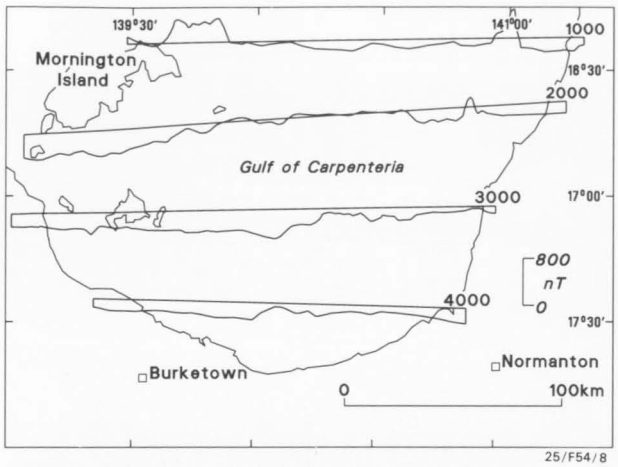


Fig. 8. Magnetic traverses across the southern part of the Gulf of Carpentaria. These show that the Mount Isa Geophysical Domain structures do not continue north into the Gulf of Carpentaria.

Within 50 km of the boundary, most of the northwest-trending magnetic anomalies end abruptly, and a broad magnetic low here is considered to be due solely to loss of magnetite resulting from metamorphism (reworking). Closer to the boundary the northwest gravity trends die out, marking the end of northwest-trending structures in the upper crust. The attenuated magnetic anomalies forming the broad magnetic low near the southern margin of the Mount Isa Domain were interpreted by H.D. Hsu (personal communication in Hawkins & Harrison, 1978) as showing that the Precambrian rocks were down-faulted at least 10 km. This interpretation seems unlikely, because there is no deep gravity low coincident with the proposed trough, and because other boundaries have similar long-wavelength magnetic lows that are known to be due to demagnetisation.

Figure 6 shows the position of the boundary of the Mount Isa Domain from three data sets – trends from short-wavelength magnetic anomalies, and the gradients of gravity and magnetic long-wavelength anomalies. In general the estimates of position of the boundary of the domain are similar. There is poorest agreement in areas A, B, and C of Figure 6. In areas A and B, the discrepancy is due to granite crossing the western margin of the Domain, giving a local gravity low. In these two areas the boundary defined by the magnetic anomalies has been adopted.

The boundaries adopted for the Mount Isa Domain are broadly similar to those adopted earlier by previous authors using less geophysical information and less satisfactory information display. The main differences are: placement of the northern domain boundary 30 km farther to the northeast; adoption of the western margin of Wellman (1986), which is farther west than that of Wellman (1976b), Tucker & others (1979), and Hone & others (1982); and placement of the southeast boundary at the major gravity gradient, not at the position 50 km to the north adopted by Wellman (1976b) and Murray & others (1989). The Mount Isa Domain is unlikely to extend to the northeast into Cape York Peninsula, because although the gravity anomalies are similar, there is a 100 km gap between the structures, and the magnetic anomalies are not similar. Magnetic anomaly profiles across the southern end of the Gulf of Carpentaria (Fig. 8) do not support an extension of the Mount Isa Domain into the Gulf.

The western boundary of the Mount Isa Domain (Fig. 6) is consistent in general with the geological evidence. There must be a break between the older rocks in most of the Mount Isa Inlier which have a northerly strike, and older rocks to the west which have different strikes; for example the Saint Ronans Metamorphics in the southwest of the inlier but outside the Mount Isa Domain strike northwest, and rocks of the Murphy Tectonic Ridge to the northwest of the inlier strike east. The western boundary of the Mount Isa Domain is close to the western extent of exposed cover sequence 2 rocks, and close to the western margin of cover sequence 2 rocks as seen in magnetic images. However, the younger rocks of cover sequence 3 continue across this domain boundary, and the boundary does not coincide with any known geological structure. Figure 6 shows that there is some uncertainty in the position of the geophysical boundary, so it may be gradational rather than sharp.

Gross subdivision of the Mount Isa Domain

Day & others (1983) and Blake & Stewart (1988) have proposed subdivisions of the Mount Isa Inlier based on geology. The short-wavelength magnetic anomalies, because they mainly reflect basement surface geology, are not an independent data source, so they cannot be used to critically evaluate the proposed sub-divisions, but long-wavelength gravity and magnetic anomalies can, as these data sets are essentially independent of geology. If a geological subdivision is fundamental, then it should be reflected in structures extending below the surface, and hence should correlate with gradients in long-wavelength gravity and magnetic anomalies.

Figure 9 shows that the long-wavelength gravity and magnetic anomalies have roughly concordant patterns, making it possible to subdivide the whole of the Mount Isa Domain. The main problems occur near 20.7°S, where

there is a change in the direction of all structures, and for some anomalies there is a change in correlation of long-wavelength magnetic anomalies with gravity anomalies. In subdividing the Mount Isa Domain as a whole, more weight has been given to gravity anomalies, because of their greater consistency and continuity than the magnetic anomalies, although they could mainly reflect the distribution of granite and closeness of the domain margin. Magnetic anomalies, because of their lack of continuity along strike, appear to reflect mainly the less continuous features of the upper crust.

The most satisfactory purely geophysical subdivision of the Mount Isa Domain is still that of Wellman (1986) (modified to extend the domain to the north), in which the Domain is subdivided using four residual gravity highs that extend the length of the Domain (Fig. 4).

Correlation of geophysical zones with previous geological subdivisions

Geological subdivisions of the Mount Isa Inlier have been based on extent of stratigraphic units, change in structural grain, and location of major fault zones. However the extent of stratigraphic units has to be the primary basis, as the significance of both the other two features is evaluated by their effect on the stratigraphy. In my view the geological subdivision of the Mount Isa Inlier into blocks should be focused on one time period. Cover sequences 1 and 3 do not crop out sufficiently widely to define a subdivision, so any subdivision has to be based on cover sequence 2 and its associated granites. The subdivision has then a well defined meaning – it is strictly the subdivision of the rocks at that time period.

The tectonic zones of Day & others (1983) and Blake (1987) have an average north-northeast trend. This is oblique to the average north trend of the geophysical zones within the inlier, so these tectonic zones are not discussed further.

Blake & Stewart (1988) defined a geological subdivision primarily based on the position of major faults, support for the subdivision coming from both the extent of major stratigraphic units (mainly cover sequence 2) and the change in structural grain. The following is a comment on each of their boundaries.

- Blake & Stewart (1988) suggested that the Mount Isa Fault Zone marks a major tectonic boundary change in cover sequence 3. This boundary, unlike the other boundaries of Blake & Stewart (1988), does not form a break in the extent of cover sequences 2 and 3, does not correspond to any gradients in long-wavelength gravity or magnetic anomalies, and does not coincide with a consistent pattern break in the short-wavelength magnetic anomaly images.

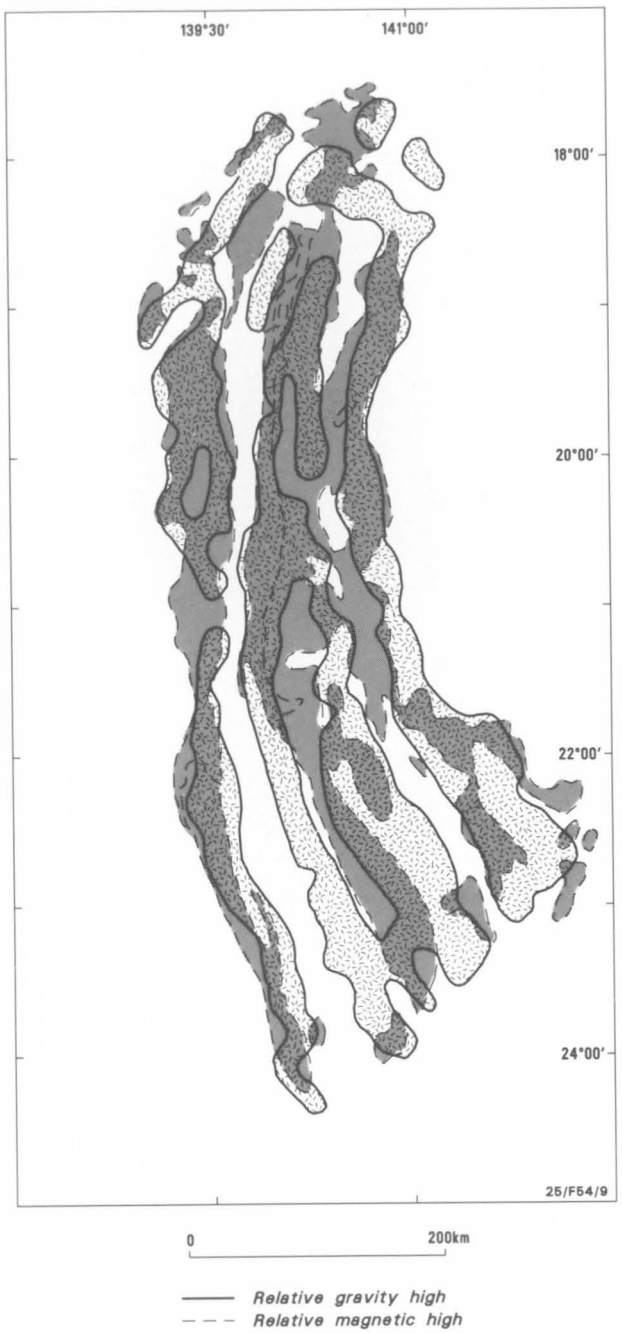


Fig. 9. Relative positions of the gravity and magnetic anomaly highs.

- The Quilalar Fault Zone (Fig. 10) closely follows major features in the short- and long-wavelength magnetic anomalies, and follows an intermittent feature in the gravity anomalies. It separates a gravity and magnetic

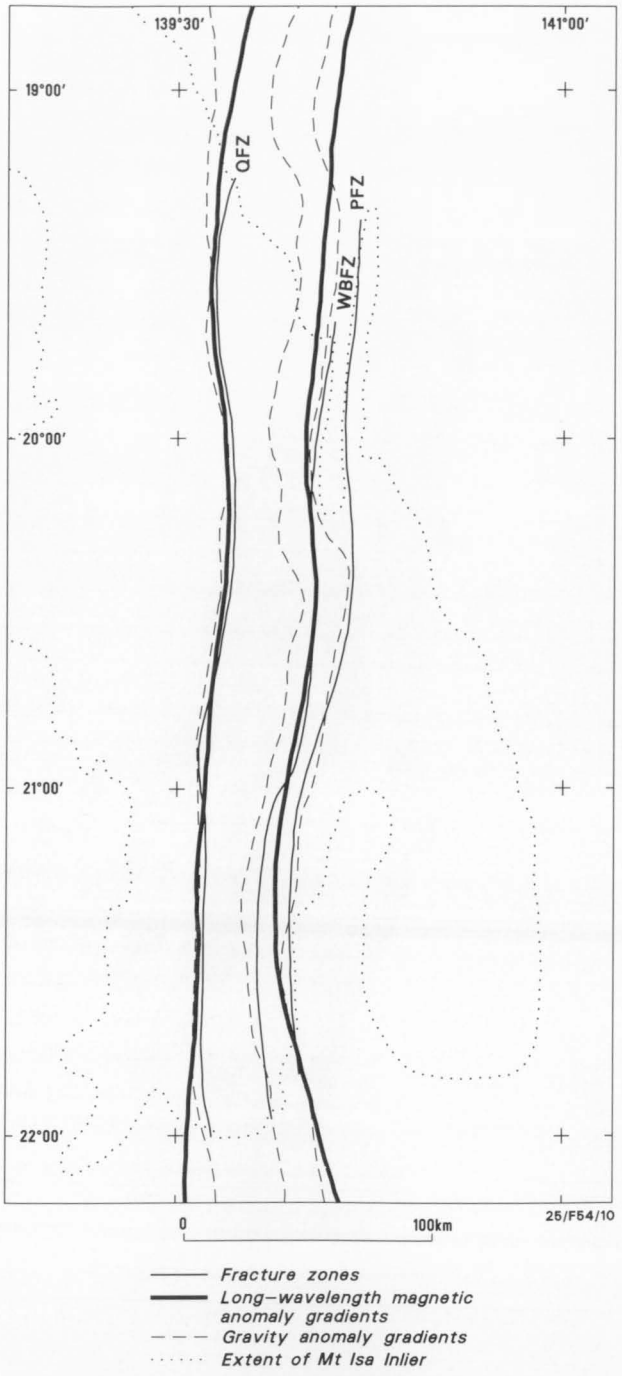


Fig. 10. Subdivisions of the Mount Isa Inlier. Thick lines give fractures zones separating the geological blocks of Blake & Stewart (1988). Thin continuous lines give the location of long-wavelength magnetic anomaly gradients. Thin dashed lines give the location of gravity anomaly gradients. Dotted line gives extent of Mount Isa Inlier.

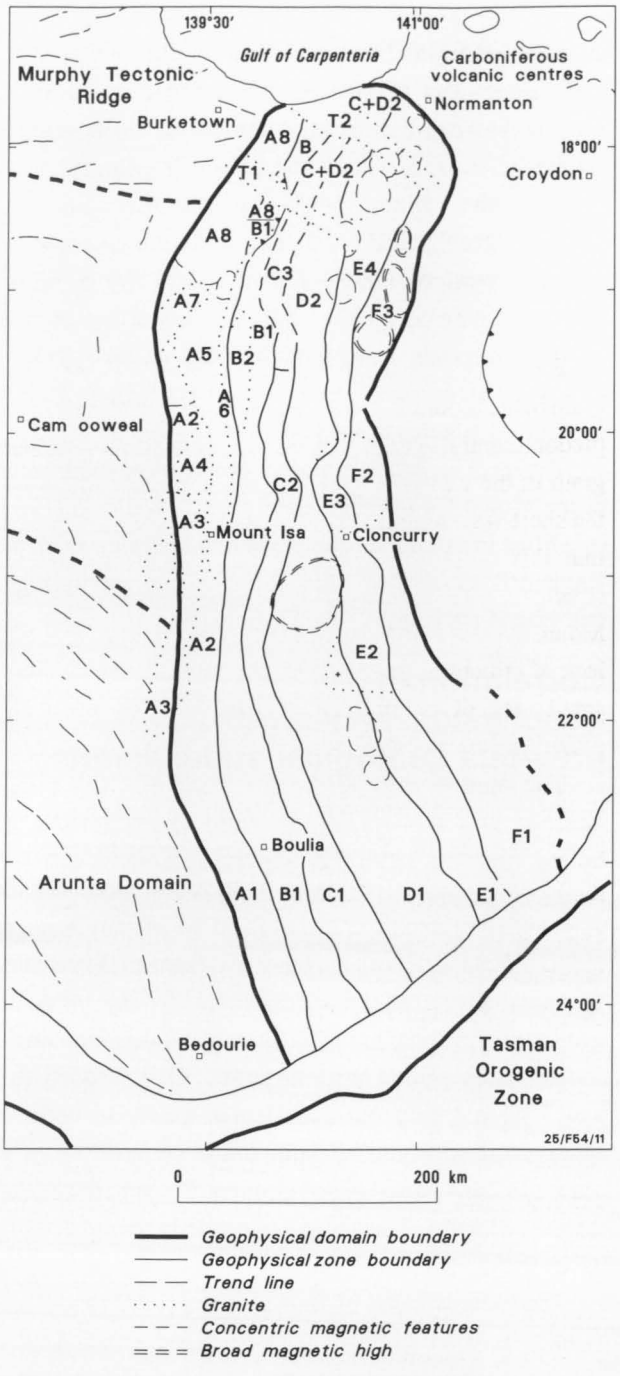


Fig. 11. Subdivision of the Mount Isa Domain on the basis of geophysics. The letters and numbers are referred to in the text.

high in the west from a gravity and magnetic low to the east. Hence, geophysics strongly supports its being a major geological boundary. This boundary is thought to follow the boundary A/B of Fig. 11.

- The Wonga Belt and Pilgrim Fault Zones (Fig. 10) are too close together for them to have independent effects on the long-wavelength gravity and magnetic anomalies. Where they are well defined geologically south of 20.2°S, they closely follow the two sides of the peak of a residual gravity high, and the Pilgrim Fault Zone roughly follows the western margin of the peak of the major central magnetic high. North of

about 20.2°S there is a lack of geological control on the position of the fault zones because key stratigraphic units are not exposed, but a likely location of the Pilgrim Fault Zone here is along the extension of the boundary between geophysical zones C and D of figure 11, to the west of the position favoured by Blake & Stewart (1988)

Blake & Stewart (1988) noted a change in structural grain in the Mount Isa Inlier at the Pilgrim Fault Zone, from predominantly longitudinal in the west, to no dominant grain in the east. The geophysical data, and in particular the short-wavelength magnetic anomalies (Fig. 5), shows that this eastern part of the inlier with no dominant structural grain is unusual, as elsewhere throughout the Mount Isa Domain there is a strong longitudinal grain. The lack of structural grain can be attributed to the relatively small area of outcrop being dominated by non-linear granitic plutons of the Naraku and Williams Batholiths.

The approximate agreement in position between geological block boundaries and geophysical zone boundaries is consistent with the geological block boundaries extending deep into the upper crust. Lack of exact agreement could be due to dip on the boundary, or uncertainty in the exact positions of the geological and geophysical boundaries. The uncertainty in the position of the geological boundaries can be evaluated by considering the discrepancy between the positions of the major faults defining the fault zones, and the position of the boundary between major stratigraphic units; this distance is in extreme cases 7 km. The uncertainty in the geophysical zone boundaries, evaluated using the difference in position of the gradients of long-wavelength gravity and magnetic anomalies, probably averages about 5 km.

Geophysical data strongly support the existence of major crustal breaks at the block boundaries of Blake & Stewart (1988), with the exception of the Mount Isa Fault Zone, and are consistent with the domain as a whole having a strongly banded structure at depth.

Detailed description of the Mount Isa Domain

The Mount Isa Domain is subdivided below using long-wavelength gravity and magnetic anomalies, and the short-wavelength magnetic anomaly pattern. The data sets are broadly concordant. The long-wavelength gravity and magnetic anomalies are similar, each indicating five bands; three highs and two lows (Fig. 9). The main difference between the two patterns is in the central highs; the gravity high is broad with a shallow dip at its centre, whereas the magnetic high is narrow and flanked by a deep wide low to the west, and a poorly developed low to the east.

Figure 11 shows the Mount Isa Domain subdivided into six zones, A to F. The zone boundaries are mainly based on concordant gravity and magnetic gradients in long-wavelength anomalies. The most confident boundaries are those based on two or more independent data sets – A/B, northern B/C, C/D, and, except in the central third, both D/E and E/F.

The short-wavelength anomalies must have a relatively shallow source; they are thought to mainly reflect the geology of the surface of the basement. Away from the inlier the type of rock causing these anomalies is not known with certainty. The most convincing way of regionally interpreting them is by correlating the patterns of magnetic anomalies on computer images with the patterns of outcrop of the mapped rock associations. In the following text, capital letters alone (e.g., F) and capital letters with numbers (e.g., F2) refer to areas in Figure 11. The distribution of rock types is based upon the 1:500 000 map of Blake (1987).

Zone A is a gravity and magnetic high. In A1 the magnetic high is broad-topped, with linear low-amplitude short-wavelength anomalies; the magnetic material is not definitely known, but is possibly Jayah Creek Metabasalt. To the north, in A2, the short-wavelength magnetic high overlies Eastern Creek Volcanics to about 20°S, where there is a transition zone, to the north of which the high overlies Myally Subgroup. Between 21.7°S and 19.2°S, there are three north-south structural bands: A2 has arcuate highs controlled in part by granite intrusion, A3 is cut by east-striking faults forming equidimensional blocks with the structural level being systematically higher to the north, and A4 has co-linear narrow outcrops. In A8 magnetic highs form an irregular pattern due to another structural style. In area A8/B1 the A8 rocks appear to be thrust eastward over B1, the gravity low of B1 extending through the area.

Zone B is a gravity and magnetic low. The important rocks within most of this zone are the Kalkadoon Batholith and Leichhardt Volcanics. B2, representing the exposed Ewen Batholith and its likely extension to the north, gives an unusual speckled pattern on the grey-scale magnetic image. South of 22°S there are some linear anomalies possibly caused by Argylla Formation and Leichhardt Volcanics.

Zone C is a gravity high. In C1 there is a regional

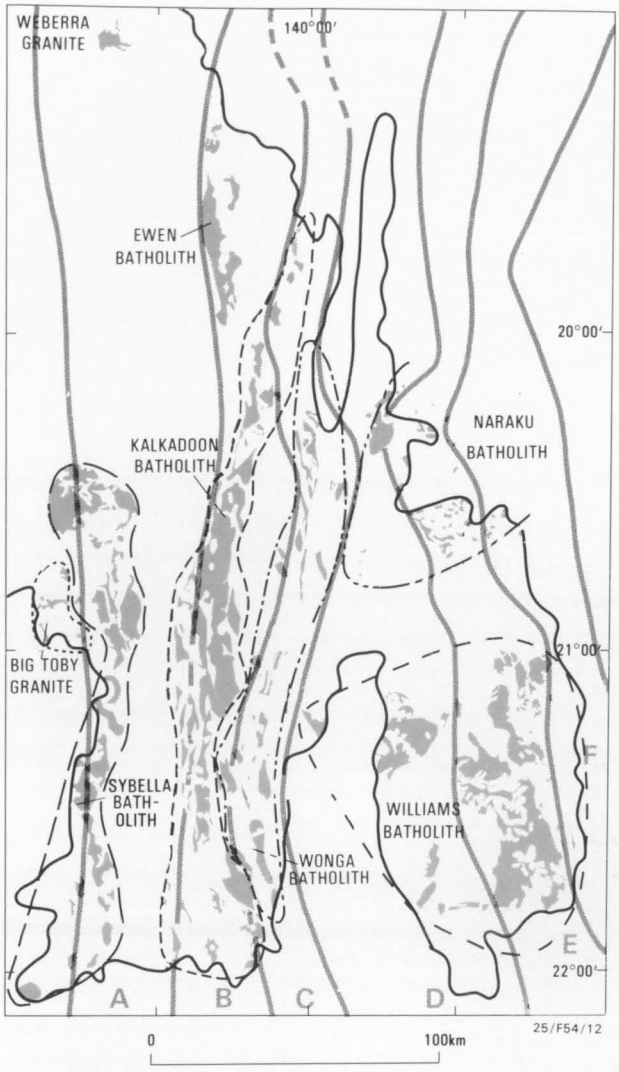


Fig. 12. Relationship between the distribution of granitic batholiths and geophysical zones.

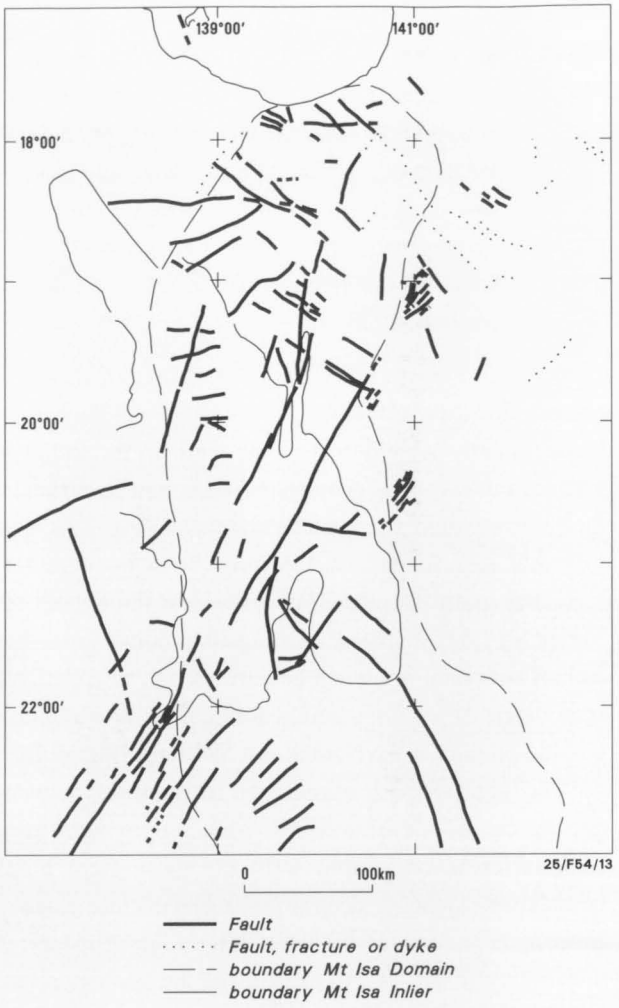


Fig. 13. Fault pattern from short-wavelength magnetic anomalies.

negative magnetic anomaly, while in C2 and C3 the anomaly is near zero. The rocks in C1 may include Plumb Mountain Gneiss, whereas C2 includes the Wonga Batholith, Argylla Formation, and Corella Formation. C3 has subparallel linear magnetic highs of uniform shape, averaging about 5 km apart, possibly correlating with Argylla Formation.

Zone D is a major magnetic and gravity high. D1 is composed of thin bands, indicated by variations in detail of the gravity and magnetic anomalies. D2 in the north has an irregular magnetic texture consistent with felsic volcanics, or possibly Corella Formation, which is exposed in the southern part of D2.

Zone E is a gravity and magnetic low. Within the Mount Isa Inlier this zone is dominated by oval geophysical structures that are largely due to the Williams and Naraku Batholiths (E2 & E3; Fig. 12). To the north and south, the gravity and magnetic low may also be due to granitic rocks, but here the gravity low does not correlate with large concentric magnetic structures or magnetic highs, so the shape and physical properties of these granitic rocks may differ from those of the Williams and Naraku Batholiths, and are possibly more like those over the Kalkadoon Batholith. In E4 there are some small, low-amplitude circular structures that may be caused by granite.

Zone F is a gravity and magnetic high. The magnetic anomalies show that the northern part of this zone, F3, contains concentric structures in magnetic rocks; the central part, F2, includes the Naraku Batholith and Soldiers Cap Group; and the southern part, F1, contains elongate magnetic highs that are interpreted to be due to volcanics.

Throughout the region there seems to be little or no correlation between metamorphic grade and the gravity and magnetic anomalies.

Post-cratonic faulting

In the Mount Isa Inlier there is a geologically-mapped major post-cratonic fault set with a strike of about 030°.

Individual faults have dextral movements of commonly 2-3 km. On the 1:500 000 map (Blake, 1987), the faults of this set are east of the Quilalar Fault Zone of Blake & Stewart (1988), and they appear to turn and merge with this fault zone. Using the magnetic data, north-northwest-striking faults can be mapped over an extensive area (Fig. 13), crossing the whole Mount Isa Domain and extending at least 100 km into domains to the west (Young, 1986) and possibly 50 km into domains to the east. Northeast-trending structures to the northeast in NORMANTON, CROYDON, and MILLUNGERA may be related to the same set. The faults defined from magnetic data have an across-strike extent of about 200 km, and their strike varies fairly systematically from 60° in the southeast to about 20° in the northwest. Features near the eastern margin of the Mount Isa Domain may be related to these structures. One of the features is a major re-entrant of the eastern margin of the domain, apparently controlled by a northeast fault nearly co-linear with the Quamby, Fountain Range, and Quartpot Faults of Blake (1987). Another feature consists of three sets of splays just to the east of the Mount Isa Domain, at 18.9-19.2°S, 19.8-19.9°S, and 20.4-20.7°S; these are interpreted as magnetised fault splays within non-magnetic pre-Mesozoic? sediments. The northern splay appears to be associated with the fault controlling the re-entrant.

North of the Mount Isa Inlier there are numerous northwest-striking faults, with up to 3 km of horizontal movement extending across the Mount Isa Domain, and also present in the crust up to 100 km to the east and north (Fig. 13). Probably related to these faults are two 15 km-wide bands crossing the Mount Isa Domain in the north (T1 and T2 in Fig. 11). These bands represent gaps in the north-trending geophysical anomalies; as the bands are gravity lows and in part magnetic highs they are interpreted as troughs with volcanic fill. The faults, which appear to have a significant extensional component, postdate cover sequence 2.

Conclusions

1. Gravity and magnetic anomalies define a Middle Proterozoic Mount Isa Geophysical Domain. The domain is about 800 km long (from north to south), 150 km wide in the north, and 250 km wide in the south. Most structures are parallel to the central axis of the domain. The domain is inferred to be younger than Proterozoic crust to the east and west, older than the crust to the north, and is older than Phanerozoic crust to the south. The margins of the domain are gravity and magnetic residual highs, consistent with the edges of the domain being denser and more magnetic than the surrounding crust.

2. The Mount Isa Domain truncates the northwest-trending Arunta basement exposed as the Yaringa and St Ronans Metamorphics in the southwest, and the east-trending Murphy Tectonic Ridge in the northwest. In the central part of its eastern margin, the Mount Isa Domain is interpreted to be thrust east over older basement. At its southern and northern margins the domain has been affected by post-Middle Proterozoic reworking.

3. The Mount Isa Domain is subdivided using gravity and magnetic anomalies into six zones extending for the entire length of the domain. Zone boundaries broadly coincide with most of the geological block boundaries identified by Blake & Stewart (1988), with boundaries of cover sequence 2 rocks, and with granite batholiths. The zones and the whole domain are arcuate, mainly because of a 20° bend at 21.5-22°S near the southern margin of the Mount Isa Inlier. At this bend the character of some of the short-wavelength anomalies and the shape and position of the long-wavelength gravity and magnetic anomalies change, consistently with changes in rock type and structure at the bend.

4. Two faulting events are recognised, both younger than cover sequence 2. The northern part of Mount Isa Domain, north of Mount Isa Inlier, is cut by a set of northwest-striking faults, and by two northwest-trending 'graben' corresponding with gravity lows and in part with magnetic highs. The faults have less than 3 km of horizontal displacement. These northwest structures appear continuous with northwest structures up to 100 km west and north of the northern part of the Mount Isa Domain. The central part of the Mount Isa Domain, and the crust up to 100 km to the west and 50 km to the east, are cut by a set of northeast-striking faults with generally dextral movements averaging 2-3 km.

Acknowledgements

I am grateful for comments on this work by D.H. Blake and A.J. Stewart. The work would not have been completed at this time without the use of images of BMR aeromagnetic data produced and made available by Geoimage Pty Ltd. Figures were drawn by H. Apps.

References

BARLOW, B.C., 1977 - Data limitations on model complexity; 2-D gravity modelling with desk-top calculators. *Bulletin of the Australian Society of Exploration Geophysics* 8, 139- 143.

BEESON, J., DELOR, C.P., & HARRIS, L., 1988 - A

structural and metamorphic traverse across the Albany Mobile Belt, Western Australia. *Precambrian Research* 40/41, 117-136.

BLAKE, D.H., 1987 - Geology of the Mount Isa Inlier and environs, Queensland and Northern Territory. *Bureau of Mineral Resources, Australia, Bulletin* 225, 83 pp.

BLAKE, D.H., & STEWART, A.J., 1988 - Block and possible terrane boundaries in the Mount Isa Inlier. *BMR Research Newsletter* 9, 2-3.

CLARK, D.A., 1980 - Magnetic properties of rocks from the Mount Isa area. *CSIRO Division of Mineral Physics, Restricted Investigation Report* 1149R.

DAY, R.W., WHITAKER, W.G., MURRAY, C.G., WILSON, I.H., & GRIMES, K.G., 1983 - Queensland geology. A companion volume to the 1:2 500 000 scale geological map (1975). *Geological Survey of Queensland, Publication* 383.

DOOLEY, J.C., 1980 - A review of the crustal structure of northeastern Australia. *In:* HENDERSON, R.A., & STEPHENSON, P.J. (Editors), The geology and geophysics of northeast Australia. *Geological Society of Australia, Queensland Division, Brisbane,* 27-45.

GEOIMAGE, 1989 - North-west Queensland, computer produced images of total magnetic intensity, 1:1 000 000 scale. Four maps. *Geoimage Pty Ltd, Queensland.*

GIBB, R.A., 1967 - Western Queensland reconnaissance gravity survey, 1957-1961. *Bureau of Mineral Resources, Australia, Report* 129, 47 pp.

GIBB, R.A., & THOMAS, M.D., 1976 - Gravity signature of fossil plate boundaries in the Canadian Shield. *Nature* 262, 199-200.

GSA, 1971 - Tectonic map of Australia and New Guinea, 1:5 000 000. *Geological Society of Australia, Sydney.*

GUNN, P.J., 1983 - Recognition of Proterozoic rift systems in the Mt. Isa - McArthur Basin area of northern Australia. *1983 Biennial Conference of the Australian Society of Exploration Geophysicists, Brisbane, Extended Abstracts,* 168-171.

HAWKINS, P.J., & HARRISON, P.L., 1978 - Stratigraphic and seismic investigations in the Lovelle Depression, western Galilee Basin. *Queensland Government Mining Journal* 79, 623-650.

HONE, I.G., 1984 - Regional geophysics. *In:* BLAKE, D.H., BULTITUDE, R.J., DONCHAK, P.J.T., WYBORN, L.A.I., & HONE, I.G., Geology of the Duchess-Urandangi Region, Mount Isa Inlier, Queensland. *Bureau of Mineral Resources, Australia, Bulletin* 219, 68-82.

HONE, I.G., CARBERRY, V.P., REITH, H.G., & WARNES, A., 1982 - Mount Isa Inlier geophysical study. *Bureau of Mineral Resources, Australia, Report* 238, 18-20.

HONE, I.G., CARBERRY, V.P., & REITH, H.G., 1987 - Physical property measurements on rock samples from the Mount Isa Inlier, northwest Queensland. *Bureau of Mineral Resources, Australia, Report* 265, 30 pp.

KLASNER, J.S., & KING, E.R., 1986 - Precambrian basement geology of North and South Dakota. *Canadian Journal of Earth Sciences* 23, 1083-1102.

MURRAY, C.G., SCHEIBNER, E., & WALKER, R.N., 1989 - Regional geological interpretation of a digital coloured residual Bouguer gravity image of eastern Australia with a wavelength cut-off of 250 km. *Australian Journal of Earth Sciences* 36, 423-449.

MUTTON, A.J., & ALMOND, R.A., 1979 - Geophysical mapping of buried Precambrian rocks in the Cloncurry area, northwest Queensland. *Bureau of Mineral Resources, Australia, Report* 210 (*BMR Microform* MF95).

RIVERS, T., MARTIGNOLE, J., GOWER, C.F., & DAVIDSON, A., 1989 - New tectonic divisions of the Grenville Province, southeast Canadian Shield. *Tectonics* 8, 63-84.

SHIRLEY, J.E., 1979 - Crustal structure of north Queensland from gravity anomalies. *BMR Journal of Australian Geology & Geophysics* 4, 309-321.

SHIRLEY, J.E., & ZADOROZNYJ, I., 1974 - Reconnaissance helicopter gravity survey, northern Queensland, 1966. *Bureau of Mineral Resources, Australia, Record* 1974/140, 13 pp., 4 pl.

TUCKER, D.H., 1975 - Cloncurry regional, and Prospector detailed, airborne magnetic and radiometric surveys, Queensland 1973. *Bureau of Mineral Resources, Australia, Record* 1975/74, 47 pp.

TUCKER, D.H., WYATT, B.W., DRUCE, E.C., MATHUR, S.P., & HARRISON, P.L., 1979 - The upper crustal geology of the Georgina Basin region. *BMR Journal of Australian Geology & Geophysics* 4, 209-226.

WELLMAN, P., 1976a - Gravity trends and the growth of Australia: a tentative correlation. *Journal of the Geological Society of Australia* 23, 11-14.

WELLMAN, P., 1976b - Regional variation of gravity, and isostatic equilibrium of the Australian crust. *BMR Journal of Australian Geology & Geophysics* 1, 297-302.

WELLMAN, P., 1978 - Gravity evidence for abrupt changes in mean crustal density at the junction of Australian crustal blocks. *BMR Journal of Australian Geology & Geophysics* 3, 153-162.

WELLMAN, P., 1979 - On the isostatic compensation of Australian topography. *BMR Journal of Australian Geology and Geophysics* 4, 373-382.

WELLMAN, P., 1986 - Mount Isa block as a 700 km-long zone of reworking of Proterozoic crust: an interpretation based on gravity and magnetic anomalies. *Bureau of Mineral Resources, Australia, Record* 1986/31, 25-28.

WELLMAN, P., 1988 - Development of the Australian Proterozoic crust as inferred from gravity and magnetic anomalies. *Precambrian Research* 40/41, 89-100.

WELLMAN, P. & MURRAY, A.S., 1979 - Free air gravity anomaly map, 1:10 000 000 scale. *Bureau of Mineral Resources Earth Science Atlas, Canberra.*

YOUNG, G.A., 1986 - Geological interpretation of geophysical results, Glenormiston special airborne survey, Queensland, 1977. *Bureau of Mineral Resources, Australia, Report* 253, 35 pp.

YOUNG, M.E., 1984 - Gravity and magnetic results from Mount Isa district, Australia. *Transactions of the Institute of Mining and Metallurgy, Section B: Applied Earth Science* 93, B78-B86.

ZUBER, M.T., BECHTEL, T.D. & FORSYTH, D.W., 1989 - Effective elastic thickness of the lithosphere and mechanisms of isostatic compensation in Australia. *Journal of Geophysical Research* 94, 9353-9367.

Deformation model and sedimentation patterns of the Proterozoic of the Paroo Range, Mount Isa Inlier, Queensland, Australia

W. Nijman [1], *J.H. van Lochem* [1], *H. Spliethoff* [1], *and J. Feijth* [1]

This paper is based on the following map: Nijman, W., 1991 - Geology of the Paroo Range and Hero/Western Fault Zone (1:20 000 scale map). Bureau of Mineral Resources, Canberra, Australia (two sheets).

This research project was supported by the Dutch Foundation 'Dr.Schurmann-fonds' with annual grants in the period 1986-1990.

A combined structural and sedimentological investigation was carried out in the 1800-1650 Ma-old rocks of the Paroo Range, situated in the centre of the Western Fold Belt of the Mount Isa Inlier at the intersection of transverse and longitudinal major block boundaries. Detailed structural mapping, restoration of cross-sections, and geometrical analysis of coarse clastic deposystems and their internal and external unconformities have led to re-assessment of the early phases of structural evolution of this part of the inlier.

Positive flower structures, spaced 4.5 km apart below the basal unconformity of the Mount Isa Group (cover sequence 3), and an en-echelon isopach pattern in the underlying Myally Subgroup (cover sequence 2) indicate early and synsedimentary transpressional wrench faulting (D^{P}_{1}) with a system of Riedel shears derived from an overall north-oriented dextral shear regime in the basement. These D^{P}_{1} faults controlled the distribution of isolated pebbly sandstone bodies in the shallow-water inshore sediments of the Bortala Formation. Transpressional tectonics formed east-verging drape folds, concurrently with block tilt with easterly and northerly components related to early interaction between the longitudinal and transverse block boundaries. This interaction also controlled sedimentation of the Lower Mount Isa Group, in which the Surprise Creek Formation is now included. The major transverse faults appear to have defined headlands in an embayed east-facing coastline with considerable tidal and wave activity, into which fan deltas fed gravel and sand from westerly source areas.

The area then underwent low-angle west-verging thrusting (D^{P}_{2}) with tiplines in the Moondarra Siltstone of the Lower Mount Isa Group. Two thrusts 10 km apart are strongly mineralised with iron oxide, particularly near the tiplines, and locally host a dolerite sill that apparently intruded wet sediment and was accompanied by soft-sediment deformation. This sets a rather early date to the initiation of thrusting.

The early thrusting was followed by the main D^{P}_{3} east-west compression and folding.

East-striking listric normal faults (D^{P}_{4}) caused substantial block rotation and tilting. Late conjugate (D^{P}_{5}) northwest-striking sinistral and northeast-striking dextral strike-slip faulting is also well known from other parts of the inlier.

It appears that the Myally Shelf, which originated at the start of this period of structurally controlled sedimentation, resembled the present-day, strike-slip dominated, offshore Californian continental platform, though of lesser average depth. During almost continuous structural deformation, the area was subject to increasing east-west compression. After the main phase, D^{P}_{3}, the regime switched to north-south transtension, which formed a linked system of east-striking normal faults and north-striking transfer faults. Final east-west shortening was mainly accomplished by conjugate strike-slip faults.

[1]Department of Geology, Institute of Earth Sciences, University of Utrecht, Postbus 80021, 3508 TA, The Netherlands.

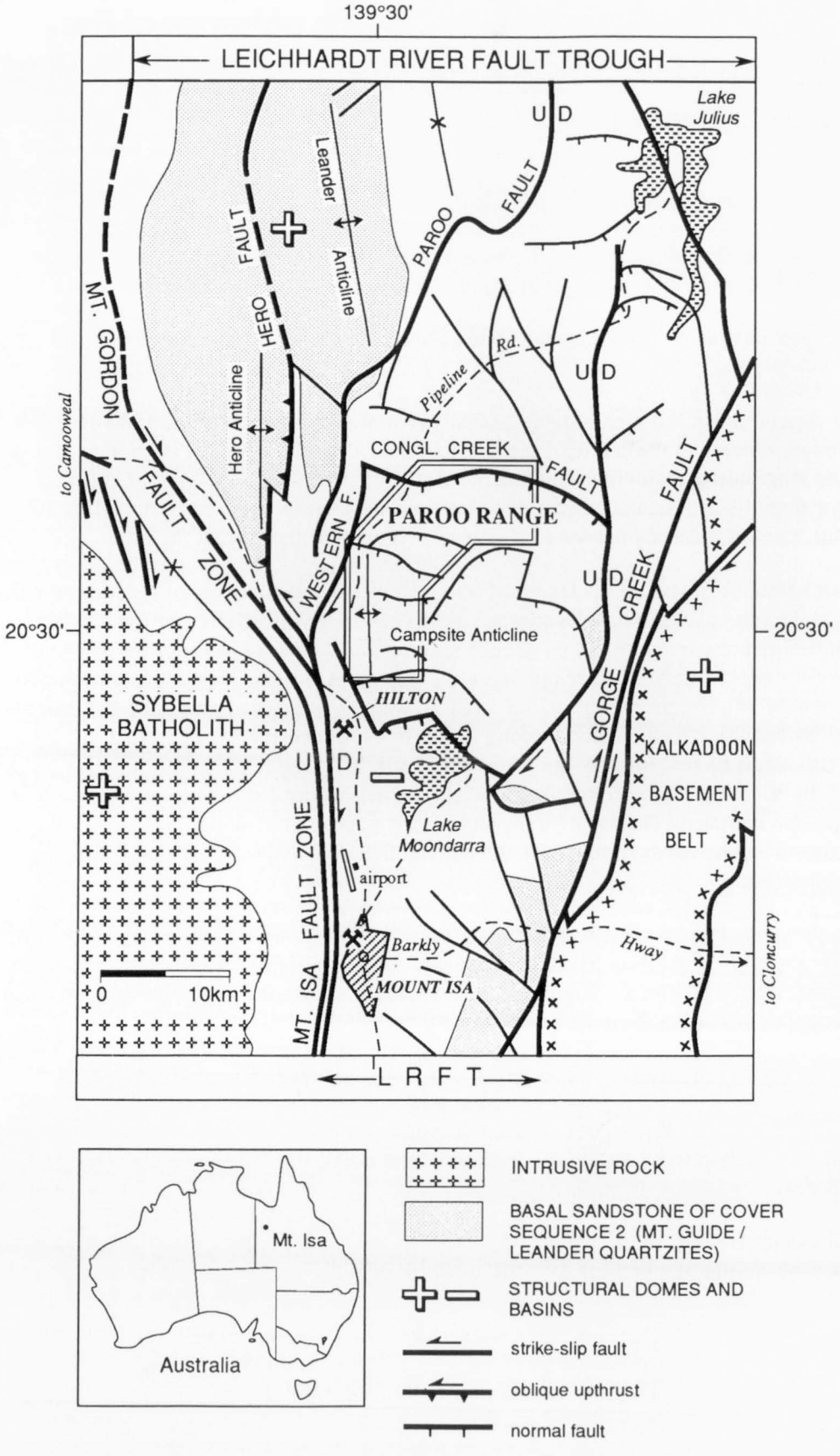


Fig. 1. Position of the Paroo Range (double frame) within Leichhardt River Fault Trough and surroundings, Mount Isa Inlier. Geology modified after Blake (1987).

Introduction

This study examines the relation between sedimentation and deformation in the Middle Proterozoic rocks of the Paroo Range, north-northeast of Mount Isa (Fig. 1; Nijman, 1991) during deposition of the Myally Subgroup and the Lower Mount Isa Group. These units respectively belong to cover sequences 2 and 3 (Blake, 1987; Blake & others, 1990) of the Leichhardt River Fault Trough (LRFT) (Fig. 2) and spanned a period of 110 Ma between the end of the extrusion of the Eastern Creek Volcanics (1780 Ma) and the intrusion of the Sybella Granite (1670 Ma; Fig. 1).

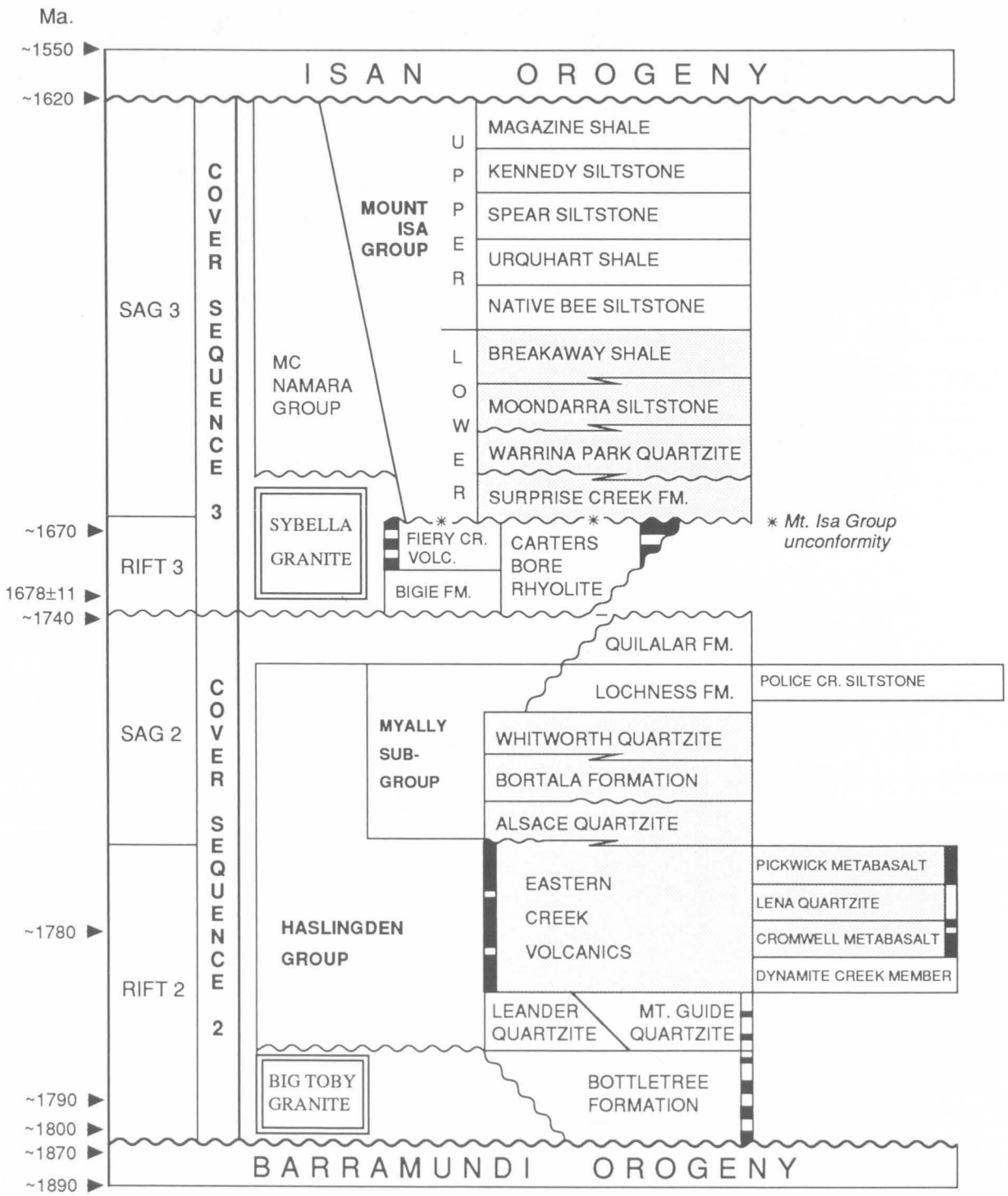


Fig. 2. Stratigraphic column of LRFT and Paroo Range. Modified after Derrick & others (1976a, b) and Blake & others (1990). Black in black-and-white bars indicates relative abundance of volcanics. Formations of Paroo Range shaded. Cover sequence 1, dated at 1870-1850 Ma in the Kalkadoon block, is not exposed in the LRFT.

The area underwent region-wide deformation during the Isan Orogeny between 1620-1550 Ma (Blake & others, 1990).

Fieldwork was carried out by a group from the Geology Department of the University of Utrecht, The Netherlands, in June-July 1986 to 1989. This paper is based on a previous report to BMR (Lochem & others, 1988) supplemented by data on D^P_2 thrusting from Feijth (1989). Mijnlieff, van Rijswijk, and Schalkwijk contributed to the mapping, and studied thermoluminescence (TL) of quartz grains in sediments of the Paroo Range and their possible source areas (Rijswijk & Schalkwijk, 1988). The aims of the study were:

- 1. Localisation of coarse clastic facies and determination of their provenance and dispersal;
- 2. Determination of the sequence of deformation and its relation to coarse clastic sedimentation patterns;
- 3. Reconstruction of the deformation history with special emphasis on the earliest recognisable phases, taking into account existing diverging opinions about the east-west faults present throughout large parts of the LRFT, variously interpreted as early growth faults (Smith, 1969; Derrick, 1982), syn- to post-sedimentary listric normal faults (spoon faults of Dunnet, 1976b), or duplex-related thrusts (Bell, 1983).

The Paroo Range was chosen because of its coarse-grained sandstone and conglomerate at several stratigraphic levels and its intra-/interformational unconformities apparently related to the intersection of major longitudinal (north-south) and transverse (east-west) structures. Longitudinal structures include the Western and Hero Faults (compare Nijman & others, this volume and Fig. 1) and the palaeogeographically inferred Mount Gordon Arch (Derrick, 1982); important transverse structures are the Conglomerate Creek Fault and the Horse's Head Syncline (compare Stewart, this volume a) bounding the Paroo Range to the north, and the North Stone Axe Fault in the south.

The 115 km^2 area (location in Fig. 1) was mapped at 1:12 500 scale, and reproduced at 1:20 000 (Nijman, 1991, sheet 1). Special attention was given to the three-dimensional sedimentological analysis of the coarsest clastic sediment bodies, which would be expected to best record structural controls.

Deformation episodes in the Paroo Range area are denoted by the superscript 'P'.

Tectono-stratigraphic framework

Tectonic setting

The Mount Isa Inlier belongs to a Proterozoic mobile belt that consists of strongly deformed sequences of mafic and, to a lesser extent, felsic volcanic rocks, epicontinental clastic and carbonate sediments, granitic to granodioritic intrusions, and mafic dyke swarms.

The Paroo Range is situated in the centre of the Leichhardt River Fault Trough (Fig. 1). Together with the Lawn Hill Platform and Ewen Block, the LRFT constitutes the Western Fold Belt of the Mount Isa Inlier (Blake, 1987), the counterpart of which is the Eastern Fold Belt, on the opposite side of an igneous and metamorphic basement high, the Kalkadoon-Leichhardt Belt. To what extent this high really played a role in Proterozoic sedimentation and how far the low-grade metamorphic sedimentary suite of the Western Fold Belt can be correlated with that of the much more metamorphosed eastern belt is as yet not fully understood (Blake & others, 1990).

The LRFT is bounded by the Gorge Creek-Quilalar Fault Zone against the Kalkadoon-Leichhardt igneous complex to the east, and by the Mount Isa and Mount Gordon Fault Zones against the Early Proterozoic North Australian craton to the west (Fig. 1). Derrick (1982) defined the LRFT as an intracontinental or continental margin rift structure, but this has been disputed as the western margin of the LRFT had not then been recognised, and may not be a rifted (faulted) margin at all (Sweet, 1983; Blake, 1987).

Dunnet (1976a) placed the Mount Isa Inlier along the eastern margin of the North Australian craton, which formed part of the Pan-Antarctic craton for much of the Proterozoic. Compositional trends of intrusive and extrusive rock suites (Glikson & others, 1976; Glikson & Derrick, 1978), the occurrence of older Precambrian basement only to the west of the inlier, and the restriction of most of the deep-water turbidite facies to its easternmost part were used as arguments for this hypothesis (Wilson, 1978). Bultitude & Wyborn (1982) could not confirm the trend in composition reported by Glikson and co-workers. Wyborn & Blake (1982) noted the continental character of the Precambrian basement below the easterly adjacent Mesozoic basins – basement that seemed to have provided the inlier sediments – and therefore concluded that most of the inlier developed in an intracratonic setting during a

mainly tensional regime. Such interpretations (compare Etheridge & others, 1987; Beardsmore & others, 1988; Loosveld, 1989) would render the tectonic setting of the Mount Isa Inlier comparable to that of most aulacogens. According to Blake (1987), east and west gravity lows flanking a high in the inlier itself, favour an intracratonic setting.

Cover sequences: rift and sag phases

At least two of the three cover sequences now recognised (Blake, 1987; Wyborn & others, 1988) are composed of rift-phase mafic and felsic lavas and clastics, succeeded by thermal sag-phase clastic deposits (Fig. 2). The sediments are mainly epicontinental alluvial to shallow marine clastics, with subordinate carbonates. Deeper-water deposits occur in the Eastern Fold Belt (Blake, 1987) and in isolated graben in the Western Fold Belt (Wilson & others, 1977).

The fill of the LRFT consists mainly of cover sequences 2 and 3 (Derrick & others, 1976a, b; Derrick & others, 1980; Blake, 1980, 1987; Blake & others, 1990). We include the Surprise Creek Formation of cover sequence 3 in the Lower Mount Isa Group for reasons given below in the section on 'Cover sequence 3, the Lower Mount Isa Group' .



Fig. 3. Infilling of cavernous top of a basalt flow (Cromwell Metabasalt) with trough cross-laminated feldspathic arenite Phc_q, just below the Lena Quartzite Member. Grid reference 436330. Pen is 14 cm long.

New data on the stratigraphy of the Paroo Range within the context of the LRFT

Cover sequence 2: Haslingden Group (Ph)

With a total thickness of up to 10 km (Derrick & others, 1976a; Derrick, 1982) the Haslingden Group of cover sequence 2 comprises from its base upwards, the Mount Guide and Leander Quartzites, the Eastern Creek Volcanics (ECV), and the Myally Subgroup, the latter being further subdivided into the Alsace Quartzite, Bortala Formation, Whitworth Quartzite, and Lochness Formation (Fig. 2). Of these, only the ECV, Alsace Quartzite, Bortala Formation, and Whitworth Quartzite are exposed in the Paroo Range. The Haslingden Group is preceded by the Bottletree Formation, the first clastic formation belonging to cover sequence 2.

The Mount Guide Quartzite consists of a lower unit with conglomerate and greywacke and an upper unit of quartz arenite and orthoquartzite, and crops out in the central-southern part of the LRFT. The Leander Quartzite of similar rock type and age is exposed in a dome northwest of the Paroo Range (Fig. 1). Each formation is up to 6000 m thick (Derrick, 1982). Derrick interpreted the basal arkose and conglomerate of these formations as alluvial rift deposits grading upwards into orthoquartzite indicative of littoral conditions. Palaeocurrent directions from the east and southeast have been reported, although little is known systematically of the source-depocentre relation. Our thermoluminescence data also suggests the Kalkadoon basement to the east as a source for these early Haslingden Group sediments, whereas clastic units younger than the Eastern Creek Volcanics show a westerly provenance (Rijswijk & Schalkwijk, 1988; compare Carter & others, 1961).

Eastern Creek Volcanics (ECV; Phe)

The thickness of the ECV in the map area, including the Hero/Western Fault Zone, is about 3200 m (compare cross-section A-E in Nijman, 1991). The total thickness of 7200 m given by Blake & others (1990) seems to be excessive. The ECV overlie the Leander and Mount Guide

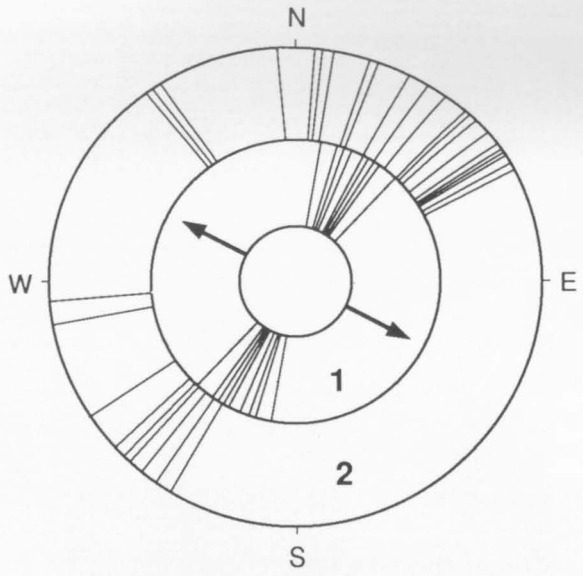


Fig. 4. Palaeocurrent pattern of a 40-m thick sequence of Lena Quartzite Member at grid reference 437343. Outer circle – restored foreset orientations of trough and planar cross-laminated megasets; inner circle – crestline orientation of wave ripple bedforms; heavy arrows – average wave oscillation directions. Combined with the mature well-rounded quartz arenitic composition, the pattern is characteristic for predominant longshore bipolar sediment-transport along a 028°– oriented coastline.

Quartzites. They are composed chiefly of basaltic lava with lesser feldspathic sandstone and some conglomerate sheets and lenses (Phe_q, Phc_q, Php_q). From bottom to top the ECV comprise the Dynamite Creek, Cromwell Metabasalt, Lena Quartzite, and Pickwick Metabasalt Members, the first of which is not exposed in the Paroo Range.

Cromwell (Phc) and Pickwick Metabasalt (Php) Members

The Cromwell and Pickwick Metabasalts below and above the Lena Quartzite Member are very similar (Wilson & others, 1977); both are mainly low-grade metabasalts of continental tholeiite composition (Glikson & others, 1976; Wilson & others, 1985). Lava flows are usually less than 40 m thick. Their sheet-like nature, the presence of stratiform amygdaloidal zones, absence of pillows, and paucity of associated basaltic tuffs indicate very shallow-water or subaerial eruption on a broad shelf or plain (Blake, 1987). Rare pillow basalts (e.g., grid reference 422330) probably erupted into lakes.

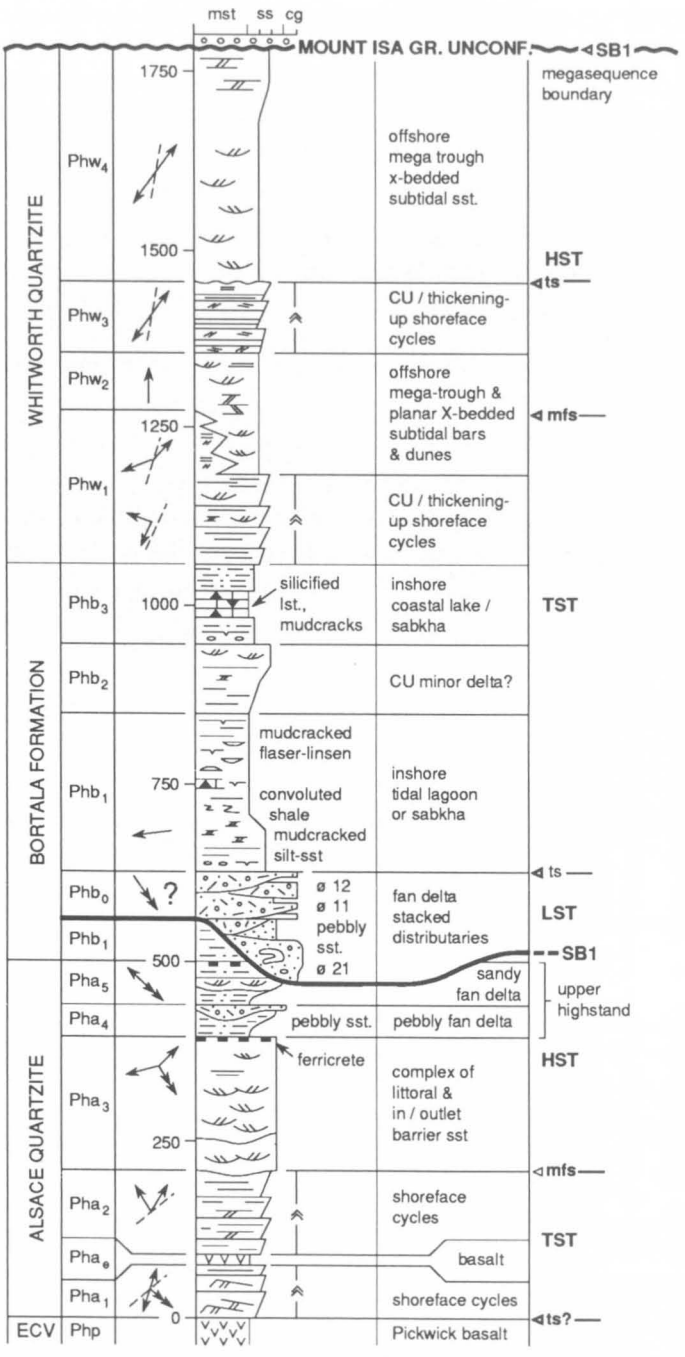
Fig. 5. (facing page). Sedimentology of Myally Subgroup: (A) Schematic sedimentary log of Myally Subgroup of eastern Paroo Range recorded along north-south gridline 46 for lower 750 m and along north-south gridline 51 for upper 1000 m. Average palaeocurrents, mainly from cross-beds (both foresets and trough axes), indicated by arrows; double-headed arrow indicates interpreted offshore direction; dashed lines indicate dominant wave ripple strike, interpreted as longshore direction. Sequence-stratigraphic notation in sixth column explained in text section on 'The Myally Shelf in the Paroo Range'. (B) Palaeocurrent distribution of Alsace and Whitworth Quartzites of Paroo Range; black – wave ripple strike; grey – trough and tabular-planar megacross-bedding. (C) Alsace Quartzite (Pha_1: grid reference 481388): 30 cm-hammer on lee face of straight-crested mega-ripple, facing east (longshore direction); stoss side covered by wave ripples (arrow); the next set consists of even-laminated shoreface facies (S_0). (D) Bortala Formation (Phb_1; grid reference 451390); heterolithic facies showing fine-grained even-laminated sets grading into climbing ripple sets with convoluted top, overlain by a shale/sandstone bed with mud cracking and curled mud flakes (arrow). Palaeocurrent to the right, i.e., southeast. Scale in centimetres. (E) Whitworth Quartzite (Phw_1: grid reference 468417); washover sandstone sheets (white layers; foresets, at arrows, towards viewer), interbedded with Bortala Formation (grey). Palaeocurrent to northwest. Hammer 30 cm long.

Arkosic to arenitic, trough cross-bedded, in places wave-rippled, sandstone bodies (Phc_q) with a tendency to increasing lateral interconnectedness precede the Lena Quartzite Member in the upper part of the underlying Cromwell Metabasalt (compare Henderson & Bain, 1991); these include channel sandstone filling the subaerial(?) cavernous surface of lava flows (Fig. 3; grid reference 436330). Comparable sandstone lenses are found in the Pickwick Metabasalt and are denoted (Php_q).

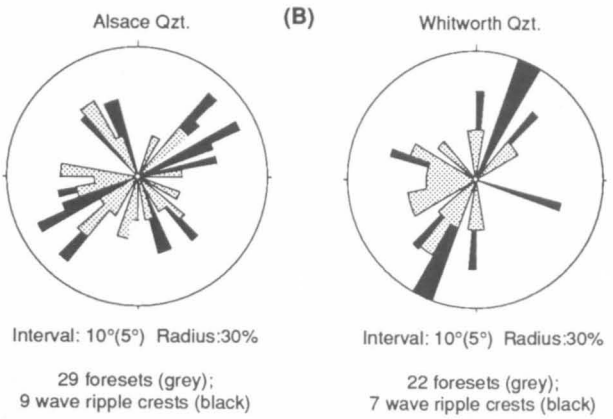
Lena Quartzite Member (Phl)

The Lena Quartzite is a sheet sandstone composed of sheets and lenses of quartz arenite to quartzite, feldspathic sandstone, and arkose, between the Cromwell and Pickwick Metabasalt Members of the ECV.

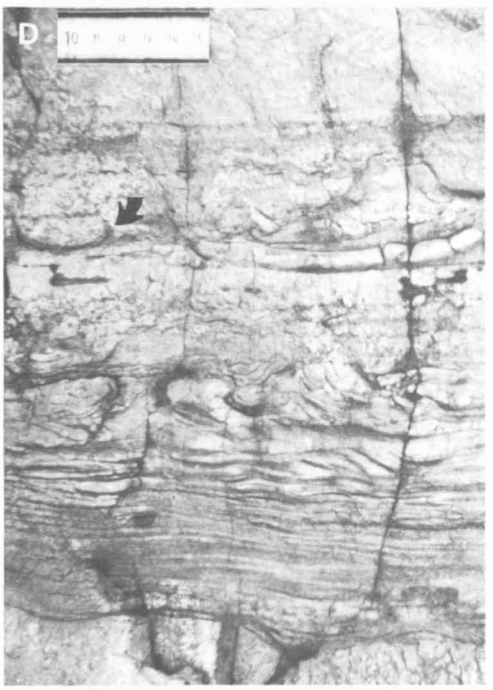
In the Paroo Range the Lena Quartzite is a lens, 250 m thick and about 2.5 km wide (see Nijman, 1991; grid reference 437343; cross-section C-E; compare restored cross-section of Fig. 11). Trough cross-bedding is ubiquitous as are symmetrical, straight-crested, and bifurcating wave ripples exposed on bedding planes. Some tabular sets of high-angle planar cross-lamination and


mst ss cg
MOUNT ISA GR. UNCONF.
SB1
megasequence boundary
WHITWORTH QUARTZITE
BORTALA FORMATION
ALSACE QUARTZITE
ECV
Phw4
Phw3
Phw2
Phw1
Phb3
Phb2
Phb1
Phb0
Pha5
Pha4
Pha3
Pha2
Pha e
Pha1
Php
1750
1500
1250
1000
750
500
250
0
offshore mega trough x-bedded subtidal sst.
HST
ts
CU / thickening-up shoreface cycles
offshore mega-trough & planar X-bedded subtidal bars & dunes
mfs
CU / thickening-up shoreface cycles
silicified lst., mudcracks
inshore coastal lake / sabkha
TST
CU minor delta?
mudcracked flaser-linsen
convoluted shale
mudcracked silt-sst
inshore tidal lagoon or sabkha
ts
ø 12
ø 11
pebbly sst.
ø 21
fan delta stacked distributaries
LST
SB1
sandy fan delta
upper highstand
pebbly sst.
pebbly fan delta
ferricrete
complex of littoral & in / outlet barrier sst
HST
mfs
shoreface cycles
TST
basalt
shoreface cycles
ts?
Pickwick basalt

(A)


Alsace Qzt.
(B)
Whitworth Qzt.
Interval: 10°(5°) Radius:30%
29 foresets (grey);
9 wave ripple crests (black)
Interval: 10°(5°) Radius:30%
22 foresets (grey);
7 wave ripple crests (black)


C
S_0


D


E

even-laminated sets with low-angle discontinuities were found.

Trough cross-beds show a wide range of current orientations best characterised as bipolar with modes to northeast and southwest, with a few measurements to northwest and west (Fig. 4). The modes coincide with the average wave ripple crest line orientation of 028°/208° ± 10° and are therefore orientated longshore. Such a palaeocurrent pattern is a common characteristic of clastic shorelines such as the Cretaceous Gallup Sandstone in the USA (McCubbin, 1982), and in the Paroo Range indicates a northeasterly coastline orientation.

The Myally Subgroup and Quilalar Formation

The predominantly arenitic to quartzitic Myally Subgroup (Fig. 2) with intervals of siltstone and shale conformably overlies the ECV. Figure 5 shows the facies sequence and stratigraphic subdivision of the Myally Subgroup in the Paroo Range; Figure 6 shows isopach and some dispersal patterns of its formations in part of the LRFT. The sequence stratigraphic notation in Figure 5 is explained in the section below on 'The Myally Shelf in the Paroo Range'.

Alsace Quartzite (Pha)

In the Paroo Range, most of the Alsace Quartzite (Pha_{1-3}) consists of repeated coarsening-up, thickening-up arenite sequences (Fig. 5A) with alternating even-laminated and wave-rippled trough and tabular-planar cross-bedding (Fig. 5C). Several of these sequences are capped by large-scale trough cross-bedded units (Pha_3). They consist of medium to coarse-grained quartz arenite and feldspathic arenite with a feldspar content of up to about 10% (Wilson & others, 1977). Heavy-mineral laminations are ubiquitous.

The polymodal palaeocurrent pattern of the formation (Fig. 5B) tends to be orthogonal to the dominant wave ripple orientation, much like that of the Lena Quartzite. The facies is characteristic for a barrier beach-inlet system. Between the first and the second unit a thin basalt sheet is found (Pha_e).

In the the upper part of the formation are coarsening-up units of a deltaic character (Pha_{4-5}; grid references 470383, 474389), some containing a top set with coarse-grained trough cross-bedded sandstone, others with a pebbly sandstone channel fill. The latter facies heralds the much larger occurrences in the base of the Bortala Formation. This transitional facies is strongly ferruginous, locally forming ferricrete. The facies transition marks the shift from littoral to inshore conditions.

In the Prospector 1:100 000 Sheet area (for location see Nijman, 1991) thickness ranges from 45 to 600 m. Maxima of over 500 m occur in a northwest-oriented en-echelon arrangement (Fig. 6A), and one of these depocentres is situated in the Paroo Range map area.

Bortala Formation (Phb)

The Bortala Formation consists mainly of siltstone and fine-grained sandstone, and is finer-grained than the adjacent formations. It is also more feldspathic and contains a larger proportion of unstable clasts. Flaser-linsen bedding and convolute laminations, mud flakes, and desiccation cracks (grid reference 451390; Fig. 5D), all point to varying depositional energy and episodic emergence. White opaque chert (grid reference 514428) possibly represents silicified lime mudstone of lacustrine(?) nature. In the Paroo Range, channel fills of pebbly sandstone and slump deposits (Phb_0) occur in the lower part of the formation (see section below on 'D^P_1 deformation and coarse-clastic deposystems'), whereas a coarsening-up sandy sequence resembling the Whitworth Quartzite forms the middle part (Phb_2).

In the Prospector 1:100 000 Sheet area, thickness is between 80 and 700 m (Wilson & others, 1977), with a local depocentre of 550 m in the Paroo Range; this pattern is comparable to that of the Alsace Quartzite (Fig. 6B).

Whitworth Quartzite (Phw)

The Whitworth Quartzite of the Paroo Range is a fine to medium-grained feldspathic arenite similar to the Alsace Quartzite in both facies and palaeocurrent pattern. The lower unit (Phw_1) interdigitates with the Bortala Formation in a facies indicative of back-barrier and washover conditions (Fig. 5E; grid reference 468417). Unit Phw_3 has north-oriented trough sets more than 10 m wide (grid reference 510440), and bars up to 2 m high, approximately parallel to the wave-ripple orientation in both directions (grid reference 515434). This interval is interpreted to be the farthest offshore subtidal exposure in an otherwise sandy littoral environment of an east-facing coastline.

In the Prospector Sheet area, thickness ranges from less than 500 m in the southwest to over 2000 m in the Paroo Creek area (Fig. 6C). True thickness can be measured only where the Lochness Formation overlies the Whitworth Quartzite. Elsewhere, as in the Paroo Range, the upper contact is an unconformity, and westward thinning and wedge-out indicate eastward tilt before

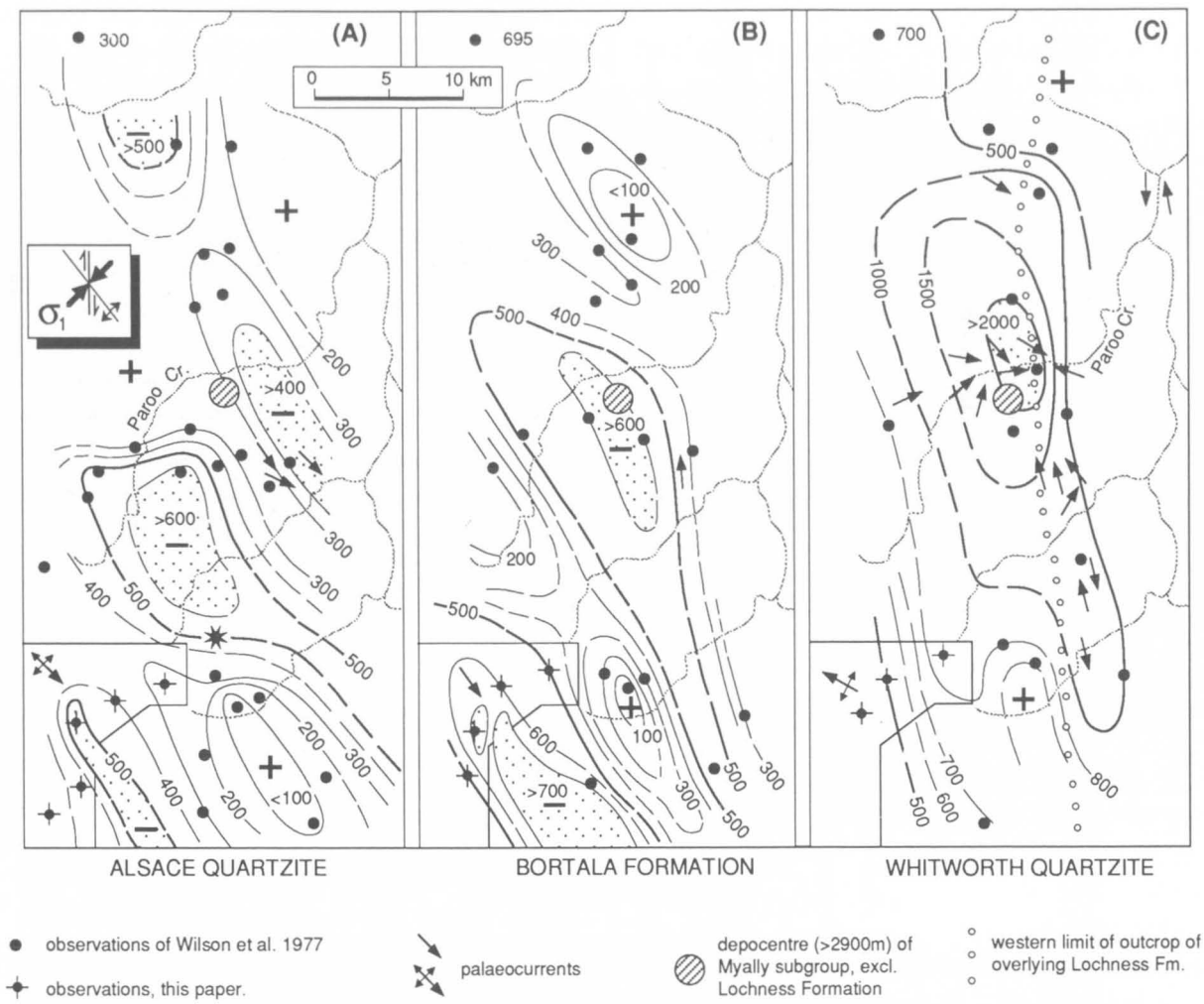


Fig. 6. Isopach maps: (A) Alsace Quartzite, (B) Bortala Formation, and (C) Whitworth Quartzite in Prospector Sheet sector of Western Fold Belt after data of Wilson & others (1977: figs. 23-25) and our data from Paroo Range area (framed in southwest corner). Bold crosses denote thinnest parts of units, bold dashes thickest parts. At this scale no corrections have been made for moderate north-south D^P_4 extension and relatively small east-west shortening during D^P_3 and D^P_5. Late transverse slike-slip may have caused juxtaposition of minima and maxima in oblique grain of pattern such as in (A) at • - site of Conglomerate Creek Fault. The depocentre of the Myally Subgroup is near Paroo Creek. En-echelon isopach pattern is interpreted to result from supracrustal folding due to northward dextral shear in basement (sigma-1: southwest-northeast in [A]).

deposition of the Mount Isa Group (Wilson & others, 1977).

Lochness Formation

Outcrop of the Lochness Formation is restricted to the eastern margin of the LRFT (Fig. 6C) and contains fine-grained feldspathic and ferruginous arenite, siltstone, and shale. Dolomitic and calcareous beds near the top of the formation have been named the Police Creek Siltstone Member by Derrick (1982). We found similar facies in the Paroo Range on top of the Whitworth Quartzite, but because their base is unconformable, they link up with the Mount Isa Group (Surprise Creek Formation).

Quilalar Formation

Elsewhere in the LRFT, especially around Lake Julius (Fig. 1), the Myally Subgroup is conformably or disconformably overlain by a sedimentary assemblage ranging from feldspathic sandstone, quartz arenite/quartzite, and conglomerate at the base, to dolomite, dolomitic silt-/sandstone, and ferruginous sandstone at the top, constituting the Quilalar Formation (Derrick & others, 1980). Its facies is very similar to that of the underlying Lochness Formation and the unconformably overlying Surprise Creek Formation and, for the finer-grained part, also reminiscent of the Bortala Formation in the Paroo Range, all sharing shallow-water to emersive features such

as desiccation cracks, small-scale heterolithic (flaser/linsen) bedding, stromatolites, and ferruginous sandstone. It is thought to have been deposited during the thermal sag phase of cover sequence 2 shortly before 1740 Ma (Jackson & others, 1990).

Because of its absence in the Paroo Range no further attention is paid to this formation.

The Myally Shelf in the Paroo Range

Extrusion of the Pickwick Metabasalt (upper ECV) was succeeded by sedimentation under coastal onlap conditions of the Alsace Quartzite (Trangressive Systems Tract [TST] + Highstand Systems Tract [HST], compare Fig. 5; sequence stratigraphic notation after Vail [1987] and Von Wagoner & others [1987]). Subsequent offlap (upper HST) of lagoonal and fan delta sediments of the Bortala Formation coincided with abrupt influx of pebbly sandstone over a locally deeply eroded surface (Lowstand Systems Tract [LST] over Type-1 Sequence Boundary [SB1]). Renewed retrogradation resulted in a TST of coastal sandstone deposition and culminated (maximum flooding, mfs) in a subtidal shelf facies of the middle Whitworth Quartzite. The subsequent HST is truncated by a major unconformity, the Mount Isa Group Unconformity, which in the Paroo Range is the megasequence boundary between cover sequences 2 and 3, and which coincides with the SB1 at the base of the Mount Isa Group.

Wilson & others (1977) stressed the blanket geometry of the Myally Subgroup, and interpreted the sedimentary environment as a shallow shelf in an epeiric sea bounded by a relatively stable block to the east; this placed the Lochness Formation in a coastline position. To the west they postulated a tectonic foreland of increasing importance as a source area. On a regional scale this shelf platform appears broadly triangular, widening to the north. Derrick (1982) referred large thickness variations of the Myally Subgroup to a block-faulted basement with synsedimentary east-west cross-faulting, transverse to the LRFT.

Facies, scale of structures, and orthogonal relations between wave ripples and subaqueous dunes and bars, such as found in the Whitworth Quartzite, resemble the configuration in the Late Precambrian shelf deposits of Finnmark, Norway (Johnson, 1977; Levell, 1980), where the depositional conditions have been interpreted as consisting of an intricate mixture of storm and tidal effects.

Cover sequence 3: Lower Mount Isa Group

The three oldest formations of cover sequence 3 are (Fig. 2): the Carters Bore Rhyolite, consisting of felsic volcanics dated by Page (1978) at 1678 Ma; hematitic sandstone and conglomerate of the Bigie Formation; and the Fiery Creek Volcanics which include felsic lava, such as rhyolite and trachyte, together with minor tuff and conglomerate. The latter two formations are primarily exposed in the far north of the LRFT, and are correlated with the Carters Bore Rhyolite of the central LRFT. The Fiery Creek Volcanics overlie the Bigie Formation conformably. This volcanic suite represents the rift phase of cover sequence 3. None of the formations are exposed in the Paroo Range.

Surprise Creek Formation (Pr)

The sequential pattern of the Surprise Creek Formation in the Paroo Range, its internal facies distribution, geometry, and relationship to adjacent stratigraphic units are described in the section below on 'The Lower Mount Isa Group and syndepositional D^{P}_{1b} deformation'.

The Surprise Creek Formation has been defined and described on a regional scale by Derrick & others (1980). Like the Quilalar Formation, which it succeeds, the Surprise Creek Formation shows a wide range of facies grading upwards from channel-fill framework conglomerate and sandstone into thin-bedded to laminated finer-grained sandstone, siltstone, and shale and, in the northern part of the LRFT, ferruginous sandstone and dolomitic siltstone. Such facies have also been encountered in the Paroo Range, though not restricted to the upper part of the formation. In the conglomerate, arenite clasts prevail with some red jasper and scarce volcanic and plutonic clasts. Unimodal current distributions in these channel-fill units (Wilson & others, 1977) indicate sediment transport to the north, northeast, and east. The lower part of the Surprise Creek Formation has been interpreted by Derrick & others (1980) as a braided stream and alluvial fan deposit, the upper part as shallow-marine.

Regionally, the Surprise Creek Formation thins towards the western margin of the LRFT against the Mount Gordon Arch. Maximum thickness is 3000 m in the Lake Julius area.

Observed interfingering relations lead us to include the Surprise Creek Formation of the Paroo Range in the Lower Mount Isa Group as part of one and the same fan deltaic and littoral deposystem.

Warrina Park Quartzite (Piw)

According to the original description of Derrick & others (1976b), the Warrina Park Quartzite is composed of white thin-bedded cross-stratified and locally ripple-marked fine-grained quartzite. Well-rounded conglomerate, well to poorly sorted, is common near the base of what has been formerly mapped as Warrina Park Quartzite (Prospector 1:100 000 Sheet area). In the Paroo Range these coarse-grained relatively poorly sorted sediments are mapped as channel-fill conglomerate of the Surprise Creek Formation. The remainder of the conglomerate, concentrated at the base of the Warrina Park Quartzite proper, is much better sorted and rounded as a result of reworking of pre-existing conglomerate and of already sorted sandstone of underlying cycles. The majority of the rock is very mature quartz arenite to orthoquartzite (Wilson & others, 1977). A detailed account of the stratigraphy and sedimentation of the Warrina Park Quartzite is given in the section below on 'The Lower Mount Isa Group and syndepositional D^{P}_{1b} deformation'.

Moondarra Siltstone (Pim) and Breakaway Shale (Pib)

The younger formations of the Lower Mount Isa Group in the Paroo Range are finer-grained and consist of alternating sequences of variably dolomitic or pyritic siltstone and shale. The Moondarra Siltstone is a thin-bedded to laminated, in places dolomitic, siltstone and laminated shale. The Breakaway Shale is a grey massive shale with pronounced cleavage, exposed in the Horse's Head Syncline and south of the North Stone Axe Fault.

In the southeast of the Paroo Range, the Moondarra Siltstone (Pim), like the Surprise Creek Formation, interdigitates with coastal sheet sandstone of the Warrina Park Quartzite (Piw_2 and Piw_3; grid references 456353 and 451314), whereas some 20 km westwards it represents the distal facies of the Hero Fan in the Lower Mount Isa Group (Nijman & others, this volume). With an overall eastward dispersion of coarse clastics in the entire area, such as discussed below in the section on 'Depositional model of the Lower Mount Isa Group Deposystem', this implies an inshore position for the Moondarra Siltstone. South of Lake Moondarra (grid reference 504223), Moondarra Siltstone facies forms the shaly parts of the Surprise Creek Formation.

This fine-grained facies also dominates the succeeding formations of the Mount Isa Group in the LRFT. Pseudomorphs of gypsum and anhydrite (McClay & Carlile, 1978), with halite casts (grid reference 466311), stromatolites, flat-pebble conglomerate, and fine-grained cross-bedded channel deposits with bimodal palaeocurrent patterns (Neudert & Russell, 1981) suggest intermittent hypersaline and emergent conditions in an intertidal-supratidal sea or ephemeral lake.

Intrusive rocks

Numerous mafic dykes and sills together with two major granitic batholiths, all of Proterozoic age, intruded the rocks of the LRFT.

Granites

Two batholiths, the Big Toby Granite and the Sybella Batholith, respectively crop out in the south and west of the LRFT (Fig. 1). The Sybella Batholith is dated at 1670 Ma , and the Big Toby Granite at 1800 Ma (Page, 1981a; Blake & others, 1990). None of these granitic plutons is exposed in the area mapped. The Sybella intrusion began just before deposition of the Mount Isa Group (Blake, 1987). According to our thermo-luminescence analysis on quartz provenance, however, detrital quartz with distinct TL characteristics of both the Sybella and Big Toby Granites already appear in the Alsace Quartzite, which should imply their surface exposure at that time (Rijswijk & Schalkwijk, 1988).

Mafic intrusions

Swarms of roughly northerly-trending (meta)dolerite dykes transect the LRFT. They are tholeiitic in composition, and geochemical analysis indicates either quartz- or olivine-normative and iron-enriched varieties (Ellis & Wyborn, 1984). Sills of a similar composition occur mainly in the Myally Subgroup. Most of the mafic intrusives are thought to have been derived from the same sources as the extensive basalt flows of the LRFT, such as the ECV, and at least two generations of these dykes are known (Ellis & Wyborn, 1984). The majority of the metadolerite dykes within the LRFT appear to intrude rocks younger than 1700 Ma (Blake, 1987). A few much younger doleritic dykes cut all regional structures and are unmetamorphosed. The youngest metamorphic event at ≈1480 Ma (Page, 1981b) sets a maximum age to these latter dykes. One dyke, the Lakeview Dolerite near Mary Kathleen, is dated at 1116 ± 12 Ma (Rb-Sr; Page, 1983). In the Paroo Range we distinguish three times of dolerite intrusion:

- (1) Dolerite (dl_1) intruded into the Myally Subgroup before the Lower Mount Isa Group was deposited (e.g., at grid reference 505442);
- (2) Dolerite (dl_2) intruded along and

subsequently sheared by the D^{P}_{2} thrust system (grid reference 456420);

- (3) Dolerite (dl) of younger age intruded along or cutting across D^{P}_{5} faults (grid reference 526447).

Deformation history of the Leichhardt River Fault Trough: a review of the problems

Pre-cover sequence 3 extension

An important issue in the structural evolution of the Mount Isa Inlier is whether any early deformation affected the older sediments such as cover sequence 2 of the LRFT before and during deposition of cover sequence 3.

Wilson & others (1977, 1979) noted the large variations (<90°) in the angle of unconformity between cover sequences 2 and 3 as evidence of an early phase of open folding.

Passchier (1986a, 1986b) and Passchier & Williams (1989) presented conclusive evidence for early deformation (pre-cover sequence 3) in the central part of the Mount Isa Inlier, outside the LRFT. This phase is characterised by low-angle brittle faulting at low-grade conditions (Passchier, 1986a), and formed early fault zones with narrow imbricate fault slices and listric faults (Passchier, 1986b). The detachment geometry of the imbricate slices (Passchier, 1986b) favour a tensional brittle regime indicating an important phase of basin-forming crustal or lithospheric extension (Passchier & Williams, 1989). Data of Pearson (1989), Stewart (1989, this volume b), Loosveld (1989), and Holcombe & others (this volume) all refer to a widespread tensional regime at about 1740 Ma, more or less coeval with the formation of the Mount Isa Group Unconformity.

East-west growth faults

Smith (1969) interpreted a large number of east-striking faults as synsedimentary, largely because of marked contrasts in thickness and character of the same stratigraphic units on either side of some faults, and because of progressive decrease in throw into younger stratigraphic horizons. He and Dunnet (1976b) suggested that normal faulting must have affected sedimentation patterns before as well as during deposition of the Lower Mount Isa Group.

Derrick (1982) also presented several examples of 'possible growth faulting' in the LRFT, and considered that they formed by basement block faulting during deposition of the Myally Subgroup and younger units. In his opinion a period of particularly intensive growth faulting occurred in the Lawn Hill Platform and LRFT during deposition of, respectively, the McNamara and Mount Isa Groups.

Dunnet (1976b) considered these faults to have developed from an early synsedimentary genesis into pre-main phase listric normal faults, called spoon faults, curving in depth to a decollement horizon. Although related to the same fault system and the same timing, his model of north-south extension and rotational domino-faulting is the complete opposite of Bell's model with early north-south compression (see next section).

Lister & others (1986 and in BMR, 1986) condensed these concepts into a structural interpretation, wherein north-striking compressional folds, transverse strike-slip, and east-striking extensional normal faults result from the same east-west compressional stress field and are therefore closely related.

Pre-main-phase thrusting

Controversial is the nature of the characteristic east to southeast-trending arcuate fault structures within the LRFT, first described by Carter & others (1961). They separate major north-tilted fault blocks, and cause southward repetition of the Haslingden-Mount Isa Group sequence. Along the western side of the LRFT they merge with the Mount Isa-Mount Gordon Fault Zone, whereas at the eastern boundary of the LRFT relationships are less clear.

Bell (1983) explained the fault blocks and fold pattern of the LRFT as a folded D_1 thrust duplex. In his interpretation, the east-west faults, now steeply north-dipping, formed as south-verging thrusts separating as many horses. Subsequent compression (D_2 of Bell, 1983) at right angles to the thrust direction folded the duplex into north-trending folds, which overprinted the east-west folds. This concept must be disputed, since many of the east-west faults intersect main phase folds and are themselves folded at a later stage.

In the Kalkadoon-Leichhardt Belt, Loosveld & Schreurs (1987) also argued in favour of pre-D_2 thrusting, not only with southward, but also with west to north-westward translation. Stewart (1989), however, related the klippen structures of these authors to early extension.

The existence of pre-D_2 thrusting was also suggested by Etheridge & others (in BMR, 1985) and by Lochem & others (1988), but there are major discrepancies in timing,

vergence, and fault expression between these and Bell's models.

Main-phase folding

Regional folding consists of north-trending open to tight upright folds with variable plunge, widely recognised as the main phase of deformation over the entire Mount Isa Inlier (D_2 of Blake, 1987). Axial plane foliation is common in pelites and volcanic rocks, but less so in quartzite. In the Lake Moondarra area, south of the Paroo Range, north-northwest (342°)-oriented folds (D_3 of Winsor, 1983, 1986) were found superposed on the D_2 folds, with a weak axial plane foliation crenulating S_2 (compare Stewart's D^H_3, this volume a). Early folds (D_1, Bell, 1983) with axes trending roughly west were found to be overprinted by the north-south folds.

Post-main phase faults

Late conjugate post-metamorphic northwest-striking sinistral, and northeast-striking dextral faults are common in the Mount Isa Inlier (Blake, 1987). They indicate continued east-west shortening. Displacements of the order of tens of kilometres are measured in the Eastern Fold Belt.

Block-bounding master faults of the LRFT

The eastern Gorge Creek-Quilalar Fault Zone (Fig. 1) ranges in width from about 3 to 8 km (Glikson & others, 1976). This zone is characterised by a varying number of northerly and north-easterly-striking faults and by strongly sheared sediments. Considerable dextral strike-slip combined with west-block down faulting juxtaposed the Kalkadoon-Leichhardt basement rocks with the LRFT sedimentary sequence.

Along the west side of the LRFT, the Mount Isa-Mount Gordon Fault Zone has accommodated large dextral strike-slip and vertical movements (Glikson & others, 1976; compare Nijman & others, this volume).

The present-day expression of these master faults is one of late fault movement (post-D_3); nevertheless their history has been long-lasting and their reactivation the rule rather than the exception (Blake & others, 1990).

Summary

To date, at least five deformation phases have been distinguished in the LRFT, which produced in chronological order:

- 1. Pre-D_1 east-striking growth faults,
- 2. D_1 thrusts,
- 3. D_2 compressional north-oriented folds and penetrative cleavage,
- 4. Local D_3 north-northwest-oriented folds,
- 5. Late conjugate strike-slip faults.

Of these, only phases 3 and 5 have been firmly established; the role of the east-west fault systems is unclear since they are variously associated with phases 1 and 2, and opinions about the timing, geometry, and character of the low-angle thrusting preceding D_1 are equivocal. The Paroo Range solved several of these questions.

In this paper the main phase of deformation, instead of D_2 , is denoted by D^P_3, to allow the introduction of early synsedimentary deformation in a scheme of five deformation events: $D^P_{1\text{-}5}$.

Correspondingly, fold axes and foliations have been denoted $B^P_{1\text{-}5}$ and $S^P_{1\text{-}5}$, respectively.

The next section deals with the younger deformations, $D^P_{3\text{-}5}$, directly evident from map and cross-sections (see Nijman, 1991). Understanding of the early, partly synsedimentary phases, $D^P_{1\text{-}2}$, depends on restoration of cross-sections by elimination of the younger deformation, and these older events are therefore discussed subsequently in the sections on 'Pre-main phase thrusting, D^P_2' and 'D^P_1 deformation and coarse clastic deposystems'. In the latter section, structural and sedimentary data are fully integrated.

Main phase and post–main phase deformation in the Paroo Range

Main-phase deformation: D^P_3

Fold style and axial planar foliation, S^P_3

D^P_3 is primarily expressed by north-trending upright horizontal to plunging folds at all scales up to hundreds of metres wavelength (cross-section C-E in Nijman, 1991). The Campsite Anticline is a major fold with a half wavelength of at least 4 km. Asymmetric parasitic folds have a westward-increasing amplitude and density. The folds have round to angular hinges and in the Warrina Park Quartzite are of the modified concentric type 1C (Ramsay, 1967). Disharmonic folding is common in heterolithic facies (Fig. 7).

The plunge of the D^P_3 fold axes increases from approximately horizontal in the south to over 40° near the



Fig. 7. D^P3 parasitic folding in heterolithic facies of Suprise Creek Formation, where overlain by quartz arenite of Warrina Park Quartzite. S^P3 axial planar foliation is visible behind 30 cm-hammer. Grid reference 442378. View to north.

Horse's Head Syncline (cross-section F-H, I-K; see Nijman, 1991). This axial curvature is thought to be related to post-main phase D^P4 normal faulting (see section below on 'Post-main phase deformation D^P4').

Axial planar foliation, S^P3, strengthens from barely perceptible in the east through spaced cleavage into pervasive foliation in the Campsite Anticline and Horse's Head Syncline in the west (Fig. 8). Stereograms in Figure 8 show that the foliation is vertical and strikes 350° for domains A-D, spread out over much of the area, and corresponds with the average fold axis, B^P3. In fine-grained rocks in the Eastern Creek Volcanics, Bortala Formation, and Moondarra Siltstone, the foliation is a slaty to closely spaced cleavage, whereas in coarser-grained rocks the spacing of the cleavage increases in proportion to grain size (e.g., 5 mm in the Alsace Quartzite). In basalt, pencil cleavage is common.

No evidence for refolding, such as crenulation of the D^P3 axial plane cleavage by a north-northwest-striking cleavage, has been found, nor a bimodal distribution of D^P3 fold axes observed. It is therefore assumed that the 342°-oriented folds observed by Winsor (1983; compare Bell, 1983; Bell & others, 1988; Stewart, this volume a) are only local and caused by variation in the regional east-west compressive stress field (compare Nijman & others, this volume).

Strain analysis

Deformed amygdales in the Eastern Creek basalt, decementation spots in Warrina Park Quartzite, stretched pebbles of the Surprise Creek Formation, and conjugate tension gashes all indicate a strain ellipsoid with X-axis horizontal, Y-axis parallel to B^P3, and Z-axis in the vertical plane; hence it is deduced that the bulk of the strain is related to the main phase, D^P3.

Strain analysis on deformed quartz + carbonate-filled basalt amygdales (grid reference 434376) yields k and d values of the strain ellipsoid of respectively 70.3 and 1.2. Hence the finite strain ellipsoid is prolate, and in a Flinn-plot located in the field of apparent uniaxial constriction. From nearby ptygmatic and buckle folds of competent rock between less competent rock, east-west shortening (e_3) is estimated to be 25-30%. This implies a volume reduction of 2-20% in addition to the stretching. These values are of course valid only for the measured specimen. Field observation, however, indicates they give at least an indication of the finite strain ellipsoid of the western part of the study area. Our data, however, are insufficient to consistently account for bulk strain in the restored sections of Figures 11 and 16. Passchier (1986a) reported a horizontal shortening of 50-80% in the Duchess Belt south of Mount Isa, and Loosveld & Schreurs (1987) estimated the strain value at 50% in the Eastern Fold Belt.

Post-main phase deformation D^P4

D^P4 listric normal faults

In cross-section F-H (see Nijman, 1991) more than ten east-striking faults offset D^P3 structures. Many of their surface traces are convex to the north, with an angle of curvature of up to 120° and lengths of several kilometres. The two largest, the Conglomerate Creek Fault and the North Stone Axe Fault, respectively delimit the Paroo

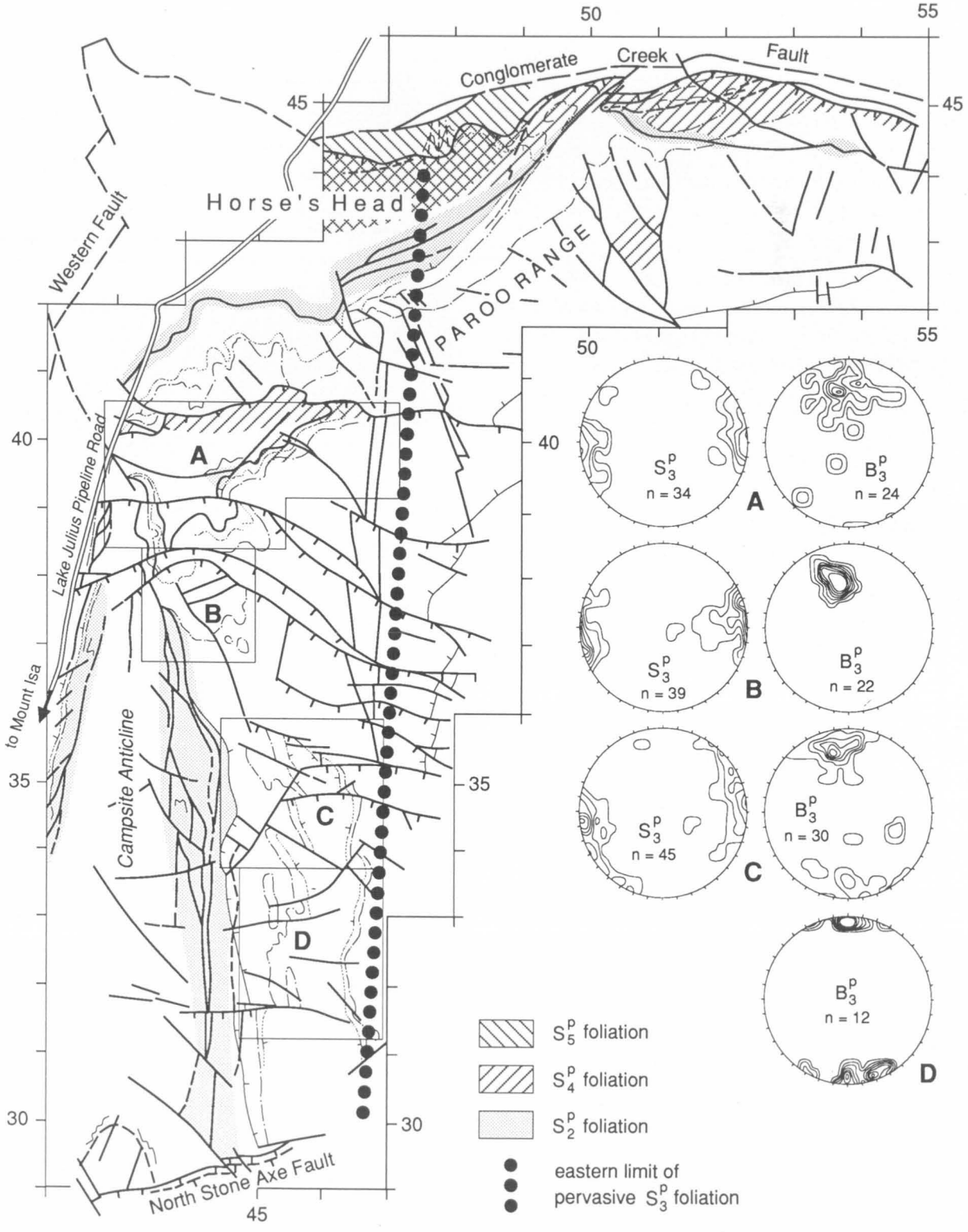


Fig. 8. Distribution of observed $S^p_{2,3,4}$ and $_5$ foliations. Pervasive axial planar S^p_3 foliation (slaty cleavage in shale, spaced fracture cleavage in sandstone and conglomerate) west of dotted line. For domains A-D inCampsite Anticline, S^p_3 and fold axes, B^p_3, closely correspond to a vertical axial plane striking circa 350° (equal-area projection with contours at 1, 4, 8, 12, 16, and 20% per 1% area).

Range Area to the north and south. They are cut by later strike-slip faults (e.g., grid references 446294, 505454, and 514455) or affected by D^P_5 folds (grid reference 481447).

Except along the major block-bounding faults, the fault zones are no wider than 3 m and are normally filled with white quartz, in places cementing rafts of country rock; many tensional quartz veins are present, and provide data on strain during brecciation. Some larger faults of this type enclose rafts of undeformed bedded sandstone of the Warrina Park Quartzite (grid reference 442403) up to several metres in length. Fault dips at the surface usually vary between 70°S to vertical, but lower values of 15° to 40° are reported from the Paroo Range by Dunnet (1976b: p. 336). South block downthrow ranges around hundreds of metres.

These data indicate that the faults are normal, and were produced by north-south tensional stress.

D^P_4 folds

In cross-section F-H (see Nijman, 1991) the fault blocks systematically increase in dip northward from horizontal at a culmination at grid reference 454326 (altitude 487 m) to over 40° near the Horse's Head Syncline, quite characteristic of a large roll-over anticlinal structure. This bending is also responsible for the curvature of the B^P_3 fold axes.

Tighter D^P_4 folds are found only along D^P_4 faults with considerable downthrow, mostly as hanging wall synclines (grid reference 442403), but in places as footwall anticlines (grid reference 485404; cross-section I-K in Nijman, 1991). The axial plane is approximately vertical. The half wave length of the folds ranges up to hundreds of metres, apparently proportional to the size and the amount of throw of the controlling fault. Spacing and amplitude of the folds along the Conglomerate Creek Fault, e.g., in the Horse's Head Syncline, are an order of magnitude larger than those along the secondary faults.

The D^P_4 fold axes are parallel to the host faults near their northernmost bending point (grid reference 442403), but oblique to their southeasterly curvature (grid reference 472404) and to their opposite western end at the Western Fault (Nijman & others, this volume). The synclines parallel or oblique to the D^P_4 faults reflect the spoon shape of the faults. It causes dip-slip drag in the heads, and oblique slip in their lateral ramps (Fig. 9A). The plunge of the fold axes varies in the Paroo Range between horizontal and 50° west.

S^P_4 cleavage is of two types (Figs. 8, 9A). Firstly, it is

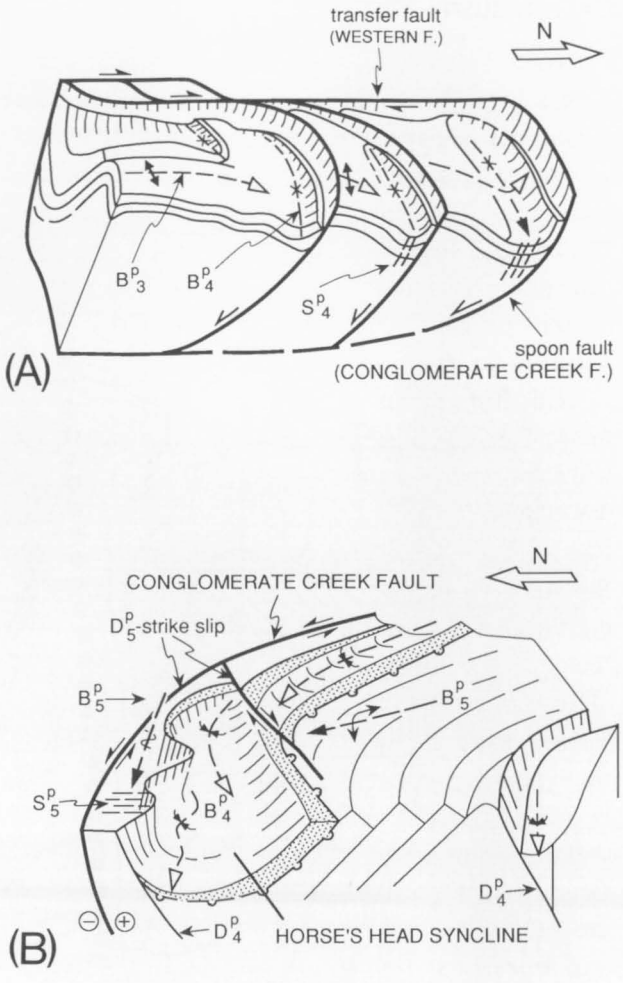


Fig. 9. Models of overprinting structures: (A) D^P_4 spoon faults and associated structures overprinting D^P_3 folds. (B) D^P_5 faults and folds overprinting D^P_4 faults and folds, as exposed in Horse's Head Syncline and adjacent central and eastern Paroo Range.

associated with the narrowest synclines, where it has a spacing of several millimetres to centimetres and crenulates S^P_3 cleavage, for instance at grid references 473441 and 447405. In the Breakaway Shale immediately south of the Conglomerate Creek Fault (grid reference 479442), S^P_4 is overprinted by S^P_5 cleavage. Secondly, where flexural slip within the tilted blocks is evident from bedding-parallel quartz-veins with fibre growth at high angles to the bedding, and from dip-slip S_0-parallel slickensides, S^P_4 cleavage dips at higher angles and tension gashes at lower angles than the bedding (grid references 454398 and 507428). This combination of features might be expected in Bell's (1983) south-verging D_1 thrust deformation, but equally well fits a model of synthetic rotation in the more strongly tilted normal fault blocks during D^P_4.

Discussion

The combination of south-block-down movement along steep southerly dipping faults with roll-over and drag folding can be explained only by normal faulting. The concave to the south curvature of the faults in map view cannot have been caused by the main-phase east-west shortening as supposed by Dunnet (1976b), because the latter precedes the faulting; only locally is later east-west shortening visible in deformation of the fault planes by steeply plunging D^P_5 folds (Fig. 9B).

If in a listric normal fault fan, new riders develop in the footwall (Wernicke & Burchfiel, 1982; Gibbs, 1984) they will show progressively increasing tilt in the direction of downthrow. If on the other hand, riders develop in the hanging wall, such as in the African rifts described by Bosworth (1985), the dip of the fault blocks decreases in the direction of downthrow. This is the case in the Paroo Range. According to Chapman & Williams (1984), displacement on the basal decollement of such a system equals the summation of the displacements of all faults of the system. Angular shear strain, which induces larger extension at the basal decollement than at the earth's surface, is necessary to conserve area in the cross-section. Oblique slip will be important on the tear faults bounding the domains, and, depending on the shape of the transfer, transpressional or transtensional effects will be produced (compare 'loaf tectonics', Gibbs, 1987). In the Paroo Range, the Conglomerate Creek Fault serves as the floor fault, and the Western Fault (compare Nijman & others, this volume) as a bounding transfer fault.

Tight drag synclines (Hamblin, 1965; Williams & Vann, 1987), increase in size proportional to the amount of downthrow, and are well developed along the three northernmost D^P_4 faults. The Conglomerate Creek Fault, by far the largest of these faults, is flanked by the correspondingly large Horse's Head Syncline. Although depth extrapolation of the curvature in cross-section is tentative, the decollement level in our reconstruction could very well be the top of the basement below the Haslingden Group at about 8 km depth below the Mount Isa Group Unconformity, measured where the latter is in subhorizontal position (Fig. 10). In fact, extension at the level of the unconformity over the cross-section F-H is practically nil, whereas that over a north-south cross-section of the LRFT like the one of Figure 10, would amount to 10%. Hence most of the movement has been accommodated along the floor faults of the linked fault systems, such as the Conglomerate Creek, Paroo, Crystal Creek, and Investigator Faults, by summation of the throw along the subvertical surface segments of the spoon faults. The exceptional tightness of the drag synclines, and the associated axial planar cleavage, may be due to space problems where the floor faults were generated at sites of previously formed planar basement faults, as suggested in Figure 10. Such early fault activity is also recorded in unconformities and facies patterns (compare sections below on 'D^P_{1a} block tilt' and 'Geometry of the Lower Mount Isa Group, D^P_{1b} drape folds and progressive unconformities').

Our model resembles that of Dunnet's (1976b) spoon faults, but the latter is different in the increase of tilt away from the outcrop of the footwall, and in the timing, which is essentially pre-east-west shortening (Dunnet, 1976b, p.344). In Dunnet's model, the boundary faults of the LRFT also delimit the listric fault system. Glikson & others (1976) provided a deformation table with the same dating of the east-west faults as we present here (compare BMR, 1986). These faults have mainly normal movements and accommodate north-south extension. Bell's (1983) model of a giant thrust duplex predating the east-west shortening is in conflict with our data and interpretation. This model does not account for the fact that the faults are at high angles to bedding and dip steeply southwards. Winsor (1984) found a weak north-striking fracture cleavage in the fault gouge of the east-west faults, which he interpreted to be associated with the main phase of deformation. This could, however, equally well be the result of the D^P_5 event.

Post-main phase deformation D^P_5: conjugate strike-slip faulting and associated steeply plunging folds

On the 1:100 000 geological maps of the Mount Isa Inlier, conjugate dextral northeast-striking and sinistral northwest-striking strike-slip faults are shown. Only a few of these subvertical D^P_5 faults are found in the study area (see Nijman, 1991) where they intersect D^P_4 faults or reactivate old faults, such as the D^P_2 fault at grid reference 500450. The fault zones are several metres wide, and contain abundant white quartz partly in extension veins.

Within the Conglomerate Creek Fault zone, D^P_5 strike-slip has been accommodated along a fault trace just north of the previous D^P_4 fault position (Fig. 9b). Sinistral sense of movement is indicated by vertically S-folded en-echelon tension gashes (grid reference 537453). The older D^P_4 fault plane is shortened by steeply plunging D^P_5 folds. At grid reference 481446, this has formed upright synformal anticlines with north-striking axial planes. An

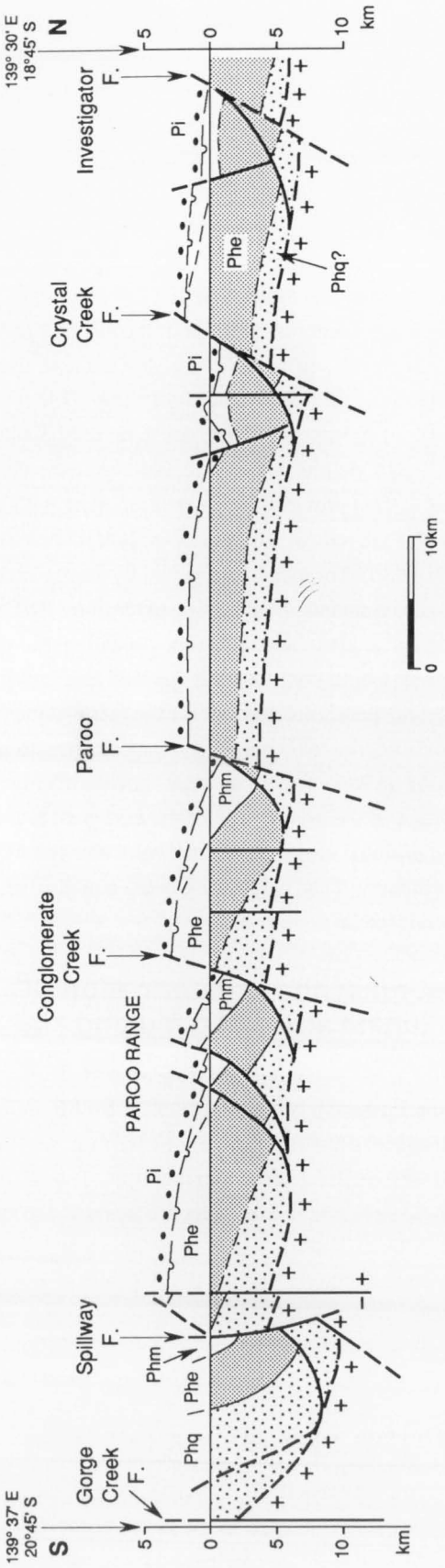


Fig. 10. Tentative north-south cross-section of $D^{P}4$ spoonfault structure over decollement on top of Barramundi basement (+ +) at an estimated 8 km below Mount Isa Group unconformity in Paroo Range. Our data (cross-section F-K; Nijman, 1991) fitted into map data of Blake (1987). Basement faults are thought responsible for recurrent movement along the major listric faults, such as Conglomerate Creek Fault, during several episodes of deformation. Extension measured at Mount Isa Group Unconformity between Investigator and Spillway Faults amounts to 10.2%.

$S^{P}5$ axial plane cleavage is subparallel to $S^{P}3$ cleavage. Unless the structural relation with $D^{P}4$ is clear, $D^{P}5$ folding and foliation are difficult to recognise (compare Stewart, this volume, a), but undoubted overprinting of a $D^{P}4$ spoon fault by near-vertical $D^{P}5$ folds has been found at grid reference 458407.

Pre-main phase thrusting, $D^{P}2$

Pre-main phase structures are of two kinds:

- 1. $D^{P}2$ low-angle fault systems: westward-ascending ramps and flats with tiplines in the Moondarra Siltstone;
- 2. $D^{P}1$ fold and fault systems: flower structures and drape folds, hanging below unconformities at the base of and within the Lower Mount Isa Group.

The geometry of these structures is obvious only from restoration of balanced oblique east-west cross-sections perpendicular to the curvature of the $D^{P}3$ fold axes (Figs. 11 and 15). No corrections have been made for bulk strain over the Campsite Anticline.

To show the geometry of the pre-main phase structures, it generally suffices to straighten the top of the Warrina Park Quartzite. As the low-angle thrust systems appear to die out in the lower part of the Moondarra Siltstone, their traces in such a restored cross-section are a reliable picture of their geometry.

The bedding-parallel to low-angle $D^{P}2$ faults described in this section affected all formations up to the Moondarra Siltstone and are themselves deformed by $D^{P}3$ and later folds. The $D^{P}2$ faults formed in two spatially separated systems: one, the Paroo Thrust, obliquely traverses the Paroo Range in the northeast; the other, the Campsite Thrust, is located on both limbs of the Campsite Anticline, east of the Pipeline Road. The geologic map (Nijman, 1991) shows the $D^{P}2$ fault systems in oblique cross-section.

Campsite Thrust

The Campsite Thrust is illustrated in cross-section C-E (see Nijman, 1991) and in Figure 11. Faulting and folding which preceded formation of the D^P_3 Campsite Anticline are evident from secondary folds preserving their west-verging asymmetry over the fold crest (compare grid reference 427399 and 439348 in the east limb respectively with grid reference 433398 and 426369 in the west limb). This negates their formation as parasitic D^P_3 folds.

Duplication of the Lena Quartzite in the east limb of the Campsite Anticline is tectonic; all upper contacts of the quartzite bodies are intensely sheared. Hanging-wall anticlines show 16°– 40° north-plunging meso-scale folds in their steep frontal limbs. Along the trailing edges of the Lena Quartzite and in the shear zones, swarms of sandstone slivers are encased in the Eastern Creek Volcanics, partly consisting of Lena Quartzite, partly of disconnected sandstone lenses from within the ECV (Phc_q, Php_q, Phe_q).

Towards its feather edge the Lena Quartzite is duplicated by the formation of an antiformal stack (* in Fig. 11) the roof thrust of which can be traced to where it finally merges with the Paroo Thrust in the Moondarra Siltstone at grid reference 436382.

The floor thrust of the Campsite system is represented by the low-angle fault below the Lena Quartzite (grid references 432370 and 440304) in the eastern limb of the Campsite Anticline, and in the Cromwell Metabasalt at the level of the Phc_q-sandstone intercalations along the entire western limb. There, a small duplex has been formed in the Lena Quartzite (grid references 429390 and 425380), and a leading imbricate fan (Butler, 1982) in the Warrina Park Quartzite. At its passage into Moondarra Siltstone it tends to flatten (grid reference 426378). Fold axes of associated southwest-plunging, S-asymmetric, 10 m-sized folds in the Warrina Park Quartzite (grid reference 425368) are too steep (70°) to tally with a restored west vergence, but they may have been rotated during D^P_4 strike slip in the west limb of the Campsite Anticline (compare Nijman & others, this volume). Similar S-folds closer to the floor thrust have 23°/034° axes that do yield a more westerly vergence (grid reference 426369).

In the Campsite Thrust, ramps through the Lena and Alsace Quartzites and Surprise Creek Formation are commonly enriched in iron oxide. In the Alsace and Lena Quartzites, the fault rock is very fine-grained and resembles a cohesive fault gouge. In this kind of rock, however, the S^P_3 cleavage is penetrative and obscures D^P_2 microstructures. D^P_2-foliated shear zones have been observed in the Eastern Creek Volcanics.

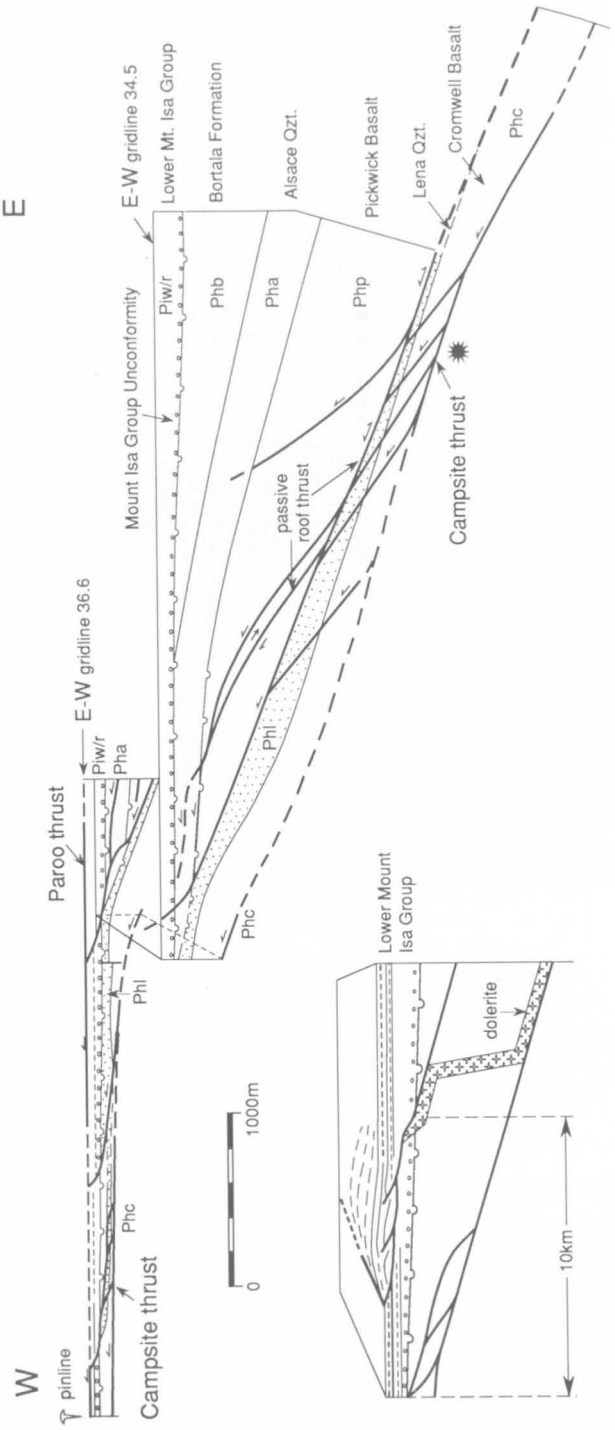


Fig. 11. Restored pre-D^P_2 cross-section through Campsite Anticline showing traces of Campsite Thrust system. During D^P_2, duplex at (*) deformed into an antiformal stack below a passive roof thrust (underthrusting). Subsequent D^P_3 folding resulted in structure shown in cross-section C-E of Nijman (1991), which served as a base to restoration. Restoration reveals a local unconformity at base of Alsace Quartzite (Pha on Phl) caused by early D^P_{1a}-tilt. Further description in text.



Fig. 12 (A) Detail of D^P_2 ramp structure in Paroo Thrust at grid reference 534444. Quartz-filled 330°/90° tension gash in Whitworth Quartzite (above 30 cm-hammer) bends into shear-foliated breccia (at hammer) oriented 357°/61°. Sense of shear indicated by arrow. View to north.

Paroo Thrust

Along the entire length of the Paroo Range (see Nijman, 1991) the Paroo Thrust shows only minor displacement. A maximum angle to bedding of 30^0 is attained in the eastern Paroo Range where the Paroo Thrust ramps through the Myally Subgroup (grid reference 524444) and the Lower Mount Isa Group (grid reference 505449). Westward, the thrust flattens in the Moondarra Siltstone, 50-300 m above the top of the Warrina Park Quartzite. At grid reference 462418 a dl_2 dolerite dyke meets the fault plane and from there forms a sill along the thrust, pinching out to the west.

Farther south, a segment of the Paroo Thrust has been mapped in the Moondarra Siltstone passing over grid reference 452399 and grid reference 406392. Other faults associated with the system are found in the southeast Paroo Range at grid reference 526425, and possibly also in the fault system at Police Creek (grid reference 487414) along which dl_2 dolerite intruded, and which appears to have been reactivated during D^P_5.

The Paroo Thrust is marked by quartz-filled shear veins along its ramp through the Myally Subgroup (Fig. 12A; grid reference 534444). Where the ramp cuts the Mount Isa Group Unconformity (grid reference 517445), a duplex 500 m long has been formed in silicified limestone and heterolithic facies of the Surprise Creek Formation.

The ramp then cuts through the overlying sandstone of the Surprise Creek Formation, where it is strongly ferruginised and contains meso-scale recumbent folds, facing west after tilt corrections (grid reference 506448). Upon reaching the northernmost bending point of the Paroo Range (grid reference 504450) the D^P_2-thrust plane has been deformed not only by the late $40^o/350^o$ plunging D^P_5-fold responsible for this bend, but also by D^P_4 drag folds (grid references 504450 and 497452) along the Conglomerate Creek Fault. The rotated and steepened thrust segment at grid reference 501452 has been subsequently reactivated into a dextral northeast-striking D^P_5 fault, which implies a reversal of offset.

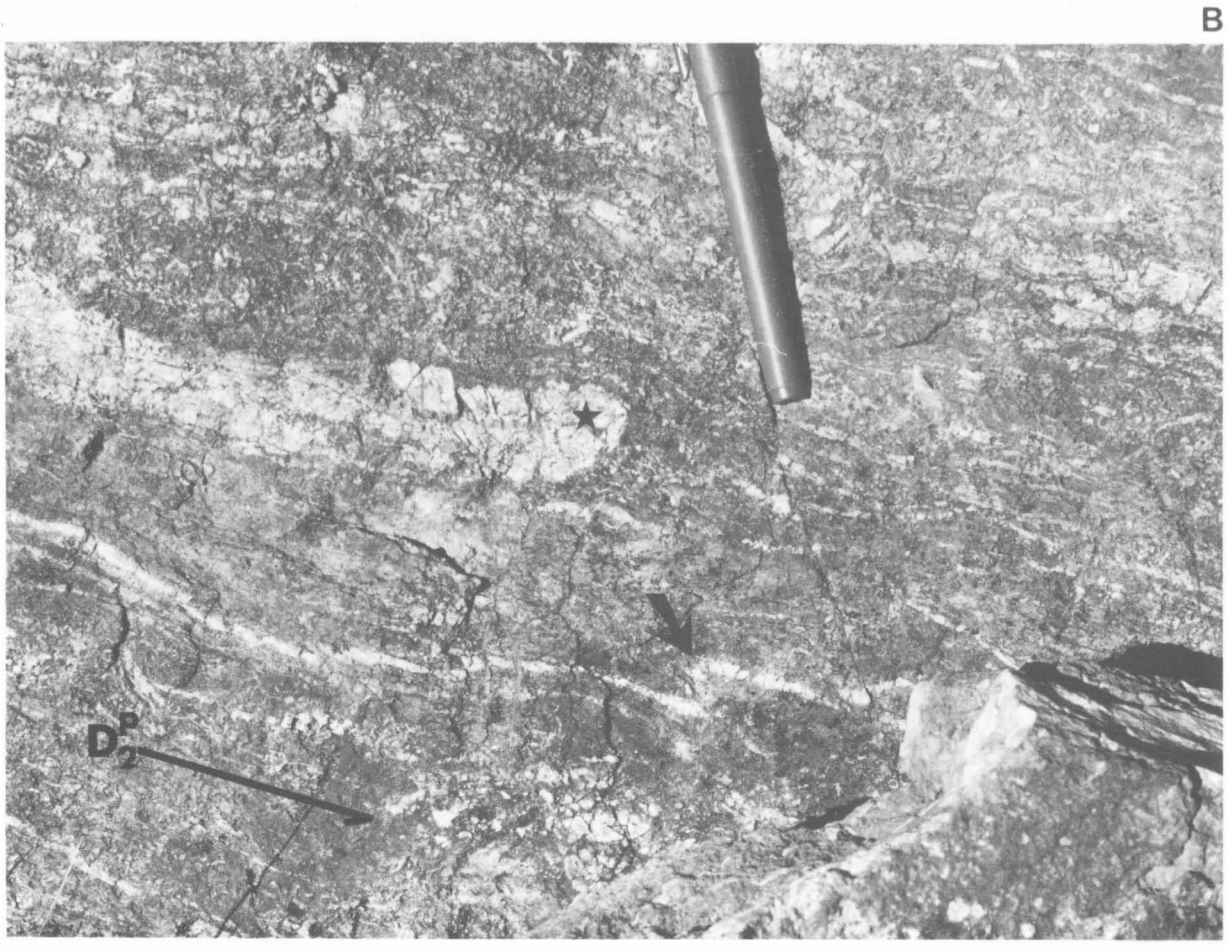


Fig. 12 (B) D^P_2 fault rock in thrust flat in Paroo Thrust in upper part of Warrina Park Quartzite at grid reference 490440, viewed to southeast in overturned position (140°/65°). Predominantly isoclinally (•) to tightly S-folded (arrow) white layers of coarse-grained quartz, separated by cataclastically deformed fine-grained quartzite define shear foliation, which is offset by later microfaults with same direction of shortening (e.g., along 14 cm-pencil orientation). Sense of shear indicated in left lower corner.

For this reason the main thrust is difficult to trace to where it merges at the top of the Warrina Park Quartzite (grid reference 490440) with a 3 m-thick layer of shear-foliated fault rock (Fig. 12B). The latter is located within Warrina Park sandstone and conglomerate below the hanging wall of Moondarra Siltstone. The fault rock is compositionally banded, with 1-10 mm-thick coarse-grained quartz layers separated from each other by 5 to 30 mm-thick cataclastically deformed quartzitic rock with red-brown iron oxide concentrations. Such shear foliation has also been observed elsewhere along D^P_2 contacts, for instance in the Eastern Creek Volcanics (grid reference 422346).

The coarse quartz laminae are asymmetrically folded (Fig. 12B), in places isoclinally in a semi-ductile mode, then brittly kink-folded and disrupted by microfaults causing stair-stepping structures. The brittle structures are west-verging because the reverse microfaults dip eastwards after reconstruction by rotation of the shear foliation to its original low-angle position. Most of the isoclinal folds also show the same vergence. Microscopically, the coarse quartz shows new growth in a previously cataclastically deformed silicate rock, evidently at a sufficiently high temperature to allow ductile deformation, during which recrystallisation took place. Cataclasis of the quartz into subgrains represents the last phase of brittle deformation.

Whatever original thrust translation may have occurred at this site, its effect has been subdued by the above-mentioned reverse dextral D^P_5 offset.

In the Moondarra Siltstone, the Paroo Thrust splays into several blind thrusts accompanied by breccia and strong iron oxide enrichment. Intraformational slump folds (grid reference 486436) suggest some of the faulting

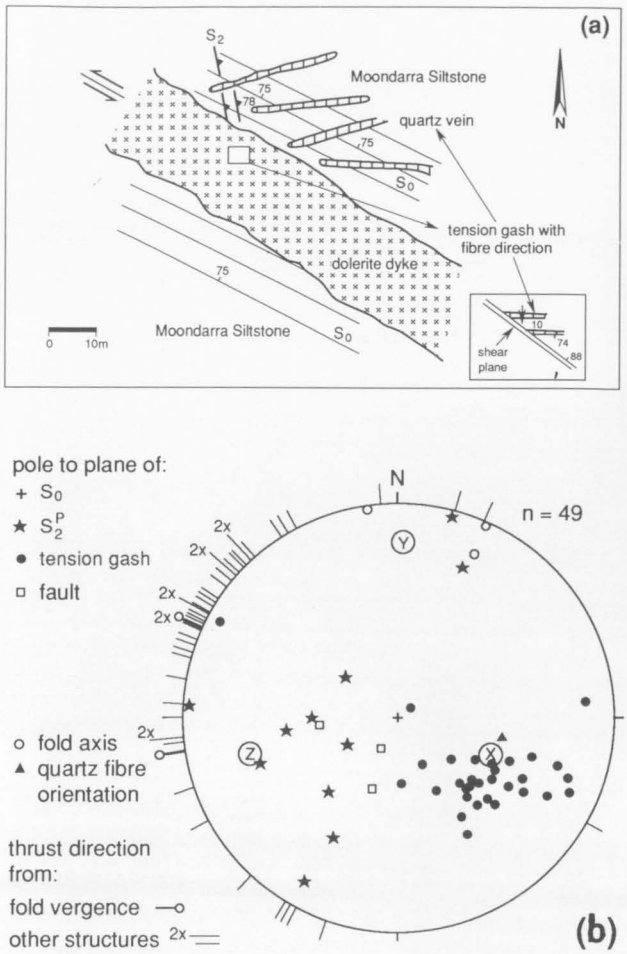


Fig. 13. Dolerite (dl_2) sill intruded along D^P_2 thrust plane: (A) Structural sketch map at grid reference 456420; (B) Stereoplot of structures in (A) after correction for post-D^P_2 rotation. To the latter are added data from nearby locations, positions of the X, Y, and Z axes, and inferred directions of thrust translation along periphery.

took place in unconsolidated Moondarra Siltstone. In thin-section, rotated or folded foliation or lamination in the breccia components is indicative of continued fault action along the same thrust. Dynamic recrystallisation results in a fabric of small angular quartz grains.

Quartz veins, partly as tension gashes, are commonly associated with the faults. They generally range in thickness from 1 to 15 cm, but in places are considerably thicker, and brecciated; iron oxide here fills cracks in vein quartz. The host Moondarra shale and siltstone are also strongly enriched in iron oxide, and resemble gossan.

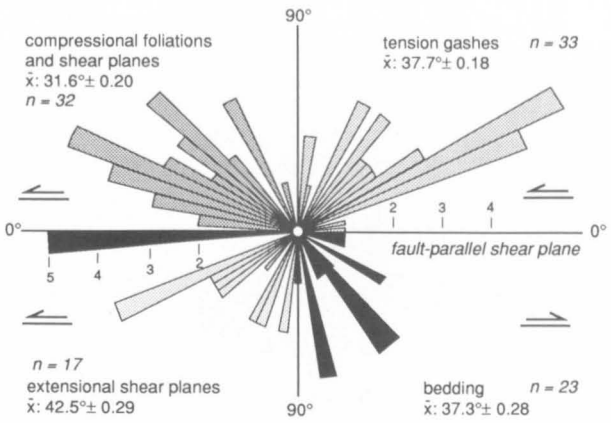
Where the dl_2 dolerite sill follows the thrust plane (Fig. 13: grid reference 456420), the dolerite is itself deformed by the fault, and numerous quartz veins are present within it and in the host rock. The rock is intensely weathered and very rich in iron oxide. Except for flow structures of minerals, such as sericitised plagioclase phenocrysts and occasional offshoots into the hostrock, the dolerite is hardly recognisable as such. Around the offshoots (grid reference 460418), dewatering structures are found in the siltstone host rock, again indicative of soft-sediment deformation during emplacement of the sill. Ankerite and siderite are found in these structures.

The dolerite therefore is thought to have been intruded along a zone of weakness formed in an initial synsedimentary or syndiagenetic D^P_2 thrust stage, while later continued translation was accommodated within and at the contacts of the sill. The conditions necessary for semiductile deformation and quartz recrystallisation may have been generated by hot fluids related to the dolerite ascending along the fault plane.

Displacement analysis

Macro- and meso-scale foliations, shear planes, folds, mesofaults, tension gashes, and fibrous veins within fault zones were used as kinematic indicators. In order to determine the direction of thrust movement, the orientation of bedding and the $D^P_{3,4,5}$ fold axes must be known at the sample locality. Bedding is assumed to have been horizontal during D^P_2. After correction for the effects of $D^P_{3\text{-}5}$, tension gashes and extensional shear planes dip in the direction of hanging-wall translation; compressive foliations (S^P_2) dip in the opposite direction, and ramps and fold axes may be assumed to have formed along a direction normal to the movement of the hanging wall. This implies an error for oblique ramps, and the assumption of subhorizontal bedding may lead to a larger angle between shear foliation and bedding than theoretically expected (Fig. 14A). In the example of Figure 13, the strain (Fig. 13A) corresponds to pure shear deformation induced by west-verging sinistral simple shear along and around the thrust plane (Fig. 13B). A data set for the entire Paroo Range is given in Figure 14, and indicates west to northwest translation (mean: 301°).

Displacement along the Paroo Thrust ranged up to hundreds of metres. Along the Campsite Thrust, displacement at the surface in the western anticlinal limb is near zero, but increases to about 2 km within the antiformal stack of the eastern limb. Restoration shows that the hanging wall behaved passively because of fixation at the tipline, and for that reason the roof thrust must have had a reverse effect, i.e., underthrusting (Fig. 11 and cross-section C-D in Nijman, 1991).



thrust direction	n	mean	σ
tension gashes	27	309.4	0.23
S_2^P compressional foliation	14	271.9	0.61
extensional shear planes	4	311.8	-
fold axes	2	258.0	-
ramps	4	321.0	-
all structures	51	301.4	0.45

Fig. 14. Rose diagram showing angular relations (with means and standard deviations) between fault-parallel shear foliation (horixontal axis) and planar tensional structures (quadrants I and III), compressional foliation (quadrant IV), and bedding (black). Data from Paroo and Campsite Thrusts and from another D^P_2 thrust in the southeasterly area adjacent to Paroo Range, north of Lake Moondarra between north-south grid lines 48 and 49. Table gives values of thrust directions for 51 of the above observations.

D^P_1 deformation and coarse clastic deposystems

Pre-Mount Isa Group deformation and pebbly sandstone occurrence

D^P_{1a} block tilt

East-west cross-sections show eastward tilt of the Haslingden Group, allowing the Mount Isa Group Unconformity to intersect progressively deeper stratigraphic levels towards the west. This continues to beyond the Hero Fault, in palinspastic sections at least 20 km west of the Paroo Range (Nijman & others, this volume), and reflects the existence of the Mount Gordon Arch. The restored section over the Campsite Anticline shows a local unconformity between the Alsace and Lena Quartzites (Fig. 11), suggesting the tilting was already active at the beginning of deposition of the Myally Subgroup.

In north-south cross-sections, the unconformable relationships of the Mount Isa Group close to the Conglomerate Creek Fault Zone indicate the existence of an early pre-Mount Isa Group drag synclinal effect along what must be considered the first recognisable downthrow effect along this lineament (compare Fig. 20).

D^P_{1a} flower structures

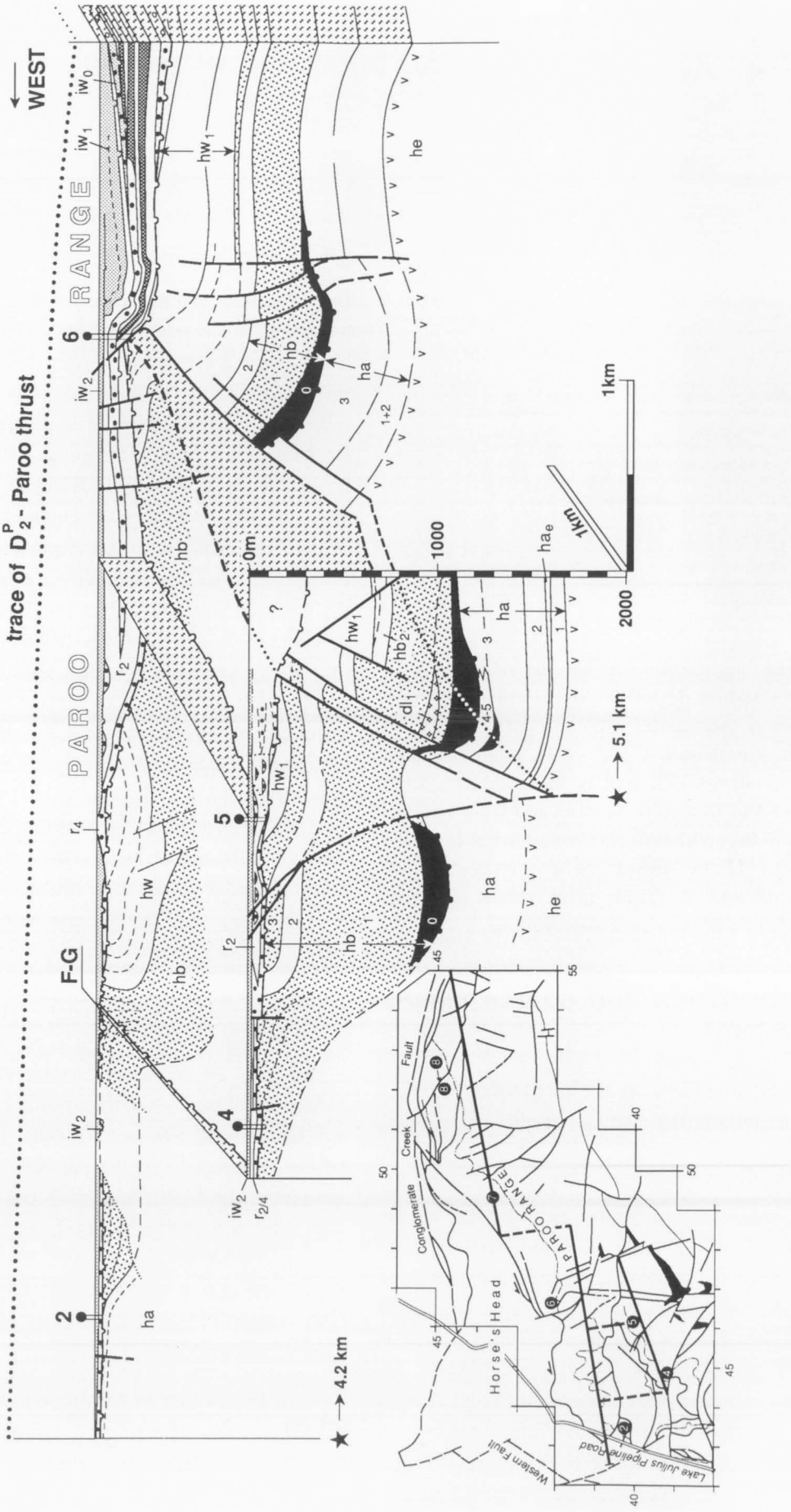
Both D^P_{1a} folds and faults are shown in restored position below the Mount Isa Group Unconformity in Figure 15. The folds are Z-symmetric, looking north, and the restored average orientation of their axes is 05°/003°. They are related to pre-unconformity faults diverging upward from the base of the Myally Subgroup. The two so-formed flower structures (Lowell, 1972; Harding & Lowell, 1979) appear on the map in elongate oblique cross-section due to D^P_4 tilt. The western structure (section locations PR5 and PR6 in Fig. 15) is a positive flower or palmtree structure (Sylvester & Smith, 1976; Harding, 1983, 1985) with rim synclines of the size and shape shown by Sylvester (1988: fig. 25b) for the Oak Ridge Fault, California. The original downwarp on the east side amounts to about 400 m and is larger than on the opposite flank. The eastern flower, just east of section location PR7, is slightly positive and almost symmetrical.

The folds at and just east of section location PR2 (west side of Fig. 19) and the faults at the extreme opposite side probably also belong to flower structures; the westernmost is asymmetric, east-verging, and with drape or forced folding, whereas the easternmost is a more neutral flower structure. The distance between the four flower centers along the Mount Isa Group Unconformity is about 4.5 km, and the flowers tend to become more positive westwards.

Not only do the faults intersect dl_1-dolerite, which intrudes all formations of the Myally Subgroup, but they also host it (grid reference 512440). The same dolerite formed depressions in the palaeorelief of the flower structure at the Mount Isa Group Unconformity, which were filled with clastic sediments of the Surprise Creek Formation (conglomerate channel fills at grid reference 501442 and coarse sandstone at grid reference 510442). Later dolerite (dl_2) intrusions again followed the faults (grid reference 480440).

Pebbly sandstone of the Bortala Formation (Phbo)

Fine-grained heterolithic facies of the lower Bortala Formation (Phb_1; see section above on 'The Myally


WEST
RANGE
PAROO
trace of D_2^P - Paroo thrust
F-G
iw0
iw1
iw2
hw1
hb
ha
he
r2
r4
r2/4
hb2
dl
hae
0m
1000
2000
1km
5.1 km
4.2 km
Horse's Head
Conglomerate Creek
Fault
PAROO RANGE
Western Fault
Lake Julius Pipeline Road

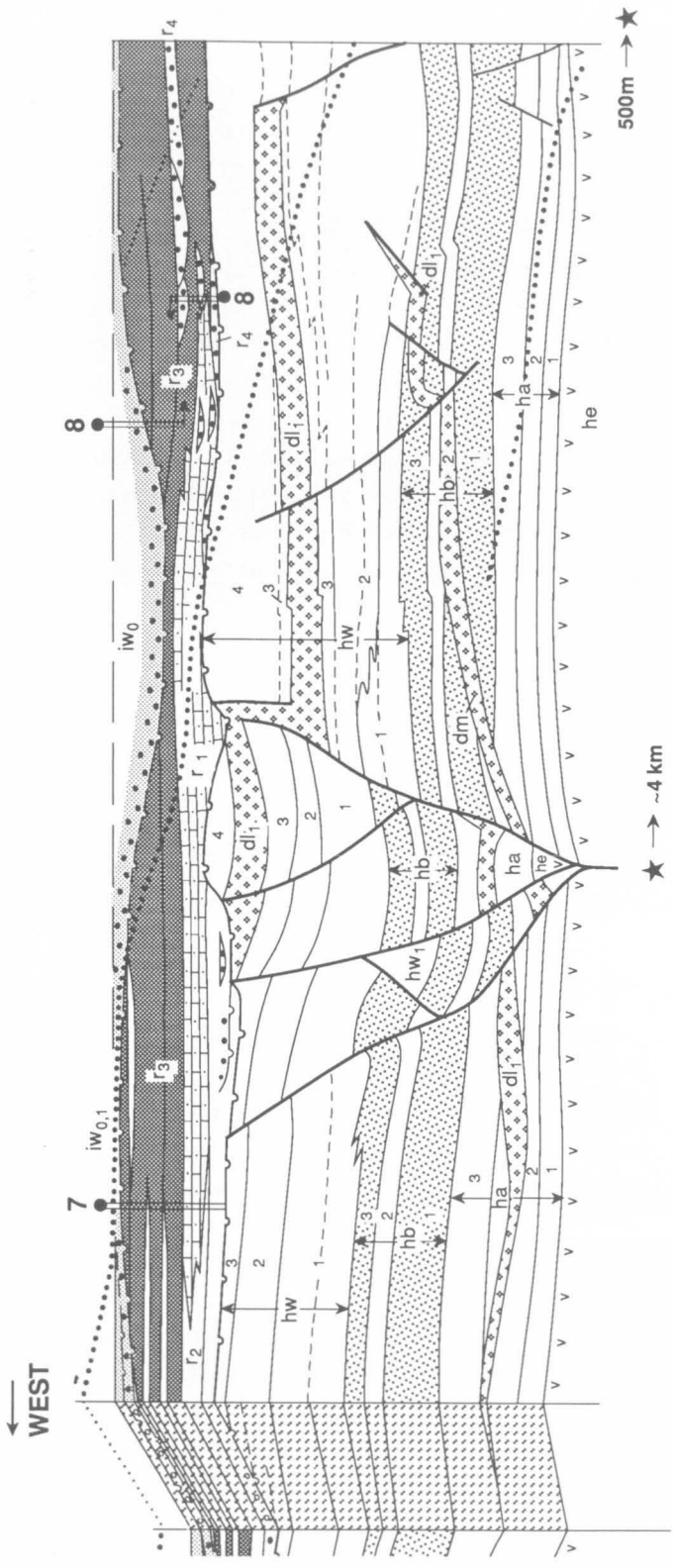


Fig. 15. (facing page and left). Restored oblique strike sections along Paroo Range constructed at right angles to D^P_3 fold axes (see inset figure), showing D^P_{1a} flower structures and drape folds below Mount Isa Group Unconformity and westward-thickening wedge of Lower Mount Isa Group with D^P_{1b} drape folding and internal unconformities, e.g., at location 6.
*** 4.5 km denotes measured distances between observed and estimated positions of cores of D^P_1 flower structures. he – Eastern Creek Volcanics; ha – Alsace Quartzite; hb – Bortala Formation (in black; hb_0 – pebbly sandstone facies); hw – Whitworth Quartzite; r – Surprise Creek Formation; iw – Warrina Park Quartzite; dl_1 – pre-Mount Isa Group dolerite dykes and sills; initial P omitted from stratigraphic letter symbols for clarity. For details of subdivisions see Figure 5 and description of Lower Mount Isa Group in text. Reference is top Warrina Park Quartzite, except for eastern part of range where Surprise Creek sandstone facies (r_3) is considered to be horizontal. Numbers 2-8 above line of reference and in inset figure refer to section locations numbered PR2-8 in text; F-G refers to cross-section in Nijman (1991).**

Subgroup and Quilalar Formation') encase pebbly sandstone bodies (Phb_0), the largest of which are located in the rim synclines of the D^P_{1a} flower structure (grid references 473390 and 466376; Figs.15-17). Geometrically, they consist of a multistorey channel fill with a basal surface deeply scouring into the upper members of the underlying Alsace Quartzite (Pha_{3-5}). Farther southwards, deep scour has not been observed, and flatter depositional contacts seem to prevail, although this impression may be biased by the longitudinal sections produced in outcrops, where D^P_3 fold axes are subhorizontal (grid reference 464357).

The facies is a matrix-supported massive pebbly wacke (Fig. 17A) or diamictite with 10-50% of subrounded coarse clastic components. The matrix varies from poorly sorted coarse feldspathic arenite to feldspathic wacke, and contains, besides the quartz and feldspar, minor amounts of rock fragments, chert, clay flakes, and heavy minerals such as the basalt-derived magnetite. The pebbles and boulders predominantly consist of sandstone from the Alsace Quartzite and Bortala Formation, with an appreciable amount of volcaniclastic material of ECV origin.

Within the multistorey channel fill, the mean maximum particle size (MPS, calculated from the ten largest pebble diameters in each outcrop; Fig. 16) decreases upwards. Several intercalated sandstone layers probably represent the final stage of single storeys. The basal part of the fill contains huge slabs, up to tens of metres in size, some of them upside down, derived from the Alsace Quartzite substratum. In the eastern outcrop (grid reference 471389), no structures other than those due to sliding, flow, dewatering, and diapirism have been found, and the only indication of bedding is given by intercalated sandstone. In the western location (grid

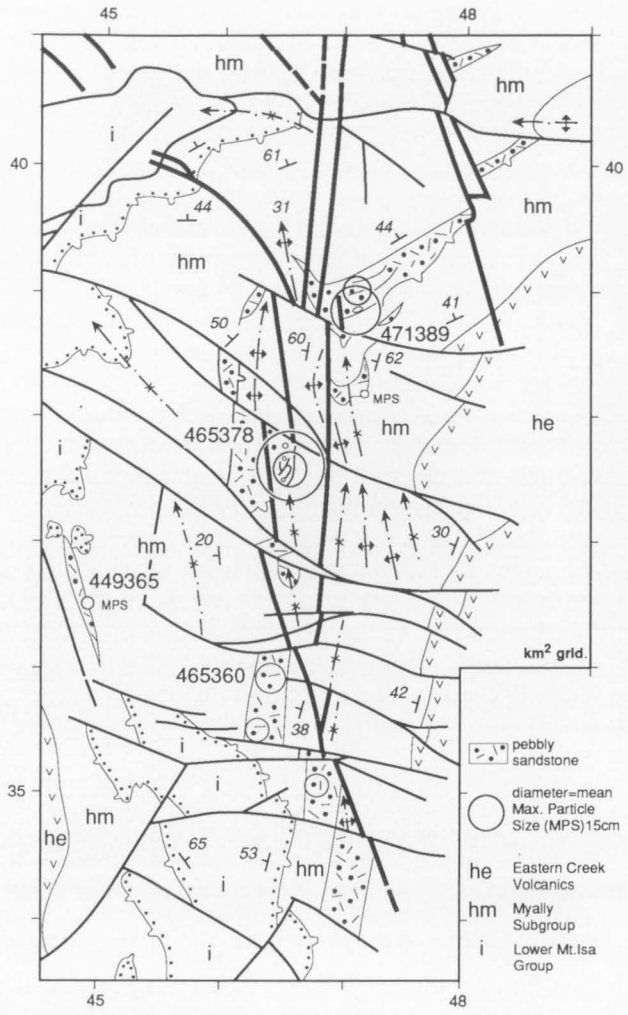


Fig. 16. Outcrop map of pebbly sandstone (hb_0) of the Bortala Formation, with locations described in the text and illustrated in Figure 17. MPS of clasts denoted by circles. Fluvial component of palaeocurrent direction of the transitional facies, immediately underlying the main body of the pebbly sandstone, is to the southeast. D^P_1 faults, in heavy lines, show flower structure in oblique section north of east-west grid 39, and in birds-eye view farther south. Initial P omitted from stratigraphic letter symbols for clarity.

reference 465378), meso-scale rootless slump folds face away from the flower crest; they are encased in inversely and normal-to-inversely graded pebbly sandstone beds.

The MPS of the pebbly sandstone occurrences tends to decrease southwards (Fig. 16), where in addition thin lenses of the same rock occur over a wider lateral extent (grid references 449365 and 451318). Framework conglomerate has been observed only in the southernmost outcrops in channel fills at the base of the sequence (grid reference 465360).

Precursors of this facies are the smaller channel fills in the underlying transitional facies ($Pha_{4,5}$) of the Alsace Quartzite. They form architectural elements at a stratigraphic level that also contains about 35 m-thick deltaic CU-FU clastic build-ups over finely wave-rippled mudstone (grid reference 474389 [Pha_5]; Fig. 5a).

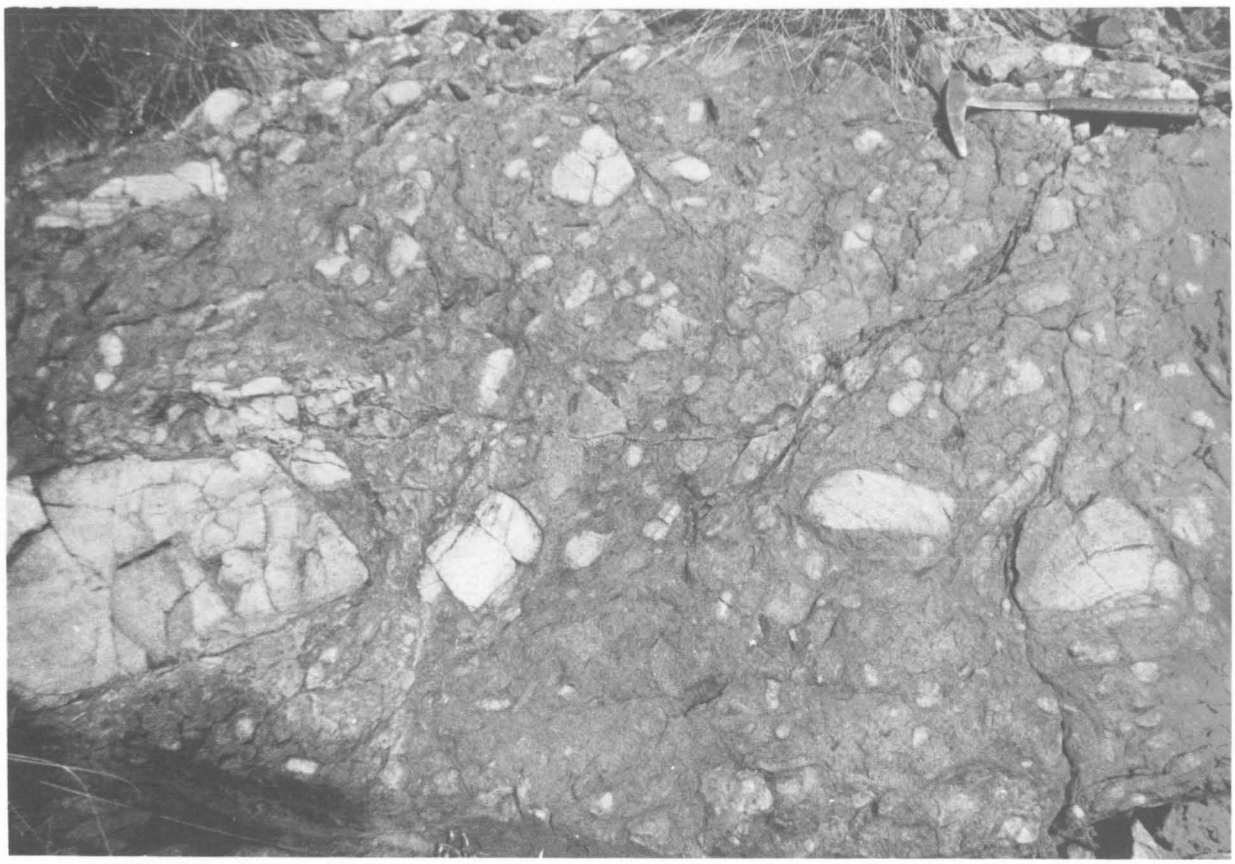
Sedimentary environment

The massive pebbly sandstone facies is identical to that found in the Hero Fan Delta (compare facies C_m of Nijman & others, this volume), which we compared with Shultz's (1984) massive matrix-supported diamictite. In the Hero Fan, this facies appears to have resulted from debris flow deposition during fan retrogradation under either subaerial or shallow subaqueous conditions. The surrounding fine-grained Bortala sediment indicates alternately dry and wet conditions in an inshore lacustrine or lagoonal environment. The Type-1 sequence boundary at the base of the pebbly sandstone, and the sandstone itself, evidently formed during a lowstand caused by a drop in sea level, or by structurally induced uplift after the highstand deposystem of the Alsace Quartzite (Fig. 5a). Both the southeasterly orientation of the minor deltas in the top of the Alsace Quartzite and the MPS distribution in the pebbly sandstone suggest the coarse clastic sediments were fed into the system from the northwest, most probably in a fan delta, where the multistorey unit filled an alluvial or estuarine valley.

Relationship between pebbly sandstone deposition and D^P_{1a} transpression

Structurally, these clastics appear to have been funnelled into the rim synclines of a rising positive flower structure. Together with the observation of sideward slumping of sandstone of the Alsace Quartzite adding to the infilling of the syncline, this proves the synsedimentary transpressive nature during early growth of the flower structure (Naylor & others, 1986; Fig. 17B). The full development of the strike-slip pattern was achieved during and after deposition of the Myally Subgroup, combining with the eastward tilt before deposition of the Lower Mount Isa Group. Hence it is definitely a cover sequence 2 event, possibly coeval with deposition of the Quilalar Formation. The positive transpressive nature is further emphasised by the forced folds, such as described by Stearns (1978) and Stearns & Stearns (1978) in the Rocky Mountains Foreland, over the high-angle reverse Riedel faults.

The flower structures observed in the Paroo Range can be interpreted to represent cross-sections of approximately northeast-striking transpressive en-echelon Riedel faults (Fig. 17B), generated by north-oriented right-lateral



A

Fig. 17 (A) Characteristic outcrop of matrix-rich pebbly sandstone of Bortala Formation (Phb_0) with flow structures around cobbles (hammer: 30 cm; grid reference 471389).

wrench faults spaced 4.5 km apart. The wrench faults may represent either the next level in a hierarchy of underlying flower structures related to deeper-seated major strike-slip faults on the scale of the block-bounding master faults, or transfer faults within north-south extensional domains, as in the 'loaf-tectonic' model of Gibbs (1987). Their regular spacing suggests the first solution, but early activity along the Conglomerate Creek Fault (see next section) the second. The northwest-oriented grain of the isopach patterns of the Alsace Quartzite and Bortala Formation (compare the 340°–360° orientation of the pre-unconformity folds in the adjacent Kennedy Gap 1:100 000 Sheet area; Wilson & others 1979, p.78 and fig. 38) may be explained by an en-echelon fold pattern preceding the surface penetration of Riedel systems in a transpressive stress field with the same northeast sigma-1 orientation (Wilcox & others, 1973), and supports the concept of overall control by north-directed dextral simple shear in the basement.

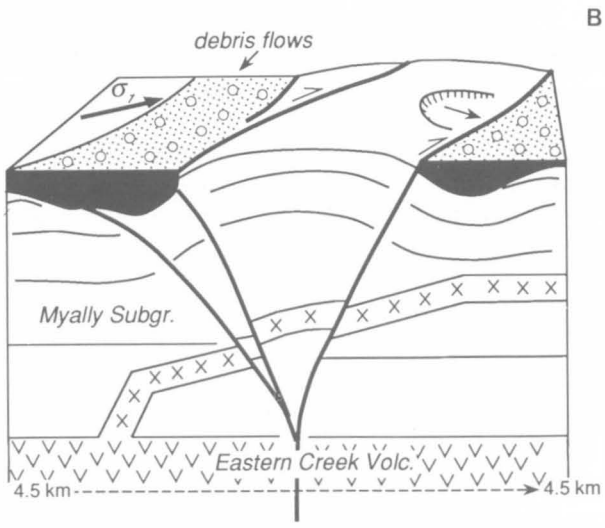


Fig. 17 (B) Model of flower structure with rim synclinal deposition of coarse clastics, and the inferred stress pattern.

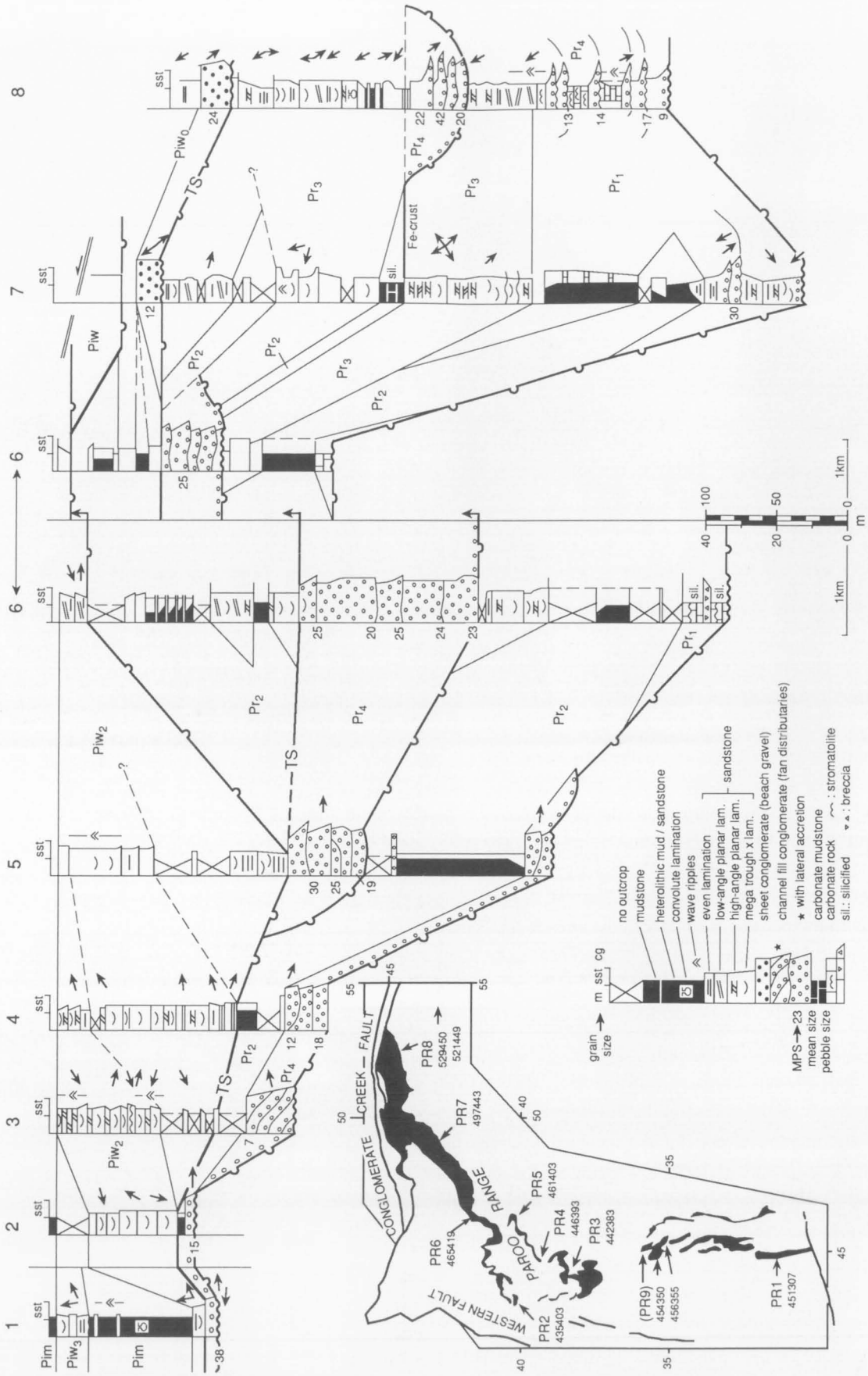


Fig. 18. Correlation of sedimentological logs of the Lower Mount Isa Group coarse clastic wedge. Correlation is based on mapping of continuous outcrop along the Paroo Range. Locations of columnar sections shown in inset figure. TS: transgressive surface at the base of the Warrina Park transgressive system tract. Stratigraphic code as in map legend (Nijman, 1991); see also text.



Fig. 19. Interpreted air photograph of the Paroo Range around grid reference 470420 showing: D^P_{1b} drape folds and antithetic thrusts (♦) overlain by Warrina Park Quartzite (iw) units with stacked unconformities (0-2); R – D^P_{1a} Riedel fault; (*) contact between Warrina Park (iw_0) beach conglomerate and Surprise Creek (r) fan delta channel-fill conglomerate; imbricate thrusts of the D^P_2 Paroo Thrust system in the Moondarra Siltstone (im). hb – Bortala Formation; hw – Whitworth Quartzite; dl – dolerite; MU – Mount Isa Group Unconformity. Initial P omitted from stratigraphic letter symbols for clarity. Numbered crosses are 1000 m intersections of Australian Map Grid Zone 54.

Lower Mount Isa Group and syndepositional D^{P}_{1b} deformation

Geometry of the Lower Mount Isa Group, D^{P}_{1b} drape folds, and progressive unconformities

The internal and external geometry of the Surprise Creek Formation and Warrina Park Quartzite are primarily derived from restored sections (Fig. 15) hung from the boundary between the Warrina Park Quartzite and the overlying Moondarra Siltstone, ignoring any primary inclination of this surface. Where the top of the Warrina Park Quartzite is not exposed in the northeastern Paroo Range, the middle Surprise Creek Formation is used for reference. Because east-west sections have been chosen within D^{P}_{4} fault blocks, no structural distortion other than those corrected for may be expected.

Sequential information comes from nine sedimentary logs (PR1-8, Fig. 18; also PR-9, not illustrated). The Surprise Creek Formation and Warrina Park Quartzite form a single clastic wedge, 440 m thick in PR7 (grid reference 497443), possibly even more near site PR8, where the top has not been preserved (grid reference 520450). Towards the west, this sedimentary wedge laps on to progressively lower levels of the Haslingden Group. Superimposed abrupt thickness changes are caused by D^{P}_{1b} structures. Internal unconformities at the base of Warrina Park sandstone units (Piw_{0-2}) partly or completely excised the Surprise Creek sequence during continued block tilt to the east, or where existing structures were reactivated.

Intraformational unconformities at the base of Warrina Park sandstone units (Piw_0 and Piw_2) around grid reference 470420 cut across the crest of a Z-asymmetric drape fold in the underlying Surprise Creek Formation (Fig. 19 and section location PR6 in Fig. 15). The fold is located over a reactivated D^{P}_{1a} Riedel fault (R in Fig. 19) whose tip was subsequently bent westward with the development of mesoscale west-verging thrust folds in the Surprise Creek Formation, antithetic to the drape fold (♦) in Fig. 19).

One kilometre east of location PR2 in Figure 18 (grid references 496411 and 441405) the iw_2-unconformity cuts away the Surprise Creek Formation over the crest of the westernmost half-flower, indicating positive relief on that structure. In some places the Warrina Park Quartzite is missing (grid references 448416 and 434390), and the Moondarra Siltstone overlies either Surprise Creek Formation or Myally Subgroup.

In Figure 20 the unconformity between sandstone (Piw_0) of the Warrina Park Quartzite over the Surprise Creek Formation (Pr) records continued sagging of the pre-existing D^{P}_{1a} drag syncline along the 'proto'-Conglomerate Creek Fault.

Since such deformation took place during deposition of the Lower Mount Isa Group, it is considered to be the after-effect or reactivation of D^{P}_{1a} structures, and classified as D^{P}_{1b} in our notation.

Internal facies distribution in the Lower Mount Isa Group clastic wedge

The Surprise Creek Formation comprises four facies: a fine-grained heterolithic facies; a Fe-sandstone/stromatolite; a relatively feldspar-rich sandstone; and a conglomerate. In contrast the Warrina Park Quartzite consists of conglomerate and sandstone of a more mature texture and composition.

Surprise Creek heterolithic facies (Pr_2)

The irregular alternation of thinly bedded to laminated (<10 cm) greenish-grey shale, siltstone, wacke, and some poorly sorted fine-grained arenite justifies the label'heterolithic' (Fig. 7). Bedding is discontinuous where it develops into flaser/linsen structures. Bed contacts are sharp. The facies overlies or encases lenses of conglomerate, and interfingers eastwards with sandstone of the Surprise Creek Formation or the Warrina Park Quartzite.

Surprise Creek Fe-sandstone/stromatolite facies (Pr_1)

The facies is restricted to the east Paroo Range, where a maximum thickness of 62 m has been measured near the Conglomerate Creek Fault (PR8). It is is made up of thin sheetlike dark-brown to reddish-grey banded carbonate bodies intercalated with dark-brown weathered ferruginous sandstone, below and laterally continuous with the heterolithic facies in the lower Surprise Creek Formation. Silicified algal plate limestones belong to the same association (grid references 471419 and 515415).

The stromatolite component contains flat, in places convex-upward, algal-laminated rocks, in which the irregular lamination consists of alternating carbonate mud (dolomicrite) and poorly sorted fine-grained quartz sandstone and siltstone with some additional micrite. In particular near the Conglomerate Creek Fault (grid reference 507448), these stromatolites are internally brecciated and contain not only stromatolitic fragments (intraclasts) but also angular feldspathic sandstone breccia and cross-bedded Fe-rich sandstone (Fig. 21A). Sand-filled polygonal cracks occur in the flat-laminated carbonate (Fig. 21B; also at grid reference 528450).



Fig. 20. Open east trending D^P_4 syncline in Lower Mount Isa Group in north-south cross-section at grid reference 508448. Contact at base of conglomerate/ sandstone sequence (iw_0) of Warrina Park Quartzite cuts away upper part of Surprise Creek Formation (r_3) in northern limb of syncline. Growth of syncline is shown by stepwise flattening of north limb from Myally Subgroup (hm) over Mount Isa Group Unconformity (MU) via Surprise Creek Formation ($r_{1,3}$) towards Warrina Park Quartzite. Unit r_1 contains the outcrop shown in Figure 21A. The Myally Subgroup is strongly brecciated and overlies a quartz reef in what probably represents the folded D^P_2 Paroo Thrust (compare Nijman, 1991). CCF – Conglomerate Creek Fault (D^P_4 trace); he – Eastern Creek Volcanics. Initial P omitted from stratigraphic letter symbols for clarity.

Surprise Creek (feldspathic) arenite facies (Pr_3)

The sandstone facies of the upper Surprise Creek Formation of the eastern Paroo Range is 265 m thick in section PR7 and 219 m in section PR8 (Fig. 18).

Sequences of cross- or even-laminated sandstone coarsen and thicken upwards (Fig. 21C; PR8 at 290 m) and grade up from arkose to feldspathic arenite and quartzitic arenite. The CU-trend is regularly interrupted by FU-sequences, preferentially though not exclusively composed of cosets of planar and trough-shaped cross-beds with bipolar palaeocurrents (Fig. 21D; PR7 at 200 m; PR8 at 170 m and 230 m). In the mature quartz arenite, sets of low-angle to even lamination are more frequently found. Wave and current ripplemarks are very common.

Surprise Creek conglomerate facies (Pr_4)

The conglomerate facies occurs in channel fills with a height/width ratio ranging from 1:5 to 1:10 i.e., ribbon geometry. The ribbons consist of poorly sorted matrix-rich framework conglomerate organised in fining-up sequences in places with lateral accretion bedding (Fig. 22A; compare PR3 in Fig. 18). The conglomerate pebbles are subrounded to rounded and invariably have a quartz arenitic to arkosic composition. The same holds for the medium to coarse-grained matrix. Imbrication is common (Fig. 22B), but gravel bar foresets are rare.

In the western part of the study area, this facies appears at the base of the Surprise Creek Formation or intercalated with the heterolithic facies, not only as ribbons but also as a conglomerate sheet formed by imbricate stacking and lateral linkage of several channel fills (e.g., between PR4 and PR5).



Fig. 21 (A) Alternation of (1) flat-laminated stromatolitic carbonate and (2) sandstone breccia in cross-bedded Fe-sandstone of the Fe-sandstone facies/stromatolite (Pr_1) of the Surprise Creek Formation. Rocks weather dark brown. Grid reference 507448. Hammer 30 cm long.



Fig. 21 (B) Detail of stromatolite facies of the Surprise Creek Formation of Figure 21A with sand dyke in crack pattern. Pencil 14 cm long.

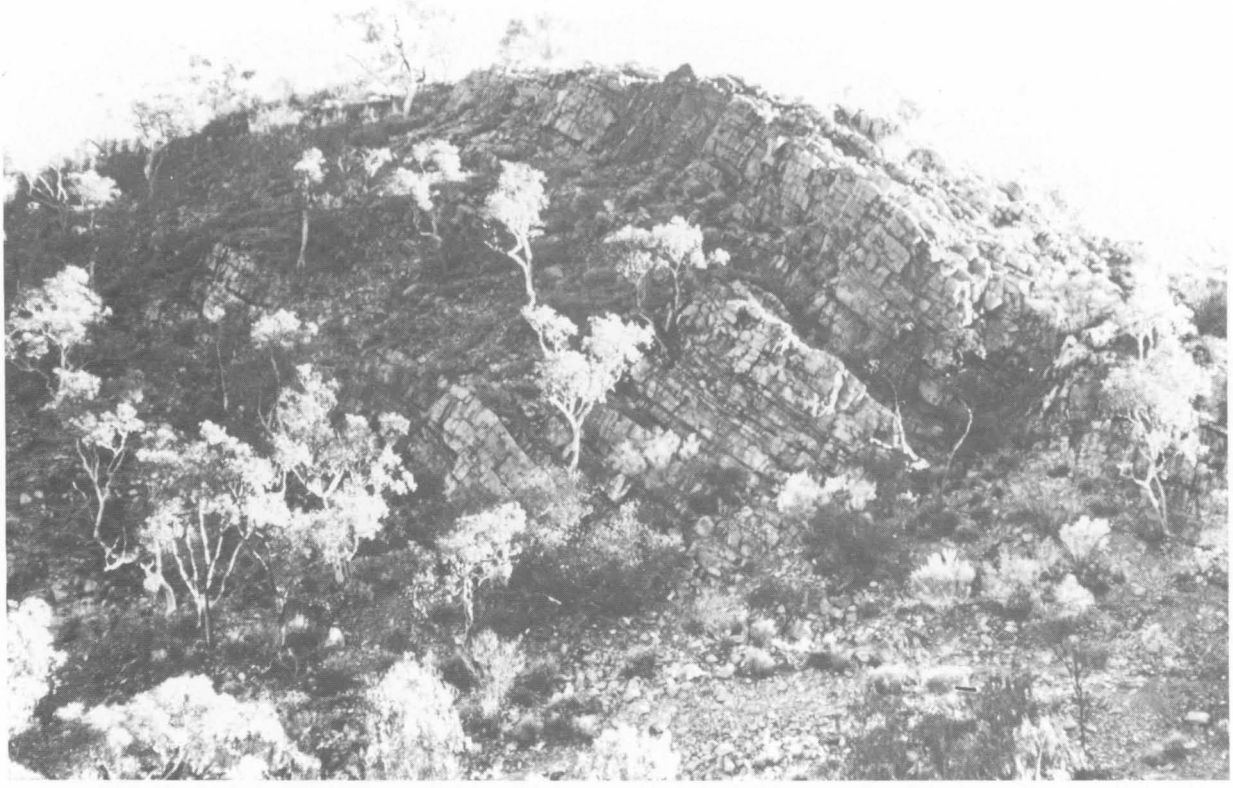


Fig. 21 (C) Stack of thickening-up shoreface sequences in feldspathic sandstone facies of Surprise Creek Formation (Pr_3). Log PR8 (235-300 m). Grid reference 520449



Fig. 21 (D) Alternation of bipolar wedge-shaped to tabular sets of tangential cross-lamination with even-laminated sets in feldspathic sandstone facies of Surprise Creek Formation (Pr_3). Log PR8 (132 m). Grid reference 528451. Pencil 14 cm long.

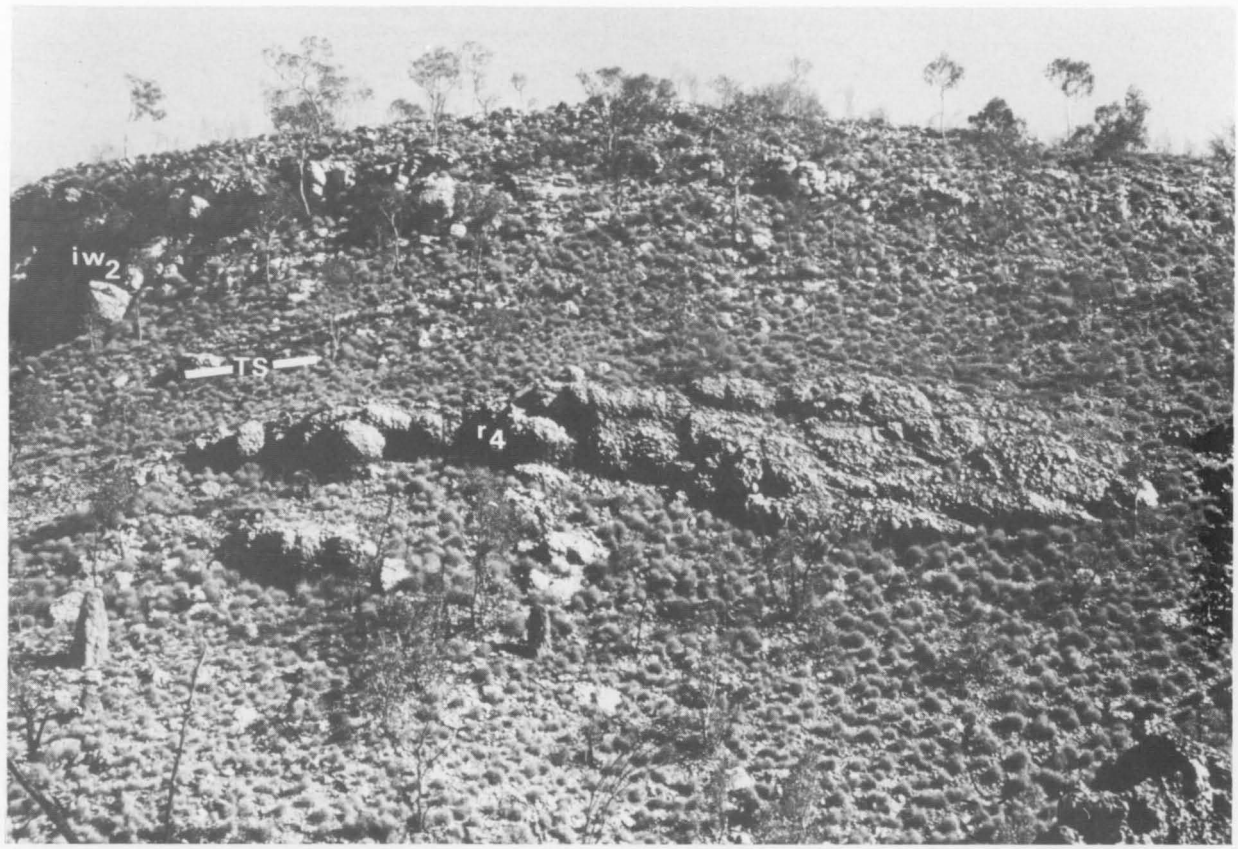


Fig. 22 (A) Cross-section of framework conglomerate ribbon with lateral accretionary bedding of Surprise Creek Formation (r_4) overlain by coastal sandstone (iw_2) of Warrina Park Quartzite, the two separated by transgressive surface (TS). Conglomerate facies of the Lower Mount Isa Group. Log PR3, grid reference 442383. Initial P omitted from stratigraphic letter symbols for clarity.



Fig. 22 (B) Poorly sorted imbricated conglomerate (Pr_4) at base of Surprise Creek Formation. Grid reference 480421. Hammer 30 cm long.



Fig. 22 (C) Well rounded beach pebble conglomerate (Piw_0) of Warrina Park Quartzite. S_0 bedding (306°/55°; with 30 cm-hammer) indicated by berm(?) sandstone veneer over beach conglomerate; landward side to right. S_0* bedding traces within conglomerate indicated by reversals in imbrication. Conglomerate slightly deformed parallel to D^P_4 axial plane. Grid reference 488436.

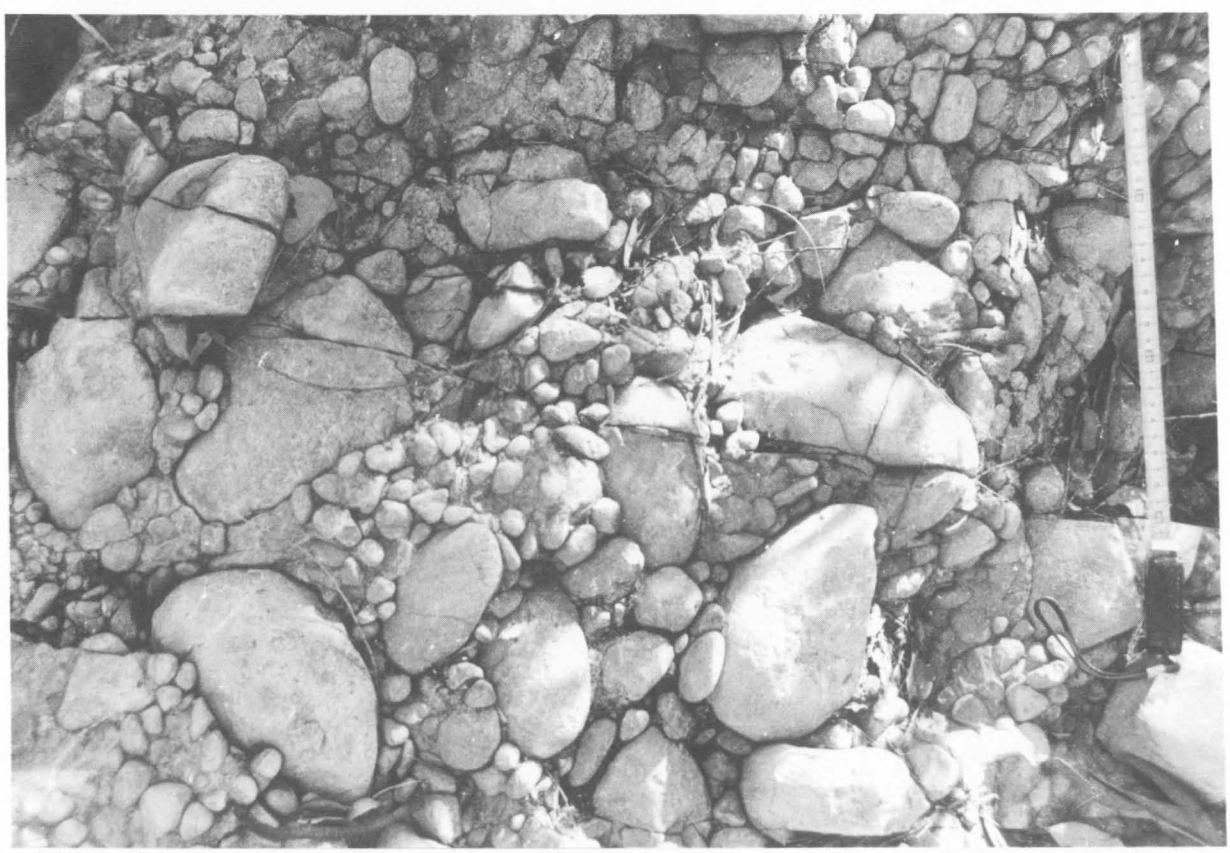


Fig. 22 (D) Bimodal sorting in bedding plane of beach conglomerate of Warrina Park Quartzite. Scale in centimetres. Grid reference 489438.

In the easternmost sector of the Paroo Range, maximum clast size is 60 cm (MPS: 42 cm) in a cluster of vertically stacked, commonly disconnected conglomerate channel fills with southeasterly palaeocurrents, more or less parallel to the Conglomerate Creek Fault Zone (PR8, Fig. 18). Here, conglomerate channel fills (Pr_4) are under and overlain by sandstone (Pr_3) and/or Fe-sandstone/stromatolite facies (Pr_1). The boulder and cobble conglomerate indicate a major edifice of coarse clastics. Towards the southern part of the range, MPS first decreases, then increases again to values of 38 cm in PR1 (grid reference 451307) and surroundings.

Warrina Park quartz arenite and conglomerate (Piw_{0-3})

Two facies have been distinguished within the Warrina Park Quartzite. Westward onlapping quartz arenite sheets form the bulk of the formation, whereas in the northeastern Paroo Range a highly rounded well-sorted quartz arenite pebble conglomerate is exposed at the base of the two lower units of Warrina Park Quartzite, Piw_0 and Piw_1 (logs PR7 and PR8). Maximum thickness of uninterrupted Warrina Park sandstone is 34 m (Piw_2 in PR9, grid reference 454350; $Piw_2 + Piw_3$: 60 m).

The well-sorted very pure quartz arenite and quartzite show irregular stacking of thickening-upward, fining-upward, or trendless sequences about 5-10 m thick (e.g., PR2 in Fig. 18). The average grain size varies between fine and medium. Bedding is even and bed contacts sharp. Sedimentary structures are very common. Trough cross-laminated and, less frequently, tabular high-angle planar sets alternate with or grade upwards to even-laminated or low-angle sets as in the underlying less mature Surprise Creek sandstone facies. Straight-crested symmetrical wave ripples abound as bedforms.

The framework conglomerate is closely packed, moderately to very well-sorted, and highly rounded. Clasts and matrix consist almost entirely of quartz arenite and feldspathic arenite, the clasts derived from the immediate substratum. MPS does not exceed 10 cm. The facies forms sheets at the base of units Piw_0 and Piw_1.

An unconformable contact between the Piw_0-sheet conglomerate of the Warrina Park Quartzite and the Pr_4-channel-fill conglomerate of the Surprise Creek Formation is found at grid reference 478424 in the central-north Paroo Range (* in Fig. 19). At grid reference 489437, alternate bedding of low-angle and high-angle reverse imbrication is combined with bimodal sorting of pebbles (Nemec & Steel, 1984; Fig. 22C, D).

Palaeocurrent patterns of the Lower Mount Isa Group

The results of palaeocurrent analysis after correction for D^P_3 folding and D^P_4 tilt are shown in Figure 23. Measurements on foresets and pebble imbrications have been distinguished for each locality, whereas wave ripple strikes have been combined because of their relatively constant orientation over the entire range, indicating the general coastline orientation.

Foresets and trough axes are unimodal eastwards to bipolar in the central west of the Paroo Range. From the rather vague trend in the data set, two dominant palaeocurrent directions could be demonstrated with the Kuiper test (Kuiper, 1960), oriented respectively 085° and 275° ± 5° at 95% confidence. In the northeast, the pattern becomes orthogonal with on/offshore and longshore components, obliquely oriented with respect to the wave-ripple strike. In the south, the vectors tend to group in three modes: onshore, offshore, and an uncertain northward longshore component.

In the relatively little deformed eastern half of the map area, most conglomerate shows a well preserved imbrication (PR1 and east of PR6). Both here and in the deformed conglomerate, imbrication has been systematically measured on flat pebbles (n = or >20). Where D^P_3 deformation resulted in bulk strain, pebbles are flattened in the axial plane. Nevertheless one would not expect the observed systematic eastward centripetal pattern of the palaeovectors (Fig. 23) to result from D^P_3 strain, since the strain ellipsoid is related to a constant 350° orientation of the D^P_3 axial plane (compare Fig. 8). So the pattern may be safely considered indicative of the sedimentary conditions.

Depositional model of the Lower Mount Isa Group Deposystem

Environmental interpretation

The environmental interpretation largely depends on the facies relationships given in Figure 24, based on the data of Figure 18 and the palaeocurrent patterns of Figure 23.

Facies end-members are the channelised polymict Surprise Creek conglomerate and the mature Warrina Park quartz arenite. The first forms an eastward-draining channel system with maximum grain size near the Conglomerate Creek Fault, where also (scarp) breccia interdigitates with the Lower Mount Isa Group. Upstream, only the heterolithic facies is directly associated with the channel conglomerate. In many aspects the heterolithic facies resembles the Bortala Formation, deposited in a

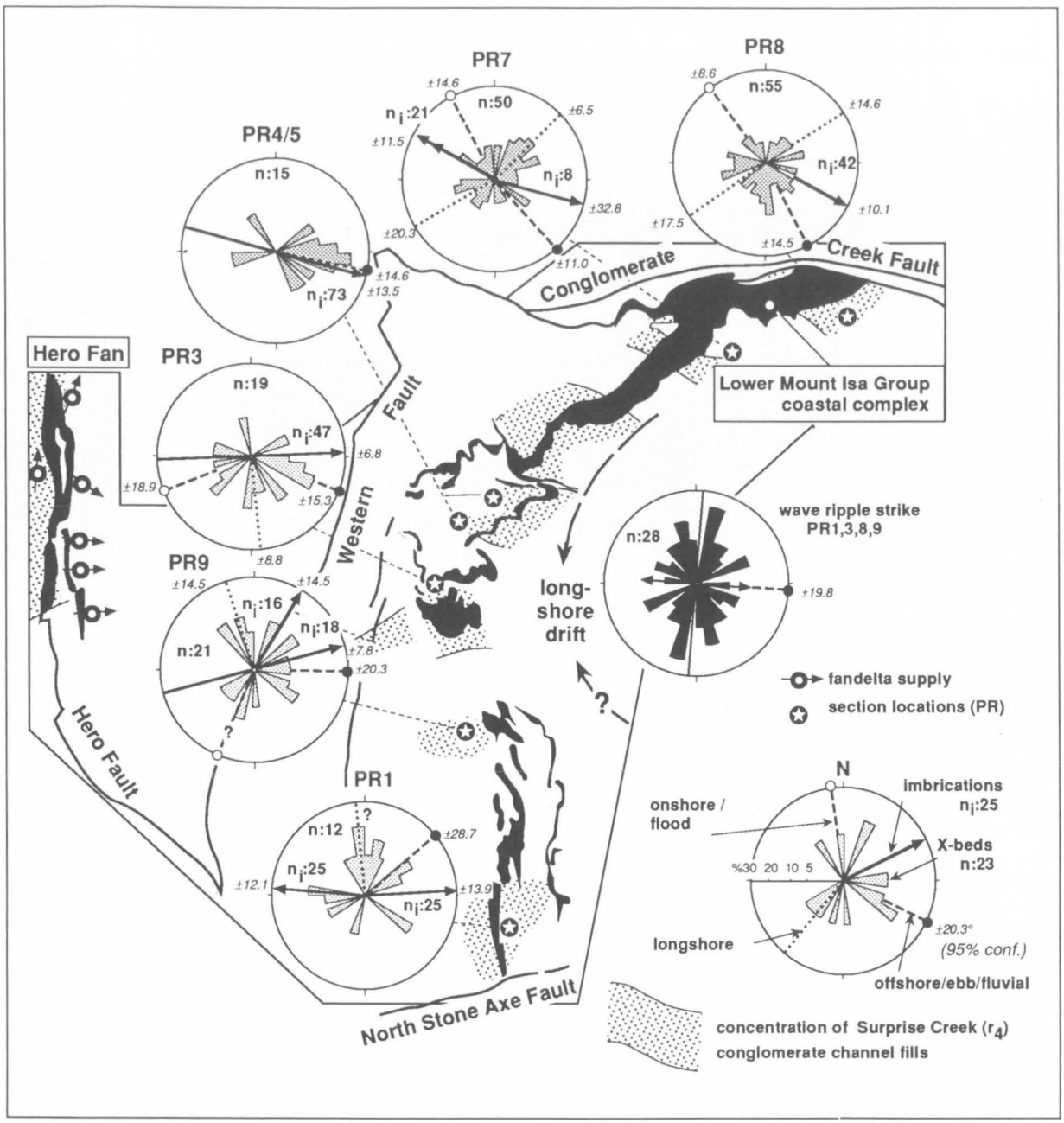


Fig. 23. Outcrop and dispersal pattern of the Lower Mount Isa Group clastic wedge (including the Hero Fan; Nijman & others, this volume). The mean palaeocurrent vectors indicate: – a fanning pattern for the inshore Hero fan delta in the west; – a centripetal supply in the coastal system of the Paroo Range. Frequency, grainsize, and thickness of the framework conglomerate increase towards the Conglomerate Creek Fault. There is also a grainsize increase in the far south. A consistent north-south wave ripple strike at various angles to the primary supply of the coarse clastics suggests an embayed coastline facing eastwards between delta fronts and/or headlands near the east-west bounding faults (Conglomerate Creek Fault, North Stone Axe Fault, i.e., Spillway Fault System). See text.

protected low-energy depositional environment, such as a coastal lake or tidal lagoon, in which the alternation of lithotypes formed by irregular variations in depositional energy, most probably with tidal influence. In the absence of palaeontologic evidence, this interpretation largely depends on the fact that, downstream towards the east, both channel and heterolithic facies meet sandstone concentrations which we interpret as coastline deposits.

The sedimentary structures, sequential trends, and palaeocurrent patterns of the upper Surprise Creek arenites strongly indicate a wave-and-tide-influenced, probable barrier-beach environment oriented northeast, wherein the FU units represent inlet and outlet channels. Major pebble to boulder-floored fan delta distributaries bypassed sand into this coastline (Fig. 24, inset). The feldspar content tallies with a direct fan delta supply from hinterlands

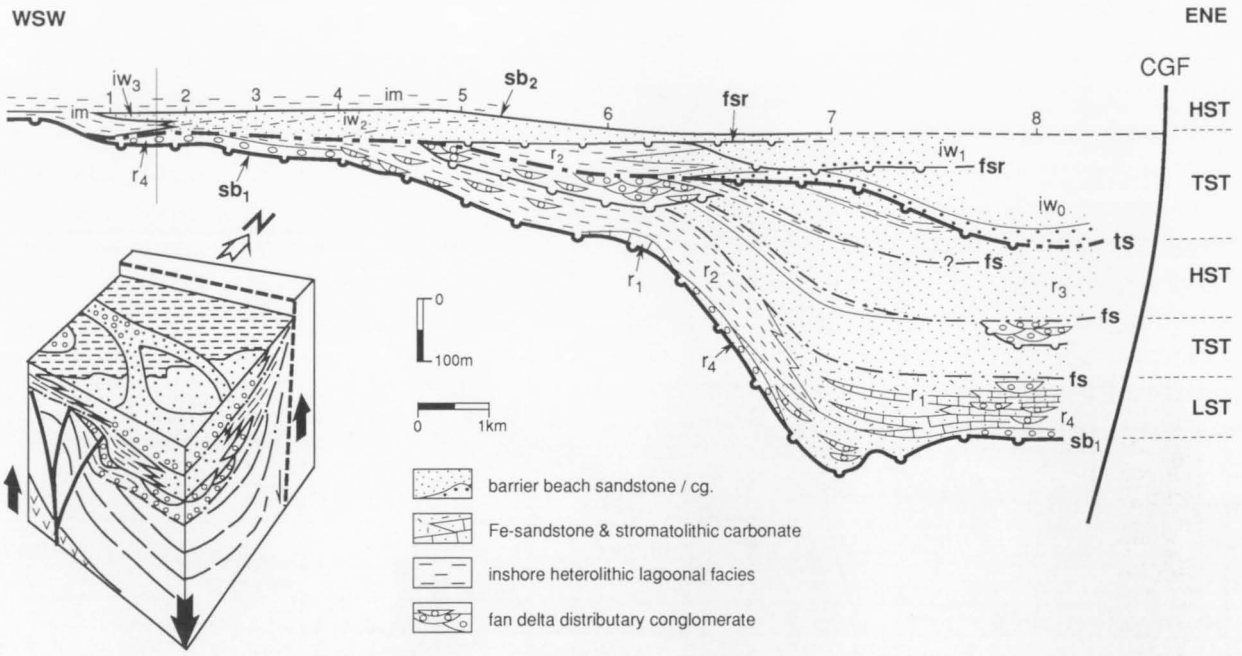


Fig. 24. Depositional model of the Lower Mount Isa Group (Breakaway Shale excluded), based on data of Figures 20 and 23. Section is oblique to inferred north-south embayed coastline and hence intersects Conglomerate Creek Fault (CCF) at right hand side of figure. Thickening of the wedge is due to combination of downthrow along the fault and eastward regional tilt, as shown in inset 3D diagram. The other element of structural control consists of reactivation of D^P_1 flower structures. iw_{0-3} – sandstone bodies of Warrina Park Quartzite; r_{1-4} – facies of Surprise Creek Formation; $sb_{1,2}$ – sequence boundaries types I and II of Vail (1987); ts – transgressive surface; fs – flooding surface; fsr – flooding surface with ravinement. Initial P omitted from stratigraphic letter symbols for clarity.

nearby to the west or northwest, where the Mount Isa Group Unconformity tapped Myally and older source rock, including granite.

Because of the lateral association with coastal sandstone (PR8) at one end and inshore heterolithic facies at the other (PR7), the most likely environment of deposition for the Fe-sandstone/stromatolite facies is the back-barrier supra-/intertidal area at the seaward side of a lagoon, probably in reach of washover deposition. The interlaminated ferruginous sandstone tallies with a sand flat environment, wherein flat-pebble carbonate breccia, some of it now silicified, indicates break-up of algal mats due to flooding or storm activity in places normally sheltered against the siliciclastic sedimentation. For the Fe-sandstone facies, nevertheless, we lack sufficient data to support this interpretation. The rare sandstone extraclast breccia may be related to nearby synsedimentary fault activity.

For the Warrina Park Quartzite, a high-energy beach environment is interpreted on several grounds. First, the compositional and textural maturity of the sedimentary material suggests winnowing in a high-energy environment. Shoreface cycles, including low-angle planar laminated sets, regularly occur. The associated sedimentary structures with the bi-/trimodal to bipolar palaeocurrent vectors and the east-west direction of wave oscillation derived from the average wave ripple orientation, indicate an overall north-oriented coastal sandstone complex. The fanning arrangement of the foreset directions of the entire Lower Mount Isa Group coastal deposystem along the Paroo Range, as well as the systematic bending of longshore transport components, suggest an embayed coastline.

The localisation of the Warrina Park conglomerate facies along the Conglomerate Creek Fault Zone fits into this model as pebble beach deposits concentrated on a headland from which sandstone was winnowed by bayward longshore currents (Fig. 23). Sedimentologic evidence for their beach character is present in the reverse and steeply landward imbrications and bimodal pebble sorting (Nemec & Steel, 1984). Our present interpretation corroborates those of Wilson & others (1977) and Plumb & others (1980), who have earlier referred to the beach character of the Warrina Park Quartzite (in the strict sense).

Depositional model and structural control

A depositional model for the Surprise Creek /Warrina Park clastic wedge consists of three distinct elements (Fig. 24): (1) a pro- to aggradational basal sequence (LST) comprising the basal Surprise Creek coarse clastic and heterolithic sediments and silicified limestones over the Mount Isa Group Unconformity (megasequence and Type-1 sequence boundary); (2) a retro- to aggradational upper sequence (TST-HST) of Surprise Creek coastal sandstone and lagoonal sediments built of at least four parasequences over a basal flooding surface (fs) below which stacked distributary channels represent the shifting active segments of a fan delta; and (3) a rapid retrogradation of transgressive coastal sandstone (TST), with ravinement and sediment reworking (parasequence boundaries: fsr), resulting in deposition of the mature quartz arenite of the Warrina Park Quartzite, followed by a Type-2 conformable sequence boundary (base Moondarra Siltstone).

The environment of deposition of the basal offlap sequence was a prograding coastal plain in which east-flowing braided streams drained an uplift area situated nearby to the west. If our correlation with the inshore Hero Fan Delta as its landward boundary is correct, the width of this plain was about 20 km (Fig. 23; compare Nijman & others, this volume). Lakes and/or narrow lagoons occupied much of its surface behind a north-oriented embayed coast of barrier islands and beaches as discussed in the previous paragraph. East of this deposystem, a wide, probably open, marine shelf must have been present to account for sufficient fetch to generate the waves capable of building a barrier coastline. This picture is not very different from that of the Myally arenites.

The axis of coarsest sediment supply was closest to the proto-Conglomerate Creek Fault, which together with the structural evidence for an early D^{P}_{1b} drag syncline indicates synsedimentary activity of these east-west faults and their capacity to control the clastic facies patterns (compare Smith, 1969; Dunnet, 1976b; Derrick, 1982). Another fanglomerate edifice was located at the Spillway Fault near Lake Moondarra, which corresponds to the increase in MPS to the extreme south of the Paroo Range area near the North Stone Axe Fault. These accumulations of coarse clastic sediment, probably of fan deltas, evidently localised at transverse faults, defined headlands where longshore currents (Fig. 23) fed sand to a wide bay the size of the entire map area during the deposition of the upper Surprise Creek Formation and Warrina Park Quartzite. Morphologically, this pattern already reflects the north-south structural compartmentation visible on the regional geologic map (compare Blake, 1987 and Figs. 1 and 10).

The upper onlap sequence incorporates two separate phases with an upward increasing content of quartz arenite at the expense of feldspathic sandstone. They mainly reflect a process of beach reworking, strongly onlapping to the west and forming ravinement surfaces, expressed as unconformities (Piw_{0-2}). How much of the stratigraphic record has been eliminated is difficult to establish.

The lacustrine(?) shale and siltstone of the Moondarra Siltstone rapidly buried this coastal sandstone, of which Piw_3 represents an inshore tidal channel sandstone (PR1 in Fig. 18; PR9).

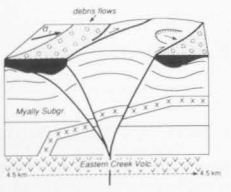
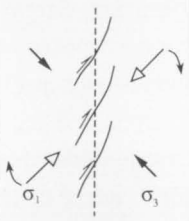
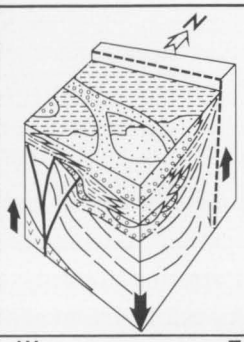
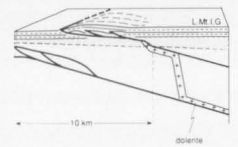
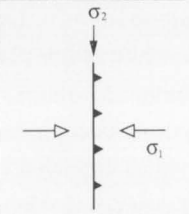
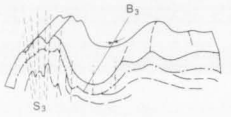
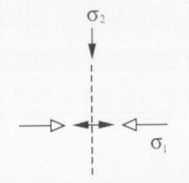
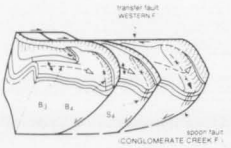
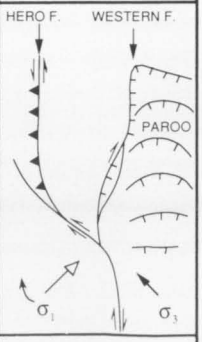
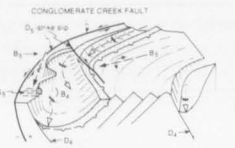
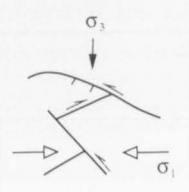
Conclusions

Table I summarises the sedimentary and structural events of the Leichhardt River Fault Trough as observed in and interpreted for the Paroo Range.

1. Early extension with a strong strike-slip component in the Eastern Fold Belt (Passchier, 1986b; Passchier & Williams, 1989; Loosveld, 1989) is dated at 1750-1730 Ma, i.e., post-Myally Subgroup and pre-Surprise Creek Formation (Blake, 1987) and hence synchronous with our phase of transpressional tectonics. Coexistence of transpression and transtension in different parts of a strike-slip belt is a common feature (Reading, 1980). In fact, the entire sequence of events in which north-south tensional and east-west compressional stress components play recurrently upon an undertone of strike-slip (compare our paper on the Hero Fault area; Nijman & others, this volume), leads one to think of the latter as the dominant structural regime for the Mount Isa Inlier.

2. Facies, facies distribution, and interpreted energy level do not differ fundamentally between the Myally Subgroup and the Lower Mount Isa Group. All sedimentary sequences and palaeocurrent patterns found in the study area indicate a relatively wide eastward-opening shelf along a rising Mount Gordon Arch in the west from which the coarsest clastics appear to be shed into the coastal area. A change in regime from a trough to a wide shelf is corroborated by TL provenance data of Rijswijk & Schalkwijk (1988), who interpret a change from an easterly Kalkadoon basement source to westerly sources with the onset of the deposition of the Myally Subgroup. During deposition of the Mount Isa Group, such a wide shelf, continuous with the sediments of the Eastern Fold Belt, is generally accepted (Derrick, 1982), but for the sedimentation realm of the Haslingden

Table 1
DEFORMATION PHASES AND SEDIMENTARY RESPONSES, PAROO RANGE

Deformation/ sedimentation events	Structures and deposystems	3D models	Inferred stress field N
D^P_{1a} pre-Mt.Isa Gr.	• NW-SE en-échelon depocenters; • N-S trending positive flower structures with 4.5km spacing; • associated east-verging upthrusts and drape folds; • eastward block tilt causing a regional unconformity at the base of the Mount Isa Group (= base Surprise Creek Formation); • dolerite dykes cut and hosted by Riedel faults	W E 	
syn-D^P_{1a} sedimentation	*Myally Subgroup coastal and shallow marine rhythmic deposits derived from hinterlands in the west. Bortala Formation inshore sedimentation with fan delta pebbly wacke restricted to rim synclinal lows of flower structures*		
D^P_{1b} syn- Lower Mt.Isa Gr.	• continued eastward tilt and drape folding; • south-down stepping, northward block tilt and drag syncline along the Conglomerate Creek Fault		**stress relaxation**
syn-D^P_{1b} sedimentation	*Lower Mt.Isa Gr.. sedimentary clastic wedge , opening to the east and composed of fan (delta) conglomerate channel fills (Surprise Creek Fm.); inshore heterolithic facies and coastal sandstone (Surprise Creek Fm) , overlain by and interdigitating with littoral quartzarenites and conglomerates of the Warrina Park Quartzite (highstand system). Progressive unconformities related to drape folds and to westward onlap over the Haslingden Group*		
D^P_2 syn-to post-Moondarra Siltstone	• west-verging, low-angle thrusting with S^P_2-cleavage close to the thrust planes; offset decreasing to nil in the Moondarra Siltstone; horizontal spacing of the thrusts ±10 km; fault breccia often strongly ferruginous; • dolerite intrusion in wet sediment along segments of the thrust plane in the Horse's Head	W E 	
D^P_3 post-Mt.Isa Gr.	• N-trending, upright, horizontal to plunging, non-cylindrical and disharmonic folds; fold amplitude increases with decreasing wave-length to the west, while S^P_3-axial plane foliation becomes penetrative	W E 	
D^P_4 post-Mt.Isa Gr.	• southblock down E-W curved normal faults (spoon faults of Dunnet, 1976b), causing pronounced curvature and progressively increasing N-plunge of B^P_3-fold axes towards the footwall; • tight to open drag synclines with axial planar S^P_4-foliation close to the spoon faults; • dextral, transtensive, oblique slip along the Western Fault as a transfer, with releasing duplexes	S N 	
D^P_5 post-Mt.Isa Gr.	• sinistral strike slip in the Conglomerate Creek Fault Zone; • steeply plunging, vertical or overturned folds in D^P_4-faults of the Paroo Range; • NE dextral/NW sinistral conjugate strike slip faults; • post-D^P_5 dolerite	N S 	

Group and Quilalar Formation the Kalkadoon Block is mostly considered the eastern boundary (e.g., Jackson & others, 1990).

We suggest that from the time of deposition of the Alsace Quartzite onward, the entire area of the LRFT and the Kalkadoon basement, together with an unknown part of the Eastern Fold Belt, at least during episodes of highstand, resembled the present-day Californian offshore continental platform (Howell & others, 1980: fig. 10), but at shallower depth. This comparison is valid for a model in which strike-slip plays a dominant role in the break-up of the basement into slivers. The isopachs of the Myally Subgroup testify to the early deformation of the cover over probably right-lateral strike-slip structures in the basement. Our study shows that these en-echelon undulations were then intersected by the Riedel patterns of the flower structures as the next step of deformation under the same regime. Shallowing and emergence of the Kalkadoon Block, as assumed by many authors, could fit in such a picture not as localised at a closed eastern margin of a symmetric trough, but as uplifted fragments of basement determining the position of coarse water-laid detritus or even aeolian deposits within a wider subsiding shelf area. The counterpart of such horsts would then be found in depressions such as the trough, filled with turbiditic deposits of Surprise Creek Formation, described by Wilson & others (1977).

3. Apart from a longitudinal (north-south) strike-slip component of the very first structures that controlled sedimentation, other early movements took place along crudely defined east-west transverse structures like the Conglomerate Creek Fault. South-block downthrow appears to have recurred from at least the formation of the Mount Isa Group Unconformity onwards, while only in the last stages (D^{P}_{5}) did the transverse fault zone accommodate strike-slip.

4. Another important component of deformation is the newly recognised west-verging low-angle thrust system, preceding the main shortening. The conditions of hot fluid migration along the fault system, interpreted from an aberrant increase in ductility in an otherwise brittle fault zone, the syntectonic dolerite emplacement, and the gossan-like ferruginisation near the tiplines of the system, may bear on the way mineralisation is understood in the area.

Acknowledgements

We thank the Bureau of Mineral Resources, Geology and Geophysics, Canberra, Australia, for the invitation to participate in the Mount Isa Regional Tectonic History Project and for providing logistics in the field. We gratefully acknowledge the yearly grants of the Dutch foundation 'Dr.Schurmannfonds' from 1986 to 1990. Special thanks are due to Prof. Peter Ypma for close cooperation during the entire project, to Prof. Gordon Lister and Drs. Dave Blake, Alastair Stewart, Bill Perkins, Jim Jackson, Ken Eriksson, and Ed Simpson for the stimulating discussions during the BMR field seasons. The manuscript benefited much from the comments and corrections by Drs. John Savage, Alastair Stewart, and Ian Sweet. At the Institute of Earth Sciences at Utrecht, Mr I.M.Santoe and Mr J.J.J.Bergenhenegouwen drafted the figures, while Mrs B.Benders prepared the photographs.

References

BEARDSMORE, T.J., NEWBERY, S.P., & LAING, W.P., 1988 - The Maronan Supergroup: an inferred early volcanosedimentary rift sequence in the Mount Isa Inlier, and its implications for ensialic rifting in the Middle Proterozoic of northwest Queensland. *Precambrian Research* 40/41, 487-507.

BELL, T.H., 1983 - Thrusting and duplex formation at Mount Isa, Queensland, Australia. *Nature* 304, 493-497.

BELL, T.H., PERKINS, W.G., & SWAGER, C.P., 1988 - Structural controls on development and localization of syntectonic copper mineralization at Mt.Isa, Queensland. *Economic Geology* 83, 69-85.

BLAKE, D.H., 1980 - The early geological history of the Proterozoic Mount Isa Inlier, North Western Queensland: an alternative interpretation. *BMR Journal of Australian Geology & Geophysics* 5, 243-256.

BLAKE, D.H., 1987 - Geology of the Mount Isa Inlier and environs, Queensland and Northern Territory. *Bureau of Mineral Resources, Australia, Bulletin* 225, 83 pp.

BLAKE, D.H., ETHERIDGE, M.A., PAGE, R.W., STEWART, A.J., WILLIAMS, P.R., & WYBORN, L.A.I., 1990 - Mount Isa Inlier - Regional geology and mineralisation. *In:* HUGHES, F.E. (Editor), Geology of the mineral deposits of Australia and Papua New Guinea. *Australasian Institute of Mining and Metallurgy, Monograph* 14, 915-925.

BLOM, J.C., 1990 - Deformation in the Leichhardt River Fault Trough, a fluid inclusion study, Mount Isa, Queensland, Australia. MSc thesis, University of Utrecht, The Netherlands, 27 pp + app. (unpublished).

BMR, 1985 - Nappe tectonics in the Mount Isa Inlier. *Bureau of Mineral Resources, Australia, Research Newsletter* 2, 11.

BMR, 1986 - Transpressional strike-slip faulting in the

Mount Isa Inlier. *Bureau of Mineral Resources, Australia, Research Newsletter* 4, 1-2.

BOSWORTH, W., 1985 - Discussion on the structural evolution of extensional basin margins (J.,141, 1984, 609-620). *Journal of the Geological Society of London* 142, 939-942.

BULTITUDE, R.J., & WYBORN, L.A.I., 1982 - Distribution and geochemistry of volcanic rocks in the Duchess-Urandangi region. *BMR Journal of Australian Geology & Geophysics* 7, 99-112.

BUTLER, R.W.H., 1982 - The terminology of structures in thrustbelts. *Journal of Structural Geology* 4, 239-245.

CARTER, E.K., BROOKS, J.H., & WALKER, K.R., 1961 - The Precambrian mineral belt of north-western Queensland. *Bureau of Mineral Resources, Australia, Bulletin* 51, 344 pp.

CHAPMAN, T.J., & WILLIAMS, G.D., 1984 - Displacement-distance methods in the analysis of fold-thrust structures and linked fault systems. *Journal of the Geological Society of London* 141, 121-128.

DERRICK, G.M., 1982 - A Proterozoic rift zone at Mount Isa, Queensland, and implications for mineralisation. *BMR Journal of Australian Geology & Geophysics* 7, 81-92.

DERRICK, G.M., 1983 - Reply to discussion: A Proterozoic rift zone at Mount Isa, Queensland, and implications for mineralisation. *BMR Journal of Australian Geology & Geophysics* 8, 164-165.

DERRICK, G.M., WILSON, I.H., & HILL, R.M., 1976a - Revision of stratigraphic nomenclature in the Precambrian of northwestern Queensland, II: Haslingden Group. *Queensland Government Mining Journal* 77, 300-306.

DERRICK, G.M., WILSON, I.H., & HILL, R.M., 1976b - Revision of stratigraphic nomenclature in the Precambrian of northwestern Queensland, III: Mount Isa Group. *Queensland Government Mining Journal* 77, 402-405.

DERRICK, G.M., WILSON, I.H., & SWEET, I.P., 1980 - The Quilalar and Surprise Creek Formations, new Proterozoic units from the Mount Isa Inlier: their regional sedimentology and application to regional correlations. *BMR Journal of Australian Geology & Geophysics* 5, 215-223.

DUNNET, D., 1976a - Some aspects of the Panantarctic cratonic margin in Australia. *Philosophical Transactions of the Royal Society, London* 280, 641-654.

DUNNET, D., 1976b - Mount Isa: reconstruction of a faulted orebody. *Philosophical Transactions of the Royal Society, London* 283, 333-344.

ELLIS, D.J., & WYBORN, L.A.I., 1984 - Petrology and geochemistry of Proterozoic dolerites from the Mount Isa Inlier. *BMR Journal of Australian Geology & Geophysics* 9, 19-32.

ETHERIDGE, M.A., RUTLAND, R.W.R., & WYBORN, L.A.I., 1987 - Orogenesis and tectonic processes in the Early and Middle Proterozoic of northern Australia. *In:* KRÖNER, A. (Editor), Proterozoic Lithospheric Evolution. *Geodynamics Series (American Geophysical Union / Geological Society of America),* 131-147.

FEIJTH, J., 1989 - Structural analysis and interpretation of D_2-thrusts in the Leichhardt River Fault Trough, Mount Isa, Queensland, Australia. MSc thesis, University of Utrecht, The Netherlands, 42 pp. (unpublished).

GIBBS, A.D., 1984 - Structural evolution of extensional basin margins. *Journal of the Geological Society of London* 141, 609-620.

GIBBS, A.D., 1987 - Development of extension and mixed mode sedimentary basins. *In:* COWARD M.P, DEWEY J.F., & HANCOCK, P.L. (Editors), Continental Extension Tectonics. *Special Publication of the Geological Society of London* 28, 19-33.

GLIKSON, A.Y., DERRICK, G.M., WILSON, I.H., & HILL, R.M., 1976 - Tectonic evolution and crustal setting of the middle Proterozoic Leichhardt River Fault Trough, Mount Isa region, northwestern Queensland. *BMR Journal of Australian Geology & Geophysics* 1, 115-129.

GLIKSON, A.Y., & DERRICK, G.M., 1978 - Geology and geochemistry of Middle Proterozoic basic volcanic belts, Mount Isa/Cloncurry, northwestern Queensland. *Bureau of Mineral Resources, Australia, Record* 1978/48, 43 pp.

HAMBLIN, W.K., 1965 - Origin of 'reverse drag' on the downthrown side of normal faults. *Geological Society of America, Bulletin* 76, 1145-1164.

HARDING, T.P., 1983 - Convergent wrench fault and positive flower structure, Arduron Basin. *In:* BALLY, A.W. (Editor), Seismic expression of structural styles Volume 3. *American Association of Petroleum Geologists Studies in Geology Series* 15, 4.2.13-16.

HARDING, T.P., 1985 - Seismic characteristics and identification of negative flower structures, positive flower structures, and positive structural inversion. *American Association of Petroleum Geologists Bulletin* 69, 582-600.

HARDING, T.P., & LOWELL, J.D., 1979 - Structural styles in petroleum provinces. *American Association of Petroleum Geologists Bulletin* 63, 1016-1058.

HENDERSON, G.A.M., & BAIN, J.H.C., 1991 - Geology of the Haslingden Group, East Moondarra Area (1: 35 000 scale map). *Bureau of Mineral Resources, Canberra, Australia.*

HOLCOMBE, R.J., PEARSON, P.J., & OLIVER, N.H.S., this volume - Structure of the Mary Kathleen Fold Belt.

In: STEWART, A.J., & BLAKE, D.H. (Editors), Detailed Studies of the Mount Isa Inlier. *Bureau of Mineral Resources, Australia, Bulletin* 243.

HOWELL, D.G., CROUCH, J.K., GREENE, H.G., McCULLOUGH, D.S., & VEDDER, J.G., 1980 - Basin development along the late Mesozoic and Cainozoic California margin: a plate tectonic margin of subduction, oblique subduction and transform tectonics. *In*: BALLANCE, P.F., & READING, H.G. (Editors), Sedimentation in Oblique-slip Mobile Zones. *Special Publication of the International Association of Sedimentologists* 4, 43-62.

JACKSON, M.J., SIMPSON, E.L., & ERIKSSON, K.A., 1990 - Facies and sequence stratigraphic analysis in an intracratonic, thermal sag basin: the Early Proterozoic, Lower Quilalar Formation and Ballara Quartzite, Mount Isa Inlier, Australia. *Sedimentology* 37, 1053-1078.

JOHNSON, H.D., 1977 - Shallow marine sandbar sequences: an example from the Precambrian of North Norway. *Sedimentology* 24, 245-270.

KUIPER, N.H., 1960 - Tests concerning random points on a circle. *Koninklijke Nederlandse Akademie van Wetenschappen Proceedings* A63, 38-47.

LEVELL, B.K., 1980 - A late Precambrian tidal shelf deposit, the Lower Sandfjord Formation, Finnmark, North Norway. *Sedimentology* 27, 539-557.

LISTER, G.S., THOMAS, A., & DUNN, J., 1986 - Tectonic processes in the Mount Isa Inlier: significance of transpressional strike-slip faulting. *Geological Society of Australia, Abstracts* 15, 127-128.

LOCHEM, J.H. van, SPLIETHOFF, H., & NIJMAN, W., 1988 - Structure and sedimentation in the Proterozoic of the Paroo Range, Mount Isa Inlier, Queensland, Australia. *Contributions to the MIRTH Project, Institute of Earth Science, University of Utrecht, Report No.2 Bureau of Mineral Resources, Australia.,* 100+xliii pp.,1:25 000 geological map.

LOOSVELD, R.J.H., 1989 - The intracratonic evolution of the central eastern Mount Isa Inlier, northwest Queensland, Australia. *Precambrian Research* 44, 243-276.

LOOSVELD, R.J.H., & SCHREURS, G., 1987 - Discovery of thrust klippen, northwest of Mary Kathleen, Mount Isa Inlier, Australia. *Australian Journal of Earth Sciences* 34, 387-402.

LOWELL, J.D., 1972 - Spitsbergen Tertiary orogenic belt and the Spitsbergen fracture zone. *Geological Society of America Bulletin* 83, 3091-3102.

McCLAY, K.R., & CARLILE, D., 1978 - Mid Proterozoic sulphate evaporites at Mount Isa Mine, Queensland, Australia. *Nature* 274, 240-241.

McCUBBIN, D.G., 1982 - Barrier island and strand plain facies. In: SCHOLLE, P.A., & SPEARING, D. (Editors), Sandstone Depositional Environments. *American Association of Petroleum Geologists, Tulsa,* 247-279.

NAYLOR, M.A., MANDL, G., & SIJPESTEIJN, C.H.K., 1986 - Fault geometries in basement-induced wrench faulting under different initial stress states. *Journal of Structural Geology* 8, 737-752.

NEMEC, W., & STEEL, R.J., 1984 - Alluvial and coastal conglomerates: the significant features and some comments on gravelly mass flow deposits. *In:* KOSTER, E.H., & STEEL, R.J. (Editors), Sedimentology of Gravels and Conglomerates. *Canadian Society of Petroleum Geologists, Memoir* 10, 1-31.

NEUDERT, M.K., & RUSSELL, R.E., 1981 - Shallow-water and hypersaline features from the Middle Proterozoic Mt Isa sequence. *Nature* 293, 284-287.

NIJMAN, W., 1991 - Geology of the Paroo Range-Hero/Western Fault Zone (1:20 000 scale map). *Bureau of Mineral Resources, Canberra, Australia* (two sheets). Available as a colour electrostatic plot on paper (AUD30), or in digital form on optical disc or Exabyte 8 mm tape (prices on application) both of which can be displayed on Intergraph Microstation software on computers that will run Unix. The digital data comprise a scanned raster image (.RLE format) of the black and white geological map, and an Intergraph vector design file containing the boundaries of coloured polygons. The coloured map and data are available from the Publication Sales Centre, Bureau of Mineral Resources, and an uncoloured Ozalar film or paper copy (AUD20) of the map is available from BMR Copy Service, both at GPO Box 378, Canberra, ACT, 2601, Australia. All orders to be prepaid to Collector of Public Monies.

NIJMAN, W., MIJNLIEFF, H.F., & SCHALKWIJK, G., this volume - The Hero Fan Delta (Lower Mount Isa Group) and its structural control: deformation in the Hero/Western Fault Zone and Paroo Range compared, Proterozoic, Mount Isa Inlier, Queensland, Australia. *In:* STEWART, A.J., & BLAKE, D.H. (Editors), Detailed Studies of the Mount Isa Inlier. *Bureau of Mineral Resources, Australia, Bulletin* 243.

PAGE, R.W., 1978 - Response of U-Pb zircon and Rb-Sr total rock and mineral systems to low-grade regional metamorphism in Proterozoic igneous rocks, Mount Isa, Australia. *Journal of the Geological Society of Australia* 25, 141-164.

PAGE, R.W., 1981a - Mount Isa project. *In*: Geological Branch Summary of Activities 1980. *Bureau of Mineral Resources, Australia, Report* 230, 155-157.

PAGE, R.W., 1981b - Depositional ages of the stratiform basemetal deposits at Mount Isa and McArthur River, Australia, based on U-Pb zircon dating of concordant tuff horizons. *Economic Geology* 76, 648-658.

PAGE, R.W., 1983 - Chronology of magmatism, skarn formation and uranium mineralization, Mary Kathleen,

Queensland, Australia. *Economic Geology* 78, 838-853.

PASSCHIER, C.W., 1986a - Proterozoic deformation in the Duchess belt, Australia: a contribution to the Bureau of Mineral Resources, Australia, Mount Isa Regional Tectonic History Program. *Geologie en Mijnbouw* 65, 47-56.

PASSCHIER, C.W., 1986b - Evidence for early extensional tectonics in the Proterozoic Mount Isa inlier, Australia. *Geology* 14, 1008-1011.

PASSCHIER, C.W., & WILLIAMS, P.R., 1989 - Proterozoic extensional deformation in the Mount Isa Inlier, Queensland, Australia. *Geological Magazine* 126, 43-53.

PEARSON, P.J., 1989 - The structural and tectonic development of the Wonga belt and surrounding Mary Kathleen Fold Belt, Mt.Isa Inlier, northwestern Queensland. PhD thesis, University of Queensland (unpublished).

PLUMB, K.A., DERRICK, G.M., NEEDHAM, R.S., & SHAW, R.D., 1980 - The Proterozoic of northern Australia. *In*: HUNTER, R.D. (Editor), Precambrian of the southern hemisphere. *Developments in Precambrian Geology* 2. *Elsevier, Amsterdam*, 205-307.

RAMSAY, J.G., 1967 - Folding and Fracturing of Rocks. *McGraw-Hill, New York*, 568 pp.

READING, H.G., 1980 - Characteristics and recognition of strike-slip systems. *In:* BALLANCE, P.F., & READING, H.G. (Editors), Sedimentation in Oblique-slip Mobile Zones. *Special Publication of the International Association of Sedimentologists* 4, 7-26.

RIJSWIJK, J.B.H. van, & SCHALKWIJK, G., 1988 - Thermoluminescence of quartz as a sedimentary provenance study technique in the Proterozoic of the Paroo Range, Mount Isa Inlier, Queensland, Australia. *Contributions to the MIRTH project, Institute of Earth Science, University of Utrecht, Report No. 3, Bureau of Mineral Resources, Australia, Canberra*, 45 pp.

SHULTZ, A.W., 1984 - Subaerial debris-flow deposition in the Upper Palaeozoic Cutler Formation, Western Colorado. *Journal of Sedimentary Petrology* 54, 759-772.

SMITH, W.D., 1969 - Penecontemporaneous faulting and its likely significance in relation to Mount Isa ore deposition. *Geological Society of Australia Special Publication* 2, 225-235.

STEARNS, D.W., 1978 - Faulting and forced folding in the Rocky Mountains foreland. *In*: MATTHEWS III, V. (Editor), Laramide Folding Associated with Basement Block Faulting in the Western United States. *Geological Society of America Memoir* 151, 1-37.

STEARNS, M.T., & STEARNS, D.W., 1978 - Geometric analysis of multiple drape folds along the northwest Big Horn Mountain front, Wyoming. *In:* MATTHEWS III, V. (Editor), Laramide Folding Associated with Basement Block Faulting in the Western United States. *Geological Society of America Memoir* 151, 139-156.

STEWART A.J., 1989 - Extensional faulting as the explanation for the Deighton 'Klippe' and other Mount Albert Group outliers, Mount Isa Inlier, northwestern Queensland. *Australian Journal of Earth Sciences* 36, 405-421.

STEWART, A.J., this volume a - Geology of the Horse's Head structure, north of Mount Isa, and its bearing on the 'roof thrust + imbricate stack' hypothesis, Mount Isa Inlier, Queensland. *In:* STEWART, A.J., & BLAKE, D.H. (Editors), Detailed Studies of the Mount Isa Inlier. *Bureau of Mineral Resources, Australia, Bulletin* 243.

STEWART, A.J., this volume b - Stratigraphy, extension, and contraction in the Ballara - Mount Frosty area, Mount Isa Inlier, Queensland. *In:* STEWART, A.J., & BLAKE, D.H. (Editors), Detailed Studies of the Mount Isa Inlier. *Bureau of Mineral Resources, Australia, Bulletin* 243.

SWEET, I.P., 1983 - Discussion: A Proterozoic rift zone at Mount Isa, Queensland, and implications for mineralisation. BMR *Journal of Australian Geology & Geophysics* 8, 163-164.

SYLVESTER, A.G., 1988 - Strike-slip faults. *Geological Society of America, Bulletin* 100, 1666-1703.

SYLVESTER, A.G., & SMITH, R.R., 1976 - Tectonic transpression and basement controlled deformation in the San Andreas fault zone, Salton Trough, California. *American Association of Petroleum Geologists, Bulletin* 60, 2081-2102.

VAIL, P.R., 1987 - Seismic stratigraphy interpretation utilizing sequence stratigraphy, Part 1: Seismic stratigraphy interpretation procedure. *In:* BALLY, A.W. (Editor), Atlas of seismic stratigraphy. *American Association of Petroleum Geologists Publications, Studies in Geology* 27, 1-10.

VON WAGONER, J.C., MITCHUM, R.M., POSAMENTIER, H.W., & VAIL, P.R., 1987 - Seismic stratigraphy interpretation utilizing sequence stratigraphy - Part 2: The key definitions of sequence stratigraphy. *In*: BALLY, A.W. (Editor), Atlas of seismic stratigraphy. *American Association of Petroleum Geologists Publications, Studies in Geology* 27,11-14.

WERNICKE, B., & BURCHFIEL, B.C., 1982 - Modes of extensional tectonics. *Journal of Structural Geology* 4, 105-115.

WILLIAMS, G., & VANN, I., 1987 - The geometry of listric normal faults and deformation in their hanging walls. *Journal of Structural Geology* 9, 789-795.

WILCOX, R.E., HARDING, T.P., & SEELY, D.R., 1973 - Basic wrench tectonics. *American Association of Petroleum Geologists Bulletin* 57, 74-96.

WILSON, I.H., 1978 - Volcanism on a Proterozoic continental margin in northwestern Queensland. *Precambrian Research* 7, 205-235.

WILSON, I.H., DERRICK, G.M., HILL, R.M., DUFF, B.A., NOON, T.A., & ELLIS, D.J., 1977 - Geology of the Prospector 1:100 000 sheet area (6857), Queensland. *Bureau of Mineral Resources, Australia, Record* 1977/4, 197 pp.

WILSON, I.H., HILL, R.M., NOON, T.A., DUFF, B.A., & DERRICK, G.M., 1979 - Geology of the Kennedy Gap 1:100 000 sheet area (6757), Queensland. *Bureau of Mineral Resources, Australia, Record* 1979/24, 104 pp.

WILSON, I.H., DERRICK, G.M., & PERKIN, D.J., 1985 - Eastern Creek Volcanics: their geochemistry and possible role in copper mineralisation at Mount Isa, Queensland. *BMR Journal of Australian Geology & Geophysics* 9, 317-320.

WINSOR, C.N., 1983 - Syntectonic vein and fibre growth associated with multiple slaty cleavage development in the Lake Moondarra area, Mount Isa, Australia. *Tectonophysics* 92, 195-210.

WINSOR, C.N., 1984 - Solution transfer syn-S_2: an inferred means of deriving fault fill in the Lake Moondarra area, Mount Isa, Queensland, Australia, based on oxygen isotope results. *Journal of Structural Geology* 6, 679-685.

WINSOR, C.N., 1986 - Intermittent folding and faulting in the Lake Moondarra area, Mount Isa, Queensland. *Australian Journal of Earth Sciences* 33, 27-42.

WYBORN, L.A.I., & BLAKE, D.H., 1982 - Reassessment of the tectonic setting of the Mount Isa Inlier in the light of new field, petrographic, and geochemical data. Abstracts 11th BMR Symposium, Canberra, 4-5 May 1982. *BMR Journal of Australian Geology & Geophysics* 7, 143.

WYBORN, L.A.I., PAGE, R.W., & McCULLOCH, M.T., 1988 - Petrology, geochronology, and isotope geochemistry of the post-1820 Ma granites of the Mount Isa Inlier: Mechanisms for the generation of Proterozoic anorogenic granites. *Precambrian Research* 40/41, 509-541.

Page 74 is blank.

The Hero Fan Delta (Lower Mount Isa Group) and its structural control: deformation in the Hero/Western Fault Zone and Paroo Range compared, Proterozoic, Mount Isa Inlier, Queensland, Australia

W. Nijman [1], *H.F. Mijnlieff* [1], *and G. Schalkwijk* [1]

This paper is based on the following map: Nijman, W., 1991 - Geology of the Paroo Range - Hero/Western Fault Zone (1:20 000 scale map). Bureau of Mineral Resources, Canberra, Australia (two sheets).

This research project was supported by the Dutch Foundation 'Dr.Schurmann-fonds' with annual grants from 1987-1990.

The Hero and Western Faults diverge northwards from a restricting double bend in the Mount Gordon-Mount Isa Fault Zone between the Sybella Batholith in the south and a Leander Quartzite-cored dome in the north. Both faults form the western boundaries of outcrops of Lower Mount Isa Group, unconformably overlying Eastern Creek Volcanics.

The detailed map of the area (Nijman, 1991) shows only the last three phases of deformation. We relate the conjugate faults of the youngest phase to D^P_5 in the easterly adjacent Paroo Range. During the preceding D^P_4 phase, the Western Fault served as a dextral transfer fault to a system of south-block- down listric normal faults in the Paroo Range. Vertical to steeply plunging drag folds and vertical duplexes are associated with this transtension. At the same time the Hero Fault Zone was subject to sinistral simple shear shown by vertical S-folds. Before this deformation, north-oriented kilometre-scale D^P_3 folds were formed by regional east-west compression recognised throughout the entire Mount Isa Inlier. During or near the end of this phase, the Hero Fault was a steep east-verging upthrust with the Hero Anticline in the hanging wall and the Hero Syncline in the footwall.

Pre-D^P_3 deformation is unclear from direct structural analysis, but is evident in the sedimentary record. Clast shape, composition, and palaeocurrent pattern of the Hero Formation (new name), a coarse alluvial fan delta facies at the base of the Lower Mount Isa Group, indicate an active fault-controlled(?) uplift nearby to the west, possibly the Mount Gordon Arch of Derrick (1982). Observed asymmetry and southward depocentre shift of this Hero Fan point to sinistral strike slip on the fault. Since the stratigraphic position of the Hero Formation is the same as that of the Lower Mount Isa Group clastic wedge in the nearby Paroo Range, this synsedimentary fault control is assigned to phase D^P_{1b}, distinguished by our group in that area.

En-echelon faults within the Eastern Creek Volcanics of the Hero Fault Zone are truncated by the Mount Isa Group Unconformity, and therefore apparently belong to the earliest D^P_1 deformation recognised in the area. When back-rotated by restoring the unconformity to horizontal, the fault pattern indicates pre-Mount Isa Group and post or syn-Haslingden Group (D^P_{1a}) north-south extension.

This sequence of events leaves the possibility open of the existence of D^P_2 low-angle thrusting, such as recognised in the Paroo Range. Intense brecciation, pebble stretching, and mineralisation at the Hero Fault suggest that D^P_1 might have been linked to D^P_3 by a low-angle D^P_2 thrust phase as a precursor to later upthrusting.

The data from the Hero/Western Fault Zone and the Paroo Range indicate almost continuous east-west compression and north-south tension, concurrent with north-south strike-slip changing from transtensive to transpressive over distances of a few tens of kilometres. Whether the fundamental regime was strike-slip with subordinate tension and compression, or alternating compression and tension with strike-slip transfer faulting as a derivative, remains at present unanswered, although we prefer the former. Our data from this western part of the Mount Isa Inlier seem to corroborate those of Loosveld (1989) from the easternmost part near Cloncurry, suggesting that these areas were the shoulders of a basin for which the Kalkadoon Basement formed the centre.

[1]Department of Geology, Institute of Earth Sciences, University of Utrecht, Postbus 80021, 3508TA, The Netherlands.

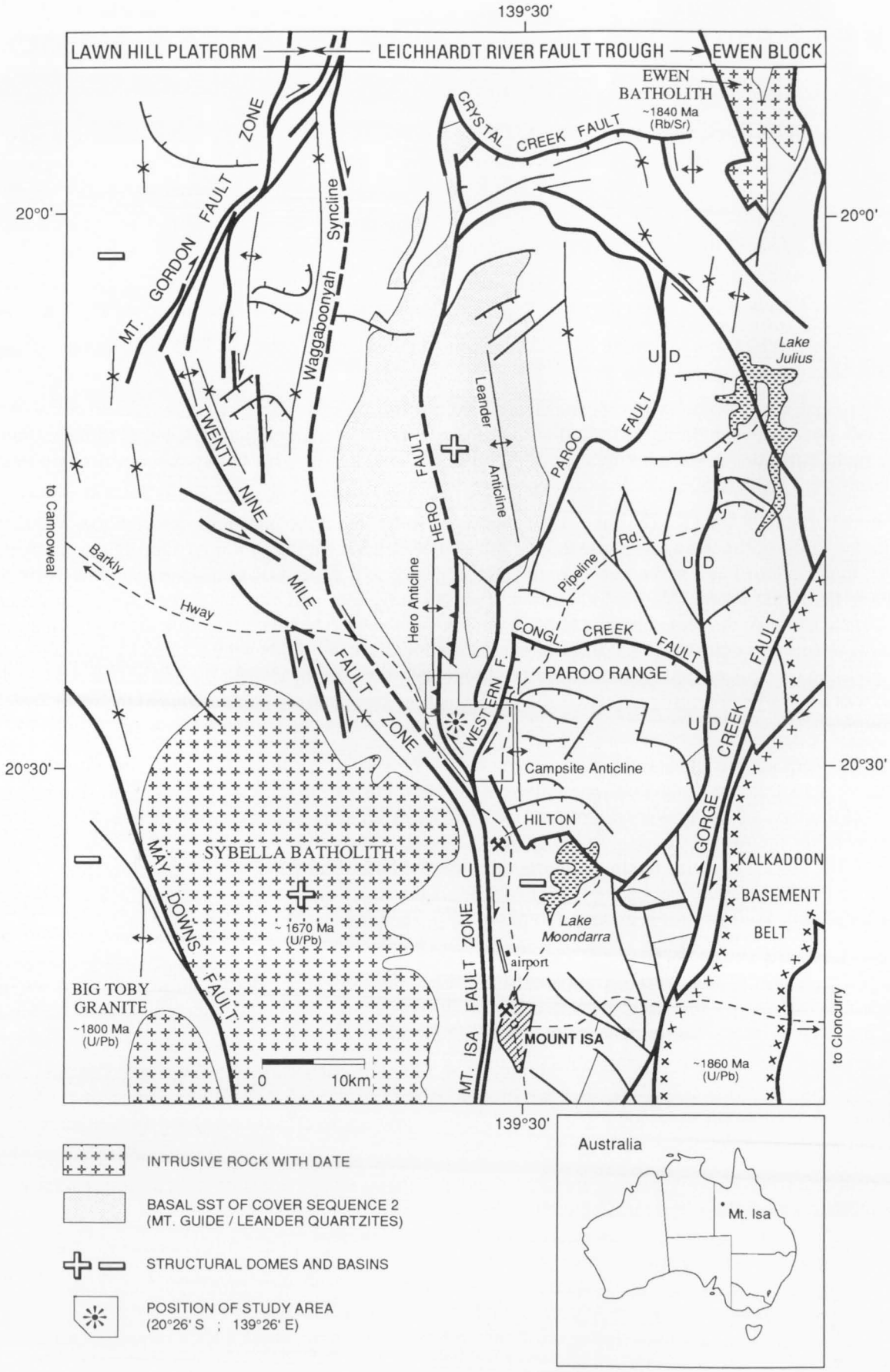


Fig.1. Location of the Hero/Western Fault Zone (asterisk) in the Mount Isa Inlier. Geology modified after Blake (1987). White areas are undifferentiated Proterozoic and Paleozoic rocks.

Introduction

This paper presents an evaluation of the relationships between the structural geology and sedimentology of the Proterozoic coarse clastics of the Hero and Western Fault Zone, 30 km north of Mount Isa (Fig. 1 and sheet 2 of Nijman, 1991). Field work was done from 1987 to 1990. The paper is complementary to Nijman & others (this volume) on the easterly adjacent Paroo Range.

The Hero/Western Fault Zone is a north-trending fault and fold complex approximately 10 km wide situated in the southeast corner of the Kennedy Gap 1:100 000 Sheet area (Wilson & others, 1979; Fig. 1). The stratigraphic sequence in the area, from oldest to youngest, comprises the Leander Quartzite and Eastern Creek Volcanics (ECV) of the Haslingden Group (cover sequence 2 of Blake, 1987), unconformably overlain by the Warrina Park Quartzite, Moondarra Siltstone, Breakaway Shale, and Native Bee Siltstone of the Mount Isa Group (cover sequence 3).

The Hero Fault (Figs. 1, 2) juxtaposes the Hero Anticline, cored by Leander Quartzite, with a tight syncline on its eastern side, the Hero Syncline, in which the Lower Mount Isa Group unconformably overlies the Eastern Creek Volcanics. Farther east, the latter surround an outcrop of Leander Quartzite in the southerly plunging Leander Anticline. The Western Fault separates this domain from a folded fine-grained sequence (Moondarra Siltstone to Native Bee Siltstone) in the western limb of the Campsite Anticline of the Paroo Range.

On a regional scale (Fig. 1), the area is situated within the north-trending Leichhardt River Fault Trough (LRFT), 60 km wide and 325 km long, in the west of the Mount Isa Inlier (Blake, 1987). Whether or when the trough was fault-bounded on both sides (Derrick, 1982; Neudert, 1983) is problematic (compare Lochem & others, 1988). Basement rocks crop out on both sides of the study area: the Yaringa Metamorphics (>1890 Ma, U-Pb zircon), the Big Toby Granite (1804 Ma, U-Pb zircon), and the Sybella Batholith (1670 Ma, U-Pb zircon) on the west side; the Kalkadoon Basement (1856/1862 Ma, U-Pb zircon) on the east side; and the Ewen Batholith (1840 Ma, Rb-Sr) to the northeast (isotopic dates from Wyborn & others, 1988; Blake & others, 1990). Intrusion of the Sybella granite started shortly before deposition of the Mount Isa Group.

Thermoluminescence of detrital and basement quartz grains indicates provenance solely from the east side of the trough for the basal part of the Haslingden Group, and solely from the west for the Myally Subgroup and Lower Mount Isa Group (Rijswijk & Schalkwijk, 1988).

Major fault zones separate the LRFT from the basement and from other adjacent structural units. The Mount Gordon Fault Zone divides the LRFT from the Lawn Hill Platform to the northwest. Stratigraphically, however, the platform sequence overlies LRFT rock. The fault zone continues southeastwards via the Twenty Nine Mile Fault Zone into the south-striking Mount Isa Fault Zone (Fig. 1). From Hilton Mine southwards, the latter fault zone is composed of a set of reverse faults (Glikson & others, 1975) dipping 75-80° west. Figure 1 illustrates that the Twenty Nine Mile Fault Zone also separates the dome of the Sybella Batholith from the one formed of Leander Quartzite and intersected by the Hero Fault.

The structural history of the Mount Gordon-Mount Isa Fault Zone is complex, since it has been demonstrated that both large dextral strike-slip and west-block-up (Sybella basement) or -down (late stage of the Lawn Hill Platform) movements have taken place (Mathias & others, 1973; Glikson & others, 1975; Blake, 1987). At the time of deposition of the Haslingden Group, the Mount Gordon and the Mount Isa Faults were probably initiated as respectively the western and eastern boundary faults of the Mount Gordon Arch (Derrick, 1982). Palaeogeographically, our study area may be thought of as situated on the eastern flank of this high.

Other structural elements known of in the region are:

- 1. Pre-main folding structures, including east-trending folds, south-verging thrusts (Bell, 1983), synsedimentary faults (Derrick, 1982), flower structures, and west-verging thrusts (Lochem & others, 1988; Nijman & others, this volume).

- 2. Post-main folding, east-striking arcuate faults with large vertical south-block-down movement such as the Crystal Creek and the Conglomerate Creek Faults (Fig. 1), and which repeat strata. The interpretation of the dip direction and angle, timing, and the type of such faults is still controversial (Dunnet, 1976; Derrick, 1982; Bell, 1983; Nijman & others, this volume; Stewart, this volume).

- 3. A later conjugate set of northwest-striking sinistral and northeast-striking dextral strike-slip faults segments the area (Blake, 1987). The large Gorge Creek Fault, separating

the Kalkadoon basement block from the LRFT in the southeast, belongs to this system.

Much attention has been paid to the coarse clastic facies of the Lower Mount Isa Group along the Hero Fault, composed of proximal fanglomerate and distal fan sandstone bodies within a Moondarra Siltstone facies. Firstly, proximal coarse clastic facies are sensitive to structural control (compare Colella & Prior, 1990) and may record early synsedimentary structural events of which little is known in the Mount Isa Inlier, and which cannot be easily detected solely by structural mapping and analysis. Secondly, proximal deposits of this sort are relatively rare because of their low preservation potential. When preserved, they add substantially to the completion of a palaeogeographic and tectono-sedimentary synthesis of a basin. In our area, they form the primary influx of sediments belonging to the Lower Mount Isa Group, the more shoreward equivalents of which have been studied by our group in the easterly adjacent Paroo Range. In this paper we compare the geologic histories of both areas to place them within the sequence of events known from other parts of the Mount Isa Inlier.

Deformation phases (D), fold axes (B), foliations (S), and faults (F) in the Hero/Western Fault Zone are denoted by a superscript 'P', like those distinguished in the Paroo Range by Nijman & others (this volume). D^P_3 refers to the main phase of north- trending upright folding, which corresponds to D_2 of Bell (1983).

Structure of the Western Fault Zone

The Western Fault Zone was mapped by Schalkwijk in 1987 (Fig. 2 and Nijman, 1991, sheet 2). Data were compared and added to those of existing maps (Perkins, 1970). Folds are mainly macro (>100 m) and mesoscale (10-100 m) in size. Microscale folds (m) are relatively rare, generally open to close, but in places tight. Faults are characterised by cataclastic ferruginous bands, quartz accumulations, heavily foliated ferruginous zones, and quartz-rich breccia.

The main structures in the area are (Fig. 2):

- a northwest-trending fold system, which interferes with a northeast-trending syncline to form a dome-and-basin structure. This pattern is obliquely truncated by :
- the Western Fault system, consisting of the Western Fault proper, which separates the folded Mount Isa Group sediments from the Eastern Creek Volcanics to the west; and

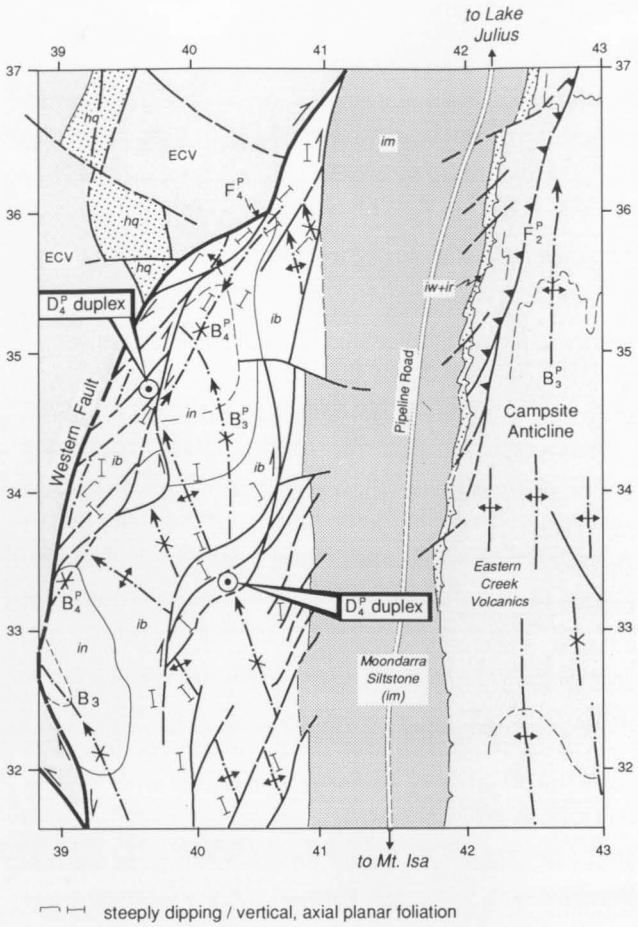


Fig. 2. Structural map of the investigated segment of the Western Fault Zone and the adjacent Campsite Anticline. Note the vertical duplex structures and the crossing of B^P_3 and B^P_4 fold axial plane traces. *iw + ir*, Warrina Park Quartzite and Surprise Creek Formation; *im*, Moondarra Siltstone; *ib*, Breakaway Shale; *in*, Native Bee Siltstone. P omitted from stratigraphic symbols for clarity. Numbered ticks are 1000 m intervals of Australian map Grid Zone 54.

associated minor northeast-striking faults, roughly parallel to it in the form of strike-slip duplexes (Woodcock & Fisher, 1986).

Three deformation phases have been recognised. The first is the main phase of folding, D^P_3; subsequent deformations can be correlated with D^P_4 and D^P_5 in the Paroo Range.

D^P_3-folding

The Western Fault truncates the western limb of a large-scale D^P_3 anticline, the Campsite Anticline in the Paroo Range. Second- order folds are found obliquely superposed on this limb. The fold axis in the centre of the fold bundle plunges 45°/325° on the basis of the S_0-girdle distribution (n = 95). Southwards, the fold pattern converges to a due north plunge outside the map area.

Mesoscale D^P_3-folds are mainly symmetric and open, with half wave-lengths between 10 and 50 m. The axial plane cleavage (S^P_3) is well-developed, but patchy. It is truncated by faults of all phases, an argument in favour of its belonging to the regional main phase of deformation (see section below on 'Interpretation and discussion').

Western Fault system

The Western Fault system consists of a 0° to 020°-oriented master fault with right-stepping double bends, with which are associated vertical strike-slip duplexes. Most structures near the faults can be related to their motion.

One set of faults parallels the Western Fault, and forms a duplex in the centre and southeast of the area (grid reference 402334). These are vertical oblique-slip faults, sharply delineated by 5-10 cm-thick ferruginous quartz breccia, or, mainly in their northeasterly segments, by strongly foliated zones 3-5 m wide. The displacement along these faults is relatively small, and in its dextral oblique south-block-down movement, compares with that of the Western Fault. Strain analysis yields sigma-1 orientations of 45°/250° and 60°/245°.

Another duplex immediately adjacent to the Western Fault (between grid reference 389333 and 405360) contains several sets of mesofaults with dextral horizontal offset and, in places, steeply (50°) south-plunging striations. Z-folds with subvertical axes along the Western Fault and sets of associated tension gashes support the inference of a northeasterly-oriented maximum compressive stress component. A fault plane solution yields a 50°?/200° orientation for sigma-1. All of these data are consistent with dextral oblique slip.

The inferred fault regime of the Western Fault System was therefore one of dextral oblique slip, west-block-up; the double bend is a releasing bend (Biddle & Christie-Blick, 1985) and the associated en-echelon fault patterns are likewise releasing duplexes. The Western Fault system truncates D^P_3-folds and foliations, and where it joins the Conglomerate Creek Fault, is offset by northwest-striking D^P_5 faults (see structural sketch in Nijman, 1991, sheet 2); it is therefore assigned to the D^P_4 phase.

D^P_4-associated fold interference patterns

A single D^P_4 syncline parallel to the northeasterly-striking segment of the Western Fault overprints the D^P_3-fold pattern, creating a structural basin (grid reference 400350; Figs. 2, 4). It is truncated by the duplex adjacent to the Western Fault, but can still be seen to interfere with the westernmost D^P_3 syncline before meeting the master fault. Small-scale open to tight, in places chevron-like, slightly asymmetric parasitic folds with wave-lengths of 6 to 10 m occur in a thin-bedded alternation of siltstone and shale. Fold axes plunge 70°/210° and 60°/030°. In places, axial plane cleavage (S^P_4) strikes 023° east with subvertical dip.

A subvertical 040°-oriented simple shear foliation transects these folds, and seems to be related to the Western Fault. Some of the activity along the fault therefore postdates the interference pattern. But since the northeast-oriented syncline and its axial plane cleavage are restricted to a domain adjacent to the Western Fault, where the latter obliquely dissects the preceding D^P_3-folds (Fig. 4), we interpret it as a syn-dipslip drag-syncline, exactly as observed in the Paroo Range in relation to D^P_4-spoon faults. This supports the idea of a close relationship between the oblique slip of the Western Fault and the D^P_4 spoon faults in the Paroo Range (see section below on 'Interpretation and discussion').

D^P_5 east-striking faults

D^P_5 is sparsely represented in the area by a set of minor east-striking faults. Vertically plunging drag folds indicate sinistral strike-slip motion.

Fracture analysis

Due to the lithological homogeneity of the predominating massive shale, strain analysis in this area of high-level brittle deformation had to rely largely upon fractures as kinematic indicators. Fracture orientations are independent of bedding plane orientation, and are commonly associated with mesofaults.

Poles to 117 fractures yield a diffuse asymmetric girdle around the perimeter of the stereogram, multimodal to the level of 3 to 4 times uniform, from which can only be concluded that the fracture orientation does not statistically deviate from a mean vertical orientation. We therefore isolated from this population 42 conjugate pairs from as many sample localities. The corresponding components of these pairs were plotted and contoured separately (Fig. 3a, b). The orientation of one set of fractures (Fig. 3a) has an elongate maximum at 3 times uniform with two submaxima at 5 and 6 times uniform, respectively. The best fitting great circle to this distribution gives a mean fracture orientation of 092°/75° and relates to a statistically significant point maximum. The second set (Fig. 3b) shows a single elongate significant maximum at 5 times uniform, corresponding to a fracture orientation of 319°/89°. Considered as shear fractures (Riedel and anti-Riedel, Fig. 3b) in direct, or in the case of stress release, indirect response to the maximum stress

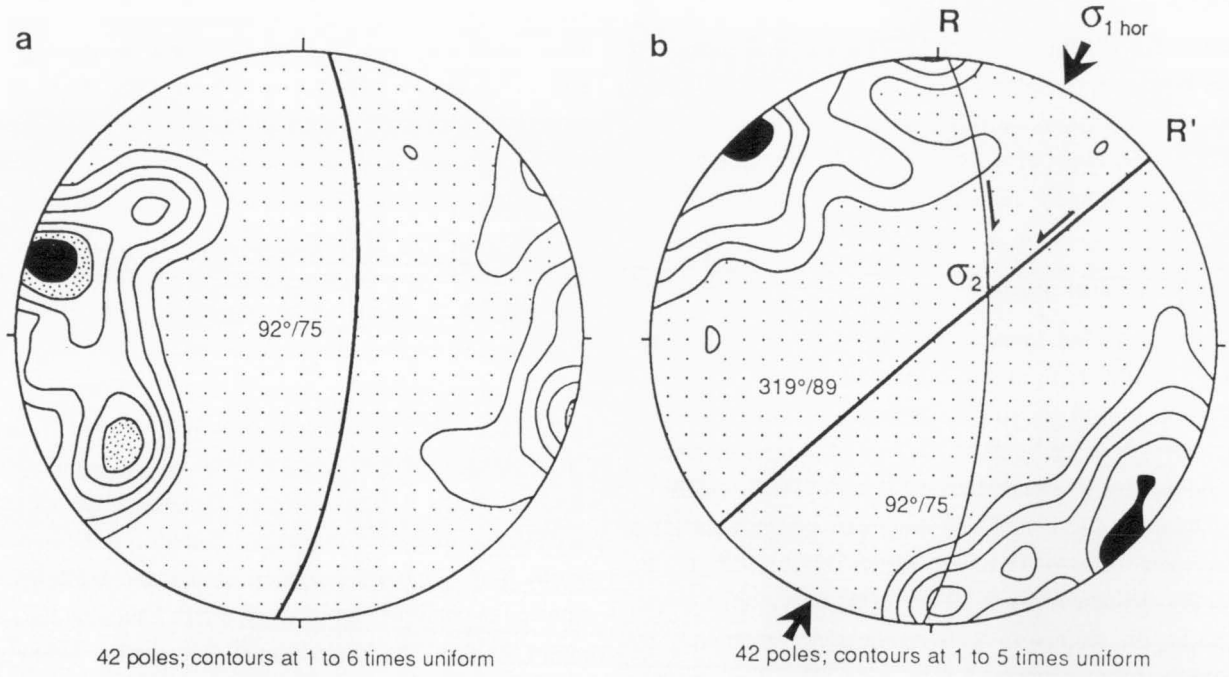


Fig. 3a. Contoured Schmidt equal-area plot of poles to fractures for one component of conjugate pairs at 42 localities in the Western Fault Zone; the plot shows an elongate maximum with two submaxima. The best-fitting great circle corresponds to a mean fracture orientation of 092°/75°. Fig. 3b. The same plot for the other component of the conjugate pairs shows a single elongate maximum and a mean fracture orientation of 319°/01° (thick line). Together with the other fracture orientation (thin line) and interpreting both as shear fractures (R: Riedel, R': anti-Riedel), this conjugate set points to a maximum horizontal compressive stress (sigma-1$_{horiz}$) oriented 22°/202°E (sigma-1 = 202°/19°) with sigma-2 oriented 049°/70°, which corresponds to dextral strike slip on the Western Fault.

component (Mandl & others, 1977; Hancock, 1985), the two mean fracture orientations yield sigma-1 at 202°/19° with sigma-2 subvertical (049°/70°) The pronounced submaxima in the Riedel distribution can be explained by rotation and flexuring during their formation (Tchalenko, 1970; Naylor & others, 1986). The deduced stress orientation fits the other observations reasonably well, and points to dextral oblique slip along the Western Fault. As described in the section below on 'The Hero Fault', fracture distribution and stress orientation along that fault are the mirror image of those along the Western Fault.

Leander Anticline

To the northwest of the Western Fault, a block of Leander Quartzite stands isolated within Eastern Creek Volcanics (grid reference 395360; Nijman, 1991, sheet 2; Fig. 1). All the contacts of this block with its surroundings are tectonic. The 1:100 000 geologic map suggests the block results from north-south extension and fragmentation of the Leander Anticline.

Interpretation and discussion

The earliest structures recognised are the northwest-trending folds. They closely resemble those generated by a post-main phase of folding recognised by others in various localities (i.e., Perkins, 1984; Winsor, 1986; Blake, 1987). Throughout the region they are of only local importance and seem to be associated with faults with a dextral strike-slip orientation. Winsor (1986) recorded this folding in the Lake Moondarra area in proximity to the Paroo and Mount Isa Faults as generally north-plunging flexures which trend north-northwest at between 8° and 15° to the north-striking faults, postdating them. He also contends that the associated slaty cleavage is strongest immediately east of the Mount Isa Fault Zone.

Post-main phase folds also occur in the Urquhart Shale at Mount Isa Mine. The so-called 'mine folds' and the Mount Isa Fold belong to this deformational phase (our D^P_4, i.e., D_3 of Bell [1983], Perkins [1984], and Bell & others [1988]). The Mount Isa Fold has an amplitude of 190 m with a wave length of 200-400 m, but the 'mine folds' normally occur in 10-20 m-wide zones, with amplitudes between one and 90 m. Fold-axis orientation in the mine ranges between 325° and due north, with plunges of up to 80° (Mathias & Clark, 1975). Wilson (1975) also mentioned folds of similar style and orientations in the Mount Isa Fault Zone.

Along the Western Fault we did not observe such overprinting by northwest-oriented folds and axial planar

foliations of pre-existing regional north-south folds and north-striking foliation. Rather the 'en-echelon' folds seem to have been superposed on and deflect into, and therefore to have been syngenetic with, larger main-phase folds. The observed fanning towards the Western Fault could just as well be explained by bending into a position at right angles to the sigma-1 component of the dextral oblique slip induced by that fault (compare the $F_{2/3}$ anticline between Lake Moondarra and the Mount Isa Fold Zone in Winsor, 1986: p.38). If elsewhere a distinct foliation has been superimposed on the main-phase folding and foliation, this merely illustrates that both phases could have developed in an east-west compressive regime (our D^P3) that gradually gave way to a strike-slip regime or became modified by it.

The Western Fault joins the Conglomerate Creek Fault in the northwest corner of the Horse's Head, northwest of the Paroo Range (Nijman & others, this volume; Fig. 1; Nijman, 1991, sheet 2); the latter fault has a long history of motion, that certainly reached a climax during D^P4 tension in the Paroo Range area. The timing of the Western Fault's main activity corresponds with that of the east-west listric normal faults of Dunnet (1976) and of Nijman & others (this volume).

Dextral oblique slip along the Western Fault threw the Mount Isa Group against the ECV, but absolute displacement cannot be calculated. The vertical component may have caused the development of a 'drag'-syncline along the fault, with associated very localised cleavage such as described and discussed for the D^P4 faults by Nijman & others (this volume). As in the Paroo Range, these drag folds interfere at right angles with the main-phase folds, but abut the spoon faults at a narrow angle where the latter curve away from a purely east-west strike (Fig. 4).

Since they transect the drag syncline related to a master fault that had already progressed almost or completely towards the surface, the vertical duplexes are relatively late-D^P4, and cannot be interpreted as precursor structures (e.g., Riedel faults).

Because of the mutual relations between tensional faulting, oblique slip, and drag synclines, all during D^P4, the Western Fault was a transfer fault (Gibbs, 1984) delimiting a domain of north-south extension in the Paroo Range area (Fig. 4). In other words, the Western Fault served as a western lateral ramp to a major listric fault block delimited to the north by the Conglomerate Creek Fault and encompassing the entire Paroo Range and the area immediately adjacent to it towards the south.

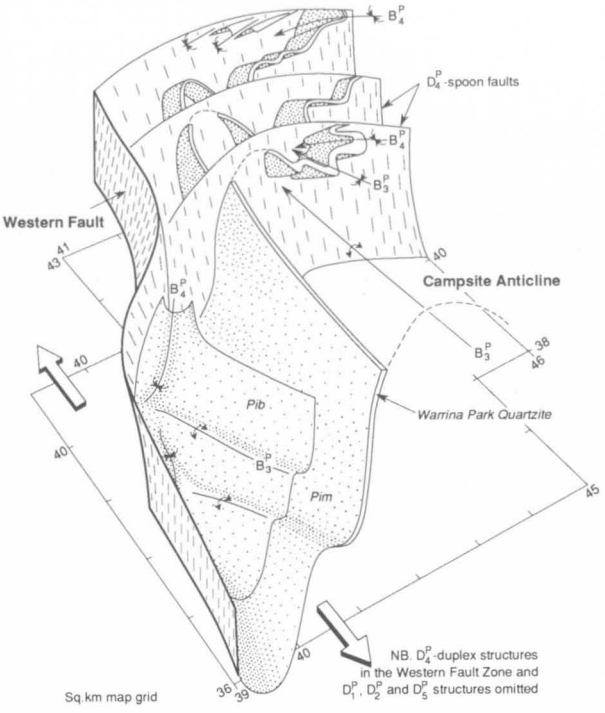


Fig. 4. Block diagram showing the relationship between dextral oblique slip at the Western Fault as transfer to D^P4 extensional faults in the Campsite Anticline/Paroo Range. Note the drag-synclines (B^P4) in en-echelon arrangement close to the curved D^P4 fault planes and at high angles to the regional north-south folds (B^P3).

The structural history of the Western Fault Zone can be summarised as follows:

- 1. Regional east-west shortening forming north-south folds (D^P3 in Nijman & others, this volume).
- 2. North-south major dextral strike-slip with an important vertical east-block-down motion; bending of D^P3-folds; subsequent development of a drag syncline and ultimately formation of vertical duplexes at bends in the master fault (D^P4).
- 3. Late east-west minor sinistral strike-slip faulting (D^P5).

Structure of the Hero Fault Zone

A 16 km^2 area along the Hero Fault was mapped in detail by Mijnliefff and Nijman (Fig. 5; Nijman, 1991, sheet 2). Depth extrapolation in the northern cross-section, X-Y (Fig. 5, inset), has been obtained from drilling data provided by Mount Isa Mines Exploration Department. The southern cross-section, A-B, is part of the east-west section A-E of Nijman (1991, sheet 1) from the Hero Fault

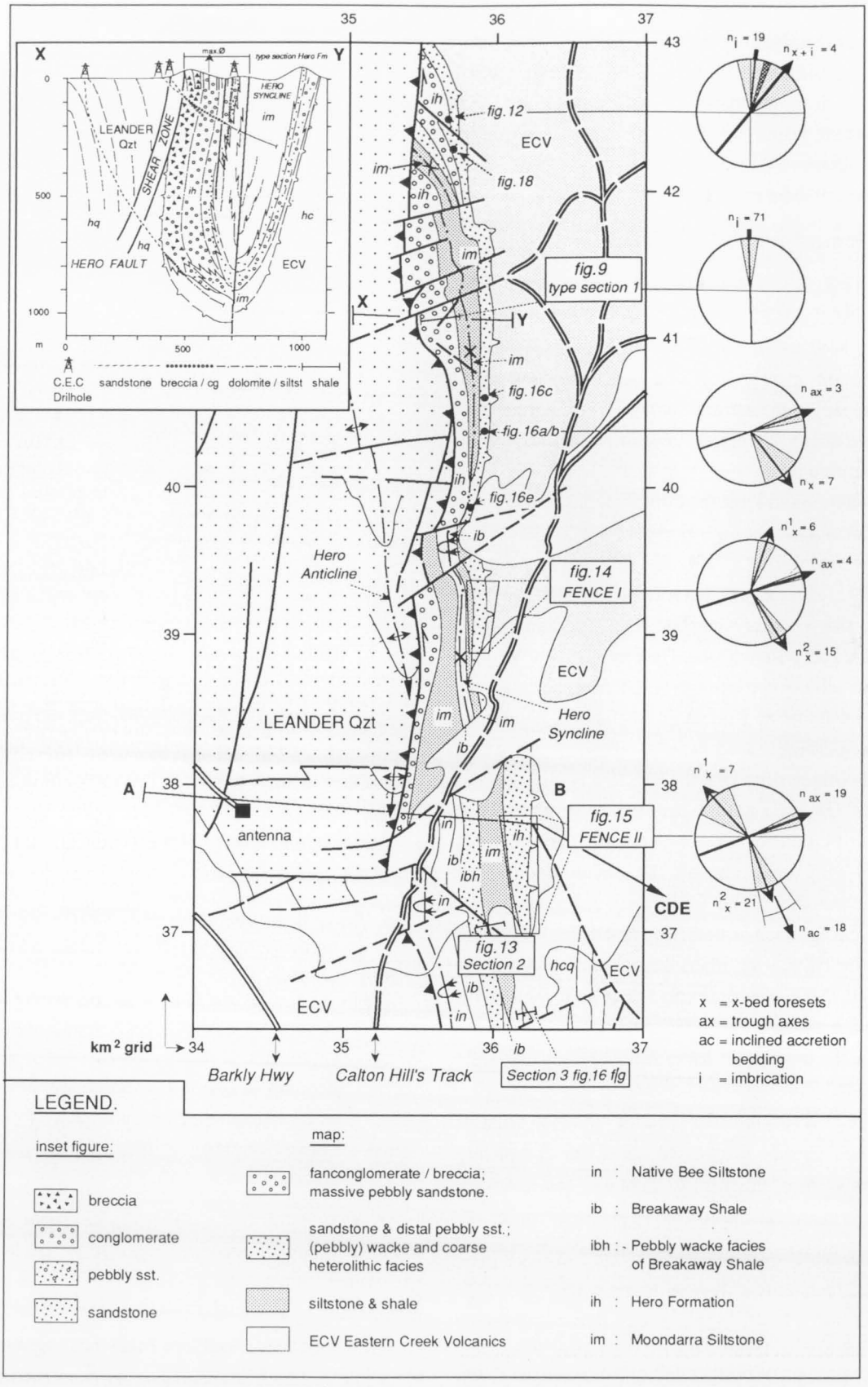


Fig. 5. Geologic map of the segment of the Hero Fault Zone that includes the outcrop of the Hero Formation, with the observation points mentioned in the text. For more detail of the facies distribution within the Hero fan delta, see Nijman (1991, sheet 2). On right, mean palaeocurrent vectors with standard deviations show a pattern of north to northeast dispersal of clastics in the north, east dispersal in the east and southeast. Inset figure shows cross-section X-Y over type locality of the Hero Formation, constructed from outcrop and borehole data. Trace A-B forms part of the east-west cross-section A-E of Nijman (1991, sheet 1). Numbered ticks are kilometre intervals of Australian Map Grid Zone 54.

to beyond the Paroo Range. The structures in the ECV between the Hero Syncline and the Western Fault have been mapped mainly from aerial photographs, augmented by photo-interpreted data from the 1:25 000 scale geological compilation sheets of the Kennedy Gap 1:100 000 geological map (BMR 1974).

Pre-/syn-Mount Isa Group structures (D^P_1)

Early deformation is shown by the Lower Mount Isa Group Unconformity truncating the ECV in the eastern limb of the Hero Syncline (Fig. 5). The palaeosurface is indicated by weathering of the ECV at the contact. The unconformity can be directly related to the one below the Surprise Creek Formation in the Paroo Range area (Nijman & others, this volume; see cross-section A-C in Nijman, 1991, sheet 1; Fig. 8).

The extensive outcrop of ECV east of the Hero Syncline has an estimated thickness of about 3 km (Fig. 6) of Cromwell Metabasalt (Phc; Nijman, 1991, sheet 2). We correlate the bundles of sandstone in the southwest corner of the outcrop area with those occurring elsewhere in the top of the Cromwell Metabasalt (Phc_q), but they could also represent the pinch-out of the Lena Quartzite.

At grid reference 363377, a northwest-striking, now vertical, quartz-rich and ferruginous fault zone traverses the ECV. Where the fault meets the Mount Isa Group Unconformity, a fault breccia occurs, composed of siltstone and fragments of weathered volcanics. The fault was active during Mount Isa Group deposition, but the offset below the Mount Isa Group Unconformity is much larger, indicating its early existence.

After the unconformity is restored to the horizontal, bedding dips 25° north and the fault 35° south or southeast, which geometrically classifies it as low-angle. The fault can be traced on aerial photographs as a structural discontinuity bending southwards below the alluvial cover of the Paroo Creek, and separating two domains: to the east the regularly steeply northwest-dipping Cromwell Metabasalt is cut by 320°-striking faults; to the west, a sequence of basalt, ferruginous and feldspathic sandstone, and siltstone (Phc_q; grid reference 367361), shows a more complicated fault pattern. Farther north, west of the Paroo Creek, this sort of discontinuity can also be observed where the uppermost level of the ECV is patchily exposed, and shows more evidence of folding (grid reference 368396) and disruption than the far more regularly dipping block-faulted domain of underlying ECV. Most of the 320°-striking faults in this monocline cannot be traced beyond the boundary between the two domains, and therefore may belong to the same early generation.

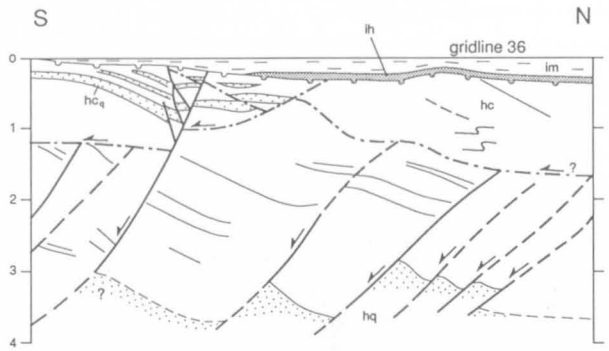


Fig. 6. Restored cross-section along north-south gridline 36 parallel to the axial plane of the Hero Syncline, showing D^P_{1a} pre-Mount Isa Group Unconformity structures in the Eastern Creek Volcanics. The cross-section suggests early south-verging extensional faulting, accompanied by block rotation and surficial collapse along low-angle detachments. *im*, Moondarra Siltstone; *ih*, Hero Formation; *hc*, Cromwell Metabasalt; *hcq*, sandstone in the top of *hc*, possibly belonging to the Lena Quartzite member; *hq*, Leander Quartzite. P omitted from stratigraphic symbols for clarity.

Because of the near-vertical bedding, the map pattern is almost a cross-section, which in Figure 6 has been restored with the base of the Breakaway Shale horizontal. The restoration strongly suggests that the structural discontinuity, observed as a gossanous fault where cut by the unconformity, could be explained as a south-facing low-angle listric detachment in the top of the Cromwell Metabasalt subject to block faulting and rotation due to a local north-south tensional regime. This phase of pre-Mount Isa Group deformation we label D^P_{1a}, analogous to the sequence of deformation of the Paroo Range (Nijman & others, this volume).

We conclude that northward tilting of the ECV before or during the formation of the Mount Isa Group Unconformity was accompanied by southward collapse tectonics along low-angle detachment planes, and that many of the northwest-striking faults in the Cromwell Metabasalt are of an early age. Some of them were reactivated during later phases. These conclusions are preliminary, and need confirmation.

Syn-Mount Isa Group deformation during this episode, apart from restricted reactivation of D^P_{1a} faults, is mainly recorded in the coarse clastic sediments along the Hero Fault, and is described below in the section on 'Mount Isa Group sedimentation in the Hero/Western Fault Zone'. There is no convincing evidence of D^P_2 pre-main phase low-angle thrusting, such as found in the Paroo Range.

Main-phase ($D^{P}3$) folds

The Hero Anticline and Syncline have all the characteristics of the regional main-phase $D^{P}3$ compressive folds. They are megascale folds, north-trending, upright to east-verging, inclined to overturned, and with a subvertical penetrative axial planar cleavage (Fig. 5).

The average fold axis orientation of the Hero Syncline is 28°/184° (parasitic folds: 46°/187°); the Hero Anticline also plunges south (grid reference 353394: 32°/192°). This south plunge in the Hero Fault Zone may be related to the sinistral sense of the post-$D^{P}3$ strike-slip component of the Hero Fault, in the same way as the north plunge near the dextral Western Fault may be related to $D^{P}4$-block rotation in the Paroo Range (compare Fig. 4).

The Hero Fault

The Hero Fault dips vertically to steeply west; in cross-section X-Y (Fig. 5, inset), borehole data (from Carpentaria Exploration Company) suggest a dip of 68° west. From north to south, the fault obliquely intersects the Hero Syncline, follows the steep limb common to the Hero fold couplet, then curves southeastwards into the Twenty Nine Mile Fault Zone, where it joins the Western Fault (Nijman, 1991, sheet 2; Fig. 5).

The Hero Fault is a very ferruginous and/or brecciated zone about 10 m thick, such as is observed in the $D^{P}2$ low-angle thrust zones of the Paroo Range (Nijman & others, this volume). At grid reference 354381, conglomerate pebbles are stretched with long axes vertical and intermediate and short axes approximately equal and horizontal. Vertical tensional quartz reefs are oriented normal to the strike of the fault.

Parallel to the Hero Fault in the north of the map area, a subvertical to steeply west-dipping fault follows the core of the syncline. The inferred relative movement is east-block-up in cross-section X-Y (Fig. 5, inset).

Further deformation related to the Hero Fault consists of small- to-mesoscale asymmetric S-folds on both limbs of the syncline (grid reference 355411). The fold axes plunge vertically to steeply south-southwest. Some of the folds break along north- northeast-striking sinistral fault planes (grid reference 358417). Such faults also diverge westwards from the Hero Fault. Several of these secondary features were observed around the type locality of the Hero Formation. At grid reference 355411, a shear zone branches off the southern hinge of a double bend in the Hero Fault proper. All these features fit an explanation by sinistral simple shear, then effective over the entire fault zone, the syncline included.

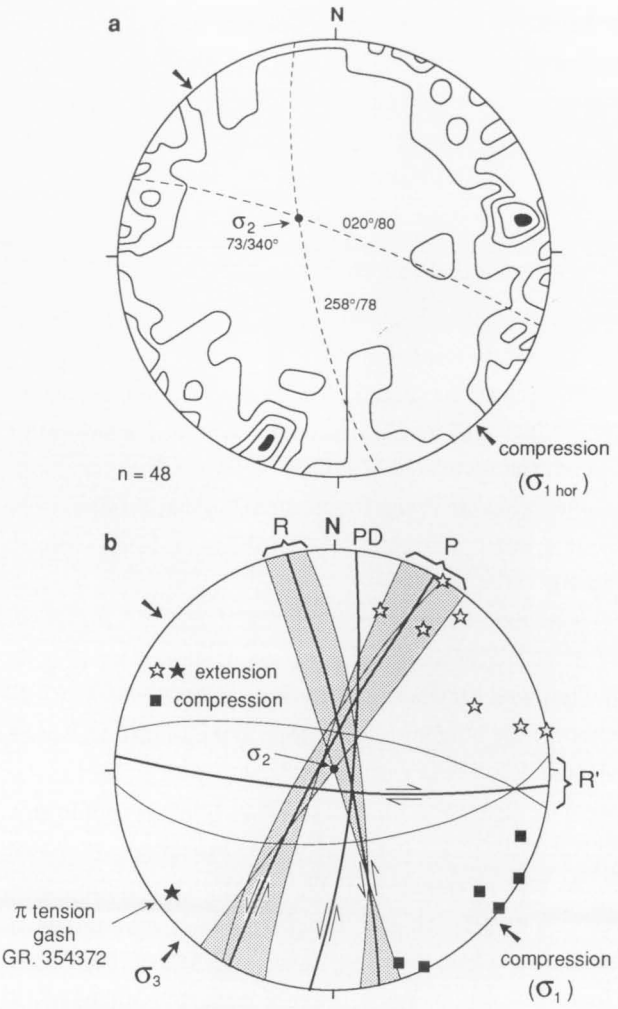


Fig. 7. Stress orientation at the Hero Fault: a. Contoured equal-area plot of poles to fractures; contours at 1, 3, 5, and 7% per 1% area. b. Plot of axes of shortening and extension derived from tension gashes at several localities along the Hero Fault, combined with great-circle projections of shear fractures at grid reference 354372. R, R', P, PD: Riedel, anti-Riedel, P shear, and Principal Displacement fractures. The stress orientations derived from the various data sets show a high degree of correlation, and indicate sinistral strike-slip on the Hero Fault.

Fracture orientations (Fig. 7a) on both sides of the Hero Fault show two distinct maxima, 258°/78° and 020°/80°. Interpreted as conjugate shear fractures (as done for the Western Fault), sigma-1 is oriented 320°, and sigma-2, the intersection of the fractures, 70°/314°. This pattern is mirrored around a north-striking vertical plane with the pattern at the Western Fault (compare Fig. 3). A sinistral simple shear regime along the Hero Fault is confirmed by measurements from tension gashes (Fig. 7b). Brittle fracturing in the fault zone at grid reference 354372 reveals

the complete set of R, R', P, and PDZ shears and tension gashes, yielding a sigma-1 orientation of 135 (Fig. 7b)

Where the Hero Fault bends towards the Western Fault, sinistral displacement is indicated by drag folding of the entire ECV-Mount Isa Group sequence.

Hence, the Hero Fault started with dip slip, which on the basis of brecciation and pebble stretching was produced by compression along a probably westward-dipping upthrust (originally an overthrust?). The pebble stretching implies ductile deformation, whereas other fault characteristics point to entirely brittle conditions. Subsequently, the Hero Fault accommodated sinistral strike-slip. The simple shear responsible for that effect generated the steeply plunging to vertical S-folds and associated faults in both limbs of the Hero Syncline.

Late faults

Both the Hero Syncline and Hero Fault are offset by 070°-striking faults, which refract into a due east strike in the Leander Quartzite of the Hero Anticline. Most of these faults have a dextral horizontal offset (grid reference 357397), but some are sinistral (grid reference 354413). Both are accompanied by mesoscale steeply to vertically plunging drag folds. Some have pronounced dip slip, such as the fault at grid reference 352376.

Summary and comparison of the deformation in the Hero Fault Zone and in adjacent areas

D^P_1-structures in the Hero/Western Fault Zone suggest local extensional south-block-down faulting superposed on a regional eastward tilt. The latter causes erosional truncation into successively deeper stratigraphic levels to the west, related to the rising of the Mount Gordon Arch. If we compare the D^P_1-faulting with coeval deformation in the Paroo Range, it resembles the early south-block-down effect along the transverse Conglomerate Creek Fault (Nijman & others, this volume). Neither in the Hero nor in the Western Fault Zone have D^P_1 structures been found directly related to early strike-slip, as they are in the Paroo Range.

D^P_2 structures, as in the Paroo Range, have not been identified in the Hero/Western Fault Zone. In the three areas, main-phase D^P_3-folds are alike in scale, geometry, and possession of a north-striking vertical axial plane cleavage.

Simple shear in the Hero Fault Zone predates D^P_5 faulting and postdates the Hero D^P_3-folds, and therefore is considered as D^P_4. Since the Hero Fault itself is deformed during this phase, its present geometry of an east-verging upthrust most probably relates to D^P_3 shortening. Structural observations alone do not clarify whether upthrusting was preceded by a D^P_1-stage of normal or strike-slip motion, and/or by a D^P_2-stage of low-angle thrusting as in the Paroo Range, although with opposite vergence. In the Paroo Range, an increase in P-T conditions towards ductility, such as suggested along the Hero Fault by pebble stretching, is also inferred and related to ferruginisation along the D^P_2-fault plane. Upthrusting probably continued during D^P_4 strike-slip given the southwest plunge of the D^P_4-folds.

By comparison, D^P_4 deformation at the Hero Fault can be summarised as left-lateral west-block-up transpressive oblique slip; at the Western Fault as east-block-down right-lateral transtensive oblique slip; and at the Mount Isa Fault - Twenty Nine Mile Fault Zone as west-block-up right-lateral transpressive oblique slip. This variation in an area of tens of square kilometres suggests strong strike-slip control during D^P_4, probably overlapping with the preceding and following phases of deformation.

Any better assessment of the behaviour of the Hero Fault depends on information derived from sedimentation patterns that were influenced by its early action (discussed below in the section on 'Deformation and sedimentation in the Hero/Western Fault Zone').

Finally, the late-stage faults, including the reactivated D^P_1 320°-fault system in the ECV, match the D^P_5 fault systems of the Paroo Range, which combine conjugate strike-slip faults due to continued east-west compression with dip-slip due to north-south tension.

Mount Isa Group sedimentation in the Hero/Western Fault Zone

The Mount Isa and McNamara Groups

The Mount Isa Group was originally defined by Bennet (1965) and redefined by Derrick & others (1976) as comprising eight formations. Only the four lowest are exposed in the area studied (Fig. 8): the Warrina Park Quartzite, which we will rename the Hero Formation in the Hero Fault Zone area, Moondarra Siltstone, and Breakaway Shale, which form a fining-upward megasequence called the Lower Mount Isa Group; and the Native Bee Siltstone, which contains coarser clastic sandstone bodies and forms the basal formation of a second fining upward megasequence, the Upper Mount Isa Group. To the Lower Mount Isa Group of the Paroo Range we have added the Surprise Creek Formation. Further details are given below in the section on 'Coarse clastic

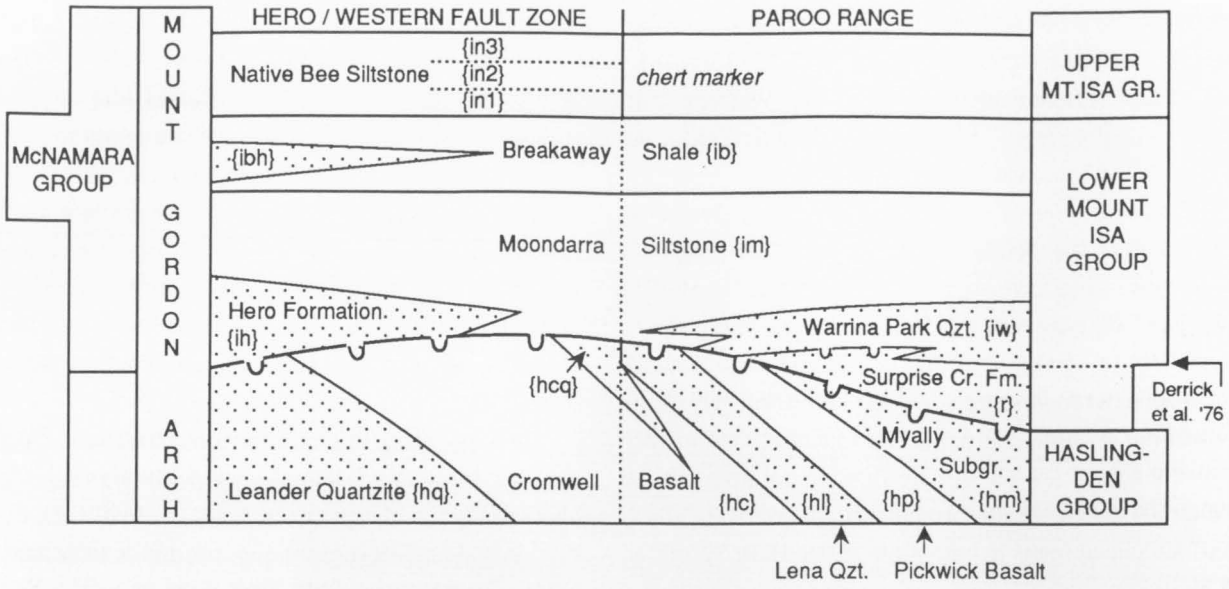


Fig. 8. Stratigraphic units in the Hero/Western Fault Zone and Paroo Range. The position of the Mount Gordon Arch (Derrick, 1982), separating the Mount Isa Group from its westerly time- equivalent, the McNamara Group, is also shown. P omitted from stratigraphic symbols for clarity.

facies of the Mount Isa Group: the Warrina Park Quartzite (Piw) and Hero Formation (new name; Pih)'

The McNamara Group is considered to be time-equivalent and lithologically comparable to the Mount Isa Group, but was deposited west of the Mount Gordon Fault Zone on the Lawn Hill Platform (Figs. 1, 8). According to Derrick (1982), this subdivision reflects the separation of the first-order basin, the LRFT, into two second-order basins by the Mount Gordon Arch, an emergent palaeohigh, active from the time of deposition of the Haslingden Group until that of the Lower Mount Isa Group. Units thin rapidly towards the arch while the sediments become more arenaceous and even conglomeratic, indicating proximity of the deposystems.

According to Derrick (1982), not only the palaeohigh, but also east-striking growth faults controlled sedimentation of the Mount Isa Group.

Fine-grained facies of the Mount Isa Group

The Moondarra Siltstone (Pim) attains a thickness of around 950 m in the Western Fault Zone, and consists of a relatively deeply weathered thin-bedded alternation of siltstone and shale, in places dolomitic. Bed thickness varies from 1-30 cm. Lamination is parallel and in places convoluted, and diagenetic iron-oxide colour banding is characteristic. Contacts with the underlying Warrina Park Quartzite and the overlying Breakaway Shale are conformable. In the Western Fault Zone, the Moondarra Siltstone probably lies immediately and unconformably upon ECV, because in the adjacent Paroo Range the underlying conglomerate and sandstone of the Warrina Park Quartzite and Surprise Creek Formation wedge out to the west and south, while onlapping the Mount Isa Group Unconformity (see cross-section B-D in Nijman, 1991). In the Paroo Range the Moondarra Siltstone also interdigitates with the Warrina Park Quartzite (Nijman & others, this volume; Fig. 8). In the Hero Fault Zone, lateral and upward transitions between Moondarra Siltstone and the coarser clastic facies of the Hero Formation are present (see section below on *'Facies G: Moondarra-type siltstone [Pim]'*).

On air photographs, the Breakaway Shale (Pib) is recognisable by its hills and ridges. Thickness varies between 400 and 650 m. The predominant rock type is a pale grey (especially in the upper part) or orange-and-purple laminated silty shale, which is vuggy, sericitic, siliceous, and includes siltstone laminae. Laminae are 1-7 mm thick. Massive shale occurs in places, and contains pyrite casts. The contacts of the Breakaway Shale with the overlying Native Bee Siltstone are gradational.

In the south of the Hero Syncline, part of the Breakaway Shale consists of a pebbly wacke facies (Pibh); this is described below together with the coarse clastic facies of the Lower Mount Isa Group in the section on *'Facies B: Fine-grained (pebbly) wacke facies (Pih_3) and (Pibh)'*.

The top of the succeeding unit, the Native Bee Siltstone (Pin), has not been preserved in the Hero/Western Fault Zone, so its thickness of 510 m is a minimum.

In the Western Fault Zone we distinguish three members ($Pin_{1,2,3}$: Nijman, 1991, sheet 2; Fig. 5) on the basis of minor lithological variations. The upper and lower members of the formation are easily eroded, and consist of thin-bedded (1-5 cm) ferruginous shaly siltstone with sandy beds, comparable to those of the Moondarra Siltstone. Channel fills, such as reported by Neudert (1983), have not been found. The middle member of the formation commonly forms low hills, and consists of massive shale with beds 10-15 cm thick, black siltstone, and, in its lower part, three or four chert beds, each about 5 cm thick (Fig. 8). According to Neudert (1983), the chert is stromatolitic wherever the primary structure survived silicification.

In the Hero Fault Zone, the formation was only briefly examined. Channel-fill sandstone was observed at the base.

Since the fine-grained facies were not a primary target of our investigation, their environmental interpretation is summarised from Neudert & Russell (1981) and Neudert (1983).

These authors interpreted the Moondarra Siltstone as a floodplain or flood basin deposit, relatively close to a clastic source. Synsedimentary faulting resulted in intercalated polymict conglomerate beds of limited lateral extent. The controlling faults are inferred to have had an east-west strike by Derrick (1982), but we shall show that north-south structures were also important.

Little is known of the Breakaway Shale, but its scarcity of current-produced structures suggests its environment was the most distal of the Lower Mount Isa Group.

In the Native Bee Siltstone, at the base of the Upper Mount Isa Group, Neudert (1983) recorded channel-fill sandy deposits within a floodplain to carbonate mudflat environment, indicating a more proximal character than that of the underlying Breakaway Shale.

The younger formations above the Native Bee Siltstone are perennial lake deposits, saline mudflats, and fan fringe deposits.

Coarse-clastic facies of the Mount Isa Group: The Warrina Park Quartzite (Piw) and Hero Formation (new name; Pih)

In our studies of the Mount Isa Inlier, we focussed on the coarse-grained clastics – conglomerate, breccia, and sandstone – as the more sensitive in recording structural control (compare Smith, 1969; Derrick, 1982). They are concentrated at the base of the Mount Isa Group, and in the existing maps and literature have been assigned to one formation, the Warrina Park Quartzite.

In the Paroo Range, the Warrina Park Quartzite consists of quartz arenite and well-sorted and rounded conglomerate deposited in a high-energy littoral environment (Nijman & others, this volume; compare Plumb & others, 1980). This description agrees with that of the type section by Derrick & others (1976). Although in places unconformities do exist at the base of the Warrina Park Quartzite in the Paroo Range, the underlying Surprise Creek Formation, the overlying Moondarra Siltstone, and the littoral sandstone of the Warrina Park Quartzite all appear to be intimately linked geometrically (Fig. 8). For this reason the Surprise Creek Formation, previously mapped as unconformably overlain by the Mount Isa Group, has been incorporated into the Lower Mount Isa Group, which thus forms an eastward-thickening clastic wedge (Nijman & others, this volume). The Mount Isa Group Unconformity, at the base of this wedge, truncates the Haslingden Group, whereas the Surprise Creek Formation, Warrina Park Quartzite, and Moondarra Siltstone onlap this surface to the west (Fig. 8).

Wilson & others (1979) described the Warrina Park Quartzite from several isolated outcrops in the Kennedy Gap Sheet 1:100 000 area as an assemblage of very immature ferruginous clastics, very different from those in the type section. One of these occurrences is found in the Hero Syncline. The conglomerate and sandstone of this area, although stratigraphically related to the littoral deposystem of the Warrina Park Quartzite of the Paroo Range, are not obviously directly connected to it. Since the two units also differ sedimentologically, we prefer to rename the clastics of the Hero Syncline the Hero Formation.

Sedimentology of the Hero Formation and Moondarra Siltstone

Terminology

The following terms are simplified from Miall (1985). Single rock types like trough cross-bedded sandstone, corresponding to the lithofacies of Miall, are named lithotypes, and we refer to Miall's (1978) and Shultz' (1984) lithofacies codes between square brackets. These lithotypes form facies, which have a geometric notion such as 'sheet' or 'ribbon' and/or a sequential trend, e.g., 'fining-upwards', and/or a genetic notion such as

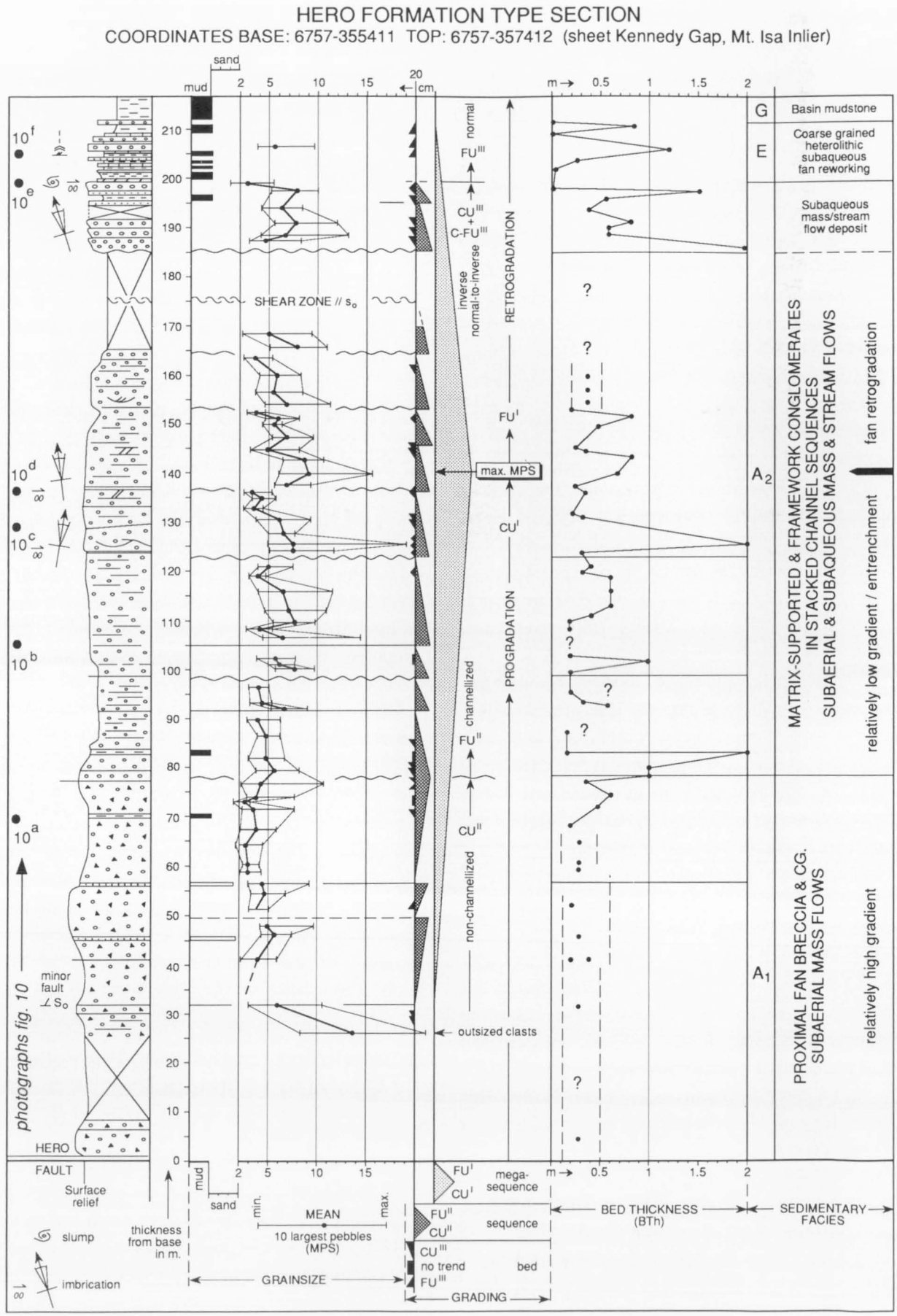


Fig. 9. Type section of the Hero Formation. Location in Figs. 5, 20. Description in text.

'fanglomerate' or 'mass flow'. The facies are indicated with italics: *Facies A-F* make up the Hero Formation (Pih), *Facies G* is the Moondarra Siltstone (Pim). *Facies B* also occurs intercalated in the Breakaway Shale (Pib), and is then denoted Pibh.

Facies combine in associations, which because of their genetic unilateral linkage, are called *(facies) tracts*, a term borrowed from the depositional system tracts of sequence stratigraphy.

Analysis of the coarse clastic facies of the Hero Formation is based on sedimentological logging at scales of 1:100, 1:200, and 1:400 at three localities (Fig. 5).

Continuous outcrop in ridges along the east limb of the Hero Syncline allowed the construction of fence diagrams at 1: 2500 scale, referred to as fences I and II. The facies description is further elaborated by palaeocurrent measurements and by determination of the ratio between MPS (Maximum Particle Size - the arithmetic mean of the ten largest clasts at a sample site) and BTh (Bed Thickness; Nemec & Steel, 1984).

The designated type locality is section 1, with the base at grid reference 355411 and the top at grid reference 357412. Paratype localities are in the finer-grained sandstone and conglomerate bodies of fences I (grid reference 358389 to 358393) and II (grid reference 362371 to 362379). All locations are indicated in Figure 5.

Type section

The type-section of the Hero Formation (Fig. 9) is composed of 212 m of conglomerate, breccia, and sandstone. This is a minimum thickness, as the base of the section is cut away by the Hero Fault. A combination of borehole data at the type locality (inset, Fig. 5), and mapping and observation at the paratype localities, indicates that only some tens of metres of the basal facies are missing from the type-section (Fig. 5, inset). At 175 m above the base of the section, a bedding-parallel shear zone occurs, related to the left-stepping bending of the Hero Fault. It does not seem to disturb the stratigraphic sequence. Some thickening might be expected from offsets along minor northeast-striking D^{P}_{4} sinistral tear faults.

Matrix-supported volcanoclastic breccia and conglomerate *(Facies A)* form the bulk of the type-section. Framework (clast-supported) conglomerate becomes increasingly important in the middle of the section, whereas heterolithic lithotypes *(Facies E)* prevail in the top 15 m (197-212 m in Fig. 9). The type-section is overlain by Moondarra Siltstone *(Facies G)*.

Facies and sedimentary environments of the Hero Formation

Facies A: Mass flow-dominated fanglomerate.

This facies dominates the lowest 197 m of the type- section (Figs. 9, 10). Based on grain-size grading, a hierarchy of trends can be identified at 100 m (megasequence), 10 m (sequence) and 1 m (bed) scale (Fig. 9). The higher-level (larger- scale) trend reflects facies tracts and fan behaviour, the intermediate trend the geometric aspects of the facies, and the lower-level (smaller-scale) trend the sedimentation mechanism (compare Heward, 1978).

The *megasequence* trend is defined by the enveloping surface of the maxima of the MPS curves. It shows a steady coarsening-up (CU) to the maximum MPS of 9 cm at 140 m from the base of the section, where it inverts to a fining-up (FU) trend to the top of the section. Omitted is an exceptionally high MPS (14 cm) at 25 m caused by outsized clasts of over 20 cm diameter in otherwise relatively fine-grained breccia and conglomerate.

The *sequence*-scale trend changes at 77 m from CU to FU and, together with a decrease in angularity of the pebbles, defines the distinction between *subfacies* A_1 and A_2.

At *bed*-scale, the first 170 m show irregular patterns of CU (inverse), CU+FU (inverse-to-normal), FU (normal), and no grading. Above 185 m, inversely graded beds are the rule.

Bedding preservation is of variable quality, and so bed thickness generally difficult to measure. BTh and MPS were nevertheless systematically recorded. A BTh/MPS plot (Fig. 11) shows the positive linear correlation indicative of mass-flow deposits according to Nemec & Steel (1984). Beds thicker than 60 cm mainly occur above the subfacies boundary at 77 m.

Subfacies A_1: CU fan breccia and conglomerate (Pih_1)

The lower 77 m of the type-section consist of a stack of three sequences, respectively 32, 24, and 21 m thick, the upper two being definitely CU. The base of the lowermost sequence is strongly affected by silicification, iron oxidation, and brecciation along the Hero Fault. Bedding structures suggest even bedding at decimetre scale, but amalgamation, fracturing, and, in places, poor outcrop hinder consistent measuring of bed thickness.

This subfacies is characterised by high angularity of the components, up to true breccia facies (Fig. 10a), and smaller MPS than the overlying interval. The sediment is matrix-rich to matrix-supported [Gms/Gm]. Strong

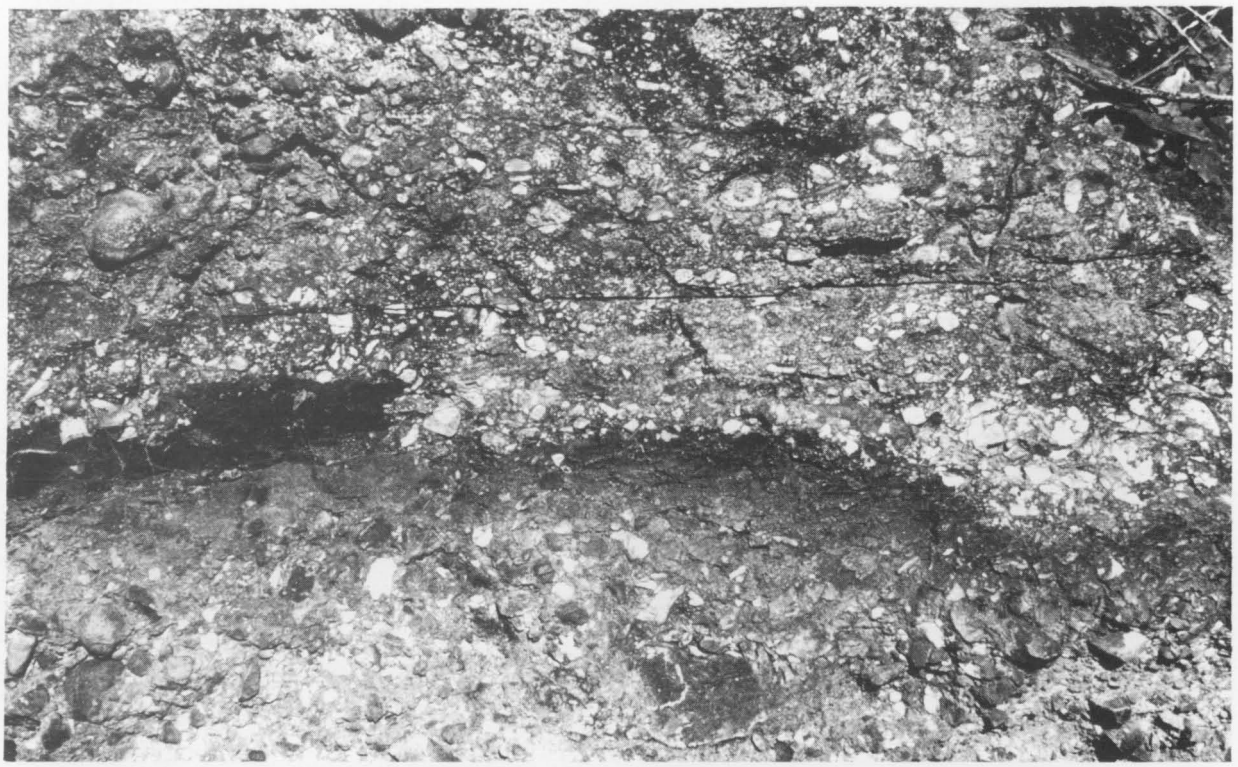


Fig. 10a. *Subfacies A_1* of the Hero Formation at the type section. Poorly sorted angular to subrounded matrix-supported debris flow conglomerate/breccia of volcanoclastic and quartzitic composition with ferruginous fine-grained sand/siltstone matrix. MPS: 3.2 cm. The photograph shows one of the rare normally graded tops of a breccia bed, strongly enriched in iron oxide. 70 m above base in Figure 9.



Fig. 10b. *Subfacies A_2* of the Hero Formation at the type section. Inverse-to-normally graded debris flow framework conglomerate overlain by ungraded matrix-supported debris flow beds with outsized clasts. 105 m above base in Figure 9.

limonite colouring relates to the high iron content of the predominantly volcanoclastic material.

Subfacies A_2: FU fanglomerate (Pih_2)

The succeeding 120 m consist mainly of varied conglomerate composing seven stacked FU sequences, on average 17 m thick, some of them being multistorey. The sixth sequence is incomplete because of faulting. CU trends occur only on the scale of bedding.

Examples of grading are illustrated in Figure 10b, c. Stratification is generally horizontal [Gm/Gms]. Gravel bar foresetting [Gp] (Fig. 10d) and mega-trough cross-bedding [Gt] have been observed at 135 m, but are otherwise rare. The clasts are subangular to well-rounded, and composed of volcanics, mudstone, and quartz wacke. The fabric shows all variety from matrix support to matrix-rich framework. The matrix is a sandy to gravelly lithic wacke, composed of quartz, opaque, and chert grains, and siltstone and volcanic rock fragments.

Pebble imbrication and bar foresetting indicate northward palaeotransport (Fig. 9).

The two FU sequences above the shear zone (185-197 m) contain a mixture of lithotypes ranging from predominant conglomerate to minor sandstone (Fig. 10e). Some conglomerate beds have a thin sandstone or gravelstone base, a pebbly sandstone in the middle, and a framework conglomerate at the top. Inverse grading is



Fig. 10c. *Subfacies A_2* of the Hero Formation at the type section. Inverse-to-normally graded subrounded to rounded matrix-supported to framework conglomerate with distinct imbrications corresponding to northward transport (i.e., to the left); transport mode transitional from mass flow to stream flow. 128m above base in Figure 9. Hammer head 15 cm.



Fig. 10d. *Subfacies A_2* of the Hero Formation at the type section. Gravel bar facies [Gp] with northward high-angle planar foresetting, indicative of a stream flow regime. 135 m above base in Figure 9. North arrow: 12 cm.

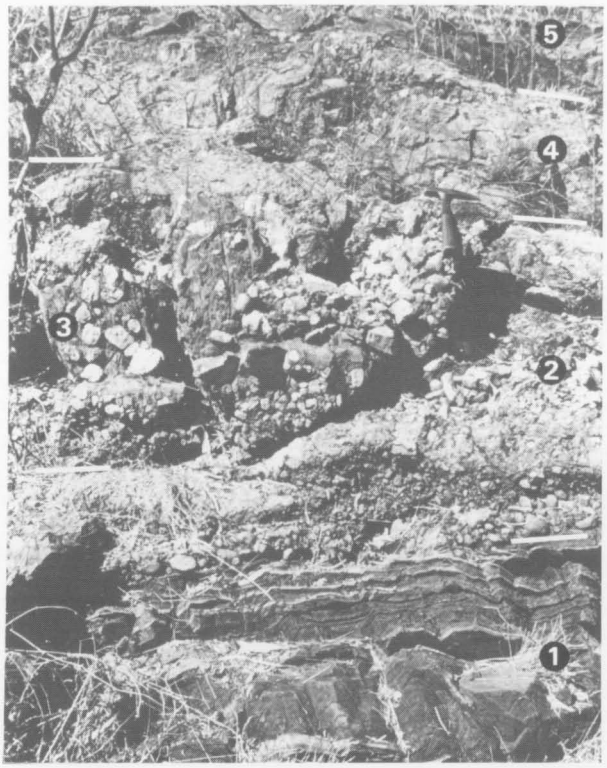


Fig. 10e. Top interval of *subfacies A2 transitional to heterolithic facies E* of the Hero Formation at the type section. Subaqueous mass/streamflow deposits:
(1) heterolithic sandstone/mudstone,
(2) imbricated framework conglomerate,
(3) contorted bed of (slumped) sandy conglomerate (MPS: 8 cm),
(4) cross-bedded sandstone and conglomerate overlain by
(5) heterolithic sandstone/ mudstone. 197 m above base in Figure 9. White bars between numbers : 20 cm.

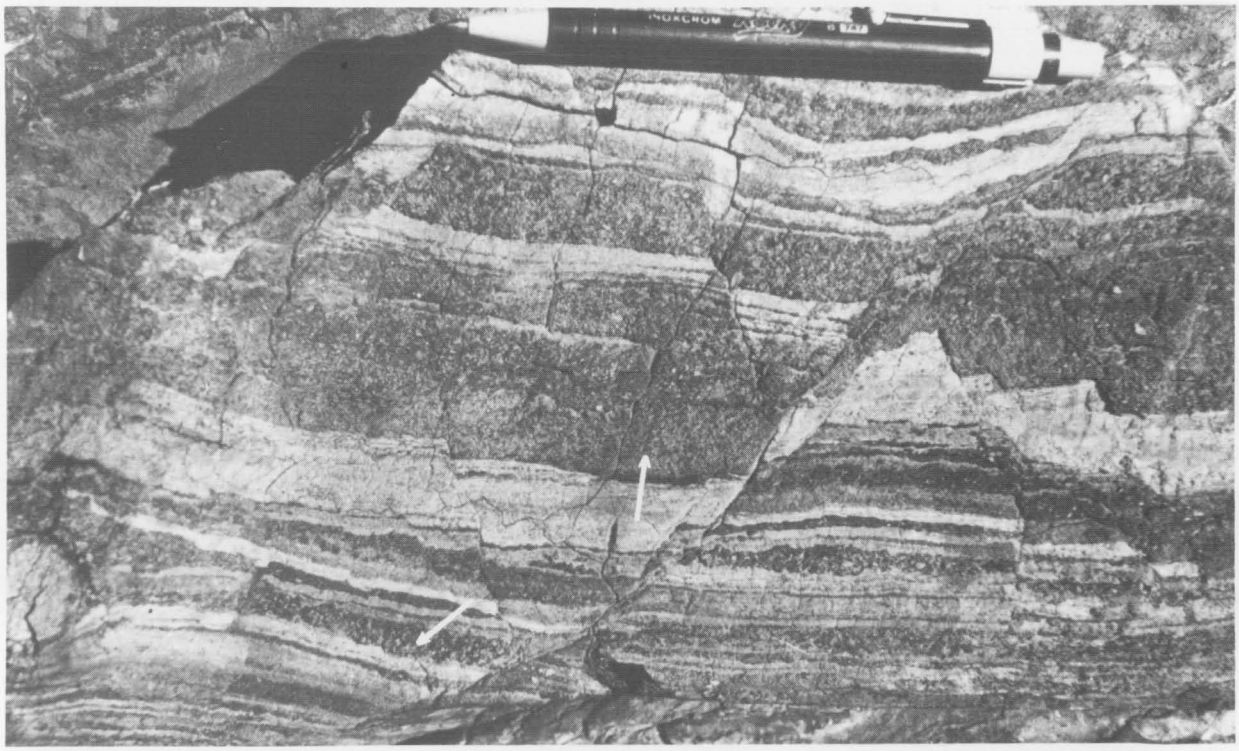


Fig. 10f. *Facies E* of the Hero Formation at the type section. Synsedimentary faults in coarse-grained heterolithic facies composed of alternating laminae of very coarse sandstone, fine-grained sandstone, and ferruginous mudstone. Coarse-grained layers FU and with cross-laminated base (white arrows); fine-grained layers predominantly even-laminated, though commonly with wavy small ripple lamination. 204 m above base in Figure 9. Pencil: 12 cm.

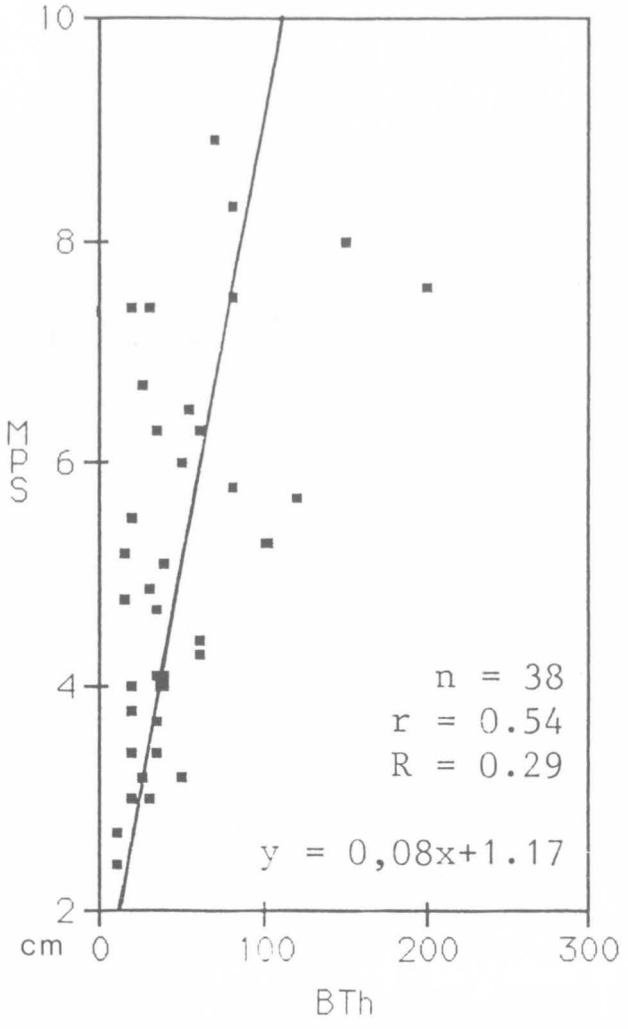


Fig. 11. Plot of Mean Particle Size (MPS) against Bed Thickness (BTh) for the Hero Formation, *facies A*. For interpretation, see text.

common. Convolutions and slumped conglomerate are also present.

Interpretation of facies A

Sporadic occurrence of scour-based discontinuous beds, the lack of internal stratification, the dominance of poorly sorted matrix-supported conglomerate and of inversely graded and ungraded beds, and the occurrence of outsized clasts all indicate that the conglomerates were deposited predominantly by debris flows and are therefore most likely of alluvial fan rather than fluvial origin (compare Nemec & Steel, 1984; McPherson & others, 1988). The angularity of *subfacies* A_1 points to a high-gradient fan depositing scarp breccia or scree slopes together with debris flows under unconfined conditions, while the coarser-grained channellised FU sequences of *subfacies* A_2 probably reflect conditions of fan head entrenchment and backward erosion at a somewhat lower gradient (compare Heward, 1978).

The continuous stacking of fanglomerate bodies, especially in the lower part of the sequence, without mud/silt interbeds between successive mass-flow events, and the absence of mudstone matrix in the matrix-supported debris flow deposits indicate subaerial transport. The high iron-oxide content could relate to original subaerial exposure (Fig. 10a).

Although the correlation coefficient of the BTh/MPS plot of Figure 11 is relatively low (0.54) the plot shows a significant linear relation, which according to Nemec & Steel (1984) indicates mass-flow deposition. The line constant (1.17) indicates cohesive debris flows. Inverse and inverse-to-normal grading of beds are indicative of subaqueous mass-flow deposition (Nemec & Steel, 1984; Nemec & others, 1984). It is observed in the interval of FU-sequences, and more frequently in its top 12 m, where it accompanies slumping and convolution. Therefore, this sort of grading (e.g., CU beds in FU sequences) probably corresponds to greater water contents of the transporting medium at lower fan gradients, after the initial stage of subaerial mass flows over the fan surface (CU-beds in CU sequences in the basal interval). In view of the regular stacking of FU sequences, however, subaqueous conditions probably have to be understood as within-channel conditions or as episodic floodings, whereas fully subaqueous conditions probably prevailed only in the last FU sequence of *facies A* and in the overlying facies.

The predominance of mass-flow deposits suggests a fan environment of relatively steep gradient, although it should be remembered that Proterozoic slopes were not consolidated by vegetation, and so gravity had full play in the supply of sediment even at low slope angles.

Facies B: Fine-grained (pebbly) wacke facies (Pih_3) and (Pibh)

A fine-grained greenish wacke with rare pebbly wacke intercalations occurs in the north and in the south of the Hero Syncline.

The wacke sequence in the north crops out for about 3 km along the east limb of the Hero Syncline (grid references 359411 to 355431). It is predominantly composed of greenish silt-/mudstone with an increasing amount of quartz wacke towards the top. There too, wacke-supported conglomerate (pebbly wacke) occurs (grid reference 357425) in isolated beds (BTh: respectively 80 and 28 cm), with relatively coarse and therefore outsize well-rounded pebbles (MPS: respectively 16.5 and 8.6 cm; Fig. 12), predominantly of quartz arenite .

Measured section 2, in the south of the Hero Syncline



Fig. 12. Pebbly wacke within wacke *facies B* of the Hero Formation at grid reference 357425. MPS: 8.6 cm. Hammer head: 17 cm.

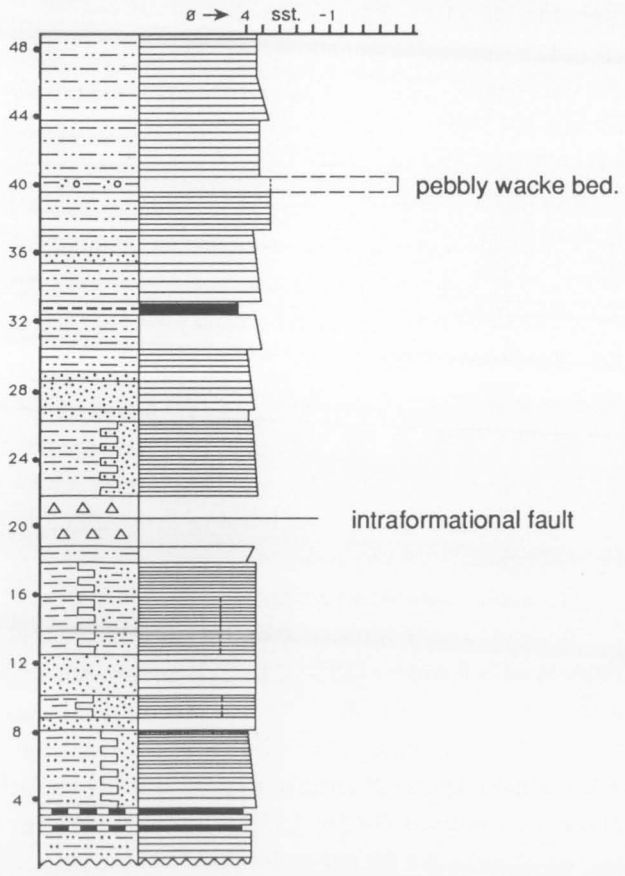


Fig. 13. Sedimentary log of the pebbly wacke facies (Pibh) of the Breakaway Shale at section location 2 (for location, see Figs. 5, 20). The intraformational fault is a listric fault, due to slope failure.

(grid reference 359371; Fig. 5), contains approximately 50 m of this facies (Fig. 13). In the Kennedy Gap 1:100 000 Sheet area and on our own map, this wacke sequence is included in the Breakaway Shale as Pibh. The wacke forms a ridge immediately west of a depression containing poorly exposed Moondarra Siltstone overlying the Hero Formation (Fig. 5).

The wacke facies of section 2 (Fig. 13) is composed of: (1) fine- to very fine-grained lithic and arkosic wackes; (2) fine-grained lithic arenite; (3) thin-bedded siltstone; (4) alternations of the previous three rock types; and (5) mudstone. These occur in FU to ungraded 4.5 m-thick sequences. Set thickness varies between 10-50 cm for the first type, and 5-20 cm for the others. Bedding is somewhat lenticular in east-west cross-section. One pebbly silt/sandstone bed, 70 cm thick, occurs 40 m from the base. The well-rounded widely scattered pebbles range between 6 and 0.5 cm in diameter. At the northern wall of the creek intersection of section 2, intraformational listric faults, facing obliquely updip, indicate synsedimentary deformation.

Interpretation of facies B

The lack of sedimentary structures, the textural immaturity, the presence of matrix-supported conglomerate and pebbly wacke, the absence of scouring, the CU trend in the sequence (northern outcrop), and the

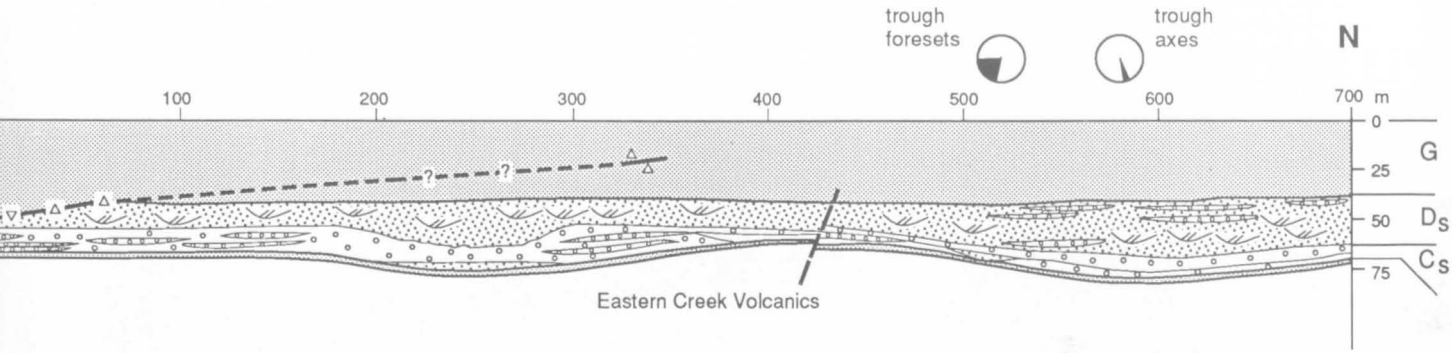


Fig. 14. Fence diagram I: erosive superposition of sheet *subfacies* C_S (pebbly sandstone, below) and sheet *subfacies* D_S (sandstone, above). Location in Figs. 5, 20.

FU trends of the beds indicate that this facies is likely to be the distal subaqueous equivalent of the mass-flow *facies A*. FU trends at bedding scale may correspond to turbulent mass flow. In this respect the facies resembles the distal facies of the Domba fan-delta in Norway (Nemec & others, 1984). Outsized clasts may have been transported by occasional dense mass flows generated during extreme flooding of the subaerial part of the fan (compare Postma, submitted). In this interpretation the wacke facies represents a subaqueous slope environment, and the observed synsedimentary deformation represents slope failure in the form of intraformational rotational listric faulting; see also the section below on 'Facies associations and the depositional model of the Hero Formation'.

Facies C: Pebbly sandstone (Pih4)

Matrix-rich pebbly sandstone occurs in a variety of subfacies:

C_S: pebbly sandstone in sheets
C_r: (pebbly) sandstone in ribbons
C_m: massive pebbly sandstone

Subfacies C_S and C_r are the first coarse-clastic facies above the Mount Isa Group Unconformity in the eastern limb of the Hero Syncline.

Subfacies C_m is found stratigraphically higher, above *facies B, D,* and *E* in the northernmost sector of the Hero Syncline, and on top of *facies A* close to the Hero Fault in the western synclinal limb.

Subfacies C_S: Pebbly sandstone sheets.

At the locality of fence diagram I (Fig. 14), this facies consists of well-bedded medium to coarse-grained pebbly lithic arenite, with appreciable amounts of clay (sericite); mudflakes and rip-up clasts are common. The pebbles are well-rounded quartzite or volcanic rock. MPS varies between 1.6 and 3.5 cm, and BTh between 20 and 100 cm. The pebble density varies widely. Ungraded beds predominate. Beds are elongate, lenticular in cross-section, lack internal sedimentary structures, and are non-erosive. Measurements of the orientation of the few foresets found suggest southeast-directed currents. Beds of relatively fine-grained framework conglomerate, sandstone, and siltstone are intercalated in the pebbly sandstone sequence. The number of siltstone beds decreases towards the top of the sequence.

Subfacies C_r: (Pebbly) sandstone ribbons.

The ribbon *subfacies* C_r is found in the southern part of fence II (Fig. 15: grid reference 362371) and in several outcrops north of fence I (grid reference 359404, Figs. 5, 16a; and grid reference 359406, Figs. 5, 16b).

In the south, ribbons are encased in even-bedded siltstone and very fine-grained silt-/sandstone *(facies F)* at the same stratigraphic level as the C_S-sheet. Lithotypes are: (1) coarse ungraded arkosic arenite with low-angle lamination and trough cross-lamination; (2) coarse-grained mostly ungraded arkosic pebbly arenite containing dispersed well-rounded pebbles (MPS not exceeding 3 cm), large mudflakes, low-angle lamination, and trough cross-lamination; (3) granule and pebble conglomerate; (4) siltstone and sandy siltstone as laterally persistent layers and streaks in the pebbly arenite.

The ribbons have a concave-up lunate cross-section (Fig. 15) with a width (≈100m)/ thickness (7m) ratio of approximately 15, indicative of ribbon architecture (compare Marzo & others, 1988). The basal surface scours the even-bedded *facies F*. Details of the vertical lithologic variation are given in four sections in Figure 15. Where they pinch out laterally, the ribbon fill increments are truncated and overlain by the last sandstone layer or by *facies F*. At least one of the ribbons suggests lateral infill to the south. Interbedded pebbly sandstone has a patchy distribution, generally restricted to the centre of the ribbon.

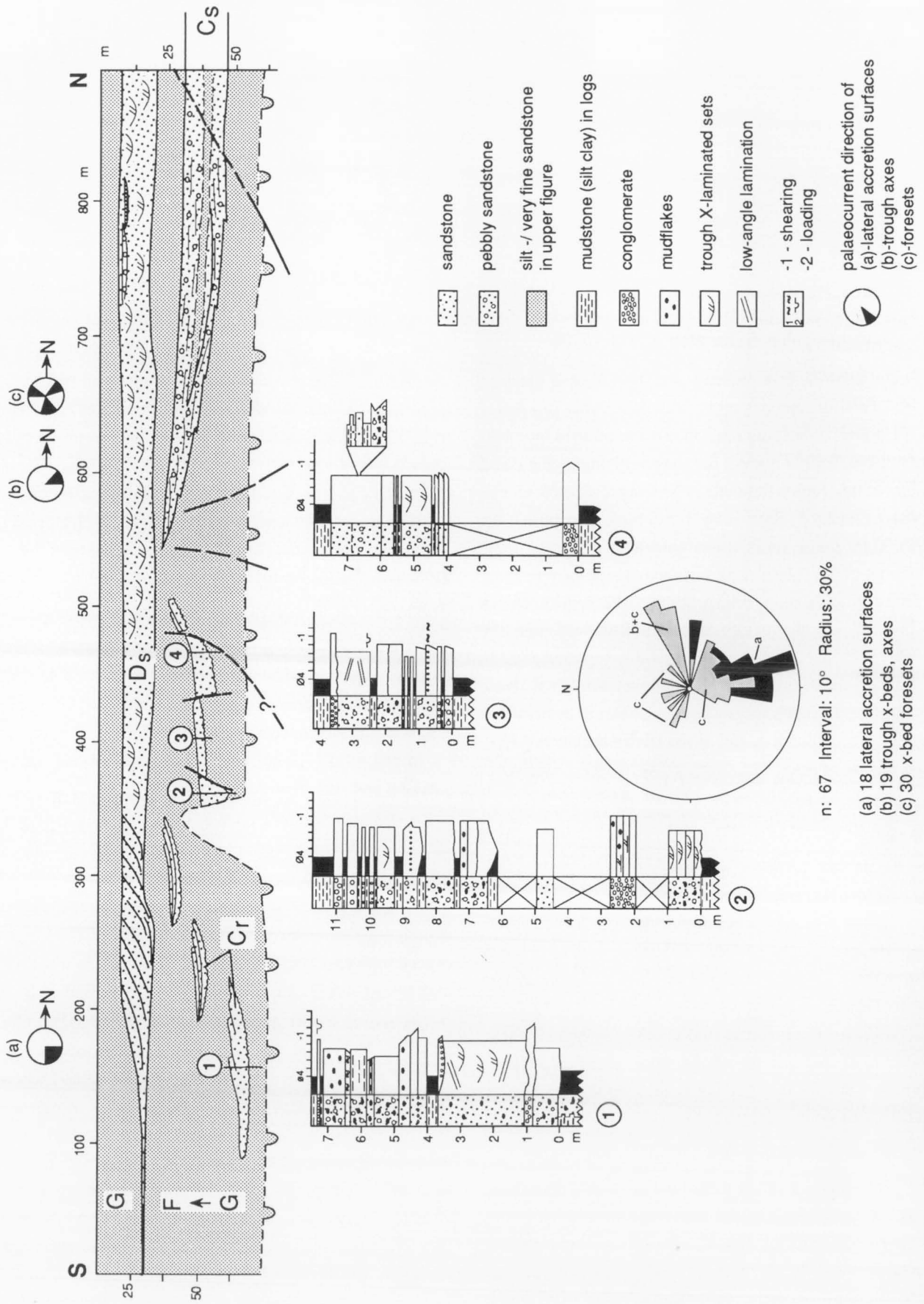


Fig. 15. Fence diagram II showing geometry of sandstone bodies of *subfacies* C_S, C_r, and D_S. Vertical columns give details of the southern exposures of *ribbon-subfacies* C_r. Location in Figs. 5, 20.

Restored bearings of trough axes trend eastwards at about right angles to the dip of the inclined accretionary bedding (rose diagram in Fig. 15; compare also Fig. 5)

Vertical sequences through some of the ribbons lateral and to the north of the pebbly sandstone sheet of fence I are shown in Figure 16a-c (locations in Fig. 5)

One example (Fig. 16a, b) is approximately 20-25 m wide in oblique cross-section and 2 m thick. It contains two pebbly sandstone beds, 68 and 67 cm thick (MPS of the 67 cm bed: 3.9; Fig. 16b), which wedge out laterally, and one ungraded 40 cm-thick sandstone bed with horizontal, cross, and convolute lamination. Interbedded sandstone and siltstone overlie the channel-fill. Palaeocurrents from ripple foresets indicate flow to the southeast, from trough axes to the east-northeast (Fig. 5).

A second example, 7 m thick, is a multistorey ribbon within a siltstone matrix. It is composed of interbedded sandstone, pebbly sandstone, and siltstone (Fig. 16c, d). An individual storey such as that of Figure 16d is composed of a 50 cm-thick FU coarse to medium-grained sandstone bed, pebbly (MPS 2.5 cm) at the base and with one intercalated pebble horizon (MPS 1.5 cm), overlying a thin sandstone and overlain by 40 cm of interbedded thin sandstone and siltstone, succeeded by a 60 cm-thick inversely graded bed with a pebbly top (MPS 3 cm).

Subfacies C_m: Massive pebbly sandstone

Massive (structureless) pebbly sandstone *(subfacies C_m)* is a chaotic mixture of rounded to angular sandstone and volcanic rock fragments floating in a greenish volcanoclastic sandstone matrix. This facies is widespread in the western limb of the Hero Syncline.

At grid reference 354381, bed thickness is several metres, and at least three of these beds have been observed in succession immediately east of the Hero Fault. In the uppermost bed, pebbles float widely dispersed in the matrix (Fig. 17). Both in fabric and in composition, this facies is identical to the pebbly sandstone of the Bortala Formation of the Paroo Range (Nijman & others, this volume). Near the fault contact, the pebbles are vertically stretched (MPS at right angles to the stretching: 7.7, 7.9 cm; stretching reaches 150%).

Tracing the C_m outcrops to the north, the subfacies appears to occur at a stratigraphic level just above *subfacies A_2* of the type-section of the Hero Formation. Two kilometres south of the type locality (grid reference 356393), interbedded conglomerate and sandstone at the top of *subfacies A_2* show an upward increase of pebbly sandstone at the expense of conglomerate. The sequence begins with a poorly sorted inversely graded matrix-supported conglomerate (MPS: 9.2 cm). Three sandstone beds follow, the lower two even to wavy laminated. The second contains a few pebbles. The third bed incorporates large clasts and shows convolute lamination. Next, an ungraded conglomerate bed, MPS: 7.2 cm, is overlain by interbedded sandstone and siltstone.

Farther north (grid reference 357399), the same facies contains outsized quartz boulders, 54, 50, and 40 cm in diameter in a matrix-rich conglomerate with MPS 21.6 (13-32) cm. Near the type locality, the pebbly sandstone beds begin to show horizontal stratification with pebble strings and convoluted lamination. The intercalated sandstone beds contain load structures, scour-and-fill structures, and planar cross-laminated sets, where *subfacies C_m* passes into *facies E.*

Relatively fine-grained subfacies C_m is found in the core of the northernmost segment of the Hero Syncline, where it overlies the imbricated sandstone channel fills of *subfacies D_r* (grid reference 356426).

Interpretation of facies C

The sheet *subfacies C_s* is a composite of lenticular non-channellised or channellised units of pebbly sandstone [Gms] with interbedded sandstone and conglomerate, some of them trough cross- bedded. Although less muddy, the preponderant part of the pebbly sandstone compares with the graded matrix-supported diamictite facies [Dmg] of Shultz (1984), interpreted to have been deposited in thin sheets from dilute, probably pseudo-plastic, slurries. The concentration of (1) thin channel-fills consisting of relatively fine-grained framework conglomerate and (2) trough-bedded sandstone in the basal part of C_s points to conditions of stream flow during which the debris flow deposits upstream were reworked at a lower level of discharge (model I of Miall, 1985). Their concentration in the base of the sheet then reflects the process of fan progradation.

The multistorey ribbons of *subfacies C_r* are interpreted to have resulted from the stacking of fills of relatively straight, very shallow, but high-energy channels with variable discharge and mixed transport modes, including stream flow (trough-bedded sandstone) and mass transport (pebbly sandstone). The concave-up shape of the fill increments and the erosion of their pinch-outs indicate that they responded to loading by downward bending. This sort of channel preservation has also been mentioned by Nami & Leeder (1978). The frequent intercalation of pebbly sandstone with rounded pebbles links this facies to *facies*

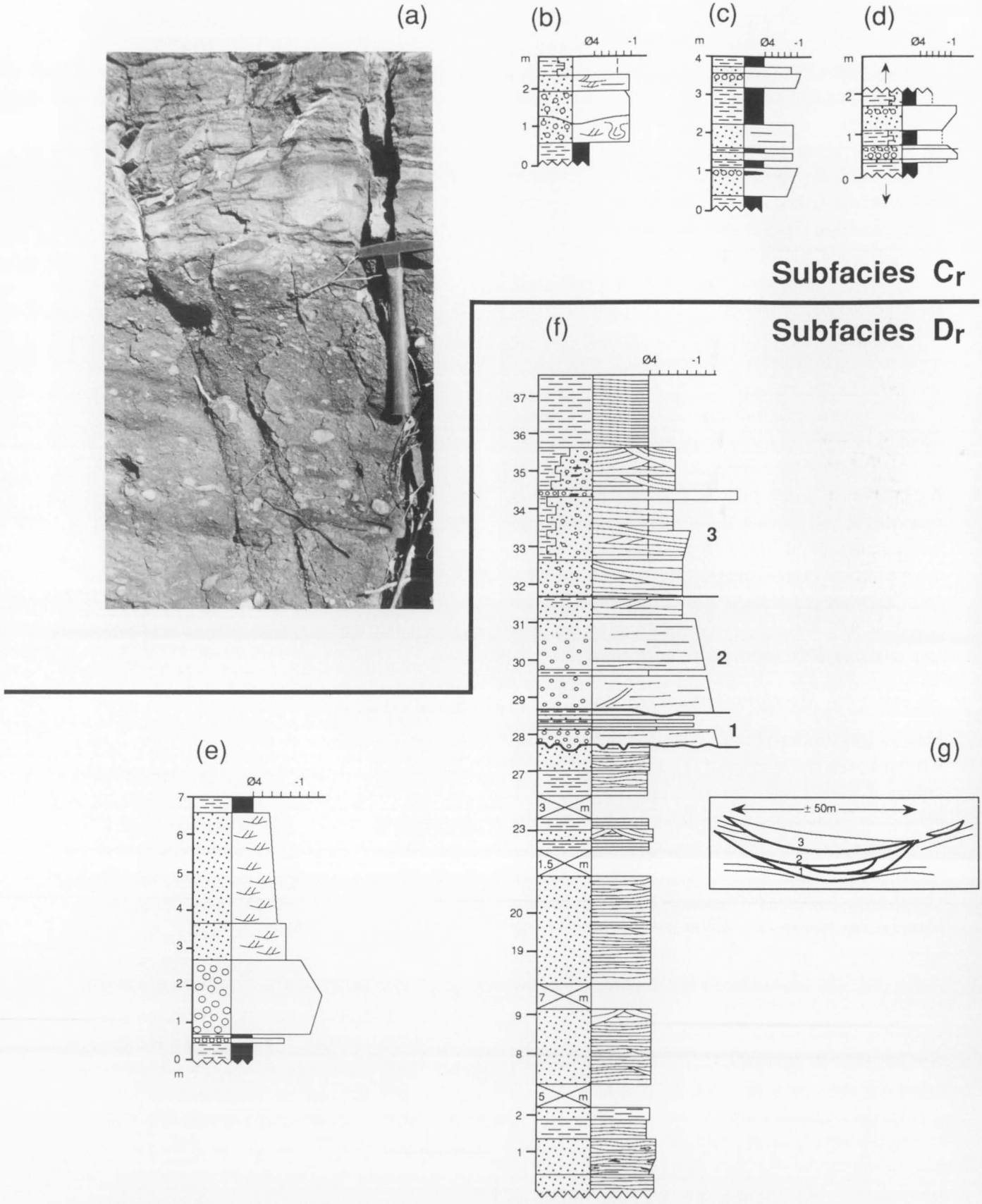


Fig. 16. Ribbon facies a: *Subfacies C_r:* pebbly sandstone facies abruptly overlain by horizontally and cross-laminated sandstone shown in b. b-d: details of ribbon sequences; see also Figure 15. e: *Subfacies D_r:* regularly FU sequence of a ribbon at grid reference 358398, north of the *D_s:* sandstone sheet. f: section 3 in the extreme south of the map area; sequence of fine-grained sandy heterolithic *facies F*, overlain by a FU multistorey *D_r* -ribbon: storeys are numbered 1-3 and the cross-section of these stacked channel fills is illustrated in g. For locations see Figs. 5, 20.



Fig. 17. Massive pebbly sandstone, *subfacies* C_m. Thick-bedded structureless unsorted mass-flow deposit of quartzitic and volcanic clasts floating in a feldspar-rich wacke matrix. Top of Hero fanglomerate facies (grid reference 354381). Pencil: 12 cm.

C, but other characteristics such as the well-structured cross-bedded sandstone compare with the ribbons of *subfacies* D_r.

The position of *subfacies* C_r laterally north and south of *subfacies* C_s, reflects the fact that the sheet geometry, by decrease of interconnectedness towards its periphery, gives way to the ribbon facies. The centre of the sheet then corresponds to the position of the fan (lobe) axis.

Finally, the massive pebbly sandstone (C_m) in the western limb of the Hero Syncline is definitely different in its chaotic aspect, coarser grain size (maximum 54 cm), and variable pebble shape. It resembles Shultz' facies [Dmm] of subaerially emplaced massive matrix-supported diamictite. Whether *subfacies* C_m is subaerial or subaqueous is not clear from the few observations made. In the Bortala Formation of the Paroo Range a similar facies occurs in an inshore transitional marine environment (Nijman & others, this volume).

Facies D: FU (conglomeratic) sandstone (Pih5)

Pebbly sandstone *facies C* is overlain by the better-sorted sandstone *facies D*, which likewise allows a subdivision into a sheet *subfacies* D_s and a *ribbon subfacies* D_r.

Subfacies D_S: Sheet sandstone.

In the east limb of the Hero Syncline, a sandstone sheet extends over a distance of about 3 km from grid reference 362370 northwards (Figs. 5, 14, 15). This facies is overlain by ferruginous micaceous Moondarra Siltstone *(facies G)*, and has an erosive contact with the underlying pebbly sandstone (fence I; Fig. 14) or with fine-grained sandstone and siltstone enveloping C_r – ribbon-type channel-fills (fence II; Fig. 15). It consists predominantly of medium to coarse-grained lithic arenite with many mudflakes, forming a tabular sandstone body wedging out to the south.

In the northern part of fence I (600 m horizontal scale mark in Fig. 14), the thickness is 25 m, and the sandstone grades upwards from coarse to fine with intercalations of very fine-grained sandstone and siltstone. Southwards, at about the 100 m mark, the sequence thins to about 15 m, fining upwards from coarse/medium to medium/fine grain size.

The southern continuation of the sheet is shown in fence II, where its thickness diminishes from 15 m in the northern part (800 m scale mark in Fig. 15) to a complete wedge-out south of this location. The sequence is well-bedded; bed thickness ranges from 15 to 45 cm.

At both localities, restored foreset orientations of meso-scale trough cross-laminated sets are oriented symmetrically to the east-northeast-oriented trough intersections, the latter therefore representing the true palaeocurrent direction (Figs. 5, 14, 15). Only in the southern part of fence II does the sheet show inclined accretionary bedding over its entire thickness; palaeodip is to the south-southeast. Accretion units show a weak upward fining, and contain trough sets in the base with axes pointing east-northeast, indicative of the lateral orientation of the accretion with respect to the dominant palaeocurrent.

Subfacies D_r: Conglomeratic sandstone ribbons.

Vertically stacked channel fills with pronounced FU-trend occur in section 3 (Fig. 16f, g), at approximately the same stratigraphic level as D_s at fence II, but south of that locality (grid reference 362365; Fig. 5; see also Fig. 20).

The upper part of section 3 (Fig. 16f: 27.7 to 36.5 m) is a multistorey channel fill composed of stacked fining-up coarse-clastic beds, lenticular in cross-section (Fig. 16g). Width-thickness ratio is 7.0. The ribbons consist of fine volcanoclastic conglomerate and arenite. The contact with the underlying fine-grained sediments *(facies F)* is erosive, the loading of the conglomerate lag generating mud flame structures.

The first storey (1) in Figure 16f consists of a horizontally stratified conglomerate lag on a scour surface, with clasts of the underlying siltstone beds, overlain by interbedded very coarse-grained lithic arenite and very fine-grained sandstone. The next storey (2) is a FU sequence composed of two conglomerate beds, the lower one horizontally stratified, in places cross-bedded [Gh/Gt], with a scoured base; the upper conglomerate bed is flat-based, and fines from gravel to very coarse lithic arenite, and in the next bed to coarse arenite The third storey (3) is composed of a coset of low-angle trough cross-laminated to horizontally laminated coarse lithic arenite [St/Ss/Sh], with dispersed pebbles and some siltstone layers. A possible fourth storey at 34.4 m is a pebbly lag with quartzite pebbles, silt flakes, and thin siltstone lenses. This is overlain by a coset of pebbly lithic arenite with trough sets about 4 m wide and 30 cm high, and by further increase of silt intercalations is transitional into the overlying siltstone.

D_r ribbons also occur at the northern margin (grid reference 358398, Figs. 5, 20) of the sheet sandstone D_s, where they can be distinguished from C_r ribbons by their better fining-up trend. The ribbon sequence of Figure 16e consists of an inverse-to-normally graded matrix-supported conglomerate, overlain by 4 m of FU trough cross-bedded sandstone. Palaeoflow is southeastwards.

In the northernmost segment of the Hero Syncline at grid reference 357425 (Figs. 5, 20), D_r ribbons (h: 5-10 m at w: 25-50 m) top the pebbly wacke of *facies B*. They are successively overlain by massive pebbly sandstone *(subfacies C_m)* and an alternation of pebbly sandstone/ sandstone *(facies E)* in an overall CU trend.

Interpretation of facies D

The predominance of trough cross-laminated sandstone [St and Ss] and the pronounced fining-up trend of the sequence are interpreted to have been caused by confined stream flow. The relatively coarse grain-size of the sandstone, the presence of framework conglomerate lenses, lags, and in places, pebbly sandstone characteristic of the previous facies *(C)* suggest bedload transport. The juxtapositon of multilateral sheet geometry with marginal ribbons places this transport mechanism in a braid plain, distal to that of the fan apex (Model II of Miall, 1985). Lateral-accretionary bedding relates to sideward growth of the sheet within one of the major fan distributaries during the last stage of D_s sheet formation. Exposure was insufficient to see an abandonment plug and/or cut bank which would indicate channel abandonment. As discussed for the underlying *facies C,* the form differentiation within this more sandy facies is explained as the sheet sandstone representing the axis of the clastic supply, whereas the isolated or stacked channel fills represent the periphery.

Facies separation and overall vertical grain size trend testify to a rather low gradient and the rapid abandonment of the entire coarse clastic system, an abandonment concurrent with flooding of the alluvial plain and onlap of the inshore basin facies of overlying Moondarra Siltstone (compare the section below on 'Facies associations and depositional model of the Hero Formation').

Facies E:. Coarse-grained heterolithic facies (Pih6)

Rounded quartzite-pebble framework conglomerate and pebbly sandstone beds are intercalated with sandstone, siltstone, and (dolomitic) mudstone in the top interval of the type section of the Hero Formation (grid reference 357423; Fig. 9, 197-212m). The conglomerate beds range in thickness from 25 to 120 cm. They wedge out laterally, have flat non-erosive bases, and are normally graded. Protruding pebbles in the top of the pebbly sandstone indicate outwash of the sand fraction followed by infilling (see also Fig. 18).

The sandstone component of this heterolithic facies consists of thin coarse-grained structureless wavy or ripple-laminated sandstone, interbedded with siltstone and mudstone (Fig. 10f). Mud flames, loadcasts, synsedimentary faults, and irregular wavy bedding planes are commonly associated. To the south, this facies grades laterally into massive pebbly sandstone *(subfacies C_m)*, whereas to the north, in a beautiful exposure of interbedded decimetre-scale sandstone and pebble layers at grid reference 357423 (Figs. 5, 18), it overlies C_m.

Interpretation of facies E

The small-scale alternation of lithotypes characteristic for this facies is found in both the braided distal fan environment and in conditions of shoreface reworking (Bourgeois & Leithold, 1984, fig. 11b; Postma, submitted). Its intermediate position between underlying proximal fan and overlying inshore basin facies (Moondarra Siltstone), and its high degree of pebble



Fig. 18. Coarse-grained heterolithic *facies E* (grid reference 357423). Centimetre to decimetre-scale interbedding of well rounded sandy conglomerate and pebbly sandstone with even-to-wavy laminated fine-grained sandstone. Protruding pebbles in the surface of the conglomerate layers (white arrows) point to outwash of the gravel beds before deposition of the sandstone; this facies is known to result from shoreface reworking of subaqueously deposited mass-flow conglomerate in distal fan deltas; see text. Hammer: 40 cm.

rounding and compositional sorting favour an interpretation by shallow subaqueous deposition as a result of shoreface(?) reworking of the associated massive pebbly sandstone of *subfacies* C_m. Its occurrence is restricted to that segment of the Hero Fan which is also characterised by the presence of wacke *facies B*, instead of the channellised pebbly sandstone of *subfacies* C_s/C_r.

Facies F: CU fine-grained heterolithic facies (Pih7)

The lower 27.7 m of the sequence illustrated in Figure 16f consist of interbedded very fine to fine-grained sandstone and greenish commonly micaceous siltstone and sandy siltstone. Bed thicknesses vary from 2 to 20 cm. Even bedding and even lamination are dominant, whereas scour-and-fill structures and planar and tangential cross-lamination are rare. Convolution and very poor lamination are characteristic of the intercalated lenticular beds. The sequence does not show grading and neither do most beds, although a few are inversely graded (e.g., at the 1 m mark in Fig. 16f).

A similar red-grey colour-banded siltstone and very fine sandstone facies underlies sandstone *facies D* in Fence II (Fig. 15). This rock is even-bedded and mainly even-laminated, with the same association of scour-and-fill structures, convolutions, current ripples, and rare wave ripples. *Facies F* here results from coarsening/thickening upwards from *facies G*, and encases sandstone ribbons C_r.

The sedimentary environment will be discussed for the two facies in combination at the end of the next section.

Facies G: Moondarra-type siltstone (Pim)

Even-bedded/-laminated, in places massive, iron-oxide colour-banded pyritic dolomitic siltstone and mudstone overlie the coarse clastic facies of the Hero Formation. This is the Moondarra Siltstone *(facies G)* referred to above in the section on 'Fine-grained facies of the Mount Isa Group'. The contact is gradational as illustrated by the occurrence of *facies E* in the top of the type section of Figure 9. Banding is caused by an alternation of structureless and very finely laminated layers, which have different weathering characteristics, the laminated layers being more resistant. Some pebble strings are intercalated. The original greyish colour weathers brown.

In the east limb of the Hero Syncline, *facies G* occurs not only above the Hero Formation, where it separates *facies D* from *facies B* in the Breakaway Shale (Pibh) in section 2, Figure 13; see Fig. 5 for location), but also at the base of the Hero Formation below *facies F*.

Interpretation of facies F and G

The dominance and lateral persistence of horizontal and ripple lamination and the fine grain size place *facies F* and *G* in a shallow subaqueous environment with suspension settling and modest wave and current action. Beach facies of some significance has not been found in the Hero area, nor indications of slopes with extensive slumping and subaqueous mass transport towards deeper water, other than indicated by the restricted occurrences of *facies B*. Instead, the data indicate an environment of shallow- water sandy shoals or mouth bars *(facies F)* in low-energy low-gradient shorelines with ephemeral input of clastics from

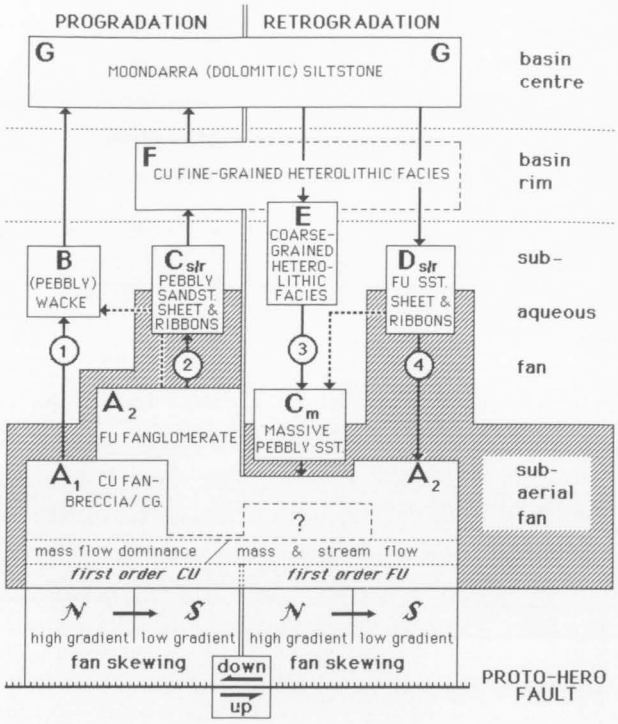


Fig.19. Facies relationship diagram of the Hero fan delta. For explanation, see text. The diagram is represented in three dimensions in Figure 20.

fan distributive systems of mixed mass flow/stream transport, as for *facies C* and *D*.

Lithologically, the more distal and basinward *facies G* is identical with the Moondarra Siltstone, and the depositional environment can be better specified in a comparison with occurrences in the Paroo Range; see next section.

Facies associations and depositional model of the Hero Formation

Facies and lithotypes, in particular the widespread occurrence of subaerial and to a lesser extent subaqueous mass flow deposits (*facies A, B,* and *C*), combined with the shallow-water distal *facies F* and *G* and the fanning of the palaeocurrents classify the Hero Formation as an alluvial fan delta in the restricted sense of McPherson & others (1988), or as a shoal-water or Hjullström-type delta with a relatively steeply sloping A-type fan feeder system as defined by Postma (1990, table 3). 'Steep' gradient in this context refers to fan slope, not basin slope.

Figures 19 and 20 illustrate the interrelations of facies observed in the Hero Formation. The model largely depends on mapping (Fig. 5; Nijman, 1991, sheet 2) and geometric analysis of the Hero Syncline, as the three-dimensional diagram of Figure 20 uses the unfolded syncline and the two strike outcrops of the steep limbs as the sides of the block diagram. Correlation of the thick sequence of the type section on the west limb of the Hero Syncline with the relatively thin sequence of sandy deposits on the east limb leads to a vertical bipartition of the fan sequence into a progradational and a retrogradational suite of facies. The surface of bipartition has been chosen at the grain-size maximum within *subfacies* A_2 of the type section (megasequence boundary at 140 m in Fig. 9) and between the pebbly sandstone *subfacies* $C_{s/r}$ and the FU sandstone *facies D* in the corresponding distal parts of the fan, exposed in fences I and II. This reference plane is considered to slightly climb in time southwards in the direction of a shift in the positions of *(sub)facies E*, C_m, *D* and *B*, as described below in this and the next section.

In both the progradational and the retrogradational stages, the facies sequences in the northern segment of the Hero Fan with northerly and northeasterly palaeocurrents differ from those in the southern segment with easterly and southeasterly palaeocurrents. It is therefore concluded that an asymmetric or skewed facies pattern appears to be another characteristic of the Hero Fan. Such a configuration is more specifically indicated by the lateral juxtaposition of distal fan *facies B* in the north to *facies F* in the south, both related to the same proximal fan *(facies A)*, and by northerly palaeocurrent directions in the fanglomerates but east to southeastward deflection of current directions in the channellised fan fringe.

The combination of both the vertical and the horizontal facies subdivisions results in the distinction of four tracts of genetically and laterally linked facies (Fig. 19):

(1) a *high-gradient progradational tract:* $A_1 \rightarrow (A_2) \rightarrow (C_r) \rightarrow B \rightarrow G$; mass-flow dominated;

(2) a *low-gradient progradational tract:* $A_1 \rightarrow A_2 \rightarrow C_{s/r} \rightarrow F \rightarrow G$; mixed transport mode;

(3) a *high-gradient retrogradational tract:* $G \rightarrow E \rightarrow C_m \rightarrow A$; mass-flow dominated;

(4) a *low-gradient retrogradational tract:* $G \rightarrow (F) \rightarrow D \rightarrow A_2$; stream-flow dominated;

in which the facies between brackets are underdeveloped or might have been expected to occur if outcrops were complete. Subaerial and subaqueous domains of deposition are also indicated. The three-dimensional distribution of facies is shown in the block diagram of Figure 20.

Mixed transport load (stream and mass flow) is strongly indicated by the intricate mixing of debris flow and stream flow conglomerate in *subfacies* A_2, and by the juxtaposition of cross-bedded sandstone and pebbly

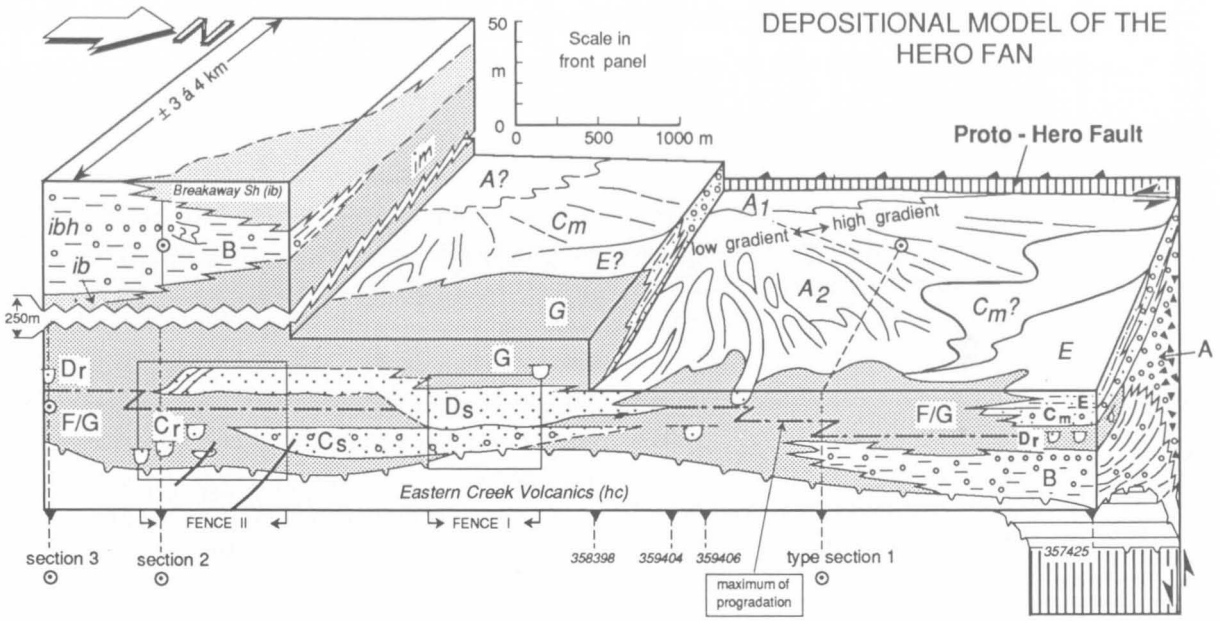


Fig. 20. Block diagram showing facies relationships, skewing (high-gradient northern, low-gradient southern fan slopes), southward depocentre shift, and inferred left-lateral strike-slip control of the Hero Formation. To the upper left, *facies B* refers to the recurrence of (pebbly) wacke in the Breakaway Shale, illustrated by the log of section 2 in Figure 13. *im:* Moondarra Siltstone; *ib:* Breakaway Shale; *ibh:* Breakaway Shale (pebbly) wacke facies; *in* : Native Bee Siltstone. P omitted from stratigraphic symbols for clarity.

sandstone in *facies C* in the more distal reaches. As long as the MPS still increases, *subfacies A_2* reflects the flattening of the fan profile with respect to that of *subfacies A_1*, resulting in increased fan progradation (compare grain size trends at sequence and megasequence scale in Fig. 9). In terms of structural control this would correspond to a decrease of differential vertical movement (compare Heward, 1978; Heller & others, 1988).

Stream-flow dominance is indicated by the linkage of the FU sandstone sheet and ribbon *facies D* with the upper part of the fanglomerate *subfacies A_2*.

The high-gradient progradational tract in the northern segment is illustrated by the occurrence of pebbly sandstone with well-rounded outsized clasts, even in the fine-grained wacke *facies B*, which we interpret as a subaqueous slope towards a shallow lagoon, incidentally fed by coarse clastics directly derived from subaerial mass flows or flood events. In its retrogradational counterpart, the concurrence of *subfacies C_m*, and of what probably is a shoreface reworking of such a deposit, *facies E*, are considered significant features of the high-gradient mass-flow-dominated environment. 'High-gradient' is meant only in a relative sense, because the slope effects on what is considered the northeastern steepest part of the fan are subdued, and certainly do not point to a deep-water environment. Unless our observations on the accretionary bedding in *subfacies D_s* are incomplete, toe set features corresponding to a deep-water setting or to progradational Gilbert-type delta foresets (compare Massari & Colella, 1988) have not been found. Also, large-scale foresets may have been missed due to the orientation of the outcrop at right angles to the palaeocurrents.

Subfacies C_m occurs along the entire exposed west limb of the Hero Syncline in the top of the fanglomerate sequence southwards, and lateral of *facies E* at the top of the type section. In the northernmost outcrops, *subfacies C_m* lies below *facies E* (Fig. 20) and, in the eastern synclinal limb, laterally of the *D_s* sheet. It suggests a slight shift of *subfacies C_m* southwards and upwards in the fan, a shift also shown by the relative positions of *subfacies D_s* and *C_s*. In this respect, it is tempting to explain the second occurrence of wacke *facies B* within the Breakaway Shale, stratigraphically above and farther south than the main body of the Hero Fan (section 2 in Figs. 5, 13), as the northern segment of the next younger fan. This argument further enhances the suggestion of a southward depocentre shift of the fan system.

As the fine-grained end-member in the depositional model, Moondarra-type *facies G* represents the local basin centre facies. These deposits are subaqueous, but with

more evidence of dessiccation could easily fit the floodplain interpretation of Neudert (1983; see section above on 'Fine-grained facies of the Mount Isa Group'). The geometric relations we observe in the Lower Mount Isa Group of the Hero/Western Fault Zone and Paroo Range (Fig. 21) allow some further speculations. Because of the intermediate position and interdigitating relations of Moondarra (-type) Siltstone between coarse clastic basin margin facies of the Hero Fault Zone in the west, and the coastal deposystem of the Paroo Range in the east, this facies, when subaqueous, seems to occupy a coastal lake or inshore lagoon (compare Nijman & others, this volume, fig. 23).

Deformation and sedimentation in the Hero/Western Fault Zone compared with the Paroo Range

Fault control of the Hero Fan

Although we realise that interpretation of the Hero Fan in terms of tectonic control may be premature with the currently available data set, some features can be reasonably inferred:

1. The Hero Fan is small; 5 x 5 km with a maximum thickness of 250 m. The coarse-grained sediments in the east limb of the Hero Syncline are related to those of the high-gradient fan deposits in the west limb as is shown by the closure of the syncline to the north. This means that about 200 m of fanglomerate are laterally equivalent to the relatively thin 25 m of distal coarse clastics. The distance between the outcrops of distal and proximal facies along cross-section X-Y amounts to 2.5 km, which allows for a realistic average slope angle of 4° (compare Rachoki, 1981), when not accounting for differential subsidence. Since the majority of coarse clastic units in the localities of fences I and II are well connected in sheets, the base level, and after a rapid progradation also the slope of the fan, must have been fairly constant. The thickness difference, therefore, has to be explained by differential tectonic subsidence in the proximal fan reaches, a common occurrence where faults control sedimentation.

2. Except for the northernmost outcrops, proximal conglomerate *(facies A)* and pebbly sandstone *(subfacies C_m)* are restricted to the west limb, while the distal and fringe facies are found in the east limb. Apart from the rapid initial progradation and terminal retrogradation, this reflects conditions of internal vertical facies stacking, as is known from areas of rapid generation of relief along boundary faults (Heward, 1978). The mixing of breccia and conglomerate and the occurrence of outsized clasts are further arguments in favour of fault activity.

3. The observed asymmetry and facies shift of the Hero Fan points to a syndepositional strike-slip control, probably with a northward tilt component, which created a steeper slope in the northern half of the fan. If the fan asymmetry and depocentre shift are compared with other known examples of fan skewing (e.g., Hooke, 1972; Steel, 1988; Nijman & Savage, 1989; Dabrio, 1990, table 1 and fig. 16C, showing a fan delta in the Murcia Basin), the setting corresponds to sinistral strike-slip. Long after sedimentation, during D^P_4, the same sense of displacement was resumed.

The above arguments favour an interpretation of oblique-slip fault control. The controlling fault must have had a north-south strike, as facies boundaries are parallel to the north-south D^P_3-structures. Such a proto-Hero Fault (Fig. 20), or proto-Mount Gordon Fault, is not likely to have been an east-verging D^P_2-low angle thrust, because such faults generally create the strongly diachronous facies boundary pattern characteristic of rapid progradation. Instead, an early east-block-down effect along a steep (D^P_1?) fault can be expected to have controlled the deposition of the Hero Formation. There is no clue to the precise regime along such a fault step other than the analogy with such steps along and over D^P_1 flowers farther eastwards in the Paroo Range (Nijman & others, this volume). The observed positive flowers tend to change by steps into half-flowers to the west, up the dip of the palaeoslope. If such a trend is extrapolated to the Hero Fault Zone, a west-block-up fault step may have been created by D^P_{1b} upthrusting along an original D^P_{1a}-strike-slip fault at or westerly adjacent to the present Hero Fault.

The relation between the Hero/Western Fault Zone and the Paroo Range

Table I summarises and compares the sequence of events in the Hero/Western Fault Zone and the Paroo Range.

Conclusions

1. The stratigraphic position of the Hero Fan with respect to the Mount Isa Group Unconformity is comparable to that of the Lower Mount Isa Group in the Paroo Range, at a restored distance of 20 km to the east (Fig. 21). Except for outsized clasts, the overall maximum grain size of the Hero Fan excludes its connection with the fan distributaries of the Surprise Creek Formation that are on average some grades coarser, but does correspond with

Deformation/ sedimentation phase	Description	Hero Fault Zone	Western Fault Zone	Correlation with Paroo Range Nijman , this volume
D^P_{1a}	# N-S extensional listric faulting (?)	• in ECV		
	# N-S positive flower structures and associated drape folds			• diverging from top ECV
	# regional eastward tilt	• reg.unconf.	• reg.unconf.	• reg.unconf.
syn-D^P_{1a} sed.	*# pebbly sandstone in rim synclines of the flower structures*			• *Bortala Fm.*
D^P_{1b}	# east-verging drape folds/upthrusts (reactivation of D^P_{1a}-structures)	? proto-Hero F.		• syn-Surprise Creek Form.
	# sinistral N-S strike slip	• proto-Hero F.		
	# south-down stepping E-W normal faults	• minor growth faults		• Congl.Creek Fault
syn-D^P_{1b} sed.	*# early syn-D^P_{1b} fandelta cg/(in)shore sst.*			• *Surprise Cr.Fm*
	# late to post syn-D^P_{1b} alluvial fan/coastal sst/cg.	• *Hero Fan.*		• *Warrina Park Qzt.*
	# southward depocentre shift	• *Hero Fan*		
D^P_2	# low-angle thrusting with restricted S^P_2-cleavage and meso/micro-scale folds	? proto-Hero F. E-verging (?)		• syn to post-Mt. Isa Group, W-verging
D^P_3	# regional N-S folding, S^P_3-ax.planar foliation	• Hero Anti- / Syncline	•	• e.g.Campsite Anticline
	# east-verging upthrusting	• Hero Fault		
D^P_4	# sinistral transpressive strike slip,vertical S-folds and NE sinistral faults	• Hero Fault & Syncline		
	# dextral transtensive strike slip; duplexes		• Western F.	
	# plunge of D^P_3 folds	• southwards	• northwards, fanning	• northwards
	# southblock-down E-W spoon faults			• e.g.Congl.Cr.F
	# drag synclines with ax. planar S^P_4		•	• Horse's Head
D^P_5	# conjugate NE dextral and NW sinistral, rare E-W, transpressive/-tensive faults	•	•	• e.g.Congl.Cr.F
	# vertical folds with S^P_5-cleavage and sinistral strike slip			• Horse's Head

TABLE I. SEQUENCE OF SEDIMENTATION AND DEFORMATION EVENTS IN THE HERO/WESTERN FAULT ZONE, COMPARED WITH THAT OF THE PAROO RANGE (NIJMAN & OTHERS, THIS VOLUME).

the coastal quartz arenite of the Warrina Park Quartzite (compare Fig. 8). Whether maximum onlap of the Warrina Park coastline correlates with maximum progradation of the Hero Fan, i.e., facies zone contraction, followed by expansion of the Moondarra Siltstone over both zones of coarse clastics or, on the contrary, coincides with fan retrogradation cannot be assessed due to lack of exposure in the intermediate zone of floodbasin deposits (Moondarra facies).

2. D^P_1-effects are visible in the Hero Fault Zone with a D^P_{1a} north-south tensional component for the pre-Mount Isa Group period, and a D^P_{1b} west-block-up fault step (inferred upthrust or half-flower structure) along a proto-Hero Fault to account for the sedimentation of the Hero Fan. Early sinistral strike-slip is indicated by the southward depocentre shift and skewing in the Hero Fan. Such a combination of east-west compression and north-south tension with strike-slip is also known from the Paroo Range, but the strike-slip motions are opposite in the two areas.

3. The low-angle west-verging D^P_2 thrust system of the Paroo Range has not been found in the Hero Fault area. Instead, the evidence supports the existence of a steep east-verging reverse fault, which, however, may have had a lower-angle D^P_2 precursor, or may have originated directly from a D^P_1 half-flower. East vergence compares

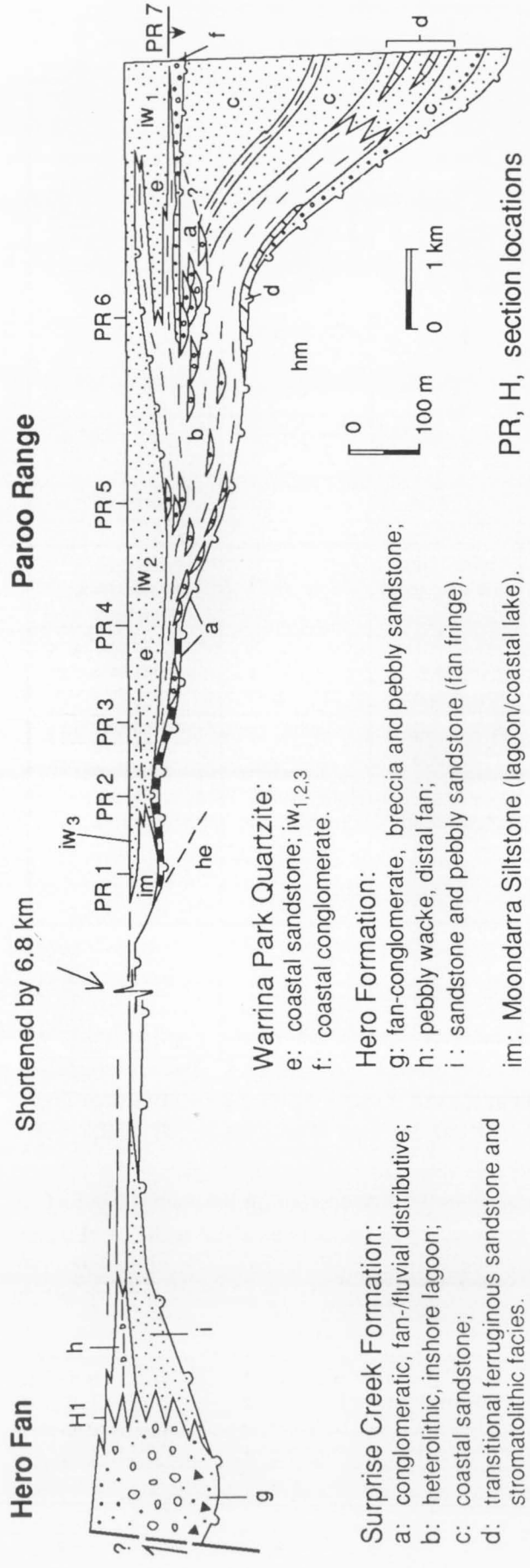


Fig. 21. Stratigraphic east-west cross-section restored at the level of maximum fan progradation, here correlated with the top of the Warrina Park depositional system of the Paroo Range. Section shortened by 6.8 km in east-west direction to fit on page. P omitted from stratigraphic symbols for clarity.

with data of Connors & others (this volume) suggesting the existence of similar but later thrusts (D^{N}_{3a} of Connors & others = D2 = D^{P}_{3}) west of the Mount Isa Fault.

4. Late-stage (D^{P}_{4}) sinistral strike-slip at the Hero Fault could mirror the transfer mechanism of differential north-south extension derived for the Western Fault. Then one would expect corresponding spoon faults in the domain between the Hero Fault and the Western Fault. Reactivation of D^{P}_{1a} faults in the ECV may have occurred at this time. The situation west of the Hero Fault points to transpression between the Hero and the Mount Gordon Faults (Fig. 1), i.e., west-block-up sinistral oblique displacement along the Hero Fault (compare BMR, 1986). Whether on the scale of the inlier the inferred strike-slip deformation was subordinate to an overall extensional tectonic regime, such as the north-south extension observed at deeper levels in the Wonga Belt by Pearson & others (this volume), or whether a fundamental deep-seated strike slip induced juxtaposed transtensive and transpressive domains in the cover rock, remains questionable. Such a basic motif of deformation is worth further discussion. Figure 22 relates the deformation sequence of Table I with known events within and to the east of the LRFT, and this illustrates a striking analogy between the deformation history of the Paroo Range and surroundings and that of the easternmost structural unit of the Mount Isa Inlier, the Soldiers Cap Belt near Cloncurry (Loosveld, 1989, this volume).

Acknowledgements

We thank the Bureau of Mineral Resources, Geology & Geophysics, Canberra, Australia, for the invitation to participate in the Mount Isa Project and for providing logistics in the field. Mount Isa Mines Exploration Department provided maps, drill hole data, and supported a fieldtrip in the Hero area in 1990, for which we thank in particular Drs Peter Forrestal and Bill Perkins. We gratefully acknowledge the annual grants of the Dutch foundation 'Dr.Schurmannfonds' from 1987 to 1989, without which our participation could never have been realised. Prof. Peter Ypma (University of Adelaide) participated during the first phase of the fieldwork. The manuscript greatly benefited from the comments and

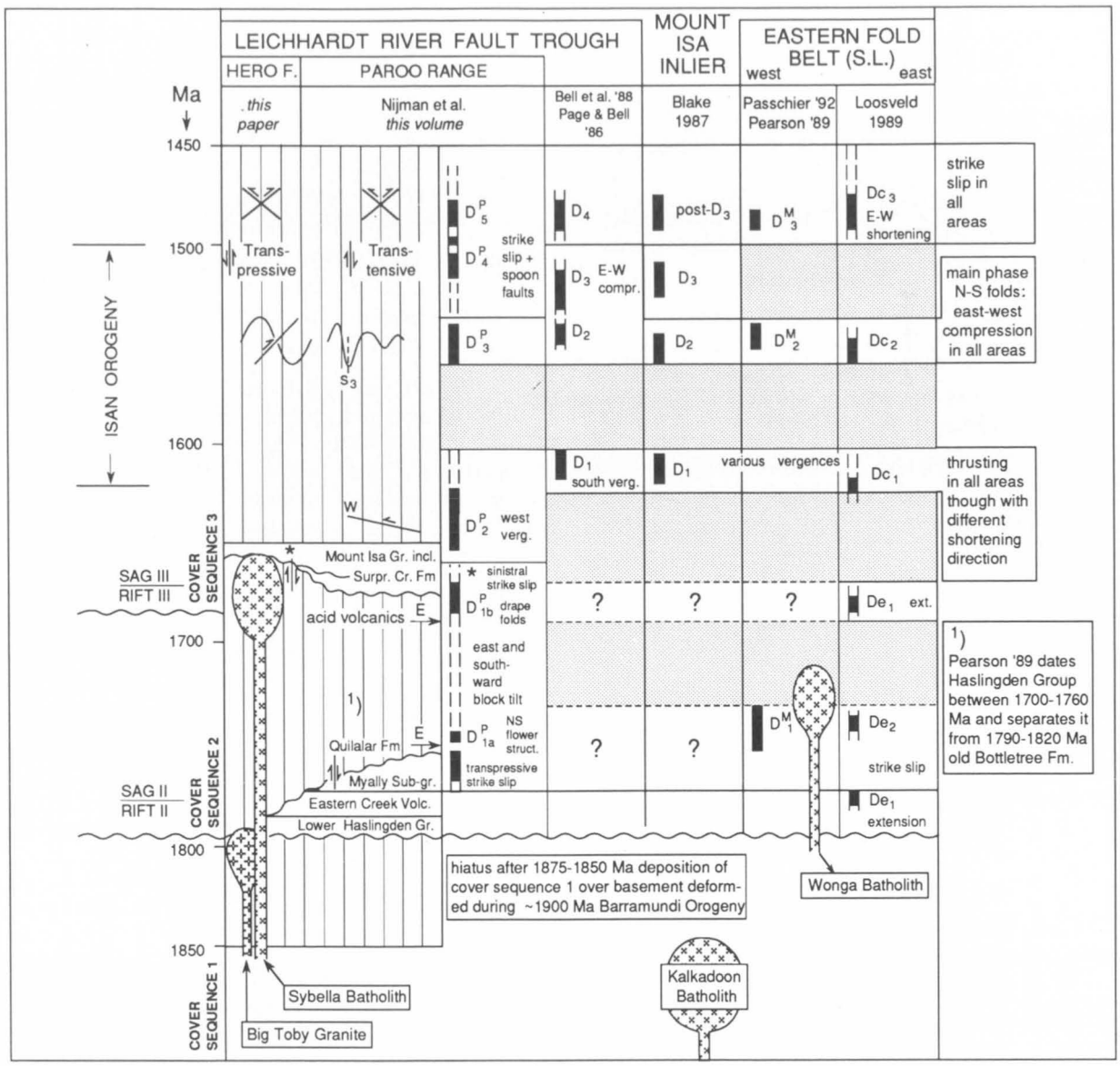


Fig. 22. Correlation scheme of deformation events in the Mount Isa Inlier. The deformation history of the Hero/Western Fault Zone and Paroo Range compares with that recorded by Loosveld (1989) from the Soldier's Cap Belt in the east of the Mount Isa Inlier near Cloncurry.

corrections by Drs Jim Jackson (BMR), John Savage (University of Utrecht), Ed Simpson (Kutztown University, Pennsylvania), and Alastair Stewart (BMR), and from discussion of the fan model with Dr George Postma (University of Utrecht). Messrs I.Santoe and J.J.J. van Bergenhenegouwen at the Institute of Earth Sciences at Utrecht drafted the figures, while Mrs B. Benders prepared the photographs.

References

BELL, T.H., 1983 - Thrusting and duplex formation at Mount Isa, Queensland, Australia. *Nature* 304, 493-497.

BELL, T.H., PERKINS, W.G., & SWAGER, C.P., 1988 - Structural controls on development and localization of syntectonic copper mineralization at Mt. Isa, Queensland. *Economic Geology* 83, 69-85.

BENNET, E.M., 1965 - Lead-zinc-silver and copper deposits of Mount Isa. *In:* J.McANDREW (Editor), Geology of Australian Ore Deposits. *8th Commonwealth Mining and Metallurgical Congress, Melbourne,* 233-246.

BIDDLE, K.T., & CHRISTIE-BLICK, N., 1985 - Glossary - Strike-slip deformation, basin formation, and sedimentation. *In:* BIDDLE, K.T., & CHRISTIE-BLICK, N. (Editors), Strike-slip deformation, basin formation, and sedimentation. *Society of Economic Paleontologists and Mineralogists, Special Publication* 37, 375-386.

BLAKE, D.H., 1987 - Geology of the Mount Isa Inlier and environs, Queensland and Northern Territory. *Bureau of Mineral Resources, Australia, Bulletin* 225, 83 pp.

BLAKE, D.H., ETHERIDGE, M.A., PAGE, R.W., STEWART, A.J., WILLIAMS, P.R., & WYBORN, L.A.I., 1990 - Mount Isa Inlier - regional geology and mineralisation. *In:* HUGHES, F.E. (Editor), Geology of the Mineral Deposits of Australia and Papua New Guinea. *Australasian Institute of Mining and Metallurgy, Monograph* 14, 915-925.

BMR, 1986 - Transpressional strike-slip faulting in the Mount Isa Inlier. *BMR Research Newsletter* 4, 1-2.

BOURGEOIS, J., & LEITHOLD, E.L., 1984 - Wave-worked conglomerates - Depositional processes and criteria for recognition. *In:* KOSTER, E.H., & STEEL, R.J. (Editors), Sedimentology of Gravels and Conglomerates. *Canadian Society of Petroleum Geologists, Memoir* 10, 331-343.

COLELLA, A., & PRIOR, D.B., 1990 - Coarse-grained Deltas. *International Association of Sedimentologists Special Publication* 10, 357 pp.

CONNORS, K.A., PROFFETT, J.M., LISTER, G.S., SCOTT, R.J., OLIVER, N.H.S., & YOUNG, D.J., this volume - Geology of the Mount Novit Ranges, southwest of Mount Isa mine. *In:* STEWART, A.J., & BLAKE, D.H. (Editors), Detailed Studies of the Mount Isa Inlier. *Bureau of Mineral Resources, Australia, Bulletin* 243.

DABRIO, C.J., 1990 - Fan delta facies associations in late Neogene and Quaternary basins of southeastern Spain. *In:* COLELLA, A., & PRIOR, D.B. (Editors), Coarse-grained Deltas. *International Association of Sedimentologists Special Publication* 10, 91-111.

DERRICK, G.M., 1982 - A Proterozoic rift zone at Mount Isa, Queensland, and implications for mineralization. *BMR Journal of Australian Geology & Geophysics* 7, 81-92.

DERRICK, G.M., WILSON, I.H., & HILL, R.M., 1976 - Revision of the stratigraphic nomenclature in the Precambrian of northwestern Queensland, III: Mount Isa Group. *Queensland Government Mining Journal* 77, 402-405.

DUNNET, D., 1976 - Mount Isa - reconstruction of a faulted orebody. *Philosophical Transactions of the Royal Society of London* A283, 333-344.

GIBBS, A.D., 1984 - Structural evolution of tensional basin margins. *Journal of the Geological Society of London* 141, 609-620.

GLIKSON, A.Y., DERRICK, G.M., WILSON, I.H., & HILL, R.M., 1975 - Tectonic evolution and crustal setting of the Middle Proterozoic Leichhardt River Fault Trough, Mount Isa Region, northwestern Queensland. *BMR Journal of Australian Geology & Geophysics* 1, 115-129.

HANCOCK, P.L., 1985 - Brittle microtectonics: principles and practice. *Journal of Structural Geology* 7, 437- 457.

HELLER, P.L., ANGEVINE, C.L., WINSLOW, N.S., & PAOLA, C., 1988 - Two-phase model of foreland-basin sequences. *Geology* 16, 501-504.

HEWARD, A.P., 1978 - Alluvial fan sequence and megasequence models: with examples from Westphalian D - Stephanian B coalfields, northern Spain. *In:* MIALL A.D. (Editor), Fluvial Sedimentology. *Canadian Society of Petroleum Geologists, Memoir* 5, 669- 702.

HOOKE, R. le B., 1972 - Geomorphic evidence for late Wisconsin and Holocene tectonic deformation, Death Valley, California. *Bulletin of the Geological Society of America* 83, 2073-2098.

LOCHEM, J.H. van, SPLIETHOFF, H., & NIJMAN, W., 1988 - Structure and sedimentation in the Proterozoic of the Paroo Range, Mount Isa Inlier, Queensland, Australia. *Contributions to the MIRTH Project, Institute of Earth Science, University of Utrecht, Report No. 2, Bureau of Mineral Resources, Canberra.* 100 + xliii pp., 1:25 000 geological map.

LOOSVELD, R.J.H., 1989 - The intracratonic evolution of the central eastern Mount Isa Inlier, northwest Queensland, Australia. *Precambrian Research* 44, 243-276.

LOOSVELD, R.J.H., this volume - Structural geology of the Central Soldiers Cap Belt, Mount Isa Inlier, Australia. *In:* STEWART, A.J., & BLAKE, D.H. (Editors), Detailed Studies of the Mount Isa Inlier. *Bureau of Mineral Resources, Australia, Bulletin* 243.

MANDL, G., de JONG, L.N.J., & MALSTHAL, A., 1977 - Shear zones in granular material. An experimental study. *Rock Mechanics* 9, 95-144.

MARZO, M., NIJMAN, W., & PUIGDEFABREGAS, C., 1988 - Architecture of the Castissent fluvial sheet sandstone, Eocene, South Pyrenees, Spain. *Sedimentology* 35, 719-738.

MASSARI, F., & COLELLA, A., 1988 - Evolution and types of fan-delta systems in some major tectonic settings. *In:* NEMEC, W.D., & STEEL, R.J. (Editors), Fan Deltas: Sedimentology and Tectonic Settings. *Blackie & Sons, London*, 103-122.

MATHIAS, B.V., & CLARK, G.J., 1975 - Mount Isa copper and silver-lead-zinc ore bodies - Isa and Hilton Mines. *In:* KNIGHT, C.L. (Editor), Economic Geology of Australia and Papua New Guinea: 1. Metals. *The Australasian Institute of Mining and Metallurgy, Melbourne, Monograph Series* 5, 351-372.

MATHIAS, B.V., CLARK, G.J., MORRIS, D., & RUSSELL, R.E., 1973 - The Hilton deposit - stratiform silver-lead-zinc mineralisation of the Mount Isa type. *Bureau of Mineral Resources, Australia, Bulletin* 141, 33-58.

McPHERSON, J., SHANMUGAM, G., & MOIOLA, R.J., 1988 - Fan deltas and braid deltas: conceptual problems. *In:* NEMEC, W.D., & STEEL, R.J.

(Editors), Fan Deltas: Sedimentology and Tectonic Settings. *Blackie & Sons, London,* 14-22.

MIALL, A.D., 1978 - Lithofacies types and vertical profile models in braided river deposits: A summary. *In:* MIALL, A.D. (Editor), Fluvial Sedimentology. *Canadian Society of Petroleum Geologists, Memoir* 5, 597-604.

MIALL, A.D., 1985 - Architectural element analysis: a new method of facies analysis applied to fluvial deposits. *Earth Science Reviews* 22, 261-308.

NAMI, M., & LEEDER, M.R., 1978 - Changing channel morphology and magnitude in the Scalby Formation (M. Jurassic) of Yorkshire, England. *In:* MIALL, A.D. (Editor), Fluvial Sedimentology. *Canadian Society of Petroleum Geologists, Memoir* 5, 431-440.

NAYLOR, M.A., MANDL, G., & SIJPESTEIJN, C.H.K. 1986 - Fault geometries in basement-induced wrench faulting under different initial stress states. *Journal of Structural Geology* 8, 737-752.

NEMEC, W., & STEEL, R.J., 1984 - Alluvial and coastal conglomerates: the significant features and some comments on gravelly mass flow deposits. *In:* KOSTER, E.H. & STEEL, R.J. (Editors), Sedimentology of Gravels and Conglomerates. *Canadian Society of Petroleum Geologists, Memoir* 10, 1-31.

NEMEC, W., STEEL, R.J., POREBSKI, S.J., & SPINNANGR, A., 1984 - Domba conglomerate, Devonian, Norway: Process and lateral variability in a mass flow-dominated, lacustrine fan-delta. *In:* KOSTER, E.H., & STEEL, R.J. (Editors), Sedimentology of Gravels and Conglomerates. *Canadian Society of Petroleum Geologists, Memoir* 10, 295-320.

NEUDERT, M.K., 1983 - A depositional model for the Upper Mount Isa Group. PhD thesis, Australian National University, Canberra (unpublished).

NEUDERT, M.K., & RUSSELL, R.E., 1981 - Shallow water and hypersaline features from the Middle Proterozoic Mount Isa sequence. *Nature* 293, 284-287.

NIJMAN, W., 1991 - Geology of the Paroo Range - Hero/Western Fault Zone (1:20 000 scale map). *Bureau of Mineral Resources, Canberra, Australia* (two sheets). Available as colour electrostatic plots on paper (AUD30), or in digital form on optical disc or Exabyte 8 mm tape (prices on application) both of which can be displayed on Intergraph Microstation software on computers that will run Unix. The digital data comprise a scanned raster image (.RLE format) of the black and white geological map, and an Intergraph vector design file containing the boundaries of coloured polygons. The coloured map and data are available from the Publication Sales Centre, Bureau of Mineral Resources, and an uncoloured Ozalar film or paper copy (AUD20) of the map is available from BMR Copy Service, both at GPO Box 378, Canberra, ACT, 2601, Australia. All orders to be prepaid to Collector of Public Monies.

NIJMAN, W., LOCHEM, J.H. van, SPLIETHOFF, H., & FEIJTH, J., this volume - Deformation model and sedimentation patterns of the Proterozoic of the Paroo Range, Mount Isa Inlier, Queensland, Australia. *In:* STEWART, A.J., & BLAKE, D.H. (Editors), Detailed Studies of the Mount Isa Inlier. *Bureau of Mineral Resources, Australia, Bulletin* 243.

NIJMAN, W., & SAVAGE, J.F., 1989 - Persistent basement wrenching as controlling mechanism of Variscan thin-skinned thrusting and sedimentation, Cantabrian Mountains, Spain. *Tectonophysics* 169, 281-302.

PAGE, R.W., & BELL, T.H., 1986 - Isotopic and structural responses to successive deformation and metamorphism. *Journal of Geology* 94, 365-379.

PASSCHIER, C.W., this volume - Geology of the Myubee area, Mount Isa Inlier, Queensland. *In:* STEWART, A.J., & BLAKE, D.H. (Editors), Detailed Studies of the Mount Isa Inlier. *Bureau of Mineral Resources, Australia, Bulletin* 243.

PEARSON, P.J., 1989 - The structural and tectonic development of the Wonga Belt and surrounding Mary Kathleen Fold Belt, Mount Isa Inlier, northwestern Queensland. Ph.D. thesis, University of Queensland (unpublished).

PEARSON, P.J., HOLCOMBE, R.J., & PAGE, R.W., this volume - Synkinematic emplacement of the Middle Proterozoic Wonga Batholith into a mid-crustal extensional shear zone, Mount Isa Inlier, Queensland, Australia. *In:* STEWART, A.J., & BLAKE, D.H. (Editors), Detailed Studies of the Mount Isa Inlier. *Bureau of Mineral Resources, Australia, Bulletin* 243.

PERKINS, W.G., 1970 - 733' to 1" map of Mine Lease 8058, A-P 582M-Area, northern position. Report for Geology Department of Mount Isa Mines Ltd (unpublished).

PERKINS, W.G., 1984 - Mount Isa silica dolomite and copper orebodies: the result of a syntectonic alteration system. *Economic Geology* 79, 601-637.

PLUMB, K.A., DERRICK, G.M., & WILSON, I.H., 1980 - Precambrian geology of the McArthur River/Mount Isa region, northern Australia. *In:* HENDERSON, R.A., & STEPHENSON, P.J. (Editors), The Geology and Geophysics of the Southern Hemisphere. *Developments in Precambrian Geology* 2, *Elsevier, Amsterdam,* 205-307.

POSTMA, G.J., 1990. - Depositional architecture and facies of river and fan deltas: a synthesis. *In:* COLELLA, A. & PRIOR, D.B. (Editors), Coarse-grained Deltas. *International Association of Sedimentologists Special Publication* 10, 13-27.

POSTMA, G.J., submitted - Origin and features of bouldery debris flow deposits in shoal-water coarse-grained deltas. *Sedimentology.*

RACHOCKI, A., 1981 - Alluvial fans. *J. Wiley & Sons Ltd., London.* 161 pp.

RIJSWIJK, J.B.H. van, & SCHALKWIJK, G., 1988 - Thermoluminescence of quartz as a sedimentary provenance study technique in the Proterozoic of the Paroo Range, Mount Isa Inlier, Queensland, Australia. *Contributions to the MIRTH Project, Institute of Earth Sciences, University of Utrecht, Report* No. 3, *Bureau of Mineral Resources, Australia,* 45 pp. (unpublished).

SHULTZ, A.W., 1984 - Subaerial debris-flow deposition in the Upper Palaeozoic Cutler Formation, Western Colorado. *Journal of Sedimentary Petrology* 54, 759-772.

SMITH, W.D., 1969 - Penecontemporaneous faulting and its likely significance in relation to Mount Isa ore deposition. *Geological Society of Australia, Special Publication* 2, 225-235.

STEEL, R.J., 1988 - CU and skewed fan bodies: symptoms of strike-slip and transfer movement in sedimentary basins. *In:* NEMEC, W.D., & STEEL, R.J. (Editors), Fan Deltas: Sedimentology and Tectonic Settings. *Blackie & Sons, London,* 75-83.

STEWART, A.J., this volume - Geology of the Horse's Head structure, north of Mount Isa, and its bearing on the 'roof thrust + imbricate stack' hypothesis, Mount Isa Inlier, Queensland. *In:* STEWART, A.J., & BLAKE, D.H. (Editors), Detailed Studies of the Mount Isa Inlier. *Bureau of Mineral Resources, Australia, Bulletin* 243.

TCHALENKO, J.S., 1970 - Similarities between shear zones of different magnitudes. *Bulletin of the Geological Society of America* 81, 1625-1640.

WILSON, C.J.L., 1975 - Structural features west of Mount Isa. *Journal of the Geological Society of Australia* 22, 457-476.

WILSON, I.H., HILL, R.M., NOON, T.A., DUFF, B.A., & DERRICK, G.M., 1979 - Geology of the Kennedy Gap 1:100 000 Sheet area (6757), Queensland. *Bureau of Mineral Resources, Australia, Record* 1979/24, 104 pp.

WINSOR, C.N., 1986 - Intermittent folding and faulting in the Lake Moondarra Area, Mount Isa, Queensland. *Australian Journal of Earth Sciences* 33, 27-42.

WOODCOCK, N.H., & FISHER, M., 1986 - Strike-slip duplexes. *Journal of Structural Geology* 8, 725-735.

WYBORN, L.A.I., PAGE, R.W., & McCULLOCH, M.T., 1988 - Petrology, geochronology, and isotope geochemistry of the post-1820 Ma granites of the Mount Isa Inlier: mechanisms for the generation of Proterozoic anorogenic granites. *Precambrian Research* 40/41: 509-541.

Geology of the Horse's Head structure, north of Mount Isa, and its bearing on the 'roof thrust + imbricate stack' hypothesis, Mount Isa Inlier, Queensland

A.J.Stewart [1]

The Horse's Head, 40 km north of Mount Isa, is the southernmost of several east-west fault-bounded blocks of Mount Isa Group which segment a large, north-plunging upright antiform of the stratigraphically lower Eastern Creek Volcanics. Bell (1983, 1991) interpreted the fault blocks as horses of a south-verging D_1 imbricate stack or contractional duplex, the bounding faults ramping up from a floor thrust below to join a roof thrust above, with some 200 km of southward translation. East-west shortening (D_2) folded the imbricate stack and overlying sheet into a north-plunging antiform, and steepened the originally north-dipping thrust faults bounding the horses, in places past the vertical to a steep south dip. The chief difficulty with this model is that the D_2 antiform is cut by, and is therefore older than, the east-west faults bounding the supposed D_1 imbricates, whereas, according to the model, the antiform should be younger than the faults.

The eastern part of the Horse's Head has a steep easterly-striking penetrative to spaced cleavage which is axial-plane to small west-southwest-plunging D_1 folds. The central and western parts have a steep northerly-striking penetrative D_2 cleavage, which is axial-plane to small north-plunging upright D_2 folds, and overprints the D_1 cleavage and folds. D_3 folds are few and are small domes or northwest-plunging folds. The western bounding fault of the Horse's Head parallels the D_2 cleavage and axial planes, but 10 km to the south, the fault truncates D_2 synforms, and so is regarded as having formed at the end of D_2. The northern bounding fault dips steeply south, and cuts the major D_2 antiform and cleavage at a large angle, and is assigned to D_4. The northern and western faults are terminated in the northwest by a steep northeast-striking fault which cuts the D_2 cleavage at a large angle and is assigned to D_5 strike-slip faulting.

The structure of the Mount Isa Group in the Horse's Head is a basin representing a Type 1 interference fold, which has been subsequently dismembered by faulting. An initial east-southeast-trending D_1 synform was deepened and elongated in a northerly direction by formation of a major north-south-trending D_2 synform; this was followed by steep overthrusting from west to east up the western bounding fault, removing the western half of the north-south D_2 synform. East-west-striking listric transtensional D_4 faulting formed the northern boundary and removed the northern part of the D_1/D_2 interference synform. Lastly, a northeast-oriented strike-slip fault removed the northwest corner of the synform, giving the present outcrop shape.

The Horse's Head is not a fault-bounded horse belonging to a D_1 imbricate stack or duplex. If a thrust sheet exists, as postulated by Bell (1983, 1991), it has no fault horses or imbricates stacked beneath it at the Horse's Head.

[1] Bureau of Mineral Resources, GPO Box 378, Canberra, ACT, 2601, Australia.

Introduction

In a major contribution to the geology of the Mount Isa Inlier, Tim Bell (1983) conceived a potentially far-reaching hypothesis on the structural evolution of the Leichhardt River Fault Trough (Fig. 1) north of Mount Isa township. His hypothesis was based on interpretation and synthesis of 1:100 000 geological maps published by the Australian Bureau of Mineral Resources, and has important consequences for exploration for ore deposits of the Mount Isa type. It also introduced a previously unconsidered deformation mechanism in Mount Isa – low-angle contractional faulting and resultant nappes, imbricates, and thrust sheets. Until then, compressional structures in the Mount Isa Inlier had been generally regarded as moderate in size and characterised by steep thrust faults and upright folds with generally shallow plunges (Mathias & Clark, 1975; Derrick & others, 1977; Plumb & others, 1981). Dunnet (1976) had, however, previously proposed low- and high-angle extensional faults (spoon faults) in the area subsequently reinterpreted by Bell (1983). Smith (1969) and Derrick (1982) had explained some of the same structures as growth faults.

The Horse's Head is an outcrop of Mount Isa Group

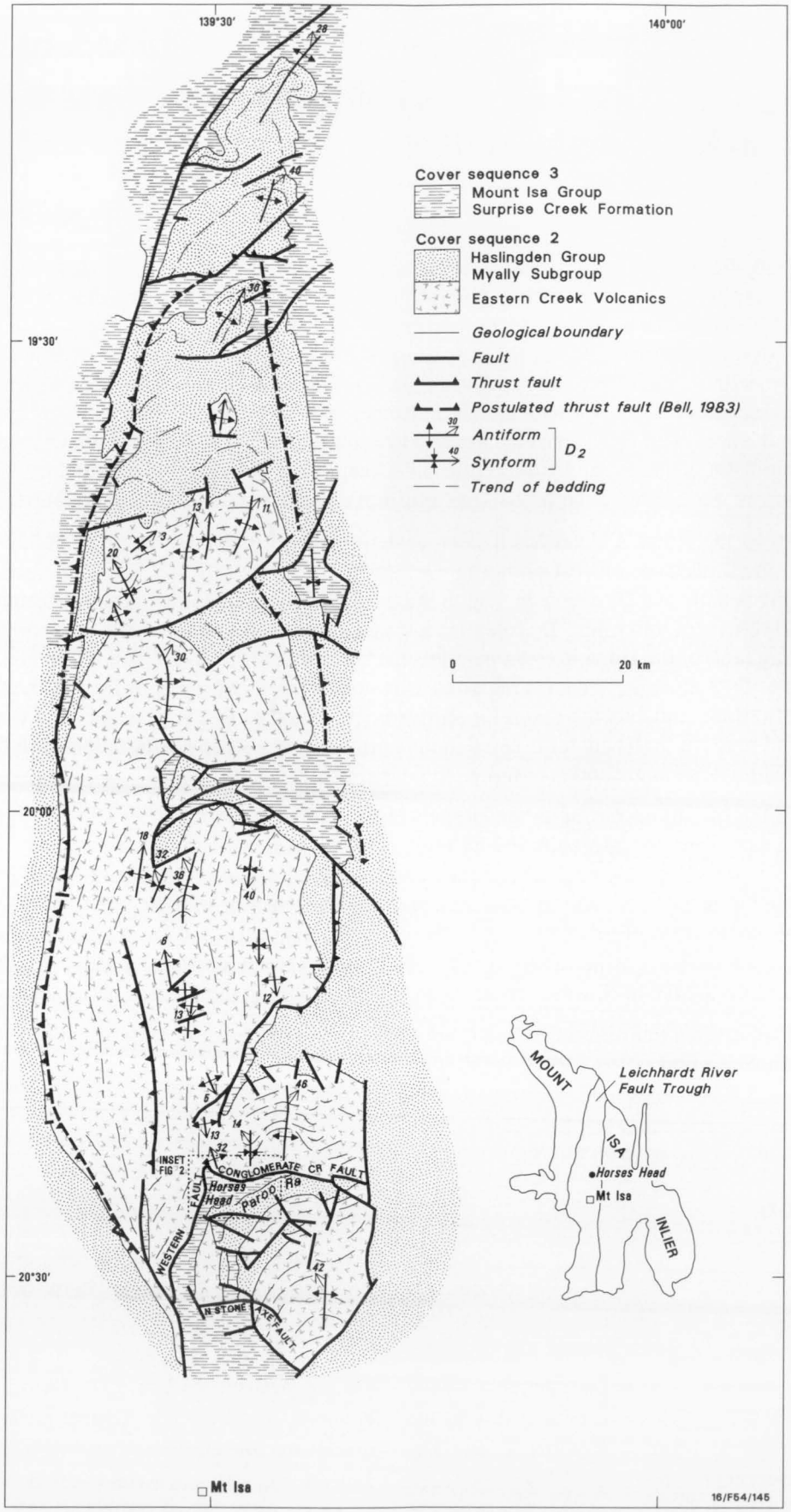


Fig. 1. Geological sketch map of Leichhardt River Fault Trough, showing location of Horse's Head and postulated roof thrust (Bell, 1983). Plunge values on folds were derived by plotting poles to bedding shown on Alsace (1982), Kennedy Gap (1980), Mammoth Mines Region (1985), Mary Kathleen (1976), Mount Oxide Region (1984), Myally (1984), and Prospector (1979) 1:100 000 geological maps of the area, published by the Bureau of Mineral Resources.

metasediments shaped like a horse's head (Figs. 1 & 2). It is located in the Leichhardt River Fault Trough 40 km north of Mount Isa, and is the southernmost of several outcrops of Mount Isa Group or Myally Subgroup (upper Haslingden Group) which are generally bounded to the north and south by east-striking faults (the spoon faults of Dunnet, 1976). The fault-bounded blocks segment a large, north-plunging upright antiform of Eastern Creek Volcanics of the middle Haslingden Group. Bell (1983, 1991) interpreted the fault-bounded blocks as horses of an imbricate stack or contractional duplex that formed during an early deformational phase, D_1. The bounding faults ramped up from a floor thrust below and flattened out to join a roof thrust above. The roof thrust is the sole of a large thrust sheet with some 200 km of southward translation. Subsequent east-west shortening (D_2) folded the imbricate stack and overlying sheet into a north-plunging antiform, which after erosion exposed the horses of the imbricate stack in the core of the antiform, and the overlying sheet on the limbs. The northward plunge steepened the originally north-dipping thrust faults bounding the horses, in places past the vertical to a steep south dip. The main, and possibly insurmountable difficulty with Bell's model is that the antiform is cut by, and is therefore older than, the east-west faults bounding the supposed D_1 imbricates, whereas, according to the model the antiform should be younger than the faults.

This paper presents a structural analysis and synthesis of the Horse's Head, to see whether or not it supports the roof thrust + imbricate stack hypothesis. To the south, in the adjoining Paroo Range area, the University of Utrecht has carried out structural mapping and sedimentological analysis of the Haslingden and Mount Isa Groups (Lochem & others, 1988; Nijman & others, this volume a, b), and their results are incorporated where appropriate. The main conclusions are:

- 1. The Horse's Head is a remnant of a D_1-D_2 basinal interference fold (Type 1 of Ramsay, 1967) whose western half was taken above the present level of erosion by overthrusting from the west at the end of D_2;
- 2. The northeastern quarter was removed by north-block-up D_4 normal faulting, leaving only the southeastern quarter of the interference fold;
- 3. The D_4 normal fault on the north side of the Horse's Head dips south, and is not a D_1 thrust connecting the floor and roof thrusts of a D_1 imbricate stack, and the western fault is not its continuation around a D_2 fold.

Hence, the roof thrust + imbricate stack hypothesis is not supported by the structural geology of the Horse's Head.

Regional Setting

The Mount Isa Inlier (Blake, 1987) comprises a basement of gneiss and migmatite older than 1870 Ma, and three overlying cover sequences of deformed and metamorphosed sedimentary and volcanic rocks. Cover sequence 1 (1870-1840 Ma) is mostly felsic volcanics, which are comagmatic with the voluminous Kalkadoon Granite intrusive into the basement complex. Cover sequences 2 (1790-1760 Ma) and 3 (1680-1670 Ma) are shallow-water sedimentary and bimodal volcanic rocks; the two sequences each formed during a rift-sag regime. An intervening period of crustal extension and low-angle normal faulting at 1740 Ma affected the central part of the Mount Isa Inlier east of Mount Isa township (Passchier, 1986; Passchier & Williams, 1989; Stewart, 1989; Holcombe & others, this volume), but is not recognised in the Horse's Head area. The Haslingden Group and Mount Isa Group of the Horse's Head area respectively belong to cover sequences 2 and 3.

Outline of Deformation History

Terminology

Deformation episodes for the Horses Head and the neighbouring Paroo Range areas are respectively denoted by superscripts 'H'and 'P'. All grid references refer to the Prospector 1:100 000 Map Sheet.

Contractional deformation

The deformational events that affected the Horse's Head-Paroo Range area are set out in Table 1. Regional shortening which affected all stratigraphic units throughout the Mount Isa Inlier took place at about 1610 Ma ($D^H_1 = D_1$) and 1544 Ma ($D^H_2 = D_2$), and several other contractional episodes of lesser extent, denoted as D^P_{1a}, D^P_{1b}, $D^H_{1.5}$, D^H_3 (= D_3; 1510 Ma), and D^H_5, affected the Horse's Head and Paroo Range area (Lochem & others, 1988; Nijman & others, this volume a, b) and also the Mount Novit area 15 km south of Mount Isa township (Connors & others, this volume). Isotopic dates on D_1, D_2, and D_3 are from Page & Bell (1986). D_1 produced folds which trend about east-west with an associated axial-plane cleavage. D_1 thrust faults are known outside the Horse's

TABLE 1. DEFORMATION EVENTS IN AND NEAR THE HORSE'S HEAD - PAROO RANGE AREA.

Time Ma	Deformation episode	Structures and events	Page & Bell 1986	Lochem & others 1988	Nyman & others this volume
1500	D^{H}_{5}	NW and NE strike-slip faults and folds plunging 0-60° N; folding of Conglomerate Creek Fault; probably result of E-W compression	D_5	$D^{P}5$	
	D^{H}_{4}	E-W transtensional normal faults with S dipand minor sinistral component, e.g. Conglomerate Creek Fault; cuts D^{H}_{2} cleavage and folds		D_4	D^{P}_{4}
1510 to 1450	D^{H}_{3}	Local NW-plunging folds, upright open to tight domes and irregular folds with no associated cleavage; folds D^{H}_{2} folds and cleavage	D_3		
1560 to 1550	D^{H}_{2}	N-plunging upright folds with axial-plane slaty cleavage; folds D_{H1} cleavage and folds. Western Fault formed at end of this episode, and truncates D^{H}_{2} axes	D_2	D_3	D^{P}_{3}
	$D^{H}_{1.5}$	Low-angle thrust faulting, upper block to W; deforms E-W D^{H}_{1} cleavage; folded by D^{H}_{2}		D_2	D^{P}_{2}
1610	D^{H}_{1}	W-plunging S-verging upright folds with axial-plane slaty cleavage which weakens S to spaced cleavage; folded by $D^{H}_{1.5}$ and D^{H}_{2}	D_1	D_4	D^{P}_{4}
1670		Deposition of Mount Isa Group			
1680 to 1670		Deposition of Surprise Creek Formation draped over flower structures; minor E and W-verging folds1670 and thrusts; second N-ward tilting and erosion; initiation of Conglomerate Creek Fault with synformal downwarping of adjoining Surprise Creek Formation south of fault		D_{1b}	D^{P}_{1b}
		Major unconformity			
		Transpressional faulting forming flower structures; E and W-verging folds and thrusts; N-ward tilting and erosion of Paroo Block		D_{1a}	D^{P}_{1a}
1740		Extension; not recognised in Horse's Head area			
1790 to 1780		Deposition of Haslingden Group of Cover Sequence 2, initiation of transpressional faulting forming flower structures			D^{P}_{1a}
1870 to 1840		Deposition of Cover Sequence 1 (not present in area)			

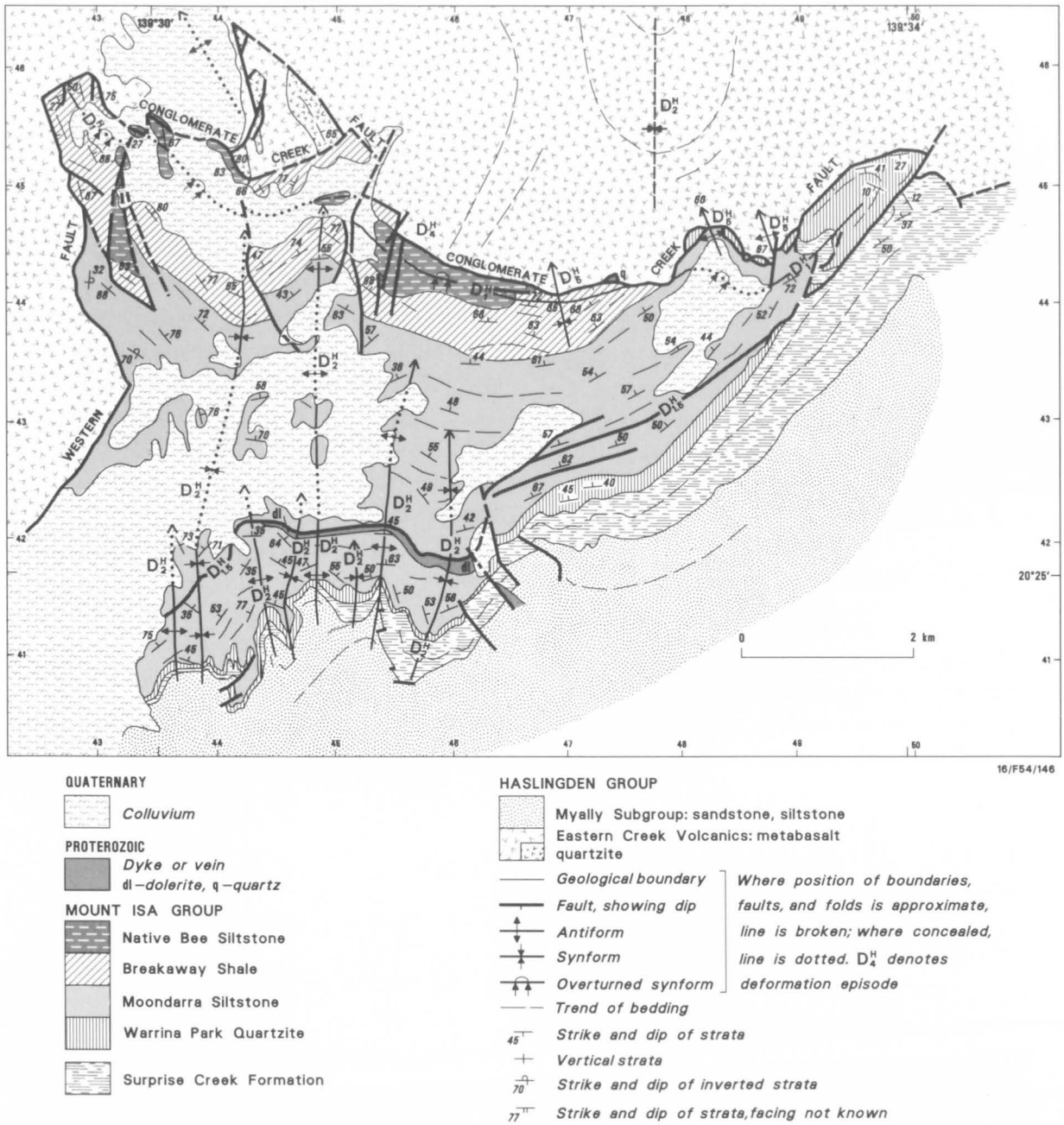


Fig. 2. Geological map of Horse's Head; mapping by Lochem & others (1988) and the author. Dip and strike values are averages of two or more measurements at each locality. Numbered ticks are 1000 m intervals of Australian Map Grid, Zone 54.

Head area, e.g., the West Leichhardt Klippe, 25 km southeast of the Horse's head (Loosveld & Schreurs, 1987; Blake, this volume). D_2 produced north-trending folds and thrust faults, and a penetrative steep to vertical schistosity; the folds dominate the map pattern of the region, and affect D_1 folds and faults. D_3 formed local folds and faults trending generally northwest. D^H_5 formed the prominent northwest and northeast strike-slip faults common throughout the Mount Isa Inlier, and also some north-plunging folds.

Before D^H_1, the Paroo Range area immediately south of the Horse's Head underwent two episodes of gentle east or west-verging open folding, faulting, and northward tilting. The first episode, D^P_{1a}, took place during and after deposition of cover sequence 2, and ended with transpressional strike-slip faulting that produced positive flower structures over which cover sequence 3 was draped unconformably (Lochem & others 1988; W.Nijman, personal communication, 1991). The second episode, D^P_{1b}, took place after deposition of the Surprise Creek Formation, the lowest unit of sequence 3 in this area (Lochem & others, 1988).

Extensional deformation

As well as the regional extensional rifting events mentioned above, the Horse's Head and Paroo Range underwent north-south extension, D^H_4, between the shortening events D^H_3 and D^H_5. This produced east-west listric normal faults, such as the Conglomerate Creek Fault (which was named by Blake [1991] and has a small sinistral strike-slip component) at the northern margin of the Horse's Head, and some two dozen others to the south, as far as the North Stone Axe Fault (Lochem & others, 1988; Nijman & others, this volume a). The faults are spaced 1-4 km apart, dip vertically or steeply south, are concave to the south, and belong to the spoonfault system of Dunnet (1976). They cut and therefore postdate D^H_3 folds, and the Conglomerate Creek Fault is folded by and therefore predates D^H_5 folds.

Geology of the Horse's Head

The oldest rocks exposed in the Horse's Head area (Fig. 2) are the *Eastern Creek Volcanics* of the *Haslingden Group* (cover sequence 2). They crop out in the north and west, and comprise greenschist-facies metabasalt and metaquartzite. To the southeast, they are overlain by feldspathic sandstone and siltstone of the *Myally Subgroup*, the upper part of the Haslingden Group. The rocks forming the Horse's Head itself belong to the lower part of the *Mount Isa Group*, and begin with the *Warrina Park Quartzite*, a shallow-marine quartz sandstone and conglomerate. This is shown on the Prospector 1:100 000 Geological Map (BMR, 1979) as making up all the ridge-forming sandstone resting unconformably on Myally Subgroup, but detailed mapping by Lochem & others (1988) restricts Warrina Park to the top 50-100 m of the sandstone, the underlying remainder (0-400 m) being assigned to the *Surprise Creek Formation* (also part of sequence 3), with an unconformity in between. The Warrina Park Quartzite is conformably overlain by the *Moondarra Siltstone* (low hills and ridges), which is followed by the *Breakaway Shale* (a prominent ridge) and *Native Bee Siltstone* (very low rises). A dyke of *dolerite* (much weathered) intrudes the Moondarra Siltstone in the south of the area. Quaternary *colluvium* covers much of the Moondarra and Native Bee Siltstones.

Macroscopic Structure

The Horse's Head (Fig. 2) is a remnant of a D^H_1-D^H_2 interference fold dismembered by late high-angle D^H_2 overthrusting from the west and by transtensional faulting in the north. The D^H_1 fold, a synform, is evident from the outcrop distribution of Breakaway Shale and Native Bee Siltstone (Fig. 2), in spite of being cut by small north-northeast and north-northwest strike-slip D^H_5 faults. At the eastern end of the area, along the northern limb of the synform, the Warrina Park Quartzite forms five boudins up to 300 m long composed of cross-bedded quartzite and pebble to boulder conglomerate (grid reference 484446). North-south D^H_2 folds are evident from the map pattern of the Warrina Park Quartzite in the south, in the undulatory traces of the upper and lower boundaries of the Breakaway Shale, and in bedding trends of the Moondarra Siltstone (Fig. 2). A D^H_2 synform in the Breakaway Shale and Native Bee Siltstone is present 10 km south of the Horse's Head, next to the Western Fault, and is shown on the Kennedy Gap 1:100 000 Geological Map (BMR , 1980).

The northern boundary of the Horse's Head, the south-dipping Conglomerate Creek Fault (Horse's Head Fault of Bell, 1991) places Eastern Creek Volcanics against the Mount Isa Group (Fig. 2). Localities where the dip of the fault can be seen are as follows:

Point No	Grid Reference	Observation
1	431458	Steeply dipping massive tabular limonite-quartz vein; sides of vein dip 75/240
2	441452	Quartz breccia, dip 85/065
3	442451	Tabular mass of quartz breccia, dip 83/225
4	443450	Quartz breccia, dip 66/215
5	466442	Quartz breccia with steep south-dipping joint faces and gentle north-dipping parting; suggestssteep south dip
6	469441	East-striking tabular ridge of quartz breccia with steep south dip of its southern side (with down-dip mineral lineation) and gently north-dipping uneven parting; south side of ridge dips 65/193
7	473442	Tabular quartz vein with steep south dip of itssouthern contact suggestive of south dip, and gently north-dipping parting
8	493450	Limonitic quartz breccia, major joints dip steeply east

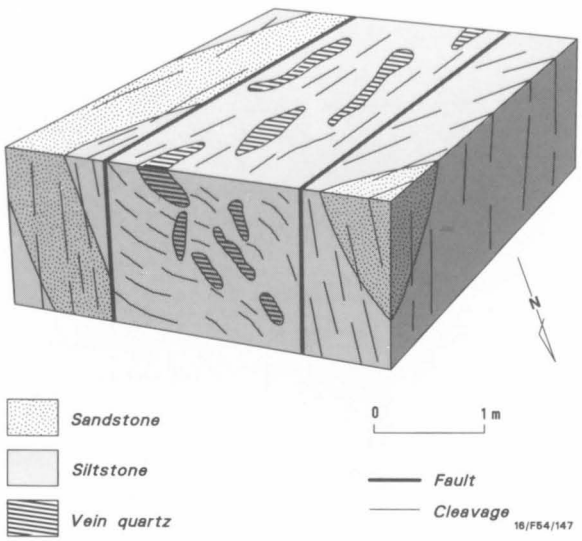


Fig. 3. Oblique view (45° down from horizontal) of $D^H_{1.5}$ fault deforming D^H_1 cleavage. Grid reference 483435.

The Eastern Creek Volcanics to the north are folded by large, moderately north-plunging upright D^H_2 folds with a steep axial-plane cleavage (Figs. 1 & 2). These folds are cut at approximately 90° by, and therefore predate, the Conglomerate Creek Fault. The fault is folded by north-plunging folds, designated D^H_5 (D_5 of Lochem & others, 1988). Nijman & others (this volume a) showed that there was also a significant sinistral strike slip component.

The eastern part of the Horse's Head has a steep easterly-striking penetrative to spaced cleavage which is axial-plane to small west-southwest-plunging D^H_1 folds. The central and western parts have a steep northerly-striking penetrative D^H_2 cleavage, which is axial-plane to small north-plunging upright D^H_2 folds, and overprints the D^H_1 cleavage and small D^H_1 folds (see below). The Conglomerate Creek Fault in the west cuts the D^H_2 cleavage at a moderate angle. The Western Fault in the Horse's Head parallels the D^H_2 cleavage and fold axial planes, but 10 km to the south, Nijman & others (this volume b) found that the Western Fault truncates D^H_2 folds. Hence, the Western Fault is regarded as having formed at the end of D^H_2. The Western Fault is terminated in the north by a steep northeast-striking fault which cuts the D^H_2 cleavage at a large angle. Hence, this northeast fault is assigned to the D^H_5 strike-slip faulting episode, which probably formed in response to east-west compression (Derrick & others, 1977; BMR, 1986).

$D^H_{1.5}$ fault

Lochem & others (1988) mapped a northeast-striking fault which ramped up from below the Surprise Creek Formation in the northeast to the Moondarra Siltstone in the southwest (Fig. 2). The western half of the fault has an undulatory trace, and was therefore interpreted as folded by, and hence older than the north-plunging D^H_2 folds (= D_3 of Lochem & others, 1988). Where seen by me (at grid reference 483435), the fault deforms, and hence is younger than D^H_1 cleavage (Fig. 3), and so it is assigned to $D^H_{1.5}$.

Mesoscopic Structure

D^H_1 cleavage

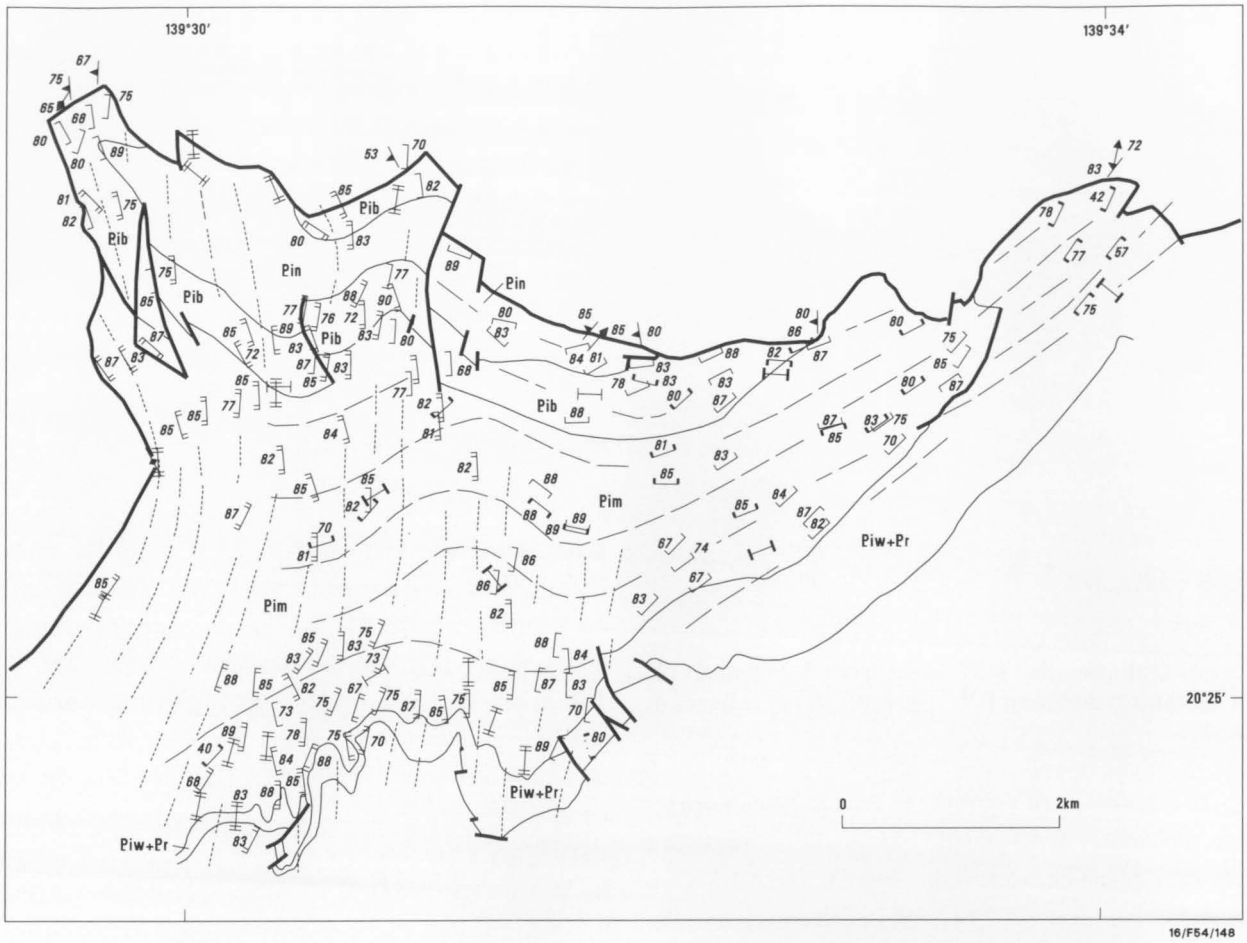
Three varieties of D^H_1 cleavage occur in the east of the Horse's Head: (i) a spaced, jointy, or fracture cleavage in the Warrina Park Quartzite in the hinge area of the main D^H_1 synform (Fig. 4); the cleavage cuts but does not deform bedding; (ii) a steeply dipping generally east-west penetrative slaty cleavage, which is present in the Mount Isa Group above the Warrina Park Quartzite (Fig. 4); it is weak and patchy in the south, but strengthens northward and spreads throughout the siltstone and shale units above the Warrina Park; and (iii) a 2-10cm–spaced cleavage (Fig. 4) which parallels the penetrative cleavage in the siltstone and shale units. Bedding is sigmoidally curved as it approaches the spaced cleavage planes, and is offset across them for up to 1 cm. The sense of offset is generally north-block-up, but at some localities it is south-block-up. In places, especially in the middle of the area, the spacing is on the mm-cm scale, and approaches a penetrative cleavage. Many of the spaced cleavage planes are lined with veinlets a few millimetres thick of quartz ± limonite. No lineation was observed on any of the cleavage planes.

D^H_2 cleavage

A penetrative slaty cleavage, D^H_2, is strongly developed throughout the western part of the Horse's Head, and generally strikes north (Fig. 4). Lineation on the cleavage surface is present only in a few places in the far northwest, where it is a fine vertical streaky mineral orientation. The D^H_2 cleavage is also present in chlorite schist in the Eastern Creek Volcanics north of the Horse's Head, and has a steep streaky mineral lineation in places.

Variously oriented cleavage

Near the Conglomerate Creek Fault in the centre and west of the area, the north-striking D^H_2 cleavage is overprinted by a steeply-dipping cleavage or by closely spaced fractures which produce slate pencils and mullions. The



Pin Native Bee Siltstone
Pib Breakaway Shale
Pim Moondarra Siltstone
Piw+Pr Warrina Park Quartzite and Surprise Creek Formation

Geological boundary
Fault
D^H_1 cleavage trend
D^H_2 cleavage trend
D^H_1 penetrative cleavage, inclined
D^H_1 penetrative cleavage, vertical
D^H_1 spaced cleavage, inclined
D^H_1 spaced cleavage, vertical
D^H_2 penetrative cleavage, inclined
D^H_2 penetrative cleavage, vertical
D^H_2 spaced cleavage, inclined
D^H_2 foliation, inclined
D^H_2 foliation, vertical
D^H_2 lineation

Fig. 4. Cleavage measurements in Horse's Head. Dip and strike values are averages of two or more measurements at each locality. Not all values shown, to avoid clutter.

orientation of the later cleavage varies from place to place, and is possibly the result of movements on the nearby Conglomerate Creek Fault.

D^H_1 folds

D^H_1 folds, like D^H_1 cleavage, are found mainly in the eastern part of the Horse's Head (Fig. 5). They are open to tight, upright, south-verging, and generally plunge moderately west or southwest; a few plunge northeast. Both penetrative and spaced D^H_1 cleavage in the siltstone units are parallel to the axial planes of the folds. Some folds have a vein of vuggy quartz + limonite near the hinge and parallel to the axial plane.

D^H_2 folds

These are upright, open to close folds and wrinkles with D^H_2 axial-plane cleavage fans. Some folds have limonite-quartz breccia veins at their hinges, parallel to the axial plane. The folds plunge moderately to steeply north or northwest (Fig. 5), and are generally symmetrical. Northeast and southwest-verging D^H_2 folds plunging 50-60° northeast or southwest, concentrated in the footwall of the Western Fault, can be explained as parts of sheath folds formed by stretching and rotation of originally gently plunging east-verging folds during ductile high-angle thrusting.

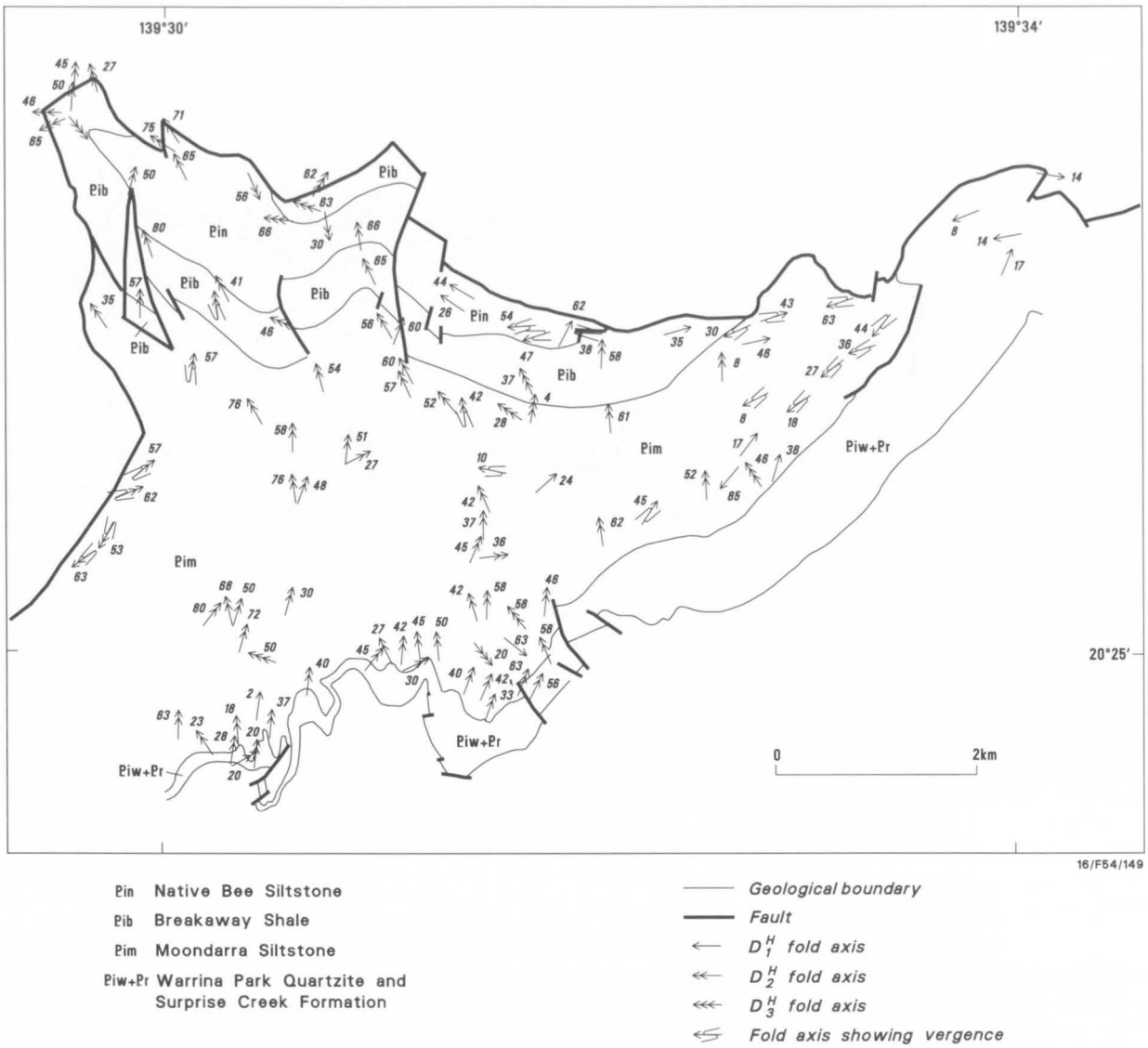


Fig. 5. Mesoscopic fold measurements in Horse's Head.

D^H_3 folds

Folds assigned to D^H_3 are open to tight domes and irregular synforms which are 1-4 m across and generally plunge northwest at 30-90° (Fig. 5). They fold D^H_2 cleavage (grid references 447450 and 441418), and are commonly associated with brecciated quartz blows. No cleavage coeval with these D^H_3 folds was observed.

D^H_5 folds (from Lochem & others, 1988)

These are steeply plunging irregular to box-like upright folds that affect the eastern half of the Conglomerate Creek Fault (Fig. 2); any associated cleavage is indistinguishable from D^H_2 cleavage.

Overprinting relationships

Clear overprinting of D^H_1 structures by D^H_2 was observed at two localities. Figure 6 shows an east-plunging D^H_1 fold remnant with east striking D^H_1 axial-plane cleavage surrounded by siltstone cleaved by north striking D^H_2 cleavage; the north-south cleavage truncates, and therefore postdates, the east-west cleavage, and the east-west cleavage is gently folded, consistent with shear along the D^H_2 cleavage. East-northeast D^H_1 cleavage is folded by a subvertical north-northeast-plunging D^H_2 fold at grid reference 463440.

Discussion

Any interpretation of the structural evolution of the Horse's Head must explain the following main features of the area:

- The consistently north-south orientation of the D^H_2 cleavage, especially in the Horse's neck (locality A, Fig. 7a).
- The cut-off by the Conglomerate Creek Fault of the axial-plane traces of the macroscopic D^H_2



Fig. 6. Photograph of Breakaway Shale showing hinge of D^{H}_{1} fold (bottom left) with D^{H}_{1} axial plane cleavage (approximately vertical in photo) surrounded and bent by later D^{H}_{2} cleavage (striking from bottom left to top right). Grid reference 441439. Scale 15 cm long.

folds in the Eastern Creek Volcanics north of the Horse's Head.

- The overprinting of the D^{H}_{1} east-west cleavage and folds by the D^{H}_{2} north-south cleavage and folds.
- The folded trace of the Conglomerate Creek Fault.

According to the 'roof thrust + imbricate stack' hypothesis of Bell (1983, 1991), the major east-west D^{H}_{1} synform of Mount Isa Group forming the Horse's Head could be a fault-bounded imbricate slice, subsequently folded by D^{H}_{3} (Bell, 1991). In this model, the Conglomerate Creek and Western Faults are parts of a single D^{H}_{1} thrust fault, folded around a northwest-trending D^{H}_{3} antiform (Fig. 7a). In this interpretation, the D^{H}_{1} synform adjacent to the Conglomerate Creek Fault is linked with the north-south synform adjacent to the Western Fault. The north-south synform is a D^{H}_{1} fold, and the Mount Isa Group outcrop represents a Type 2 crescentic interference fold (Ramsay, 1967), later disrupted. This model predicts the existence of D^{H}_{1} cleavage striking north-northeast (because it's been rotated by D^{H}_{3}) in the neck of the Horse's Head (locality A in Fig. 7a), and of a northwest- striking D^{H}_{3} cleavage in the same area. While any pre-existing D^{H}_{1} cleavage at locality A could well have been obliterated by D^{H}_{2} or D^{H}_{3} deformation, the observed cleavage (assigned by me to D^{H}_{2}) strikes north to north-northeast, at about 70° to the predicted northwest direction. The model also predicts westward vergence of folds at locality B in Figure 7a, although the folds evident in the map at this locality show eastward vergence (Fig. 4). A detailed discussion of the structure of the Horse's Head described in Bell (1991) appears in Stewart (in press).

The synform of Mount Isa Group in the Horse's Head is more likely a basin representing a Type 1 interference fold, which has been subsequently faulted. In this interpretation, the main synform in the Horse's Head was originally an east-southeast-trending D^{H}_{1} synform (Fig. 7b). It was deepened and elongated in a northerly direction by formation of a D^{H}_{2} synform (Fig. 7c) that links with the synforms next to the Western Fault 10 km south of the Horse's Head, and with a narrow synform of Mount Isa

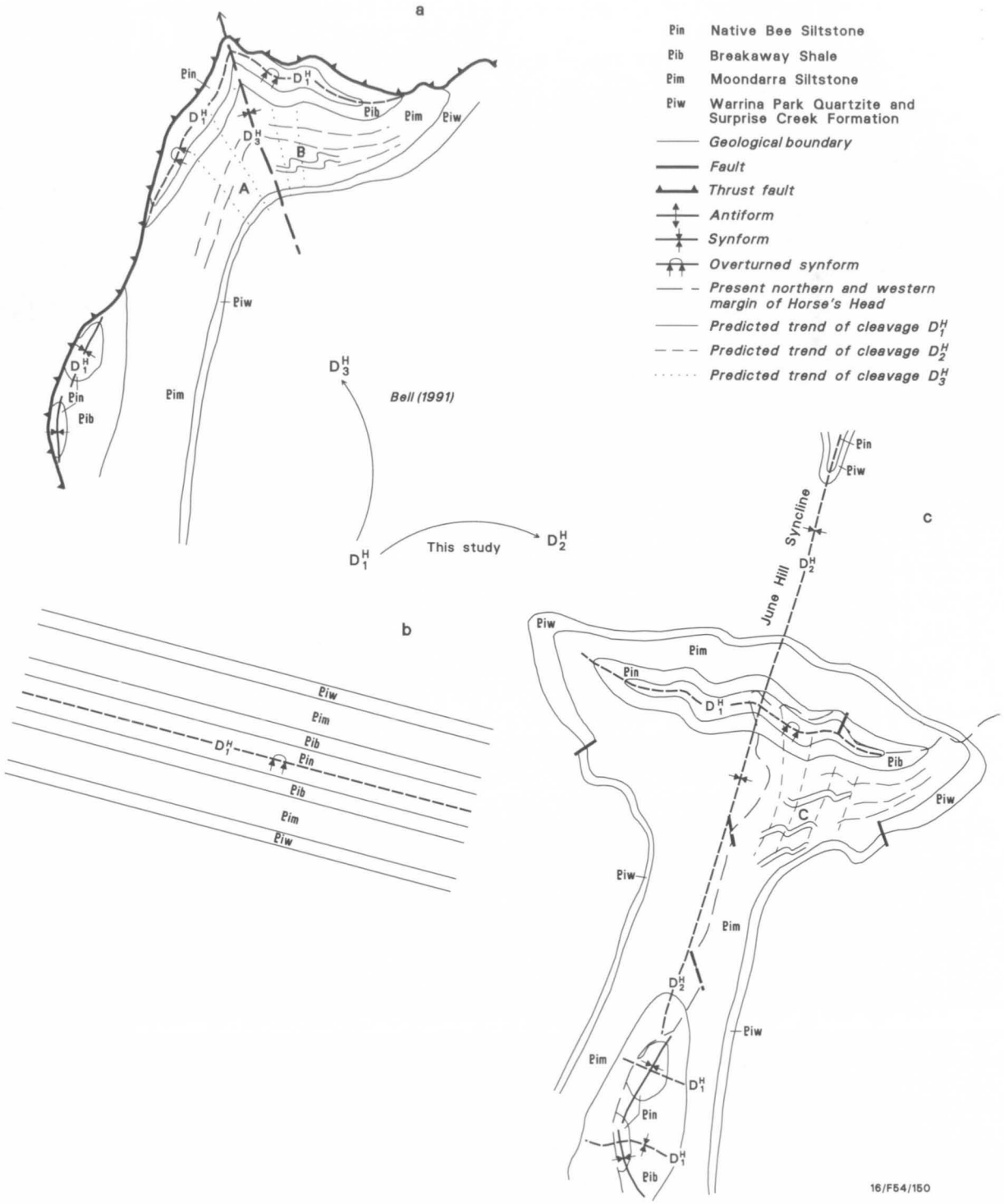


Fig. 7. Sketches illustrating possible models of formation of the Horse's Head. (a) Folded imbricate slice model, showing: D^H_1 synform folded into Type 2 crescentic interference fold by northwest-trending D^H_3 antiform; predicted D^H_1 and D^H_3 cleavages at localities A and B; west-verging minor D^H_3 folds at locality B. Effects of later faulting removed. (b) and (c) Type 1 basin and saddle interference fold model, showing: D^H_1 synform (stage 5 in evolution of Horse's Head - see text) folded by north-northeast-trending D^H_2 synform (stage 7 in text); predicted D^H_1 and D^H_2 cleavages; east-verging minor D^H_2 folds at locality C. Present outline of Horse's Head also shown.

Group 6 km north of the Horse's Head (informally known as the 'June Hill Syncline'). This model honours the essentially north-south D^H_2 cleavage throughout the Horse's Head and neck, and also the observed eastward-verging folds at locality C (Fig. 7c).

A possible variation on this model is to regard the Conglomerate Creek Fault as a D^H_1 high-angle thrust fault that was reactivated during D^H_4. The objection to this is found in the large angular discordance between the Conglomerate Creek Fault and the bedding trends in the

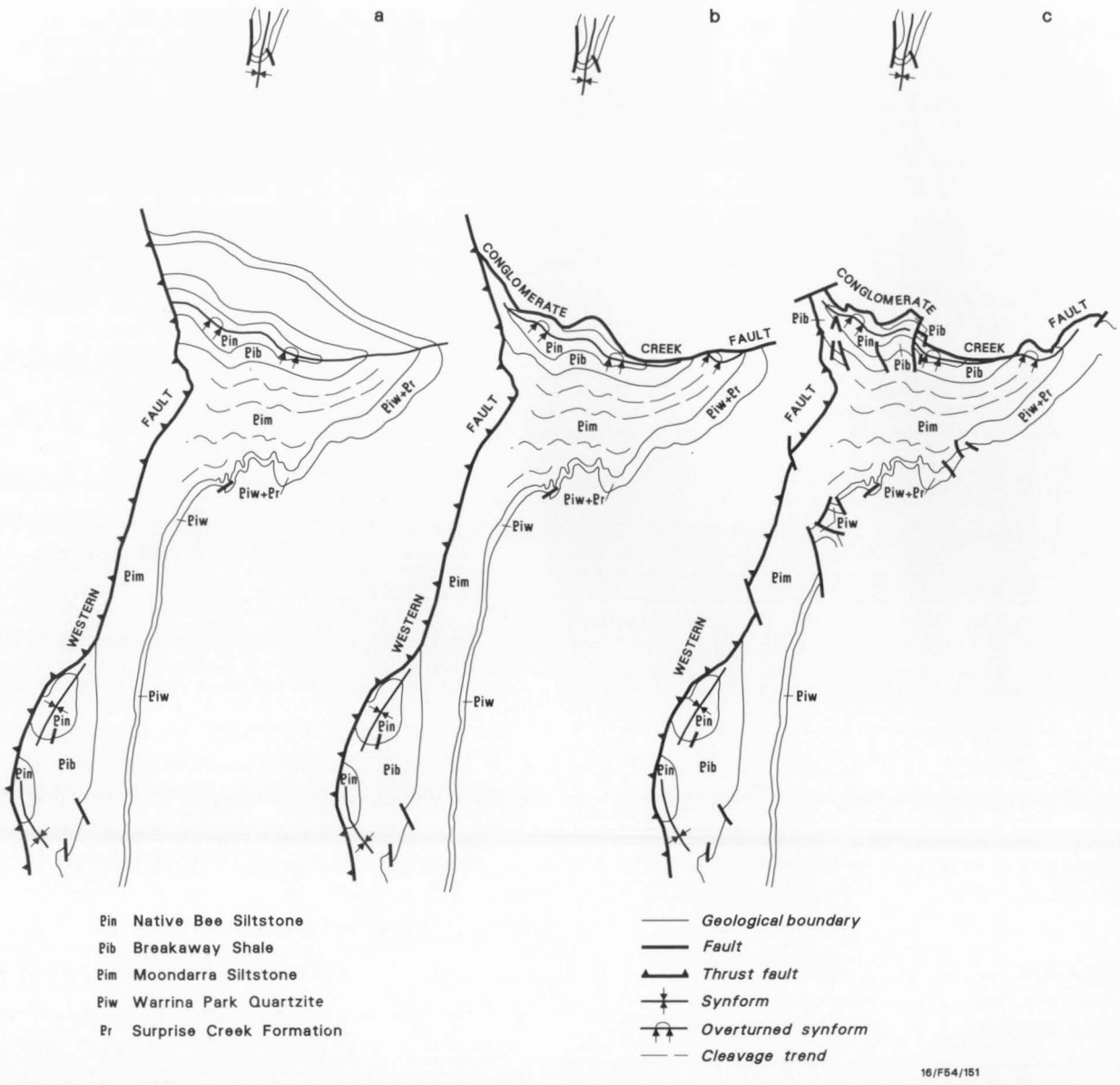


Fig. 8. Later stages of evolution of Horse's Head. (a) end of stage 7, after D^H_2 folding and steep overthrusting from west to east forming Western Fault. (b) end of stage 9, after transtensional normal faulting in north forming Conglomerate Creek Fault. (c) end of stage 10, after D^H_5 folding and formation of northwest and northeast-oriented folds and of northwest and northeast-oriented strike-slip faults.

Eastern Creek Volcanics to the north (Figs. 1 & 2). If the Conglomerate Creek Fault were a late high-angle north-dipping D^H_1 thrust fault which formed parallel or subparallel to an adjacent D^H_1 synform, then the strike of the fault and the strike of the beds should be (sub)parallel, even though the dips would differ. After synformal D^H_2 folding and steepening of the beds to a moderate north plunge, the bedding trends and fault trace would both be concave when viewed from the north, with the beds dipping synformally around a moderate north-plunging axis, and the fault dipping antiformally south around a steeply south-plunging axis. Their strikes would still be subparallel. The strike of bedding in the Eastern Creek Volcanics is, however, at large angles (up to 90°) to the strike of the Conglomerate Creek Fault, thus negating this possibility.

Still another possibility is that the Conglomerate Creek Fault was a steep south-dipping backthrust during D^H_1, which was further steepened during D^H_2, and then reactivated as a normal fault during D^H_4. This is negated by the following observations:

- there is no north-dipping thrust fault – the 'main thrust' from which the backthrust would rise – at or near the southern margin of the Horse's Head;
- D^H_2 steepening was northward, which would have lessened, not steepened the dip on a south-dipping D^H_1 backthrust.

The following history of formation of the Horse's Head using the Type 1 interference fold model is consistent with the field evidence.

- 1. Deposition of lower part of cover sequence 2 (Haslingden Group) during extensional rifting.
- 2. Initiation of D^{P}_{1a} folding and transpressional faulting during deposition of upper part (Myally Subgroup) of the Haslingden Group (W.Nijman, personal communication, 1991), early northward tilting of the Paroo Block (Lochem & others, 1988), and erosion.
- 3. Deposition of Surprise Creek Formation (initial part of Cover Sequence 3) during minor east-verging folding and thrusting (D^{P}_{1b}), followed by further northward tilting and erosion (Lochem & others, 1988).
- 4. Deposition of Mount Isa Group (Cover Sequence 3).
- 5. First major contractional deformation, D^{H}_{1}, which formed a macroscopic synform trending east-southeast (Fig. 7b) with Mount Isa Group occupying the core, plus associated mesoscopic east-trending folds and axial-plane cleavage.
- 6. Low-angle thrust-faulting $D^{H}_{1.5}$ with westward displacement of a few tens of metres (Lochem & others, 1988); local deformation of D^{H}_{1} cleavage beside this fault.
- 7. Second major contractional deformation D^{H}_{2}; formation of a north-south synform (the Horse's neck) and mesoscopic north-plunging folds with axial-plane cleavage on the north-dipping southern limb of the major D^{H}_{1} synform (Fig. 7c); folding of D^{H}_{1} cleavage; steep overthrusting from west to east up the Western Fault, removing the western part of the north-south D^{H}_{2} synform (Fig. 8a).
- 8. Formation of D^{H}_{3} mesoscopic domes and northwest-plunging synforms.
- 9. East-striking listric transtensional D^{H}_{4} faulting, forming the Conglomerate Creek Fault and removing the northern part of the D^{H}_{1}/D^{H}_{2} interference synform (Fig. 8b), with the production of closely spaced fractures and localised variously oriented steep cleavage in adjacent Mount Isa Group.
- 10. D^{H}_{5} folding of the Conglomerate Creek Fault and formation of northwest and northeast-oriented strike-slip faults, leading to the removal of the northwest corner of the Horse's Head, giving the present outcrop shape (Fig. 8c).

Conclusions

- The Horse's Head was formed by Type 1 interference of macroscopic D^{H}_{1} and D^{H}_{2} synforms, followed by erosion of upfaulted segments in the west, north, and northwest after D^{H}_{2}, D^{H}_{4}, and D^{H}_{5} faulting, respectively.
- The northern bounding fault of the Horse's Head is a D^{H}_{4} transtensional normal fault, not a D^{H}_{1} thrust.
- The Horse's Head is not a fault-bounded horse belonging to a D^{H}_{1} imbricate stack or duplex. If a thrust sheet exists, as postulated by Bell (1983, 1991), it has no fault horses or imbricates stacked beneath it at the Horse's Head.

Acknowledgements

I thank Tim Bell, Bill Perkins, and Gordon Lister for discussions on the geology of the Horse's Head, Wouter Nijman for permission to include data gathered by his University of Utrecht group, and Dave Blake, Peter Pieters, Wouter Nijman, and Ramon Loosveld for reviews of the manuscript.

References

BELL, T.H., 1983 - Thrusting and duplex formation at Mount Isa, Queensland, Australia. *Nature* 304, 493-497.

BELL, T.H., 1991 - The role of thrusting in the structural development of the Mount Isa mine and its relevance to exploration in the surrounding region. *Economic Geology* 86, 1602-1625.

BLAKE, D.H., 1987 - Geology of the Mount Isa Inlier and environs, Queensland and Northern Territory. *Bureau of Mineral Resources, Australia, Bulletin* 225, 83 pp.

BLAKE, D.H. this volume - Stratigraphy, folding, and faulting within the Quilalar Fault System, Mount Isa Inlier. *In*: STEWART, A.J., & BLAKE, D.H. (Editors), Detailed Studies of the Mount Isa Inlier. *Bureau of Mineral Resources, Australia, Bulletin* 243.

BMR, 1986 - Transpressional strike-slip faulting in the Mount Isa Inlier. *BMR Research Newsletter* 4, 1-2.

CONNORS, K.A., PROFFETT, J.M., LISTER, G.S., SCOTT, R.J., OLIVER, N.H.S., & YOUNG, D.J., this volume - Geology of the Mount Novit Ranges, southwest of Mount Isa Mine. *In*: STEWART, A.J., & BLAKE, D.H. (Editors), Detailed Studies of the Mount Isa Inlier. *Bureau of Mineral Resources, Australia, Bulletin* 243.

DERRICK, G.M., 1982 - A Proterozoic rift zone at Mount Isa, Queensland, and implications for mineralisation. *BMR Journal of Australian Geology & Geophysics* 7, 81-92.

DERRICK, G.M., WILSON, I.H., HILL, R.M., GLIKSON, A.Y., & MITCHELL, J.E., 1977 - Geology of the Mary Kathleen 1:100 000 Sheet area, northwest Queensland. *Bureau of Mineral Resources, Australia, Bulletin* 193, 114 pp.

DUNNET, D., 1976 - Mt Isa -- reconstruction of a faulted ore body. *Philosophical Transactions of the Royal Society of London* A283, 333-344.

HOLCOMBE, R.J., PEARSON, P.J., & OLIVER, N.H.S., this volume - Structure of the Mary Kathleen Fold Belt. *In*: STEWART, A.J., & BLAKE, D.H. (Editors), Detailed Studies of the Mount Isa Inlier. *Bureau of Mineral Resources, Australia, Bulletin* 243.

LOCHEM, J.H. van, SPLIETHOFF, H., & NIJMAN, W., 1988 - Structure and sedimentation in the Proterozoic of the Paroo Range Mt. Isa Inlier - Queensland, Australia. *University of Utrecht, Institute of Earth Sciences, Contributions to the MIRTH Project, BMR, Canberra, Australia, Report* 2, 100 pp. (unpublished).

LOOSVELD, R.J.H., & SCHREURS, G., 1987 - Discovery of thrust klippen, northwest of Mary Kathleen, Mount Isa Inlier, Australia. *Australian Journal of Earth Sciences 34, 387-402.*

MATHIAS, B.V., & CLARK, G.J., 1975 - Mount Isa copper and silver-lead-zinc orebodies - Isa and Hilton mines. *In*: KNIGHT, C.L. (Editor) - Economic Geology Of Australia And Papua New Guinea: 1. Metals. *The Australasian Institute of Mining and Metallurgy, Melbourne, Monograph Series* 5, 351-372.

NIJMAN, W., LOCHEM, J.H. van, SPLIETHOFF, H., & FEIJTH, J., this volume a - Deformation model and sedimentation patterns of the Proterozoic of the Paroo Range, Mount Isa Inlier, Queensland, Australia. *In:* STEWART, A.J., & BLAKE, D.H. (Editors), Detailed Studies of the Mount Isa Inlier. *Bureau of Mineral Resources, Australia, Bulletin* 243.

NIJMAN, W., MIJNLIEFF, H.F., & SCHALKWIJK, G., this volume b - The Hero Fan Delta (Lower Mount Isa Group) and its structural control: deformation in the Hero/Western Fault Zone and Paroo Range compared, Mount Isa Inlier, Queensland, Australia. *In:* STEWART, A.J., & BLAKE, D.H. (Editors), Detailed Studies of the Mount Isa Inlier. *Bureau of Mineral Resources, Australia, Bulletin* 243.

PAGE, R.W., & BELL, T.H., 1986 - Isotopic and structural responses of granite to successive deformation and metamorphism. *Journal of Geology* 94, 365-379.

PASSCHIER, C.W., 1986 - Evidence for early extensional tectonics in the Proterozoic Mount Isa inlier, Australia. *Geology* 14, 1008-1011.

PASSCHIER, C.W., & WILLIAMS, P.R., 1989 - Proterozoic extensional deformation in the Mount Isa Inlier, Queensland, Australia. *Geological Magazine* 126, 43-53.

PLUMB, K.A., DERRICK, G.M., NEEDHAM, R.S., & SHAW, R.D., 1981 - The Proterozoic of northern Australia. *In*: HUNTER, D.R. (Editor), Developments in Precambrian Geology, 2, 205- 307. *Elsevier, Amsterdam.*

RAMSAY, J.G., 1967 - Folding And Fracturing of Rocks. *McGraw-Hill, New York,* 568 pp.

SMITH, W.D., 1969 - Penecontemporaneous faulting and its likely significance in relation to Mount Isa ore deposition. *Geological Society of Australia, Special Publication* 2, 225-235.

STEWART, A.J., 1989 - Extensional faulting as the explanation for the Deighton 'Klippe' and other Mount Albert Group outliers, Mount Isa Inlier, northwestern Queensland. *Australian Journal of Earth Sciences* 36, 405-421.

STEWART, A.J., in press - The role of thrusting in the structural development of the Mount Isa mine and its relevance to exploration in the surrounding region: a discussion. *Economic Geology.*

Stratigraphy, structure, and metasomatism of the Haslingden Group, east Moondarra area, Mount Isa: a deformed and mineralised Proterozoic multistage rift-sag sequence

J.H.C. Bain [1], *C.A. Heinrich* [1], *& G.A.M. Henderson* [1]

This paper is based on the following map:

Henderson, G.A.M., & Bain, J.H.C., 1991 - Geology of the Haslingden Group, East Moondarra Area (1:35 000 scale map). Bureau of Mineral Resources, Canberra.

Detailed mapping and stratigraphic subdivision of the Eastern Creek Volcanics have revealed three episodes of deformation involving faulting and folding. The earliest structure is a steep north-dipping cleavage which indicates the existence of a large south-verging steeply inclined antiform-synform pair trending east-northeast through the area. This was accompanied by a major sequence repetition, caused either by south-directed thrusting or normal faulting. The second episode produced major north-trending upright open folds with local axial plane cleavage, and numerous conjugate strike-slip faults (commonly with a significant tilt to the northwest as well) that segmented the area immediately after the folding. The third episode formed steep north-striking faults and shatter zones that cut earlier structures.

Regional greenschist facies metamorphism produced three types of hydrothermal alteration assemblages, which can be tentatively correlated with the paragenetic history of 'silica-dolomite' alteration at the Mount Isa mine. The first two, respectively dominated by albite-actinolite and epidote-sphene, involved $CaCl_2$-rich fluids, and accompanied the main east-west shortening. The third, dominantly a carbonate-hematite-magnetite assemblage, is concentrated along the north-striking shatter zones, and involved mainly NaCl-rich brine very similar to the main stage ore fluid associated with copper mineralisation at the Mount Isa mine.

The shatter zones may have been infiltration channels for downward-flowing solutions derived from evaporites which interacted with basalt and ascended as the main ore fluid at Mount Isa, depositing Cu by reaction with dolomitic and pyritic shale meta-sediments of the Mount Isa Group.

[1] Bureau of Mineral Resources, GPO Box 378, Canberra, ACT, 2601, Australia.

Introduction

Geochemical studies by Smith & Walker (1971) revealed extreme alteration and copper depletion in Eastern Creek Volcanics (ECV) immediately beneath the Mount Isa copper orebodies, and led them to suggest that the copper deposits were epigenetic and had derived much of their copper content from the underlying greenstone. Structural and other studies by Swager (1985), Perkins (1984), and Bell & others (1988), provided further evidence of the epigenetic nature of the copper deposits and led to a model for their genesis suggesting formation during regional deformation and associated metamorphism.

Petrological and geochemical studies by Wyborn (1987) suggested that distinctive regional geochemical and mineralogical changes in the ECV took place during several cleavage-forming structural and metamorphic events of regional extent, and that the associated fluids mobilised copper and some other elements which formed the orebodies.

To test the metamorphic genesis model of the copper deposits, geochemical, petrological, and structural studies were undertaken to determine the structural history, alteration processes near the Mount Isa ore deposit, and their relation to copper metallogeny. An area of ECV in the northwest of the Mary Kathleen 1:100 000 Sheet area (extending from 5 to 30 km from the Mount Isa mine; Fig. 1) was chosen for detailed study because it exposes complex relationships between alteration, folding, faulting, and possibly early thrusting (Bell, 1983, 1991).

The 1:35 000 scale map by Henderson & Bain (1991) was compiled from information derived from numerous ground traverses plotted on 1:10 000 scale enlargements of 1969 colour airphotos, and from stereographic airphoto interpretation at 1:25 000 scale. This information was augmented with field data from mapping by A.Y. Glikson in 1970, and with Thematic Mapper Simulator (NSOO1) and Thermal Infrared Multispectral Scanner (TIMS)

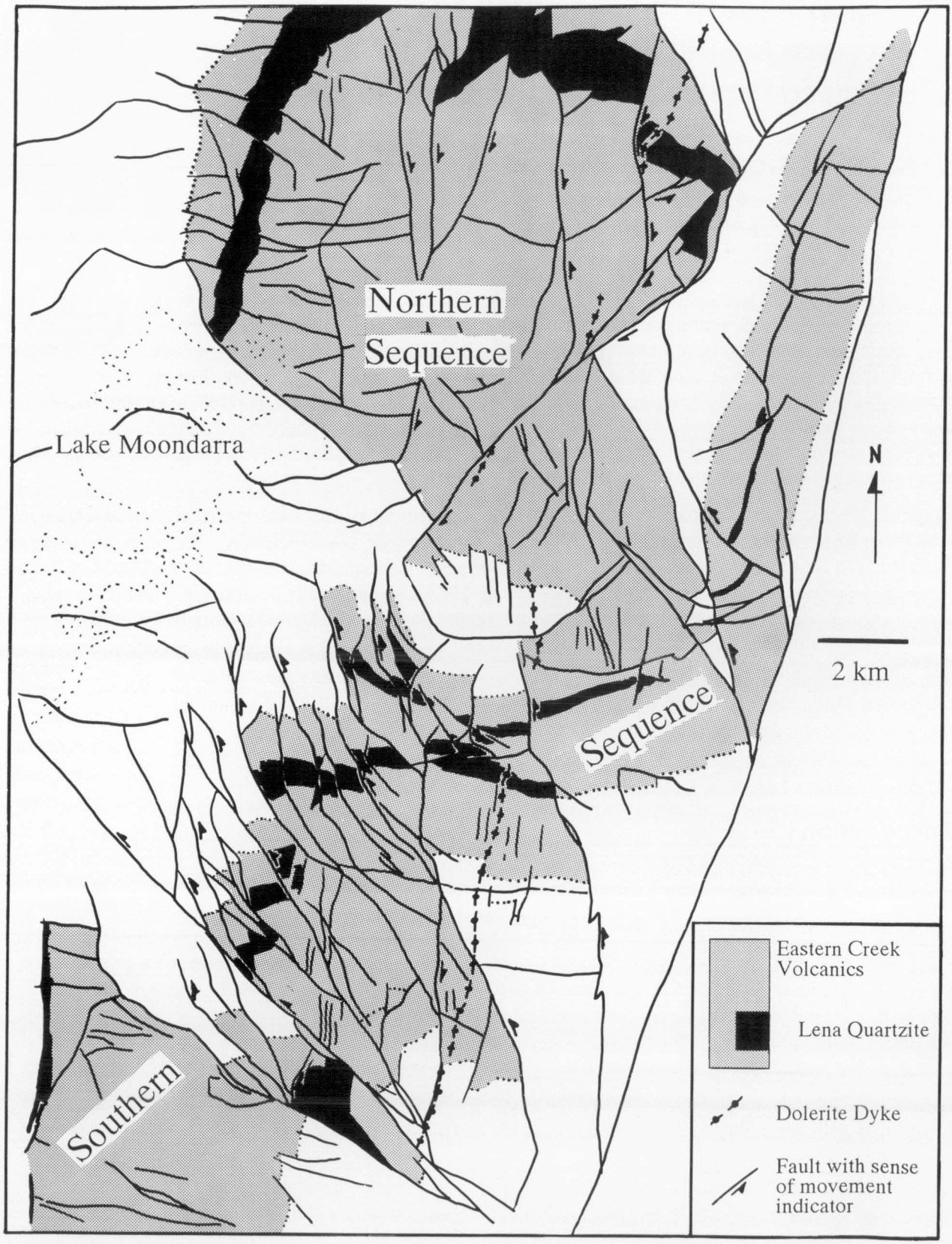


Fig. 1. Geological sketch of the east Moondarra area showing the northern and southern ECV sequences and principal faults. Most faults in the southern sequence are sinistral and northwest-striking, whereas those in the northern sequence are mostly dextral and north- or northeast-striking. East-west faults generally mark minor sequence repetitions resulting from 22% north-south extension during fault-accommodated east-west shortening. The discontinuous north-northeast-trending dolerite dyke post-dates all significant fault movement.

imagery from the 1985 US-Australia Joint Scanner Project. The following notes explain and augment the information contained in the map (Henderson & Bain, 1991).

The chemical processes of alteration and copper deposition at the mine-scale have been investigated by Heinrich & others (1989, 1990), Andrew & others (1989), and Waring (1990a,b) using fluid inclusion, stable isotope, mineralogic, and geochemical mass balance studies. Regional petrological and geochemical studies by Wyborn (1987) and Bain & others (1989) provided the regional context for the geochemical aspects of this district-scale study.

Deformation episodes in the East Moondarra area are denoted by the superscript 'A'.

Stratigraphy

Mount Guide Quartzite

The Mount Guide Quartzite (maximum estimated thickness at least 6200 m) is the lowermost formation in the Haslingden Group, and the oldest formation in the area mapped. Derrick & others (1977) subdivided the unit into two members, the lower (Phgr) consisting mainly of greywacke, conglomerate, and micaceous feldspathic sandstone, and the upper (Phg_1) of white quartzite and feldspathic sandstone.

The Mount Guide Quartzite conformably underlies the Eastern Creek Volcanics in the east and southeast of the mapped area. The topmost beds of the formation appear to have been indurated by the overlying volcanics. However many contacts with the volcanics are faulted, and in places the Quartzite is faulted against formations younger than the Eastern Creek Volcanics. The Mount Guide Quartzite is intruded by numerous north-striking metadolerite dykes which may represent feeders for the overlying volcanics.

Eastern Creek Volcanics

The Eastern Creek Volcanics consist of metabasalt flows and interflow sedimentary rocks. The volcanics were formally defined by Carter & others (1961), and informally subdivided by Robinson (1968) into the Cromwell beds (base), Paroo beds, Lena quartzite, and Pickwick beds (top). The two lowermost units were separated by Robinson on the basis of abundance of sedimentary intercalations between the metabasalt flows, but were later combined as the formally named Cromwell Metabasalt Member by Derrick & others (1977), who found difficulty in mapping a boundary between them. Derrick & others (1977) also renamed the two uppermost units the Lena Quartzite Member and the Pickwick Metabasalt Member.

Cromwell Metabasalt Member

The Cromwell Metabasalt Member (Phc) consists of successive metabasalt flows ranging from a few metres to about 140 m thick, interbedded in the upper half of the Member with sedimentary units ranging up to about 200 m thick. A few lenses of white quartzite similar to that in the upper part of the Mount Guide Quartzite crop out in some places near the base of the Member. A distinctive and persistent porphyritic metabasalt noted by Robinson (1968) and shown as C_p on the map forms a useful marker unit near the top of the Member. The total thickness of the member in the area mapped ranges from about 1200 m to about 4500 m and increases from east to west.

Each metabasalt flow commonly consists of a dark greenish-grey massive lower part passing up into metabasalt with increasingly abundant amygdales and capped by a stacktop-breccia. The breccia consists of angular fist-sized and larger fragments of dark grey metabasalt in a yellowish-green aphanitic matrix of silica and epidote. The metabasalts generally consist of fine-grained aggregates of tremolite-actinolite, epidote, chlorite, quartz, albite, minor biotite, and some calcite. The amygdales are composed of quartz, epidote, chlorite, and/or calcite (Derrick & others, 1977). The porphyritic metabasalt unit contains large white or clear euhedral laths of plagioclase 1-5 mm long in a fine-grained groundmass. Epidotisation of the metabasalts is generally concentrated in the flow-top breccias, and at one or two levels midway up the lower non-sedimentary part of the Member, where entire flows are epidotised.

The sedimentary interbeds in the upper half of the Cromwell Metabasalt Member consist of impure sandstone, quartzite, siltstone, and minor conglomerate. Some of the sandstone is feldspathic, and some of the coarser beds contain a few pebbles and cobbles of sandstone or quartzite. Much of the sedimentary material is, or was, originally calcareous, with pitted rock as evidence of calcite solution. The coarse sandstones are commonly cross-bedded and many contain dark laminae rich in heavy minerals. A distinctive sedimentary breccia towards the top of the Member above the level of the porphyritic metabasalt consists of either small angular clasts of metabasalt or large angular and subrounded clasts of metabasalt and quartzite in a sandy or silty matrix. Many of the clasts are composed of the porphyritic metabasalt.

The sedimentary units can be correlated between separate fault blocks on the basis of composition, relative thickness, and position in the sequence above the lowermost sedimentary unit. Sedimentary units are numbered on the map according to position in the sequence, C_1 being the lowest, C_2 the next above, and so on. Some units near the top of the sequence have been given letter subscripts. Only the main units have been labelled on the map.

The most distinctive lithological units are C_1 and C_2 in the central part of the area, C_b in the central and northern part, and C_s throughout the area. Unit C_1 is grey calcareous siltstone; C_2 is coarse-grained dark grey sandstone (in contrast to pale sandstone higher in the sequence) and conglomerate containing an appreciable proportion of metabasalt clasts; C_b is the sedimentary breccia described above; and C_s is slaty sericitic siltstone. The other sediment units are mainly sandstone or quartzite with or without siltstone interbeds.

Units C_2, C_5, C_8, C_{13}, and C_{14} are distinguished on the basis of relative thickness in most of the area. The thickness of each unit is proportional to the total thickness of the Member. Thus unit C_2 is about 100 m thick in the central north of the area, where the total thickness of the Member is about 4500 m, but is only about 30 m thick in the central part, where the total thickness is around 1800 m. Units C_{13} and C_{14}, easily identifiable because they are separated from each other by the porphyritic metabasalt (C_p), are thickest in the central north of the area. Unit C_{13} commonly contains interbeds of siltstone up to 10 m thick between the sandstone beds wherever the total thickness of the unit exceeds about 30 m. Unit C_{13} is absent in the southwest near Mount Isa, where the porphyritic metabasalt (C_p) appears to directly overlie an earlier metabasalt flow.

Where the Cromwell Metabasalt Member is at its thinnest, in the far northeast of the area, many of the sedimentary beds are missing or occur as very thin lenses. It is not possible to correlate most of these lenses with the beds elsewhere, except near the top of the Member where unit C_{13} forms a prominent quartzite ridge immediately east of the porphyritic metabasalt, and slate of unit C_s is also readily identified.

Lena Quartzite Member

The Lena Quartzite Member (Phl) conformably overlies the Cromwell Metabasalt Member, and consists of quartzite and feldspathic sandstone, with minor siltstone and cobble conglomerate at the base in places, mainly east of the Police Creek Fault. Cross-bedding and heavy mineral laminae are common. The Member ranges from about 80 to 900 m thick, increasing westwards, and is generally much thicker than any of the sedimentary beds within the Cromwell Metabasalt Member. Only to the east of the Police Creek Fault is the Lena Quartzite Member of comparable thickness to underlying sedimentary units in the Cromwell Metabasalt Member. Identification there is based on its position in the total sequence of Eastern Creek Volcanics.

Siltstone occurs mainly in the central south of the mapped area at the base of the Member. In places the siltstone is separated from the main quartzite body by a metadolerite sill. Conglomerate east of the Police Creek Fault contains clasts of felsic volcanics possibly derived from a basement source to the east.

Pickwick Metabasalt Member

The Pickwick Metabasalt Member (Php) conformably overlies the Lena Quartzite Member, and consists of metabasalt flows similar to those in the Cromwell Metabasalt Member, separated in places by lenses of quartzite. The total thickness ranges from about 400 m in the northeast to 1200 m in the northwest. The Member is missing in the southwest immediately east of Mount Isa, where the Lena Quartzite Member is unconformably overlain by the Mount Isa Group.

The metabasalt flows, although tending to be less altered than those in the Cromwell Member, are not readily distinguishable as Pickwick Member in the field. In some places, moderately porphyritic metabasalts, not represented in the Cromwell Member, were observed. Chemical differences between the metabasalts of the two members are discussed in Wilson & others (1985). The thin quartzite lenses, as opposed to the thicker and more lithologically variable sedimentary units in the Cromwell Member, are the main distinguishing feature of the Pickwick Member. The lenses range in thickness up to about 10 m but are commonly about 2 or 3 m thick. Many of them form the crests of ridges. The quartzites are typically coarse-grained and cross-bedded.

Myally Subgroup

The Myally Subgroup (Derrick & others, 1977) conformably overlies the Pickwick Metabasalt Member of the Eastern Creek Volcanics. Three of the four formations making up the subgroup are represented in the area mapped. They are the Alsace Quartzite at the base, overlain by the Bortala Formation, and at the top the Whitworth Quartzite (Derrick & others, 1977). The

Alsace Quartzite contains cross-bedded medium to coarse-grained quartz sandstone, feldspathic sandstone, and minor mud-flake conglomerate, and is about 300 m thick. The Bortala Formation is a recessive unit of fine-grained highly feldspathic sandstone and minor amounts of grey siltstone, about 200 m thick. The Whitworth Quartzite consists of feldspathic sandstone, pebble beds, and minor siltstone partings, and is extensively cross-bedded; it ranges in thickness from 300 to 650 m, but is up to 2000 m thick in the Prospector 1:100 000 Sheet area to the north.

Only the Alsace Quartzite (Pha) and the Whitworth Quartzite (Phw) have been differentiated on the map. Undifferentiated Myally Subgroup (Phm) is probably mainly Bortala Formation or Bortala Formation equivalent, but commonly consists of medium to coarse-grained sandstone and quartzite, and forms more rugged hills than the typical Bortala Formation. The Alsace Quartzite at the base of the Subgroup cannot be differentiated from Myally Subgroup in most places in the northeast of the area.

Surprise Creek Formation

Thinly bedded siltstone (Ps_Z) overlying the Whitworth Quartzite south of Lake Moondarra was mapped as basal Mount Isa Group by Derrick & others (1977), but later correlated with the Surprise Creek Formation by Wilson & others (1983). It consists mostly of thin-bedded siltstone with a few thin conglomerate and sandstone interbeds, and is 300 to 650 m thick. In two places a prominent thick conglomerate mapped as Ps occurs at the base. One is 2 to 3 km southeast of Lake Moondarra dam, and the other is on the microwave tower hill near the Barkly Highway 8 km east of Mount Isa. At the latter locality, boulder-sized clasts at the base of the conglomerate consist of basalt and quartzite that appear to be derived from the Pickwick Metabasalt Member and the Myally Subgroup. The conglomerate there is overlain by siltstone (Ps_Z) and underlain by a much reduced thickness of Myally Subgroup. Thus, although the Surprise Creek Formation in the mapped area appears in many places to be almost conformable on the Whitworth Quartzite, it is almost certainly unconformable on the older formations.

Mount Isa Group

The basal formation of the Mount Isa Group, the Warrina Park Quartzite (Piw), is the youngest unit mapped in the area studied. It lies on the Alsace Quartzite of the Myally Subgroup and on the Pickwick Metabasalt Member of the ECV in the northwest, on the Surprise Creek Formation south of Lake Moondarra, and on the Lena Quartzite Member east of Mount Isa, and is therefore unconformable on these older units. The formation commonly forms prominent ridges.

Intrusive rocks

Numerous metadolerite dykes and some sills intrude the Mount Guide Quartzite and Eastern Creek Volcanics; a few dykes also penetrate the Myally Subgroup. Most of the dykes strike north and are generally not more than about 20 m wide. However a few are much wider than this, and one that crosses the Barkly Highway 5 km east of Mount Isa is about 500 m wide.

The dykes are of similar mineralogical composition to the metabasalts, but are generally coarser-grained. Some of the very narrow dykes are no coarser than the metabasalts and are only obvious where they cut sedimentary interbeds. Many dykes have a coarse-grained core and finer-grained chilled margin.

A metadolerite sill mapped as Do_1 occurs in most places at the base of the Lena Quartzite Member in the western half of the area. Metadolerite intruding the Pickwick Metabasalt Member in the northwest corner of the area also appears to be a sill, but farther north, in the Prospector 1:100 000 Sheet area, it cuts obliquely across the upper boundary of the Pickwick Member, and intrudes the Alsace Quartzite and Bortala Formation.

The metadolerite intrusions have been divided into two groups according to degree of alteration and inferred relative age. Most belong to the older group, which includes all the narrow dykes, as well as some wider dykes and sills mapped as Do_1. They show comparable alteration to the metabasalts, and are truncated by all generations of faults. A leucodolerite? sill, mapped as Dl, which occurs at the base of the Myally Subgroup 7 km southeast of Lake Moondarra Dam, is probably related to the Do_1 group.

The younger group, mapped as Do_2, is essentially one semi-continuous dyke about 80 m wide which extends north-northeast across the entire mapped area. This dyke is uniformly coarse-grained, relatively unaltered, and crosses many major faults without displacement or apparent interruption. In contrast to the Do_1 dykes, it crops out as spheroidally weathered boulders. It may be a correlative of the 1116 Ma-old Lakeview Dolerite to the east.

Structure

The Haslingden Group within the mapped area is folded about widely spaced axial planes with axes that plunge

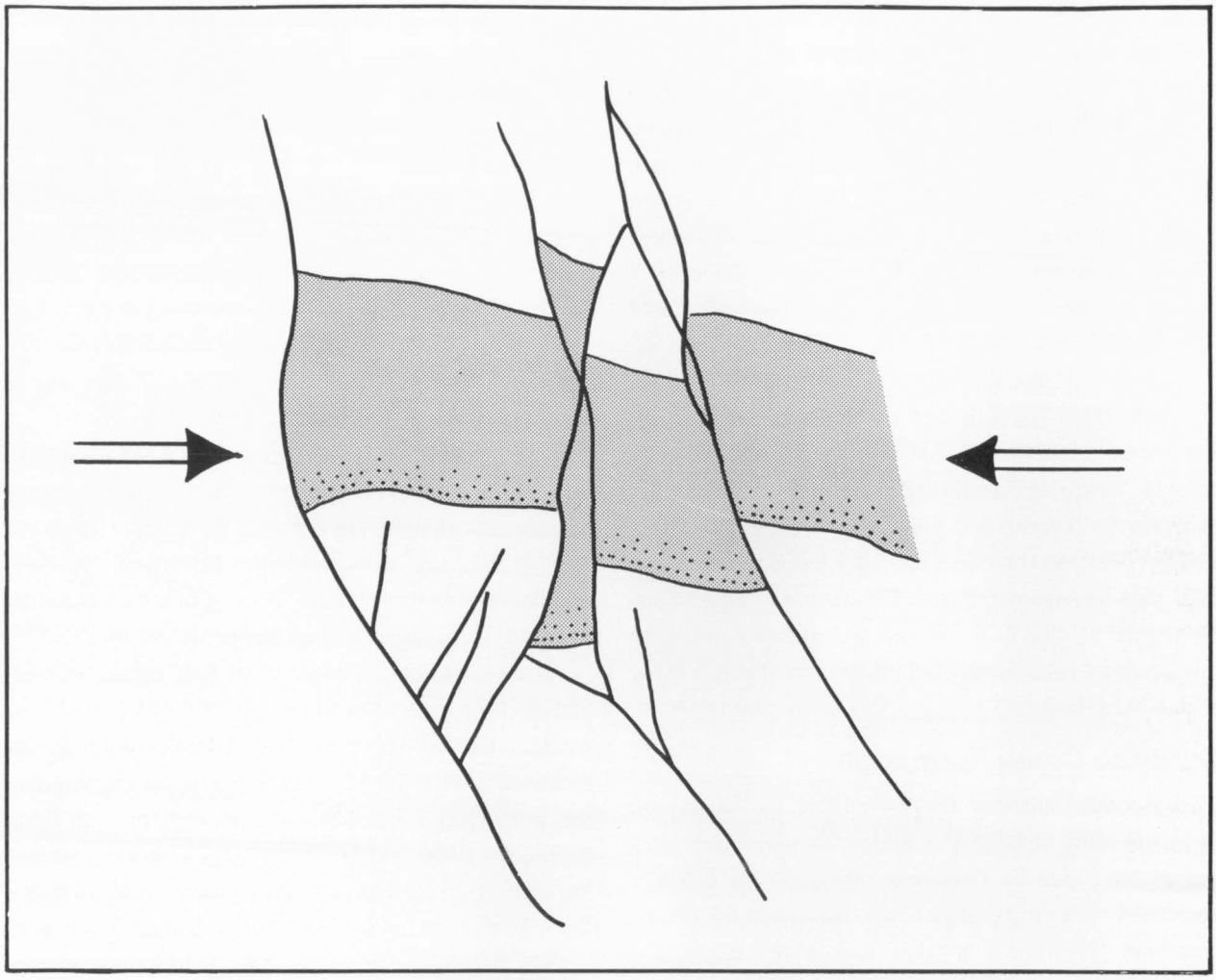


Fig. 2. X-shaped faults and popouts affecting the Lena Quartzite Member, indicative of east-west shortening.

steeply north or northwest, and is extensively disrupted by a complex pattern of intersecting faults. Southeast of Lake Moondarra, the dominant fault systems are curvilinear and strike northwesterly, whereas to the northeast the sequence is cut by generally northerly and easterly-striking straight faults and a major northeast-striking strike fault. Although almost all the faults in this region have been active during the main compressive deformation of the Haslingden Group (Isan Orogeny), there is some evidence of two earlier periods of faulting.

Abrupt changes in thickness of the Whitworth Quartzite, and the local development of fault-bounded massive conglomerate at the base of the Surprise Creek Formation (Ps in the microwave tower hill and Lake Moondarra dam areas) are indicative of syndepositional faulting in the period following deposition of the ECV and preceding deposition of the Mt Isa Group. Such faulting would have been extensional and associated with a small depocentre in the vicinity of the present Lake Moondarra. The original orientation of the faults is unknown.

The other early faulting is indicated by a major sequence repetition revealed by partially reconstructing the pre-Isan Orogeny configuration of the Haslingden Group as discussed below. The nature of this early (but post-Mount Isa Group) faulting is, however, not known; exposed field relationships are ambiguous and may be explained by southward thrusting (compare Bell, 1983) or by north-south extension on south-dipping normal faults.

The earliest and most extensive mesoscopic structural fabric identified is a moderate to strong cleavage (S_1 in the map area) in the ECV. It is mostly a closely-spaced to slaty cleavage in the metabasalt and a slaty cleavage in the pelitic to psammopelitic parts of the interflow sediment beds. This cleavage is most prominent in some interflow sediments and immediately adjacent parts of the enclosing flows, and in the upper parts of the southern sequence repetition. This cleavage dips steeper than bedding, consistently maintains a south vergence, and strikes at an angle of 5 to 15° greater than the strike of bedding at the same locality; it also cuts the generally orthogonal

north-trending mafic dykes. It is not parallel to any of the observed fold axial planes in the region, and no mesoscopic fold closures to which the cleavage could be axial-plane have been observed. The relationship between bedding and S_1 cleavage indicates that the exposed beds may be the upright northwest-dipping limb of a large subhorizontal east-northeast-trending D^A_1 antiform. This fold has been subsequently folded around an upright north-trending D^A_2 synform extending through Mount Isa.

Considerable east-west D^A_2 shortening of the sequence occurred during two distinguishable, but probably closely related episodes, resulting in open folding of bedding and S_1 cleavage around north and north-northwest-trending axes, and development of conjugate north-northwest and northeast-striking strike-slip and arcuate east-west normal faults. The north-northwest strike-slip faults generally exhibit sinistral displacements, whereas the northeast-striking faults generally have dextral displacements. Many intersecting faults resulting in X-shaped sequence repetitions (Fig. 2) reflect east-west shortening and concomitant north-south extension. These faults connect with or terminate at the northwest-southeast strike-slip/dip-slip faults, suggesting formation during the same event. The east-west faults cause other minor sequence repetitions resulting from local north-south extension. S_1 cleavage is cut, and in a few places crenulated, by locally developed S_2 fracture cleavages associated with the larger, particularly north-striking faults. In northerly-trending sections of the ECV, such as in the southwest and northeast of the map area, these two cleavages are at low angles to each other and are generally more pervasive than elsewhere.

The resultant mosaic of variously oriented fault-blocks was subsequently cut by well-spaced shatter zones generally along north-striking faults. These zones were probably formed by minor extension during rebound after the earlier shortening event. Brecciation was accompanied by calcite veining and calcite-hematite-magnetite alteration. The shattered rocks have a characteristic 'hackly' surface, and are locally a distinctive reddish brown (see section below on 'Carbonate alteration').

To model the deformation history of the mapped area, the pre-faulting configuration of fault blocks was partially reconstructed by cutting the map of the present configuration along fault lines and repositioning fault blocks to achieve best fit. The resultant reconstruction reveals two similarly open-folded northwest-dipping sequences, presumably separated by either a pre-folding D^A_1 thrust (compare Bell, 1983, 1991) with several kilometres of north-over-south displacement, or by a south-dipping normal fault associated with north-south extension. The reconstruction also demonstrates that separation occurred before the main compressional D^A_2 deformation took place.

Fault block matching is mostly good to excellent. Locally poor matches necessitated minor adjustments to the overall post-folding configuration of the reconstruction. These adjustments were made by using the reconstructed configuration in best controlled areas as the basis for reconstruction in poorly controlled areas. Generally this resulted in moving fault blocks apart to allow for compression, and rotating them a few degrees to fit the better established configuration. Some very small blocks provide insufficient clues for accurate repositioning. In areas of intersecting fault sets, trial and error revealed which set to restore first (i.e., which is the youngest). For example, in the Cromwell Metabasalt Member north and east of the Lake Moondarra spillway, the east-west faults are the youngest faults, and so need to be restored first. These faults terminate, or change direction, at northerly-striking faults, and repeat sections of the intervening strata in such a way as to indicate that they are normal faults with a consistent south-block-down sense of movement. The northerly-striking faults have acted as transfer faults for blocks with different strike-slip movements. In reconstruction, failure to reverse movement on the east-west faults before reversing movement on the major north and northeasterly faults results in major space problems.

Northwest-striking faults have mostly sinistral displacements. Those terminating in the Myally and Surprise Creek sequences provide problems for reconstructions that use only simple strike-slip movements. Better reconstruction (i.e., better matching of fault blocks) is obtained if individual fault blocks are tilted at different angles, southeast end up, implying some scissor movement. Such tilting gives a better match of apparently different stratigraphic thicknesses in adjacent blocks. The type and amount of fault movement required to restore the current map configuration to a simpler form (Fig. 3), largely devoid of fault-related discontinuities, provides a useful guide to the faulting history of the region.

Regional metamorphism and alteration

The mafic rocks in the map area are the subject of an ongoing study aimed at understanding the history of

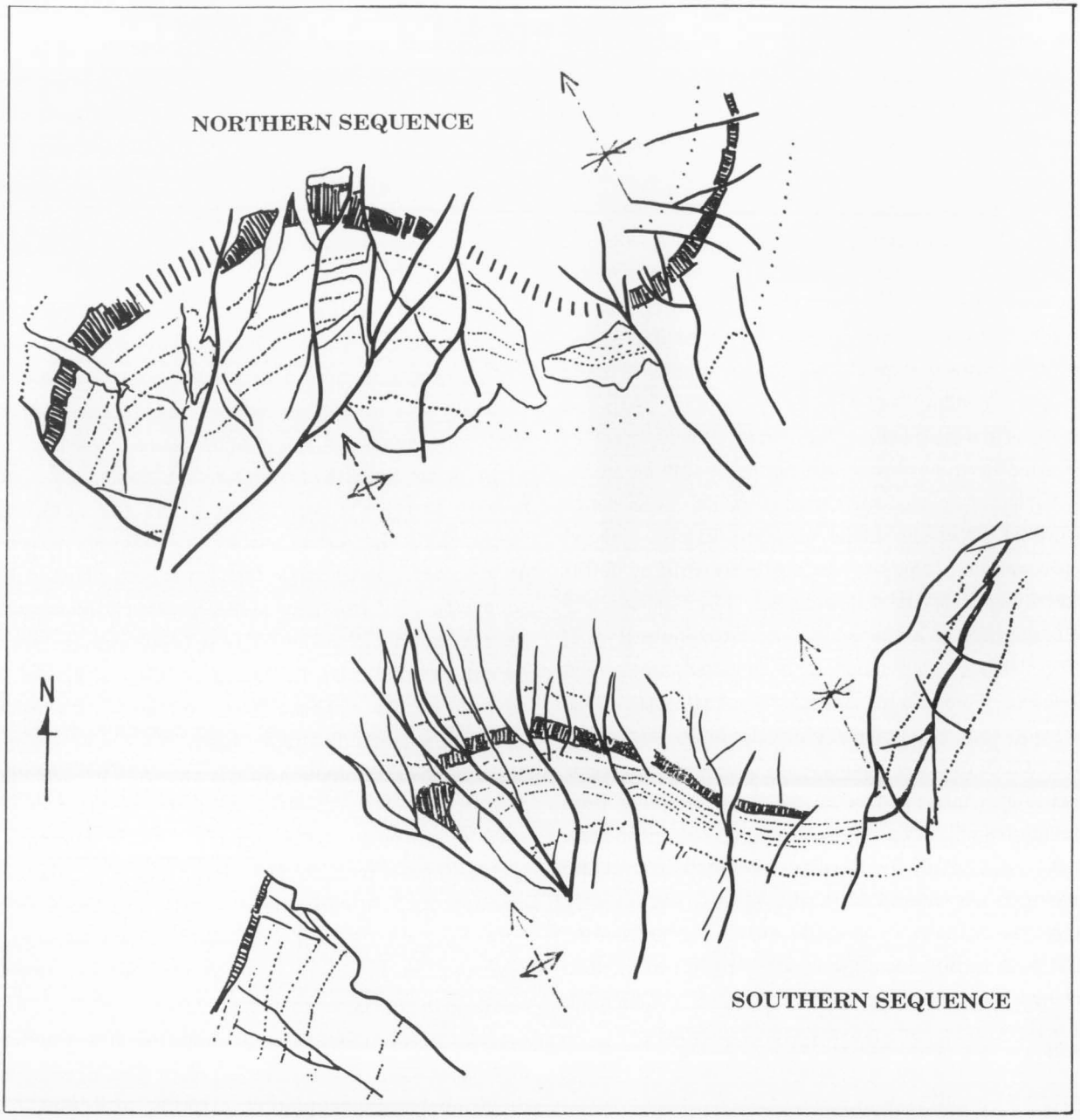


Fig. 3. Partial reconstruction of the east Moondarra area to a pre-D^A_2 configuration. This was achieved by restoring most pre-faulting relationships between fault blocks, and shows north-northwest-trending open folding of a repeated east-thinning ECV sequence, and D^A_1 cleavage.

regional fluid flow and fluid-rock interaction, and their possible relation to copper mineralisation at Mount Isa mine (Bain & others, 1989; Heinrich & others, submitted; in preparation). The stratigraphic and structural data presented in Henderson & Bain (1991) and discussed above provide a framework for the relative timing of veining and alteration events.

Regional metamorphism east of Mount Isa

East of the Mount Isa Fault Zone, regional metamorphic grade reaches upper greenschist facies, characterised by albite + chlorite + actinolite + epidote + sphene + magnetite + quartz ± biotite ± calcite in mafic rocks. These assemblages have been referred to as the albite-actinolite alteration type by Wyborn (1987) in order to distinguish them from less thoroughly hydrated, but otherwise chemically similar rocks containing relict magmatic clinopyroxene, occurring near Mammoth Mines 100 km north of the map area. Penetrative schistosity is restricted to the vicinity of faults and where lithologic contacts provide a competency contrast. The metamorphic minerals generally pseudomorph earlier magmatic minerals (albite laths after igneous plagioclase, chlorite-epidote clots after

pyroxene, sphene-rimmed magnetite after titanomagnetite, etc.).

Fluid inclusions trapped in quartz within undeformed amygdales record the earliest fluid recognised in the area, but their timing relative to peak metamorphism is not established. These inclusions are highly saline brines, commonly with a small halite daughter crystal, and probably have a high $CaCl_2$ content.

Epidote – sphene alteration

Epidote-dominant rocks – epidosites – are widespread within the ECV. Two types of occurrence – in flow-top breccias and as vein-related alteration are common, but not always clearly distinguishable. Structures in flow-tops are ambiguous as to whether the epidosites originated by metamorphism of a deuterically oxidised protolith, or by synmetamorphic metasomatism, or by syn-eruptive burial/hydrothermal alteration of propylitic alteration. Vein-related epidosites in the interior of flows and dykes, however, are clearly products of alteration at high temperatures. They occur as closely-spaced millimetre-thick sheeted epidote veinlets, or as sharply bounded or diffuse haloes up to 1 m wide around discrete veins filled with euhedral or fibrous (crack-seal) crystals of quartz ± epidote ± alcite. Locally, these veins and haloes crosscut metamorphic textures, and in other places they occur as boudins within foliated, less altered, and less competent metabasalt. These relationships indicate that epidote-alteration overlapped in time with the main regional deformation and metamorphism (probably D2 of Bell, 1983).

The most intensely epidotised rocks (both types of occurrence) consist of Fe-rich (near-stoichiometric) epidote + quartz + pale green actinolite + sphene ± chalcopyrite ± pyrite ± occasional blades of hematite. Minor magnetite, green chlorite, and biotite are apparently stable in less altered epidosite samples.

Fluid inclusions, some of them probably primary, in associated quartz veins are identical to the $CaCl_2$-rich inclusions occurring in amygdales. Oxygen isotope compositions of quartz are around 12 permil SMOW. Water extracts from fluid inclusions and from epidotes have dD of about -20 permil, which could indicate a seawater or meteoric water component. These characteristics are similar to those of the apparently earliest $CaCl_2$-rich fluids associated with dolomitic alteration in the 'silica-dolomite' breccia at Mount Isa mine (Heinrich & Cousens, 1989; Heinrich & others, 1989). Mass balance comparison of vein-related epidosites with less-altered protoliths nearby indicate net oxidation at constant total Fe content, a large gain in Ca, and almost complete loss of Mg and alkalies.

Carbonate–Fe–oxide alteration

Later carbonate alteration is most intense in kilometre-scale shatter zones, the more prominent of which are shown on the map (Henderson & Bain, 1991). Less intense carbonate veining of similar textural character (the calcite-magnetite alteration type of Wyborn, 1987) is more widespread. The major shatter zones cut D^A_2 faults and thus postdate the main compressional deformation, and at all scales the fracturing, veining, and carbonate-oxide alteration clearly postdate regional metamorphic cleavage and all types of epidote – sphene alteration. Carbonate-Fe-oxide alteration is locally associated with brittle-ductile fault displacements up to about 100 m (e.g., south of Millicent Martha prospect), but generally the fracturing involves only minimal deformation and no penetrative cleavage formation in the altered rock, as shown by the common preservation of magmatic pseudomorph textures even in extremely altered rocks. Irregular discontinuous calcite (-quartz-chlorite) veinlets up to a few millimetres wide typically make up several volume percent of the altered bulk rock, and give weathered exposures their characteristic 'hackly' appearance. Zones of most intense alteration show red hematite staining, and veinlets commonly merge to irregular breccia zones. Zones of intense hematitic alteration commonly show elevated gamma-radiation intensity, and uranium mineralisation occurs at intersections of the shatter zones with interflow sediments (e.g., Anderson's Prospect; Fig. 4 discussed below; Brooks, 1960; other occurrences shown in Henderson & Bain, 1991).

The mineral composition of the most intensely altered metabasic rocks is calcite + albite + magnetite + hematite (all increasing in modal abundance relative to the less-altered protoliths) + quartz ± chlorite ± biotite. The presence of minor stable biotite indicates that this alteration occurred at elevated (greenschist facies) temperatures. Mass-balance data indicate major oxidation at constant Fe_{tot}, net gain in Na, Ca, and CO_2, and major loss of K, Rb, Mg, and SiO_2 in some samples. These gains and losses are the opposite of those associated with Mg-chlorite-rutile alteration immediately below Mount Isa mine and in 'retrograde' mafic schists close to the Mount Isa Fault Zone west of Mount Isa (Smith & Walker, 1971; Wyborn, 1987; Heinrich & others, in preparation).

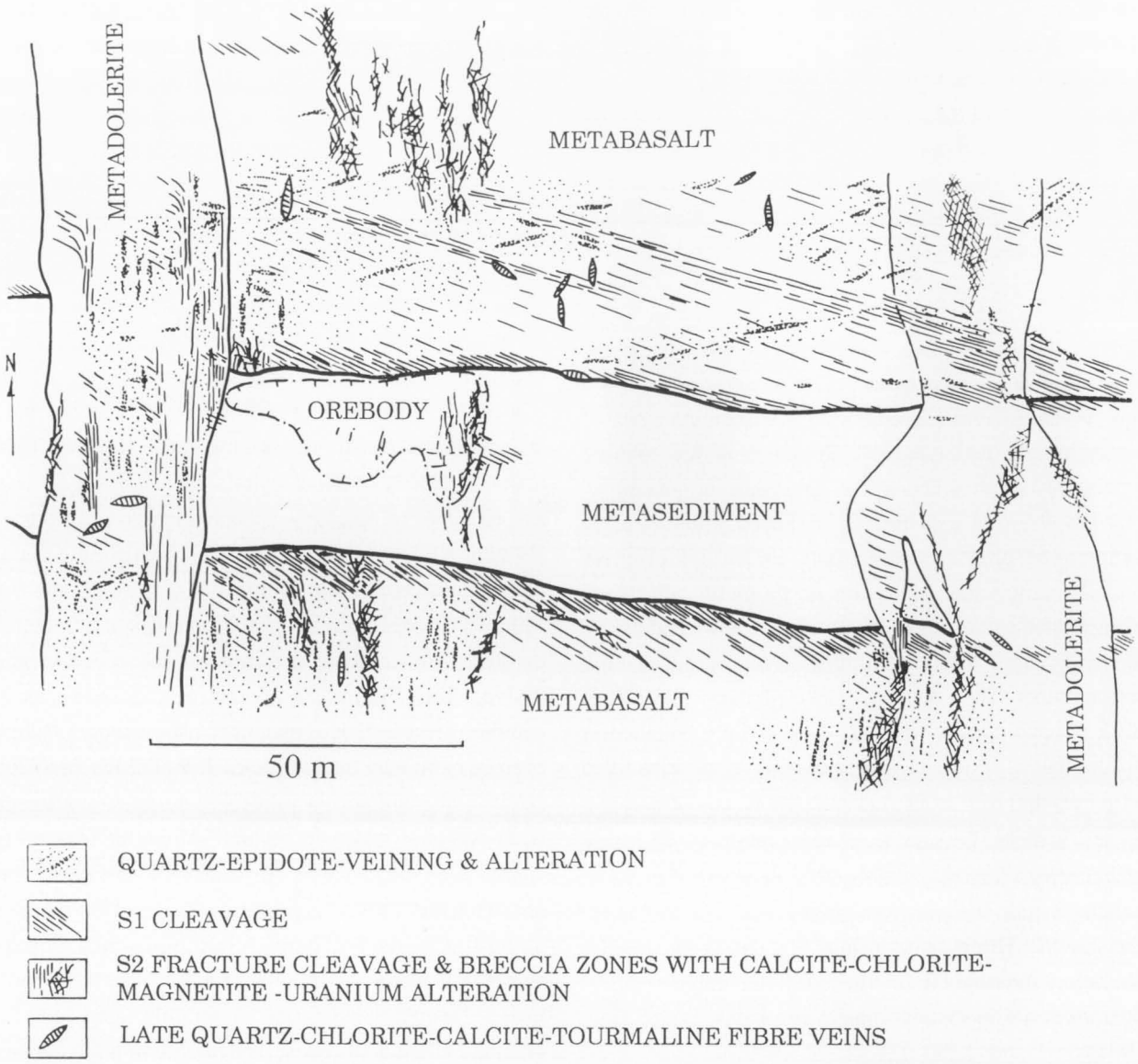


Fig. 4. Geological relationships in the vicinity of Anderson's Lode, showing that the metadolerite dykes that cross the sequence are cut by S_1 cleavage, and that the uranium deposit is located within an interflow sediment unit Phc_5 where cut by north-trending breccia-hosted calcite-chlorite-magnetite-hematite-uranium alteration zones associated with sporadic east-dipping S_2 fracture cleavage.

Fluid inclusions comprise CO_2-, NaCl-, and $CaCl_2$-rich types, but moderate-salinity NaCl-rich inclusions are most consistently associated with the calcite-albite-magnetite-hematite alteration. Microthermometric properties of these fluid inclusions, their Br/Cl ratios as determined by neutron activation analysis, and oxygen and hydrogen isotopic signatures, are all identical to the respective properties of the main-stage copper-depositing ore fluids at Mount Isa mine (Heinrich & others, 1989, submitted).

Geological relationships at Anderson's prospect

A detailed map of the Andersons Lode (also known as Counter uranium prospect) and surroundings (Fig. 4) documents the typical geological history, from rock emplacement to deformation and alteration, as it was observed in many other locations in the East Moondarra map area.

All mafic rocks are pervasively hydrated and metamorphosed to chlorite-albite-epidote-magnetite -sphene-quartz ± biotite ± calcite assemblages. A penetrative east-southeast-striking regional metamorphic schistosity is restricted to contacts against the more competent interflow sandstones. Epidote alteration occurs in discrete or diffuse haloes around discontinuous quartz-epidote veins, predominantly in areas of less schistose and more competent metabasalt. Some epidote

veins cut the metamorphic fabric, and some epidosites form boudins in the metamorphic foliation, indicating that epidote alteration, regional metamorphism, and semi-ductile deformation overlapped in time.

A north-south fracture cleavage with steep east dip associated with calcite (quartz-chlorite) veining is restricted to two semicontinuous zones of carbonate-magnetite (-biotite-chlorite-hematite) alteration. These fracture zones show no displacement or penetrative foliation, and clearly cross-cut regional metamorphic fabric and epidote alteration veins. One of the zones occurs within and along the contacts of a mafic dyke, and the other cuts through metabasalt flows. The latter is related to uranium mineralisation occurring at the intersection of the alteration and fracture zones with the metasediments, which is a carbonated quartz, chlorite, biotite and plagioclase-rich greywacke with minor pyrite and other opaques (Brooks, 1960). The uranium orebody has a cigar shape with a steep northerly plunge, parallel to the intersection of the north-striking fracture cleavage S_2 and the earlier penetrative cleavage S_1. It has been drilled to a depth of 320 m, and a resource of 590,000 t at 0.2% U_3O_8 has been identified (Brooks, 1960; unpublished report of Queensland Mines NL to Queensland Geological Survey, 1974). The ore zone is enriched in biotite and calcite, but the uranium mineral assemblage is not known.

Veins of white quartz ± tourmaline up to 1 m wide and a few metres long, and irregular quartz-calcite-hematite breccia veins postdate metamorphism and epidote alteration and, probably, carbonate-oxide alteration and U-mineralisation as well.

Conclusions

The combination of detailed mapping and related geochemical studies has provided some insight into the link between regional structural, metamorphic and metasomatic processes and mine-scale ore depositional processes.

The relative timing between deformation and fluid-rock interaction events at a regional scale can be correlated with the sequence of hydrothermal events recorded by the deformation and paragenetic history of the copper-mineralised 'silica- dolomite' at Mount Isa mine. This correlation is based on 'robust' geochemical tracers such as oxygen and hydrogen isotopes of alteration minerals and fluid inclusions, on major-element compositions of altered rocks, and Br/Cl ratios of fluid inclusions. The similarity of fluid histories provides a tentative link between fluid flow at mine and regional scale. The north-oriented shatter zones showing carbonate-oxide alteration may be the infiltration channels for NaCl-rich oxidised brines derived from evaporitic sediments. They may represent recharge channels for downward-flowing solutions which, after extensive interaction with metabasalt and possibly underlying rocks, were refocussed and ascended as the main ore fluids through Mount Isa mine, where reaction with reduced, dolomitic, and pyrite-rich metasediments of the Urquhart Shale provided a chemical trap for chalcopyrite precipitation.

Acknowledgements

We would like to thank Stewart Needham and Taro Macias for their contributions to the field mapping. Vic Wall, Chris Waring, and Lesley Wyborn helped with stimulating discussions about 'mouldy basalt' alteration. We are most grateful to Dave Blake, Alastair Stewart and Lesley Wyborn for helpful reviews of the manuscript.

References

ANDREW, A.S., HEINRICH, C.A., WILKINS, R.W.T., & PATTERSON, D.J., 1989 - Sulfur isotope systematics of copper ore formation at Mount Isa, Australia. *Economic Geology 84, 1614-1626.*

BAIN, J.H.C., HENDERSON, G.A.M., & HEINRICH, C.A., 1989 - Structural and metasomatic history of the Eastern Creek Volcanics, east Moondarra area, Mount Isa. *Geological Society of Australia, SGTSG Conference on Australasian Tectonics, Kangaroo Island, February 1989, Abstracts* 24, 3-4.

BELL, T.H., 1983 - Thrusting and duplex formation at Mount Isa, Queensland, Australia. *Nature* 304, 493-497.

BELL, T.H., 1991 - The role of thrusting in the structural development of the Mount Isa Mine and its relevance to exploration in the surrounding region. *Economic Geology* 86, 1602-1625.

BELL, T. H., PERKINS, W. G., & SWAGER, C. P., 1988 - Structural controls on development and localization of syntectonic copper mineralization at Mount Isa, Queensland. *Economic Geology* 83, 69-85.

BROOKS, J.H., 1960 - The uranium deposits of north-western Queensland. *Geological Survey of Queensland, Publication* 297, 44 pp.

CARTER, E.K., BROOKS, J.H. & WALKER, K.R., 1961 - The Precambrian mineral belt of northwestern Queensland. *Bureau of Mineral Resources, Australia, Bulletin* 51, 344 pp.

DERRICK, G.M., WILSON, I.M., HILL, R.M., GLIKSON, A.Y., & MITCHELL, J.E., 1977 - Geology of the Mary Kathleen 1:100 000 Sheet area, northwest

Queensland. *Bureau of Mineral Resources, Australia, Bulletin* 193, 114 pp.

HEINRICH, C. A., ANDREW, A. S., WILKINS, R. W. T. & PATTERSON, D. J., 1989 - A fluid inclusion and stable isotope study of synmetamorphic copper ore formation at Mount Isa, Australia. *Economic Geology* 84, 529-550.

HEINRICH, C. A., & COUSENS, D. R., 1989 - Semiquantitative electron microprobe analysis of fluid inclusion salts from the Mount Isa copper deposit, Queensland, Australia. *Geochimica et Cosmochimica Acta* 53, 21-28.

HEINRICH, C.A., WARING, C.L., & WALL, V.J., 1990 - Essential chemical ingredients for Mount Isa-style copper mineralisation. *Monash University and Victorian Institute of Earth and Planetary Sciences, Mount Isa Inlier Geology Conference, Monash University, November 1990, Melbourne,* 72-73.

HEINRICH, C.A., BAIN, J.H.C., FARDY, J.J., & WARING C.L., submitted - Bromine/chlorine geochemistry of hydrothermal brines associated with Proterozoic sediment-hosted copper mineralisation at Mount Isa, northern Australia. *Geochimica et Cosmochimica Acta.*

HEINRICH, C.A., BAIN, J.H.C., ANDREW, A.S., & others, in preparation - Regional metabasalt alteration and source processes for metamorphic copper mineralisation at Mount Isa. Tentative title for BMR Record and/or Economic Geology.

HENDERSON, G.A.M., & BAIN, J.H.C., 1991 - Geology of the Haslingden Group, East Moondarra Area (1:35 000 scale map). *Bureau of Mineral Resources, Canberra, Australia* . Available as a colour electrostatic plot on paper (AUD30), or in digital form on optical disc or Exabyte 8 mm tape (prices on application) both of which can be displayed on Intergraph Microstation software on computers that will run Unix. The digital data comprise a scanned raster image (.RLE format) of the black and white geological map, and an Intergraph vector design file containing the boundaries of coloured polygons. The coloured map and data are available from the Publication Sales Centre, Bureau of Mineral Resources, and an uncoloured Ozalar film or paper copy (AUD20) of the map is available from BMR Copy Service, both at GPO Box 378, Canberra, ACT, 2601, Australia. All orders to be prepaid to Collector of Public Monies.

PERKINS, W.G., 1984 - Mount Isa silica-dolomite and copper orebodies: The result of a syntectonic hydrothermal alteration system. *Economic Geology* 79, 601-637.

ROBINSON, W.B., 1968 - Geology of the Eastern Creek Volcanics in the Mount Isa district. *Proceedings of the Australasian Institute of Mining and Metallurgy*, 226, 89-96.

SMITH, S.E., & WALKER, K.R., 1971 - Primary element dispersions associated with mineralisation at Mount Isa, Queensland. *Bureau of Mineral Resources, Australia, Bulletin* 131, 64 pp.

SWAGER, C.P., 1985 - Syndeformational carbonate-replacement model for the copper mineralisation at Mount Isa, northwest Queensland: A microstructural study. *Economic Geology* 80, 107-125.

WARING, C.L., 1990a - Genesis of the Mount Isa Cu ore system. Ph.D. thesis, Monash University, Melbourne, 297 pp. (unpublished)

WARING, C.L., 1990b - The Mt. Isa Cu system: alteration, fluid flow, and pre-disposing factors. *Monash University and Victorian Institute of Earth and Planetary Sciences, Mount Isa Inlier Geology Conference, Monash University, November 1990,Melbourne,* 69-71.

WILSON, I.H., DERRICK, G.M., & PERKIN, D.J., 1985 - Eastern Creek Volcanics: their geochemistry and possible role in copper mineralisation at Mount Isa, Queensland. *BMR Journal of Australian Geology & Geophysics 9, 317-328.*

WILSON, I.H., GRIMES, K.G., & DERRICK, G.M., 1983 - Cloncurry 1:250 000 Geological Sheet, 2nd edition. *Bureau of Mineral Resources, Australia.*

WYBORN, L.A.I., 1987. The petrology and geochemistry of alteration assemblages in the Eastern Creek Volcanics, as a guide to copper and uranium mobility associated with regional metamorphism and deformation, Mount Isa, Queensland. *In* PHARAOH, T. C., BECKINSDALE, R. D., & RICKARD, D. (Editors), Geochemistry and mineralisation processes of Proterozoic volcanic suites. *Geological Society of London Special Publication* 33, 425-434.

Geology of the Mount Novit Ranges, southwest of Mount Isa mine

K.A. Connors [1], *J.M. Proffett* [2], *G.S. Lister* [1], *R.J. Scott* [1], *N.H.S. Oliver* [1], *& D.J. Young* [1]

This paper is based on the following map:

Connors, K.A., Proffett, J.M., Lister, G.S., Scott, R.J., Oliver, N.H.S., & Young, D.J., 1991 - Geology of the Mount Novit Area (1:25 000 scale map), Bureau of Mineral Resources, Canberra. (two sheets).

Southwest of Mount Isa Mine, deformation has resulted in a succession of fold/cleavage generations, ductile faults, and shear zones which reflect continued east-west to northeast-southwest shortening in the Proterozoic Mount Isa Inlier. Kinematic indicators and stratigraphic/metamorphic relationships across the faults demonstrate west-over-east movement throughout this history. Pre-D^N_2 fabrics remain enigmatic, and are recognised only on the microscale. Macroscopic structures suggested by previous workers to be D_1 (Bell, 1983) in origin have been shown to be younger or older. The dominant fabric and fold generation developed during D^N_2, synchronously with low pressure – high temperature metamorphism. Peak conditions reached upper amphibolite facies, and peak temperatures outlasted D^N_2 deformation. Most of the major faults and shear zones (including the Mount Isa Fault) were initiated during D^N_3, accompanied by continued folding, as the low pressure – high temperature metamorphic event began to wane. Early shear zone fabrics (S_{3a}) are overprinted by mesoscopic asymmetrical non-cylindrical F_{3b} folds. Larger scale upright F_{3b} folds were followed by continued displacement on some faults and shear zones. Further shortening resulted in local development of at least two additional fold generations involving upright symmetrical folds and crenulations; faulting continued throughout this period. Thus the deformation history of the Mount Novit Ranges involved a complex period of folding and faulting which has not previously been documented.

[1] Victorian Institute of Earth and Planetary Sciences, PO Box 2729X, Melbourne, Victoria 3001

[2] Hunt, Ware, and Proffett, P.O. Box 111 253, Anchorage, Alaska 99511, USA

Introduction

The Mount Novit Ranges are situated south-southwest of Mount Isa within the Western Fold Belt (Blake, 1987) and consist largely of Haslingden and Mount Isa Group units. The oldest rocks exposed in the mapped area are banded gneiss and schist of the *May Downs Gneiss* (Table 1), which may represent either the Yaringa Metamorphics or a basal unit of the *Mount Guide Quartzite* (Blake, 1987). Overlying units of the Haslingden Group include metabasalt and interbedded metasediments of the *Eastern Creek Volcanics*, and a sequence of alternating quartzite and pelite to psammopelite interpreted as the *Myally Subgroup* (Table 1). The younger *Mount Isa Group* units and/or *Surprise Creek Formation* consist of metashale, metasiltstone, and quartzite sequences.

Units from both the Mount Isa and Haslingden Groups crop out on both sides of the Mount Isa Fault, which cuts north-south through the Mount Novit Ranges. However, detailed correlation of strata is difficult due to differences in metamorphic grade, alteration, and intensity of deformation which alter both the appearance and the thickness of individual units. Lateral facies variations further hamper correlation.

The Haslingden Group is intruded by the *Sybella Batholith*, pegmatites, and various mafic intrusions (see Connors & others, 1991). Hill & others (1975) reported that the batholith is overlain unconformably by the *McNamara Group,* seen as equivalent to the Mount Isa Group (Blake, 1987). They noted clasts of porphyritic microgranite, quartz-tourmaline pegmatite, and granite in the basal conglomerate of the McNamara Group. Most contacts between the batholith and the McNamara Group are either faulted or not exposed, but 11.5 km northwest of Carter's Bore (grid reference 6756 - 162930), the basal conglomerate lies unconformably upon Carter's Bore Rhyolite and contains pebbles of this rock type. Just north of this locality the contact is poorly exposed, but the conglomerate appears to lie unconformably on the granite. It contains abundant coarse angular clasts of feldspar and quartz similar to that found in the Sybella Batholith (Proffett, 1989b).

TABLE 1. LITHOLOGY AND STRATIGRAPHIC RELATIONSHIPS OF UNITS EXPOSED WITHIN THE MOUNT NOVIT RANGES. Stratigraphic relationships taken in part from Blake (1987).

UNIT		LITHOLOGY	STATIGRAPHIC RELATIONSHIPS
Mount Isa Group	Native Bee Siltstone	buff to yellow, leached dolomitic metasiltstone, rare chert beds	conformably overlies Breakaway Shale
(east of the Mount Isa Fault)	Breakaway Shale	grey to buff, siliceous to silty metashale, graphitic metashale	conformably overlies Moondarra Siltstone
	Moondarra Siltstone	grey to purple, leached dolomitic metasiltstone, finely laminated metasiltstone, carbonaceous phyllites, and feldspathic, mica-rich psammite to psammopelite	?conformably overlies Surprise Creek Formation
Surprise Creek Formation ±		laminated metasiltstone to graphitic phyllite	conformably overlies psammite + metasiltstone unit
Basal Mount Isa Group Equivalents		fine grained, brown psammite to metasiltstone	comformably overlies and is gradational with quartzite
(west of the Mount Isa Fault)		orthoquartzite to micaceous quartzite	conformably overlies conglomerate
		basal metaconglomerate	unconformably overlies units of the Myally Subgroup
Haslingden Group	Myally Subgroup	quartzite, psammite, pelite to psammopelite	conformably overlies Eastern Creek Volcanics intruded by pegmatites, dykes, and ?Sybella
	Eastern Creek Volcanics	amphibolite, metabasalt, metagabbro, and chlorite schist all with interbedded pelites, quartzite, and psammite	conformably overlies Mount Guide Quartzite intruded by Sybella, pegmatites, and ?younger mafic dykes
	Mount Guide Quartzite	coarse grained quartzite and psammite	conformably or unconformably overlies May Downs Gneiss
Haslingden Group or basement?	May Downs Gneiss	banded quartzo-feldspathic gneiss, biotite and muscovite schists, minor quartzite and psammite	base not exposed may represent basement metamorphics or basal Mount Guide intruded by Sybella, pegmatites, and mafic dykes

U-Pb zircon ages of 1671 ± 8 Ma for the Sybella Batholith and 1678 ± 1 Ma for the Carter's Bore Rhyolite (Page & Bell, 1986; Page, 1978) are older than the revised age of 1656 ± 10 Ma obtained by ion microprobe analysis of zircons from a tuff bed in the Urquhart Shale of the Mount Isa Group (R.W. Page, BMR, unpublished data), which was previously dated as 1670 +20-17 Ma (Page, 1981). Additional ion microprobe analyses and geologic work are in progress to resolve the significance of the 1610 ± 10 Ma U-Pb zircon result obtained for the Queen Elizabeth Pluton by Page & Bell (1986). They interpreted the pluton as a separate, younger phase of the Sybella Batholith, although recent field work (this study) suggests that it is part of the main batholith.

Structural domains recognised in this study

The map area has been divided into the following five structural domains (Fig. 1) :

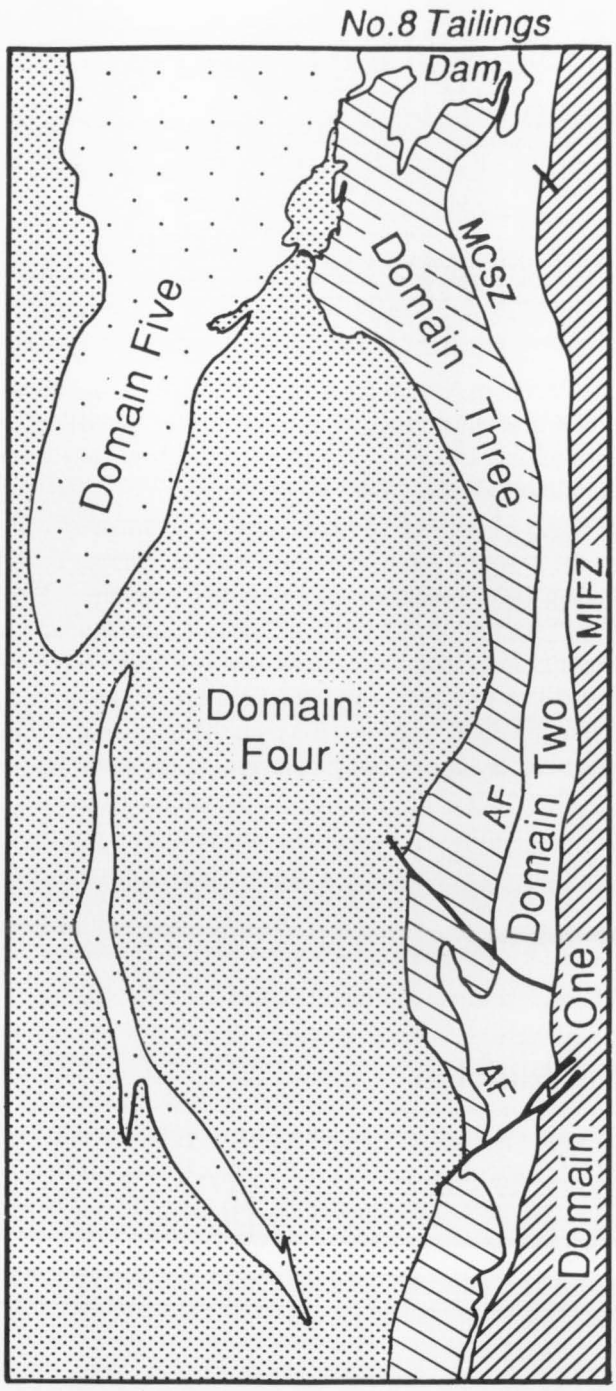


Fig. 1. Summary map of the field area outlining the five structural / lithological domains. Mount Isa is approx. 5 km to the north. MIF = Mount Isa Fault, AF = Adelheid Fault, and MCSZ = Mica Creek Shear Zone.

- Domain One - East of the Mount Isa Fault;
- Domain Two - Mount Isa Fault to the Adelheid Fault / Mica Creek Shear Zone;
- Domain Three - Adelheid Fault / Mica Creek Shear Zone to the Sybella Batholith;
- Domain Four - Sybella Batholith;
- Domain Five - 'Vortex' structure.

The major differences in structural style between these domains are due to such factors as variation in the competency of units, and in pressure and temperature during deformation and metamorphism. The rocks in Domain Two and parts of Domains Three and Five provide the best evidence for the sequence of deformation events west of the Mount Isa Fault, and the structural histories for the other domains are based on correlation with these domains. The sequence of fold and fault generations is summarised in Figure 2. Deformation episodes in the Mount Novit area are denoted by the superscript 'N'.

Domain One

The easternmost domain (Fig. 1) consists of greenschist facies-chlorite zone (Wilson, 1972) metasiltstone/shale of the Moondarra Siltstone, Breakaway Shale, and Native Bee Siltstone of the Mount Isa Group, and metabasalts and quartzites of the Eastern Creek Volcanics. Alteration and deformation of the metabasalts have formed chlorite schist interlayered with metasediment and quartzite. These westward dipping units are upward facing. Other units of the Mount Isa and Haslingden Groups crop out east of the study area.

D^N_2 structures

Throughout much of this domain, only one pervasive cleavage can be identified in outcrop. This slaty cleavage is very tentatively correlated with S_2 in Domain Two. It dips steeply west and consistently displays eastward vergence with respect to bedding. The intersection lineation between bedding and this cleavage generally plunges north, but minor variations in the orientation of either surface results in significant plunge variations in the intersection lineation, due to the small angle between bedding and cleavage in these rocks.

D^N_3 structures

A zone of mesoscopic to macroscopic east-verging similar folds, tentatively correlated with F_{3b}/S_{3b} of Domain Two, occurs within metashale south of the Double Peak Fault (see Connors & others, 1991). The north-striking axial planar fabric forms a strong schistosity, and overprints a slaty cleavage with which it maintains eastward vergence. The older slaty cleavage, tentatively correlated with S_2, is parallel or subparallel to bedding, and also verges eastward. In thin section, the younger schistosity is clearly a crenulation cleavage defined by recrystallised strain-free micas which overgrew the crenulated slaty cleavage, and by aligned opaque minerals and new mica growth parallel to the new cleavage. These crenulations are rarely evident in outcrop.

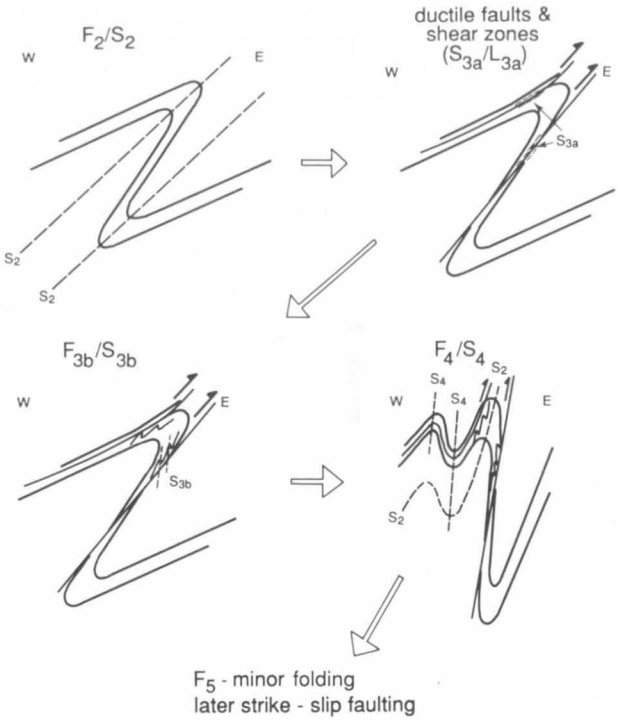


Fig. 2. Schematic diagrams depicting the sequence of fold and fault episodes recognised in the Mount Novit Ranges. The asymmetrical east- to northeast-verging F_2 folds formed on all scales from centimetres to hundreds of metres. The overturned limbs are generally attenuated, but actual fault and shear zone development post-dates F_2/S_2. S_{3a} forms a strong fabric or mylonitic fabric, associated with the down-dip mylonitic L_{3a} mineral lineation, in and adjacent to the fault and shear zones. As fault/shear zone movement slowed or ceased, strongly asymmetrical non-cylindrical F_{3b} folds with an axial planar crenulation cleavage formed. Further shortening resulted in additional displacement on faults and shear zones, and in several generations of north to northwest-trending upright symmetrical folds and crenulations including late F_{3b}, F_4, and possibly F_5. The youngest structures are strike-slip faults.

D^N_5 structures

In the north of Domain One, the pervasive slaty cleavage is locally folded by northwest-plunging folds and steeply dipping axial planar crenulation cleavage. These also fold and crenulate mylonites associated with the Mount Isa Fault, and can be traced across the fault into Domain Two where they overprint S_{3b} and L_{3b}. These northwest-plunging structures are interpreted to correlate with F_5/L_5 in Domain Two (see below).

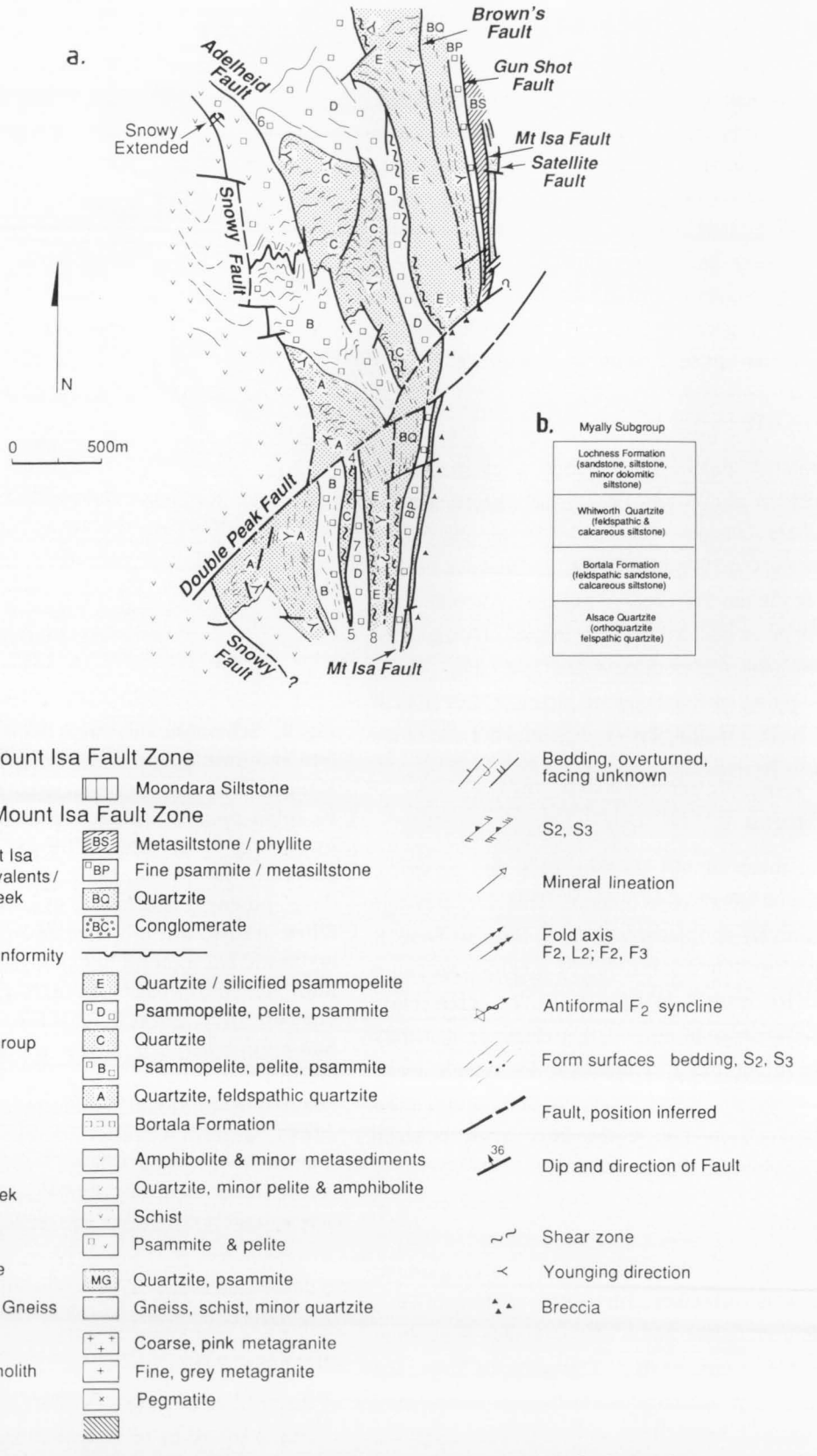


Fig. 3. (a) Geologic map south of Snowy Extended mine (see Connors & others, 1991) depicting the sequence of quartzite, psammite, and pelite (units A to E) which are correlated with the Myally Subgroup. See text for more details. Locations 4, 5, and 6 refer to Figure 5, and locations 7 and 8 refer to Figure 7. Generalised from mapping by K.A. Connors 1988-1990 (Ph.D. thesis, Monash University). (b) Stratigraphy of the Myally Subgroup east of the Mount Isa Fault. In comparison to this stratigraphy, the sequence observed in Figure 3a includes two extra units (either B + C or C + D) between the lower Alsace Quartzite (unit A) and upper Whitworth Quartzite (unit E). Unit C represents either a quartz-rich horizon within the pelites and psammites of the Bortala Formation, or part of the stratigraphy has been repeated along bedding-parallel faults.

Faults

There are many north-striking faults in Domain One, which dip steeply west at a low angle to bedding and juxtapose older units to the west against younger units to the east (see Connors & others, 1991). Some faults (e.g., the Crystallena Fault; Proffett, 1989a) are overprinted by the pervasive slaty cleavage tentatively correlated with S_2 of Domain Two as discussed above.

The boundary between Domains One and Two is marked by the Mount Isa Fault, which includes both ductile and brittle features. Ductile deformation associated with the fault is most pervasive in Domain Two. Zones of brittle deformation occur mainly along later faults that cut and offset the ductile Mount Isa Fault at low angles. Within the metashale/siltstone of Domain One, zones of brittle deformation are defined by quartz vein complexes which grade into breccia zones up to 1 m wide containing metashale or metasiltstone fragments in a quartz matrix. In some breccias, rotation of the clasts is minimal and many clasts appear to fit back together. In others, clasts are clearly rotated as the orientation of the strong cleavage varies from clast to clast. Many of the late brittle faults belong to a set of northwest-striking left lateral faults and northeast-striking right lateral faults discussed below.

Domain Two

The western part of Domain Two consists of quartzite, psammite, psammopelite, and schist correlated with the Myally Subgroup (Table 1). North of Mica Creek, fine-grained psammite and schist are exposed directly below the basal Surprise Creek /Mount Isa Group unconformity, and these may represent the Bortala Formation (see Connors & others, 1991). Interpretation of the Myally Subgroup sequence exposed in the south (Fig. 3a) is more difficult due to deformation and/or facies variations.

South of the Double Peak Fault, amphibolite and interlayered metasediment of the Eastern Creek Volcanics are stratigraphically overlain by a unit interpreted as the Alsace Quartzite (unit A of Figure 3a). In turn this is overlain by a sequence of interbedded pelite and psammite interpreted as the Bortala Formation (unit B of Figure 3a). The overlying sequence: quartzite unit C, pelite and psammite unit D, and silicified 'quartzite' unit E, does not match the known stratigraphy of the Myally Subgroup east of the Mount Isa Fault (Fig. 3b). It is not certain that these units are in stratigraphic continuity, but no evidence has been found for a major fault.

The unconformity at the base of the Surprise Creek Formation and/or basal Mount Isa Group equivalents, previously interpreted as a fault (Wilson, 1973; BMR, 1978; Bell, 1989), is typically marked by a conglomerate or an angular discordance with the underlying Haslingden Group (Proffett, 1990). In other localities the unconformity has been faulted out. North of Mica Creek, the unconformity and overlying metasediments dip steeply west and are overturned, younging to the east (Perkins & Poole, 1980). These units above the unconformity in Domain Two are referred to as 'Surprise Creek Formation and/or basal Mount Isa Group' as correlation of these units is unclear. Older rocks of the Myally Subgroup are truncated by the unconformity at angles of up to 90°.

The basal conglomerate consists of subangular to subrounded quartzite cobbles and pebbles in a quartz-mica matrix, and is up to 35 m thick. The Bortala Formation, unconformity, and overlying conglomerate are truncated by the east branch of the Mica Creek Shear Zone (Proffett, 1990), 0.9 km north of Mica Creek (see Connors & others, 1991). South of this point, the quartzite unit of the Surprise Creek Formation and/or basal Mount Isa Group equivalents is in fault contact with Eastern Creek Volcanic units to the west.

Near Sybella Creek, the exposed section of quartzite of the Surprise Creek and/or basal Mount Isa Group equivalents is much thicker than immediately to the north or south (see Connors & others, 1991). Sporadic, but locally continuous, lenses of deformed conglomerate occur in roughly the same stratigraphic position as the basal conglomerate exposed north of Mica Creek. Clean to micaceous quartzite crops out both above and below the conglomerate lenses, and bedding orientation is generally consistent across these lenses. These discontinuous lenses continue south of Sybella Creek and are interpreted to represent the basal unconformity (see Connors & others, 1991).

Pebbles (5 to 15 cm) in the southern conglomerate exposures are flattened within the strong fabric ($S_2 \pm S_{3a}$) and stretched parallel to L_{3a} ; aspect ratios for X:Y range from 2-5 and for Y:Z from 3-12). Farther south the lenses occur sporadically, and the pebbles are smaller (1- 4 cm). The most southerly noted occurrence of scattered pebbles is about 1 km north of Brown's Waterhole Creek (see Connors & others, 1991). The unconformity has not been positively identified south of this locality, although faulted angular discordances east of the King prospect probably mark its location.

The basal conglomerate of the Mount Isa Group

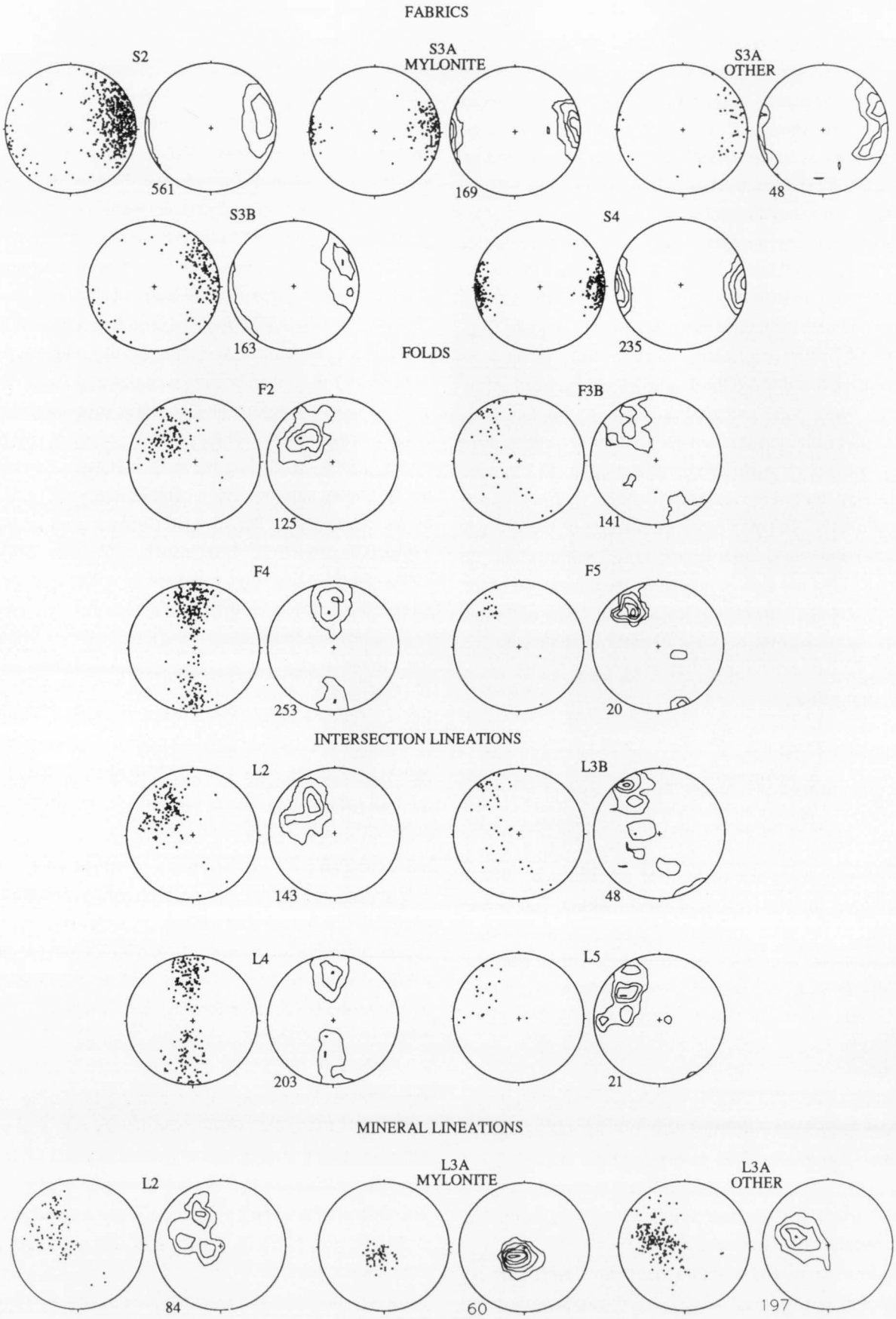


Fig. 4. Equal-area stereoplots of (a) fabrics, (b) fold axes, (c) intersection lineations, and (d) mineral lineations for the different deformation episodes. Contours are: 2%, 6%, 10%, 14%, and 18% per 1% area. All structural data are from mapping by K.A. Connors 1988-1990 (area 4 on index map beside the main map; Connors & others, 1991).

equivalents is overlain by cross-bedded orthoquartzite, micaceous quartzite, and psammite. These rocks are overlain by fine-grained brown psammite and metasiltstone across an interbedded gradational contact 2 to 14 m wide (see Figure 6a below). South of Mica Creek, this contact is usually faulted (see Connors & others, 1991). The fine-grained brown psammite and metasiltstone are conformably overlain by thinly bedded metasiltstone and graphitic phyllite. These rocks are faulted against Domain One units along the Mount Isa Fault.

D^N_1 structures

There is no unequivocal field evidence of pre-D^N_2 folds or fabrics. In thin section, however, relict crenulation hinges defined by decussate mica textures (i.e., abundant cross micas between septa) within S_2 microlithons preserve evidence of a pre-S_2 fabric. No mesoscopic or macroscopic folds that formed with this fabric as axial plane have been identified. We have shown that two structures (the Adelheid and Tailings Dam Faults) previously interpreted as D_1 thrusts (Bell, 1989) are in fact D^N_3 and pre-D^N_1, respectively.

D^N_2 structures

The pervasive S_2 cleavage is dominant throughout most of the study area. S_2 forms a finely differentiated schistosity in micaceous rocks. In mica-poor units, S_2 forms a finely spaced cleavage defined by oriented micas. In contrast to statements by previous workers (e.g., Bell, 1983; Bell & others, 1988), S_2 orientation is variable due to refraction and effects of later deformation. In areas of little subsequent deformation, S_2 dips moderately to steeply west to southwest (Fig. 4a).

F_2 folds generally plunge gently to moderately northwest but vary from southwest- to west- to north-plunging (Fig. 4b) and in most areas are northeast- to east-verging. Asymmetrical antiforms have a gentle west-dipping upper limb and a steeply dipping overturned lower limb. Folds of all scales (from 10 cm to 0.5 km) commonly display attenuation of the steeply overturned limb. Rarely the lower limb dips gently southwest resulting in a tight recumbent fold.

The L_2 mineral lineation generally plunges west-northwest or northwest, and is commonly parallel to the S_0/S_2 intersection and F_2 fold axes (Figs. 4b-d) where all three are observed in one outcrop. L_2 is defined by the same minerals and same microstructures as S_2.

D^N_3 structures

S_{3a} and S_{3b} are interpreted to result from progressive deformation within and adjacent to ductile faults and shear zones. Therefore they have not been labelled as separate generations despite local overprinting. S_{3a} and L_{3a} developed within the ductile faults or shear zones, whereas S_{3b}/F_{3b} occur throughout the map area, but formed most pervasively adjacent to some faults and shear zones.

The S_{3a} fabric (Fig. 4a) is a strong cleavage or mylonitic fabric. Along the Adelheid Fault (see Connors & others, 1991) S_{3a} is confined to a 5 to 15 m zone. It decreases in intensity away from the fault zone. S_{3a} forms a pervasive mylonitic fabric in quartzite exposed in the hanging wall of the Mount Isa Fault (see Connors & others, 1991). The mylonite obscures bedding in the quartzite over a zone 20 to 100 m wide (and up to 400 m wide south of Double Peak Fault, where the Gun Shot and Brown's Faults merge with the Mount Isa Fault; see Connors & others, 1991).

In the quartz mylonites, L_{3a} plunges steeply south or southwest (Fig. 4d); elsewhere it plunges west-northwest similar to L_2. L_{3a} is typically defined by the same minerals as L_2, but coarse muscovite flakes and radial clusters of fibrolitic sillimanite that grew post-S_2/L_2 (Connors, 1990b) are stretched parallel to L_{3a}. In highly deformed zones such as the Adelheid and Mount Isa Faults, L_{3a} is typically parallel to the S_2/S_{3a}, and more rarely S_2/S_{3b}, intersection lineations .

The steeply west- to southwest-dipping S_{3b} fabric (Fig. 4a) commonly forms a fine to coarse (1 to 10 mm) discrete crenulation cleavage (using the terminology of Gray, 1977). This locally approaches a differentiated layering. These variations are dependent upon rock type, grain size, and intensity of S_2, as well as on the heterogeneous nature of the F_{3b}/S_{3b} deformation event.

Tight east- to northeast-verging F_{3b} folds are strongly asymmetrical and highly non-cylindrical (Fig. 5a-b) adjacent to many D^N_3 ductile faults and shear zones. In these high-strain zones there is marked variation in fold axis orientation within the axial plane, ranging from subhorizontal to steeply plunging and trending in the range 315°-360° and 135°-180° (Fig. 4b). Hinge lines of the most non-cylindrical folds vary from perpendicular to subparallel to the strong mineral lineation L_{3a} ($\pm L_2$) (Fig. 5a-b). In other areas F_{3b} folds are upright, gently doubly-plunging or almost cylindrical, and roughly symmetrical.

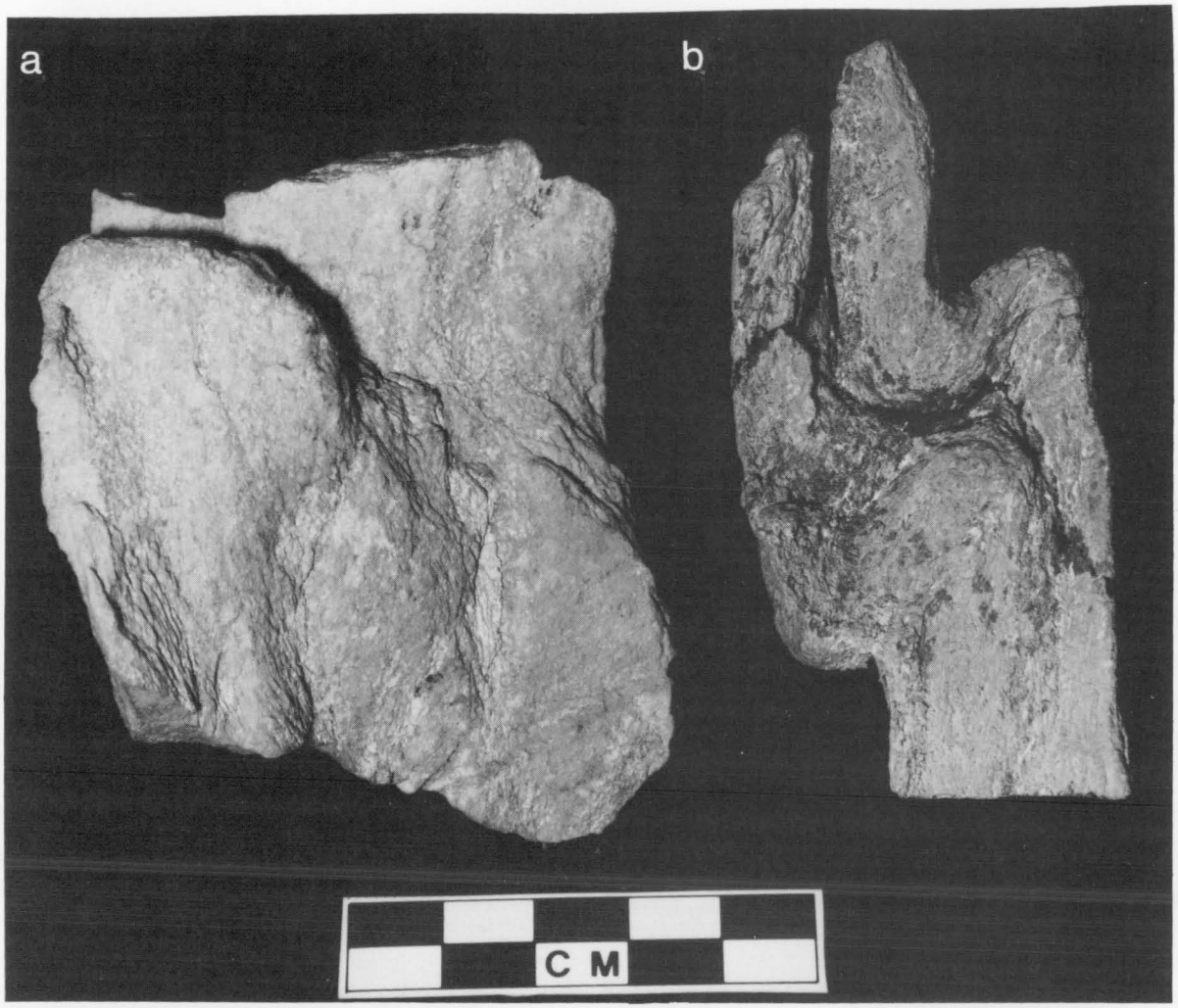


Fig. 5. (a) Non-cylindrical F_{3b} fold in strongly deformed micaceous quartzite (looking east). The fold axis changes orientation by 90° and then dies out over a short distance; location 4 in Figure 3a (quartzite unit C). (b) Asymmetrical east-verging F_{3b} fold in strongly deformed psammite (looking south); location 5 in Figure 3a (pelite and psammite of unit D).

D^N_4 structures

A near vertical north-striking S_4 fabric (Fig. 4a) forms a zonal crenulation cleavage defined by strong symmetrical crenulations with angular hinges. Asymmetrical crenulations on the limbs of large-scale folds locally develop into a discrete crenulation cleavage. The gently north- to south-plunging F_4 folds (Fig. 4b) are open, upright, and vary from roughly symmetrical to slightly asymmetrical and east-verging.

D^N_5 structures

Northwest-plunging F_5 folds and L_5 crenulations (Fig. 4b-c) are upright and roughly symmetrical, but are not widely distributed. Fold style varies from similar to concentric, and as a result locally develop accommodation problems in hinge zones. North of Mica Creek, northwest-plunging F_5 folds with a weak crenulation cleavage fold the Mount Isa Fault mylonite as well as S_{3b} in rocks of Domain Two (Proffett, 1989a).

Faults

Early syndepositional faults

South of the No. 8 Tailings Dam (Fig. 6a), a steep east-west fault dextrally offsets the base of the Surprise Creek and/or basal Mount Isa Group equivalents, but does not offset the fine-grained psammite + metasiltstone unit 300-400 m above the unconformity. This indicates that fault movement had ceased before deposition of the psammite/metasiltstone unit (Proffett, 1990). Where the fault is overlain by the psammite/metasiltstone unit there is no angular unconformity, but on the down-thrown side there is a thin conglomerate consisting of reworked subangular pebbles of the underlying quartzite (Fig. 6a). This fault is overprinted by S_2, and is folded by F_3 (Fig. 6a).

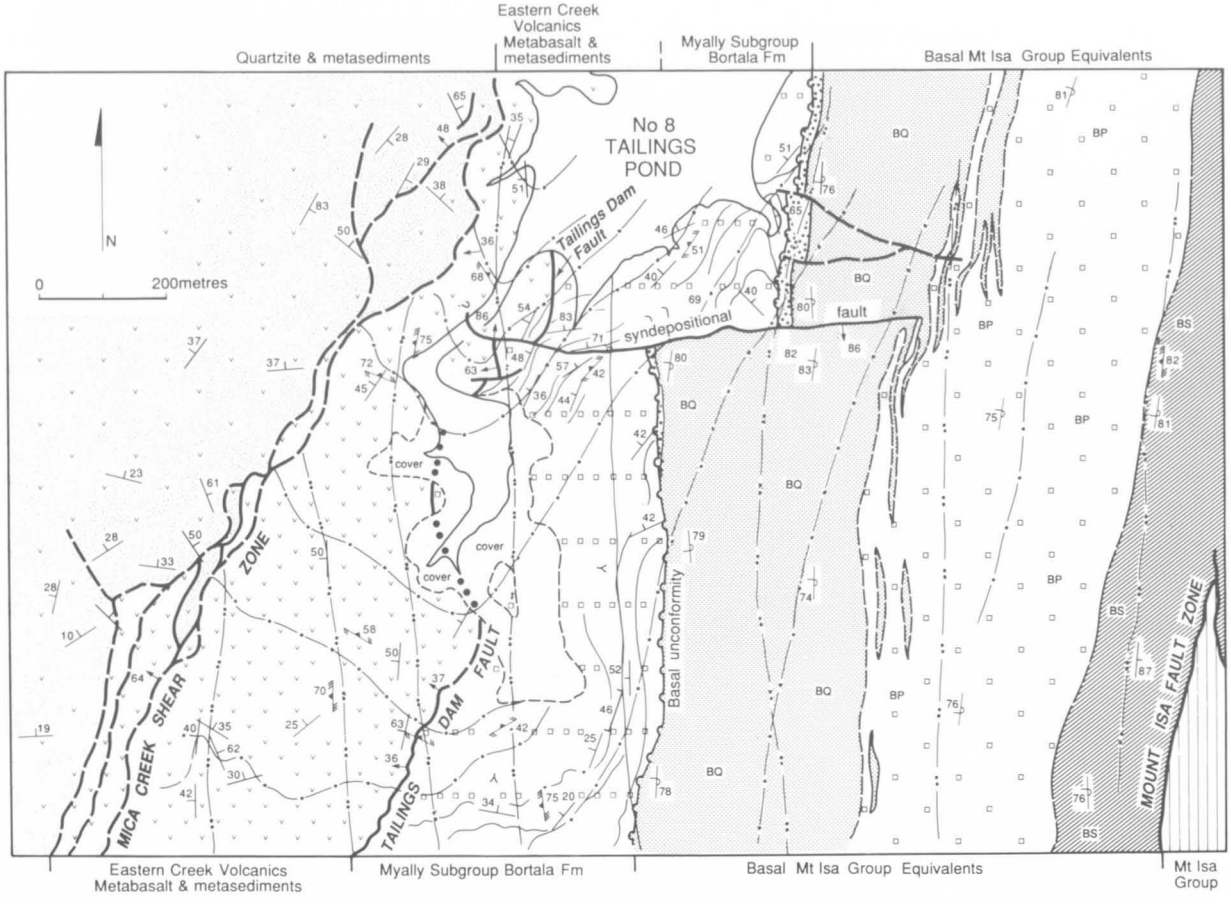


Fig. 6(a). Geologic map south of the No 8 Tailings Dam showing syndepositional fault displacing Tailings Dam Fault, basal conglomerate, and quartzite, but overlain by unit of fine-grained brown psammite and metasiltstone. A small lens of conglomerate occurs on the down-thrown southern side of the syndepositional fault. S_2 appears axial planar to the fold exposed immediately below the unconformity, but this could be coincidence and the fold may predate the unconformity. Refer to Figure 3a for the stratigraphic column and legend. Generalised from mapping by J.M Proffett, 1989-1990, for Mount Isa Mines.

A similar east-striking fault 1.5 km south of Mica Creek offsets the contact between the Surprise Creek and/or basal Mount Isa Group quartzite and overlying psammite + metasiltstone unit by about 100 m, but to the east the younger metasiltstone + phyllite unit is not affected (Fig. 6b). Nor does this fault offset the faulted contact between Eastern Creek Volcanics and quartzite of the Surprise Creek and/or basal Mount Isa Group (i.e., Mica Creek Shear Zone, Fig. 6b).

Tailings Dam Fault

The west-dipping Tailings Dam Fault crops out north of Mica Creek (see Connors & others, 1991), where it separates Bortala Formation to the east from Eastern Creek Volcanics to the west. The fault zone is 1 to 3 m thick and consists of breccia, commonly either silicified or altered to quartz + biotite + tourmaline, overprinted by S_2 (early schistosity of Proffett, 1990). The Tailings Dam Fault is displaced by the northernmost of the two syndepositional faults discussed above (Fig. 6a), and thus is also older than the psammite + metasiltstone unit (Proffett, 1990). There is no evidence (such as erosional surfaces of high relief or thick conglomerate) that a fault such as the Tailings Dam Fault was active between the time of the basal unconformity and the time of deposition of the psammite + metasiltstone unit. Therefore it is likely that the Tailings Dam Fault predates the unconformity. Restoring the unconformity to horizontal reveals that at the time of the unconformity, the Tailings Dam Fault must have been a younger over older fault dipping at a low to moderate angle to the north (Proffett, 1990).

Mount Isa Fault

The west-dipping Mount Isa Fault separates greenschist to amphibolite facies Haslingden Group units and Surprise Creek and/or basal Mount Isa Group equivalents of Domain Two in the west, from lower greenschist facies Mount Isa Group and Haslingden Group units of Domain One to the east (see cross section in Connors & others, 1991). This position for the Mount Isa Fault, which is east

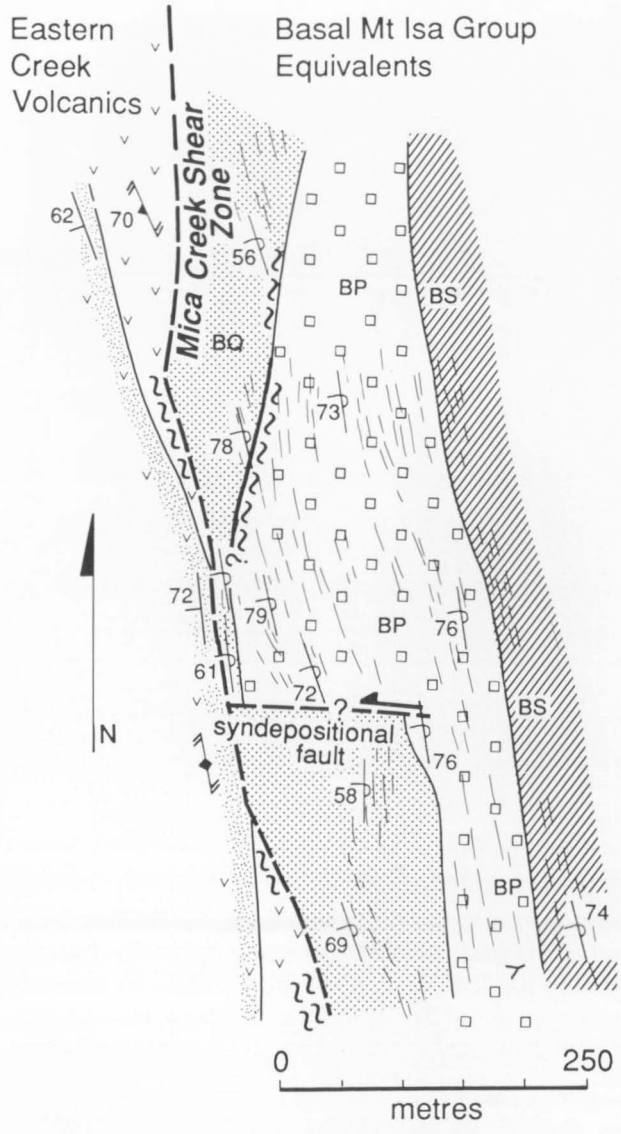


Fig. 6(b). Geologic map south of Mica Creek showing another east-west syndepositional fault which offsets the contact between quartzite and fine-grained brown psammite and metasiltstone, but is overlain by the younger metasiltstone and phyllite. Refer to Figure 3a for the stratigraphic column and legend. Generalised from mapping by D.J. Young 1989 (Monash Earth Science Survey) and P.J. Davoren 1990 (B.Sc. [Hons.] thesis, Monash University).



Fig. 7(a). Shear bands overprinting the mylonitic fabric in strongly deformed quartzite (looking north); location 7 in Figure 3a (quartzite unit C).

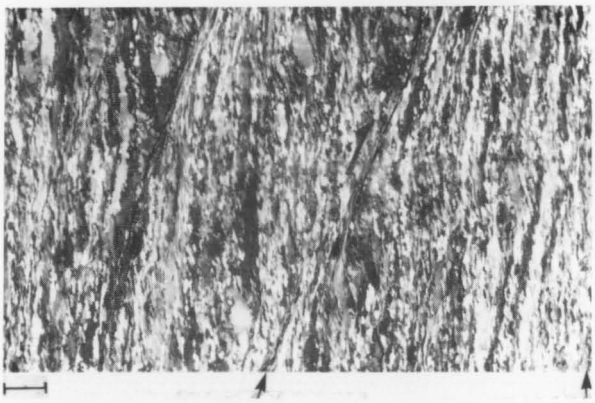


Fig. 7(b). Photomicrograph of shear bands (left arrow) overprinting the mylonitic fabric (right arrow) in the hanging wall quartzite of the Mount Isa Fault (looking north). Micas and opaque grains are concentrated along the shear bands as well as the mylonitic fabric. Location 8 in Figure 3a (quartzite unit E).

of previous interpretations (e.g., BMR, 1978), was first demonstrated by Perkins & Poole (1980). In the south, the fault occurs on the steeply overturned eastern limb of a map scale F_2 anticline (Connors, 1989, 1990a).

Approaching the fault zone from the west, the prominent cleavage ($S_2 \pm S_{3a}$) intensifies and parallels attenuated bedding, bedding becomes obliterated, and a strong mylonitic fabric (S_{3a}) with a steeply south- to southwest-plunging mineral lineation (L_{3a}) develops within the quartzite. Strongly asymmetrical highly non-cylindrical F_{3b} folds with an axial planar crenulation cleavage (Fig. 5a-b) overprint both S_2 and the S_{3a} mylonitic fabric. S_2 and the mylonites are also overprinted by a set of consistently west-dipping shear bands (Fig. 7) which demonstrate west-over-east movement (Connors, 1989, 1990a). Similar ductile fabrics are evident in quartz veins along the fault zone and in silicified quartzite just east of the fault. In the north, approaching the Mount Isa Fault from the west, the nearly bedding-parallel S_{3b} cleavage (late crenulation cleavage of Proffett, 1990) intensifies slightly and a steeply southwest-plunging mineral lineation forms. The main evidence for large

displacement on the Mount Isa Fault in this area is the metamorphic grade change across the fault.

Many of the contacts between major rock units, especially in the south of Domain Two, are structural rather than stratigraphic, due to shearing along unit boundaries (see Connors & others, 1991). South from the King prospect, deformation intensifies and Domain Two is significantly thinned (see Connors & others, 1991 and Fig. 3a). Bedding is obliterated by a strong S_2 fabric, and an anastomosing shear fabric (S_{3a}) develops in proximity to the mylonite zones of the Mount Isa Fault and related faults (see Connors & others, 1991). Some units are 25% of their thickness in less deformed areas.

Gun Shot Fault

The west-dipping Gun Shot Fault is located west of the Mount Isa Fault and juxtaposes the overturned west-dipping quartzite unit and the younger metasiltstone/phyllite unit, both of the Surprise Creek Formation and/or basal Mount Isa Group. It cuts out part of both of these units as well as the intervening fine-grained brown psammite (Fig. 8). The fault displays evidence of ductile deformation similar to the Mount Isa Fault, including a mylonitic fabric, mineral lineation, and shear bands which indicate west-over-east reverse displacement. To the north, the fault cuts east into the metasiltstone unit, and cannot be traced due to lack of exposure. Local shear bands and mylonite farther north along the eastern edge of the Surprise Creek Formation and/or basal Mount Isa Group quartzite may represent the continuation of this fault. Alternatively it could merge with the Mount Isa Fault to the east. The Gun Shot Fault continues south at about the same stratigraphic level (see Connors & others, 1991).

Brown's Fault

South of Brown's Waterhole Creek, Brown's Fault approximately coincides with the western boundary of the Surprise Creek Formation and/or basal Mount Isa Group quartzite (see Connors & others, 1991). The Myally Subgroup units to the west consist of fine-grained micaceous psammite, which is commonly silicified and therefore resembles quartzite east of the fault. Bedding west of the fault is at a high angle to the fault in some zones, but bedding to the east has been largely obliterated by the strong fabric ($S_{3a} \pm S_2$) which parallels the fault. A mylonitic foliation, mineral lineation, and rare shear bands displaying west-over-east movement, are developed along the fault zone.

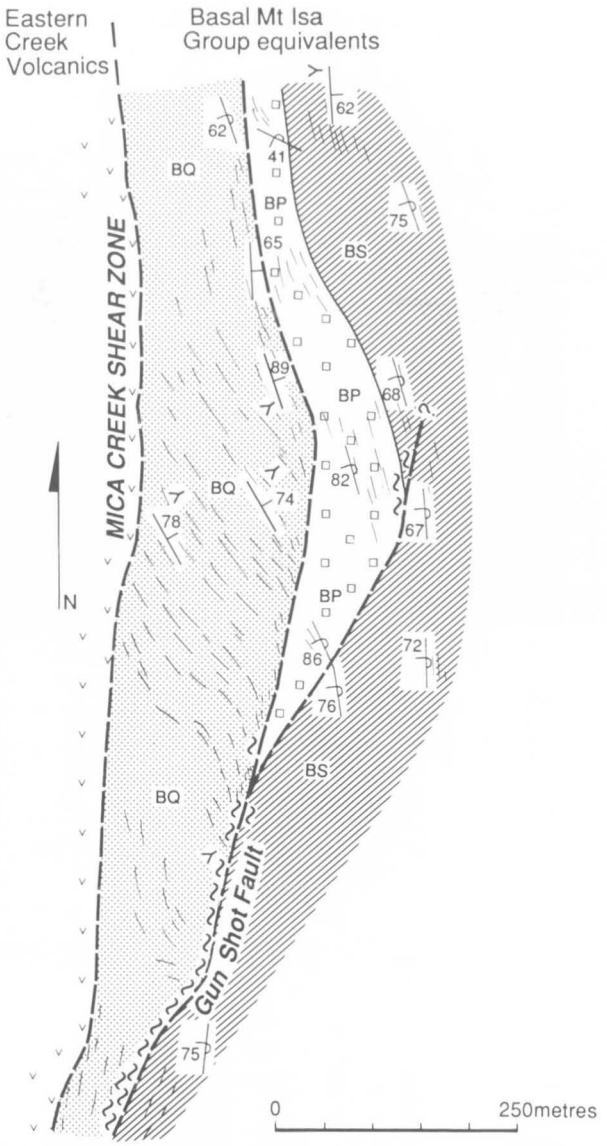


Fig. 8. Geologic map about 2.5 km south of Mica Creek showing the stratigraphic relationships across the Gun Shot Fault. Refer to Figure 3a for the stratigraphic column and legend. Generalised from mapping by D. Close 1989 (Monash Earth Science Survey) and P.J. Davoren 1990 (B.Sc. [Hons.] thesis, Monash University).

Adelheid Fault

In the south, the west-dipping Adelheid Fault places Eastern Creek Volcanics of Domain Three over the younger Myally Subgroup and Surprise Creek Formation and/or basal Mount Isa Group equivalents of Domain Two (see Connors & others, 1991 and map cross section). Intensity of deformation and alteration along the fault are variable. Assemblages of coarse-grained quartz + white mica or chlorite, chlorite or biotite + feldspar ± quartz, and chlorite ± biotite ± white mica overprint and in part, completely obscure the original rock types. The strong

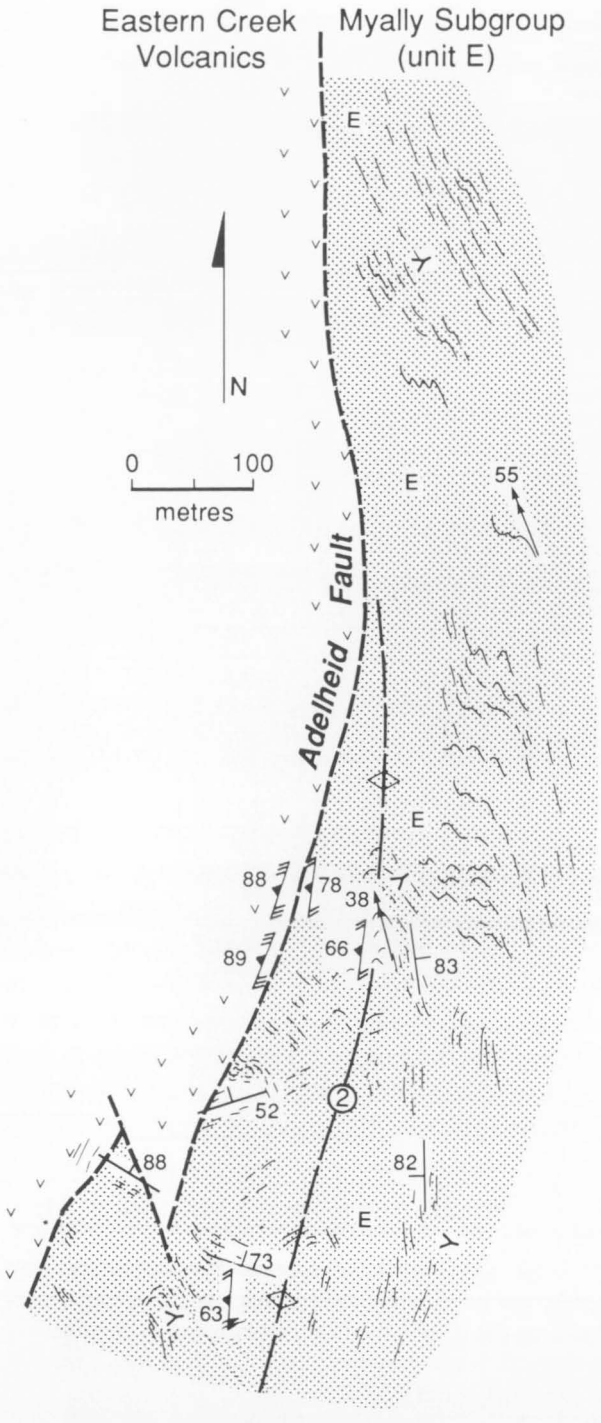


Fig. 9. Geologic map north of Brown's Waterhole Creek showing truncation of the hinge zone of a large north-plunging F_2 anticline by the Adelheid Fault. Refer to Figure 3a for the stratigraphic column and legend. Generalised from mapping by K.A. Connors 1990 (Ph.D. thesis, Monash University).

fault zone fabric, S_{3a}, is approximately parallel to the fault, and is overprinted by asymmetrical non-cylindrical F_{3b} folds and S_{3b} crenulation cleavage. The steeply west-plunging L_{3a} mineral lineation is well developed in adjacent metasediments, especially between the King prospect and the Snowy Extended mine (see Connors & others, 1991).

The Adelheid Fault cuts across the hinge zone of map-scale F_2 anticlines (Connors, 1990a) east of Snowy Extended and near Brown's Waterhole Creek (see Connors & others, 1991 and Fig. 9). In the latter area the fault cuts from the western limb across the entire hinge zone of the megascopic F_2 fold such that only the steeply overturned eastern limb is exposed north of Brown's Waterhole Creek (Fig. 9). The fault was subsequently folded by a map-scale F_4 anticline.

South and east of Snowy Extended (see Connors & others, 1991), two branches of the Adelheid Fault are truncated by the north-northwest-striking Snowy Fault, a poorly exposed structure 0.5 to 3 m wide, with quartz breccia and fine chloritic gouge.

Mica Creek Shear Zone

North of Mica Creek, the west-dipping Mica Creek Shear Zone (see Connors & others, 1991) juxtaposes quartzite to the west and amphibolite + chlorite schist of the Eastern Creek Volcanics to the east (Proffett, 1990). Both the Tailings Dam Fault and basal unconformity are truncated by the eastern strand of the shear zone (Proffett, 1990). South of this truncation, the east strand of the shear zone places amphibolite and chlorite schist to the west against quartzite of the Surprise Creek Formation and/or basal Mount Isa Group equivalents to the east (see Connors & others, 1991).

The shear zone consists mainly of shear-foliated chlorite schist and less commonly relict biotite schist. A mylonitic lineation plunges west, down-dip of the shear-foliated chlorite schist (Proffett, 1990). Drag folding and shear bands indicate west-side-up (reverse) displacement. The biotite schist, but not the chlorite schist, is overprinted by S_{3b} (late crenulation cleavage of Proffett, 1990). The shear zone cuts off S_2 and several map-scale F_{3b} folds (Proffett, 1990). The map-scale anticline in the hanging wall with shear foliation parallel to its axial plane is interpreted as a drag fold (Proffett, 1990; see Connors & others, 1991).

Domain Three

This domain, bounded to the east by the Adelheid Fault - Mica Creek Shear Zone and to the west by the metagranite, consists of amphibolite, chlorite schist, interbedded pelitic schist, and quartzite. Most of these units are thought to belong to the Eastern Creek Volcanics, but the stratigraphy is poorly constrained due to faulting and lack of distinctive stratigraphic markers. Metasedimentary interbeds within

the metabasalt and amphibolite of Domain Three are generally thicker and more abundant than in the Cromwell and Pickwick Metabasalt members to the east of the Mount Isa Fault. Metabasalt flows thin and pinch out within surrounding metasediments throughout this domain.

Mafic igneous units include both metadolerite/gabbro and metabasalt. Metadolerite/gabbro occurs as sills, stocks, plugs, or rarely as dykes. Relict ophitic to subophitic textures or amygdales and flow-top breccias are commonly preserved in massive pods surrounded by anastomosing zones of strongly cleaved or sheared ($S_2 \pm S_{3a}$) very fine- to medium-grained chlorite ± quartz schist. At higher metamorphic grade (i.e., sillimanite facies) the chlorite schist includes orthoamphibole, and Downing (1986) reported assemblages of orthoamphibole + cordierite.

Typical assemblages within the pelitic or psammopelitic units include quartz + muscovite + biotite ± chlorite ± cordierite ± sillimanite + minor tourmaline, apatite, and opaques. Unaltered cordierite porphyroblasts occur in association with coarse biotite laths, but retrogression to aggregates of quartz + pinite + Fe-oxides is common. Sillimanite, and less commonly andalusite, occur in pelitic and psammitic rocks. The two minerals occur together at several locations.

D^N_2 structures

The main foliation in Domain Three is a strong S_2 schistosity, which has an obvious decussate texture in chlorite schist. In fine-grained pelite and psammopelite, S_2 is a finely differentiated schistosity, and in psammitic units S_2 is defined by oriented micas. In amphibolite, S_2 forms a strong foliation or finely differentiated layering defined by hornblende needles and plagioclase laths.

A regionally continuous north-south syncline mapped by previous workers (e.g., Bell, 1989) has been difficult to clearly define. North of Mica Creek, a tight F_2 syncline with a subhorizontal axis occurs between the 7600E and Big Beryl Faults (see Connors & others, 1991). Tracing this syncline to the north it becomes a steeply-plunging antiformal syncline and dies out about 1 km east of the north end of the metagranite. South of Mica Creek, younging changes across a schist unit, but a change in F_2 vergence cannot be demonstrated due to poor S_2 development in the east- and west-younging quartzites on either side of this schist. These quartzites differ in rock type, colour, and sedimentary structures, suggesting that they are not the same unit. It is therefore interpreted that the west-younging limb of the F_2 syncline is truncated by the 7600E Fault, and that west-younging units from east of the fault are placed against the east-younging limb of the F_2 syncline (see Connors & others, 1991).

D^N_3 structures

A strong schistosity in the coarse quartz + phyllosilicate alteration zone along the 7600E Fault may correlate with S_{3a} (or possibly S_2). This cleavage is very similar to S_{3a} in quartz + phyllosilicate alteration assemblages along the Adelheid Fault. The L_{3a} mineral lineation in amphibolite is typically weak where S_2 is well developed, and strong where S_2 is weak; in the latter case a spaced fracture cleavage, interpreted as S_{3b}, is present in places. A weak down-dip lineation and a strong north- or south-plunging lineation occur together in some amphibolites. West of the Adelheid Fault near the Snowy mine (see Connors & others, 1991), the strong mineral lineation plunges gently north-northwest in amphibolite. This lineation is parallel to the strong L_{3a} mineral lineation defined by sillimanite in adjacent psammite. Thus the strong mineral lineation in the amphibolites is interpreted as L_{3a}, and the weak down-dip lineation as L_2.

S_{3b} is a northwest- to north-striking medium to coarse (2 to 7 mm) discrete crenulation cleavage. The crenulations are asymmetrical and verge eastward with respect to S_2. S_{3b} locally forms a spaced fracture cleavage in amphibolite, especially in the north. Meso- to macroscopic F_{3b} folds vary from upright to inclined, symmetrical to asymmetrical, and are commonly doubly-plunging. North of Mica Creek, F_3b folds are better developed and consistently north-plunging.

D^N_4 structures

D^N_4 structures include north-trending symmetrical folds, kinks, and crenulations. A zonal to discrete crenulation cleavage is developed in fold hinges in pelite, but cleavage is rare in amphibolite. These D^N_4 structures are present in restricted zones throughout this domain.

Faulting

Fault II of Wilson (1973)

No evidence for a fault previously mapped 500 m west of the Mica Creek Shear Zone, between quartzite to the east and schistose metasediments to the west (Wilson, 1973; BMR, 1978; Downing, 1986) has been found. The two units appear to be interbedded along a conformable depositional contact (Proffett, 1990).

7600E Fault

North of Mica Creek, the west-dipping 7600E Fault (see Connors & others, 1991) crops out 1.2 km west (but only

400 to 500 m structurally above) the Mica Creek Shear Zone. This structure separates quartz-mica schist (± cordierite) to the east from amphibolite with metasedimentary interbeds to the west (Proffett, 1990). A coarse schistosity, interpreted as S_{3a} or possibly S_2, overprints coarse biotite + chlorite + quartz alteration in the fault zone. This schistosity is in turn overprinted by the S_{3b} crenulation cleavage. The amount and direction of displacement are unknown.

Big Beryl Fault

The west-dipping Big Beryl Fault is exposed approximately 2 km west of the Mica Creek Shear Zone, north of Mica Creek (Proffett, 1990). In the north, it truncates north-northwest-plunging F_{3b} folds in amphibolite and metasediment, and places them against pegmatite sills, metasediments, and mafic meta-intrusives to the west (Proffett, 1990). Farther south this fault separates amphibolite to the west from quartzite to the east (see Connors & others, 1991), and here it may be equivalent to Fault III of Wilson (1973). The fault zone contains coarse shear-foliated quartz-mica schist and sheared pegmatite. The amount and direction of displacement are uncertain, but similarity in orientation and timing to the Mica Creek Shear Zone suggest west-side-up movement.

Domain Four

The large elliptical 'pod' of metagranite within this domain appears to be almost isolated from the main body of the Sybella Batholith (Mount Isa 1:100 000 Sheet area, BMR 1978). As a result, this 'pod' is informally referred to as the Queen Elizabeth Pluton (Page & Bell, 1986). However, geometrical analyses (this study) suggest that it is continuous with granitic rocks to the west. The metagranite intruded as a tabular or lens-shaped sheet within the lower part of the Haslingden Group, and is generally overlain by amphibolite of the Eastern Creek Volcanics and underlain by the Mount Guide Quartzite (see cross section in Connors & others, 1991).

The metagranite margin, which marks the boundary of this domain, is roughly parallel to adjacent stratigraphic boundaries, but locally cross-cuts them at a small angle. The metagranite/country rock contact is generally sharp and appears intrusive. However, intense foliation, shearing, and mylonites occur in some locations along the margin, and rare mylonitised pegmatite occurs in the north.

Evidence of contact metamorphism has not been documented, but could be obscured by regional metamorphism. Metamorphic grade increases across the metagranite from Domain Three, where sillimanite is stable, to Domain Five, where partial melting has occurred (see below).

The main body of metagranite varies in composition from metagranodiorite to alkali-feldspar metagranite (Wyborn & others, 1988). It consists of quartz + plagioclase + K-feldspar + biotite ± hornblende + minor sphene, muscovite, opaques (magnetite and ilmenite), apatite, and zircon. Wilson (1972) reported accessory fluorite. Grain size varies from uniformly fine (average 1 to 3 mm) to coarse (5 to 10 mm) with K-feldspar augen up to 20 mm.

Distinct fine-grained hornblende-free grey metagranite to metagranodiorite occurs as sills and irregular pods along the western edge of the pluton and within the country rocks of Domain Five. This rock type contains stretched and flattened xenoliths of amphibolite and metasediment.

Pegmatite dykes and sills are common in the country rocks along the pluton margins, but less common within the metagranite. McGowan (1991) recognised eight mineralogical types, but only two pegmatite generations were distinguished in this study. In a highway cutting 6 km southwest of the King prospect (see Connors & others, 1991), pegmatites that are parallel to bedding and the main foliation (probably $S_2 \pm S_{3a}$), are deformed into boudins with axes perpendicular to the southwest-plunging mineral lineation ($L_{3a} \pm L_2$). Approximately 20 m farther south, a late pegmatite cuts the strong foliation (Proffet, 1989a) and small S_{3a}-related shear zones. The older pegmatites consist of white or pink feldspar + quartz + muscovite ± biotite ± tourmaline ± beryl and are commonly zoned with quartz + muscovite rich margins and feldspar-rich cores. East of the King prospect and at the north end of the pluton (see Connors & others, 1991) similar pegmatites have been folded by F_2. The later pegmatite consists of graphic intergrowths of pink feldspar and quartz plus minor muscovite.

Segregations consisting of quartz + K-feldspar + albite + muscovite (McGowan, 1991) occur within the metagranite north of Mica Creek, and are locally abundant along the eastern contact (location 1, Fig. 10a). They are coarser-grained than adjacent metagranite and locally have a biotite-rich selvedge. Biotite in the selvedges is parallel or subparallel to S_2 in the metagranite. They form elongate discontinuous lenses or blebs (Fig. 10b-e) cross-cutting the pervasive S_2 metagranite fabric at a low to moderate angle. S_2 is commonly reoriented adjacent to the segregations (Fig. 10b). Rare folded segregations appear to have S_2 as

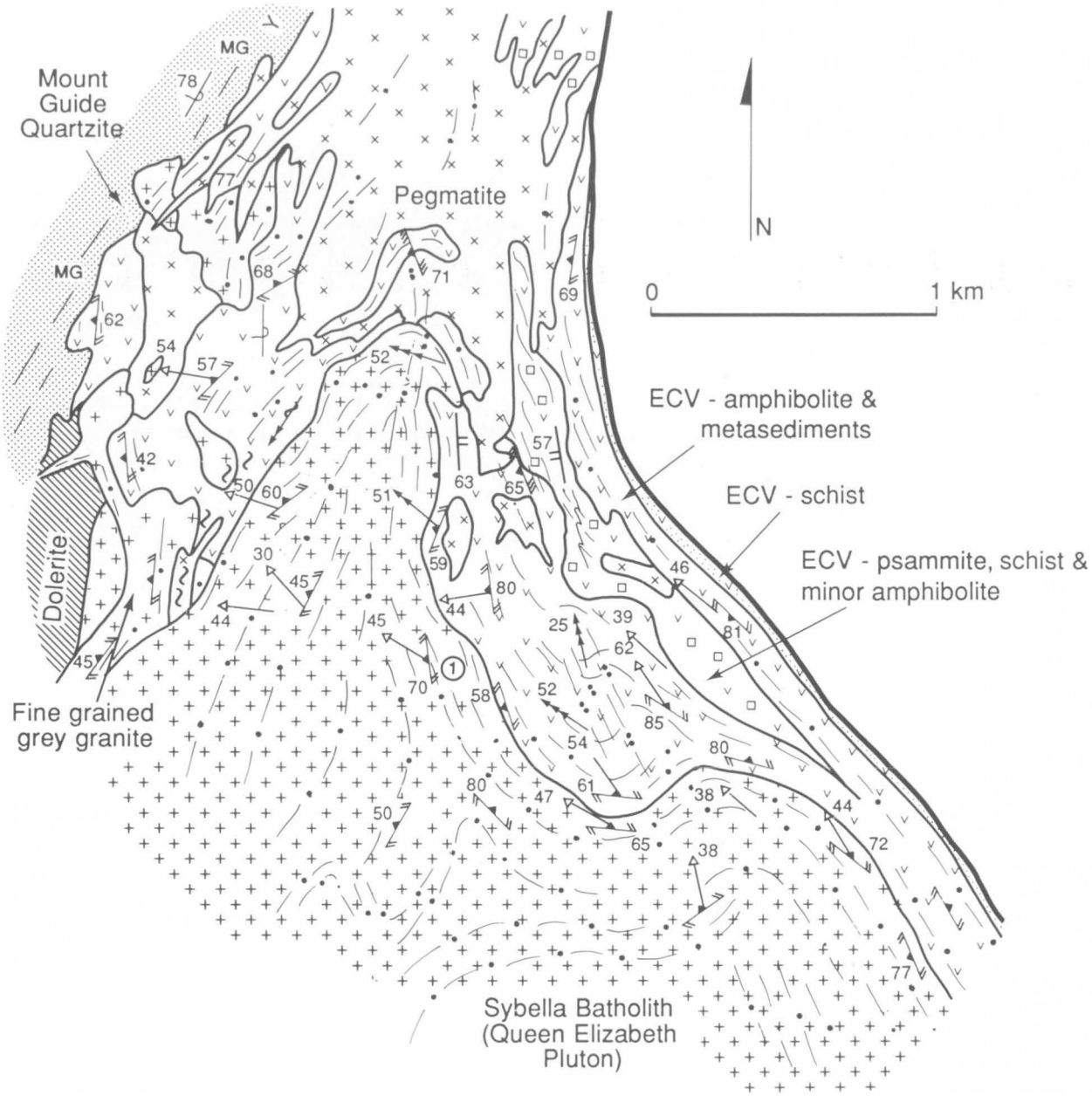


Fig. 10 (a). Geologic map of folded nose of the Sybella metagranite of Domain Four showing folding of the metagranite margin, S_2 within both the metagranite and country rocks, bedding within the country rocks, and some of the pegmatites. Refer to Figure 3a for the stratigraphic column and legend. Generalised from mapping by J.M. Proffett, 1989-1990, for Mount Isa Mines, R. Askew 1989 (Monash Earth Science Survey), M. Leake 1989 (Monash Earth Science Survey), and Wilson (1972). (b-e) Quartz + feldspar segregations within the metagranite (segregations = stippled pattern, metagranite = blank). All sketches from location 1 in Figure 10a.

an axial planar fabric. In some areas these segregations are arranged in two orientations forming a ladder-like pattern (Fig. 10c) with the weak set approximately parallel to S_2.

D^N_2 structures

The pervasive S_2 foliation and west-plunging mineral lineation ($L_2 \pm L_{3a}$) in the metagranite are defined by biotite ± hornblende. Fabric intensity varies from weak in coarse-grained zones to very strong in fine- or medium-grained zones, especially near the margin. The metagranite most commonly forms an L-S tectonite, although some zones are dominated by either L or S fabrics. S_2 is defined by fine biotite laths and flattened stretched xenoliths within the finer-grained grey metagranitoid.

F_2 folds are rarely observed, but in places S_2 is axial planar to rare structures which fold wispy biotite-rich zones (Fig. 10f).

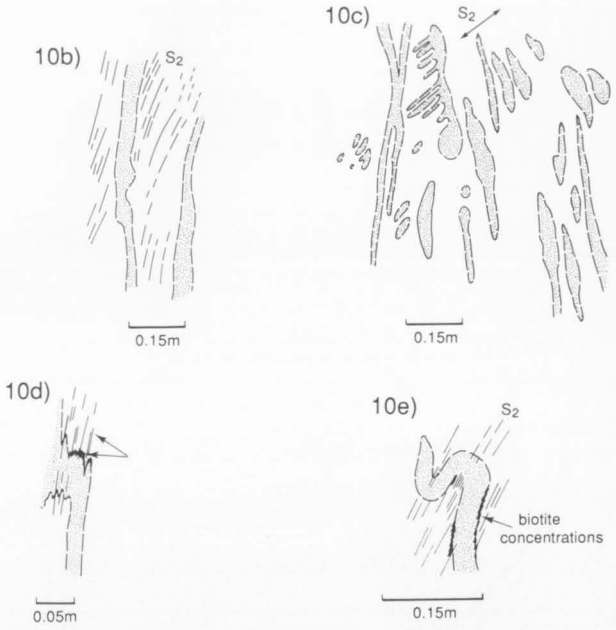


Fig. 10(b-e). (b) Vertical east-west section looking north, showing deflection of S_2 adjacent to the segregations which may lie within S_{3a} or S_{3b}. (c) Quartz + feldspar segregations on subhorizontal erosion surface; the less prominent set of segregations is roughly parallel to S_2. (d) Folding of a quartz + feldspar segregation with the S_2 fabric roughly axial planar; biotite flakes in concentrations along the margin and in wispy stringers within the metagranite appear to parallel S_2; vertical, approximately east-west surface, looking north. (e) Fold with axial planar S_2 overprinting quartz + feldspar segregation; biotite occurs in a selvedge along part of the contact, and laths are generally aligned in S_2.

D^N_3 structures

The F_{3b} closure at the northern end of the pluton (Fig. 10a) folds S_2 within the granite and country rocks, bedding, and some pegmatites (Proffett, 1990). The fold axis plunges west, down the dip of the axial planar fabric which appears to be the S_{3b} crenulation cleavage (Proffett, 1990).

On the western edge of Domain Four, a large-scale synform-antiform pair folds S_2 in the metagranite. The antiform is cored by Mount Guide Quartzite and May Downs Gneiss (see Connors & others, 1991) in Domain Five where overprinting relationships confirm that this fold is F_{3b}. The synform, which is cored by amphibolite, may correlate along trend with the west-plunging F_{3b} fold closure at the nose of the metagranite. More detailed mapping is required in the intervening zone to evaluate this hypothesis. Although the metagranite is less than 1 km thick on the middle limb of this fold pair, this is probably a result of thinning during deformation, and the original thickness is unknown.

D^N_3 fabrics have been recognised in only a few

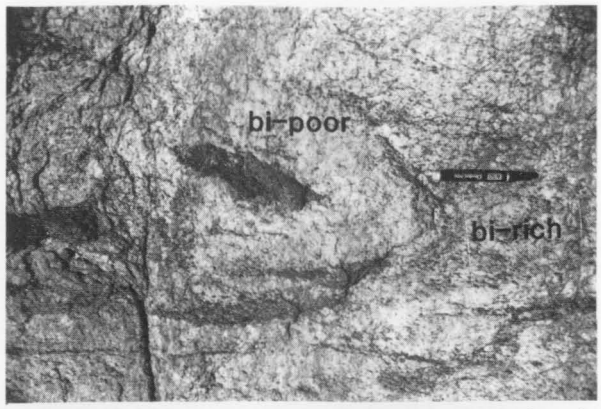


Fig. 10(f). Fold in metagranite defined by variations in the proportion of biotite (fold closes to the south); north-striking S_2 foliation is axial planar. Grid reference 379942.

restricted areas in Domain Four: (i) near the northern fold closure (Fig. 10a), (ii) south of the map-scale F_{3b} antiform of Domain Five (see Connors & others, 1991), and (iii) in the zone of F_{3b} folding near the northeastern margin (Fig. 10a). In the first area a spaced fracture cleavage overprints S_2, and in the second a strong sheared fabric is developed. However, in the third area S_2 is overprinted and deflected by the north-striking spaced (5 to 15 cm) quartz + feldspar segregations described above (Fig. 10c), which may be related to either S_{3a} or S_{3b}.

Domain Five

The 'Vortex' structure is a complex zone of large-scale folding bounded by the Sybella Batholith (see Connors & others, 1991). Rock types include the May Downs Gneiss, Mount Guide Quartzite, and minor amphibolite of the Eastern Creek Volcanics. Various small felsic and mafic intrusions occur throughout the domain. At the northern end of this domain the Mount Guide Quartzite youngs to the east and overlies the May Downs Gneiss to the west. However facing directions are generally unknown within the core of the 'vortex'.

Layering within the gneiss is defined by alternating biotite-rich layers and quartzo-feldspathic relatively biotite-poor layers which vary from 5 to 100 mm thick. Young (1990) interpreted this gneissic banding as bedding rather than the result of chemical differentiation, based on the variable thickness and mineral proportions between layers of similar composition. Furthermore, this layering parallels bedding in the overlying Mount Guide Quartzite.

Rare sillimanite is present in pelite and psammopelite of the May Downs Gneiss (Young, 1990). North of the study area, Rubenach (1992) reported assemblages of sillimanite + K-feldspar + biotite in the Mount Guide Quartzite, and sillimanite + muscovite in the May Downs

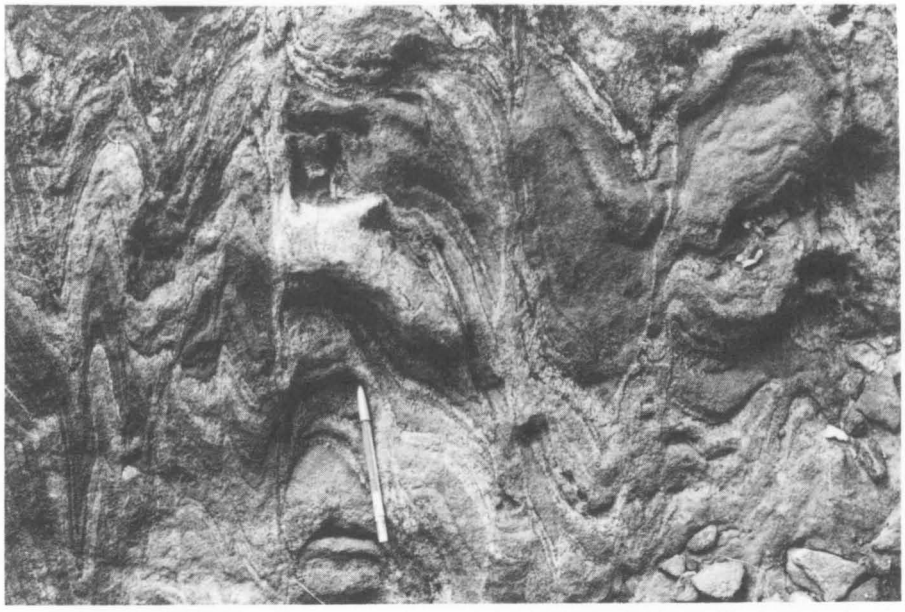


Fig. 11 (a). Thin stringers consisting of quartz + feldspar approximately parallel to the axial plane of F_2 folds in the May Downs Gneiss (looking north). Grid reference 312942.

Gneiss, which he interprets to reflect variations in water activity rather than temperature.

Quartz + feldspar segregations within the gneiss have mafic biotite-rich selvedges. Some segregations are approximately axial planar to F_2 folds (Fig. 11a); others are folded by F_2 and contain mafic segregations subparallel to S_2 (Fig. 11b). Pegmatites appear similar to these felsic segregations, but lack mafic selvedges or segregations. The pegmatites are folded by F_2 and commonly display pinch and swell structures.

D^N_2 structures

The dominant, layer-parallel cleavage within the May Downs Gneiss is interpreted as S_2. It is defined by a preferred orientation of strain-free biotite ± muscovite and by a grain-shape preferred orientation of quartz and feldspar (Young, 1990). In the hinges of associated folds the predominant orientation of unstrained biotite laths is parallel to the axial plane, but some laths occur at moderate and high angles to the axial plane, forming a weak decussate texture (Young, 1990). F_2 folds are tight to isoclinal and commonly display thickened hinges and attenuated limbs. Just west of the northern end of the metagranite, an antiformal F_2 syncline appears to be refolded around the pluton nose during D^N_3 (Proffett, 1990). In restricted areas shearing parallel to the S_2 axial plane has resulted in local transposition zones (Young, 1990).

D^N_3 structures

S_{3b} is defined by the orientation of quartz grains which

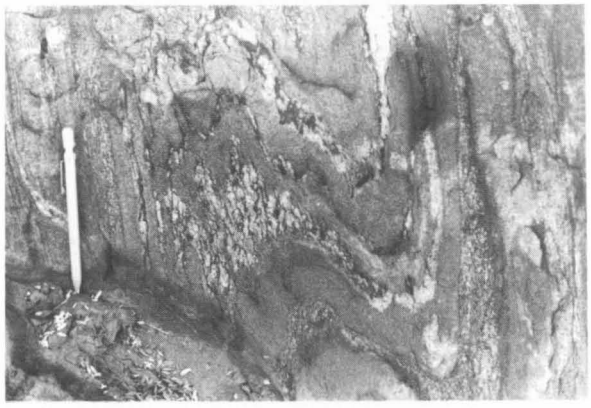


Fig. 11 (b). Irregular quartz + feldspar segregation in the hinge zone of an F_2 fold in May Downs Gneiss (looking north); biotite within the segregation is concentrated in thin zones roughly parallel to the S_2 axial plane. Grid reference 312942.

display strong undulose extinction, subgrain development, and irregular sutured boundaries in thin section, and by coarsely spaced fractures in outcrop (Young, 1990). In the gneissic rocks, S_{3b} forms a crenulation foliation overprinting the S_2 biotite schistosity. F_{3b} and F_2 are approximately coaxial resulting in Type 3 (Ramsay, 1967) interference patterns where mesoscopic folds of both generations are well developed.

The map pattern in Domain Five is dominated by a doubly-plunging F_{3b} antiform (see Connors & others, 1991). At the south-plunging end, the F_{3b} fold overprints a sequence consisting of two quartzites on either side of a gneissic unit. Three interpretations have been considered (Fig. 12): (1) the lithological repetition represents original

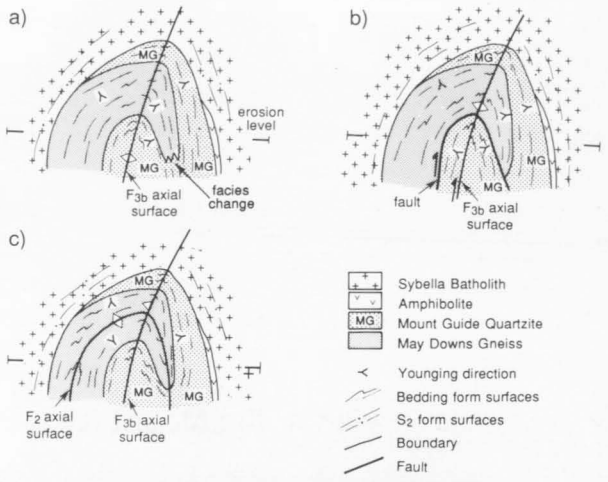


Fig. 12. Schematic cross-sections depicting structural relationships and facing directions for three hypotheses that can account for the layer of gneiss within the Mount Guide Quartzite of Domain Five (see text for discussion). Modified after Young (1990).

stratigraphy (i.e., the gneissic unit is interbedded with quartzite of the lower Mount Guide; (2) the stratigraphy has been repeated by bedding-parallel thrust faults, and (3) the gneiss occurs in the core of an F_2 or older fold (Young, 1990). Younging indicators are absent, and weak fabrics in the quartzites hamper geometrical analysis. No evidence of a change in vergence across the gneiss has yet been recognised, nor has an obvious closure been found at the poorly exposed northern termination of the gneissic unit (Young, 1990). Although it is difficult to favour one hypothesis at this time, we have used the third one for the cross-section accompanying the map (Connors & others, 1991), because mesoscopic refolding of F_2 folds by F_{3b} occurs in several locations, and S_2 is folded around the main F_{3b} antiform.

D^N_4 structures

Asymmetrical east-verging F_4 folds overprint F_{3b}/S_{3b} in the core of the map-scale F_{3b} antiform (see Connors & others, 1991). These younger folds have a coarsely spaced fracture cleavage (Young, 1990).

Strike-slip faults

Northeast and northwest strike-slip faults, with offsets up to several hundred metres, occur in all domains and cross-cut all other structures. The northeast-striking faults are typically dextral, and the northwest-striking faults are sinistral (see Connors & others, 1991). A dip-slip component is inferred from structural and stratigraphic changes across these faults. This systematic offset pattern is similar to strike-slip fault patterns elsewhere in the inlier (e.g., BMR, 1986).

Metamorphism and metasomatism

Prograde metamorphic assemblages display a westward increase in grade from lower greenschist to upper amphibolite facies. The Mount Isa and Haslingden Group units east of the Mount Isa Fault are characterised by chlorite zone assemblages (Wilson, 1972). In the biotite zone, immediately west of the Mount Isa Fault, strain-free laths of intergrown biotite and muscovite define the S_2 schistosity. In the biotite and biotite + cordierite zones, andalusite and cordierite porphyroblasts deflect S_2 and are accompanied by low-strain pressure-shadows. In rare cases, however, S_2 cleavage traces are continuous between cordierite porphyroblasts and the matrix. The sillimanite isograd, which occurs 1.5 to 3 km west of the fault, is marked by radiating clusters of fibrolitic sillimanite which overgrow the S_2 cleavage. East of the metagranite, sillimanite (typically fibrolite) and white mica commonly occur together in the absence of K-feldspar. To the west, however, Rubenach (1992) reports prismatic sillimanite + K-feldspar + biotite in the Mount Guide Quartzite, and muscovite + microcline + sillimanite in the May Downs Gneiss, north of the study area.

Several metasomatic events occurred during deformation and metamorphism (Connors, 1990b). This resulted in a wide variety of alteration assemblages such as: quartz, quartz + tourmaline, tourmaline, quartz + chlorite or white mica, feldspar + chlorite ± biotite, biotite only, sillimanite ± muscovite, actinolite ± clinopyroxene, and quartz + plagioclase. Copper mineralisation at the King prospect (see Connors & others, 1991) is related to the actinolite ± clinopyroxene stage of alteration (Connors, 1990b). Extensive pre- to syn-D^N_2 metasomatism of basalt has resulted in chlorite + quartz + rutile ± plagioclase schist at lower grades, and chlorite + orthoamphibole ± cordierite assemblages in the sillimanite zone after subsequent metamorphism (Downing, 1986; Proffett, 1989b; Davoren, 1991).

Discussion

Structural history of the Mount Novit Ranges

Previous interpretations of the structural and tectonic history of the Mount Isa area have defined three main periods of deformation which affected the mid-Proterozoic cover sequences (e.g., Bell, 1983; Winsor, 1986; Blake, 1987). D_1 involved north-south shortening and resulted in southerly-directed thrust faults and associated east-west folds. D_2 involved east-west shortening and vertical

extension resulting in north-south upright folds and axial plane cleavage. D_3 produced north-northwest-oriented folds (Bell, 1983; Winsor, 1986) or normal, reverse, and thrust faults and folds resulting from transpressional wrenching (BMR, 1986). Some of these interpretations have come into question during this study.

We found no evidence to support north-south D_1 thrusting west of the Mount Isa Fault. In fact, little information regarding the nature and significance of pre-D^N_2 deformation has been uncovered in this area. A pre-S_2 fabric is evident only in thin section, and there are no mesoscopic or macroscopic structures demonstrably associated with this fabric. The origin of S_1 is unclear. It could reflect alignment of detrital mica by compaction and/or early diagenetic effects.

D^N_2, D^N_3, and D^N_4 of this study all resulted from east-west to northeast-southwest shortening and west-over-east movement. These events may correspond, in part, to D_2 and D_3 of other workers in the Mount Isa region, but there are significant differences. In the Mount Novit Ranges, asymmetrical F_2 folds vary from west- to north-plunging with moderately west- to southwest-dipping axial planes which are reoriented by subsequent deformation. Attenuation on the overturned limbs of F_2 folds in areas where subsequent events are weak or absent indicates that this attenuation predates D^N_{3a} shear zones. D^N_2 folds in the Mount Novit area contrast significantly with the symmetrical north-trending F_2 folds with steep axial planes described elsewhere in the inlier.

In this area the D^N_3 event includes significant faulting/shearing (D^N_{3a}) as well as folding (D^N_{3b}), in contrast to the single fold/cleavage generation described by other workers (e.g., Bell, 1983; Winsor, 1986; Bell & others, 1988). S_{3a} and L_{3a} structures developed in the high-strain fault/shear zones, whereas F_{3b}/S_{3b} occur throughout the area. Mesoscopic non-cylindrical F_{3b} folds are most commonly adjacent to D^N_{3a} faults and shear zones, and meso- to megascopic upright F_{3b} folds occur in the north and west. These younger D^N_{3b} structures may reflect the waning stages of fault/shear zone movement and/or the accommodation of strain over a larger volume of rock. Reorientation of non-cylindrical F_{3b} fold axes in high-strain zones may reflect stretching within the axial plane during progressive deformation (e.g., Sanderson, 1973). Stretching and fracturing of fibrolite clusters adjacent to the Adelheid Fault demonstrate that L_{3a} is a stretching lineation (Connors, 1990b). The lineation is thus interpreted to define the extension direction during fault movement.

Continued east-west shortening and west-over-east movement resulted in post-F_{3b} movement on the Mica Creek Shear Zone, Big Beryl Fault, and the Mount Isa Fault. Further post-D^N_3 shortening resulted in mesoscopic to macroscopic, north-trending F_4 folds and tightening and steepening of earlier structures. Mesoscopic F_5 folds formed only in local zones, and could be related to strike-slip faulting.

Age of deformation in the Mount Isa region

Ages for the D_1-D_2-D_3 regional deformation scheme have been respectively interpreted as 1610 ± 13, 1544 ± 12, and 1510 ± 13 Ma based on Rb/Sr whole rock analyses and supposed identification of S_1, S_2, and S_3 within different zones of the Sybella Batholith, west of Mount Isa (Page & Bell, 1986). They interpreted the pervasive fabric within the Queen Elizabeth Pluton of Domain Four as S_1, and described it as west-northwest-striking throughout the pluton (Figure 1 of Page & Bell, 1986). Form-surface mapping throughout the pluton, however, has demonstrated that the pervasive foliation strikes north-south overall, but locally strikes northwest (or northeast) mimicking the orientation of the metagranite margin (see Connors & others, 1991). This orientation is inconsistent with S_1 of Bell (1983) or Page & Bell (1986). In addition, geometrical analyses indicate that the pervasive metagranite fabric is S_2, not S_1 (see section above on Domain Four). Thus the 1610 ± 13 Ma date obtained from the Queen Elizabeth Pluton site probably indicates the age of D^N_2 not D^N_1. Furthermore, any imprint of D^N_1 deformation and greenschist facies metamorphism on the Rb-Sr isotopic system is likely to have been obliterated by upper amphibolite facies conditions (600-650°C see below) syn- to post-D^N_2.

The significance of major faults in the area

Various interpretations have been proposed for the Mount Isa Fault, many involving significant strike-slip movement (e.g., Carter & others, 1961). The Mount Isa Fault was interpreted as the western boundary of the Leichhardt River Fault Trough by Glikson & others (1976), but Derrick (1982) suggested that the trough extends farther west, based on stratigraphic correlations across the fault. More recently the fault has been interpreted as a strike-slip major block boundary which

extends through the crust to the mantle (BMR, 1988; Blake, 1990), but no evidence of strike-slip motion has been found within the fault zone. All the ductile features (i.e., mylonites with down-dip lineations, asymmetrical folds, shear bands, and S-C fabrics) demonstrate dip-slip, west-over-east movement.

Hydrothermal breccias adjacent to the Mount Isa Fault could result from late strike-slip movement, but these appear insufficient to account for the tens of kilometres of horizontal displacement postulated by these workers. These breccias generally are not continuous for more than 20-30 m, the same rock types occur on both sides, and adjacent fragments commonly appear to fit back together suggesting that deformation was largely dilational and significant displacement was not accommodated by these breccia zones.

Early displacement along the Mica Creek Shear Zone formed shear-foliated biotite schist which is overprinted by S_{3b}. This movement is similar in age to that along the Adelheid Fault (see below), but much of the displacement occurred post-S_{3b} and resulted in the younger shear-foliated chlorite schist (Proffett, 1990).

The Tailings Dam Fault is offset by, and therefore predates, an east-striking syndepositional fault (Fig. 6a). The Tailings Dam Fault is therefore unrelated to D^N_1 thrusting as previously interpreted (e.g., Bell, 1989). At the time of the unconformity, this fault originally juxtaposed younger units over older units and may be related to early extension.

Brown's Fault occurs approximately along strike with conglomerate lenses that define the unconformity at the base of the Surprise Creek Formation and/or basal Mount Isa Group (see Connors & others, 1991). The changes in rock type and angular discordance across this structure are similar to those across the unconformity, which is thus interpreted to be truncated by this fault 2 to 3 km north of Brown's Waterhole Creek (see Connors & others, 1991). Furthermore, pebbles within the southernmost conglomerate lenses are flattened and stretched parallel to the strong fabric ($S_{3a} \pm S_2$) and L_{3a} mineral lineation, reflecting proximity to this high-strain zone.

The Adelheid Fault has been mapped in detail from the south of the map area to about 1 km north of Brown's Waterhole Creek (see Connors & others, 1991). It can be traced north to Mica Creek, where it either correlates with, at least in part, or is truncated by the Mica Creek Shear Zone. The youngest displacement on the Mica Creek Shear Zone post dates S_{3b} (Proffett, 1990) and is therefore younger than the Adelheid Fault, but earlier movement on the shear zone, represented by shear-foliated biotite schist that is overprinted by S_{3b}, has age relationships similar to the Adelheid Fault. The Big Beryl Fault is similar in age and orientation to the youngest movement on the Mica Creek Shear Zone.

The 7600E Fault separates rocks similar to those affected by the Adelheid Fault, and is characterised by similar alteration. The 7600E Fault, however, may be older if it correlates with the fault that cuts the F_4 (or F_{3b}) synform southwest of the King prospect, as tentatively postulated on the map (Connors & others, 1991).

The Gun Shot Fault may merge with or truncate the Adelheid Fault in the area where these two structures cross the Diamantina Development Road (see Connors & others, 1991). In this zone it is not possible to separate the two faults, and so it is unclear whether the Adelheid Fault exists north of this point.

Metamorphism

Metamorphism began pre- or early syn-D^N_2, and occurred throughout this period of east-west to northeast-southwest shortening. In Domains Two and Three, andalusite and cordierite porphyroblasts grew pre- or syn- D^N_2. Rare instances where inclusion trails are continuous with S_2 in the matrix suggest that porphyroblast growth occurred, or at least continued, until syn-S_2. The broad laths of strain-free biotite which define S_2 grew (or recrystallised) after D^N_2 deformation had ceased. Fibrolitic sillimanite clusters grew after S_2 and before L_{3a}. These metamorphic assemblages indicate low pressure / high temperature metamorphism.

In Domain Four, deflection of S_2 adjacent to the quartz + feldspar segregations suggests that the segregations are associated with S_{3a}, or possibly S_{3b}, both of which formed during faulting and shearing. These segregations may therefore be related to localised shearing in the metagranite. In contrast to this evidence, the biotite-rich selvedges typically display alignment of biotite flakes parallel or subparallel to S_2, and S_2 appears axial planar to rare folded segregations (Figs. 10 d-e). Either these folded segregations resulted from an earlier unrelated event (e.g., pegmatite intrusion), or they indicate that partial melting began early syn-S_2 (or pre-S_2) and continued to post-S_2. In Domain Five, some quartz + feldspar segregations with mafic selvedges occur parallel to the axial plane of F_2 folds and others are folded by F_2. This therefore suggests segregation during D^N_2 deformation. This difference in timing for partial melting in Domains Four (syn- to post-D^N_2) and Five (syn-D^N_2) suggests that Domain Five

may have been at a deeper structural level and thus reached conditions for partial melting slightly earlier during deformation.

Experimental melting of a biotite-bearing granite, similar to the Sybella, in the presence of excess water and at a pressure greater than 200 Ma (Wyllie, 1983) indicates a minimum temperature of 625° to 650°C for partial melting in Domain Four during peak metamorphism . However, experimental studies on the system Qz-Ab-Or at 1 MPa by Manning & Pichavant (1983), demonstrate a significant drop in melting temperature in the presence of a boron- and/or fluorine-bearing aqueous phase. Both boron and fluorine are present in various mineral phases of the metagranite, pegmatites, and adjacent metasediments. Thus the melting temperature may have been even lower than Wyllie's (1983) experimental estimate of 625° to 650°C. This temperature is similar to the estimate of 600°C for sillimanite-bearing assemblages (Richardson & others, 1969; Holdaway, 1971) and suggests that partial melting may have occurred at sillimanite facies conditions.

Conclusions

This study has defined a complex succession of fold generations, ductile faults, and shear zones that formed during east-west to northeast-southwest shortening and west-over-east displacement. D^N_2 and D^N_3 structures formed in association with the low P / high T metamorphic event which began pre- or early syn-S_2 and reached peak conditions post-S_2 but pre-L_{3a}. West-over-east directed movement occurred on D^N_3 faults and shear zones as metamorphic conditions began to wane. Fluids were introduced predominantly along the faults and shear zones, resulting in retrogression. D^N_4 structures formed at lower metamorphic grades during this same event as faulting continued. D^N_5 structures could be related to strike-slip faulting (i.e., D_3 of BMR, 1986).

This structural history defined for the Mount Novit Ranges shows few similarities to other areas. We found no evidence that supports north-south D_1 thrusting west of the Mount Isa Fault, and demonstrated that one of Bell's (1989) D_1 thrust faults is in part an older pre-D^N_1 fault (Tailings Dam Fault) and in part a younger D^N_{3a} fault (Adelheid Fault). Furthermore we found that east-west to northeast-southwest shortening in the Mount Novit area resulted in three (or four) fold generations and a series of major faults and shear zones (D^N_2, D^N_{3a}, D^N_{3b}, and D^N_4 ± D^N_5) in contrast to the two fold/cleavage generations (D_2 and D_3) associated with approximately east-west shortening in the simplified D_1-D_2-D_3 scheme.

This study highlights the complexities and variations in the structural history of the inlier resulting from heterogeneous deformation, and demonstrates the dangers inherent in attempting broad structural correlations in the absence of very detailed geometrical analyses. Although it is sometimes desirable to simplify and correlate deformation schemes across the inlier in order to make comparisons, these correlations are tenuous at best and can lead to significant errors in interpretation if such correlations are relied upon in the absence of detailed mapping (e.g., Williams, 1985). We have found it very difficult to even correlate fold/cleavage generations across the Mount Isa Fault due to differences in lithology and metamorphic grade, and possible variations in the local structural histories.

Geologists have long recognised and accepted the numerous problems involved in correlating stratigraphic units across the inlier (e.g., Blake, 1987) owing to the complicated history of sedimentation, intrusion, metamorphism, and metasomatism. Accurate age determinations are required to unravel the relative age relationships and absolute ages of units. Similarly, geochronological constraints and careful geometrical analyses are required before reliable structural correlations can be made across the inlier. Detailed structural histories have been determined for several areas (see other papers in this volume), but more geochronological data are required.

In Table 2, the regional metamorphic event has been used as a datum for correlating structural events. It is foolish to assume, however, that peak metamorphic conditions were attained at the same time over a volume of rock as large as the Mount Isa Inlier. Thus the timing of peak metamorphism is likely to vary. Even if metamorphism is not significantly diachronous, any, or all, of the deformation events may have occurred at different times in different areas (e.g., Williams, 1985). Thus, timing of deformation events from one area to the next may have varied with respect to both time and metamorphism. A further problem in using regional metamorphism as a datum to correlate structures is that two metamorphic events, both amphibolite facies grade, have been recognised in some areas (e.g., Hill & others, this volume).

We have made tentative correlations (Table 2) between the deformation history preserved in the Mount Novit Ranges and that presented by other workers for the benefit

Table 2. Tentative correlation of deformation episodes in Mount Novit and neighbouring areas.

Mount Novit Ranges	Page & Bell, 1986	BMR, 1986	Bell & others, 1988	Nijman & others, this volume a	Stewart, this volume a
Minor strike-slip faulting				D^{P}_{5}	
F_5/L_5 minor folds					
Continued faulting					
F_4/S_4 north-south folds		D_3			
Continued faulting				D^{P}_{4}	
F_{3b}/S_{3b} megascopic north-south folds	D_2 & D_3		D_2 & D_3	D^{P}_{3}	D^{H}_{2}
S_{3a}/L_{3a} faulting/ shearing (strike-slip and reverse)		D_2			
Peak metamorphism				D^{P}_{2}?	
F_2/S_2 north-south folds					D^{H}_{1}?
D^{N}_{1}?	D_1	D_1	D_1		D^{H}_{1}

of those who wish to use it. We stress that these correlations are tenuous, and ongoing research continues to reveal surprising complexities in the structural/tectonic history of the Mount Isa Inlier.

Acknowledgements

Mapping was conducted as part of the 1988 and 1989 Monash Earth Science Survey field camps with the support of the Australian Bureau of Mineral Resources and Mount Isa Mines. We thank all students involved for their valuable contribution. June Hill provided considerable input during the 1988 field camp; Mike Rickard, stimulating discussions in the field; and Bill Perkins, constant encouragement and many discussions. Diane Perkins helped in more ways than we could possibly list. Draga Gelt drafted the figures. KAC was funded by a 1967 Natural Science and Engineering Research Council of Canada Postgraduate Scholarship and in part by Mount Isa Mines. We thank Mount Isa Mines for permission to publish consulting work by JMP.

References

BELL, T.H., 1983 - Thrusting and duplex formation at Mount Isa, Queensland, Australia. *Nature* 304, 493-497.

BELL, T.H., 1989 - Geological Review. Mount Isa Mines Ltd. Report , 23 pp. (unpublished).

BELL, T.H., PERKINS, W.G., & SWAGER, C.P., 1988 - Structural controls on development and localization of syntectonic copper mineralization at Mount Isa, Queensland. *Economic Geology* 83, 69-85.

BLAKE, D. H., 1987 - Geology of the Mount Isa Inlier and environs, Queensland and Northern Territory. *Bureau of Mineral Resources, Australia, Bulletin* 225, 83 pp.

BLAKE, D. H., 1990 - A terrane analysis of the Mount Isa Inlier. *Mount Isa Inlier Geology Conference, Victorian Institute of Earth and Planetary Sciences, Monash University,* 8.

BMR, 1978 - Mount Isa 1:100 000 Geological Series, Sheet 6756. *Bureau of Mineral Resources, Australia.*

BMR, 1986 - Transpressional strike-slip faulting in the

Mount Isa Inlier. *Bureau of Mineral Resources Research Newsletter* 4, 1-2.

BMR, 1988 - Block and possible terrane boundaries in the Mount Isa Inlier. *Bureau of Mineral Resources Research Newsletter* 9, 2-3.

CARTER, E.K., BROOKS, J.M., & WALKER, K.R., 1961 - The Precambrian mineral belt of northwestern Queensland. *Bureau of Mineral Resources, Australia, Bulletin* 51, 344 pp.

CONNORS, K.A., 1989 - Implications of an early fold/thrust event in the western Mount Isa Inlier. *Geological Society of Australia, Abstracts* 24, 25-26.

CONNORS, K.A., 1990a - D_2 fault and shear zone development in the Mount Isa area. *Geological Society of Australia, Abstracts* 25, 175-176.

CONNORS, K.A., 1990b - Metasomatism and structurally controlled fluid pathways. *Mount Isa Inlier Geology Conference, Victorian Institute of Earth and Planetary Sciences, Monash University,* 53-55.

CONNORS, K.A., PROFFETT, J.M., LISTER, G.S., SCOTT, R.J., OLIVER, N.H.S., & YOUNG, D.J., 1991 - Geology of the Mount Novit Area (1:25 000 scale map), *Bureau of Mineral Resources, Canberra, Australia.*(two sheets), Available as colour electrostatic plots on paper (AUD30), or in digital form on optical disc or Exabyte 8 mm tape (prices on application) both of which can be displayed on Intergraph Microstation software on computers that will run Unix. The digital data comprise a scanned raster image (.RLE format) of the black and white geological map, and an Intergraph vector design file containing the boundaries of coloured polygons. The coloured map and data are available from the Publication Sales Centre, Bureau of Mineral Resources, and an uncoloured Ozalar film or paper copy (AUD20) of the map is available from BMR Copy Service, both at GPO Box 378, Canberra, ACT, 2601, Australia. All orders to be prepaid to Collector of Public Monies.

DAVOREN, P.J., 1991 - Structural, metamorphic, and metasomatic study west of the Mount Isa Fault, Mount Isa, northwest Queensland. B.Sc. (Hons.) thesis, Monash University (unpublished)

DERRICK, G.M., 1982 - A Proterozoic rift zone at Mount Isa, Queensland, and implications for mineralisation. *BMR Journal of Australian Geology & Geophysics* 7, 81-92.

DOWNING, J.G., 1986 - Structural and metamorphic geology of the Mica Creek area, Mount Isa, northwest Queensland. B.Sc. (Hons.) thesis, James Cook University, 134 pp. (unpublished)

GLIKSON, A.Y., DERRICK, G.M., WILSON, I.H., & HILL, R.M., 1976 - Tectonic evolution and crustal setting of the middle Proterozoic Leichhardt River fault trough, Mount Isa region, northwestern Queensland. *BMR Journal of Australian Geology & Geophysics 1, 115-129.*

HILL, E.J., LOOSVELD, R.J.H., & OLIVER, N.H.S., this volume - Structure and geochronology of the Tommy Creek Block, Mount Isa Inlier. *In* STEWART, A.J., & BLAKE, D.H. (Editors), Detailed Studies of the Mount Isa Inlier. *Bureau of Mineral Resources, Australia, Bulletin* 243.

GRAY, D.R., 1977 - Morphological classification of crenulation cleavages. *Journal of Geology* 85, 229-235.

HILL, R.M., WILSON, I.H., & DERRICK, G.M., 1975 - Geology of the Mount Isa 1:100 000 sheet area, northwest Queensland. *Bureau of Mineral Resources Australia, Record* 1975/175, 112 pp.

HOLDAWAY, M.J., 1971 - Stability of andalusite and the aluminum silicate phase diagram. *American Journal of Science* 271, 97-131.

MANNING, D.A.C. & PICHAVANT, M., 1983 - The role of fluorine and boron in the generation of granitic melts. In ATHERTON, M.P., & GRIBBLE, C.D. (Editors), Migmatites, melting and metamorphism. *Proceedings of the Geochemical Group of the Mineralogical Society, Shiva Publishing Ltd., Cheshire,* 94-109.

MCGOWAN, G.E., 1991 - The geology of Mica Creek, northwest Queensland. B.Sc. (Hons.) thesis, University of Queensland, 167 pp. (unpublished)

NIJMAN, W., LOCHEM, J.H. van, SPLIETHOFF, H., & FEIJTH, J., this volume. Deformation model and sedimentation patterns of the Proterozoic of the Paroo Range, Mount Isa Inlier, Queensland, Australia. *In* STEWART, A.J., & BLAKE, D.H. (Editors), Detailed Studies of the Mount Isa Inlier. *Bureau of Mineral Resources, Australia, Bulletin* 243.

PAGE, R. W., 1978 - Response of U-Pb zircon and Rb-Sr total-rock and mineral systems to low grade regional metamorphism in Proterozoic igneous rocks, Australia. *Journal of the Geological Society of Australia* 25, 141-164.

PAGE, R.W., 1981 - Depositional ages of the stratiform base metal deposits at Mount Isa and Mcarthur River, Australia, based on U/Pb zircon dating of concordant tuff horizons. *Economic Geology* 76, 648-658.

PAGE, R.W. & BELL, T.H., 1986 - Isotopic and structural responses of granite to successive deformation and metamorphism. *Journal of Geology* 94, 365-379.

PERKINS, W.G. & POOLE, J.R., 1980 - The structure and stratigraphic relationship of the Mount Isa Group across the Mount Isa Fault. Mount Isa Mines Ltd. Report, 13 pp. (unpublished).

PROFFETT, J.M., 1989a - Progress report, geological mapping in the Mount Isa district, Queensland. Mount Isa Mines Ltd. Report, 110 pp. (unpublished).

PROFFETT, J.M., 1989b - Second progress report,

geological mapping in the Mount Isa district, Queensland. Mount Isa Mines Ltd. Report, 30 pp. (unpublished).

PROFFETT, J.M., 1990 - Some new observations on the geologic structure southwest of Mount Isa. *Mount Isa Inlier Geology Conference, Victorian Institute of Earth and Planetary Sciences, Monash University,* 29-31.

RAMSAY, J.G., 1967 - Folding and Fracturing of Rocks. *McGraw Hill Book Company, New York,* 568 pp.

RICHARDSON, S.W., GILBERT, M.C., & BELL, P.M., 1969 - Experimental determination of kyanite-andalusite and andalusite-sillimanite equilibria: the aluminum silicate triple point. *American Journal of Science* 267, 259-272.

RUBENACH, M.J., 1992 - Proterozoic low-pressure/high-temperature metamorphism and anticlockwise P-T-t path for the Hazeldene area, Mount Isa Inlier, Queensland, Australia. *Journal of Metamorphic Geology 10, 333-346.*

SANDERSON, D.J., 1973 - The development of fold axes oblique to the regional trend. *Tectonophysics* 16, 55-70.

STEWART, A.J., this volume - Geology of the Horse's Head structure, north of Mount Isa, and its bearing on the 'roof thrust + imbricate stack' hypothesis, Mount Isa Inlier, Queensland. *In:* STEWART, A.J., & BLAKE, D.H. (Editors), Detailed Studies of the Mount Isa Inlier. *Bureau of Mineral Resources, Australia, Bulletin* 243.

WILLIAMS, P.F., 1985 - Multiply deformed terrains - problems of correlation. *Journal of Structural Geology* 7, 269- 280.

WILSON, C.J.L., 1972 - The stratigraphic and metamorphic sequence west of Mount Isa, and associated igneous intrusions. *Australasian Institute of Mining and Metallurgy, Proceedings* 243, 27-42.

WILSON, C.J.L., 1973 - Faulting west of Mount Isa Mine. *Australasian Institute of Mining and Metallurgy, Proceedings* 245, 3-15.

WINSOR, C.N., 1986 - Intermittent folding and faulting in the Lake Moondarra area, Mount Isa, Queensland. *Australian Journal of Earth Sciences* 33, 27-42.

WYBORN, L.A.I., PAGE, R.W., & McCULLOCH, M.T, 1988 - Petrology, geochronology, and isotope geochemistry of the post-1820 Ma granites of the Mount Isa Inlier: mechanisms for the generation of Proterozoic anorogenic granites. *Precambrian Research* 40/41, 509-541.

WYLLIE, P.J., 1983 - Experimental studies on biotite- and muscovite-granites and some crustal magmatic sources. *In:* ATHERTON, M.P. & GRIBBLE, C.D. (Editors), Migmatites, melting and metamorphism. *Proceedings of the Geochemical Group of the Mineralogical Society, Shiva Publishing Ltd., Cheshire,* 12-26.

YOUNG, D.J., 1990 - Aspects of structure and metamorphism of the vortex, Mount Isa. M.Sc. preliminary thesis, Monash University, 67 pp. (unpublished).

Stratigraphy, folding and faulting within the Quilalar Fault System, Mount Isa Inlier

D.H.Blake [1]

This paper is based on the following maps:

Blake, D.H., 1991a - Geology of the West Leichhardt Klippe and the Gorge Creek Sector of the Quilalar Fault Zone (1:50 000 scale map). Bureau of Mineral Resources, Canberra.

Blake, D.H., 1991b - Geology of the Rifle Creek region (1:50 000 scale map). Bureau of Mineral Resources, Canberra (two sheets).

The Quilalar Fault System, a north-trending band of major strike-slip faults, includes the Quilalar Fault Zone which forms the boundary between the Leichhardt River Fault Trough (LRFT) to the west and the Kalkadoon-Leichhardt Belt to the east. This fault zone postdates the main folding events, D_1 (north-south shortening) and D_2 (east-west shortening), of the 1620-1520 Ma Isan Orogeny; dextral strike-slip movement along it probably exceeded 50 km.

Anastomosing faults in the Gorge Creek sector of the Quilalar Fault Zone mainly enclose Myally Subgroup, Quilalar and Surprise Creek Formations, and Mount Isa Group. To the east, in the West Leichhardt Klippe, Eastern Creek Volcanics and Myally Subgroup of the Haslingden Group, and overlying Quilalar Formation form a D_1 imbricate thrust stack above a decollement possibly in metabasalt of the Eastern Creek Volcanics, which was folded into a major syncline during D_2. The folded klippe is cut by a mafic dyke that shows the effects of Isan metamorphism.

A sector of the Quilalar Fault Zone farther south forms the western part of the fault-bounded Rifle Creek Block, which consists of basement, cover sequence 1 (Leichhardt Volcanics and newly named Orient beds), Kalkadoon Granite, mafic dykes, and unconformably overlying cover sequence 2 (Eastern Creek Volcanics, Myally Subgroup, Quilalar Formation) and cover sequence 3 (Bigie and Surprise Creek Formations, Mount Isa Group). These rocks were affected by D_1 thrusting along a decollement zone well below cover sequence 2, and were later folded to form a major D_2 north-plunging anticline before the Rifle Creek Block and a subsidiary block on its northeastern side, the Orient Block, were transported tens of kilometres southward, relative to the LRFT, along the Quilalar Fault Zone. The Rifle Creek and Orient Blocks are separated by major strike-slip faults, probably dextral, on their eastern sides from the rest of the Kalkadoon-Leichhardt Belt.

[1]Bureau of Mineral Resources, GPO Box 378,Canberra, ACT, 2601, Australia.

Introduction

The Quilalar Fault System is a north-trending band of faults several kilometres wide and more than 200 km long in the central part of the Mount Isa Inlier. It includes the Quilalar Fault Zone (Fig. 1), which forms the boundary between the Leichhardt River Fault Trough (LRFT) of the Western Fold Belt and the Kalkadoon-Leichhardt Belt to the east (Blake & Stewart, 1988). The Quilalar Fault Zone ranges from a single band of negligible width to a zone up to 2.5 km wide, as in the Gorge Creek sector (see below), and coincides with a major magnetic and gravity feature (Wellman, this volume). Movements along this fault zone and other major north-striking faults in the system appear to be largely dextral strike-slip, with displacements of many kilometres – probably more than 50 km along the Quilalar Fault Zone – but some vertical displacements are also likely. However, no convincing structural evidence indicating movement directions has been found by the author on any of the faults. Most movements on the major faults postdate the main folding event of the 1620-1520 Ma Isan Orogeny (Blake & others, 1990), and have juxtaposed blocks that were originally many kilometres apart, as the faults mark abrupt changes in stratigraphy, depositional environment, and structural style.

Detailed mapping of the Quilalar Fault Zone and the area immediately to the east in the Mary Kathleen 1:100 000 Sheet area (abbreviated to MK in grid references) and adjoining parts of the Prospector (PR) and Duchess (DU) 1:100 000 Sheet areas (Fig. 1) was carried out in 1986-1988. The aims were to determine the stratigraphy and regional significance of the cover

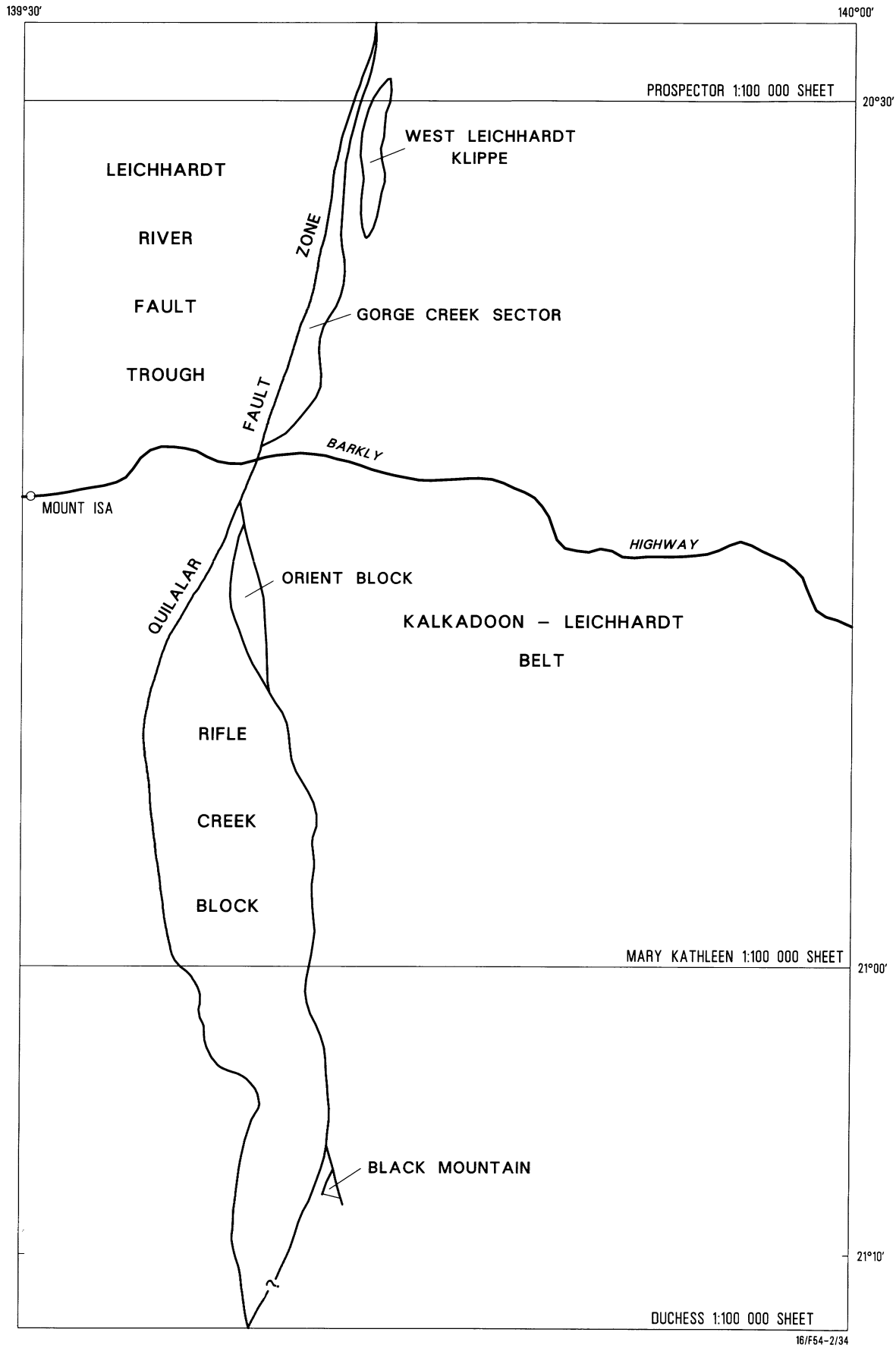


Fig. 1. Locality map

sequences exposed in this western part of the Kalkadoon-Leichhardt Belt, to unravel the complex structural history in the area, and to determine as far as possible the types and amounts of movements along the Quilalar Fault Zone and associated major faults of the Quilalar Fault System.

The stratigraphy in this part of the Kalkadoon-Leichhardt Belt (Fig. 1) – in the Gorge Creek sector of the Quilalar Fault Zone, in the West Leichhardt Klippe, in the Rifle Creek and Orient Blocks, and also in the Black Mountain outlier – was not well established before 1986. Most of the sedimentary rocks were previously mapped as Surprise Creek beds (Derrick & others, 1977), Surprise Creek Formation (Bultitude & others, 1982), or Quilalar Formation (GSQ, 1983; Blake, 1987), although some other units (Eastern Creek Volcanics and Myally Subgroup of the Haslingden Group, Bigie Formation, and Warrina Park Quartzite and Moondarra Siltstone of the Mount Isa Group) were also known to be present. Similarly, the structure was known to involve complex folding and faulting, but how these fitted into the regional picture was not clear.

In the area described, faults of the Quilalar Fault System displace stratigraphic units assigned to the basement and cover sequences 1, 2, and 3 of Blake (1987), and also granites of the Kalkadoon Batholith and mafic dykes. The stratigraphy is summarised in Table 1. In most cases the thicknesses given are estimates, because of the unknown effects of mapped and unmapped faults subparallel to bedding. The basement was deformed and metamorphosed during the Barramundi Orogeny, 1900-1875 Ma ago. The granites, all mapped as Kalkadoon Granite, were emplaced around 1860 Ma ago (Wyborn & Page, 1983). Most of the mafic dykes, except those in the westernmost part of the area, post-date Kalkadoon Granite and cover sequence 1 (1870-1860 Ma), but predate cover sequences 2 (1790-1760 Ma) and 3 (1680-1670 Ma).

Away from areas of strong shearing, the Proterozoic rocks generally show well-preserved primary textures and relatively little recrystallisation. Where there is no diagnostic mineralogical evidence available, these features, as in other parts of the Mount Isa Inlier (Blake, 1987), are taken to indicate regional metamorphism to greenschist, rather than amphibolite, facies. Upper greenschist to perhaps lower amphibolite facies, however, are suggested by metamorphic green amphibole and sodic plagioclase in metabasalt and metadolerite throughout the area. None of the major faults correspond to any marked change in regional metamorphism; the grade of metamorphism within the Quilalar Fault Zone, for example, appears to be similar to that in the adjacent LRFT and Kalkadoon-Leichhardt Belt.

Gorge Creek sector of the Quilalar Fault Zone

The Gorge Creek sector of the Quilalar Fault Zone consists of intensely faulted ridge-forming Proterozoic sedimentary rocks extending south for 27 km from latitude 20° 27'S, in the Prospector 1:100 000 Sheet area, to 1 km north of the Barkly Highway in the Mary Kathleen 1:100 000 Sheet area (Fig. 2; Blake, 1991a). It is up to 2.5 km wide, and separates northerly to westerly-dipping cover sequence 2 rocks (Bottletree Formation and Haslingden Group) in the LRFT to the west from older rocks (Kurbayia Migmatite and Kalkadoon Granite) of the Kalkadoon-Leichhardt Belt to the east.

The Gorge Creek sector contains fault-bounded outcrops of basement (Kurbayia Migmatite), Kalkadoon Granite, cover sequence 2 (Haslingden Group – Eastern Creek Volcanics and undivided Myally Subgroup – and Quilalar Formation), and cover sequence 3 (Surprise Creek Formation and Mount Isa Group – Warrina Park Quartzite and Moondarra Siltstone). Bedding within the sector is commonly steep to subvertical, and in places overturned, as shown by locally preserved facing criteria, mainly cross-bedding. Bedding trends are generally close to north-south, subparallel to most of the faults, except in the hinge areas of two large northerly-plunging folds, a syncline and an anticline, in the southern half of the sector. A pervasive north-striking subvertical cleavage is subparallel to the axial planes of these folds.

Rock units

Quartz-veined and brecciated migmatitic gneiss assigned to the basement *Kurbayia Migmatite,* veined by *Kalkadoon Granite,* is exposed at the southern end of the Gorge Creek sector in a band up to 200 m wide. Kalkadoon Granite also crops out within the Gorge Creek sector to the north (at grid reference MK642305), where altered porphyritic granite is surrounded by quartzite; both the granite and quartzite here are brecciated, sheared, and quartz-veined.

Metabasalt assigned to the *Eastern Creek Volcanics* of the *Haslingden Group* crops out in two small fault blocks within the Gorge Creek sector, one in the north (at grid reference PR647343) and the other in the south (at grid reference MK618175). Undivided *Myally Subgroup,* the upper part of the Haslingden Group, forms some of the highest ridges in the sector. It is represented mainly by

TABLE 1. SUMMARY OF PROTEROZOIC STRATIGRAPHY, QUILALAR FAULT SYSTEM IN THE MARY KATHLEEN AND DUCHESS 1;100 000 SHEET AREAS, MOUNT ISA INLIER

Unit	Distribution (max. thickness in m)	Lithology	Relationships	Remarks
COVER SEQUENCE 3	Crops out only to E of LRFT in area described			Ranges in age from about 1700 to 1670 Ma (e.g., Blake, 1987)
MOUNT ISA GROUP				1670±20 Ma (Page, 1981)[17]
Moondarra Siltstone	Gorge Creek sector (400), Rifle Creek Block (300)	Thin-bedded to laminated siltstone, commonly phyllitic; minor thin beds of fine-grained quartz sandstone	Inferred to overlie Warrina Park Quartzite conformably	
Warrina Park Quartzite	Gorge Creek sector (150), Rifle Creek Block (150)	Medium to thinly bedded and platy quartz sandstone (quartzite) and quartzite-pebble conglomerate; minor lithic or feldspathic sandstone and phyllitic siltstone	Inferred to overlie Surprise Creek Fm conformably	Forms prominent ridges
Surprise Creek Formation	Gorge Creek sector (150), Rifle Creek Block (300)	Thinly-bedded quartz sandstone and siltstone; subordinate thicker-bedded quartz sandstone, phyllitic siltstone; non calcareous	Generally fault-bounded; inferred to overlie Bigie Fm conformably or disconformably	
Bigie Formation	Rifle Creek Block (300)	Medium to thin-bedded lithic and/or feldspathic sandstone, commonly with Fe-stained joint surfaces; also micaceous sandstone, greywacke, conglomerate, siltstone, mudstone	Concordant, presumably disconformable, on Quilalar Fm	
COVER SEQUENCE 2				Ranges in age from about 1790 to 1760 Ma (e.g., Blake, 1987)
Quilalar Formation	Crops out only to E of LRFT in area described: Gorge Creek sector (1000), West Leichhardt Klippe (1500), Rifle Creek and Orient Blocks (1000), Black Mountain (400)	Lower part: mainly sandstone - silicified to friable, highly lithic or feldspathic to quartzose, some calcareous beds with porous/gossanous iron-stained weathered surfaces; minor siltstone. Upper part: variably calcareous greywacke and siltstone, marble, subordinate quartzose sandstone	Concordant/conformable on Myally Subgroup; unconformable on Kalkadoon Granite at Black Mountain	Correlated with Ballara Quartzite and Corella Formation to E, which are intruded by 1740-1720 Ma granites (e.g., Blake, 1987)

Haslingden Group				
Myally Subgroup	LRFT (500+), Gorge Creek sector (300), West Leichhardt Klippe (1000), Rifle Creek and Orient Blocks (500)	Quartzose to lithic or feldspathic sandstone, conglomerate; minor greywacke and subgreywacke, mainly near base	Conformable on Eastern Creek Volcanics	Not subdivided into constituent formations in this area
Eastern Creek Volcanics	LRFT (1000+), Gorge Creek sector (~100), West Leichhardt Klippe (500), Rifle Creek and Orient Blocks (500)	Basaltic lavas and interlayered fluvial sediments, including conglomerate; basal quartzose to arkosic sandstone and conglomerate commonly present E of LRFT	Conformable on Mt Guide Quartzite in LRFT; unconformable on Kalkadoon Granite and Kurbayia Migmatite to E	No individual members recognised in this area
Mount Guide Quartzite	Restricted to LRFT (2000+)	Upper part: quartzose sandstone, commonly sericitic. lower part (= Yappo Member): greywacke, siltstone, conglomerate	Conformable on Bottletree Formation; intruded by mafic dykes and sills	
Bottletree Formation	Restricted to LRFT (1000+)	Felsic and mafic volcanics, greywacke, siltstone, conglomerate	Unconformable on Kalkadoon Granite and Kurbayia Migmatite; intruded by mafic dykes	Dated at 1790±10 Ma (Page, 1983)
KALKADOON GRANITE	LRFT and to E: Gorge Creek sector, West Leichhardt Klippe, Rifle Creek and Orient Blocks, Black Mountain	Porphyritic to even-grained granodiorite, granite, tonalite, leucogranite, aplite, pegmatite; partly recrystallised and commonly foliated; xenoliths common. Main mafic mineral present is biotite	Intrudes Leichhardt Volcanics, Orient beds, Kurbayia Migmatite; cut by mafic dykes	Emplaced at around 1860 Ma (e.g., Wyborn & Page, 1983)
COVER SEQUENCE 1				
Leichhardt Volcanics	Only to E of LRFT: E side of West Leichhardt Klippe (1000+), Rifle Creek Block (100+), Black Mountain (1000+)	Grey non-magnetic felsic volcanics, mainly ignimbrites, with small quartz and feldspar phenocrysts and clots of biotite; variably foliated and recrystallised	Base not seen; intruded by Kalkadoon Granite, mafic dykes	Dated at 1870-1850 Ma (Page, 1988)
Orient beds	Restricted to Orient Block (500+)	Quartzitic to schistose metasediments representing sandstone, greywacke, siltstone, conglomerate; minor marble, possible felsic and mafic metavolcanics	Intruded by Kalkadoon Granite	May be correlative of Candover Metamorphics (exposed in LRFT to north)
BASEMENT				
Kurbayia Migmatite	LRFT, Gorge Creek sector, West Leichhardt Klippe, Rifle Creek Block	Thinly banded, micaceous, quartzo-feldspathic gneiss and migmatite (metasediments); fine-grained rhyolitic and dacitic gneiss (metavolcanics); nebulitic gneiss, amphibolite	Intruded by Kalkadoon Granite and mafic dykes	Protoliths predate 1900-1875 Ma Barramundi Orogeny (Blake & Page, 1988)

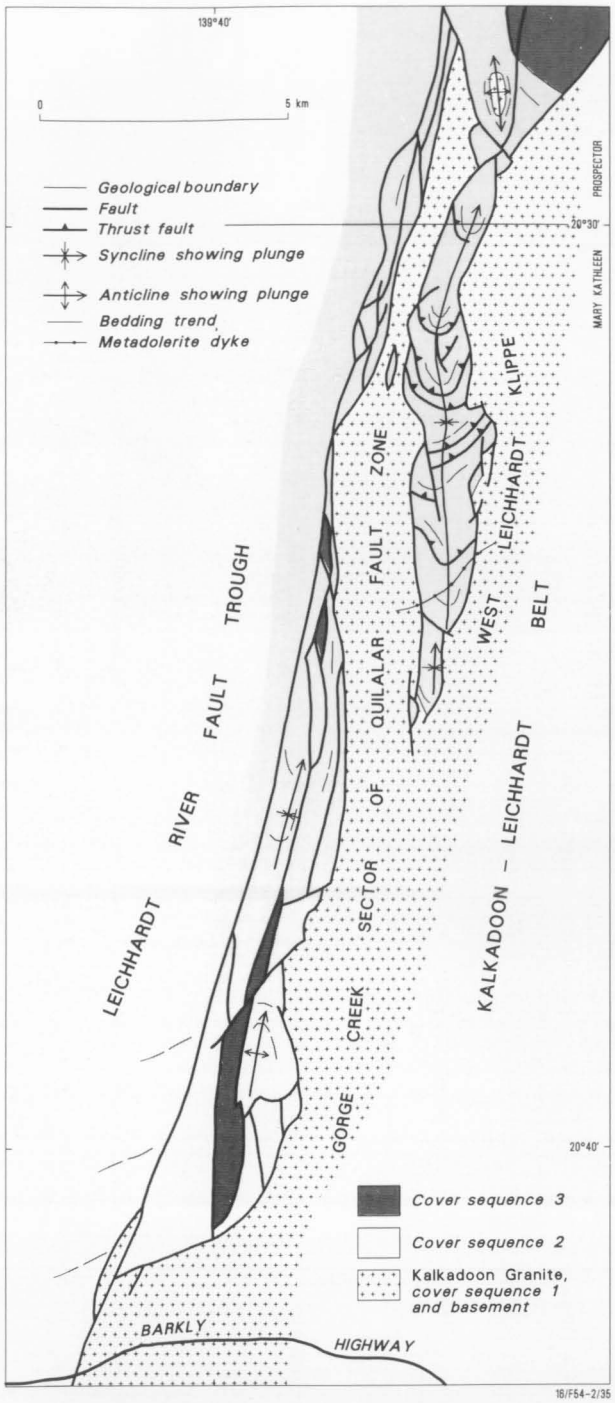


Fig. 2. Geological map of the Gorge Creek sector of the Quilalar Fault Zone and the West Leichhardt Klippe.

medium to thick-bedded and commonly cross-bedded quartzose to feldspathic sandstone, but also includes some pebbly and conglomeratic beds. Ridges of Myally sandstone in the sector, and in the West Leichhardt Klippe and Rifle Creek area described below, have much smoother crests than ridges of overlying Quilalar sandstone, which are typically sharp and uneven.

The *Quilalar Formation* is the most extensive stratigraphic unit in the Gorge Creek sector. The lower part consists of pale ridge-forming sandstone which ranges from quartzose to highly feldspathic or lithic, and invariably includes some calcareous beds; also present are thin beds of siltstone and rare calcareous conglomerate. The upper part is generally recessive, although it includes a few bands of ridge-forming sandstone. Typical rock types in this part are grey marble, which ranges from bedded to massive and is commonly brecciated, and variably calcareous grey siltstone and greywacke.

Cover sequence 3 is represented by the Surprise Creek Formation, which consists of siliceous sandstone and siltstone, and the Warrina Park Quartzite and Moondarra Siltstone of the Mount Isa Group. The Warrina Park Quartzite forms prominent ridges, wheras the other two formations are relatively recessive.

Structures

The oldest structures identified are two northerly-plunging folds more than 1 km across, a syncline and an anticline, in the southern half of the sector (Fig. 2). Both are cut by, and hence predate, several faults, most of which are subparallel to the axial planes of the folds and to the regional cleavage. The more southerly fold, the anticline, is cut off to the south by an apparent low-angle fault (thrust?). There are no comparable folds in the adjacent part of the LRFT to the west, where westerly to northerly dips prevail (Blake, 1991a; Henderson & Bain, 1991).

The many faults in the Gorge Creek sector form a complex anastomosing pattern, with an overall trend close to north-south. Most appear to be subvertical. Many more are present than can be shown at 1:50 000 scale, as some fault slices are less than a metre wide. The faults are marked by sheared, boudinaged, and brecciated rocks; by intense quartz-veining and secondary silicification; by irregular mesoscopic folds (especially in Surprise Creek Formation and Moondarra Siltstone); by kinked and crenulated cleavage; and by irregular masses of marble that appear to be tectonically emplaced.

Discussion

The two main folds in the Gorge Creek sector and the pervasive cleavage subparallel to their axial planes are correlated with D_2 of Bell (1983), the second major deformation phase of the Isan Orogeny (Blake & others, 1990) and dated at around 1550 Ma (Page & Bell, 1986). This phase is characterised by upright north-trending folds resulting from east-west compression. The two folds are cut by, and hence predate, the main faults of the sector.

The amount of fault movement represented by the

Gorge Creek sector of the Quilalar Fault Zone is unknown, but is probably in the order of many kilometres. This is suggested by (1) the presence of Quilalar Formation and cover sequence 3 units within the sector, but not in the LRFT immediately to the west; (2) the absence within the sector and to the east of Bottletree Formation, Mount Guide Quartzite, and most of the Eastern Creek Volcanics, units which are thousands of metres thick in the adjacent LRFT; and (3) the cut-off in the south of northerly-dipping Bottletree Formation and Mount Guide Quartzite which before faulting must have continued for a considerable distance to the east. Because the sector does not correspond to a marked change in metamorphic grade, most of the fault displacement is thought to have been horizontal, rather than vertical.

West Leichhardt Klippe

The West Leichhardt Klippe, so named by Loosveld & Schreurs (1987), is a narrow fault-bounded complex structural feature 12 km long and up to 1.5 km wide in the western part of the Kalkadoon-Leichhardt Belt, less than 3 km to the east of, and aligned parallel to, the Gorge Creek sector of the Quilalar Fault Zone. It is located northeast of Mount Isa, mainly in the Mary Kathleen 1:100 000 sheet area, but extends north into the Prospector 1:100 000 Sheet area (Figs. 1, 2; Blake, 1991a), and gives rise to a prominent range of steep-sided hills and strike ridges up to 150 m high (Fig. 3). The hills and ridges are formed of steeply dipping sandstone and conglomerate, and intervening valleys are eroded into less resistant siltstone, greywacke, carbonate rocks, basalt, and fault gouge. Adjacent plains are developed on older granite, migmatitic rocks, felsic volcanics, and mafic dykes.

In plan, the strike ridges and valleys of the klippe show general arcuate to horseshoe trends, concave to the north, outlining a major north-plunging syncline. Bedding dips steeply northward and faces north along the fold hinge. The klippe is bounded to the east and west by faults, and numerous faults occur within it. Its southern termination is inferred to be a north-dipping thrust, and to the north it terminates against a northwest-striking fault.

The West Leichhardt Klippe was mapped in the Mary Kathleen 1:100 000 Sheet area by Derrick & others (1977) as a fault-bounded syncline of Surprise Creek beds, comprising conglomerate, sandstone, pelite, and carbonate, but was thought to possibly include lateral equivalents of their upper Myally Subgroup, subsequently named the Quilalar Formation. It is shown as Quilalar Formation on the Prospector 1:100 000 geological map to the north (BMR, 1979), on the 2nd edition of the Cloncurry 1:250 000 geological sheet (GSQ, 1983), and on the 1:500 000 map of the Mount Isa Inlier and environs (Blake, 1987).



Fig. 3. View of the southern part of the West Leichhardt Klippe from the west.

In a recent structural investigation, Loosveld & Schreurs (1987) interpreted the klippe as a northward-dipping imbricate stack of thrust sheets underlain by a floor thrust, the whole being subsequently folded into a northerly-plunging tight upright syncline; an axial plane cleavage and a series of north-striking shear zones with subvertical extension lineations formed during the folding. According to this interpretation, the floor thrust of the imbricate stack crops out as the major faults that form the eastern and western sides of the klippe. Loosveld & Schreurs did not attempt to elucidate the stratigraphy of the klippe beyond concluding that a fining upwards sequence of conglomerate, sandstone, and siltstone was repeated tectonically at least seven times, twice in its entirety. They reported the presence of quartz-filled faults and breccia at contacts between imbricates, and of phyllonite locally developed along the eastern and western boundary faults (i.e., the floor thrust), with the phyllonitic layering being parallel to these faults and also to bedding, which is rotated into parallelism with the faults. As the imbricates dip steeply north along the entire length of the syncline, they were thought to have been northerly dipping before the folding event, implying that the direction of thrusting was from the north.

The present study supports the general conclusion of Loosveld & Schreurs (1987), that the klippe represents a folded set of imbricate thrust slices, but shows, not

unexpectedly, that the stratigraphic and structural picture is somewhat more complex than previously indicated.

Stratigraphy

The West Leichhardt Klippe comprises sedimentary rocks and subordinate metabasalt of cover sequence 2 of Blake (1987). These are assigned to the Eastern Creek Volcanics and undivided Myally Subgroup of the Haslingden Group and to the overlying Quilalar Formation, and hence are probably between 1780 and 1760 Ma old (Blake, 1987). Stratigraphic relationships within the klippe are generally uncertain, as contacts between units, and between contrasting rock types within them, are commonly marked by faults.

The klippe is in fault contact to the west with Kalkadoon Granite containing inclusions of basement Kurbayia Migmatite, and to the east with Kalkadoon Granite and the comagmatic felsic Leichhardt Volcanics of cover sequence 1. These rocks, but not the klippe, are intruded by numerous foliated and metamorphosed mafic dykes.

Repetitions within the West Leichhardt Klippe of distinctive rock types, such as arkosic conglomerate (mapped as Myally Subgroup) and calcareous sandstone (mapped as Quilalar Formation), bounded by faults subparallel to bedding, are indicative of thrust faulting. However, nowhere is the stratigraphic sequence of Eastern Creek Volcanics to Quilalar Formation repeated in its entirety (contrast Loosveld & Schreurs, 1987). Overall, the fault (thrust)-bounded blocks become progressively younger northward, in the direction of sedimentary facing – the oldest formation, the Eastern Creek Volcanics, crops out only in the south, the succeeding Myally Subgroup is confined to the southern and central parts of the klippe, and the youngest unit, the Quilalar Formation, is restricted to the central and northern parts (Blake, 1991a). Because of the extensive thrusting and other faulting, the stratigraphic thicknesses of the units cannot be determined with any certainty; estimates are Eastern Creek Volcanics 0 to perhaps 500 m, and Myally Subgroup and Quilalar Formation each about 1000 m.

The *Eastern Creek Volcanics*, not previously identified within the klippe, are represented by recessive metabasalt, minor interflow clastic sedimentary beds, and, mainly at the base, ridge-forming feldspathic and lithic sandstone and conglomerate. At the southern end of the klippe, the basal sandstone and conglomerate are up to 300 m thick, and unconformably overlie (rather than being in faulted contact with) Kalkadoon Granite to the



Fig. 4. Deformed conglomerate of the Myally Subgroup in the West Leichhardt Klippe (grid reference MK273667). The large clasts showing a vertical stretching lineation are of resistant grey quartzite and friable felsic volcanics. The foliation here strikes north-northeast.

southwest. Here arkosic grit passes down into altered regolithic granite and up into cross-bedded sandstone with some conglomerate bands. A similar unconformity, with basal pebbly sandstone separating schistose metabasalt from underlying felsic Leichhardt Volcanics, is exposed to the north-northeast (at grid reference MK664282 and MK662277). A distinctive deformed conglomerate occurs with metabasalt on the northern side of the Leichhardt River (near grid references MK654245); it contains subvertically elongated clasts, some more than 1 m long, of quartzite, leucogranite, altered felsic volcanics, probable metabasalt, and vein quartz in a foliated dark grey to black biotite-rich matrix.

The Eastern Creek Volcanics appear to be much thicker at the southern tip of the klippe than to the north. This may be attributed to repetition by thrusting in the south (Blake, 1991a) and tectonic thinning in the north.

The overlying *Myally Subgroup* consists of ridge-forming sandstone and conglomerate. Sandstone appears to predominate in the lower part of the subgroup and conglomerate in the upper part. The sandstone ranges from quartzose to feldspathic or lithic and is mainly pale greyish or pinkish, cross-bedded, and less commonly, ripple marked. The conglomerate contains deformed clasts up to boulder size, mainly of altered felsic volcanics (pale pinkish or buff, friable, finely micaceous) and grey quartzite, in a pale arkose matrix. Pebbles and larger clasts are flattened parallel to the regional northerly-striking subvertical cleavage, and generally show a pronounced

elongation, in places greater than 5:1, plunging vertically or steeply south (Fig.4).

The youngest formation in the West Leichhardt Klippe, the *Quilalar Formation*, overlies the Myally Subgroup either conformably (e.g., Derrick & others, 1980) or disconformably. The lower part consists of ridge-forming sandstone, most of which is more siliceous than typical Myally sandstone; its main distinguishing feature, though, is the invariable presence of some calcareous beds. Cross-bedding is common. In the upper part, which is generally less resistant to erosion, the main rock types are variably calcareous and feldspathic sandstone, greywacke, and siltstone (commonly phyllitic), and impure marble. Similar calcareous beds also crop out about 200 m west of the klippe in a northerly-trending fault sliver a few tens of metres wide within Kalkadoon Granite (centred at grid reference MK646300).

Numerous *mafic dykes* intrude Kalkadoon Granite and older rocks adjacent to the West Leichhardt Klippe, but only two mafic intrusions are known to occur within it (see below).

Structure

Three phases of deformation are recognised in the West Leichhardt Klippe: early faulting, folding to form the major syncline, and later faulting. All three postdate deposition of cover sequence 2 and, on regional grounds (e.g., Blake, 1987), also postdate cover sequence 3. Some of the early faults were probably reactivated during the folding and later faulting.

The early faults include arcuate transverse faults, concave to the north, which, following Loosveld & Schreurs (1987), are considered to form a stack of imbricate thrusts, as they separate repetitions of the stratigraphic sequence. These faults are folded by the major syncline and are cut by the later faults. Their traces are mostly parallel or subparallel to bedding, which dips steeply north along the hinge of the syncline, and although no dips have been measured on any of them, the faults are interpreted as originally north-dipping thrusts that were steepened to subvertical faults during subsequent folding. (If they were originally normal faults their traces would be strongly oblique, rather than parallel, to bedding on the sides of the syncline.) The thrusts are inferred to be listric, rising southwards from a floor thrust to progressively higher stratigraphic levels (Blake, 1991a). A general direction of tectonic transport from north to south is indicated, implying north-south shortening.

The floor thrust for this imbricate stack may be represented by faults along the eastern and western sides of the klippe, as suggested by Loosveld & Schreurs (1987). If so, these faults would be expected to be nearly tangential to all the arcuate thrust imbricates. Such is not the case, but this could be due to reactivation of the bounding faults during and after subsequent folding.

The decollement surface (floor thrust) of the imbricate stack may lie within metabasalt of the Eastern Creek Volcanics. This is suggested by basal sandstone of the Eastern Creek Volcanics resting unconformably on granite in the far southwest and on granite and felsic volcanics on the eastern side of the klippe, and the absence of granite and felsic volcanics in any of the thrust repetitions. If this is so, the southernmost thrust of the imbricate stack may lie within the metabasalt at the southern end of the klippe. In contrast, in the Rifle Creek Block to the south (see below) and in the Lake Mary Kathleen Fold and Thrust Zone to the southeast (Blake, this volume), the main decollement for the mapped thrusts appears to be in granite and metamorphics underlying cover sequence 2.

The imbricate stack was folded into a north-plunging syncline during subsequent east-west shortening. A vertical to steeply east-dipping cleavage, indicative of ductile deformation, is axial planar to the syncline. The cleavage is well developed in conglomerate, metabasalt, greywacke, and siltstone, and is subparallel to the foliation in granite, felsic volcanics, and mafic dykes east and west of the klippe. The subvertical stretching lineation shown by pebbles in conglomerate is attributed to this deformation phase. The folding of the klippe probably also involved some brittle fracturing, leading to block-faulting and brecciation.

The boundary faults of the klippe are marked by vertical to steeply east-dipping zones up to a few metres wide of intense shearing, quartz-veining, and local phyllonite development. Some calcareous rocks in the western fault zone are represented by streakily banded and boudinaged calcite-actinolite rock (Fig. 5). Both faults cut, and hence at least partly postdate, the major syncline, and both are displaced by some later faults.

Although numerous north and northwest-striking dykes of foliated amphibolite and mafic schist intrude adjacent granite and felsic volcanics, none cut the klippe sequence, and so these mafic dykes are inferred to predate the oldest rocks of the klippe, the Eastern Creek Volcanics. However, in the south the klippe is cut by a northeast-striking mafic dyke. This dyke consists mainly of metamorphic green amphibole and sodic plagioclase, indicating metamorphism to lower amphibolite or upper

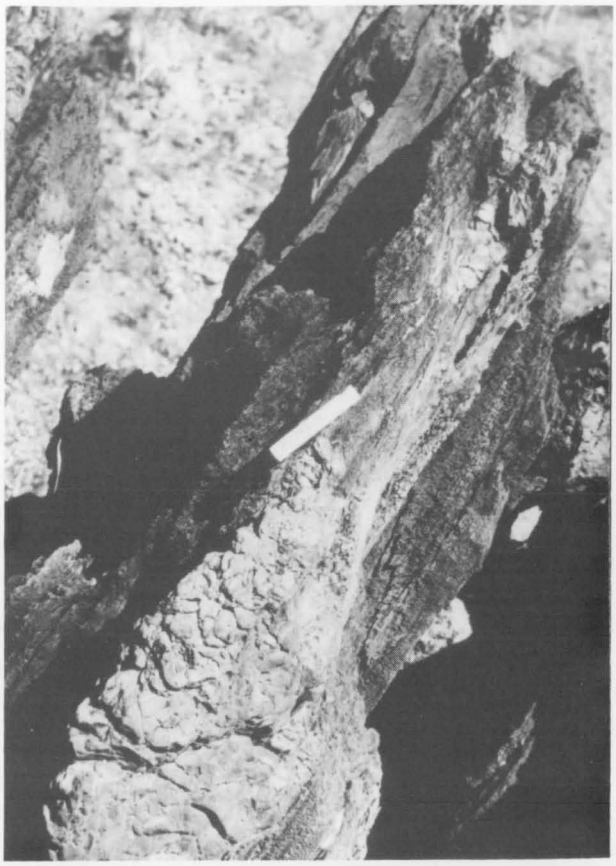


Fig. 5. Boudinaged calcite-actinolite rock on the western side of the West Leichhardt Klippe.

greenschist facies, but is not foliated, unlike the rocks it cuts, and it clearly postdates the major syncline and associated cleavage. The dyke, which crops out as distinctive rounded core-stones, can be traced along strike, with no apparent displacement, to the southwest and northeast of the klippe, cutting Kalkadoon Granite and foliated mafic dykes. Thus most, if not all, movement on the klippe-bounding faults appears to have taken place before the dyke was intruded, but, as the dyke is metamorphosed, before the cessation of the last significant metamorphic event to affect this part of the Mount Isa Inlier.

Discussion

The deformation and metamorphism of the West Leichhardt Klippe are attributed to the Isan Orogeny of Blake & others (1990), which lasted from about 1620 Ma to about 1520 Ma. Apart from the emplacement of granite batholiths in the east at around 1500 Ma, the intrusion of some younger dolerite dykes, and strike-slip movements along major faults, the tectonic events associated with this orogeny were the last to directly affect the Mount Isa Inlier to any marked degree, and certainly the last to result in region-wide metamorphism and cleavage development.

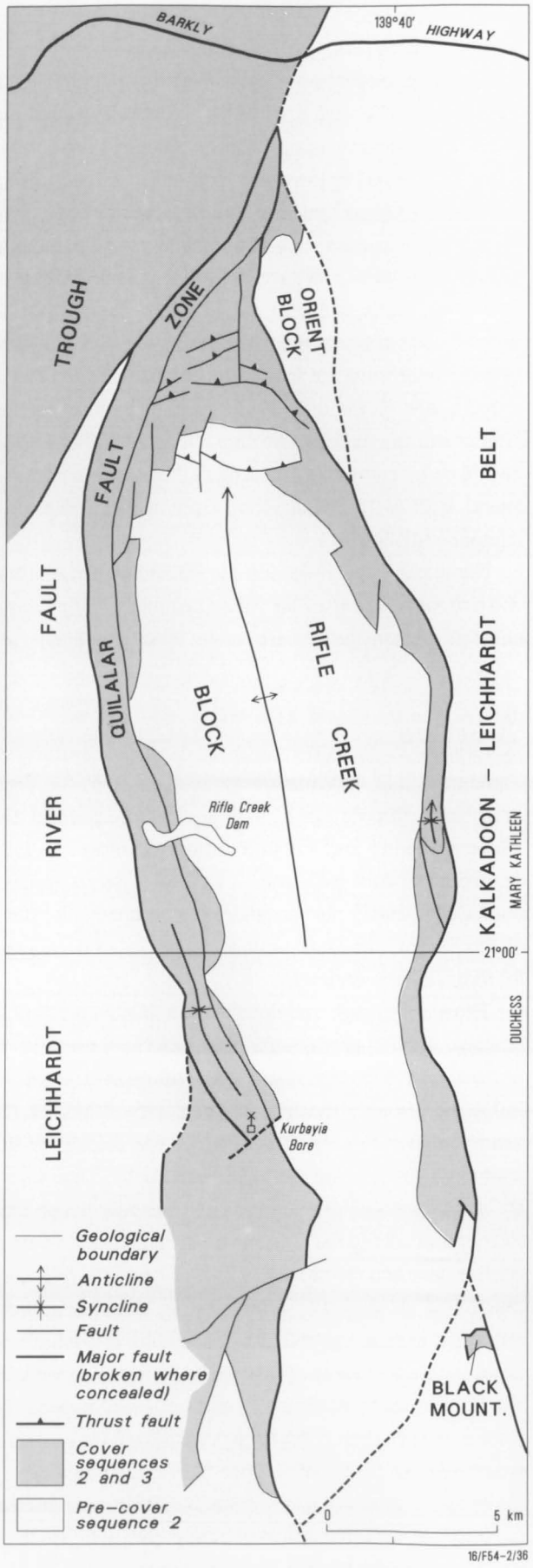


Fig. 6. Geological map of the Rifle Creek area.

The early north to south thrusting in the klippe is similar to that envisaged by Bell (1983) for his postulated much larger thrust duplex in the LRFT to the west, west of the Quilalar Fault Zone. The suggested age for this north-south compressional event, D_1 of Bell (1983), is about 1610 Ma (Page & Bell, 1986).

The subsequent deformation of the thrust imbricates to form the major upright syncline and axial planar cleavage are correlated with the D_2 deformation of Bell (1983), a phase of east-west compression and regional metamorphism at around 1550 Ma (Page & Bell, 1986). Parts of the early floor thrust of the West Leichhardt Klippe may have been reactivated during or shortly after D_2 to form the subvertical faults on either side of the klippe. Both the folding and faulting predate the northeast-striking metamorphosed mafic dyke cutting the southern part of the klippe.

Rifle Creek Area

This area includes the Rifle Creek and Orient Blocks and part of the LRFT (Figs. 1, 6; Blake, 1991b). The fault-bounded Rifle Creek Block, located in the west of the Kalkadoon-Leichhardt Belt, extends from 2 km south of the Barkly Highway in the Mary Kathleen 1:100 000 Sheet area (grid reference MK575070) southward for at least 40 km into the Duchess 1:100 000 Sheet area. It has a maximum width of 10 km, and is partly outlined by a tuning-fork pattern of ridges, apex to the north. The ridges forming the two prongs or arms of the fork consist predominantly of outwardly facing metasedimentary rocks belonging to cover sequences 2 and 3, and older migmatitic and meta-igneous rocks crop out between the two arms. The block differs significantly in stratigraphy and structure from the LRFT immediately to the west and from the adjacent part of the Kalkadoon-Leichhardt Belt to the east.

A band of closely spaced anastomosing faults along the western side of the Rifle Creek Block, forming much of the western arm of the tuning fork, is part of the Quilalar Fault Zone (Fig. 6). The most westerly fault of this zone is taken as the western boundary of the block, separating it from the LRFT. Hence the block incorporates a sector of the fault zone that is similar in many respects to the Gorge Creek sector described above. A major fault diverging southeastwards from the Quilalar Fault Zone in the north forms the eastern boundary of the block. The western and eastern bounding faults are inferred to join up again in the south, at the southern tip of the block (exact location uncertain) in the Duchess 1:100 000 Sheet area.

The main part of the Rifle Creek Block, east of the Quilalar Fault Zone, is a broad northerly-plunging anticline with subvertical parallel limbs, the oldest rocks in the core being overlain by cover sequences 2 and 3 on the two limbs – the arms of the tuning fork – and in the fold hinge in the north. Stratigraphic repetitions in the hinge area are considered to result from thrusting before formation of the anticline.

The smaller Orient Block, on the northeast side of the Rifle Creek Block, is made up of metasediments assigned to cover sequence 1 (Orient beds, new name), Kalkadoon Granite, and cover sequence 2 (in the north). The eastern boundary of this block is inferred to be a concealed major fault.

Stratigraphy

The Proterozoic stratigraphy of the Rifle Creek Block and adjacent area is summarised in Table 1 and Figure 7.

Basement

Inclusions of *Kurbayia Migmatite,* some more than 100 m across, are present within the Kalkadoon Granite in the core of the Rifle Creek Block and also east and west of the block. The sedimentary and volcanic protoliths were deformed and metamorphosed to migmatite during the 1900-1870 Ma Barramundi Orogeny (Blake & Page, 1988).

Cover sequence 1

Cover sequence 1 in the area is represented by the Orient beds and Leichhardt Volcanics.

The *Orient beds* are confined to the Orient Block, where they form a prominent north-striking ridge about 7 km long and up to 1 km wide, surrounded by Kalkadoon Granite. Quartzitic to schistose metasediments predominate, but the unit also includes marble and possibly some felsic and mafic volcanics. The sedimentary rocks are somewhat similar to those of the Quilalar Formation of cover sequence 2, but differ in being generally more pelitic, and they are intruded by, rather than overlie, Kalkadoon Granite. However, the Orient beds probably postdate the Barramundi Orogeny, as they are much less deformed and metamorphosed than the Kurbayia Migmatite, and they are inferred to be similar in age to the Leichhardt Volcanics. The unit may be a correlative of the Candover Metamorphics that crop out on the eastern side of the LRFT 80 km north of the Rifle Creek Block. The Candover Metamorphics are lithologically similar to the Orient beds, are intruded by granite possibly related to the Kalkadoon Granite, and are presumed to be

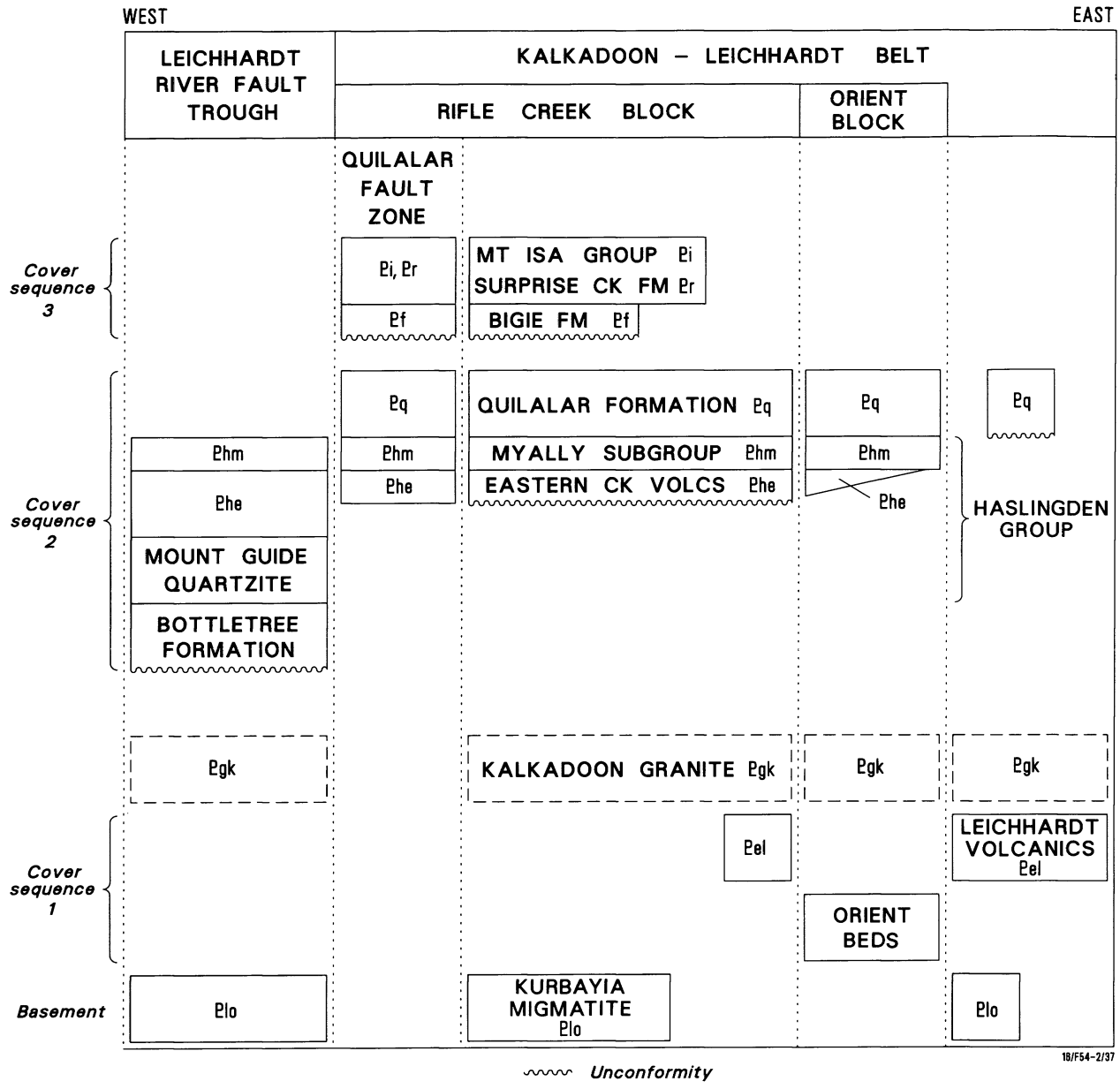


Fig. 7. Distribution of stratigraphic units in the Rifle Creek area.

overlain unconformably by Eastern Creek Volcanics (Wilson & Derrick, 1983) of cover sequence 2.

The *Leichhardt Volcanics* crop out in the Rifle Creek Block only at the southern tip of the eastern arm of the tuning fork, where they are overlain by sandstone (basal Eastern Creek Volcanics?). The predominant rock type is pale grey nonmagnetic felsic meta-ignimbrite. The formation crops out extensively to the east, where it is intruded by Kalkadoon Granite and mafic dykes.

Cover sequence 2

The two oldest formations of cover sequence 2 in the LRFT, the *Bottletree Formation,* dated at 1790 Ma (Page, 1983), and the conformably overlying *Mount Guide Quartzite* of the Haslingden Group, are not present in the Rifle Creek Block, but are several kilometres thick just to the west, in the LRFT. Eriksson & Simpson (1990) and Simpson & Eriksson (1991) consider that the upper part of the Mount Guide Quartzite represents shallow subtidal to tidal-flat sands probably deposited over a period of 20-25 Ma, indicating that the overlying Eastern Creek Volcanics and Myally Subgroup of the Haslingden Group may be younger than 1770 Ma.

In the Rifle Creek Block, the oldest cover sequence 2 formation present is the *Eastern Creek Volcanics*. This formation rests directly on Kalkadoon Granite, is up to

about 500 m thick, and consists of ridge-forming basal quartzose to lithic or arkosic sandstone and conglomerate and overlying recessive metabasalt, much of which is strongly cleaved. In the Orient Block the formation is represented by lenses of cleaved metabasalt a few metres thick. In marked contrast, in the LRFT to the west, the Eastern Creek Volcanics are up to 7000 m thick and are separated from underlying Kalkadoon Granite by several thousand metres of Bottletree Formation and Mount Guide Quartzite.

The upper part of the Haslingden Group, the *Myally Subgroup*, overlies Eastern Creek Volcanics and is overlain, probably conformably, by Quilalar Formation. The Myally Subgroup in the Rifle Creek area is about 500 m thick, and consists predominantly of pale pink to pale grey quartzose to feldspathic or lithic sandstone. In the Rifle Creek Block it also includes conglomerate, micaceous greywacke, and subgreywacke, especially near its base. The sandstone is commonly cross-bedded, and ripple marks are present locally. Conglomerate forms lenses up to several metres thick and also a band at least 200 m thick in the southeast; it is made up of pebbles, cobbles, and boulders of grey quartzite, altered porphyritic felsic volcanics, granitic rocks, basalt, and vein quartz in an arkosic matrix; pebbles and larger clasts generally show a pronounced subvertical elongation and a flattening parallel to the regional north-striking cleavage.

The Myally Subgroup in the eastern part of the Rifle Creek Block includes some interbedded calcareous sandstone, a rock type that elsewhere in the area is regarded as diagnostic of the overlying Quilalar Formation. It is mapped as Myally Subgroup here because it also includes Myally-type polymictic conglomerate and it directly overlies metabasalt of the Eastern Creek Volcanics.

The *Quilalar Formation* crops out in the Rifle Creek and Orient Blocks overlying Myally Subgroup, and also at Black Mountain in the southeast (Williams & Blake, this volume), where it rests on Kalkadoon Granite, but is not present in the LRFT to the west. In the Rifle Creek and Orient Blocks the lower part of the formation consists of ridge-forming sandstone, whereas much of the upper part is formed of less resistant, variably calcareous greywacke and siltstone and impure limestone or marble. Sandstones range from quartz-rich to highly lithic/feldspathic and/or calcareous; however, some beds of calcareous sandstone are invariably present, even in the lower part of the formation, where quartz-rich sandstone predominates. The calcareous sandstone is characterised by porous and commonly iron-stained (gossanous) weathered surfaces. Cross-bedding is common, and ripple marks are present in places, as also are siltstone laminae. Highly calcareous rocks in the upper part of the formation are commonly contorted or brecciated, and in places have been mobilised to form space-filling lenses and irregular bodies along faults; however, primary sedimentary features, including stromatolites, are preserved in places.

The lower Quilalar Formation in the Rifle Creek and Orient Blocks corresponds to the tide-dominated shelf deposits of Jackson & others (1990), laid down on the western side of the Quilalar depositional basin. In contrast, the Quilalar Formation at nearby Black Mountain (Williams & Blake, this volume), east of the Rifle Creek Block, belongs to the storm-dominated shelf type that characterises the central part of the Quilalar basin (Jackson & others, 1990).

Cover sequence 3

Rocks assigned to cover sequence 3 are confined to the western part of the Rifle Creek Block, mainly within the Quilalar Fault Zone north of Rifle Creek Dam, where contacts between units are invariably fault-bounded. Units distinguished are the Bigie and Surprise Creek Formations, and the Warrina Park Quartzite and Moondarra Siltstone of the Mount Isa Group.

The *Bigie Formation* appears to lie concordantly between Quilalar Formation below and Surprise Creek Formation or Warrina Park Quartzite above. Main rock types are feldspathic or lithic sandstone, micaceous sandstone, greywacke, polymictic conglomerate, and dark grey siltstone and mudstone. Cross-bedding and convolute bedding indicate facing.

The *Surprise Creek Formation* is characterised by non-calcareous thinly bedded (platy) silicified sandstone and siltstone in which cross-bedding and other facing criteria are rare. The *Warrina Park Quartzite* forms ridges of pale quartzite and conglomerate containing pebbles and cobbles of quartzite and rare vein quartz; the pebbles are generally highly deformed, being flattened parallel to the prevailing north-striking cleavage and elongated subvertically. The *Moondarra Siltstone* is less siliceous and generally finer-grained than the Surprise Creek Formation. Minor folds, crenulations, and irregular contortions are present in the Surprise Creek Formation and Moondarra Siltstone near faults.

Igneous intrusions

Kalkadoon Granite crops out within and on both sides of the Rifle Creek and Orient Blocks, intruding Kurbayia Migmatite, Leichhardt Volcanics, and Orient beds. It

consists of partly recrystallised and commonly foliated biotite-bearing granitic rocks, some of which contain feldspar phenocrysts. Xenoliths are common, schlieren occur locally, and net-veined complexes of granite and more mafic rocks (Blake, 1981) are present in places. The granite was emplaced at around 1860 Ma (e.g., Wyborn & Page, 1983).

In the Rifle Creek Block, numerous *metadolerite dykes* cut Kalkadoon Granite and Kurbayia Migmatite, but none intrude the overlying cover sequences 2 and 3. The dykes appear to be subvertical and show a variety of trends, with the majority being close to north-south. Few, if any, are magnetic, unlike many mafic flows in the Eastern Creek Volcanics, and they are inferred to be older than these extrusives. Mafic dykes of probably similar age, also nonmagnetic, intrude Kalkadoon Granite, Leichhardt Volcanics, and Kurbayia Migmatite east of the Rifle Creek Block, except in the Orient Block, where no dykes have been found. In the LRFT west of the Rifle Creek Block, a swarm of north-northeasterly-striking mafic dykes – some of which are magnetic – cut the Bottletree Formation and Mount Guide Quartzite, and a sill of metadolerite (nonmagnetic) at least 100 m thick intrudes the Mount Guide Quartzite; most of these mafic intrusions could be intrusive equivalents of the Eastern Creek Volcanics, and younger than most of the mafic dykes within the Rifle Creek Block.

Mylonites and phyllonites

Intensely sheared rocks, represented by mylonite and phyllonite, are widespread along the western arm of the tuning fork in the Rifle Creek Block, within and also to the east of the Quilalar Fault Zone. For example, near Rifle Creek Dam and to the south, the Eastern Creek Volcanics are represented by basal mylonitic quartzite and conglomerate and overlying phyllonitic metabasalt, and mylonitic quartzite and conglomerate form much of the Myally Subgroup (Fig. 8). The mylonitic foliation is generally subvertical, parallel to bedding, and in places is folded; observed lineations and pebble elongations are subvertical. No mylonite has been reported from the eastern arm of the tuning fork.

Structural features

The oldest structural features observed are small tight irregular folds in Kurbayia Migmatite. These are cut by, and hence predate, Kalkadoon Granite and mafic dykes, and are considered to have formed at the time of migmatisation, during the Barramundi Orogeny, about 1870 Ma ago (Blake & Page, 1988).



Fig. 8. Highly deformed (mylonitic) conglomerate of the Myally Subgroup on the western side of the Rifle Creek Block (grid reference MK860528).

All other structures identified in the area postdate deposition of the Mount Isa Group of cover sequence 3; they include major thrusts and folds attributed to the Isan Orogeny (1620-1520 Ma) and the later mainly strike-slip faults of the Quilalar Fault System.

The earliest Isan structures are a series of thrusts in the Rifle Creek Block, which repeat parts of the stratigraphic sequence several times. These are attributed to D_1 of Bell (1983). The thrust slices are part of a broad northerly-plunging anticline which formed during the D_2 deformation phase. A region-wide cleavage is parallel to the axial plane of this anticline, and is considered to have formed during the same phase of deformation. The thrusts in the hinge area of the D_2 anticline are offset by several small faults which are subparallel, and probably similar in age, to this regional cleavage.

North-south D_2 folds, but no D_1 structures, are evident in the limbs of the major D_2 anticline and also in the Orient Block to the east and the LRFT to the west. In contrast, both D_1 and D_2 folds are present at Black Mountain (Williams & Blake, this volume).

Isan thrusts (D_1)

Several D_1 thrusts have been mapped in the Rifle Creek Block (Fig. 6; Blake, 1991b). Although they now appear to be subvertical, they are inferred to have had mainly gentle dips before becoming steepened during subsequent folding. They are interpreted as thrusts because they are subparallel to bedding and they separate bands of similar strata; i.e., they repeat, rather than omit, strata, unlike extensional normal faults. As the thrusts displace Kurbayia Migmatite and Kalkadoon Granite, in addition to cover sequences 2 and 3, a major decollement zone was presumably present at some depth below the base of cover sequence 2 during the thrusting. When allowance is made for the later folding, the thrusts strike roughly east-west and dip north, indicating general north-south shortening

and north over south movement. The thrusts are marked in places by zones of quartz veining and brecciation in which the regional north- striking D_2 cleavage can be recognised.

The mylonites in the western part of the Rifle Creek Block may have been formed during D_1 thrusting, as at least some were folded during D_2.

Isan folds (D_2)

The main D_2 fold in the Rifle Creek Block is the broad anticline outlined by the tuning-fork pattern of ridges. This anticline, which folds and therefore postdates the D_1 thrusts, is north-plunging, upright, and has steep subparallel limbs and an axial plane approximately parallel to the regional cleavage.

Smaller upright folds with north-south trends on the limbs of the major D_2 anticline are also regarded as D_2 structures; they include a north-plunging syncline on the eastern limb east of Rifle Creek Dam, and a syncline on the western limb extending from Rifle Creek Dam south to Kurbayia Bore (Fig. 6). The western syncline folds mylonitic Myally Subgroup and Eastern Creek Volcanics.

Folds in the Orient Block, affecting the Orient beds, Myally Subgroup, and Quilalar Formation, have north-south trends, and hence are probably D_2 structures, as also are the folds in the LRFT to the west. In the LRFT opposite the northern part of the Rifle Creek Block, the Bottletree Formation and Haslingden Group generally dip and face west, towards a presumed synclinal hinge well to the west of the area mapped. To the south, though, the cover sequence 2 rocks of the LRFT lie on the eastern limb of a broad anticlinal D_2 structure, and dip eastwards towards the Rifle Creek Block.

The upright D_2 folds and axial planar cleavage indicate east-west shortening, in contrast to the earlier D_1 thrusts, which resulted from north-south shortening.

Later major faults

The major northerly-striking faults along the eastern and western sides of the Rifle Creek Block cut, and therefore postdate, the D_2 folds. These faults separate areas of markedly different stratigraphy and structure, implying displacements of many kilometres. They are steeply dipping to vertical, and, like other faults of the Quilalar Fault System, do not correspond to marked changes in regional metamorphic grade. Hence they are presumed to be essentially strike-slip faults.

No stretching lineations related to the late faults have been found, perhaps indicating that these faults are brittle, rather than ductile, features at the present level of exposure. The vertical to steeply plunging stretching lineation evident in deformed conglomerate within the Rifle Creek Block, and characteristic of much of the Mount Isa Inlier, is a ductile feature related to D_1 or D_2 of the Isan Orogeny, and hence predates the late faults, as also do mylonites on the western side of the Rifle Creek Block.

The eastern boundary fault diverges from the Quilalar Fault Zone at the northern apex of the Rifle Creek Block (Fig. 6), and is inferred to join up with this fault zone again in the south, passing to the west of Black Mountain. In the north a postulated offshoot forms the eastern boundary of the subsidiary Orient Block.

The western boundary fault of the Rifle Creek Block is the most westerly, and probably the largest, of the anastomosing faults making up the Quilalar Fault Zone in this area. The exact position of this fault zone south of Kurbayia Bore is unclear; the zone appears to be offset northeastwards by a younger fault, parallel to the Yappo Fault, and may correspond to a narrow ridge of subvertical mylonitic quartzite that terminates to the south near Yarraman Tank (at grid reference DU577560). This ridge separates metabasalt of the Eastern Creek Volcanics to the west, underlain farther west by Mount Guide Quartzite, from Kalkadoon Granite and Kurbayia Migmatite to the east. The mylonite here, though, if similar in age to folded mylonite in the west of the Rifle Creek Block farther north, predates D_2, and hence is not related to movement along the Quilalar Fault Zone.

Discussion and speculation

The fault-bounded Rifle Creek Block has stratigraphic and structural features that are significantly different from those in the adjacent areas (e.g., Fig. 7). These differences suggest that the block was transported to its present site alongside the LRFT after the main phases of the Isan Orogeny (D_1 and D_2) had taken place, and could be regarded as an allochthonous terrane. The following stratigraphic, sedimentological, and structural evidence, taken together, indicate lateral displacement of many tens of kilometres along the western side of the Rifle Creek Block, and a similar displacement on the major fault marking the eastern boundary of the Rifle Creek Block and subsidiary Orient Block.

Stratigraphic evidence

- The two oldest formations of cover sequence 2 in the LRFT, the Bottletree Formation and Mount Guide Quartzite, are each more than 1000 m thick in the LRFT alongside the Rifle Creek Block, but are cut off abruptly by, and nowhere occur east of, the Quilalar Fault Zone.

This fault zone also marks the western limit of the Leichhardt Volcanics, which crop out extensively in the western part of the Kalkadoon-Leichhardt Block.

- The Eastern Creek Volcanics are conformable on Mount Guide Quartzite in the LRFT, but lie unconformably on Kalkadoon Granite in the Rifle Creek Block (and also in the West Leichhardt Klippe area to the north).
- The Eastern Creek Volcanics and Myally Subgroup of the Haslingden Group have a combined thickness of probably less than 1000 m in the Rifle Creek and Orient Blocks, compared with a thickness of several kilometres to the west, in the adjacent LRFT.
- The Quilalar Formation overlies the Haslingden Group in the Rifle Creek and Orient Blocks and is overlain by Bigie Formation in the Rifle Creek Block. However, the Quilalar and Bigie Formations are not present in the LRFT to the west, as here the Haslingden Group is overlain unconformably by Surprise Creek Formation and Mount Isa Group; either they were never deposited in this part of the LRFT, or they were removed by erosion before the younger sediments were laid down.
- At Black Mountain, just to the east of the Rifle Creek Block in the south, the Quilalar Formation, the youngest unit preserved, was laid down directly on Kalkadoon Granite (Williams & Blake, this volume). Haslingden Group rocks, if originally present here, were removed by erosion before deposition of the Quilalar Formation.
- The Orient beds are confined to the Orient Block, where they are intruded by Kalkadoon Granite. Their most likely correlatives are the Candover Metamorphics, the only known outcrop area of which is 80 km to the north, within or on the western side of the Quilalar Fault Zone.

Sedimentological evidence

- The lower part of the Quilalar Formation in the Rifle Creek Block corresponds to the tidal shelf type of Jackson & others (1990), laid down on the western side of the Quilalar depositional basin. In contrast, at nearby Black Mountain to the east, the Quilalar Formation is represented by deeper-water trough-type sediments, deposited in the central part of the Quilalar basin. It is inferred that the two areas, now close together, were many kilometres apart at the time of Quilalar deposition.

Structural evidence

- The east-striking thrusts identified in the northern part of the Rifle Creek Block are not present to the west in the LRFT, nor to the east in the Kalkadoon-Leichhardt Belt. Farther north, in the LRFT, Bell (1983) has proposed a major D_1 thrust duplex, involving cover sequences 2 and 3 and north to south transport, but this duplex does not appear to extend south of the Barkly Highway. Somewhat similar but much smaller sequences of thrusts have been identified east of the Quilalar Fault Zone to the north of the Rifle Creek Block (for example, in the West Leichhardt Klippe), but not to the south.
- The D_2 folds in the Rifle Creek Block do not match up with the D_2 folds in the adjacent LRFT. (Not surprisingly, no folds have been identified in the Kalkadoon Granite and Leichhardt Volcanics east of the Rifle Creek and Orient Blocks).
- North and south of the Barkly Highway, northerly-dipping Bottletree Formation and lower Haslingden Group, several kilometres thick, are cut off to the east by the Quilalar Fault Zone (Blake, 1991a, 1991b; Henderson & Bain, 1991); i.e., before faulting this sequence extended many kilometres farther east. This gives an indication of the size of fault displacement, and also shows that here the Quilalar Fault Zone does not coincide with the eastern margin of the rift or basin in which the sequence was deposited.

The faults bounding the Rifle Creek and Orient Blocks cut, and therefore postdate the D_2 folds of the Isan Orogeny. They were probably active for a considerable time, as large displacements are involved, like some other major north-south faults in the Mount Isa Inlier. Those of the Pilgrim Fault Zone to the east and the Mount Isa Fault Zone to the west, for example, were active well into the

Phanerozoic, although most displacement took place during the Proterozoic (e.g., Blake, 1987). Perhaps, for an unknown period commencing after the D_2 folding, the Kalkadoon-Leichhardt Belt moved southwards, relative to the LRFT of the Western Fold Belt, along the Quilalar Fault Zone, and as movement proceeded, parts of the western margin of the Kalkadoon-Leichhardt Belt, including the Gorge Creek sector and Rifle Creek and Orient Blocks, became detached and lodged against the LRFT, so that they were not transported as far south as the rest of the Kalkadoon-Leichhardt Belt.

Summary of geological history

The earliest deformational event recognised in the area is that represented by the metamorphism, partial melting, and tight folding of a mixed package of sediments and volcanics which form the Kurbayia Migmatite. This event took place about 1870 Ma ago (Blake & Page, 1988), during the compressional Barramundi Orogeny (Page, 1988).

The Barramundi Orogeny and associated uplift and erosion were closely followed by deposition of the Orient beds in the Orient Block, and by widespread felsic magmatism represented by the Leichhardt Volcanics and Kalkadoon Granite. This magmatism, which took place between about 1870 and 1850 Ma (Page, 1988), and the subsequent intrusion of mafic dykes before deposition of cover sequence 2, indicate probable crustal extension.

Following substantial erosion and resulting unroofing of the Kalkadoon Batholith, further crustal extension created a major basin or rift in the west, corresponding to the Leichhardt River Fault Trough (LRFT), and the deposition of cover sequence 2 (1790-1760 Ma). The Bottletree Formation and the lower part of the Haslingden Group were confined to the depositional LRFT, but the upper part of the Haslingden Group onlapped eastwards on to the Kalkadoon-Leichhardt Belt. The overlying Quilalar Formation extended the whole way across this belt (Jackson & others, 1990), with shallow platform sediments being deposited on the western and eastern sides and deeper-water trough sediments in between.

Cover sequence 2 was overlain 80-100 Ma later, between 1680 and 1670 Ma ago, by cover sequence 3, represented in the Rifle Creek Block by the Bigie Formation, Surprise Creek Formation, and Mount Isa Group. The contact between the two cover sequences here is concordant, indicating overall tectonic stability between the two periods of deposition in this part of the Mount Isa Inlier.

The cover sequences of the Mount Isa Inlier do not appear to have been regionally deformed and metamorphosed until the Isan Orogeny, which began at around 1620 Ma ago (Page & Bell, 1986) and lasted for about 100 Ma. The earliest event of this orogeny identified in the area was thrusting and associated mylonite formation, brecciation, and quartz veining in the West Leichhardt Klippe and Rifle Creek Block – a result of north-south compression. This phase can be correlated with the north-south thrusting and associated east-trending folds recognised by Bell (1983) in the LRFT north of Mount Isa – the D_1 event dated at 1610 Ma by Page & Bell (1986). A subsequent change to east-west compression resulted in major upright folding about upright north-trending axes and formation of a pervasive axial planar cleavage, accompanied by regional metamorphism. This second phase of deformation corresponds to the regional D_2 event of Bell (1983), dated at about 1550 Ma (Page, 1988).

Faulting in the Gorge Creek sector of the Quilalar Fault Zone, along the western and eastern boundaries of the Rifle Creek Block, and along the eastern boundary of the Orient Block, commenced either shortly after the D_2 folding, towards the end of the Isan Orogeny, or sometime later. Repeated reactivation of the faults during the Proterozoic, and possibly continuing into the Phanerozoic, resulted in the Rifle Creek and Orient Blocks being transported in a general southerly direction, relative to the LRFT, for tens of kilometres to their present position. The Quilalar Fault Zone may be the reactivated eastern margin of the rift or basin in which the Bottletree and Mount Guide Quartzite of cover sequence 2 were deposited. However, there is no convincing sedimentological or structural evidence to suggest that this margin was a narrow belt of faults like the present day Quilalar Fault Zone; in the southern part of the Gorge Creek sector and northern part of the Rifle Creek Block, this fault zone cuts northerly dipping Bottletree Formation and Mount Guide Quartzite, which before faulting must have continued for a considerable, though unknown, distance eastwards.

Summary of conclusions

1. The Quilalar Fault System includes the Quilalar Fault Zone which separates the Leichhardt River Fault Trough of the Western Fold Belt from the Kalkadoon-Leichhardt Belt to the east. Displacement along this zone, and along other major faults of the Quilalar Fault System, postdates the main folding event (D_2) of the Isan Orogeny, and was probably of dextral strike-slip type.

2. The Gorge Creek sector of the Quilalar Fault Zone is a complex of anastomosing faults displacing mainly Myally Subgroup and Quilalar Formation of cover sequence 2 and Surprise Creek Formation and Mount Isa Group (Warrina Park Quartzite and Moondarra Siltstone) of cover sequence 3.

3. The West Leichhardt Klippe, to the east of the Gorge Creek sector, is an imbricate thrust stack underlain by a floor thrust, which has been folded into a major syncline and complexly faulted. The rocks of the klippe are assigned to the Eastern Creek Volcanics and Myally Subgroup of the Haslingden Group and to the Quilalar Formation. The thrusts, possibly propagated from a decollement within metabasalt of the Eastern Creek Volcanics, indicate north over south movement and north-south compression. In contrast, folding of the imbricate stack to form the major syncline resulted from east-west compression. Both the thrusting and subsequent folding took place during the Isan Orogeny, the thrusting being correlated with D_1, and the folding and associated cleavage with D_2 of Bell (1983). Faults along the eastern and western sides of the klippe may represent in part the floor thrust of the imbricate stack, but some movement along them postdates the D_2 syncline; however, these faults predate a northeast-striking mafic dyke which was metamorphosed before the end of the Isan Orogeny.

4. The fault-bounded Rifle Creek Block consists of basement, cover sequence 1 (Leichhardt Volcanics), Kalkadoon Granite, and mafic dykes, and overlying cover sequence 2 (Eastern Creek Volcanics, Myally Subgroup, Quilalar Formation) and cover sequence 3 (Bigie Formation, Surprise Creek Formation, Mount Isa Group). During the Isan Orogeny, these rocks were affected first by thrusting resulting from north-south compression (D_1), with a decollement zone at some depth beneath cover sequence 2, and then by folding about upright north-striking axial planes indicative of east-west compression (D_2). Subsequently the block was transported many kilometres along the Quilalar Fault Zone, probably in a dextral sense, to its present position alongside the Leichhardt River Fault Trough to the west. The smaller Orient Block, made up of cover sequence 1 (Orient beds), Kalkadoon Granite, and cover sequence 2 (Quilalar Formation), was transported from probably the same general area at about the same time. The two blocks are bounded to the east by another major strike-slip fault (also dextral?), separating them from the adjacent part of the Kalkadoon-Leichhardt Belt. Movement on the strike-slip faults began after the D_2 folding event, although possibly before the end of the Isan Orogeny, and may have continued into the Phanerozoic.

Acknowledgements

Discussions with P.R.Williams and A.J.Stewart, and reviews of the original manuscript by two anonymous referees, are gratefully acknowledged.

References

BELL, T.H., 1983 - Thrusting and duplex formation at Mount Isa, Queensland, Australia. *Nature* 304, 493-497.

BLAKE, D.H., 1981 - Intrusive felsic-mafic net-veined complexes in north Queensland. *BMR Journal of Australian Geology & Geophysics 6, 95-99.*

BLAKE, D.H., 1987 - Geology of the Mount Isa Inlier and environs, Queensland and Northern Territory. *Bureau of Mineral Resources, Australia, Bulletin* 225, 83 pp.

BLAKE, D.H., 1991a - Geology of the West Leichhardt Klippe and the Gorge Creek Sector of the Quilalar Fault Zone (1:50 000 scale map). *Bureau of Mineral Resources, Australia.* Available as a colour electrostatic plot on paper (AUD30), or in digital form on optical disc or Exabyte 8 mm tape (prices on application) both of which can be displayed on Intergraph Microstation software on computers that will run Unix. The digital data comprise a scanned raster image (.RLE format) of the black and white geological map, and an Intergraph vector design file containing the boundaries of coloured polygons. The coloured map and data are available from the Publication Sales Centre, Bureau of Mineral Resources, and an uncoloured Ozalar film or paper copy (AUD20) of the map is available from BMR Copy Service, both at GPO Box 378, Canberra, ACT, 2601, Australia. All orders to be prepaid to Collector of Public Monies.

BLAKE, D.H., 1991b - Geology of the Rifle Creek Region (1:50 000 scale map). *Bureau of Mineral Resources, Australia* (2 sheets). Available as colour electrostatic plots on paper (AUD30), or in digital form on optical disc or Exabyte 8 mm tape (prices on application) both of which can be displayed on Intergraph Microstation software on computers that will run Unix. The digital data comprise a scanned raster image (.RLE format) of the black and white geological map, and an Intergraph vector design file containing the boundaries of coloured polygons. The coloured map and data are available from the Publication Sales Centre, Bureau of Mineral Resources, and an uncoloured Ozalar film or paper copy (AUD20) of the map is available from BMR Copy Service, both at GPO Box 378, Canberra, ACT, 2601, Australia. All orders to be prepaid to Collector of Public Monies.

BLAKE, D.H., this volume - The compressional Lake Mary Kathleen Fold and Thrust Zone, Mount Isa Inlier. *In:* STEWART, A.J., & BLAKE, D.H. (Editors),

Detailed Studies of the Mount Isa Inlier. *Bureau of Mineral Resources, Australia, Bulletin* 243.

BLAKE, D.H., ETHERIDGE, M.A., PAGE, R.W., STEWART, A.J., WILLIAMS, P.R., & WYBORN, L.A.I., 1990 - Mount Isa Inlier - regional geology and mineralisation. *In:* HUGHES, F.E. (Editor), Geology of the Mineral Deposits of Australia and Papua New Guinea. *Australasian Institute of Mining and Metallurgy, Monograph* 14, 915-925.

BLAKE, D.H., & PAGE, R.W., 1988 - Early Proterozoic migmatitic basement in the Kalkadoon-Leichhardt Belt of the Mount Isa Inlier, northwest Queensland. *BMR Journal of Australian Geology & Geophysics* 10, 323-328.

BLAKE, D.H., & STEWART, A.J., 1988 - Block and possible terrane boundaries in the Mount Isa Inlier. *BMR Research Newsletter,* 9, 2-3.

BMR, 1979 - Prospector, Queensland - 1:100 000 Geological Series, Sheet 6857. *Bureau of Mineral Resources, Australia.*

BULTITUDE, R.J., BLAKE, D.H., MOCK, C.M., & DONCHAK, P.J.T., 1982 - Duchess region, Queensland. *Bureau of Mineral Resources, Australia, 1:100 000 Geological Map Commentary,* 35 pp.

DERRICK, G.M., WILSON, I.H., HILL, R.M., GLIKSON, A.Y., & MITCHELL, J.E., 1977 - Geology of the Mary Kathleen 1:100 000 Sheet area, northwest Queensland. *Bureau of Mineral Resources, Australia, Bulletin* 193, 114 pp.

DERRICK, G.M., WILSON, I.H., & SWEET, I.P., 1980 - The Quilalar and Surprise Creek Formations - new Proterozoic units from the Mount Isa Inlier: their regional sedimentology and application to regional correlations. *BMR Journal of Australian Geology & Geophysics 5, 215-223.*

ERIKSSON, K.A., & SIMPSON, E.L., 1990 - Recognition of high- frequency sea-level fluctuations in Proterozoic siliclastic tidal deposits, Mount Isa, Australia. *Geology 18, 474-477.*

GSQ, 1983 - Cloncurry, Queensland - 1:250 000 Geological Series, Sheet SF/54-2, 2nd Edition. *Department of Mines, Queensland.*

HENDERSON, G.A.M., & BAIN, J.H.C., 1991 - Geology of the Haslingden Group, East Moondarra area (1:35 000 scale map). *Bureau of Mineral Resources, Australia.*

JACKSON, M.J., SIMPSON, E., & ERIKSSON, K.A., 1990 - Facies and sequence stratigraphic analysis in an intracratonic, thermal-relaxation basin: the Early Proterozoic, Lower Quilalar Formation and Ballara Quartzite, Mount Isa Inlier, Australia. *Sedimentology* 37, 1053-1078.

LOOSVELD, R., & SCHREURS, G., 1987 - Discovery of thrust klippen, northwest of Mary Kathleen, Mount Isa Inlier, Australia. *Australian Journal of Earth Sciences* 34, 387-402.

PAGE, R.W., 1983 - Timing of superposed volcanism in the Proterozoic Mount Isa Inlier, Australia. *Precambrian Research* 21, 223-245.

PAGE, R.W., 1988 - Geochronology of Early to Middle Proterozoic fold belts in northern Australia: a review. *Precambrian Research* 40/41, 1-19.

PAGE, R.W., & BELL, T.H., 1986 - Isotopic and structural responses of granite to successive deformations and metamorphism. *Journal of Geology* 94, 365-379.

SIMPSON, E.L., & ERIKSSON, K.A., 1991 - Depositional facies and controls on parasequence development in siliclastic tidal deposits from the early Proterozoic, upper Mount Guide Quartzite, Mount Isa Inlier, Australia. *Canadian Society of Petroleum Geologists, Memoir* 16, 371-387.

WELLMAN, P., this volume - Structure of the Mount Isa region inferred from gravity and magnetic anomalies. *In:* STEWART, A.J., & BLAKE, D.H. (Editors), Detailed Studies of the Mount Isa Inlier. *Bureau of Mineral Resources, Australia, Bulletin* 243.

WILLIAMS, P.R., & BLAKE, D.H., this volume - Black Mountain - a strike-slip pull-apart structure in the Quilalar Fault System, Mount Isa Inlier. *In:* STEWART, A.J., & BLAKE, D.H. (Editors), Detailed Studies of the Mount Isa Inlier. *Bureau of Mineral Resources, Australia, Bulletin* 243.

WILSON, I.H., & DERRICK, G.M., 1983 - Definitions of two new stratigraphic units in the Alsace and Myally 1:100 000 Sheet areas, northwestern Queensland. *Queensland Government Mining Journal* 84, 112-115.

WYBORN, L.A.I., & PAGE, R.W., 1983 - The Proterozoic Kalkadoon and Ewen Batholiths, Mount Isa Inlier, Queensland: source, chemistry, age, and metamorphism. *BMR Journal of Australian Geology & Geophysics* 8, 51-69.

Page 180 is blank.

The compressional Lake Mary Kathleen Fold and Thrust Zone, Mount Isa Inlier

D.H.Blake [1]

This paper is based on the following map:

Blake, D.H., 1991. Geology of the Lake Mary Kathleen Zone (1:50 000 scale map). Bureau of Mineral Resources, Canberra.

The Lake Mary Kathleen Fold and Thrust Zone is a north-trending band in the Kalkadoon-Leichhardt Belt characterised by steeply east-dipping fault-bounded stratigraphic repetitions, interpreted as thrust imbricates and, in the north, tight northerly-plunging upright folds. The imbricates are formed of Leichhardt Volcanics (felsic, dated at around 1865 Ma), Kalkadoon Granite (emplaced about 1860 Ma ago), mafic dykes, and unconformably overlying eastward-facing Magna Lynn Metabasalt, Argylla Formation (felsic volcanics, 1783 Ma), and Ballara Quartzite (in east). The folds in the north affect metasediments, mapped as Quilalar Formation, that overlie Argylla volcanics to the south and are fault-bounded to the east and west. A regional foliation is subparallel to the axial planes of these folds and also to the thrust imbricates. The folding, thrusting, and foliation are attributed to a single phase of east-west compression - the 1550 Ma D_2 event of the Isan Orogeny. The main thrusts are presumed to connect at depth with a decollement well below the Magna Lynn Metabasalt unconformity, and to have been mainly gently dipping initially, before becoming steepened as deformation continued. Post-D_2 faults, with trends mainly between north and northwest, are predominantly strike-slip features that may be related to the Quilalar Fault System to the west.

[1]Bureau of Mineral Resources, GPO Box 378, Canberra, ACT, 2601, Australia.

Introduction

The Lake Mary Kathleen Fold and Thrust Zone is centred on Lake Mary Kathleen in the Mary Kathleen 1:100 000 sheet area, where it extends for at least 30 km from north to south in the Kalkadoon-Leichhardt Belt, and is up to 7 km wide (Figs. 1, 2; Blake, 1991). It is characterised by fault-bounded repetitions, aligned parallel to the length of the zone, of three volcanic units (Leichhardt Volcanics, Magna Lynn Metabasalt, and Argylla Formation); these repetitions are interpreted as thrust imbricates. Major north-plunging folds are present in the north, affecting overlying sedimentary rocks of the Quilalar Formation. The Ballara Quartzite and Corella Formation, correlatives of the Quilalar Formation, crop out to the northeast and east. All these units are regionally metamorphosed to upper greenschist/lower amphibolite facies, and generally show a strong subvertical foliation subparallel to the main faulting direction and to the axial planes of the major folds in the north.

Stratigraphy

The stratigraphy of the Lake Mary Kathleen Zone is summarised in Figure 3. The oldest rocks exposed belong to the felsic Leichhardt Volcanics of cover sequence 1 (Blake, 1987). This formation was intruded by comagmatic granite of the Kalkadoon Batholith and subsequently by mafic dykes before being overlain unconformably by cover sequence 2, represented by Magna Lynn Metabasalt, Argylla Formation, Quilalar Formation, Ballara Quartzite, and Corella Formation. The Leichhardt Volcanics and Kalkadoon Granite are dated at around 1860 Ma and the Argylla Formation at about 1780 Ma (Page, 1983a).

Intrusions of felsic porphyry probably related to the Argylla volcanism cut the Leichhardt Volcanics, Magna Lynn Metabasalt, and the lower part of the Argylla Formation. Younger metadolerite dykes intrude the Argylla Formation in the east, and much younger dykes of unmetamorphosed dolerite crop out near Lake Mary Kathleen (e.g., in the northern part of the spillway). The youngest dykes postdate the regional metamorphism and cleavage, and may be correlated with the unmetamorphosed Lakeview Dolerite exposed to the east, which has been dated by Rb/Sr at about 1115 Ma (Page, 1983b). No intrusions have been found within the Quilalar Formation or Ballara Quartzite in the Lake Mary Kathleen Zone.

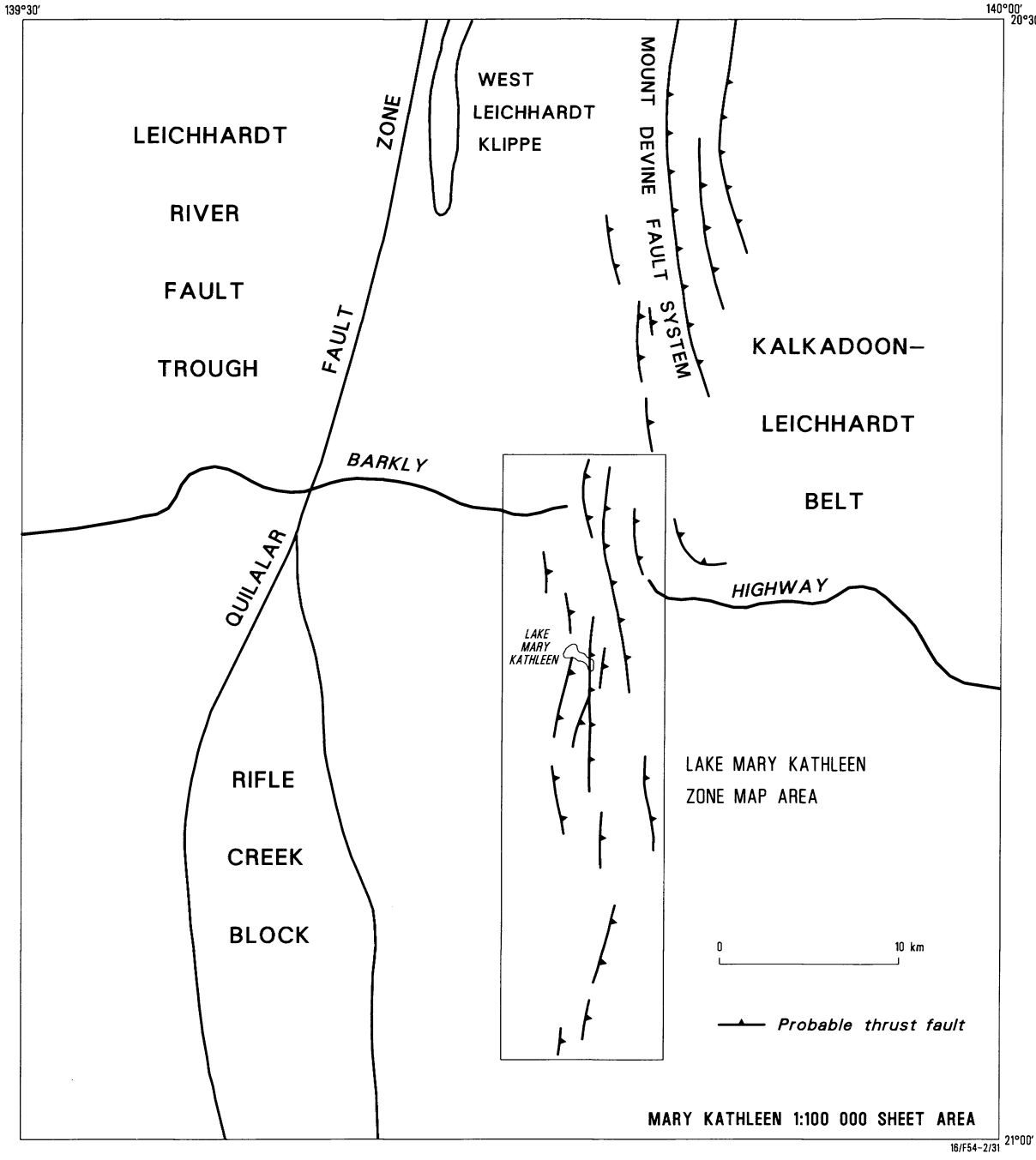


Fig. 1. Locality map.

The *Leichhardt Volcanics* (Pel), which are probably several kilometres thick, consist of recrystallised, gneissic to locally schistose, dacitic to rhyolitic metavolcanics. These are pale to medium grey where fresh, and typically contain small quartz and white feldspar phenocrysts and streaky clots of fine biotite set in a fine-grained recrystallised groundmass; the biotite clots commonly show a subvertical lineation. The felsic volcanics, unlike those of the younger Argylla Formation, are either nonmagnetic or only weakly magnetic. Most are probably ignimbrites, although flow-banded lava flows and bands of bedded feldspathic sandstone (fluvial?), tuff (air-fall?), and agglomerate or conglomerate are present in places (Figs. 4, 5). Highly altered rocks formed largely of fine white mica are common along shear zones and faults, and also at the unconformity with the overlying Magna Lynn Metabasalt, where they may represent a palaeoregolith.

The *Magna Lynn Metabasalt* (Pem) consists mainly of metabasalt lava flows, but also includes generally minor interlayered sedimentary and pyroclastic beds and, locally

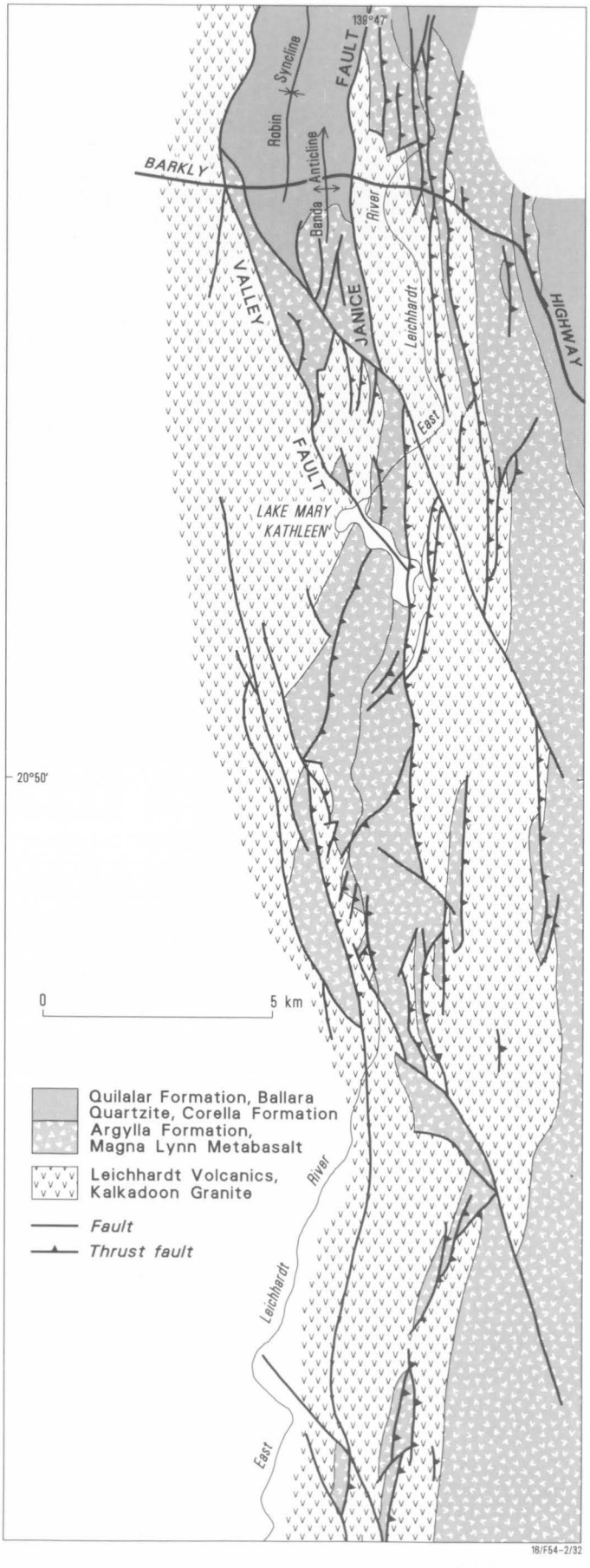


Fig. 2. Simplified geological map of the Lake Mary Kathleen Fold and Thrust Zone (after Blake, 1991a).

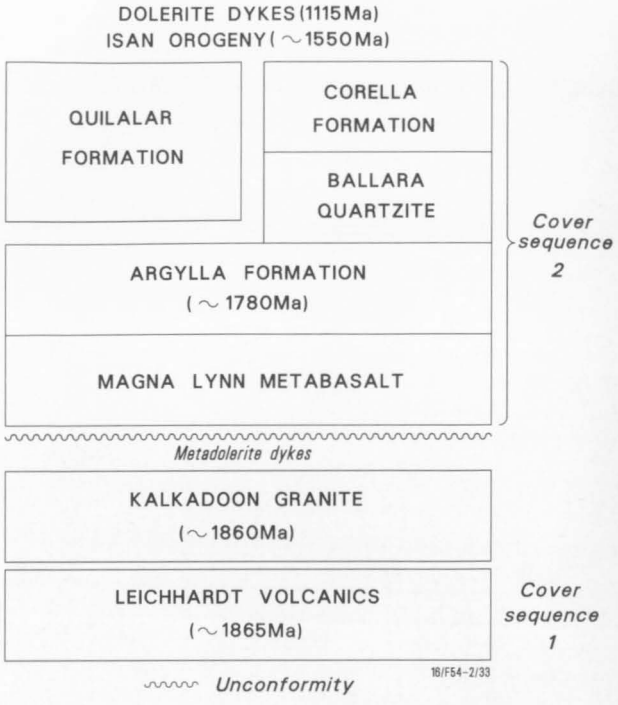


Fig. 3. Stratigraphy, Lake Mary Kathleen Fold and Thrust Zone.



Fig. 4. Thinly bedded tuff in Leichhardt Volcanics east of Lake Mary Kathleen (at grid reference 756026). Bedding is parallel to the regional D_2 foliation.

near the top, metadacite lava of Argylla type. A range in apparent thickness from less than 100 m to more than 100 m can be attributed, at least in part, to later faulting and thrusting. The mafic lavas give rise to smooth dark tones on airphotos, in marked contrast to adjacent felsic and quartz-rich rocks. They vary from massive to amygdaloidal, scoriaceous, or autobrecciated (Fig. 6), are mostly strongly magnetic, and generally show the regional subvertical north-south foliation. Fragmental and amygdaloidal metabasalt is commonly calcareous, actinolitic, and epidotic.

Where the formation is dominated by mafic lava, there are commonly one or two bands up to 10 m thick of variably lithic sandstone metamorphosed to white, greenish (epidotic), or greyish (lithic) quartzite. These bands form upstanding ribs which are white on airphotos. Some of them are boudinaged and contorted. Cross-bedding indicates younging, almost invariably to the east. Most lithic clasts in the quartzite bands appear to be of locally derived basalt. There are also local lenses of thinly bedded biotite-rich metasediments possibly representing palagonite tuff, pale grey to pinkish felsic tuff, and impure calcareous metasediments. Porphyroblasts of garnet and actinolite are present in some of the schistose mafic metasediments.

In the west of the Lake Mary Kathleen Zone, the Magna Lynn Metabasalt includes a metasedimentary sequence more than 100 m thick, mapped as unit Pem_s. This unit comprises quartzose to highly lithic and feldspathic sandstones of various shades of pink and grey, epidotic quartzite, calcareous sandstone and siltstone, impure marble, calc-silicate rock, conglomerate with felsic volcanic and quartzite clasts, and minor metabasalt flows.

Rock types present at the unconformity with underlying Leichhardt Volcanics include massive, amygdaloidal, and fragmentary mafic lava; bedded mafic tuff; quartzose sandstone; and regolithic breccia in which angular fragments of felsic rock are enclosed in a dark, fine-grained, 'basaltic' matrix.

The Magna Lynn Metabasalt is overlain conformably by felsic volcanics of the Argylla Formation. The contact ranges from sharp to a 100 m-thick transition zone of interbanded metabasalt, dacitic lava, ignimbritic felsic porphyry, and mafic to felsic bedded tuff. At one locality (grid reference 766022), veins of leucogranite cut the Magna Lynn Metabasalt.

The *Argylla Formation* (Pea) crops out in the east and north of the Lake Mary Kathleen Zone, where it is characterised by moderately to strongly magnetic massive

felsic volcanics. These appear to be ignimbrites rather than lavas, as they do not show any flow-banding. They are mostly purplish pink to purplish grey, and typically contain phenocrysts of pink feldspar which are appreciably larger than the feldspar phenocrysts in the older Leichhardt felsic volcanics. Also present, mainly in the lower part of the formation, are highly magnetic flows of metabasalt, sparsely porphyritic, dark grey metadacite containing scattered amygdales and sparse feldspar phenocrysts, and pink and grey bedded felsic tuff. Planar and cross-bedded volcaniclastic rocks and quartz sandstone occur in the upper part of the formation in the east; the volcaniclastics range from very fine-grained to conglomeratic, and from thick-bedded to laminated.

The Argylla Formation is overlain either conformably or disconformably by Quilalar Formation in the north and Ballara Quartzite in the east. The contact with Quilalar Formation is complicated by faulting, but the presence at the base of the Quilalar Formation at one locality (grid reference 718073) of conglomerate consisting of pebbles and cobbles of Argylla porphyry in a calcareous mudstone matrix suggests an erosional contact, at least at this locality, between the two formations. A small body of diorite and gabbro intrudes the Argylla Formation at grid reference 770010 (Blake, 1991) .

The thickness of the Argylla Formation in the Lake Mary Kathleen Zone is uncertain, because of structural complexities, but is probably of the order of 1 km.

The *Quilalar Formation* (Pq) crops out in the Robin Syncline and Banda Anticline area, in the northern part of the Lake Mary Kathleen Zone, bounded to the east and west by major faults (Fig. 2; Blake, 1991). It was mapped as Charley Creek Formation by Carter & others (1961), and as Ballara Quartzite by Derrick & others (1977); however, the unit is generally finer-grained and more calcareous than typical Ballara Quartzite, and is considered by Jackson & others (1990) to represent trough deposits of the Quilalar Formation, whereas the Ballara Quartzite represents correlative platform deposits.

The Quilalar Formation here consists of calcareous, lithic, and feldspathic sandstones, variably calcareous siltstone and mudstone, calc-silicate rock, impure marble, and minor basal conglomerate (all map unit Pq), and four bands, each less than 50 m thick, of ridge-forming quartzite (Pq_q). It appears to have a total thickness of at least 1000 m. Sedimentary facing is given by graded bedding, cross-bedding, slumps, and scours. The sequence has been folded into upright northerly-plunging anticlines and synclines, and an axial planar cleavage is generally well

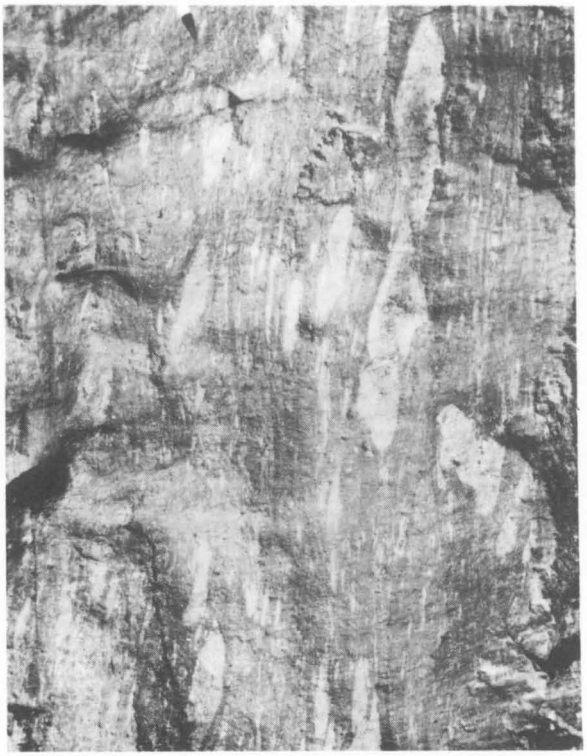


Fig. 5. Coarse pyroclastic rock within the Leichhardt Volcanics east of Lake Mary Kathleen (at grid reference 758028). The felsic rock fragments are flattened parallel to the D_2 foliation.



Fig. 6. Margin of mafic lava flow, with fragments of scoriaceous metabasalt in a matrix of quartzose arenite. Foliated Magna Lynn Metabasalt overlying Leichhardt Volcanics below the East Leichhardt Dam (at grid reference 734018).

developed. The two largest folds are the Robin Syncline and Banda Anticline. The formation is conformable or disconformable on Argylla Formation (see above).

The Ballara Quartzite (Pkb) forms prominent ridges on the eastern side of the Lake Mary Kathleen Zone, where it consists of steeply dipping well bedded white quartz sandstone metamorphosed to quartzite. It conformably or disconformably overlies felsic volcanics of the Argylla Formation to the west, and corresponds to the platform deposits of the Quilalar Formation (Jackson & others, 1990).

The Corella Formation (Pkc) crops out in the northeast of the Lake Mary Kathleen Zone. It is conformable on Ballara Quartzite, and consists mainly of calcareous metasediments not unlike those of the Quilalar Formation in the Robin Syncline.

Igneous intrusions

Several phases of *Kalkadoon Granite* (Pgk) intrude the Leichhardt Volcanics in the north and west of the Lake Mary Kathleen Zone. Most of this granite in the northeast, near the Barkly Highway, is a pink medium to coarse-grained apparently non-foliated leucocratic variety, similar to the Wills Creek Granite in the Duchess 1:250 000 sheet area to the south (Blake & others, 1984), and is probably a high-level granite. In the west the Kalkadoon Granite is represented by grey porphyritic granodiorite, richly xenolithic granite, leucogranite, and pegmatite, all weakly to strongly foliated and partly recrystallised.

Numerous dykes of metamorphosed dolerite, now *amphibolite,* intrude the Leichhardt Volcanics and Kalkadoon Granite. They range from less than a metre to several tens of metres in thickness, and have fine-grained and commonly schistose margins merging into coarser interiors. Some have feldspar phenocrysts and a few contain abundant felsic rock fragments (pebble dykes), as at grid references 737076 and 761913. At the last locality, angular to subangular fragments of felsic volcanic rocks and vein quartz, up to a metre or more across, are concentrated on the west side of a vuggy 40 m-wide mafic dyke cutting Leichhardt Volcanics.

The great majority of the mafic dykes probably predate the Magna Lynn Metabasalt; they are nonmagnetic, unlike the mafic lavas of this unit, and some are seen to be overlain unconformably by metabasalt. However, a few may be intrusive equivalents of the Magna Lynn Metabasalt, and some may be of similar age to mafic dykes intruding Argylla Formation east of the map area.

Several intrusions of foliated purplish grey to grey weakly to strongly magnetic *feldspar porphyry* cut the Leichhardt Volcanics, Magna Lynn Metabasalt, and the lower part of the Argylla Formation, forming discordant and concordant sheets, pods, and irregular bodies. These intrusions are most voluminous in the south of the Lake Mary Kathleen Zone, where they are up to 1000 m thick. Intrusive contacts are highly irregular in places, and some are marked by streaky hybrid or mixed zones. The intrusions are considered to be subvolcanic equivalents of petrographically similar Argylla extrusives.

Distinction between mafic intrusions and extrusions

A major problem in the Lake Mary Kathleen Zone, and in other parts of the Mount Isa Inlier where there are abundant deformed and metamorphosed mafic igneous rocks, is the distinction between mafic intrusions and mafic lava flows and pyroclastics. Features to bear in mind in interpreting which is which in the Mount Isa Inlier include the following:

Mafic lavas are typically heterogeneous – in a single exposure they can range from massive to amygdaloidal to scoriaceous to autobrecciated; this heterogeneity is commonly evident even in the most metamorphosed and deformed areas, as amygdales in particular can usually be identified, and many flow-margin breccias have a recognisable sedimentary matrix. Lava flows are also commonly interlayered with thin sedimentary bands.

Mafic tuffs are typically well bedded, with sedimentary layering marked by abrupt changes in grain-size and composition, and some show cross-bedding.

Mafic intrusions are typically homogeneous overall, although, like lavas, they may be streaky in highly deformed zones. They normally show a gradual increase in grain-size from their margins, which are commonly schistose, to their generally more massive centres. Several intrusions, but few lavas, contain tabular feldspar phenocrysts 5-10 mm long. Intrusions are rarely amygdaloidal, unlike lavas.

Deformation

All the Proterozoic rocks in the Lake Mary Kathleen Zone except the young dolerite dykes, as in other parts of the Mount Isa Inlier, were deformed and metamorphosed during the Isan Orogeny (Blake & others, 1990). This orogeny is generally considered to consist of two main phases, an early phase at about 1610 Ma (D_1) associated with north-south compression, and a later phase (D_2) of

east-west compression at around 1550 Ma. Only structures related to the later phase have been recognised in the Lake Mary Kathleen Zone. These include major folds in the north, numerous faults interpreted as early D_2 thrusts that were steepened later in D_2, and the regional north-trending subvertical foliation. The D_2 structures are cut by younger faults.

Regional metamorphism probably accompanied the D_2 folding and thrusting. Metamorphic mineral assemblages of plagioclase (albite-andesine) ± quartz, microcline, biotite, muscovite, green hornblende, epidote, garnet, and chlorite in mafic rocks, and of quartz + microcline + biotite + muscovite ± sodic plagioclase, chlorite, and epidote in felsic rocks, indicate upper greenschist or lower amphibolite facies. Much or all of the chlorite present in these rocks may be retrogressive.

No evidence has been found in the Lake Mary Kathleen Zone of a post-1800 Ma extensional event predating the Isan Orogeny, such as that identified in some parts of the Kalkadoon-Leichhardt Belt (e.g., Passchier, 1986; Passchier & Williams, 1989; Stewart, 1989; Holcombe & others, this volume). Nevertheless, the possibility that some of the thrusts in the zone were originally low-angle normal (extensional) faults that were later reactivated as reverse faults cannot be discounted.

Folding

The Quilalar Formation in the north is folded into northerly-plunging anticlines and synclines, the largest of which are the Robin Syncline and Banda Anticline. These folds have steeply dipping limbs and subvertical north-striking axial planes, and are presumed to have formed in response to east-west compression during D_2. They are cut by, and hence predate, major faults to the east and west.

A small tight northerly-trending syncline in Magna Lynn Metabasalt on the southwest side of Lake Mary Kathleen (at grid reference 730003) is possibly related to the east-west thrusting described below.

Faulting/thrusting

Two main phases of faulting are apparent in the Lake Mary Kathleen Zone: an early phase predating or synchronous with the regional D_2 foliation, and a later phase postdating this foliation. The amount of displacement on individual faults is conjectural in all cases.

The **early faults** are commonly marked by breccia, quartz veining, and alteration zones showing the D_2 foliation. Most of these faults strike north, parallel or subparallel to bedding and stratigraphic contacts, and are downthrown to the west. Many can be traced for several kilometres. Individual fault slices range in thickness from less than 10 m to more than a kilometre. Within each slice the strata dip and young eastwards, with bedding dips ranging from 20-90°, but generally being steeper than 60°. Stretching lineations in rocks adjacent to the faults, and elsewhere in the Lake Mary Kathleen Zone, are generally steep down-dip on the foliation, implying dip-slip rather than strike-slip movement.

The early faults are inferred to be subvertical or steeply east-dipping, like most bedding, but no dips or dip directions have been measured on any of them. Because they cause stratigraphic repetitions, rather than omissions, and are mostly subparallel to bedding, they are considered to represent a series of thrusts resulting from east-west compression. These thrusts are presumed to have been mainly gently dipping before becoming steepened as compression continued. No roof or floor thrusts have been identified, so an imbricate stack, rather than a thrust duplex, is proposed. Lateral thrust ramps may be represented by relatively short early faults oblique to bedding.

The thrusts are inferred to be listric at depth, flattening out eastwards to join a floor thrust (decollement zone) located somewhere within underlying Leichhardt Volcanics or Kalkadoon Granite (Blake, 1991), perhaps within what was the brittle/ductile transition zone at the time of thrusting.

The thrusted repetitions of stratigraphic units are clearly evident where contrasting rock types, such as mafic and felsic volcanics, are juxtaposed, or where a distinctive rock, such as a band of bedded tuff, is repeated, but not where the thrust lies within massive mafic or felsic volcanics. Consequently, many more thrusts may be present than shown on the map. Unmapped thrusts could account for some apparently excessive stratigraphic thicknesses in parts of the area, such as that of the Magna Lynn Metabasalt south of Lake Mary Kathleen.

Major **late faults**, tens of kilometres long and striking mainly between north and northwest, cut across and displace the earlier thrusts. Many of these late faults are marked along parts of their length by ridge-forming quartz veins that post-date the regional foliation; the most prominent quartz ridge marks a northwest-striking fault in the south of the zone. The late faults include the Valley and Janice Faults, which mark the western and eastern boundaries, respectively, of the Quilalar Formation outcrop. The Valley Fault joins southwards with an anastomosing series of faults, one of which swings

southeast to join the Janice Fault 2 km north of the East Leichhardt Dam.

The major late faults do not correspond with abrupt changes in metamorphic grade, and are therefore inferred to have had mainly strike-slip, rather than vertical, movements. Some, such as the Janice Fault, may have horizontal displacements of tens of kilometres. These large faults could be related to the Quilalar Fault System of the Rifle Creek area to the west (Blake, this volume) and the Lake Julius area to the north (BMR, 1986). Their ages are uncertain; the faults postdate D_2 folds and thrusts, but could have been initiated before the end of the Isan Orogeny, perhaps during the D_3 phase that was synchronous with the Cu mineralisation at Mount Isa mine (Perkins, 1984; Swager & others, 1987; Bell & others, 1989). Some may have been D_2 thrusts subsequently reactivated as strike-slip faults. The larger faults, such as the Leichhardt and Janice Faults, may have remained active well into the Phanerozoic, like some of the other major north-striking faults in the Mount Isa Inlier (Blake & Stewart, 1988).

Discussion

Both the folding and thrusting in the Lake Mary Kathleen zone are attributed to east-west compression, and are considered to have formed during the same deformation event – the regional D_2 phase of the Isan Orogeny, dated at about 1550 Ma (e.g., Page, 1988). The well-bedded sedimentary rocks of the Quilalar Formation responded to the compression by folding about north-trending axes while thrusts developed in underlying mainly nonbedded igneous rocks (see Blake, 1991). The thrusts in the Lake Mary Kathleen Zone, therefore, differ from those identified to the west – in the Leichhardt River Fault Trough by Bell (1983) and in the West Leichhardt Klippe and Rifle Creek Block by Blake (this volume), as these are attributed to north-south compression during D_1. Thrusts recognised in the Eastern Fold Belt to the east, in the Tommy Creek area (Hill, 1987; Hill & others, this volume) and the Soldiers Cap area (Loosveld, 1989 and this volume), are also ascribed to D_1.

The thrusts mapped in the Lake Mary Kathleen Zone probably extend to the north and east, north of the Barkly Highway, to join the Mount Devine Fault System (Fig. 1) of Derrick & others (1977). This fault system is marked by several repetitions of eastward-facing cover sequence 2 units (mainly Argylla, Ballara, and Corella formations), and is described by Derrick & others as a series of north-trending normal or perhaps high-angle reverse faults or thrusts that may have been steepened during subsequent folding.

Conclusions

- Fault-bounded stratigraphic repetitions from west to east across the Lake Mary Kathleen Zone, involving mainly Leichhardt Volcanics and east-dipping and east-facing Magna Lynn Metabasalt and Argylla Formation, are attributed to thrusting. The thrusts generally strike north, implying east-west compression.

- Upright north-plunging folds of Quilalar Formation sediments in the north, and the regional foliation subparallel to the axial planes of these folds, are indicative of similar east-west compression.

- The thrusting, folding, and foliation probably took place during the same compressional phase, the thrusts forming in mainly massive igneous rocks while folds developed in overlying well-bedded Quilalar Formation. This phase is correlated with the D_2 event of the Isan Orogeny (1550 Ma).

- Most of the thrusts probably dipped gently to the east initially, and later, as compression continued, became steepened to subvertical attitudes. They are presumed to be listric at depth, propagating upwards from a decollement situated well below the base of the Magna Lynn Metabasalt.

- Later strike-slip faults post-date the D_2 deformation, but may have been initiated before the end of the Isan Orogeny. Movement along some of these faults may have continued into the Phanerozoic.

Acknowledgements

Discussions with P.R.Williams and A.J.Stewart, and a critical review by A.J.Stewart, are gratefully acknowledged.

References

BELL, T.H., 1983 - Thrusting and duplex formation at Mount Isa, Queensland, Australia. *Nature* 304, 493-497.

BELL, T.H., PERKINS, W.G., & SWAGER, C.P., 1989 -

Structural controls on development and localization of syntectonic copper mineralization at Mount Isa, Queensland. *Economic Geology* 83, 69-85.

BLAKE, D.H., 1987 - Geology of the Mount Isa Inlier and environs, Queensland and Northern Territory. *Bureau of Mineral Resources, Australia, Bulletin* 225, 83 pp.

BLAKE, D.H., 1991 - Geology of the Lake Mary Kathleen Zone (1:50 000 scale map). *Bureau of Mineral Resources, Canberra, Australia.* Available as a colour electrostatic plot on paper (AUD30), or in digital form on optical disc or Exabyte 8 mm tape (prices on application) both of which can be displayed on Intergraph Microstation software on computers that will run Unix. The digital data comprise a scanned raster image (.RLE format) of the black and white geological map, and an Intergraph vector design file containing the boundaries of coloured polygons. The coloured map and data are available from the Publication Sales Centre, Bureau of Mineral Resources, and an uncoloured Ozalar film or paper copy (AUD20) of the map is available from BMR Copy Service, both at GPO Box 378, Canberra, ACT, 2601, Australia. All orders to be prepaid to Collector of Public Monies.

BLAKE, D.H., this volume - Stratigraphy, folding, and faulting within the Quilalar Fault System, Mount Isa Inlier. *In:* STEWART, A.J., & BLAKE, D.H. (Editors), Detailed Studies of the Mount Isa Inlier. *Bureau of Mineral Resources, Australia, Bulletin* 243.

BLAKE, D.H., BULTITUDE, R.J., DONCHAK, P.J.T., WYBORN, L.A.I., & HONE, I.G., 1984. Geology of the Duchess-Urandangi region, Mount Isa Inlier, Queensland. *Bureau of Mineral Resources, Australia, Bulletin* 219, 96 pp.

BLAKE, D.H., ETHERIDGE, M.A., PAGE, R.W., STEWART, A.J., WILLIAMS, P.R., & WYBORN, L.A.I., 1990 - Mount Isa Inlier - regional geology and mineralisation. *In:* HUGHES, F.E. (Editor), Geology of the mineral deposits of Australia and Papua New Guinea. *Australasian Institute of Mining and Metallurgy, Monograph* 14, 915-925.

BLAKE, D.H., & STEWART, A.J., 1988 - Block and possible terrane boundaries in the Mount Isa Inlier. *BMR Research Newsletter* 9, 2-3.

BMR, 1986 - Transpressional strike-slip faulting in the Mount Isa Inlier. *BMR Research Newsletter* 4, 1-2.

CARTER, E.K., BROOKS, J.H., & WALKER, K.R., 1961 - The Precambrian mineral belt of north-western Queensland. *Bureau of Mineral Resources, Australia, Bulletin* 51, 344 pp.

DERRICK, G.M., WILSON, I.H., HILL, R.M., GLIKSON, A.Y., & MITCHELL, J.E., 1977 - Geology of the Mary Kathleen 1:100 000 Sheet area, northwest Queensland. *Bureau of Mineral Resources, Australia, Bulletin* 193, 114 pp.

HILL, E.J., 1987 - Structural geology of the Tommy Creek area, Mount Isa Inlier, NW Queensland. *Bureau of Mineral Resources, Australia, Record* 1987/20, 51 pp.

HILL, E.J., LOOSVELD, R.J.H, & PAGE, R.W., this volume - Structure and geochronology of the Tommy Creek Block, Mount Isa Inlier. *In:* STEWART, A.J., & BLAKE, D.H. (Editors), Detailed Studies of the Mount Isa Inlier. *Bureau of Mineral Resources, Australia, Bulletin* 243.

HOLCOMBE, R.J., PEARSON, P.J., & OLIVER, N.H.S., this volume - Structure of the Mary Kathleen Fold Belt. *In:* STEWART, A.J., & BLAKE, D.H. (Editors), Detailed Studies of the Mount Isa Inlier. *Bureau of Mineral Resources, Australia, Bulletin* 243.

JACKSON, M.J., SIMPSON, E.L., & ERIKSSON, K.A., 1990 - Facies and sequence stratigraphic analysis in an intracratonic, thermal-relaxation basin: the Early Proterozoic, Lower Quilalar Formation and Ballara Quartzite, Mount Isa Inlier, Australia. *Sedimentology* 37, 1053-1078.

LOOSVELD, R.J.H., 1989 - The intra-cratonic evolution of the central eastern Mount Isa Inlier, northwest Queensland, Australia. *Precambrian Research* 44, 243-276.

LOOSVELD, R.J.H., this volume - Structural geology of the central Soldiers Cap Belt, Mount Isa Inlier, Australia. *In:* STEWART, A.J., & BLAKE, D.H. (Editors), Detailed Studies of the Mount Isa Inlier. *Bureau of Mineral Resources, Australia, Bulletin* 243.

PAGE, R.W., 1983a - Timing of superposed volcanism in the Proterozoic Mount Isa Inlier, Australia. *Precambrian Research* 21, 223-245.

PAGE, R.W., 1983b - Chronology of magmatism, skarn formation and uranium mineralization, Mary Kathleen, Queensland, Australia. *Economic Geology* 78, 838-853.

PAGE, R.W., 1988 - Geochronology of Early to Middle Proterozoic fold belts in northern Australia: a review. *Precambrian Research* 40/41, 1-19.

PASSCHIER, C.W., 1986 - Evidence for early extensional tectonics in the Proterozoic Mount Isa inlier, Australia. *Geology* 14, 1008-1011.

PASSCHIER, C.W., & WILLIAMS, P.R., 1989 - Proterozoic extensional deformation in the Mount Isa Inlier, Queensland, Australia. *Geological Magazine* 126, 43-53.

PERKINS, W.G., 1984 - Mount Isa silica dolomite and copper orebodies: the result of a syntectonic hydrothermal alteration system. *Economic Geology* 79, 601-637.

STEWART, A.J., 1989 - Extensional faulting as the explanation for the Deighton 'Klippe' and other Mount Albert Group outliers, Mount Isa Inlier, northwestern Queensland. *Australian Journal of Earth Sciences* 36, 405-421.

SWAGER, C.P., PERKINS, W.G., & KNIGHTS, J.G., 1987 - Stratabound phyllosilicate zones associated with syntectonic copper orebodies at Mt Isa, Queensland. *Australian Journal of Earth Sciences* 34, 463-476.

Black Mountain – a strike-slip pull-apart structure in the Quilalar Fault System, Mount Isa Inlier

P.R. Williams [1] *& D.H. Blake* [1]

This paper is based on the following map:

Blake, D.H., 1991. Geology of Black Mountain, Duchess (1:5000 scale map). Bureau of Mineral Resources, Canberra.

Black Mountain is a small outlier of Quilalar Formation, surrounded by older Kalkadoon Granite, which was folded and cleaved during the Isan Orogeny. It lies within an array of linked strike-slip, hinge, and steep normal faults interpreted as a fan-shaped graben – a pull-apart structure formed within an overall dextral strike-slip environment.

[1]Bureau of Mineral Resources, Geology & Geophysics, GPO Box 378, Canberra, ACT, 2601.

Introduction

Pop-up structures, flower structures, and duplexes are characteristic features of strike-slip fault complexes (Woodcock & Fischer, 1986; Willcox & others, 1973). In the Mount Isa Inlier there are several such complexes involving large and small faults that post-date the last regional folding event; movements on the large faults were predominantly horizontal (e.g., Blake, 1987), whereas those on many of the small faults were mainly vertical. The first to recognise these features here was Lister (in BMR, 1986), who demonstrated the presence of a pop-up flower structure (largely vertical movement) related to one of several strike-slip faults in the Lake Julius area, 60 km north-northeast of Mount Isa. In this paper we suggest that the Black Mountain outlier is preserved as a pull-apart (or negative flower) structure resulting from vertical movements within the same broad zone of north-south strike-slip faults – the Quilalar Fault System.

The Black Mountain outlier is located in the west of the Kalkadoon-Leichhardt Belt 48 km south-southeast of Mount Isa, in the Duchess 1:100 000 Sheet area. It consists of well-bedded sedimentary rocks which were laid down on granite of the Kalkadoon Batholith. This batholith was emplaced at about 1860 Ma (Wyborn & Page, 1983). The sedimentary rocks were previously mapped as Surprise Creek Formation (Bultitude & others, 1982), but are now assigned to the Quilalar Formation, part of cover sequence 2 of Blake (1987), deposited at around 1760 Ma. Mafic dykes intrude the granite, but not the sedimentary rocks, and are inferred to be older than the Quilalar Formation. Cover sequence 2 was folded and metamorphosed during the 1620-1520 Ma Isan Orogeny (Blake & others, 1990).

Two phases of Isan folding are evident at Black Mountain: D_1, represented by an east-west syncline in the central west, and D_2, represented by two large northerly-plunging synclines, an intervening anticline, and several smaller folds along the D_2 synclinal axial plane traces (Fig. 2). The youngest part of the Quilalar Formation at Black Mountain is preserved in the centre of the D_1 syncline, which is folded by the western D_2 syncline. A well developed regional cleavage is axial planar to the D_2 folds, and is attributed to the same episode of deformation. D_1 and D_2 are correlated respectively with the north-south shortening D_1 event and east-west shortening D_2 event of Bell (1983). The Quilalar Fault System of major north-striking strike-slip faults developed after the folding. This fault system includes the Quilalar Fault Zone, which marks the boundary between the Leichhardt River Fault Trough of the Western Fold Belt to the west and the Kalkadoon-Leichhardt Belt to the east (Fig. 1; Blake & Stewart, 1988), and the eastern boundary fault of the Rifle Creek Block (Blake, this volume) just to the west of Black Mountain (Fig. 1).

Rock Units

The oldest rocks exposed in the Black Mountain area (Fig. 2; Blake, 1991) are felsic extrusives of the *Leichhardt Volcanics* in the east. These are separated by a major fault from *Kalkadoon Granite* to the west. Both the volcanics and granite are cut by metamorphosed mafic dykes. A palaeoregolith of rubbly and disaggregated granite is present locally at the unconformity with overlying Quilalar Formation.

The *Quilalar Formation* is represented by alternating bands 20 m to more than 100 m thick of ridge-forming

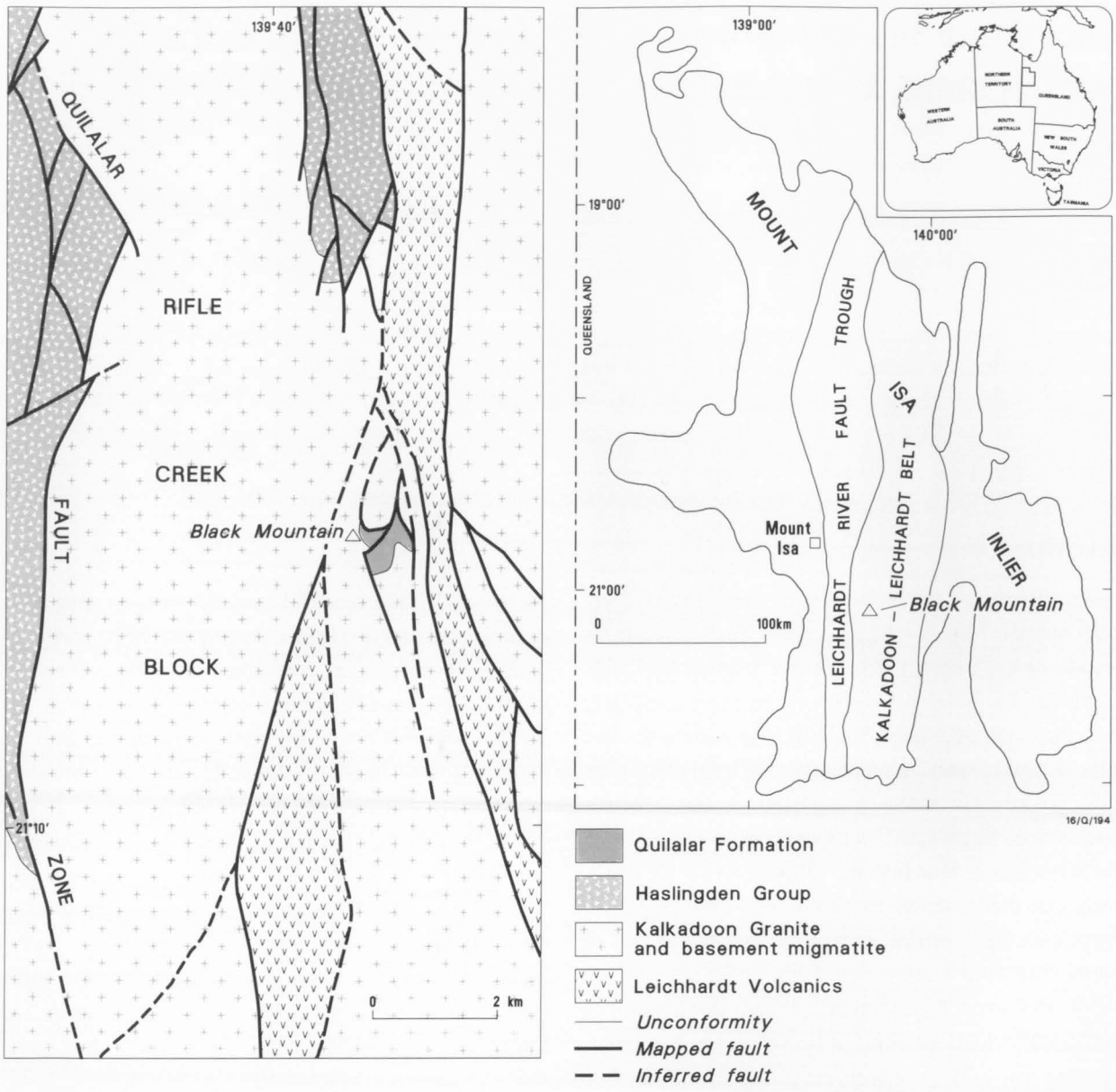


Fig. 1. Location of the Black Mountain outlier, showing the major regional faults in the immediate vicinity of the down-faulted cover sequence.

sandstone and less resistant finer-grained clastics dominated by black siltstone/mudstone. The lowest ridge-forming band, directly overlying granite, consists of basal gritty and pebbly sandstone with conglomerate lenses, overlain by interbedded iron-stained sandstone and siltstone, including some porous (calcareous?) beds, and at the top, feldspathic sandstone; cross-bedding and ripple marks are common. Conglomerate lenses near the base contain clasts of pink feldspar, vein quartz, and grey quartzite. This lowest band corresponds to the continental depositional system of Jackson & others (1990). It is overlain by a band of thinly bedded dark grey to black siltstone and paler graded-bedded and ripple-bedded sandstone. This band is separated from a higher band of similar lithology, but also including some feldspathic sandstone and highly calcareous beds, by a ridge-forming band of cross-bedded variably feldspathic sandstone with minor siltstone, silty sandstone ('wacke') and porous iron-stained (calcareous) sandstone. The succeeding ridge-forming band, the youngest preserved, consists predominantly of cross-bedded feldspathic sandstone, some of which is also calcareous. The two recessive bands and the upper two ridge-forming bands represent the storm-dominated shelf depositional system of Jackson & others (1990), laid down in the central part of the Quilalar depositional basin.

The Quilalar Formation at Black Mountain differs from that exposed in the nearby Rifle Creek Block to the west (Blake, this volume) in that it overlies Kalkadoon Granite, rather than the Haslingden Group of cover



Fig. 2. Generalised geological map of Black Mountain based on field work by DHB, showing the detailed fault array. Letters A-G refer to individual fault blocks and points W,X,Y,Z are fault intersection points referred to in the text.

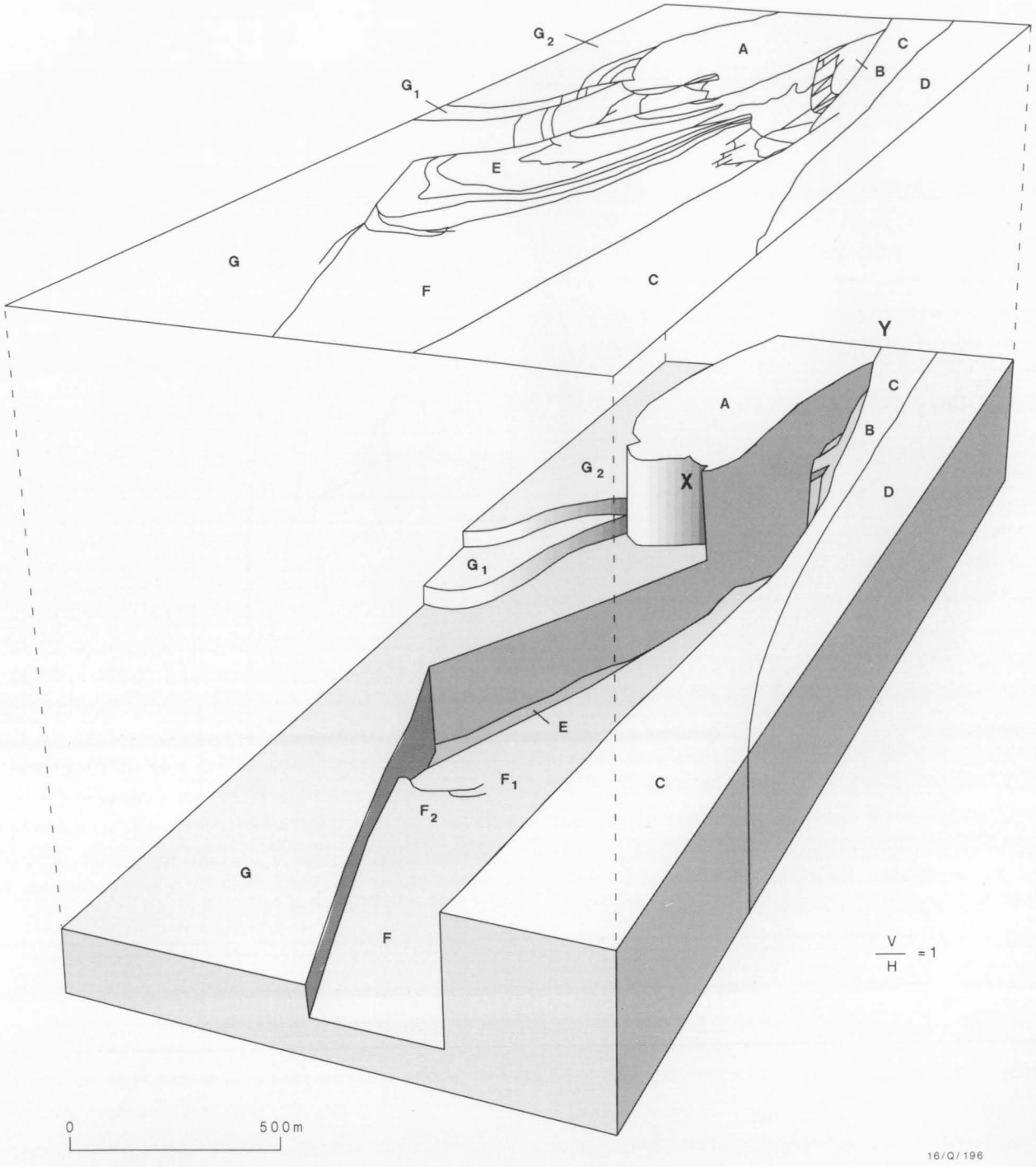


Fig. 3. Interpretation of the fault array as a pull-apart graben, using offsets consistent with the geology shown in Figure 2. Levels determined mainly from displacement of the nonconformity and the lower beds of the Quilalar Formation. Although the faults are shown as vertical, they may fan out at depth to form a negative flower structure.

sequence 2, and is characterised by feldspathic sandstone and black siltstone of storm-dominated shelf (or trough) type rather than quartz-rich sandstone of tide-dominated shelf (or platform) type. These differences indicate that Black Mountain and the Rifle Creek Block were probably many kilometres apart when the Quilalar Formation was deposited, implying subsequent major strike-slip movement along the eastern boundary fault of the Rifle Creek Block.

Fault geometry at Black Mountain

The Black Mountain area is divided by faults into seven major blocks, within which are a number of subsidiary faults. The major blocks are labelled A to G in Figures 2

and 3. Block E represents the lowest structural region. Individual faults are identified according to the blocks they separate (e.g., fault A/B separates blocks A and B).

Age of faulting

Several straight to gently curved faults cut the D_2 structures. One example is fault G/E-A/E-A/B, which crosses Black Mountain from southwest to north-northeast (Fig. 2). Displacement of the Quilalar Formation and the D_1 syncline across this fault indicates either dextral or east-side-down movement. This fault and faults to the east are not folded or rotated by D_2 folds; faults B/E and E/F offset D_2 folds and B/C and C/F truncate D_2 fold limbs. Thus all these faults post-date the regional folding.

In contrast to these straight to gently curved faults, the mapped portion of fault A/G, on the northwest side of Black Mountain, is markedly arcuate, the curvature apparently being consistent with folding during the formation of the western D_2 syncline. However, when either strike-slip or dip-slip displacement on the northeast-striking fault G/E-A/B is restored, the implied D_2 fold hinge trace defined by the curvature on fault A/G lies well to the west of the D_2 fold hinge trace defined by bedding in block E (Figs. 2, 3). Also, in block G, bedding is not rotated in harmony with the curvature on fault A/G, and the beds are clearly truncated by this fault. These observations show that the curved fault A/G either post-dates the D_2 folding or was a curved fault before to D_2. The younger age is considered the more likely, especially as the fault truncates quartz veins within the Kalkadoon Granite which were cleaved during D_2, although conclusive evidence is lacking because no cleavage has been observed parallel to this fault, and so there are no clear overprinting relationships.

Offsets

The age relationships indicate that the faults are likely to be contemporaneous, and therefore linked. The fault array can be reconstructed as a complex of hinge faults connected by subperpendicular normal fault segments forming a fan-shaped pull-apart graben within an overall dextral strike-slip setting. On this basis, geologically consistent fault offsets are shown diagramatically in Figure 3; hinge points are labelled W to Z in Figures 2 and 3. In this reconstruction the prominent northeast-striking fault G/E-A/B is inferred to have a dominantly vertical rather than horizontal movement; the apparent horizontal displacement of the basal beds of Quilalar Formation in the west by approximately 150 m implies a vertical throw of close to 200 m, east-block-down. The displacement on this fault is considered to become progressively less to the northeast, because there is no northwest-striking fault north of B/E to compensate for the downthrow of block B with respect to blocks A and C. There is also an average increase in dip of beds to the north of fault E/F (55° to 70°), which suggests a rotation on a southeast-northwest hinge between blocks E and B. Hinge point Y (Figs. 2, 3) could be located farther northeast; the zero vertical displacement between blocks A and D is arbitrary, because no Quilalar Formation is preserved on block C to provide constraints. Two smaller northeast-striking faults which offset the curved fault A/G have a better constrained hinge fault geometry. Both faults arise from the same point X and suggest an upwarp of block G2 with respect to G1, along an approximately east-west hinge, of about 90 m (30 m on the western fault and 60 m on the eastern fault). This upwarp is consistent with the change of dip of the unconformity across the faults (75° to 50°).

Block E represents the lowest structural level of the fault complex, faults to the west having east-side-down movement and faults to the east having west-side-down movement. Block F is uplifted with respect to block E, but downthrown with respect to blocks G and C. Note that the west-northwesterly segments of faults E/F and E/B define a west-northwesterly-trending segment of the central downthrown block. A secondary tear commencing at hinge point W is the locus of uplift of block F2 with respect to block F1, and a similar tear arises from the intersection of the two segments of fault E/F (point Z in Fig. 3). The overall downthrow of north-side-down blocks on faults E/F and E/G is less than the southerly downthrow across A/G and B/E. Consequently, block G in the south of the area is lower than the Kalkadoon Granite of blocks A, B, and C.

There is no direct evidence of the movement direction on the fault marking the western margin of block C, nor on the fault C/D. Fault C/B-F may have a significant vertical component of movement, as the Quilalar Formation is downthrown with respect to the Kalkadoon Granite, but the unconformity is not exposed east of the fault, and so the movement could be largely strike-slip. Similarly, there is no control on the movement direction on fault C/D. The regional geology, however, suggests that these faults are predominantly strike-slip, as the Quilalar Fault System, to which these faults belong, is a strike-slip zone (Blake, 1987, and this volume).

Style of faulting

The Black Mountain fault array thus appears to be a series

of splay faults (C/B - C/F, A/B - E/G, northeast-striking part of E/F, and A/G) with transverse step faults (B/E, F/G and northwest-striking part of E/F) and downwarps (G1/G2, F1/F2), arising from a bounding strike-slip fault to the east (possibly C/D). The splay faults strike southwest to south-southwest, whereas the main boundary faults strike north-south. The overall fan shape of the fault array is clear from Figure 2, and the lower level of Kalkadoon Granite in the south of the area compared to the north suggests an overall hinge fault geometry, unless there is an unrecognised bounding fault to the west of Black Mountain with a significant vertical component of movement. The dominant control on the fault pattern is dextral strike-slip movement within the Quilalar Fault System. The fan-like shape of the array of southwesterly-striking faults with a hinge geometry defines the array as a negative flower structure (Woodcock & Fischer, 1986). However, the associated northwesterly-striking cross faults and down-warps which link the normal faults add complexity to the fault geometry. These faults indicate that there has also been significant transtension across Black Mountain. This could account for up to 25% of the down-throw in the central graben, block E, (compare Eyal & others, 1986; Aydin & Nur, 1982). An implication of this model is that there has been a matching transfer of strike-slip motions from the faults southeast of Black Mountain to those to the northwest.

Complex fault patterns which can be ascribed to the post-D_2 strike-slip fault event are now recognised over a wide area of the central Mount Isa Inlier (e.g., BMR, 1986). Normal and reverse faults are associated with the strike-slip fault arrays, which means that criteria for the relative timing of fault structures is essential before fault geometries can be reconstructed confidently.

Conclusions

Black Mountain is an outlier formed of Quilalar Formation sediments unconformably overlying Kalkadoon Granite. These sediments were laid down in the central part of the Quilalar depositional basin.

During the Isan Orogeny the Quilalar Formation was folded first about east-west axes (D_1) and then about north-south axes (D_2). A well developed subvertical cleavage is axial planar to the D_2 folds.

Younger hinge faults and connecting normal faults form an array interpreted as a pull-apart (negative flower) structure linked to a major strike-slip fault within the Quilalar Fault System.

Acknowledgements

This paper has benefited from comments by P.G. Stuart-Smith, R.J. Korsch, A.J.Stewart, and two anonymous reviewers.

References

AYDIN, A., & NUR, A., 1982 - Evolution of pull-apart basins and their scale independence. *Tectonics* 1, 91-105.

BELL, T.H., 1983 - Thrusting and duplex formation at Mount Isa, Queensland, Australia. *Nature* 304, 493-497.

BLAKE, D.H., 1987 - Geology of the Mount Isa Inlier and environs, Queensland and Northern Territory. *Bureau of Mineral Resources, Australia, Bulletin* 225, 83 pp.

BLAKE, D.H., 1991 - Geology of Black Mountain, Duchess (1:5000 scale map). *Bureau of Mineral Resources, Australia.* Available as a colour electrostatic plot on paper (AUD30), or in digital form on optical disc or Exabyte 8 mm tape (prices on application) both of which can be displayed on Intergraph Microstation software on computers that will run Unix. The digital data comprise a scanned raster image (.RLE format) of the black and white geological map, and an Intergraph vector design file containing the boundaries of coloured polygons. The coloured map and data are available from the Publication Sales Centre, Bureau of Mineral Resources, and an uncoloured Ozalar film or paper copy (AUD20) of the map is available from BMR Copy Service, both at GPO Box 378, Canberra, ACT, 2601, Australia. All orders to be prepaid to Collector of Public Monies.

BLAKE, D.H., this volume - Stratigraphy, folding, and faulting within the Quilalar Fault System, Mount Isa Inlier. *In:* STEWART, A.J., & BLAKE, D.H. (Editors), Detailed Studies of the Mount Isa Inlier. *Bureau of Mineral Resources, Australia, Bulletin* 243.

BLAKE, D.H., ETHERIDGE, M.A., PAGE, R.W., STEWART, A.J., WILLIAMS, P.R., & WYBORN, L.A.I., 1990 - Mount Isa Inlier -- regional geology and mineralisation. *In:* HUGHES, F.E. (Editor), Geology of the mineral deposits of Australia and Papua New Guinea. *Australasian Institute of Mining and Metallurgy, Monograph* 14, 915-925.

BLAKE, D.H., & STEWART, A.J., 1988 - Block and possible terrane boundaries in the Mount Isa Inlier. *BMR Research Newsletter* 8, 2-3.

BMR, 1986 - Transpressional strike-slip faulting in the Mount Isa Inlier. *BMR Research Newsletter* 4, 1-2.

BULTITUDE, R.J., BLAKE, D.H., MOCK, C.M., & DONCHAK, P.J.T., 1982 - Duchess region, Queensland. *Bureau of Mineral Resources, Australia, 1:100 000 Geological Map Commentary.*

EYAL, Y., EYAL, M., BARTOV, Y., STEINITZ, G., &

FOLKMAN, Y, 1986 - The origin of the Bir Zrier rhomb-shaped graben, Eastern Sinai. *Tectonics* 5, 267-277.

JACKSON, M.J., SIMPSON, E.L., & ERIKSSON, K. A., 1990 - Facies and sequence stratigraphic analysis in an intracratonic, thermal-relaxation basin: the early Proterozoic, lower Quilalar Formation and Ballara Quartzite, Mount Isa Inlier, Australia. *Sedimentology* 37, 1053-1078.

WILCOX, R.E., HARDING, T.P., & SEELY, D.R., 1973 - Basic wrench tectonics. *Geological Society of America, Bulletin* 57, 74-96.

WOODCOCK, N.H., & FISCHER, M., 1986 - Strike-slip duplexes. *Journal of Structural Geology* 8,725-735.

WYBORN, L.A.I., & PAGE, R.W., 1983 - The Kalkadoon and Ewen Batholiths, Mount Isa Inlier, Queensland: Source, chemistry, age, and metamorphism. *BMR Journal of Australian Geology & Geophysics* 8, 53-69.

Page 198 is blank.

Geology of the Myubee area, Mount Isa Inlier, Queensland

C. W. Passchier [1]

This paper is based on the following map:

Passchier, C.W., 1991a - Geology of the Myubee Area (1:25 000 scale map), Bureau of Mineral Resources, Canberra.

In the southern Mount Isa Inlier near Duchess, cover sequence 2 (1790-1760 Ma) was affected by regional extension at around 1760-1730 Ma. The extension can be subdivided into an early brittle stage (D^{M}_{1a}), mainly recognised in the Kalkadoon-Leichhardt Block, and a later ductile stage (D^{M}_{1b}), mainly in the Mary Kathleen Zone. In the Mary Kathleen Zone, the Revenue Granite pluton predates D^{M}_{1b}, while a net-veined granite-gabbro pluton (Myubee Pluton) postdates D^{M}_{1b}. Both plutons probably belong to the 1750-1730 Ma Wonga Batholith and predate D^{M}_{2} at around 1550 Ma. D^{M}_{2} substantially shortened the whole area east-west and extended it vertically. D^{M}_{3} is an episode of strike-slip faulting.

[1]Instituut voor Aardwetenschappen, Budapestlaan 4, Utrecht, The Netherlands.

Introduction

An area around the Myubee Pluton, 10 km north of Duchess in the Mount Isa Inlier, was studied in detail during the period 1983-1986 as part of the BMR Mount Isa Project in order to determine the sequence of deformational and intrusive events. Previous results of this study have been published by Passchier (1986a, 1986b, 1987) and Passchier & Williams (1989). This paper summarises results of the mapping project. Deformation episodes in the Myubee area are denoted by the superscript 'M'.

Outline of stratigraphy

The area studied consists mainly of low-pressure amphibolite facies metasediments intruded by granite and gabbro plutons (Bultitude & others, 1982; Blake, 1987). The area straddles the boundary of two major north-trending tectonic units of the Mount Isa Inlier, the central Kalkadoon-Leichhardt Belt and the Mary Kathleen Zone of the Eastern Fold Belt (Fig. 1; Passchier, 1986b; Blake, 1987). These tectonic units are separated in the Myubee area by the Shinfield Zone, a north-trending anticline which exposes highly strained rocks (Fig. 1; see Passchier, 1991a). The Shinfield Zone is the southern extension of the similarly highly deformed Wonga Belt (Derrick & others, 1980; Pearson & others, 1987; Passchier & Williams, 1989; Holcombe & others, this volume). The Kalkadoon-Leichhardt Belt consists of various highly deformed granite plutons, felsic metavolcanics, and gneisses classified as basement, and cover sequence 1, all older than 1850 Ma (Page, 1978; Wyborn & Page, 1983; Blake, 1987). These rocks are overlain in the Kalkadoon-Leichhardt Belt by cover sequence 2 (Fig. 1), dated at about 1790-1760 Ma (Blake & others, 1984; Blake, 1987). The Mary Kathleen Zone in the Myubee area consists entirely of cover sequence 2 rocks. Cover sequence 3,

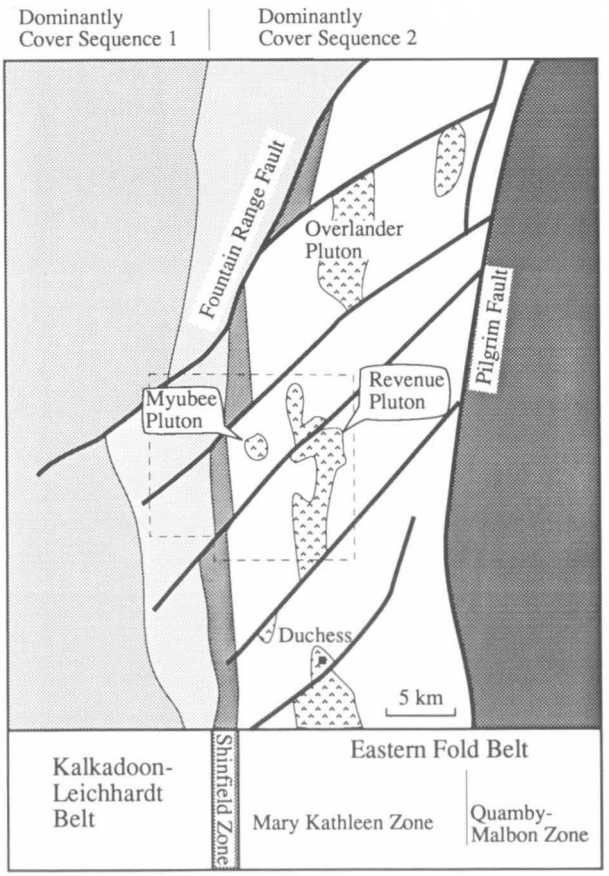


Fig. 1. Schematic map of the central part of the Mount Isa Inlier surrounding the Myubee and Revenue Plutons.

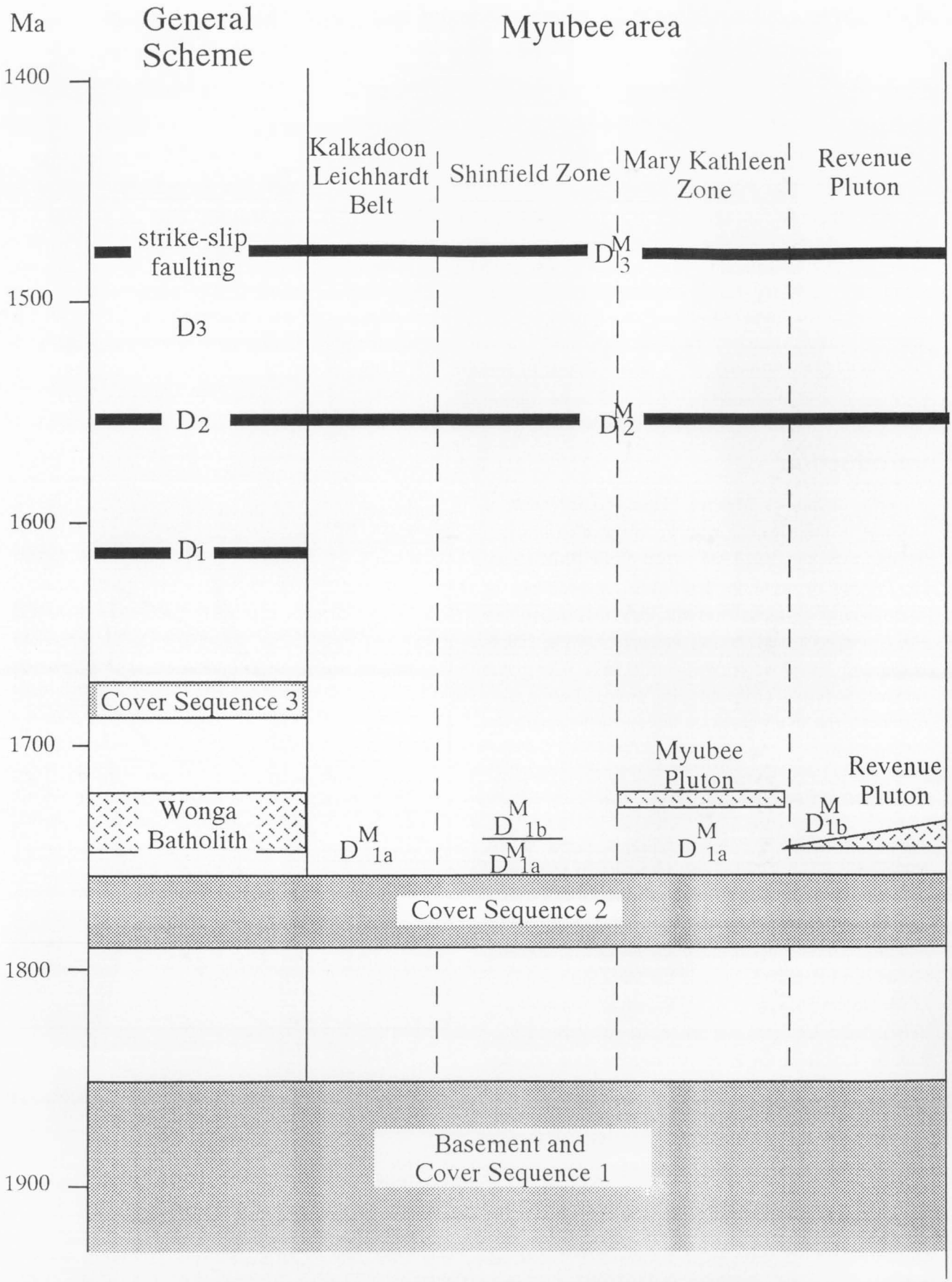


Fig. 2. Relative age scheme of cover sequences, deformation and intrusion phases in the Myubee area, and their relation with the regional scheme of events. D – Isan deformation; D^M – deformation phases recognised in the Myubee area.

dated at 1680-1670 Ma (Blake, 1987), does not occur in the mapped area.

In the Myubee area, the only rocks which may predate cover sequence 2 are strongly deformed lenses of porphyritic biotite granite in the Shinfield Zone (Passchier, 1986b). Blake (1987) grouped this rock type and associated leucogranite as Bushy Park Gneiss of the Wonga Batholith, which postdates deposition of cover sequence 2. The leucogranite in the Shinfield Zone, however, has intruded both cover sequence 2 and the porphyritic biotite granite (Passchier, 1986b); the porphyritic biotite granite shows no intrusive contacts and may be older than cover sequence 2.

Cover sequence 2 is represented in the Myubee area by the following formations (in ascending order; Blake, 1987):

(1) *Magna Lynn Metabasalt*, mainly amphibolitised metabasalt with minor intercalated quartzite and felsic porphyry;

(2) *Argylla Formation*, comprising lower and upper sequences. The lower sequence consists mainly of layered felsic metavolcanics, dominantly rhyolitic to dacitic ignimbrite and bedded tuff, intercalated with thin layers and lenses of banded quartzite (1-50 m thick). Minor lenses of felsic porphyry and amphibolite are also present (Passchier, 1986a). The upper sequence consists of quartz-rich fine-grained metasandstone with relict large scale cross-bedding, possibly a continental deposit (Passchier, 1986a; BMR, 1990), and minor lenses and layers of quartzite, felsic porphyry, and amphibolite (Passchier, 1986a). This metasandstone has also been found in the Ballara-Mount Frosty area, which is the continuation of this area but displaced 28 km to the northeast along the dextral Fountain Range Fault (BMR, 1990; Stewart, this volume), and there mapped as part of the newly named Mount Frosty Member;

(3) *Ballara Quartzite*, a mainly homogeneous massive quartzite of shallow-marine origin (Blake, 1987). The boundary between the Ballara Quartzite and the top of the Argylla Formation is difficult to find in the Myubee area because of the similar rock types and brittle faulting; consequently, sandstone and quartzite from both formations are grouped together on the map;

(4) *Corella Formation*, which comprises alternating banded calc-silicate rocks, banded amphibolite, and massive amphibolite with minor lenses of quartzite, felsic metavolcanics, and sillimanite – white mica schist. Some cordierite-anthophyllite rock is present at the base of the formation. The calc-silicate rocks consist of microcline, scapolite, carbonate, hornblende, diopside, grossularite, and allanite (compare Carter & others, 1961).

Sequence of deformational and intrusive events

The following sequence of events is reconstructed for the Myubee area, based on established field relationships for the period after deposition of cover sequence 2 (Fig. 2).

Intrusion of granite and pegmatite

In the east of the Myubee area, a major granite body, the *Revenue Pluton*, intruded the Corella Formation before ductile deformation (Passchier, 1991b). It consists of a leucogranite rim up to 300 m wide, and a core of homogeneous biotite granite. The pluton intruded parallel to layering; similar sill-like granite plutons of the same relative age are reported by Holcombe & others (this volume) in the northern Mary Kathleen Zone. Pegmatite veins intruded both the granite and the country rock (Passchier, 1986b). In the Shinfield Zone, veins and lenses of leucogranite intruded porphyritic biotite granite and rocks of cover sequence 2 before ductile deformation. As no granite veins occur in the centre of the Myubee area between the Revenue Pluton and the Shinfield Zone, the relative age of the Revenue Pluton and granite veins in the Shinfield Zone is unknown.

D^M_{1a} deformation

Early low-angle brittle faulting affected cover sequence 2 throughout the Myubee area (Passchier, 1986a, 1986b; Passchier & Williams, 1989), and has been called D_{1a} (Passchier, 1986b), Alligator phase (Passchier & Williams, 1989), D_{e2} (Loosveld, 1989), and pre-D_2 faulting (Stewart, 1989; BMR, 1990). D^M_{1a} is older than the regional D_1 of Bell (1983; Table 1).

The most spectacular brittle fault structures are found in the Alligator Syncline in the Kalkadoon-Leichhardt Belt (see Passchier, 1991a), where quartzite and sandstone lenses in the Argylla and Ballara formations are locally truncated by subparallel, planar breccia zones up to several metres wide and spaced 5-100 m apart, with a matrix rich in tourmaline (Passchier, 1986a, 1987; Passchier & Williams, 1989). The most important of these faults have been shown on the map (Passchier, 1991a). Breccia zones have been ductilely deformed during D^M_2, mainly by tight folding and by an overprinting D^M_2 axial planar cleavage. As a result, the present orientation of fault imbricates cannot be used to assess the contractional or extensional nature of the fault system. However, the geometry of the fault imbricates, and their displacement direction with

TABLE 1. CORRELATION SCHEME OF DEFORMATION EPISODES IN THE MYUBEE AREA AND REGIONALLY RECOGNISED EPISODES OF BELL (1983).

Myubee area	Bell (1983)	Remarks
D^M_{1a}		Brittle pre-D2 event, probably 1750-1730 Ma
D^M_{1b}		Ductile pre-D2 event, probably 1750-1730 Ma
	D_1	
D^M_2	D_2	
	D_3	
D^M_3		Strike-slip faulting, probably 1480 Ma

respect to fault-bedding intersection lines can give an indication of its nature. The breccia zones steeply truncate bedding, and delimit narrow fault imbricates, which strongly resemble those described from extensional fault systems elsewhere (e.g., Davis & Hardy, 1981; Wernicke & Birchfiel, 1982; Davis & others, 1986). Displacement on breccia zones ranges from less than 1 m on zones spaced less than 10 m apart, to 500 m on zones spaced 100 m apart. Displacement of bedding along the breccia zones indicates the original movement was dominantly normal to the intersection line of faults and bedding, although some faults seem to have had a significant original strike-slip component of displacement (Passchier & Williams, 1989). Lenses and dykes of amphibolite are common in the Argylla and Ballara Formations, commonly at a high angle to bedding. Many of these amphibolite bodies intruded along the breccia zones (Stewart, 1987; Passchier & Williams, 1989). At two localities in the Alligator Syncline, dykes of K-feldspar porphyry intrude D^M_{1a} breccia zones. These dykes both pre- and post-date dolerite intrusion.

Brittle faults as described above also occur in the Shinfield Zone and the Mary Kathleen Zone (see Passchier, 1991a). In the Shinfield Zone, quartzite beds have been truncated by early brittle faults rich in tourmaline, especially near grid reference 760455. In the Mary Kathleen Zone, breccia zones have been recognised in the Corella Formation north of the Myubee Pluton and west of the Revenue Pluton, and consist of fragments of banded calc-silicate and amphibolite up to 0.5 m in diameter in a structureless matrix. Both breccia zones separate massive amphibolite from calc-silicate rocks within the Corella Formation, and are folded by D^M_2. The breccia zones are mostly parallel to bedding in calc-silicate rocks, but locally 10 m-scale ramps occur where bedding is truncated against the breccia zones. Although no breccia has been found locally, the ramp-like shape of the alternating amphibolite and calc-silicate bands near grid reference 805505 is probably also an effect of D^M_{1a}.

The data discussed above, and in more detail in Passchier (1986a, 1987) and Passchier & Williams (1989), indicate that a brittle fault system in the Myubee area is dominantly extensional in nature, with movement of the hanging wall towards the south or southeast. The Shinfield Zone may have been the locus of this deformation. The Shinfield Zone is a D^M_2 anticline which exposes highly strained juxtaposed kilometre-scale fragments of porphyritic biotite granite and cover sequence 2 rocks, some separated by ductilely deformed tourmaline-rich breccias. The thickness of Argylla and Ballara Formation rocks changes from 1 km on the western limb of this anticline to less than 100 m on the eastern limb. The strain intensity of ductile deformation which postdates the imbrication, as assessed from xenoliths in porphyritic biotite granite, is insufficient to explain this amount of thinning; it is better explained as an effect of D^M_{1a}.

D^M_{1b} deformation

A D^M_{1b} ductile shape fabric has been found in the Revenue Pluton and in the Shinfield Zone. In the Revenue Pluton, the shape fabric is usually linear and locally planar (see Passchier, 1991a, b), and parallel to the contact of the pluton with the country rock. Xenoliths in the pluton are deformed to an oblate or prolate shape in accordance with the type of shape fabric present. The linear shape fabric component has an east-west or southeast-northwest orientation (see Passchier, 1991a). In the northernmost lobe of the Revenue Pluton, the D^M_{1b} linear shape fabric has a persistent east-west trend, discordant to the pluton shape (see Passchier, 1991a). This shows that the fabric is

not associated with pluton ascent and intrusion, but that D^{M}_{1b} is a deformation phase of regional significance (Passchier, 1991b). In the centre of the pluton, east of Green Creek Tank, a kilometre-scale D^{M}_{1b} mullion-structure formed in the contact zone, parallel to the D^{M}_{1b} linear shape fabric (Fig. 3; Passchier, 1991b). The original shape of this mullion-structure after D^{M}_{1b} and before D^{M}_{2} was probably as shown in Figure 3a.

In the Shinfield Zone and in the westernmost kilometre of the Mary Kathleen Zone, a north-trending D^{M}_{1b} linear shape fabric is present, mostly in porphyritic biotite granite but also locally in Argylla felsic metavolcanics, microgranite dykes, Magna Lynn Metabasalt, quartzite, and calc-silicate rocks (D_{1b} in Passchier, 1986b). In quartzite lenses, D^{M}_{1a} brittle faults with ramp-like structures are overprinted by this stretching lineation (Passchier, 1986b; Passchier & Williams, 1989). The plunge of the D^{M}_{1b} lineation varies strongly along strike on a 10 m scale, but is usually rather shallow. This variable plunge is interpreted as an effect of overprinting by D^{M}_{2}, which locally forms steep mineral lineations. Similar sets of early lineations have been found in the Wonga Belt 70 km farther north, which can be considered as the northern equivalent of the Shinfield Zone (Holcombe & others, this volume), the two being separated by dextral strike-slip movement on the Fountain Range Fault.

Intrusion of the Myubee Pluton

The *Myubee Pluton* intruded the Corella Formation in the centre of the Mary Kathleen Zone (see Passchier, 1991a). The pluton consist of an outer zone of coarse leucogranite surrounding a core of olivine gabbro. Fragments of gabbro are common in the granite, but the reverse is also observed, suggesting that both magma types intruded synchronously. Similar relationships in the Myubee and other plutons in the Mary Kathleen Zone have been described by Blake (1981) and Holcombe & others (this volume) as net-veined complexes. The Myubee pluton differs markedly from the Revenue Pluton by the absence of a D^{M}_{1b} shape fabric.

D^{M}_{2} deformation

D^{M}_{2} is an episode of ductile deformation, dated at approximately 1550 Ma (Table 1; Page & Bell, 1986), which strongly affected all units in the studied area, and which has been recognised over large parts of the Mount Isa Inlier (Blake & others, 1984; Blake, 1987; Loosveld, 1989). It corresponds to regional D_2 (Bell, 1983) and to the Duchess phase of Passchier & Williams (1989). In the Myubee area it is synchronous with the peak of metamorphism, which formed low-pressure amphibolite facies assemblages in all the studied units (Reinhardt, 1990). Extensive static recrystallisation of scapolite, diopside, and hornblende in calc-silicate rocks indicates that these conditions outlasted D^{M}_{2}.

D^{M}_{2} produced tight to isoclinal folds with steeply west-dipping axial surfaces in all units. Detailed investigation in Corella calc-silicate rocks has shown that D^{M}_{2} folds are strongly disharmonic and non-cylindrical (Passchier, 1986a). Vergence mapping of parasitic folds, with correction for the variable plunge of fold axes, reveals the existence of kilometre-scale D^{M}_{2} folds with north and south-plunging fold axes (see Passchier, 1991a). The Shinfield Zone coincides with a major tight D^{M}_{2} anticline. In the Kalkadoon-Leichhardt Belt, a major D^{M}_{2} syncline (Alligator Syncline) has been recognised (Bultitude & others 1982; Passchier, 1986a).

A steep D^{M}_{2} foliation and subvertical D^{M}_{2} mineral lineation, defined by a preferred orientation of hornblende and biotite, are present in amphibolite of the Corella and Magna Lynn formations. The biotite lineation arises where biotite crystals have variable orientation but share a common axis, thus defining a bulk linear fabric. Planar and linear D^{M}_{2} shape fabric elements of the same orientation occur in Argylla felsic metavolcanics, porphyry, and quartzite, and in the plutons. The mineral and stretching lineations are oblique to D^{M}_{2} fold axes.

The present elongate domal shape of the Revenue Pluton is an effect of large-scale D^{M}_{2} folding (Fig. 3); the north-trending lobes in the northern part of the pluton coincide with kilometre-scale D^{M}_{2} folds in the contact and in layering in the surrounding Corella Formation rocks (see Passchier, 1991a, and Fig. 3b). The large embayment in the western side of the Revenue Pluton (see Passchier, 1991a) is caused by large-scale D^{M}_{1b}-D^{M}_{2} fold interference; the northern part of the embayment is interpreted as a large D^{M}_{1b} mullion structure (Passchier, 1991b). The southern part of the embayment is an asymmetric kilometre-scale D^{M}_{2} fold, parasitic on a major synform to the west. The fold axis of this D^{M}_{2} structure is gently northwest-plunging (see Passchier, 1991a). The D^{M}_{1b} fabric in the pluton is folded by D^{M}_{2} on a centimetre-metre scale.

In the Myubee pluton, a linear-planar D^{M}_{2} shape fabric is present. The shape fabric in the granitic component of the pluton is generally stronger than in the gabbro; a subvertical linear D^{M}_{2} fabric is dominant. The contact between granite and gabbro is deformed into 10 m-scale

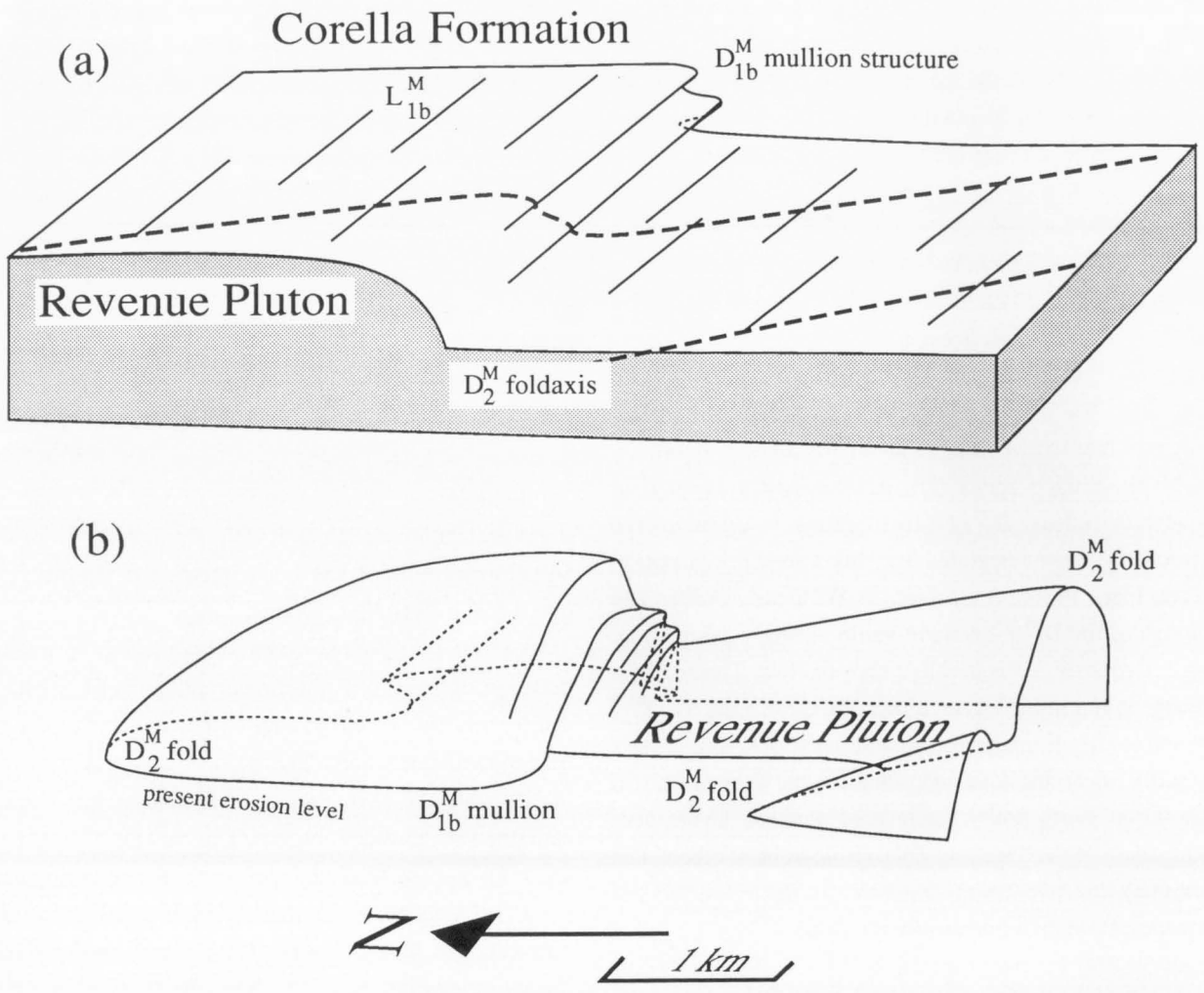


Fig. 3. Schematic interpretation of the deformation of the Revenue Pluton. (a) shape of the roof of the pluton after D^M_{1b}; a kilometre-scale mullion structure exists parallel to the D^M_{1b} stretching lineation. (b) Inferred shape of the Revenue Pluton above the present erosion level. D^M_3 faults have been omitted. The refolded D^M_{1b} mullion structure and an asymmetric D^M_2 fold form a major embayment in the western side of the pluton.

mullions with subvertical axes, indicating relatively competent behaviour of the gabbroic component. In cuspate and lobate folds of the mullions, a subvertical planar D^M_2 shape fabric is locally developed on a metre scale, with a gradual transition to the linear D^M_2 shape fabric in the surrounding rocks. In lobate folds, this foliation is parallel to the contact; in cuspate folds it is axial planar. The irregular distribution of planar and linear shape fabric elements can be attributed to inhomogeneous internal D^M_2 deformation of the pluton in response to the presence of two rock types. The dominance of steep linear fabrics can be attributed to constrictional deformation in the pluton, whereas a planar shape fabric formed in the surrounding Corella Formation. The constrictional nature of deformation in the pluton may be due to the large amount of gabbro present.

The axial planes of kilometre-scale D^M_2 folds in Corella Formation rocks wrap around the Myubee Pluton (see Passchier, 1991a). To the west and east, strain intensity is high as determined from tightly to isoclinally folded dykes which radiate from the pluton, and from attenuated D^M_2 folds in layered calc-silicates. To the north and south, areas of low strain intensity occur which can be regarded as strain shadows.

Intrusion of dolerite dykes

North-south dolerite dykes intruded after D^M_2. One truncates the Myubee Pluton (see Passchier, 1991a) and apparently intruded parallel to the regional trend of D^M_2. These dykes have undergone no ductile deformation or metamorphism.

D^M_3 deformation

All structural elements mentioned so far are truncated by northeast-striking brittle strike-slip faults (D^M_3; Fig. 2 and

Passchier, 1991a) with dextral offset, usually recognisable as cataclasite zones up to 30 m wide (Lister & others, 1986). D^M_3 is equivalent to D_4 of Page & Bell (1986) and is referred to as the Fountain Range phase in Passchier & Williams (1989). The fault zones are rich in vein quartz which is commonly affected by the cataclasis. Quartz veins occur in the country rock up to several hundreds of metres away from the main faults. Similar fault systems have been dated at approximately 1480 Ma elsewhere in the Mount Isa Inlier (Blake, 1987).

Discussion

Significance of D^M_{1a} and D^M_{1b}

D^M_{1a} in the Myubee area represents an important episode of regional extension which has now been recognised over most of the Mount Isa Inlier (Passchier, 1986a; Pearson & others, 1987; Passchier & Williams, 1989; Stewart, 1989, this volume; Loosveld, 1989; BMR, 1990; Holcombe & others, this volume). Brittle extensional faulting took place before the 1610 Ma thrusting (D_1 of Bell, 1983; Malbon phase of Passchier & Williams, 1989) reported elsewhere in the Mount Isa Inlier, and after deposition of cover sequence 2 was completed around 1760 Ma (Fig. 2; Stewart, 1989; BMR, 1990). Extension is probably associated with intrusion of the Wonga Batholith around 1750-1730 Ma (Pearson & others, 1987; Holcombe & others, this volume; Loosveld, 1989; Passchier & Williams, 1989).

The regional significance of D^M_{1b} as recognised in the Myubee area is difficult to assess with the scanty data available. The following observations are of relevance. D^M_{1b} certainly postdates intrusion of the Revenue granite and D^M_{1a} brittle extension, and predates D^M_2. D^M_{1b} linear shape fabrics are east- or southeast-trending in the Revenue Pluton, and north-trending in the Shinfield Zone. Although the orientation of D^M_{1b} fabrics is probably strongly affected by later deformation, the difference in orientation between fabrics in the Revenue Pluton and in the Shinfield Zone must date from before D^M_2; D^M_2 causes folding of D^M_{1b} fabrics in the Revenue Pluton, but not in the Shinfield Zone. If any planar D^M_{1b} fabric were present in the Shinfield Zone, it must have had a relatively steep orientation, since no D^M_2 crenulation of an older planar fabric has been found (Passchier, 1986b; BMR, 1990).

Structures similar to the D^M_{1b} fabric in the Shinfield Zone are common in the Wonga Belt, the northern continuation of the Shinfield Zone, the two being separated by the Fountain Range Fault (Fig. 1; Pearson & others, 1987; Holcombe & others, this volume). These structures were formed by north-south ductile extensional deformation contemporaneous with Wonga Batholith granite intrusion and brittle extension at higher crustal levels (Holcombe & others, this volume). D^M_{1b} in the Shinfield Zone can therefore be interpreted as an episode of ductile extensional movement during or after intrusion of the Wonga Batholith (Fig. 2; Passchier & Williams, 1989; Passchier, 1991b). In contrast to the Wonga Belt where brittle and ductile extension are reported to be contemporaneous (Holcombe & others, this volume), D^M_{1b} ductile fabrics overprint D^M_{1a} brittle structures in the Shinfield Zone.

The D^M_{1b} fabric in the Revenue Pluton is difficult to date with respect to fabrics in the Shinfield Zone, but similar structures in granite sills in the Wonga Belt are also interpreted as belonging to the 1750-1730 Ma extension event (Holcombe & others, this volume). If the D^M_{1b} fabric in the Revenue Pluton formed at the same time as that in the Shinfield Zone, the original difference in orientation between fabric elements in both units can be explained by dominant ductile north-south transcurrent movement in the the Shinfield Zone during oblique ductile extension in the top of the Revenue granite.

Age of the plutons

The granite plutons in the Mary Kathleen Zone are grouped together as part of the Wonga Batholith (Blake, 1987). Some plutons in the Wonga Batholith have been dated and give zircon U-Pb ages between 1750 and 1730 Ma, before D_2 (Page, 1978, 1979, 1983; Blake, 1987; Loosveld, 1989). Holcombe & others (this volume) suggest that Wonga Batholith plutons in the northern Mary Kathleen Zone intruded as sills along brittle fractures during regional extension. Parallelism of the roof of the Revenue pluton to layering in the Corella Formation, and the presence of D^M_{1a} breccia zones in the Corella formation parallel to this contact, support this interpretation. The Revenue Pluton was subsequently overprinted by D^M_{1b}.

Unlike the Revenue Pluton, the Myubee Pluton is not affected by D^M_{1b}, and probably postdates this event. In its well-exposed southern strain shadow, the Myubee pluton intrudes and cuts through open north-trending folds in Corella Formation calc-silicates, and granite offshoots intrude the metasediments along foliation planes axial planar to these folds (Passchier, 1986b). Passchier (1986b) interpreted these structures as early D^M_2, implying that the Myubee Pluton is syn-D^M_2. However, the presence of foliations associated with the extension phase in the northern part of the Mary Kathleen Zone (Holcombe &

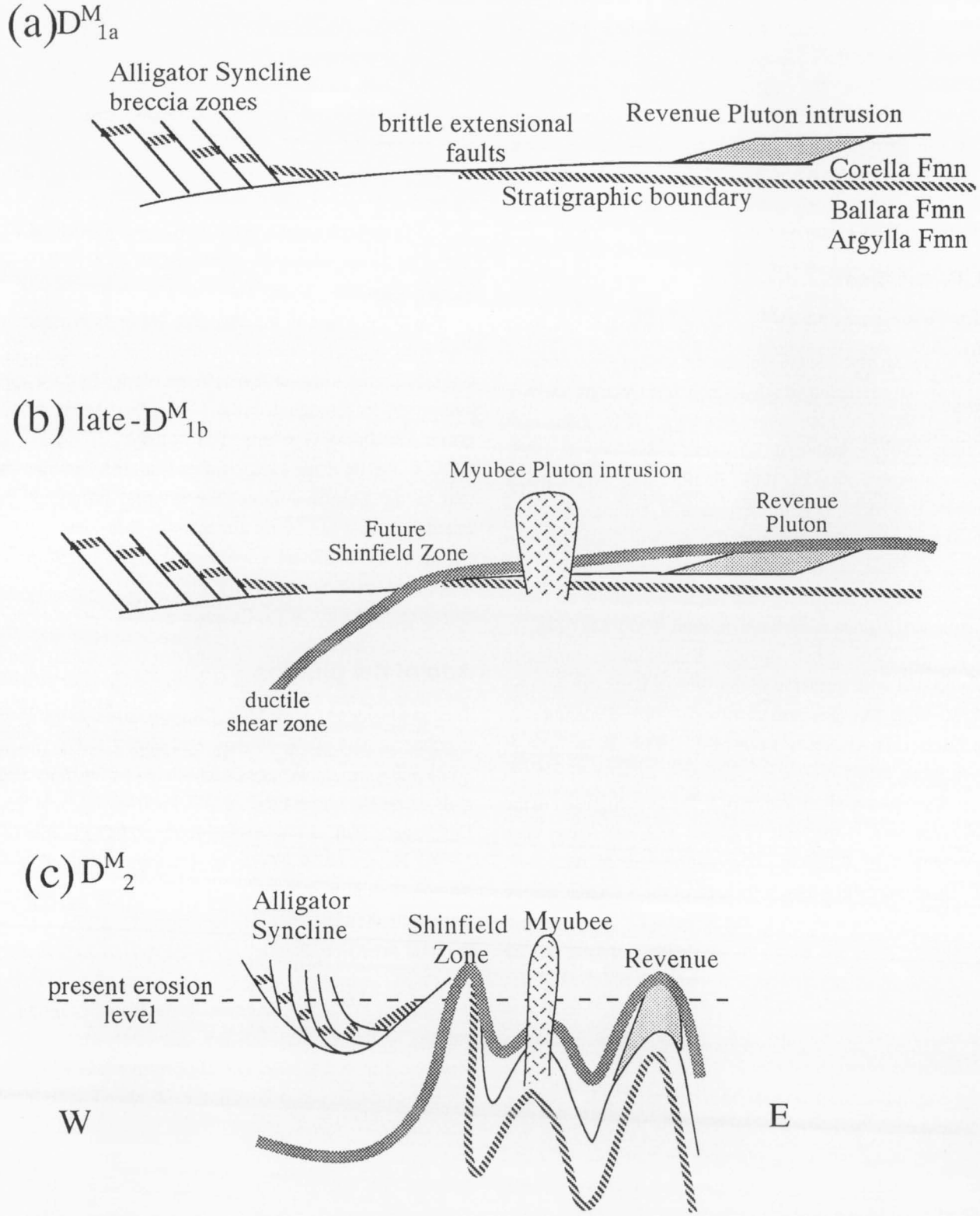


Fig. 4. Schematic reconstruction of the geological history of the Myubee area, shown in east-west cross-section, looking north; (a) Brittle extensional deformation during D^M_{1a}, resulting in breccia zones and intrusion of the Revenue Pluton. (b) D^M_{1b} ductile extensional deformation, affecting the Shinfield zone and the Revenue Pluton; the Myubee Pluton intrudes after this deformation. (c) D^M_2 east-west shortening brings units into their present position.

others, this volume) implies that these structures in the southern strain shadow may also belong to D^{M}_{1a} or D^{M}_{1b}. The Myubee Granite is very similar to other net-veined plutons in the northern Mary Kathleen Belt, which also lack an early shape fabric (Holcombe & others, this volume). These data, and the fact that no other syn-D_2 granites have been reported to date, suggest that the Myubee Pluton also belongs to the Wonga Batholith. If this is so, it must have intruded relatively late at the end of the regional extension event.

Conclusions

The following sequence of events is proposed for the Myubee area (Fig. 4). Rocks of cover sequence 2 (1790-1760 Ma) were affected by brittle extensional faulting (D^{M}_{1a}), especially in the Alligator Syncline and Shinfield Zone, but also in the Mary Kathleen Zone (Fig. 4a). Breccia zones were formed during this period, and the Revenue Pluton may have intruded along one of the faults (Fig. 4a). Subsequent ductile deformation (D^{M}_{1b}) during ongoing regional extension affected the Revenue Pluton and the Shinfield Zone; deformation in the Shinfield Zone had a large component of north-south transcurrent movement. The Myubee pluton intruded after the end of D^{M}_{1b} (Fig. 4b). D^{M}_{1a}, D^{M}_{1b}, and intrusion of both plutons probably took place in the 1750-1730 Ma time-bracket suggested by Holcombe & others (this volume). Subsequent east-west shortening during D^{M}_{2} (1550 Ma) brought all units to their present positions (Fig. 4c). D^{M}_{3} strike-slip faulting around 1480 Ma separated the Shinfield Zone and the Wonga Belt.

Acknowledgements

Funding for this research project was given by the Royal Society of London (1983) and by the Schurmann fund (1984, 1985, 1986). Extensive logistic and financial support was obtained from BMR, Canberra. I further wish to thank Peter Williams, Gordon Lister, Dave Blake, Ide van der Molen, and Mike Etheridge for useful discussions in the field. The manuscript was improved by comments of Alastair Stewart, Russell Shaw, and an anonymous reviewer.

References

BELL, T.H., 1983 - Thrusting and duplex formation at Mount Isa, Queensland, Australia. *Nature* 304, 493-497.

BLAKE, D.H., 1981 - Intrusive felsic-mafic net-veined complexes in north Queensland. *BMR Journal of Australian Geology and Geophysics* 6, 95-99.

BLAKE, D.H., 1987 - Geology of the Mount Isa Inlier and environs, Queensland and Northern Territory. *Bureau of Mineral Resources, Australia, Bulletin* 225, 83 pp.

BLAKE, D.H., BULTITUDE, R.J., DONCHACK, P.J.T., WYBORN, L.A.I., & HONE, I.G., 1984 - Geology of the Duchess-Urandangi region, Mount Isa Inlier, Queensland. *Bureau of Mineral Resources, Australia, Bulletin* 219, 96 pp.

BMR, 1990 - New Results from the Mount Isa Geotraverse. *BMR Research Newsletter* 12, 6-8.

BULTITUDE, R.J., BLAKE, D.H., & DONCHACK, P.J.T., 1982 - Duchess Region, Queensland. *Bureau of Mineral Resources, Australia, 1:100 000 Geological Map and Commentary*, 35 pp.

CARTER, E.K., BOOKS, J.H., & WALKER, K.R., 1961 - The Precambrian mineral belt of north-western Queensland. *Bureau of Mineral Resources, Australia, Bulletin* 51, 344 pp.

DAVIS, G.A., LISTER, G.S., & REYNOLDS, S.J., 1986 - Structural evolution of the Whipple and South Mountain shear zones, southwestern United States. *Geology* 14, 7-10.

DAVIS, G.H., & HARDY, J.J., 1981 - The Eagle Pass detachment, southern Arizona: product of mid-Miocene listric(?) normal faulting in the southern Basin and Range. *Geological Society of America, Bulletin* 92, 749-762.

DERRICK, G.M., WILSON, I.H., & SWEET, I.P., 1980 - Quilalar and Surprise Creek Formations - new Proterozoic units from the Mount Isa Inlier: their regional sedimentology and application to regional correlations. *BMR Journal of Australian Geology and Geophysics* 5, 215-223.

HOLCOMBE, R.J., PEARSON P.J., & OLIVER N.H.S., this volume - Structure of the the Mary Kathleen Fold Belt. *In*: STEWART, A.J., & BLAKE, D.H. (editors), Detailed Studies of the Mount Isa Inlier. *Bureau of Mineral Resources, Australia, Bulletin* 243.

LISTER, G.S., THOMAS, A., & DUNN, J., 1986 - Tectonic processes in the Mount Isa Inlier: significance of transpressional strike-slip faulting. *Geological Society of Australia, Abstracts* 15, 127-128.

LOOSVELD, R.J.H., 1989 - The intra-cratonic evolution of the central eastern Mount Isa Inlier, Northwest Queensland, Australia. *Precambrian Research* 44, 243-276.

PAGE, R.W., 1978 - Response of U-Pb zircon and Rb-Sr total rock and mineral systems to low-grade regional metamorphism in Proterozoic igneous rocks, Mount Isa, Australia. *Journal of the Geological Society of Australia* 25, 141-164.

PAGE, R.W., 1979 - Mount Isa Project. *In* Geological Branch Summary of Activities 1978. *Bureau of Mineral Resources, Australia, Report* 212, 181-182 .

PAGE, R.W., 1983 - Chronology of magmatism, skarn

formation and uranium mineralization, Mary Kathleen, Queensland, Australia. *Economic Geology* 78, 838-853.

PAGE, R.W., & BELL, T.H., 1986 - Isotopic and structural responses of granite to successive deformation and metamorphism. *Journal of Geology* 94, 365-379.

PASSCHIER, C.W., 1986a - Evidence for early extensional tectonics in the Proterozoic Mount Isa inlier, Australia. *Geology* 14, 1008-1011.

PASSCHIER, C.W., 1986b - Proterozoic deformation in the Duchess Belt, Australia - *Geologie en Mijnbouw* 65, 47-56.

PASSCHIER, C.W., 1987 - Reply to comment by A.J. Stewart on 'Evidence for early extensional tectonics in the Proterozoic Mount Isa inlier, Australia'. *Geology* 15, 977-979.

PASSCHIER, C.W., 1991a - Geology of the Myubee Area (1:25 000 scale map), Bureau of Mineral Resources, Canberra, Australia. Available as a colour electrostatic plot on paper (AUD30), or in digital form on optical disc or Exabyte 8 mm tape (prices on application) both of which can be displayed on Intergraph Microstation software on computers that will run Unix. The digital data comprise a scanned raster image (.RLE format) of the black and white geological map, and an Intergraph vector design file containing the boundaries of coloured polygons. The coloured map and data are available from the Publication Sales Centre, Bureau of Mineral Resources, and an uncoloured Ozalar film or paper copy (AUD20) of the map is available from BMR Copy Service, both at GPO Box 378, Canberra, ACT, 2601, Australia. All orders to be prepaid to Collector of Public Monies.

PASSCHIER, C.W., 1991b - Deformation in the Revenue granite pluton, Mount Isa Inlier, Australia. *Geologie en Mijnbouw* 70, 275-285.

PASSCHIER, C.W., & WILLIAMS, P.R., 1989 - Proterozoic extensional deformation in the Mount Isa Inlier, Queensland, Australia. *Geological Magazine* 126, 43-53.

PASSCHIER, C.W., MYERS, J.S., & KRONER, A., 1990 - Field Geology of High-grade Gneiss Terrains. *Springer Verlag, Berlin,* 160 pp.

PEARSON, P.J., HOLCOMBE, R.J., & OLIVER, N.H.S., 1987 - The Mary Kathleen Fold Belt, northwest Queensland: D1 - a product of crustal extension? *Geological Society of Australia, Abstracts* 19, 37-38.

REINHARDT, J., 1990 - Low-pressure/high-temperature metamorphism, crustal shortening and isobaric cooling in the Mary Kathleen Fold Belt, northeast Australia. *Terra Abstracts* 2, 31.

STEWART, A.J., 1987 - Comment on 'Evidence for early extensional tectonics in the Proterozoic Mount Isa inlier, Australia'. *Geology* 15, 976-977.

STEWART, A.J., 1989 - Extensional faulting as the explanation for the Deighton 'Klippe' and other Mount Albert Group outliers, Mount Isa Inlier, northwestern Queensland. *Australian Journal of Earth Sciences* 36, 405-421.

STEWART, A.J., this volume - Stratigraphy, extension, and contraction in the Ballara-Mount Frosty area, Mount Isa Inlier. *In*: STEWART, A.J., & BLAKE, D.H. (Editors), Detailed Studies of the Mount Isa Inlier. *Bureau of Mineral Resources, Australia, Bulletin* 243.

WERNICKE, B., & BURCHFIEL, B.C., 1982 - Modes of extensional tectonics. *Journal of Structural Geology* 4, 105-115.

WYBORN, L.A.I., & PAGE, R. W., 1983 - The Proterozoic Kalkadoon and Ewen Batholiths, Mount Isa Inlier, Queensland: source, chemistry, age, and metamorphism. *BMR Journal of Australian Geology and Geophysics* 8, 51-69.

Stratigraphy, extension, and contraction in the Ballara – Mount Frosty area, Mount Isa Inlier, Queensland

A J . Stewart [1]

This paper is based on the following map:

Stewart, A.J., 1991 - Geology of the Ballara-Mount Frosty Region (1:25 000 scale map), Bureau of Mineral Resources, Canberra (two sheets).

The rocks of the Ballara-Mount Frosty region belong to cover sequence 2 (1790-1760 Ma) of the Mount Isa Inlier, comprising, from bottom to top: Magna Lynn Metabasalt, Argylla Formation, Ballara Quartzite, Corella Formation, Deighton Quartzite, and White Blow Formation, intruded by dolerite and granite. Much of the shallow-marine Ballara Quartzite of earlier mapping is probably fluviatile, and makes up the major part of the newly named Mount Frosty Member of the Argylla Formation; the member also includes lenses of calc-silicate, conglomerate, tuffaceous sandstone, and basalt. The overlying Corella Formation passes gradationally up into the Deighton Quartzite, disproving an earlier suggestion that the Deighton Quartzite and White Blow Formation are a thrust repetition of the (former) Ballara Quartzite and Corella Formation.

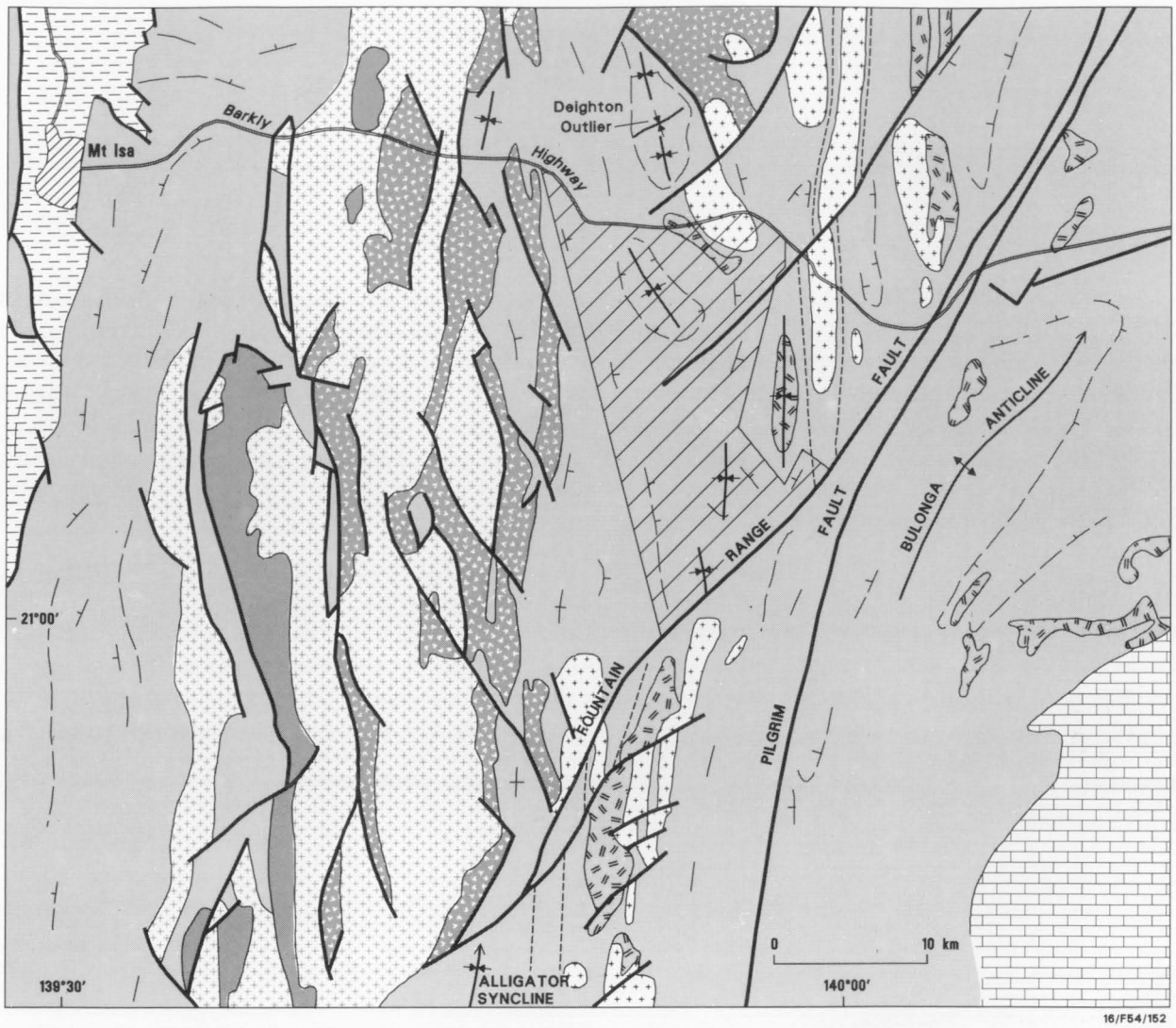
Early tension generally oriented north-south affected all stratigraphic units, and formed low to high-angle normal faults (and in the northwest, a bedding-parallel fault), many of which were intruded by dolerite. This faulting is correlated with the mid-crustal extension dated at 1760-1730 Ma in the adjoining Mary Kathleen area to the east. North-south compression at about 1610 Ma formed a large south-dipping thrust fault and an adjoining tight synform in the centre of the area, and also deformed and rotated pre-existing extensional faults. Subsequent east-west compression at about 1550 Ma formed a thrust sheet in the northeast of the area, an antiformal stack duplex in the central-north, and then the major northerly oriented upright folds of the area. Large post-1500 Ma strike-slip faults segmented the region, and were accompanied by tectonic injection of carbonate-shale of the Corella Formation into fault openings.

[1] Bureau of Mineral Resources, GPO Box 378, Canberra, ACT, 2601, Australia.

Introduction

Extensional tectonics in the Mount Isa Inlier were first suggested as a possible orogenic process by Dunnet (1976), who proposed low and high-angle extensional faults north of Mount Isa township. Passchier (1986) made a notable contribution to the geology of the Mount Isa Inlier when he documented low-angle extensional faulting in the Alligator Syncline in the central part of the Inlier (Fig. 1). The extensional faults in the Alligator Syncline are folded by and therefore predate a major regional contractional deformation, D_2 of Bell (1983), which affected the Mount Isa Inlier at about 1550 Ma (Page & Bell, 1986; Connors & Page, 1992). In the Bulonga Anticline (Fig. 1) 10 km east of the Ballara-Mount Frosty area, Williams (1989) described early extensional fault imbricates which have been affected by three episodes of compressional folding and cleavage formation, correlated with D_1 (1610 Ma), D_2, and D_3 (1510 Ma) of Bell (1983). The brittle extension in the Alligator and Bulonga areas is correlated with ductile deformation, interpreted by Holcombe & others (this volume) as extensional, which formed a mid-crustal mylonite zone in the Wonga Belt (Fig. 1) to the east; granite emplaced into the zone synchronous with the mylonitisation is dated at about 1740 Ma (Holcombe & others, this volume).

This paper describes the stratigraphy and structure of the Ballara-Mount Frosty area, which is the northerly continuation of the Alligator Syncline, from which it is now separated by some 28 km of dextral strike-slip displacement along the Fountain Range Fault. The area was selected for detailed mapping to see if the extensional structures described in the Alligator Syncline continued northward, and also to verify the presence or otherwise of a large klippe of a major D_1 thrust nappe in the area, as postulated by Loosveld & Schreurs (1987). The study found evidence of pre-D_1 extensional faulting, disproved the existence of a major D_1 thrust nappe, and also found



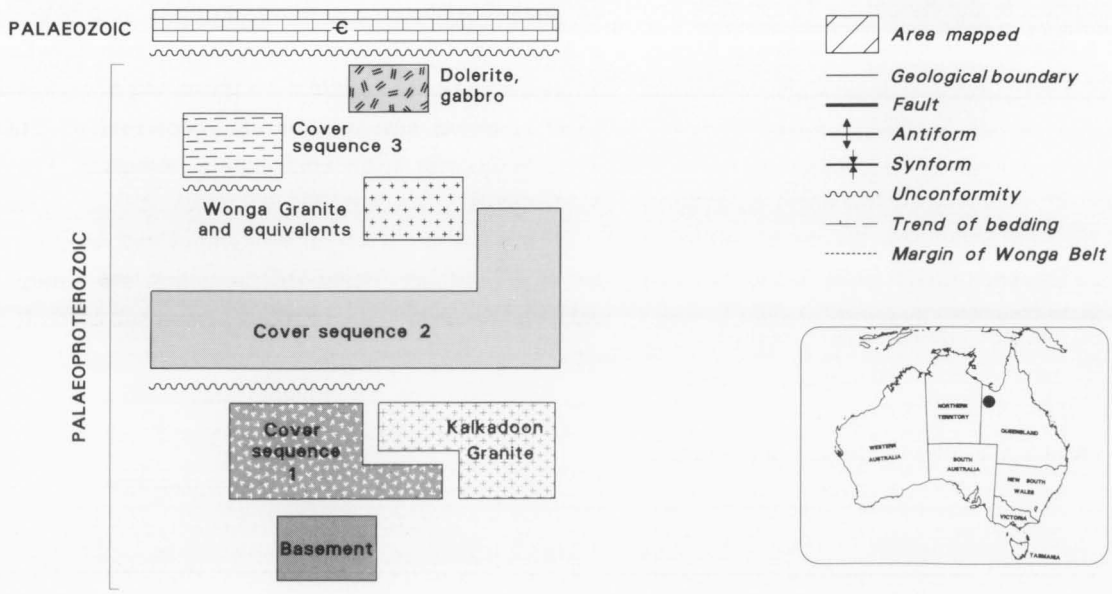


Fig. 1. Locality map of central part of Mount Isa Inlier.

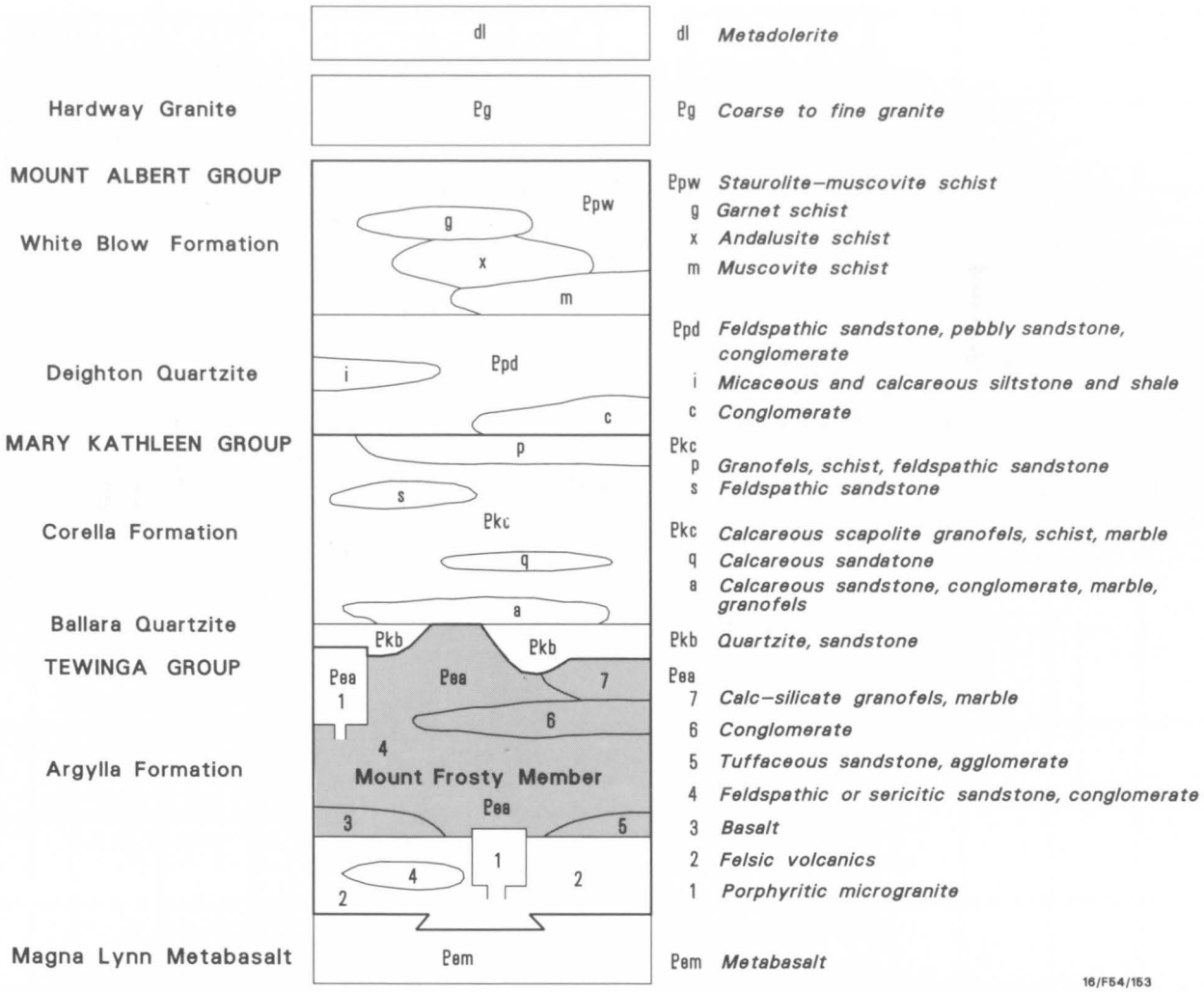


Fig. 2. Stratigraphic sequence in Ballara-Mount Frosty area.

low-angle D_1 and early D_2 thrust faults with displacements of several kilometres.

Terminology

Deformation episodes in the Ballara-Mount Frosty area are denoted by a superscript 'F'.

Regional setting

The Mount Isa Inlier (Blake, 1987) comprises a metamorphic basement of gneiss and migmatite older than 1875 Ma, and three overlying cover sequences of deformed and metamorphosed sedimentary and volcanic rocks. Cover sequence 1 (1875-1850 Ma) is mostly felsic volcanics, which are comagmatic with the voluminous Kalkadoon Granite intrusive into the basement complex. Cover sequences 2 (1790-1760 Ma) and 3 (1680-1670 Ma) comprise shallow-water sedimentary and bimodal volcanic rocks that formed during crustal rifting and sagging of the region. The period between the two rift-sag cycles included the episode of crustal extension and normal faulting at about 1740 Ma documented in the Alligator Syncline (Passchier, 1986), Bulonga Anticline (Passchier & Williams, 1989; Williams, 1989), Wonga Belt (Holcombe & others, this volume), Deighton Outlier (Stewart, 1989), and Ballara-Mount Frosty area. Granite and dolerite or gabbro were emplaced at various times after deposition of the cover sequences.

Proterozoic stratigraphy

The stratigraphic sequence in the Ballara-Mount Frosty area (Fig. 2) is conformable throughout, and comprises felsic and mafic volcanics, sandstone, carbonate, siltstone, and shale, variably metamorphosed to greenschist or amphibolite facies. The sequence begins with the Magna Lynn Metabasalt, the oldest unit of cover sequence 2 in the

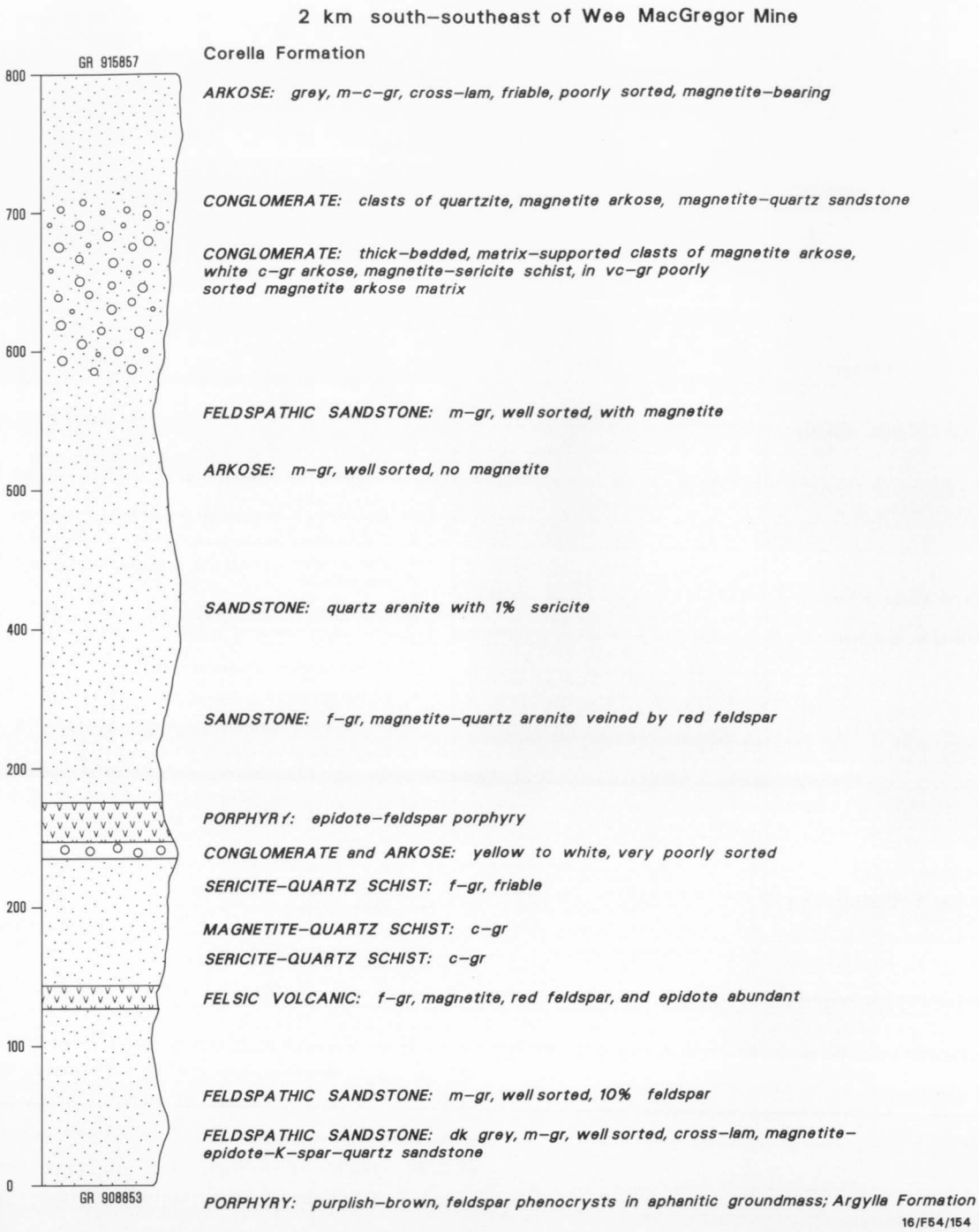


Fig. 3. Stratigraphic type section of Mount Frosty Member of Argylla Formation, 2 km south-southeast of Wee MacGregor mine.

area. The base of the Magna Lynn is not exposed, but elsewhere it is unconformable on the Leichhardt Volcanics of cover sequence 1 (Blake, 1987). Succeeding formations are felsic volcanics and sandstone of the Argylla Formation, the Ballara Quartzite, carbonate, siltstone, and shale of the Corella Formation, and then the Deighton Quartzite and aluminous schist of the White Blow Formation. The Hardway Granite (Derrick & others, 1977) intrudes the Magna Lynn Metabasalt and Corella Formation in the northeast of the area, and numerous metadolerite dykes and sills intrude all older units except the Deighton Quartzite. The Deighton Quartzite and White Blow Formation were tentatively placed in cover sequence 3 by Blake (1987), but were later transferred to cover sequence 2 (Blake & others, 1990) because the Deighton Quartzite is conformable on Corella Formation.

The stratigraphy of the Ballara-Mount Frosty area is summarised in Table 1.

TABLE 1. PALAEOPROTEROZOIC STRATIGRAPHY AND IGNEOUS INTRUSIONS, BALLARA-MOUNT FROSTY AREA, MOUNT ISA INLIER

Unit	Distribution (max thickness m)	Lithology	Relationships	Remarks
IGNEOUS INTRUSIONS				
Metadolerite dl	Throughout area; concentrated in Argylla Fm and Hardway Granite	Amphibolite: m-f.gr, massive to schistose, laced and bordered by biotite schist; bodies narrower than 2 m consist of schist only; abundant inclusions of hornfelsed sandstone	Intrudes all older units except Deighton Quartzite; small plug intrudes White Blow Fm at GR 888881	Dykes, sills, plugs, irregular masses, stockworks; magmatic cross-bedding at GR 888959
Hardway Granite Pg	In NE	Granite: massive m-c.gr; some f.gr and leucocratic granite and microgranite (Derrick & others, 1977)	Intrudes Corella Fm; faulted against Magna Lynn Metabasalt	Regarded as S-tilted pluton coeval with 1760-1730 Ma-old Wonga Granite (Page, 1990; Pearson & others, 1990)
COVER SEQUENCE 2				
MOUNT ALBERT GROUP				
White Blow Formation				
Ppw	In centre and W of Staurolite Syncline in S (870)	Staurolite-muscovite schist: carbonaceous in S; garnet pods in NW; garnet-pyrite amphibolite ovoids in NE	Conformable on Deighton Quartzite	Staurolite forms specimen-quality cruciform twins
Ppw_g	In S, SE, and NE of Staurolite Syncline (500)	Garnet schist: with biotite + muscovite	Lenses in Ppw and Ppw_m	Thickness value is outcrop width
Ppw_x	In E of Staurolite Syncline (200)	Andalusite schist: andalusite p'blasts in biot-musc-qtz g'mass; grades to carbonaceous slate and graphite schist with andalusite p'blasts	Lens between Ppw and Ppw_m	Thickness value is outcrop width
Ppw_m	In S and E of Staurolite Syncline (500)	Muscovite schist: includes biot-musc schist, micaceous metasandstone, and metasiltstone	Lens adjoining Ppw_x and Ppw_g	Thickness value is outcrop width

Deighton Quartzite				
Ppd	In Campbell Outlier (1880); in Charley Creek Outlier; S limb of Staurolite Syncline (327)	Feldspathic sandstone, pebbly sandstone, conglomerate: m-c.gr, cross-lam in thick sets; weakly metamorphosed, chlorite, biotite, actinolite common; pebbles are vein quartz and lutite; calc-silicate interbed near base in NW	Conformable on Corella Formation	Closely fractured in Charley Creek Outlier; actinolitized in centre of Charley Creek Outlier and near faults elsewhere
Ppd_i	In SE of Campbell Outlier (450)	Micaceous and calcareous siltstone, shale,: calcareous and biotitic in lower part; includes felds sst interbed with lutite clasts; grades up through biotitic granofels to metasiltstone at top	Lenticular subunit in middle of sandstone (Ppd) of Deighton Quartzite	Dark-weathering, valley-forming
Ppd_c	S end of Staurolite Syncline (150)	Conglomerate: angular to subrounded clasts of feld sst, lithic sst, and Corella Fm rock types in poorly sorted matrix of clayey and felds sst	Lens below sandstone (Ppd) of Deighton Quartzite	Quartz and feldspar partly replace some clasts
MARY KATHLEEN GROUP				
Corella Formation				
Pkc_p	Around Campbell Outlier (285 at S margin of outlier)	Granofels, schist, feldspathic sandstone: biotite, scapolite, and calcareous granofelses, plag-actin rock, marble, feld metasst with musc + biot + actin, pyritic siltstone	Conformable and gradational below Deighton Quartzite	Upper passage beds
Pkc_S	In NW (120); 3 km E of Mt Aimorn (50); SW limb of Staurolite Syncline (150)	Feldspathic sandstone: m-c.gr, cross-bedded, commonly contains up to 40% feldspar, but little or no feldspar SW of Staurolite Syncline	In middle of Corella Formation	Metamorphosed to epid-calc-biot-qtz granofels S of Campbell Outlier; altered to c.gr actin-qtz rock at GR 852962
Pkc	Throughout area (1270 in NW; 2400 between Mt Dorothy and S margin of Campbell Outlier; 1400 on SW limb of Staurolite Syncl)	Calcareous scapolite granofels, schist, marble: black biotitic metasiltstone +/- scapolite p'blasts, calc-scap granofels, marble, schist, micaceous metasandstone	Conformable on Ballara Quartzite and on sandstone (Pea_4) of Mt Frosty Member	Forms about 95% of Corella Formation; eqivalent to Pkc_1, Pkc_2, and Pkc_3 on Mary Kathleen 1:100 000 Geological Map (BMR, 1976)

Pkc_q	Between Mt Aimorn and Campbell Outlier in W (60)	Calcareous sandstone: grades to quartzite	Lenses in Pkc	Lenses up to 2 km long
Pkc_a	W limbs of Rosebud and Staurolite Synclines; 4 km SE of Mt Frosty mine (230)	Calcareous sandstone, conglomerate, marble, granofels: interbedded biot granofels or schist, quartzose marble, calc sst (conglomeratic), feld sst	Conformable and gradational on sandstone (Pea_4) of Mt Frosty Member	Lower passage beds
Ballara Quartzite				
Pkb	In NW, N, centre, and S (500)	Quartzite, sandstone.: In NW, three feld sst ridges, f-m-c.gr, cross-lam, separated by valley-forming very feld sst; in centre, m-c.gr feld sst, cross-lam, 2 m of red-brown porous sst with white clay spots at top; in S, m.gr cross-bedded qtzt with magnetite-rich cross-lam	Conformable on sandstone (Pea_4) or on calc-silicate granofels and marble (Pea_7) both of Mt Frosty Member, or on felsic volcanics (Pea_2) of Argylla Fm	In S, difficult to distinguish from sandstone (Pea_4) of Mt Frosty Member
TEWINGA GROUP				
Argylla Formation				
Mount Frosty Member				
Pea_7	In W at Mt Aimorn (40)	Calc-silicate granofels, marble: lower part v.c.gr biot-qtz-calc-actin granofels interbedded with v.c.gr cross-lam actin-calc-biot-qtz granofels; upper part felds sst, siltst, qtz wacke, arkose; some masses of c.gr calcite marble and interbeds of epid-scap-K-feld-qtz granofels	Conformable on conglomerate (Pea_6) of Mt Frosty Member	Lens 4 km long; granofels layers grade from quartz-rich at bottom to actinolite-rich at top
Pea_6	In W, on SE side of Mt Aimorn (160)	Conglomerate: interbedded c.gr feld to lithic metasst and cong with ang to subround clasts of qtz, feld sst, lutite, qtz sst, and magnetite in supporting matrix of v.c.gr epidotic lithic sst	Conformable on feld sst (Pea_4) and conformable below calc-silicate granofels and marble (Pea_7), both of Mt Frosty Member	S of Mt Aimorn, conglomerate includes felsic volcanic clasts

Pea_4	Throughout area (900)	Feldspathic or sericitic sandstone: m-thk bedded felds sst, arkose, pebble to boulder cong, rare qtz sst, and feldspar porphyry; poorly sorted, cross-bedded, m-c.gr, friable; abundant magnetite-rich cross-laminae	Conformable and gradational on felsic volcanics (Pea_2) of Argylla Formation	Max thickness near Mt Frosty mine; variably metamorphosed to musc-qtz granofels or schist, and rare quartzite; feldspar porphyry layers identical to felsic volcanics (Pea_2) of Argylla Formation
Pea_3	In S, 1 km NW of Fountain Mountain	Basalt: f.gr massive amphibolite with plagioclase phenocrysts and K-feld-actin-pyrite amygdales	Conformable below feld sst (Pea_4) of Mt Frosty Member, and conformable on felsic volcanics (Pea_2) of Argylla Fm	Single outcrop 700 m x 300 m
Pea_5	In S, W of Non Pareil mine (600)	Tuffaceous sandstone, agglomerate: qtz-musc schist with clasts of c.gr qtz-musc schist, magnetite-musc schist, musc-biot-qtz schist, quartzite +/- musc	Interfingers with feld sst (Pea_4) of Mount Frosty Member and with felsic volcanics (Pea_2) of Argylla Fm	Includes two interlayers 50-100 m thick of porph felsic volc 1 km S of Non Pareil mine; clasts interpreted as former volc fragments, and schist as former tuff and/or tuffaceous sst
Unnamed intrusions of Argylla Formation				
Pea_1	In NE, centre, and S	Microgranite: porphyritic; in NE at GR 915020, blue qtz + pink K-feldspar phenocrysts in v.f.gr g'mass; in NE at GR 908015, K-feldspar-phyric porphyry grades to musc-qtz augen schist; in centre at GR 838918, white, with qtz phenocrysts only; in S at GR 850830, magnetite-feld-musc-qtz schist	Cross-cuts enclosing feld sst (Pea_4) of Mt Frosty Member	In S, only one outcrop visited, others photo-interpreted; in NE and S, outcrops resemble felsic volcanics (Pea_2) of Argylla Fm, but are clearly intrusive
Unnamed member of Argylla Formation				
Pea_2	Throughout area (min 1700, 1.5 km S of Wee MacGregor mine)	Felsic volcanics: purple-brown rhyolite with K-feld, plag, and qtz phenocrysts in felsitic g'mass with magnetite and biot	Interfingers with Magna Lynn Metabasalt below	Commonly deformed to feldspar augen schist or gneiss with epid + musc + chlor; dated at about 1780 Ma (Page, 1983)
Magna Lynn Metabasalt				
Pem	In NE (300)	Metabasalt: c.gr foliated amphibolite with relict pyrox + epid + biot; veinlets of qtz, qtz-hornbl, qtz-chlor, red feldspar, and calcite	Base not exposed	At GR 899040, amygdales, bedded tuff, and scoria present (D.H.Blake, BMR, pers. comm.)

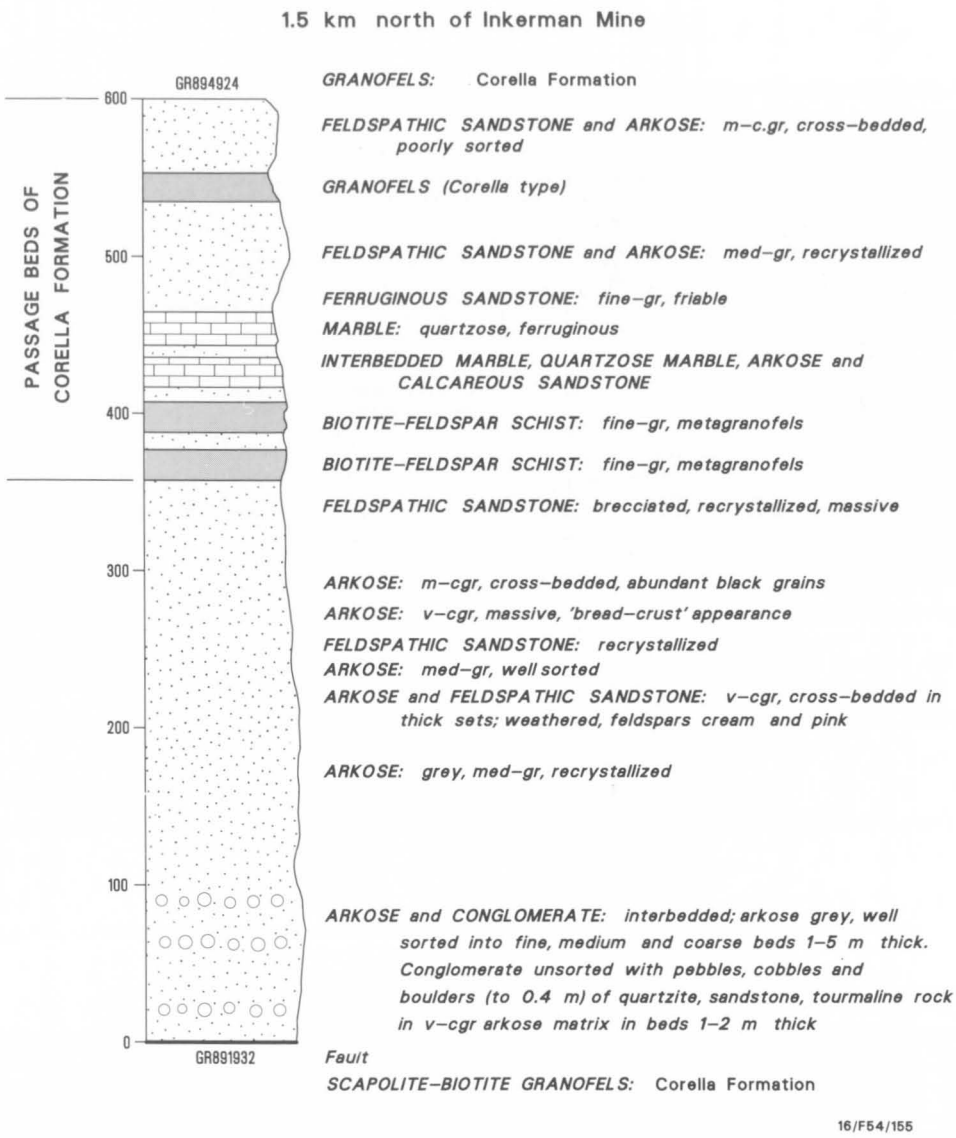


Fig. 4. Stratigraphic section through sandstone of the Mount Frosty Member and overlying passage beds of Corella Formation, 1.5 km north of Inkerman mine.

Tewinga Group

The Tewinga Group comprises the Magna Lynn Metabasalt and the overlying Argylla Formation. The Argylla Formation is a unit of sandstone and felsic volcanics, with lesser amounts of calc-silicate granofels and marble, conglomerate, tuffaceous sandstone and agglomerate, basalt, and small intrusions of porphyritic microgranite presumed to be subvolcanic equivalents of the felsic volcanics. A complete sequence through the Argylla Formation is nowhere exposed in the map area, but Derrick & others (1977, fig. 10, section j) measured 3600 m 13 km west of Ballara, just west of the map area; this estimate took no account of east-west shortening, and the true thickness is probably greater.

The Argylla Formation comprises a lower unit of felsic volcanics with subordinate lenses of feldspathic sandstone, and an upper unit, the newly named Mount Frosty Member, composed mostly of feldspathic sandstone (Fig. 2) with subordinate lenses of calc-silicate granofels and marble, conglomerate, tuffaceous sandstone and agglomerate, and basalt. A formal stratigraphic definition of the Mount Frosty Member is set out in Appendix 1. The type section is located 2 km south-southeast of the Wee MacGregor mine, and is shown in Figure 3. The sandstone of the member forms the highest hills and ridges in the area, although the sandstone and arkose are commonly friable and in places incoherent. The member rests conformably on felsic volcanics of the

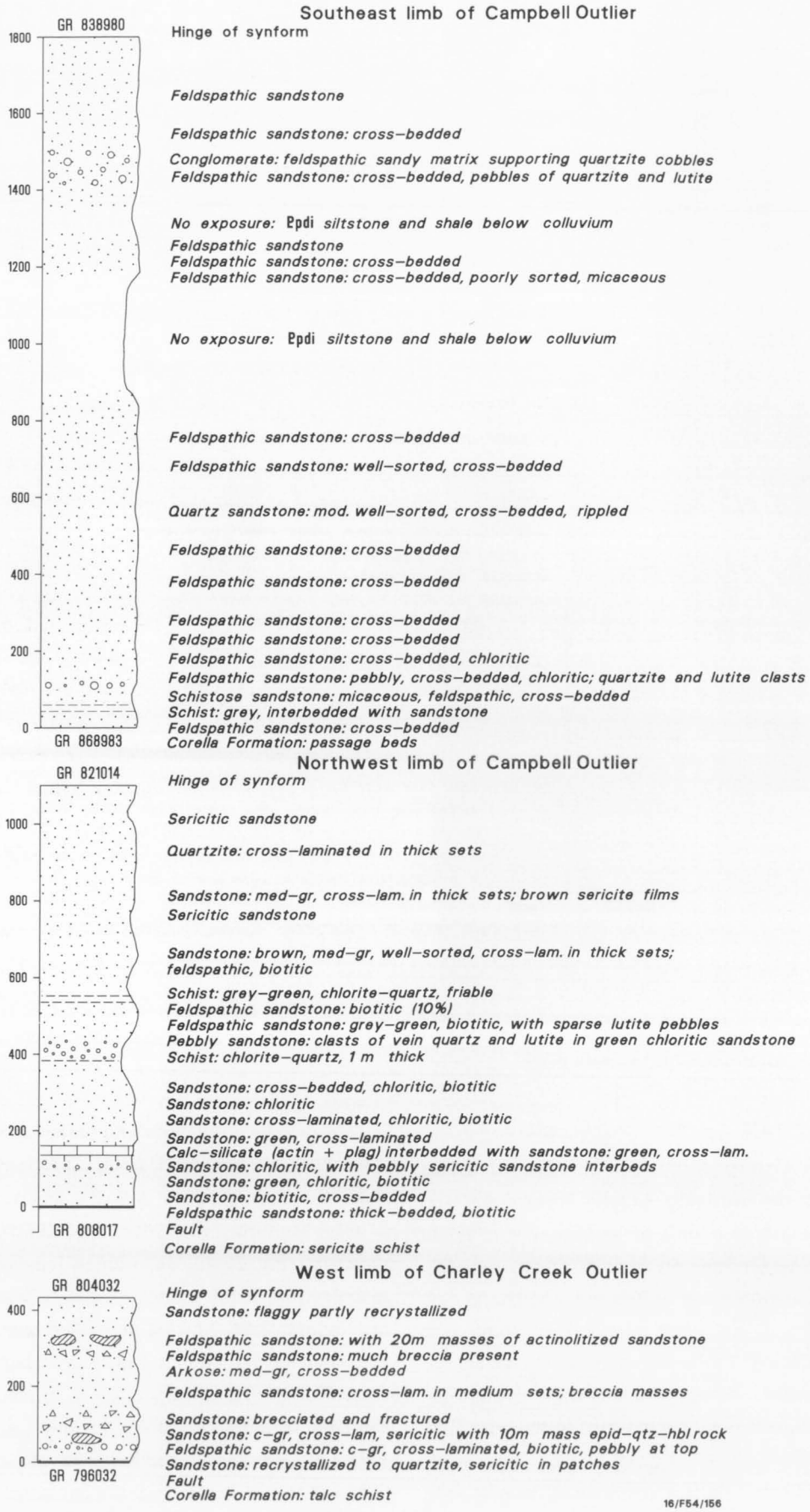


Fig. 5. Stratigraphic sections through Deighton Quartzite.

Argylla Formation at grid reference 838910, where purple feldspar porphyry is overlain by 5 m of interbedded crystal tuff and friable heavy-mineral-bearing sandstone with siltstone pebbles, then by a body of porphyry about 10 m thick, which is in turn overlain by the main sequence of cross-bedded friable feldspathic sandstone.

The abundance of feldspar, or muscovite where metamorphosed, heavy-mineral laminae, conglomerate beds, thick bedding, and high-angle cross-bedding suggest that the sandstone of the Mount Frosty Member is a fluvial or fluvio-deltaic deposit formed of detritus derived from nearby felsic volcanics of the Argylla Formation.

The sandstone of the Mount Frosty Member is shown as part of the Ballara Quartzite on the Mary Kathleen 1:100 000 Geological Map (BMR, 1976), but its sedimentological characteristics are very different from the shallow-marine environment of the Ballara Quartzite (Jackson & others, 1990). Hence, it is regarded as a different entity. On the Duchess Region 1:100 000 Geological Map (BMR, 1982), the sandstone was included near the top of the Argylla Formation. The sandstone was included in the lowest part of the Mary Kathleen Group by BMR (1990), and by Stewart (1990).

Mary Kathleen Group

The Mary Kathleen Group comprises the Ballara Quartzite and the overlying Corella Formation. The Ballara Quartzite forms up to four narrow parallel white strike ridges of resistant sandstone separated by valley-forming friable sandstone, which distinguishes the formation from the much wider plateau-forming feldspathic sandstone of the Mount Frosty Member.

The basal part of the Corella Formation is commonly an interval of passage beds comprising interbedded calcareous sandstone, conglomerate, marble, and granofels, and a similar interval occurs at the top of the formation, comprising interbedded granofels, schist, and feldspathic sandstone (Table 1). A reference section through the lower passage beds on the western limb of the Rosebud Syncline is shown in Figure 4.

Mount Albert Group

The Mount Albert Group comprises the Deighton Quartzite and the overlying White Blow Formation. The Deighton Quartzite of the Campbell Outlier and Staurolite Syncline conformably overlies the Corella Formation, but in the Charley Creek Outlier the two formations are joined by a bedding-parallel fault. Representative sections through the Deighton Quartzite are shown in Figure 5. The White Blow Formation crops out only in the Staurolite Syncline in the south of the map area, and forms low rises mantled with loose staurolite twin crystals.

Proterozoic igneous intrusions

Igneous intrusions in the map area include the Hardway Granite and numerous metadolerite dykes, sills, and stockworks (Table 1). The dolerite was emplaced along bedding planes, joints, faults, and 1 km north of Wee MacGregor, along breccia zones as found by Passchier (1986) in the Alligator Syncline.

Structure

The deformational events that affected the Ballara-Mount Frosty area are set out in Table 2. Figure 6 shows the major faults and fold traces in the area.

Extensional deformation

Extensional faulting D^{F}_{1}, the earliest deformation in the Ballara-Mount Frosty area, produced high-angle normal faults, low-angle normal faults, and bedding-parallel extensional faults. The normal faulting was accompanied by emplacement of voluminous dolerite stockworks (see Stewart, 1991). The extensional deformation is correlated with the 1760-1730 Ma extension described in the Wonga Belt to the east and in the Little Beauty Syncline to the north (Pearson & others, this volume).

D^{F}_{1} structures and associated intrusions

Metadolerite dykes and sills in the Wee MacGregor area on the southwestern limb of the Rosebud Syncline were injected along breccia zones and faults which cut the sandstone of the Mount Frosty Member at a large angle to bedding. The dykes are not brecciated, but are cleaved by the D^{F}_{3} foliation and metamorphosed to biotite schist. Hence, the dykes are pre-D^{F}_{3}, but post-breccia. Passchier (1986) attributed similar dykes and breccia zones in the Alligator Syncline 28 km to the southwest to early extensional faulting followed by dolerite intrusion along the fault and breccia zones. In the Wee MacGregor area, however, the dolerite-filled faults and breccia zones are associated with a double thickness of sandstone of the Mount Frosty Member, indicating contractional faulting. The doubled section is, however, succeeded to the north by a 1-km gap in the sandstone of the Mount Frosty Member (grid reference 887903), indicating extension. It appears that the sandstone underwent north-south D^{F}_{1} extensional faulting, and the angular fault blocks (Fig. 7a,

TABLE 2. DEFORMATION EVENTS IN THE BALLARA-MOUNT FROSTY AREA, SHOWING CORRELATION WITH REGIONAL EVENTS

Time Ma	Deformation episode	Structural Events	Page & Bell 1986
post 1500	D^F_4	NE and NW strike-slip faulting; injection of Corella Formation into fault openings; late normal faulting on NW side of Mt Aimorn	
1544	D^F_3	E-W-directed folding and cleavage, e.g., Staurolite and Rosebud Synclines; folding of Melba Fault and of D^F_2 synform at Mt Aimorn, with crenulation of D^F_2 cleavage; cleavage, metamorphism and rotation of dolerite stockworks, sills, and dykes to present attitude; formation of thrust sheet on W limb of Rosebud Syncline, followed by antiformal folding of sheet; antiformal folding of synformal White Blow Formation and of rotated normal fault at S end of Staurolite Syncline; normal faulting along NE side of Campbell Outlier	D_2
1610	D^F_2	N-S-directed thrust faulting, e.g., Melba Fault, and folding, e.g., synform at Mount Aimorn with tight folds and cleavage between Melba Fault and Mount Aimorn; formation of antiformal stack duplex 3 km W of Mt Frosty; reassembly of separated fault blocks on future SW limb of Rosebud Syncline; rotation to N dip of normal fault at S end of future Staurolite Syncline, and tight synformal folding of White Blow Formation N of fault	D_1
1760 to 1730	D^F_1	N-S-directed high-angle extensional faulting, e.g., on future SW limb of Rosebud Syncline and at S end of future Staurolite Syncline; intrusion of dolerite stockworks, sills, and dykes; formation of bedding-parallel fault beneath Charley Creek Outlier and at N end of Campbell Outlier; formation of low-angle extensional imbricate fan at S end of Campbell Outlier; S-ward tilt of Hardway Granite	

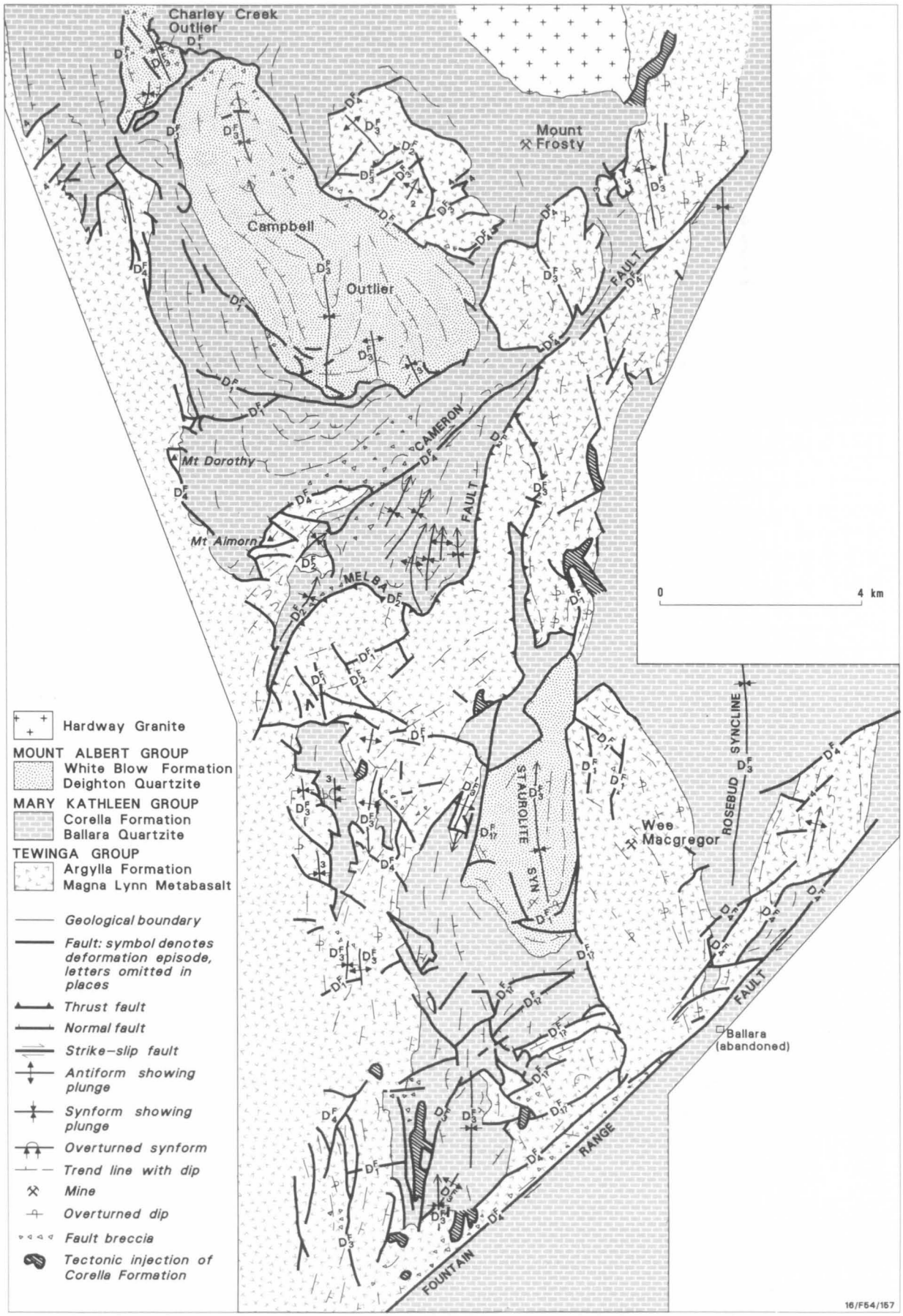


Fig. 6. Structural map of Ballara-Mount Frosty area; microgranite of Argylla Formation and metadolerite omitted.

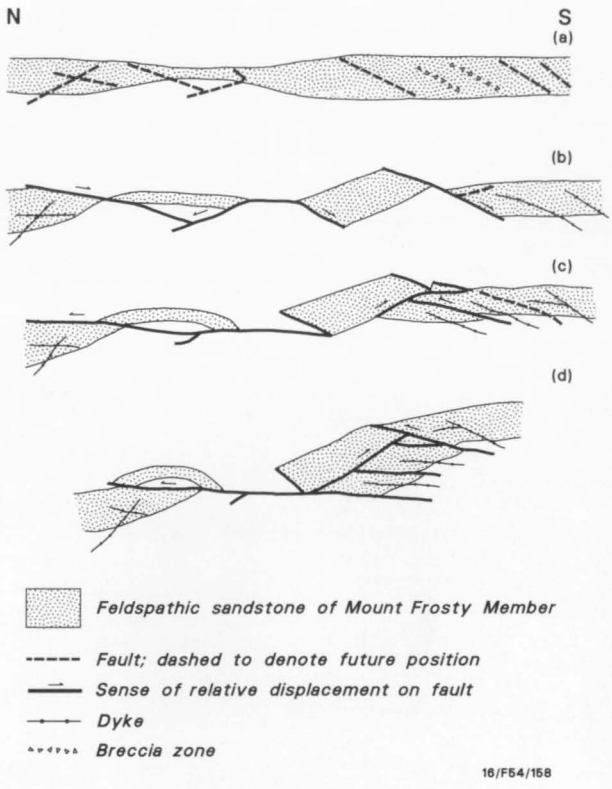


Fig. 7. Extensional and contractional faulting in southwest limb of Rosebud Syncline; dashes and triangles respectively denote future faults and breccia zones.

b) were later jammed back together during D^F_2 contraction (Fig. 7c, d).

The *Charley Creek Outlier* is in largely bedding-parallel fault contact with the underlying Corella Formation, but in detail the eastern fault margin of the outlier locally cuts bedding, and patches of fault breccia along the contact are cleaved by D^F_3 (Fig. 8). Hence, the fault at the base of the Outlier is pre or early-D^F_3. It is interpreted here as a D^F_1 extensional fault because it puts the younger Deighton Quartzite over the older Corella Formation. This is supported by the similarly fault-bounded Deighton Outlier, 4 km northeast of the map area, where the fault below the outlier is folded by and therefore predates a gently west-plunging $D_1 = D^F_2$ fold (Stewart, 1989).

The *Deighton Quartzite on the western limb of the Campbell Outlier* is conformable on the underlying Corella Formation. This negates the thrust-nappe hypothesis of Loosveld & Schreurs (1987), who suggested that the Deighton Quartzite was the stratigraphic equivalent of the Ballara Quartzite, thrust over Corella Formation. The *fault on the eastern side of the outlier* is a steeply west-dipping normal fault with pockets of massive breccia; the absence of cleavage shows that the last normal fault movements were post-D^F_3. At the northern end of the outlier, however, the fault breccia is cleaved by and therefore predates D^F_3 foliation dipping 80°W, showing that extensional faulting began pre or syn-D^F_3. The same relationships prevail on the eastern side of the Scorpion Outlier of Deighton Quartzite, 12 km to the north-northwest (Stewart, 1989). By analogy with the Charley Creek and Deighton Outliers, the extensional faulting probably began during D^F_1.

Two D^F_1 *extensional faults* are present at the southern end of the Campbell Outlier (Fig. 9). The faults root in the upper Corella passage beds, and cut down westward through the Corella Formation, forming an extensional imbricate fan. The larger fault is associated with an actinolitic alteration zone in the passage beds, and its western half has been intruded by dolerite. North of the fan, the lower Deighton Quartzite below the siltstone subunit has thinned by brittle extensional faulting.

A south-dipping *isoclinally folded fault* is present at the southern end of the Staurolite Syncline (Fig. 6 and Stewart, 1991). Bedding in the White Blow Formation north of the fault dips south, forming a downward-facing antiform. Bedding in the Deighton Quartzite south of the fault dips north, at a large angle to the fault. Hence, the fault is interpreted as a D^F_1 normal fault which originally dipped north, but was rotated to a southerly dip during D^F_2 contraction, and then isoclinally folded during D^F_3 (Fig. 10). During D^F_2 the White Blow Formation was folded into a tight east-trending north-verging synform with an inverted upper limb, and during D^F_3 it was refolded into a close south-plunging upright antiform. The final shape is a crescentic interference fold (Type 2 of Ramsay, 1967). (The interpretation of the fold shown in cross-section EF [Stewart, 1991] is superseded by that shown in Figure 10.)

A possible D^F_1 *fault* marked by abundant massive sandstone breccia and with a sinuous trace suggestive of D^F_3 folding, can be traced from the northern end of the Campbell Outlier to the eastern margin of the Charley Creek Outlier (Fig. 6).

Contractional deformation

Regional shortening which affected all stratigraphic units throughout the Mount Isa Inlier took place during the Isan Orogeny (Blake & others, 1990) at about 1610 Ma = D^F_2

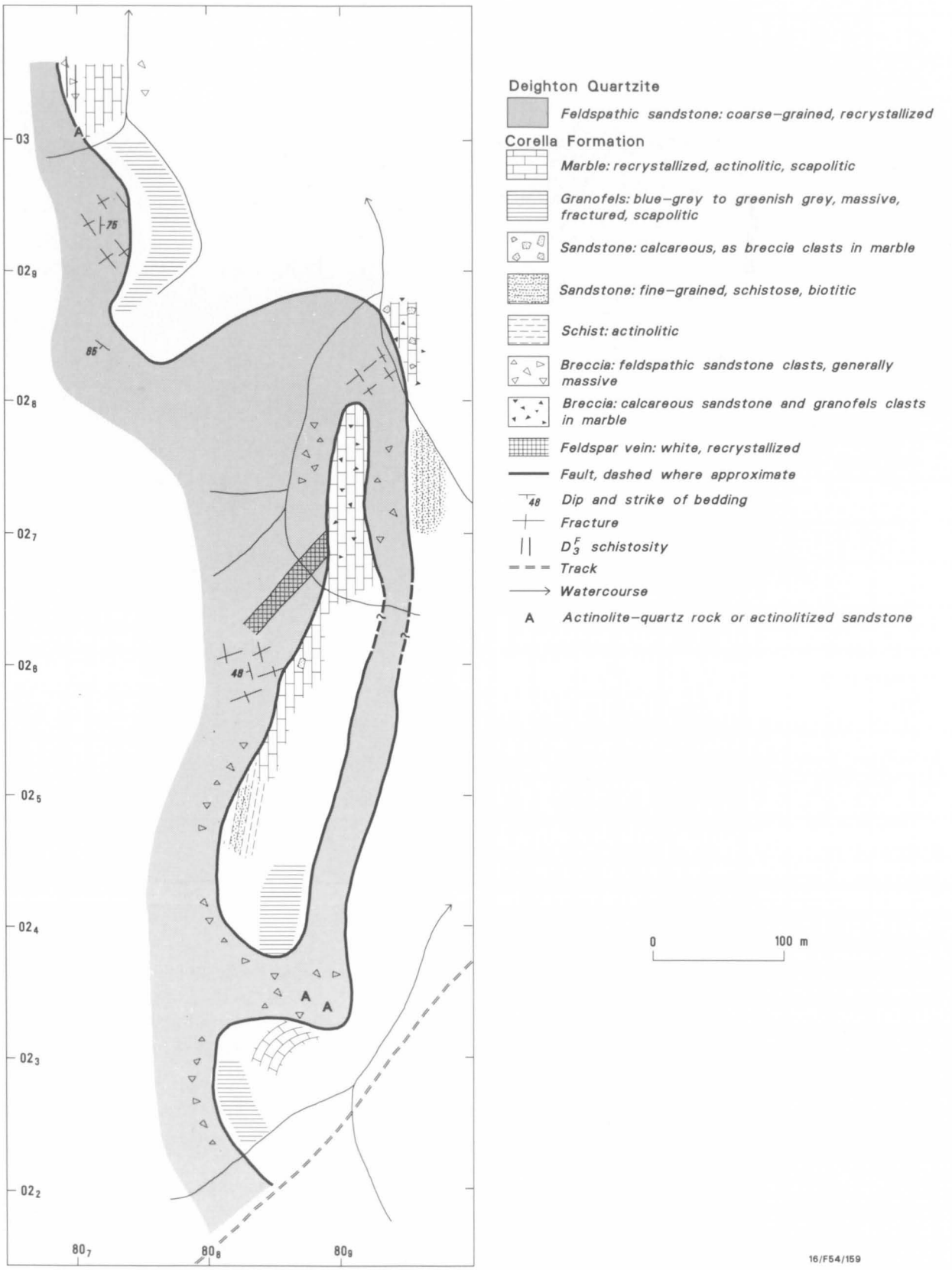


Fig. 8. Detailed map of eastern margin of Charley Creek Outlier; numbered ticks are 100 m intervals of Australian Map Grid, Zone 54.

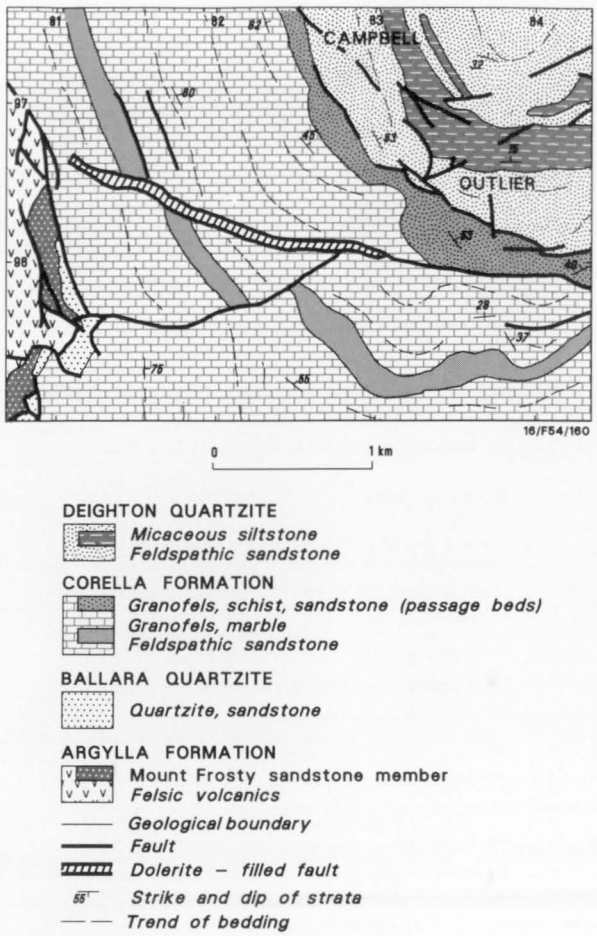


Fig. 9. D^F_1 extensional faults at south end of Campbell Outlier; numbered ticks are 1 km intervals of Australian Map Grid, Zone 54.

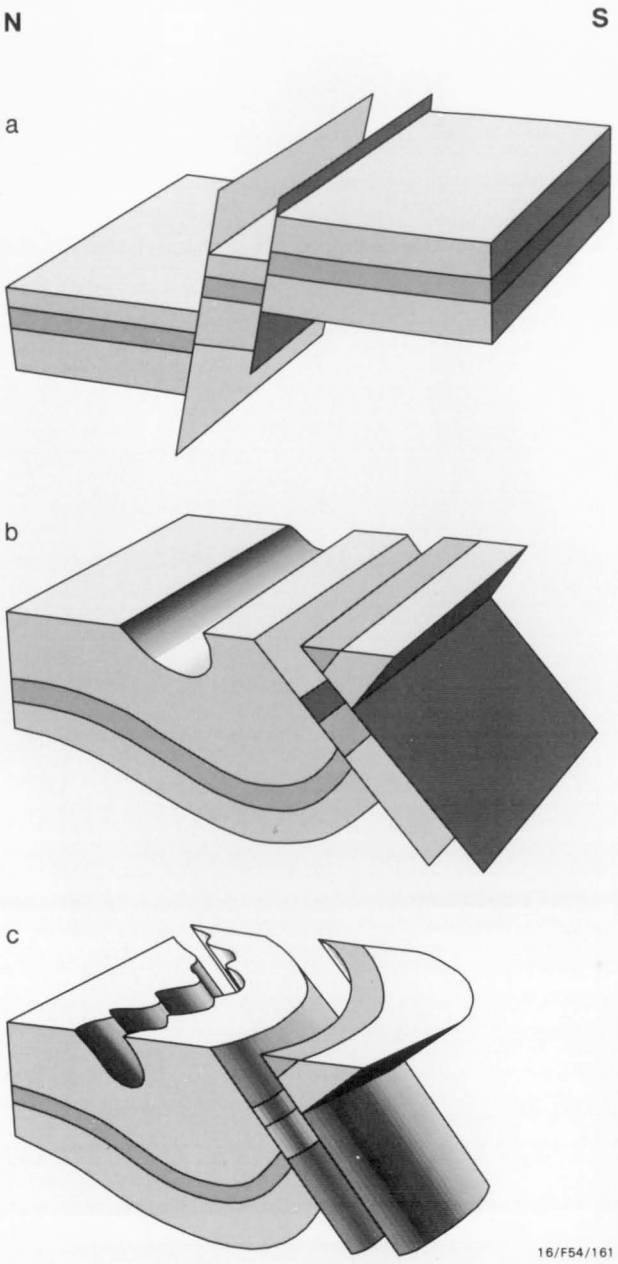


Fig. 10. Evolution of Staurolite Syncline; (a) north-south D^F_1 extensional faulting; (b) north-south D^F_2 contraction rotates faults to south dip; (c) east-west D^F_3 contraction folds faults and beds to Type 2 interference fold (Ramsay, 1967).

(D_1 of Bell, 1983) and 1544 Ma = D^F_3 (D_2 of Bell), as dated by Page & Bell (1986). D^F_2 produced east-west folds, an associated axial-plane cleavage, and several east-striking thrust faults. D^F_3 produced north-trending folds and thrust faults, and a penetrative steep to vertical north-striking schistosity; the folds dominate the map pattern of the region. Three large synforms in the Ballara-Mount Frosty area – the one through the Campbell Outlier in the northwest, the Staurolite Syncline in the south, and the Rosebud Syncline extending up the eastern side of the area – all formed during D_{F3}. The antiforms between the synforms are so damaged by faults and dolerite stockworks as to be nearly unrecognisable.

D^F_4 formed major strike-slip faults. The two largest, the Cameron Fault (2 km displacement) and Fountain Range Fault (28 km) strike northeast; northwest-striking faults are shorter and of lesser displacement than the northeast faults.

D^F_2 structures

The *Melba Fault* is a large folded fault which juxtaposes Argylla and Corella Formations in the centre of the area (Fig. 6 and Stewart, 1991). The fault is folded by, and therefore older than the major north-trending D^F_3 folds. A very tight gently arcuate synform parallels the fault at its western end, and is cut by two cleavages: a north-northwest-striking crenulation which is assigned to D^F_3 because it crenulates an earlier northeast-striking axial

plane cleavage. The earlier cleavage and the synform to which it is axial-plane are assigned to D^F_2. If the synform formed at the same time as the Melba Fault, this would indicate that the Melba Fault is D^F_2, contractional, and therefore south-dipping. This is supported by a southeast dip of 77° on the fault at grid reference 830910, and is the basis for construction of the western part of cross-section EF, the Melba Fault being shown as a south-dipping low-angle thrust fault.

A small *antiformal stack duplex* (cross-section AB; Stewart, 1991) forms the mass of sandstone of the Mount Frosty Member 3 km west of the Mount Frosty mine, and explains the excessive thickness of the sandstone in this particular area. The duplex comprises a single lenticular imbricate or horse of sandstone of the Mount Frosty Member, and an overlying thrust sheet of Argylla Formation volcanics. Indicated translation of the imbricate is 2.2 km, and of the overlying sheet 1.6 km. A stretching lineation observed at the southwestern margin of the allochthonous volcanics plunges southeast, indicating northwest translation of the thrust sheet. This direction is parallel to neither the usual D^F_2 north-south shortening nor to the usual D^F_3 east-west shortening. It is, however, parallel to the shortening direction for D^F_2 folds in the Mount Aimorn area, and in the Deighton Outlier (Loosveld & Schreurs, 1987; Stewart, 1989), and at a large angle to the shortening direction for the D^F_3 synform forming the neighbouring Campbell Outlier. Hence, the duplex is assigned to D^F_2. It is segmented by numerous small northeast-striking faults which are confined to the duplex and so are regarded as unrelated to the through-going D^F_4 strike-slip faults; they may be late-D^F_3.

D^F_3 structures

A small *thrust sheet* is located on the western limb of the Rosebud Syncline in the northeast of the map area, and is shown at the eastern end of cross-section AB (Stewart, 1991). The sheet places Argylla volcanics, preserved as a small klippe at grid reference 897005, 2 km east-southeast of the Mount Frosty mine, over Corella Formation calc-silicate, and has an indicated westward translation of 3 km. The thrust sheet is assigned to early D^F_3, and is folded by a D^F_3 antiform parallel to the Rosebud Syncline.

D^F_4 structures

The major D^F_4 structures are *northeast-striking strike-slip faults,* namely, the Fountain Range and Cameron Faults (Fig. 6). Where it cuts the sandstone of the Mount Frosty Member, the Fountain Range Fault is bordered by a zone several hundred metres wide of shattered and brecciated sandstone. Smaller D^F_4 faults form the northwest and southeast margin of the block of sandstone of the Mount Frosty Member and Argylla volcanics 3 km south of the Mount Frosty mine. This block is entirely surrounded by marble and calc-silicate rocks of the Corella Formation, which appears to have been tectonically injected along the D^F_4 fault margins. Similar *injections of Corella Formation,* most with northeast or northwest-striking boundaries, are shown in Figure 6.

The gently arcuate *fault on the northwest side of Mount Aimorn* (Fig. 6) has a massive fault breccia along it, comprising angular clasts of feldspathic sandstone in a black aphanitic mylonite matrix cut by veinlets of mylonite. The fault is apparently undeformed, and may be a D^F_4 normal fault, as the most prominent fractures in the breccia dip steeply northwest. The north-northwest-striking fault along the Argylla-Corella contact north of Mount Dorothy mine has about 2 km of sinistral strike-slip along it, and may be a tear-fault at the western end of the D^F_4 normal fault.

The interpreted sequence of structural events in the Ballara-Mount Frosty area is set out in Table 2.

Conclusions

The rocks of the Ballara-Mount Frosty area form a conformable sequence from Argylla Formation up through Ballara Quartzite, Corella Formation, Deighton Quartzite, and White Blow Formation, with transitional sequences (passage beds) of alternating rock types at the Argylla-Corella and Corella-Deighton boundaries.

A new unit, the Mount Frosty Member, is mapped at the top of the Argylla Formation, and comprises mainly feldspathic sandstone with associated lenses of calc-silicate granofels, conglomerate, tuffaceous sandstone and agglomerate, and basalt. The poorly sorted nature of the sandstone, and the abundant conglomerate, agglomerate, and tuff indicate a continental (fluviatile) depositional environment.

Most of the Ballara Quartzite in the area is now mapped as sandstone of the Mount Frosty Member, and the Ballara Quartzite is restricted to small areas of clean well sorted quartzite and feldspathic sandstone which form ridges and valleys, in contrast to extensive plateaus of sandstone of the Mount Frosty Member.

There is no major thrust nappe duplicating the Mary Kathleen Group (Ballara Quartzite and Corella Formation); the Mount Albert Group (Deighton Quartzite

and White Blow Formation) is a valid stratigraphic entity conformable above the Mary Kathleen Group.

There is abundant evidence of extensional faulting D^F_1 older than the north-south D_1 (1610 Ma) contraction of the Isan Orogeny, and oriented north-south in the east of the area, and northeast-southwest in the west. The extensional faulting is equated with that dated at 1760-1730 Ma in the neighbouring Wonga Belt, and affected all stratigraphic units up to and including the White Blow Formation. The 1760-1730 Ma time of this faulting sets a possible younger limit to the stratigraphic age of the Mount Albert Group.

D_1 (D^F_2) north-south contraction formed a large thrust sheet in the centre of the area, and a smaller antiformal stack duplex in the north.

Early D_2 (D^F_3) east-west contraction formed a small thrust sheet on the western limb of the Rosebud Syncline.

The tectonically mobile calcareous rocks of the Corella Formation were injected into numerous fault openings during strike-slip faulting D^F_4, the last deformation of the area.

Acknowledgements

I thank Dave Blake and Peter Stuart-Smith for reviews of the manuscript. The diagrams were drawn by Heicke Apps and Joe Mifsud of the Bureau of Mineral Resources' Cartographic Services Unit.

References

BELL, T.H., 1983 - Thrusting and duplex formation at Mount Isa, Queensland, Australia. *Nature* 304, 493-497.

BLAKE, D.H., 1987 - Geology of the Mount Isa Inlier and environs, Queensland and Northern Territory. *Bureau of Mineral Resources, Australia, Bulletin* 225, 83 pp.

BLAKE, D.H., ETHERIDGE, M.A., PAGE, R.W., STEWART, A.J., WILLIAMS, P.R., & WYBORN, L.A.I., 1990 - Mount Isa Inlier -- regional geology and mineralisation. *In:* HUGHES, F.E. (Editor), Geology of the Mineral Deposits of Australia and Papua New Guinea. *Australasian Institute of Mining and Metallurgy, Melbourne,* 915-925.

BMR, 1990 - New results from the Mount Isa Geotraverse. *BMR Research Newsletter* 12, 6-8.

CONNORS, K.A., & PAGE, R.W., 1992 - Age relationships between granite intrusion, metamorphism, and deformation in the Mount Isa Inlier. *Geological Society of Australia, 11th Australian Geological Convention, Ballarat, 1992, Abstracts* 32, 229-230.

DERRICK, G.M., WILSON, I.H., HILL, R.M., GLIKSON, A.Y., & MITCHELL, J.E., 1977 - Geology of the Mary Kathleen 1:100 000 Sheet area, northwest Queensland. *Bureau of Mineral Resources, Australia, Bulletin* 193, 114 pp.

DUNNET, D., 1976 - Mt Isa - reconstruction of a faulted ore body. *Philosophical Transactions of the Royal Society of London* A283, 333-344.

HOLCOMBE, R.J., PEARSON, P.J., & OLIVER, N.H.S., this volume - Structure of the Mary Kathleen Fold Belt. *In*: STEWART, A.J., & BLAKE, D.H. (Editors), Detailed Studies of the Mount Isa Inlier. *Bureau of Mineral Resources, Australia, Bulletin* 243.

JACKSON M.J., SIMPSON, E.L., & ERIKSSON, K.A., 1990 - Facies and sequence stratigraphic analysis in an intracratonic, thermal-relaxation basin: the Early Proterozoic, Lower Quilalar Formation and Ballara Quartzite, Mount Isa Inlier, Australia. *Sedimentology* 37, 1053-1078.

LOOSVELD, R.A.H., & SCHREURS, G., 1987 - Discovery of thrust klippen, northwest of Mary Kathleen, Mt Isa Inlier, Australia. *Australian Journal of Earth Sciences* 34, 387-402.

PAGE, R.W., 1983 - Timing of superposed volcanism in the Proterozoic Mount Isa Inlier, Australia. *Precambrian Research* 21, 223-245.

PAGE, R.W., 1990 - Developments in U-Pb zircon geochronology in the Mount Isa Inlier. *Monash University and Victorian Institute of Earth and Planetary Sciences, Mount Isa Inlier Geology Conference, November 1990*, 4-5.

PAGE, R.W., & BELL, T.H., 1986 - Isotopic and structural responses of granite to successive deformation and metamorphism. *Journal of Geology* 94, 365-379.

PASSCHIER, C.W., 1986 - Evidence for early extensional tectonics in the Proterozoic Mount Isa inlier, Australia. *Geology* 14, 1008-1011.

PASSCHIER, C.W., & WILLIAMS, P.R., 1989 - Proterozoic extensional deformation in the Mount Isa Inlier, Queensland, Australia. *Geological Magazine* 126, 43-53.

PEARSON, P.J., PAGE, R.W., & HOLCOMBE, R.J., 1990 - Geochronology of the Wonga Granite, northwest Queensland: implications for the timing of deformation in the Mary Kathleen Fold Belt. *Monash University and Victorian Institute of Earth and Planetary Sciences, Mount Isa Inlier Geology Conference, November 1990,* 13-15.

RAMSAY, J.G., 1967 - Folding and Fracturing of Rocks. *McGraw-Hill, New York,* 568 pp.

STEWART, A.J., 1989 - Extensional faulting as the explanation for the Deighton 'Klippe' and other Mount Albert Group outliers, Mount Isa Inlier, northwestern Queensland. *Australian Journal of Earth Sciences* 36, 405-421.

STEWART, A.J., 1990 - Extension and contraction in the Ballara-Mount Frosty area, Mount Isa Inlier. *Monash*

University and Victorian Institute of Earth and Planetary Sciences, Mount Isa Inlier Geology Conference, November 1990, 11-12.

STEWART, A.J., 1991 - Geology of the Ballara-Mount Frosty Region (1:25 000 scale map). *Bureau of Mineral Resources, Canberra, Australia* (two sheets). Available as colour electrostatic plots on paper (AUD30), or in digital form on optical disc or Exabyte 8 mm tape (prices on application) both of which can be displayed on Intergraph Microstation software on computers that will run Unix. The digital data comprise a scanned raster image (.RLE format) of the black and white geological map, and an Intergraph vector design file containing the boundaries of coloured polygons. The coloured map and data are available from the Publication Sales Centre, Bureau of Mineral Resources, and an uncoloured Ozalar film or paper copy (AUD20) of the map is available from BMR Copy Service, both at GPO Box 378, Canberra, ACT, 2601, Australia. All orders to be prepaid to Collector of Public Monies.

WILLIAMS, P.R., 1989 - Nature and timing of early extensional structures in the Mitakoodi Quartzite, Mount Isa Inlier, northwest Queensland. *Australian Journal of Earth Sciences* 36, 283-296.

Appendix 1: Stratigraphic Definition of Mount Frosty Member

Derivation of name: Mount Frosty mine (lat. 20° 46' 57"S, long. 139° 55' 13"E, grid reference 878015, Mary Kathleen 1:100 000 Sheet area).

Distribution: southeastern part of Mary Kathleen 1:100 000 Sheet area, in central part of Mount Isa Inlier.

Type section: 2 km south-southeast of Wee MacGregor mine, from base at lat. 20° 55' 46"S, long. 139° 57' 04"E (grid reference 908850) northeastward to top at lat. 20° 55' 33"S, long. 139° 57' 25"E (grid reference 915857); see Figure 3. Here the member is a ridge (bedding dips 85° northeast) consisting mainly of feldspathic sandstone and arkose with two intervals of volcanic feldspar porphyry, respectively about 17 m (lower) and 35 m (upper) thick in lower part of member, and with 130 m of conglomerate in upper part. Total thickness including porphyry and conglomerate is 800 m. Overlies volcanic feldspar porphyry of Argylla Formation, and is overlain by interbedded calcareous and biotitic granofels and marble of the Corella Formation.

Lithology: The member comprises the following mapped units:

- ridge-forming interbedded feldspathic sandstone, arkose, and conglomerate, making up most of the member and containing kilometre-sized separate lenses of:
- calc-silicate granofels and marble (valley-forming) at the top of the member; reference locality is northern slope of ridge capped by Ballara Quartzite, and extends from grid reference 836_0937_7 (base) to 837_5937_0 (top);
- conglomerate (ridge-forming) below the calc-silicate/marble unit; reference locality is southern half of ridge (northern half is feldspathic sandstone unit), and extends from grid reference 836940 (base) to 837937 (top);
- tuffaceous sandstone and agglomerate (low to moderate ridges) at base; reference locality is ridge immediately west of Non Pareil mine, from grid reference 840781 (bottom) to 844780 (top); and
- basalt (valley) at base; reference locality is in bed of creek at grid reference 886_5823_0.

Thickness: generally between 500 m and 900 m (maximum); thins to zero in northwest.

Relationships: forms upper part of Argylla Formation of Mount Isa Inlier; rests conformably on felsic volcanics of Argylla Formation, and is overlain conformably by lenses of Ballara Quartzite, or where this is absent, by the Corella Formation. The base of the member is taken at the first appearance of feldspathic (or sericitic where metamorphosed) sandstone above felsic porphyry of the Argylla Formation, and the top at the first appearance of calcareous or pelitic metasediments of the Corella Formation. The relationships of the subsidiary lenses of the member are shown diagrammatically in Figure 2.

Synonymy: Mapped as Ballara Quartzite on Mary Kathleen 1:100 000 Geological Map (BMR, 1976); mapped as an unnamed unit near the top of the Argylla Formation on Duchess Region 1:100 000 Geological Map (BMR, 1982); was included in the lowest part of the Mary Kathleen Group by BMR (1990) and by Stewart (1990).

Age: About 1780 Ma (Page, 1983) by U-Pb conventional zircon method on felsic volcanics of Argylla Formation.

Page 228 is blank.

The Corella Formation of the Rosebud Syncline (central Mount Isa Inlier): deposition, deformation, and metamorphism

Jürgen Reinhardt [1]

This paper is based on the following map:

Reinhardt, J., 1991 - Geology of the Rosebud Syncline (1:25 000 scale map), Bureau of Mineral Resources, Canberra.

The Corella Formation of the Rosebud Syncline is a sequence of interlayered Al- and Mg-rich metapelites (andalusite-sillimanite schist, cordierite schist, cordierite-orthoamphibole rock, and talc-bearing rocks), Ca-rich rocks (calcschist, para-amphibolite, calc-silicate rock, and marble), feldspathic schist, and scapolite schist. The original pelite-carbonate-evaporite sequence was deposited in a Mid-Proterozoic ensialic rift basin, and represents the final stage of rift sedimentation in a hypersaline shallow-water environment.

The major deformation events are: southward thrusting accompanied by strike-slip shearing (D_1), strong east-west shortening characterised by tight upright folding and heterogeneous vertical extension (D_2), a weaker contractional event with minor north-northwest-striking folds (D_3), and late dextral northeast- to north-northeast strike-slip faulting. Foliations and mineral lineations with characteristic orientations formed during D_1 and D_2.

The main metamorphic episode was synchronous with D_2. The rocks record prograde low-pressure reactions, and sequential mineral growth correlates with progressive stages of deformation, from early- to late-D_2. Peak conditions were reached at 580-640°C and 400-500 MPa. The study area lies completely within the sillimanite-muscovite zone, but isograds in the calc-silicate rocks and the decreasing proportion of andalusite to sillimanite indicate a temperature gradient from west to east. The metamorphic fluid compositions were heterogeneous with respect to $X_{(H2O-CO2)}$ and were locally highly saline. Infiltration metasomatism was restricted to local zones of enhanced permeability. The post-D_2 cooling history is constrained by retrograde kyanite and andalusite. Accordingly, the prograde-retrograde P-T path is anticlockwise.

[1]Geology Department, James Cook University of North Queensland, Townsville, Queensland 4811, Australia

Present address: Institut für Mineralogie, Ruhr-Universität Bochum, D-4630 Bochum, Germany

Introduction

The Rosebud Syncline, 25 km long and up to 6 km wide, is situated approximately halfway between Cloncurry and Mount Isa. It is crossed by the Barkly Highway close to the Mary Kathleen townsite, 5 km southwest of the Mary Kathleen U-REE deposit. The town was dismantled in 1983, after mining operations had ceased in 1982.

In the framework of regional tectono-stratigraphic zones, as first devised for the Mount Isa Inlier by Carter & others (1961) and later redefined by Glikson & others (1976) and Derrick & others (1977), the Rosebud Syncline belongs to the 'Eastern Succession'. The western part of the Eastern Succession, which includes the Rosebud Syncline, is now referred to as the Mary Kathleen Fold Belt (Oliver & others, 1985), a zone of tightly folded metasedimentary and meta-igneous rocks. (Note: Blake's [1987] definition of the 'Mary Kathleen Zone' is more restrictive, but is not followed here for reasons discussed in the section on 'Regional correlation and age of deposition').

After the reconnaissance survey of the Cloncurry-Mount Isa region by Carter & others (1961), detailed studies in the Mary Kathleen area were undertaken by students from the University of Queensland (Hill, 1968; Ramsay, 1968; Barlow, 1969; Bavinton, 1969; Clifford, 1969; Rowley, 1969; Rayner, 1975). Ramsay & Davidson (1970) discussed the origin of scapolite in the Mary Kathleen region. In a second paper, Ramsay & Davidson (1974) described occurrences of cordierite-anthophyllite rock west of Mary Kathleen as part of the metasedimentary sequence. Derrick & others (1977) provided an updated and comprehensive account of the geology between Mary Kathleen and Mount Isa, which includes the Mary Kathleen 1:100 000 geological map.

The general aim of the present study was to investigate



Fig. 1. Beds transitional between Ballara Quartzite and Corella Formation. Light-coloured layers are quartzitic. Interlayers are para-amphibolite, some of which contain hornblende porphyroblasts.

a portion of the Mary Kathleen Fold Belt, where, despite previous studies, no coherent picture yet existed of metamorphism or deformation history. The objectives of this investigation were (1) to constrain the pressure and temperature history, (2) to provide a structural analysis and establish a sequence of deformation events, (3) to study the interrelations of metamorphism and deformation, and (4) to investigate the origin of the metamorphosed sequence in terms of protoliths and sedimentary facies.

This paper is a summary of the regional-geological, structural, and petrological work, with some emphasis on the field-related aspects. Detailed studies on specific topics have either been published separately, or are in preparation.

Lithology and stratigraphic relationships

The rock units forming the Rosebud Syncline are, from base to top (see Reinhardt, 1991): Argylla Formation (Pea; upper Tewinga Group), Ballara Quartzite (Pkb; lower Mary Kathleen Group), Corella Formation (Pkc; upper Mary Kathleen Group), and Ortho-amphibolite. The Proterozoic Argylla, Ballara, and Corella Formations were originally defined by Carter & others (1961), and overviewed by Derrick & others (1977). The present study is mainly concerned with the Corella Formation. The over- and underlying rock units have been examined only briefly.

The topmost *Argylla Formation* consists of felsic metavolcanics (lava and possible ignimbrite), some of them flow-banded. Beds rich in brecciated volcaniclastic material are present in the upper Argylla Formation of the Rosebud Syncline. According to Derrick & others (1977), the majority of the Argylla volcanics are alkali-rhyolitic to rhyolitic, with a few exceptions approaching andesite in composition.

Most of the *Ballara Quartzite* in the Rosebud Syncline is relatively pure quartzite, with minor quartz-mica schist. Feldspathic layers occur close to the Argylla contact. Conglomerate horizons have not been observed in the study area, but are present elsewhere as the lowermost member of the Ballara Quartzite (Derrick & others, 1977). Cross-bedding is common, although in places obscured by strong deformation and recrystallisation. At a few localities, sedimentary ripples with wavelengths of about 5 cm are preserved. The quartzite thins markedly from

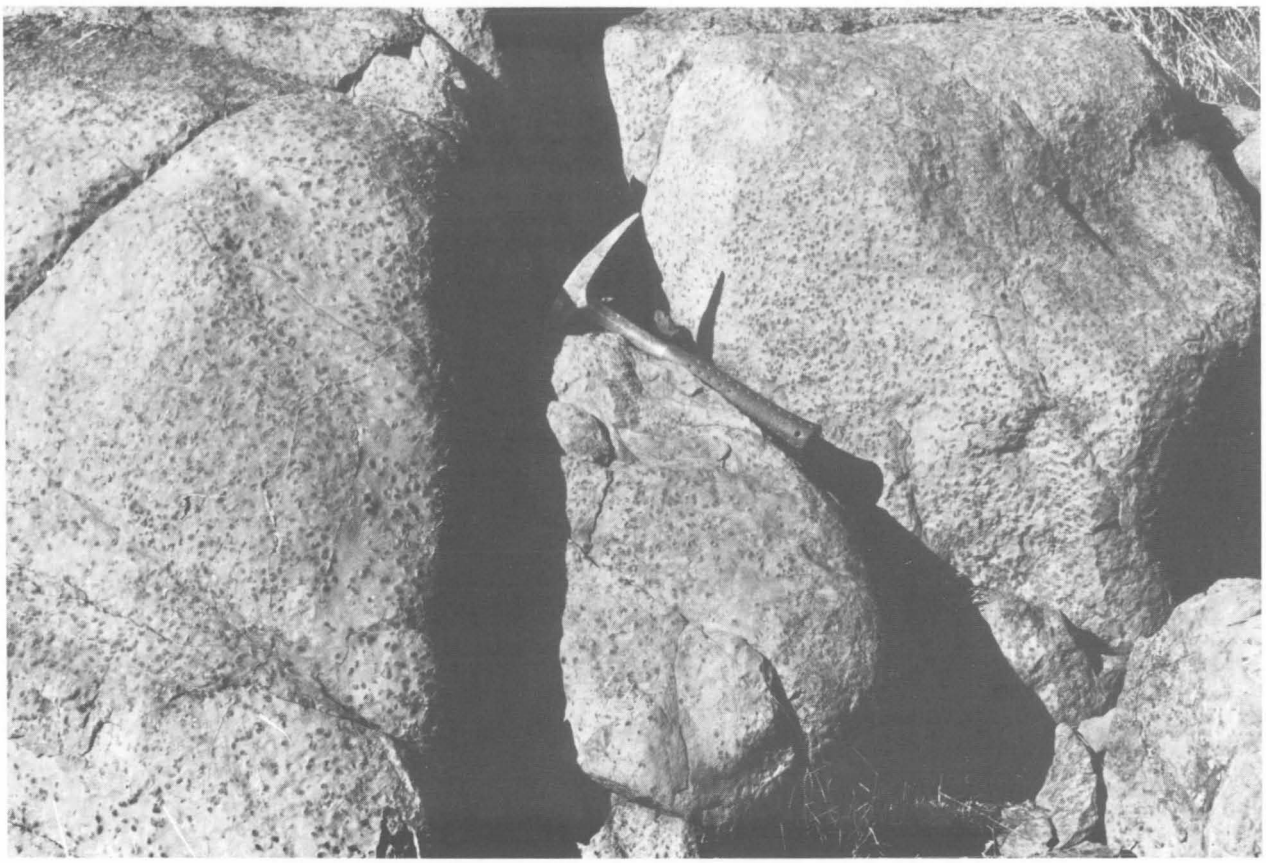


Fig. 2. Para-amphibolite with hornblende porphyroblasts in lowermost Corella Formation.

west to east. Derrick & others (1977) and Blake (1980) interpreted this variation in thickness as depositional, caused by a basement high in the vicinity of the Wonga Belt, a zone of highly deformed intrusives and volcanics in the centre of the Mary Kathleen Fold Belt, just to the east of the Rosebud Syncline.

The *Corella Formation* comprises a considerable variety of rock types, largely derived from originally calcareous and pelitic sediments. The main metamorphic types are calc-silicate rock, calcite marble, calcschist, para-amphibolite, scapolite schist, feldspathic schist, andalusite-sillimanite schist, cordierite schist, and cordierite-orthoamphibole rock.

The Corella Formation in the Rosebud Syncline can be subdivided into a lower calcareous unit, a middle schist unit, and an upper calcareous unit (see cross-section in Reinhardt, 1991) as previously proposed by Derrick & others (1977). However, the lower and upper calcareous units are similar, and this causes problems in structurally complex areas where individual outcrops cannot be assigned with certainty to either the lower or upper subunit. Stratigraphic discontinuity is common, and can be related to polyphase deformation which involved thrusting, possible extension, and tight folding (see below). Furthermore, the Corella Formation is lithologically heterogeneous, both along and across strike, due to lateral facies changes over relatively short distances (compare fig. 23 in Derrick & others, 1977). The lack of marker horizons within the three main units, and the internal structural complexity of the Rosebud Syncline make a detailed lithostratigraphic subdivision impracticable.

The Corella Formation conformably overlies the Ballara Quartzite. A transitional zone is commonly present with interlayers of quartzite and para-amphibolite (Fig. 1), and, locally, garnet-bearing scapolite-K-feldspar-biotite schist. Metapsammite continues into the Corella sequence, but purely quartzitic beds are rare. Thin beds of quartzo-feldspathic-micaceous rock are more common than quartzite, possibly representing silty rather than sandy layers. In places, graded bedding is preserved.

The calcareous units are composed mainly of calc-silicate rock, marble, para-amphibolite, calcschist, and calcite-free, feldspathic or scapolitic schist (Figs. 2, 3, 4). Bedding typically occursc at the centimetre to decimetre scale. Convolute bedding has been observed at one locality.

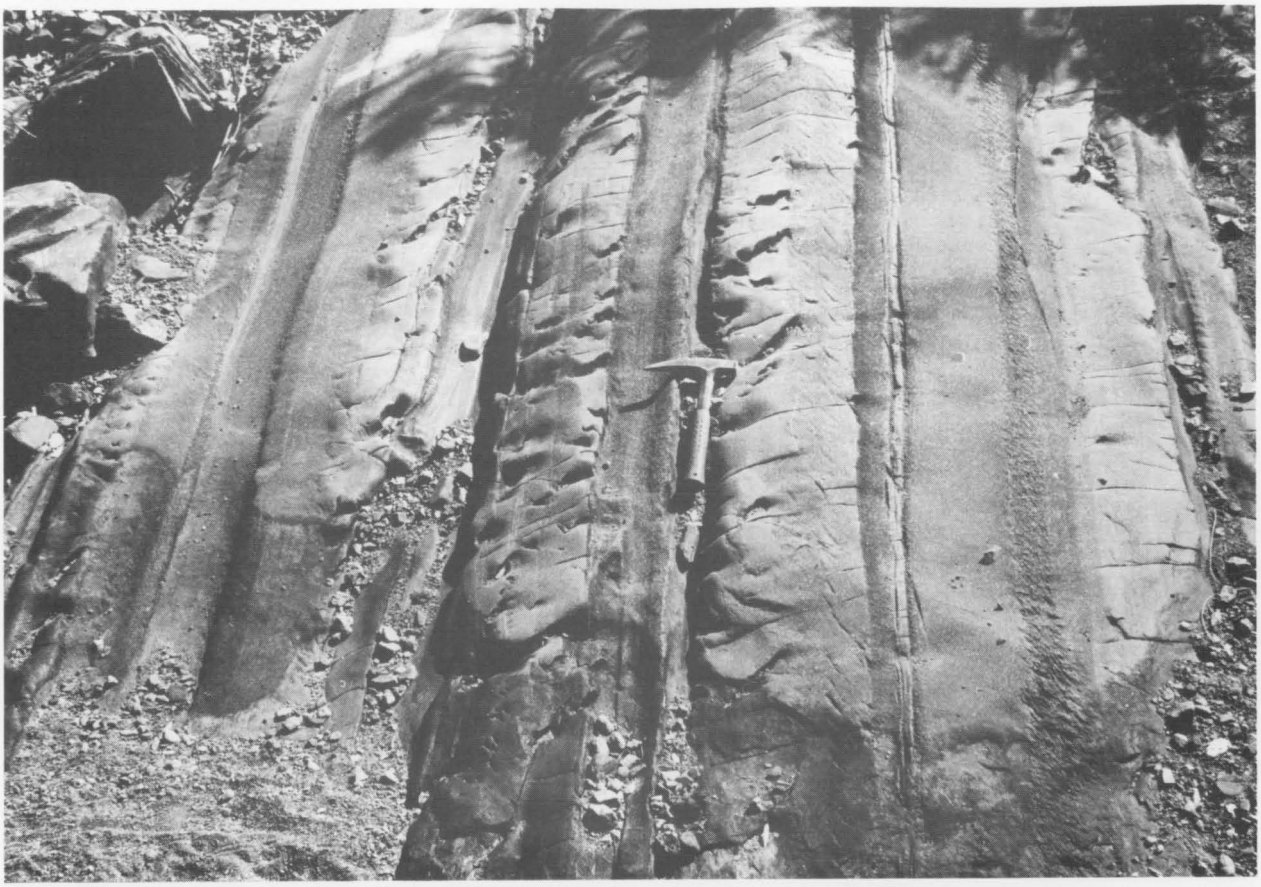


Fig. 3. Interlayered calc-silicate rock and marble in creek pavement. Calcite-rich beds show deeper erosion and have no fracture patterns. Fractures cutting the competent beds nearly at right angles are ac-fractures. Dip of S_0 is near-vertical.

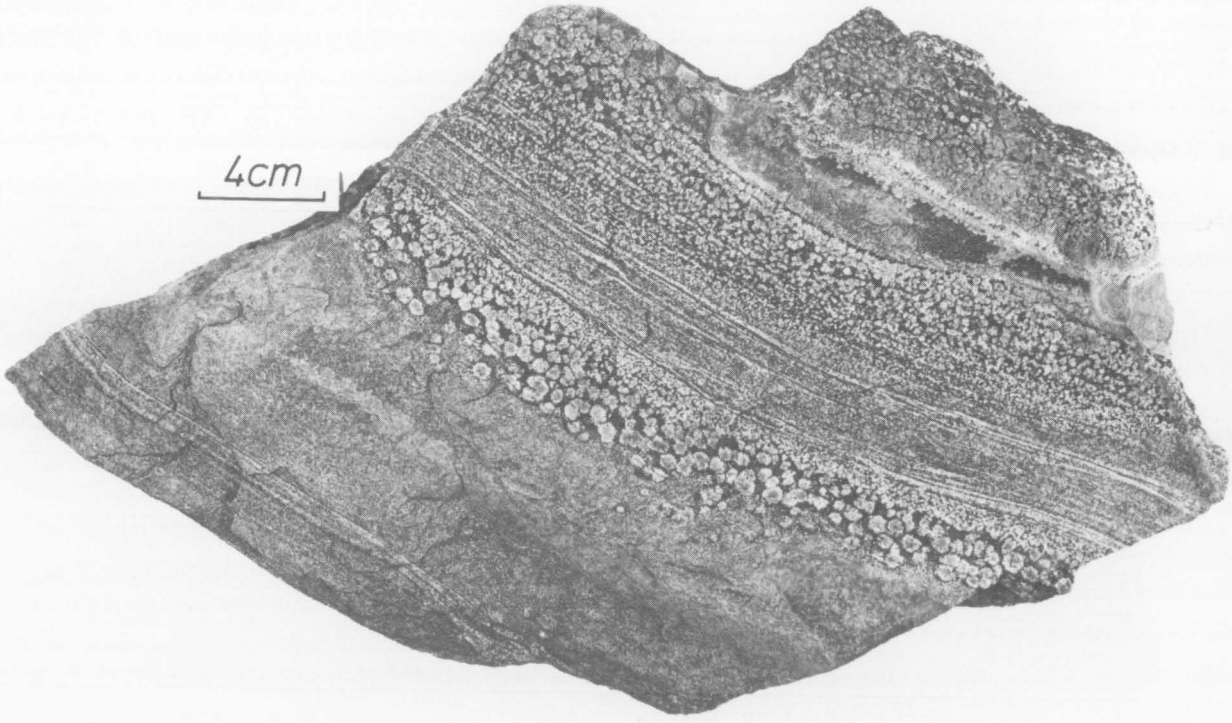


Fig. 4. Scapolite-biotite-K-feldspar rock with abundant scapolite porphyroblasts.

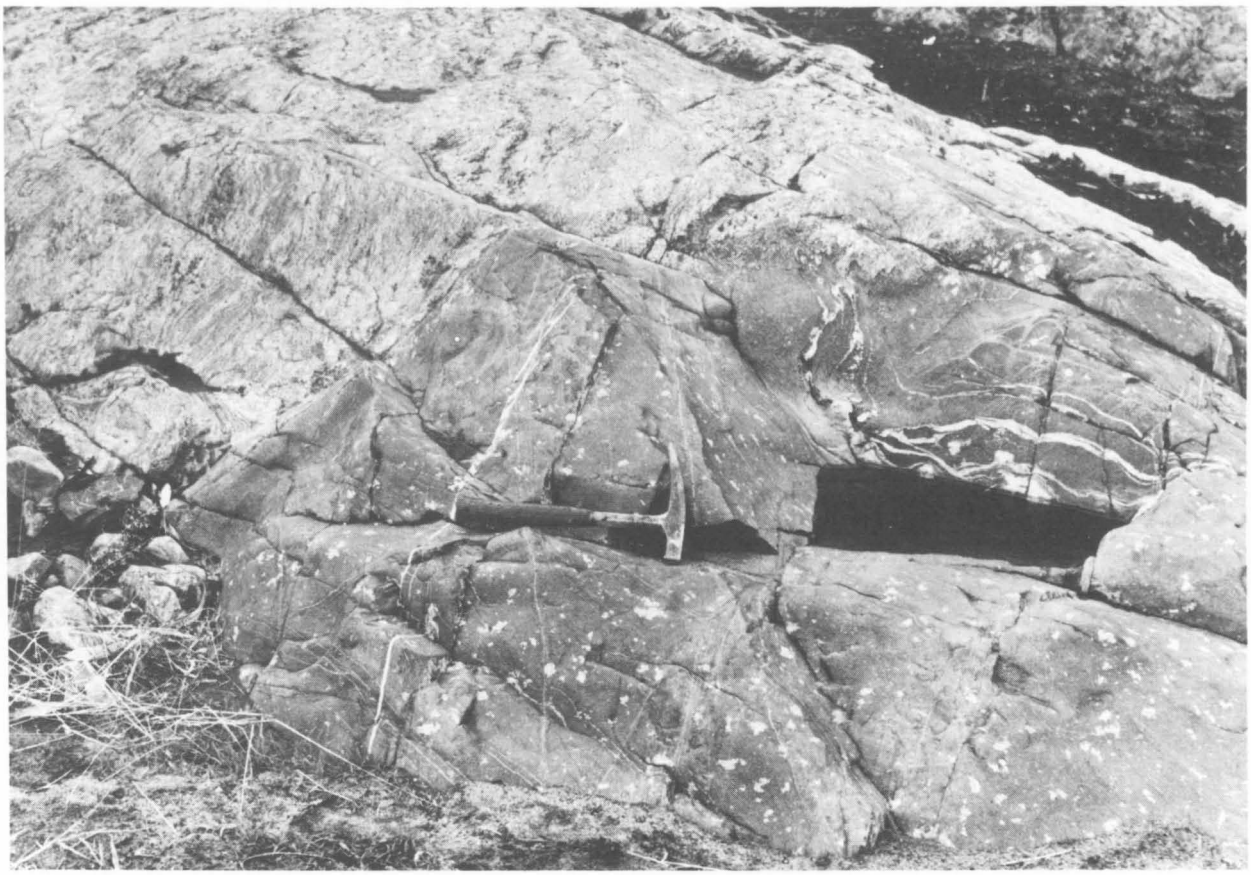


Fig. 5. Metasomatised dolerite in calc-silicate rock. White patches are aggregates of scapolite.

The calc-silicate rocks are fine to medium-grained, granoblastic, and contain Ca-amphibole and/or clinopyroxene, K-feldspar, quartz, and, in most samples, calcite, scapolite, and/or plagioclase (see the section below on 'Calcschist and calc-silicate rock' for more details on assemblages). Compositions range from calcite-poor calc-silicate rock through calc-silicate marble to relatively pure marble. The lowest-grade area is characterised by mica-bearing calcareous rock. Rocks transitional between calcareous and pelitic have hornblende-biotite assemblages and are here referred to as para-amphibolite (Fig. 2).

Scapolite is abundant in the calcareous units of the Corella Formation. It occurs in the matrix of calc-silicate rock, or as prismatic crystals ('matchstick scapolite') in calcite marble, and as spherical porphyroblasts in scapolite-K-feldspar-biotite rock (Fig. 4). Some small dolerite intrusions in calcareous rock are also rich in scapolite (Fig. 5). Edwards & Baker (1954) originally proposed a regional metasomatic origin of all the scapolite in the Mount Isa-Cloncurry region. This has been supported for metavolcanics and intrusive rocks by Ramsay & Davidson (1970) and by Oliver & Wall (1987), and is the most likely explanation for the scapolite in metadolerite bodies, as in Figure 5. However, much of the scapolite in the metasedimentary Corella Formation is rather locally derived from evaporitic minerals (see the section below on 'Sedimentary facies').

The characteristic rock type of the middle unit is andalusite-sillimanite schist (Fig. 6). Andalusite porphyroblasts are abundant, usually as short-prismatic crystals with the strongly foliated muscovite-biotite-quartz matrix anastomosing around them. In the east and north of the study area, pseudomorphs of sillimanite needles after andalusite are common. Sillimanite is also present as fibrolite in the matrix. Rare garnet is present in some pelitic layers.

Other varieties of metapelite contain porphyroblastic cordierite. These are either mica-poor, rather massive cordierite-andalusite/sillimanite rock (Fig. 7), or cordierite andalusite/sillimanite-biotite schist, or layers and lenses of cordierite-orthoamphibole-biotite rock (Fig. 8). Associated with the latter, but less abundant, are talc- and chlorite-bearing assemblages, as well as cordierite-free anthophyllite rock. A list of assemblages is given in Reinhardt (1987a). In the field, all these rocks appear to

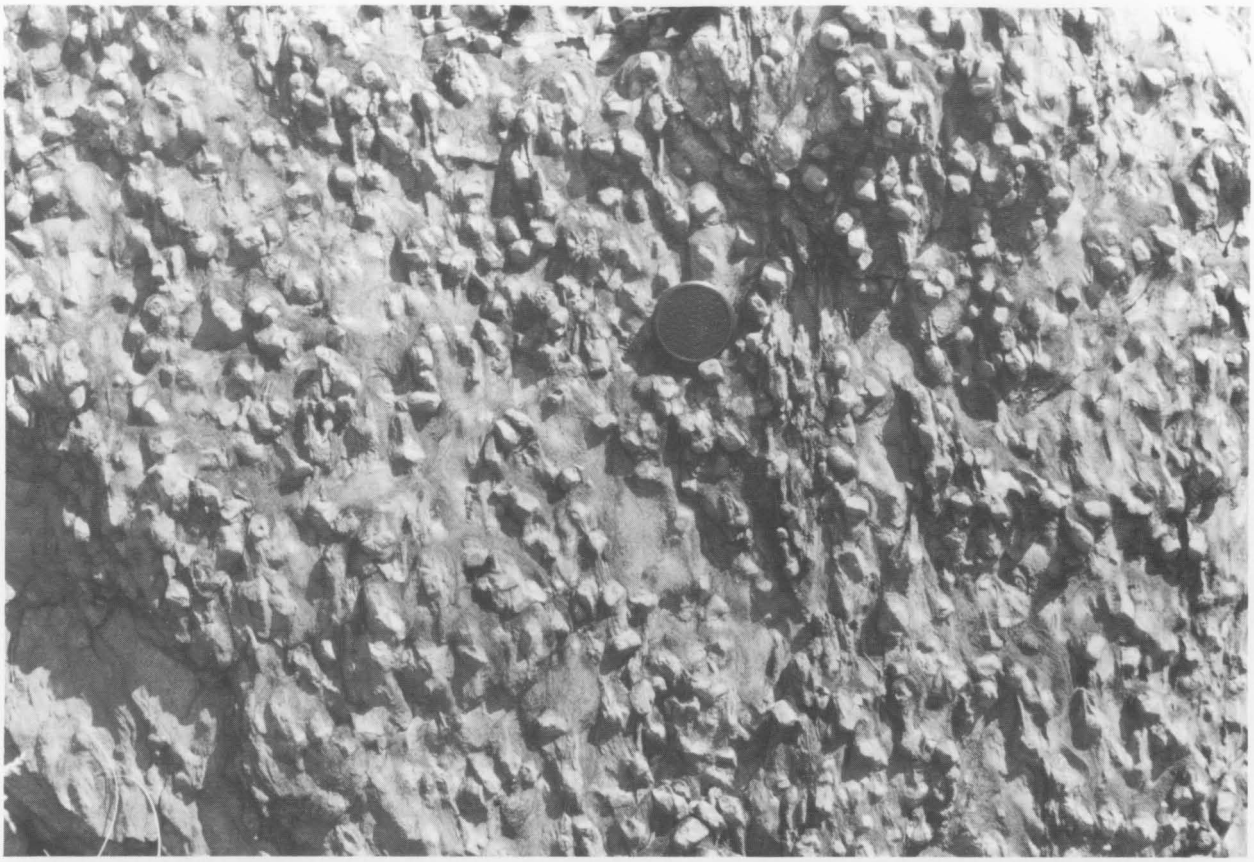


Fig. 6. Andalusite schist. View on to S_2 plane. Lens-cap is 5 cm across.



Fig. 7. Bed of massive cordierite-andalusite-sillimanite-biotite rock. Andalusite (white patches) is partly converted to sillimanite.

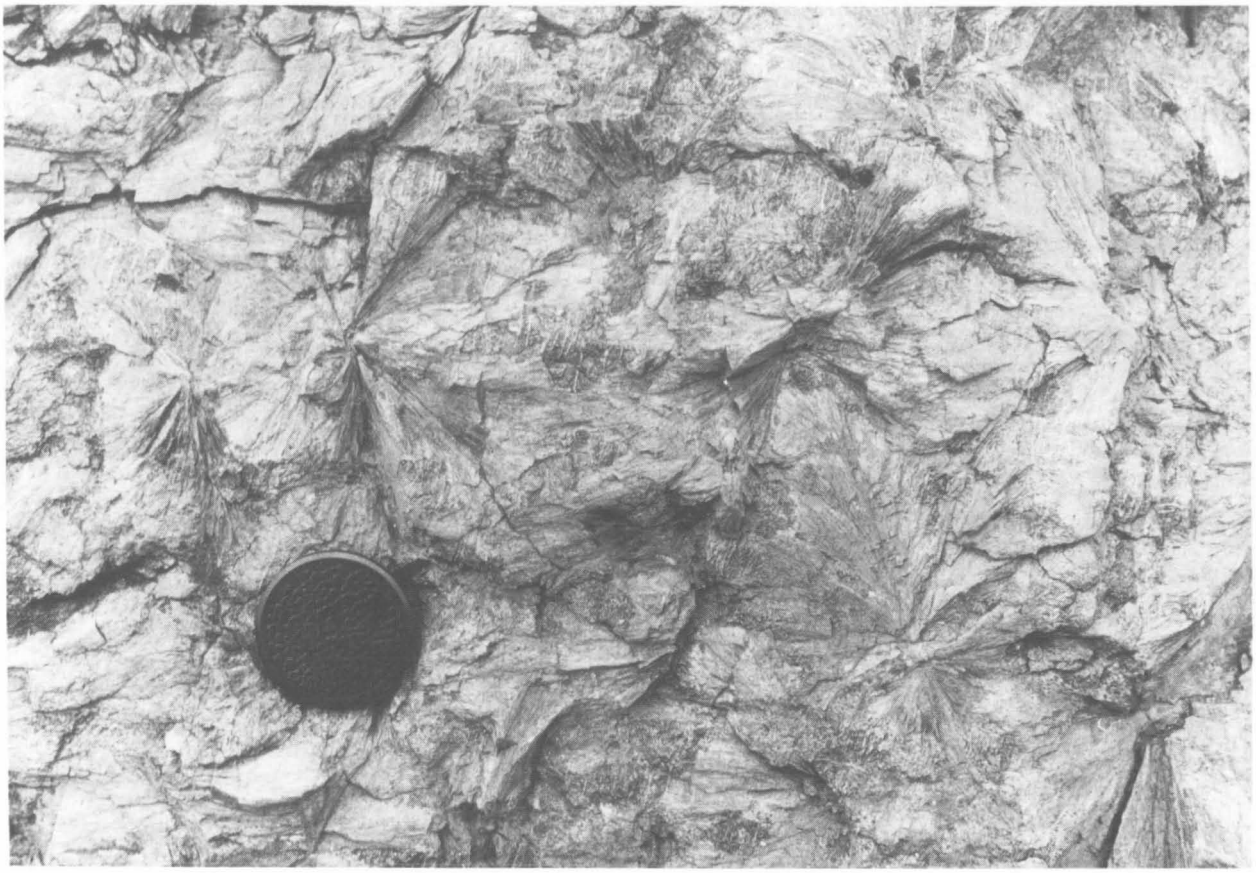


Fig. 8. Cordierite-anthophyllite rock with large rosettes of anthophyllite.

be part of the metasedimentary sequence. Compositional layering is typically present (Fig. 9). Ramsay & Davidson (1974) examined some occurrences of cordierite-anthophyllite rock west of Mary Kathleen and suggested that they are isochemically metamorphosed, Mg-rich pelites.

Rocks with similar composition are known from chloritic alteration zones, which, under amphibolite-facies conditions, will also yield cordierite-orthoamphibole rock. Such rocks are not uncommon in association with volcanogenic massive sulphides formed in sub-seafloor hydrothermal systems (e.g., De Rosen-Spence, 1969; Froese, 1969; see review of literature in Reinhardt, 1987a). The host sequences are dominated by volcanics and so are completely different from the Corella Formation in the Rosebud Syncline.

A comparative study of major and trace elements revealed that the cordierite-, orthoamphibole-, and talc-rich rocks in the Rosebud Syncline fall into the compositional range of clays and shales from evaporitic environments (Reinhardt, 1987a). These generally have high Mg/Fe ratios, unlike chloritic alteration products, which tend to be more Fe-rich (Figs. 5 and 6 in Reinhardt, 1987a; Beeson, 1988).

In addition to the metasedimentary Mg-rich rocks, chemically altered, *Mg-enriched intrusives* occur in the Rosebud Syncline. The outer zones of some small metadolerite bodies and also some narrow bands within the main mafic body in the centre have orthoamphibole- and talc-bearing assemblages. In contrast to the metasedimentary cordierite-orthoamphibole rock, transitions into pristine metadolerite are present over distances of a few metres at the most. The rock is massive and unlayered. This Mg-metasomatism is interpreted as the result of chemical exchange between dolerite and adjacent magnesian pelite or Mg-rich, saline formation water.

Intrusive rocks in the Rosebud Syncline are mostly mafic. *Dolerite* is abundant (Fig. 5). The large stratiform *amphibolite body* in the core of the syncline has previously been described as a sill (Derrick & others, 1977), and there is no clear evidence such as flow structures, pillow structures, or amygdales to suggest otherwise. A breccia layer of mixed rock fragments in a mafic matrix at the base of the ortho-amphibolite body could have formed during either extrusion or intrusion. Only a few of the mafic bodies have been sampled, but it appears that all of them predate the main amphibolite-grade metamorphism. The



Fig. 9. Bedded cordierite-anthophyllite rocks. Eastern limb of the Rosebud Syncline, view to south.

metadolerite samples contain hornblende-plagioclase assemblages, unless metasomatised, and are commonly foliated.

Felsic intrusives are rare. A small *granodiorite* intrusion is exposed at the western edge of the main ortho-amphibolite body. Some thin, strongly deformed *pegmatite dykes and sills* are present in schist zones. No larger igneous body which would be approximately synchronous with the main metamorphic episode is exposed in the vicinity of the syncline.

Depositional model

Regional correlation and age of deposition

The Corella Formation covers much of the Mary Kathleen Fold Belt and extends to the east of Cloncurry in the eastern Mount Isa Inlier. Possible lateral stratigraphic equivalents are the Doherty Formation of the Cloncurry-Selwyn Zone, and the Quilalar Formation, which crops out over a large area west of the Mary Kathleen Fold Belt (Blake, 1987).

The Corella Formation of the Rosebud Syncline is part of the Corella Formation of Zone A of Blake (1980, 1982), which he regarded as different from a lithologically similar formation in the eastern Mary Kathleen Fold Belt (Corella Formation of Zone B). This interpretation was criticised by Derrick & Wilson (1981) and Wilson (1983), who believe the two are correlatives in age and facies. Considering the new evidence for both extension and thrusting in the Mary Kathleen Group (Passchier, 1986; Pearson & others, 1987; Williams & others, 1987; this study; Bell & others, 1992), previous thickness estimates and regional comparison of such thicknesses between the formations in question (as in Blake, 1982) must be viewed with caution. The stratigraphic succession Argylla-Ballara-Corella is the same in the Rosebud and Mary Kathleen Synclines, and hence suggests the Corella Formation immediately east of the Wonga Belt has the same age as that on the western side.

The time of deposition of the Corella Formation is bracketed by the extrusion age of the underlying Argylla volcanics and by the age of the Burstall Granite and Lunch Creek Gabbro, which intruded the Corella Formation in the Mary Kathleen Syncline. U-Pb zircon ages are 1783 ±

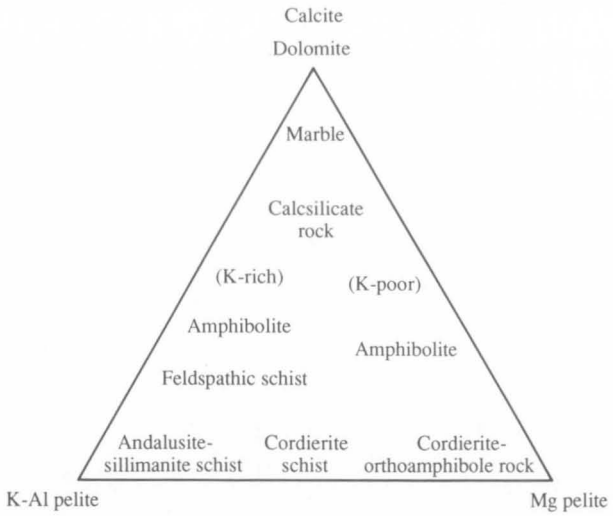


Fig. 10. Schematic presentation of rock-compositional variation within the Corella Formation as a function of variable proportions of some primary sedimentary components.

5 Ma for the Argylla Formation and 1740- 1730 Ma for the intrusions (Page, 1983a, 1983b).

Sedimentary facies

The compositional heterogeneity of the Corella Formation reflects vertical and horizontal facies changes between aluminous-pelitic, magnesian-pelitic, psammopelitic, and calcareous-dolomitic sediments, represented by andalusite-sillimanite schist, cordierite- and orthoamphibole-rich rocks, quartzo-feldspathic-micaceous beds, and calcite marble or calcsilicate rock, respectively (Fig. 10).

Aluminous schist and cordierite-orthoamphibole metapelite have generally low to intermediate Fe/Mg ratios. Magnesian pelite is characteristic of an alkaline-evaporitic environment (Moine & others, 1981; Chamley, 1989). In an evaporitic basin, detrital clay minerals can chemically transform to magnesian minerals, and certain Mg-rich clay minerals precipitate directly from hypersaline solutions (Lucas, 1962; Millot, 1970). Facies changes between 'normal' pelitic sedimentation and magnesian clay sedimentation are controlled by the proportion of chemical sedimentation and transformation versus clastic influx (Chamley, 1989). In the metamorphic sequence, andalusite-sillimanite schist and cordierite-orthoamphibole rock represent pelitic-clastic and pelitic-chemical sedimentation, respectively, whereas cordierite-aluminosilicate-rich rock represents a transitional facies (Fig. 10).

The occurrence of Cl-scapolite is regarded as further evidence for the evaporitic character of parts of the Corella Formation, in accordance with the conclusions of Ramsay & Davidson (1970). In some beds it is the predominant mineral (Fig. 4). The presence of SO_3 in much of the scapolite is most likely derived from former sulphates, such as gypsum and anhydrite.

The change of sedimentary facies within the Mary Kathleen Group from the lower Ballara member to the Corella Formation indicates a change from a high-energy to a low-energy depositional regime. The stratigraphic record shows a coarse-clastic stage (conglomerate of the lower Ballara Quartzite), followed by dominantly sandy sedimentation with few pelitic and carbonatic intercalations (upper Ballara member). The detritus of the Ballara sequence is largely derived from the Argylla and Leichhardt volcanics, but gradually changes from arkosic at the bottom to relatively pure quartzitic at the top (Derrick & others, 1977).

The general decrease of clast size and the increasing maturity of the clastic sediments from the lower to the upper Ballara sequence, plus the change from sandy-clastic to calcareous-pelitic and evaporitic sedimentation of the Corella Formation, indicate a successive reduction of topographic relief between the source and depositional regions, and perhaps increasing distance from the source area. Cross-bedding and short-wavelength sedimentary ripples in the uppermost Ballara Quartzite suggest shallow-water deposition. A change from shallow to deep-water sedimentation is not indicated in the sedimentary record of the Corella Formation.

Tectonic model

The relationship of depositional trends, basin formation, and magmatism to tectonic processes has been discussed by various authors. Extensional models for the Leichhardt River Fault Trough in the western Mount Isa Inlier have been proposed by Glikson & others (1976) and Derrick (1982). The geochemistry of the volcanic suites in the Mount Isa Inlier, and in particular their bimodal character, is typical of extensional regimes (Bultitude & Wyborn, 1982; Wyborn & others, 1987).

Wyborn & Blake (1982) and Blake (1987) listed the evidence for an intracratonic setting of the whole Mount Isa Inlier during a tensional regime lasting from about 1880 to 1670 Ma. For this period, Blake (1987) defined three cover sequences which overlie an older basement. The upper Tewinga Group and the Mary Kathleen Group are part of cover sequence 2. Beardsmore & others (1988) outlined a rift cycle model for the oldest volcano-

TABLE 1. STRATIGRAPHIC POSITION AND TECTONIC SIGNIFICANCE OF THE CORELLA FORMATION AND ITS UNDERLYING UNITS.

Stratigraphic unit			Main rock types (pre-metamorphic)	Tectonic interpretation
Pkc Corella Formation	Cover sequence 2 sensu Blake (1987)	Mary Kathleen Group	Calcareous-dolomitic and pelitic rocks, evaporite	Thermal subsidence
Pkb_2 Ballara Quartzite			Quartz sandstone	
Pkb_1 Ballara Quartzite			Conglomerate, arkose	Initial subsidence
Pea Argylla Formation			Felsic volcanics	
Pem Magna Lynn Metabasalt		Tewinga Group	Basalt	Early rifting stage
				- Erosion -
Pel Leichhardt Metamorphics			Felsic volcanics	Pre-rift stage
Pgk + Kalkadoon Granite			Granite, granodiorite	

Units Pkb_1, Pem, Pel, and Pgk are not exposed in the mapped area, but occur close by (compare Derrick & others, 1977).

sedimentary cover sequence 1 in the eastern Mount Isa Inlier. Jackson & others (1990) presented a detailed sedimentological facies analysis of the Ballara Quartzite and the Quilalar Formation to the west of the Mary Kathleen Fold Belt, supporting a rift-sag model for cover sequence 2.

With reference to general models of basin evolution, and subsidence history in particular, during and after stretching of continental lithosphere (e.g., McKenzie, 1978; Watts & others, 1982; White & McKenzie, 1988), lithostratigraphic criteria can be applied to identify ancient zones of extension, even in highly deformed and metamorphosed areas. The metavolcanics and metasediments of the upper Tewinga Group and the Mary Kathleen Group show many characteristics of a rift basin sequence (Table 1).

The mafic and felsic volcanics of the upper Tewinga Group (Magna Lynn Metabasalt and Argylla Formation) represent a period of extensive volcanic activity during early rifting (compare Wyborn & others, 1987). The restricted occurrences of coarse clastic deposits at the base of the sediment column indicate erosion and deposition controlled by local topographic highs and lows (rift-generated tilt-blocks or horsts and graben). The upper Ballara Quartzite member with its marked change of thickness across the Mary Kathleen Fold Belt would correspond to a transition from the initial subsidence stage to the thermal subsidence stage. The thin sheet of Ballara Quartzite overlying the Argylla volcanics in the eastern Rosebud Syncline and in the Mary Kathleen Syncline is interpreted as the stratigraphic onlap at a slowly subsiding basin margin. This need not be a main rift shoulder, but could also be a local topographic high in a more complexly structured rift basin.

The Corella Formation with its fine-clastic and chemical sediments would then represent the final stage of thermal subsidence, when the rift topography had largely been smoothed out, and the area of deposition reached its maximum extent. Thus, the sedimentary record of the Ballara-Corella sequence fits the expected vertical and lateral facies variations in a simple rift basin model.

Deformation

Large-scale structures (D_1, D_2, post-D_2)

Regional structural relationships show that three sets of map-scale structures can be assigned to different events (Table 2). As it was not possible (even through microstructural criteria) to separate out more than one deformation event predating the main folding, the latter is referred to as D_2 and the earlier structures as D_1. This is in accordance with the terminology in adjacent areas (e.g., Passchier, 1986), except that the late faults are not assigned to D_3 here, as at least one post-D_2 ductile deformation can be recognised in the field (see below).

TABLE 2. SUMMARY OF DEFORMATION EVENTS AND RELATED STRUCTURES IN THE ROSEBUD SYNCLINE.

	Folds Fold axes	Foliations Lineations	Faults Shear Zones	Correlation with Isan events
D_1	Rare intrafolial folds Ramp folds	Flatlying S_{1h} Subvertical N-striking S_{1v} Steeply N-dipping S_{1EW} Subhorizontal L^1_1 stretching lineation in S_{1h} and S_{1v}	Thrust planes Strike-slip shear zones Ramp faults	D_1 (1610 +/- 13 Ma)
D_2	Upright tight to isoclinal strongly non-cylindrical folds; fold axes N-oriented with variable plunge	Subvertical N-striking S_2 Subvertical L^2_2	?Reactivation of S_{1v} shear zones	D_2 (1544 +/- 12 Ma)
D_3	Crenulations and folds in S_2 and other pre-existing structures (veins, etc.)	(Subvertical NNW-striking S_3 axial plane)		D_3 (1510 +/- 13 Ma)
D_4	Rare kinks	(Vertical E-striking axial plane)		-
D_5			Major NE-striking strike-slip faults	-

Isan events refer to the notation and isotopic dates of Bell (1983) and Page & Bell (1986).

The Rosebud Syncline is shaped like a boat, with steep fold limbs and an F^0_2 fold axis plunging about 60° at each end (see Reinhardt, 1991). The north-south axial plane is characteristic of the regional-scale D_2 folds throughout the Mary Kathleen Fold Belt, a trend imposed during major east-west ductile shortening.

Map-scale structural complexity in the syncline reveals at least one earlier deformation. Extreme and locally abrupt changes in thickness of units within the Corella Formation along strike can be explained by shear zones or faults, some of which had originally a subhorizontal to northerly dipping orientation, and others which had an approximately north-striking vertical orientation. Although the presence of such structures is inferred from the geological map, they are difficult to locate in the field, except where lithological boundaries are displaced. However, many of these fault planes or shear zones are oriented at a low angle to bedding. Related microfabrics, apart from those preserved in porphyroblasts (see below), have been almost entirely wiped out by the strong D_2 deformational-metamorphic overprint.

The early structures are interpreted as interfingering thrust and strike-slip faults, which developed during south-directed D_1 thrusting (Fig. 11; Bell & others, 1992). Evidence for the compressive nature of D_1 deformation and for the top-to-the-south sense of movement are the faults along the Ballara-Corella contact on the western limb of the Rosebud Syncline, between Corella Creek and the Cameron Fault. They are interpreted as originally steeply north-dipping reverse faults of a frontal thrust ramp (compare Butler, 1982). The discontinuity of these structures at higher stratigraphic levels implies the presence of another detachment surface above this ramp. Folds which are considered as asymmetric D_1 ramp folds, and stratigraphic repetition occur to the south of the ramp 'nose'. On the eastern limb of the Rosebud Syncline, a corresponding set of structures at the equivalent stratigraphic level is not present. Hence, a strike-slip shear zone (or a lateral ramp) should exist in between, unless the structure dies out gradually to the east.

Some of the D_1 shear zones are closely associated with cordierite-orthoamphibole rocks and other cordierite- and talc-rich rocks. This is not surprising, since, at the low metamorphic grade of D_1 (see below), these were highly ductile chlorite- and talc-rich rocks, and hence were zones of low shearing resistance.

The evidence for extensional deformation is rather poor in the study area. A possible early extensional structure is the fault on which the Rosebud Mine is located. If this fault predates D_2, it must have been a low-angle normal fault.

Late brittle faults cross the syncline, and most are parallel to the prominent set of northeast to north-northeast-striking faults dissecting the Mary Kathleen Fold Belt and adjacent areas. The Cameron Fault is one of these major faults and offsets the northernmost part of the

syncline by about 1.5 km to the northeast. The northwest-striking Green's Creek Fault near the Barkly Highway is an earlier brittle structure which is cut by the Cameron Fault. The northernmost segment of the Rosebud Syncline was uplifted at the Green's Creek Fault (throw unknown) with only minor sinistral displacement.

D_1: folds and microstructures

Folds that predate the main D_2 north-south folds are rare. Intrafolial F^0_1 folds transected by S_2 are locally preserved. The large-scale parasitic folds in the western limb north of Corella Creek are interpreted as thrust ramp folds (as explained above).

D_1 microfabrics are largely obliterated in the matrix of the metamorphic rocks, but are preserved in porphyroblasts from pelitic schist. Part of the andalusite and cordierite porphyroblasts contain S_1 inclusion trails of fine-grained quartz, mica, hematite, and ilmenite. Where the inclusion trail (internal foliation, or 'S_i') has a different orientation from the S_2 foliation of the schist matrix (external S, or 'S_e'), S_1 is either truncated by or bends into S_2 at the porphyroblast margin. Whereas truncation does not allow distinction between pre- and early syn-D_2 growth, a continuous S_i-S_e transition puts tighter constraints on the timing of mineral growth. Accordingly, such andalusite and cordierite porphyroblasts have grown synchronously with S_2 formation (compare Reinhardt & Rubenach, 1989).

A three-dimensional picture of the inclusion trail geometry has been obtained by comparison of thin sections cut in different directions, from single samples. Procedures and various examples are discussed in detail in Bell & others (1992).

The deformation imposed on the S_1 fabric as preserved in early-D_2 porphyroblasts is relatively weak, and the inclusion trail orientations are fairly consistent within single samples. However, samples from different localities may show entirely different S_i orientations. Three main types of fabric orientations have been identified:

- S_{1h}, shallow-dipping to flatlying,
- S_{1v}, subvertical north-striking, and
- S_{1EW}, north-dipping east-west striking.

The h, v, and EW subscripts imply no sequence of formation, but refer to the orientations of the S_1 foliations. Both S_{1h} and S_{1v} have a subhorizontal, north-oriented linear mineral shape fabric ('L^1_1') associated. S_{1EW} is commonly represented by aligned biotite and, in two

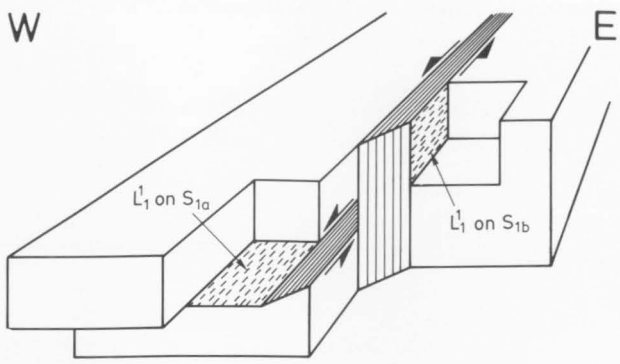


Fig. 11. Schematic block diagram showing the pre-D_2 geometric relationships between thrusts and strike-slip shears, as well as the orientation of related foliations and lineations.

samples, also by the axial plane of a differentiated crenulation cleavage in S_{1v}. The S_{1EW} biotites crosscut and overgrew the S_{1h}-L^1_1 and S_{1v}-L^1_1 fabrics. Hence, S_{1EW} appears to be the latest imprint prior to D_2. These microfabrics are developed with varying intensity. A number of samples show texturally isotropic pre-D_2 inclusion fabrics.

As discussed in Bell (1985) and Reinhardt & Rubenach (1989), the orientation of fabric elements within porphyroblasts is retained during ductile coaxial deformation (such as D_2 here), and, as Bell (1985) argues, even during non-coaxial deformation. The consistent S_1 orientations within single samples, and the generally consistent orientation of L^1_1 support the view that a significant rotation of porphyroblasts did not take place and that the inclusion fabric orientation reflects the original geometrical relationships.

Evidence for both thrusting and strike-slip shearing has been presented above, and is further substantiated by the microfabrics discussed here. If, as a result of differential lateral movement, thrusting and ductile strike-slip shearing occurred simultaneously, subhorizontal as well as subvertical fabrics should be found, both with a subhorizontal stretching lineation (see also Bell & others, 1992). S_{1h}, S_{1v}, and L^1_1 are entirely consistent with such a geometric framework, and fit the map-scale shear zone pattern described above (Fig. 11).

The lack of a D_1 fabric anisotropy in various porphyroblast-bearing samples indicates the strong partitioning of deformation during D_1. The S_{1EW} crenulation cleavage is regarded as a north-south compressional feature which developed at the end of D_1, probably after thrusting had ceased. The crystallisation of biotite aligned in S_{1EW} represents the thermal peak at the end of D_1.

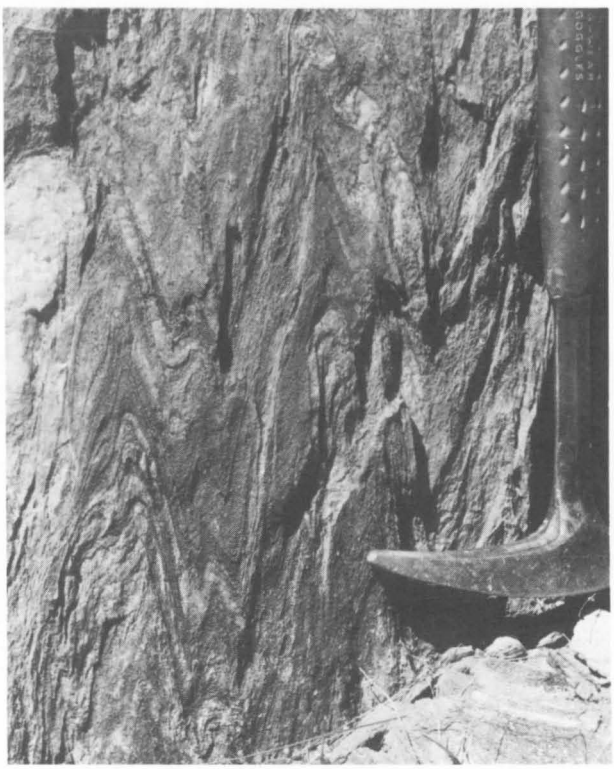


Fig. 12. Small-scale folding in thin-bedded metapelitic and quartzo-feldspathic rocks. View approximately parallel to fold axes.

D_2: folds, S-L fabric, boudinage

The characteristic D_2 fold in the western Mary Kathleen Fold Belt is tight to isoclinal, with a subvertical, north-trending axial plane (Fig. 12). Fold axes plunge north or south, as exemplified on a regional scale by the shape of the Rosebud Syncline. The northerly strike of the steeply dipping beds and the tightness of the fold hinges is shown in the S_0 orientation density plot in Figure 13a. Fold axes of meso- and small-scale F^0_2 folds form a north-south girdle (Fig. 13b), indicating the non-cylindrical character of D_2 folding.

The axial plane foliation of F^0_2 folds is a pervasive, steep to vertically dipping S_2 schistosity in mica-rich rocks, but is less strongly developed in other, more massive rock types (Figs. 14, 15a). Almost invariably associated with S_2 is a steeply plunging mineral elongation lineation L^2_2 (Fig. 15b). High-grade metamorphic minerals (sillimanite, amphiboles, micas) are generally aligned in S_2 and L^2_2. The S_2-L^2_2 fabric anastomoses around early-D_2 porphyroblasts, whereas it is overgrown by late-D_2 minerals (Reinhardt & Rubenach, 1989; Reinhardt, 1992; see 'Metamorphism' below).

The F^0_2-S_2-L^2_2 geometry indicates east-west bulk coaxial shortening with vertical inhomogeneous

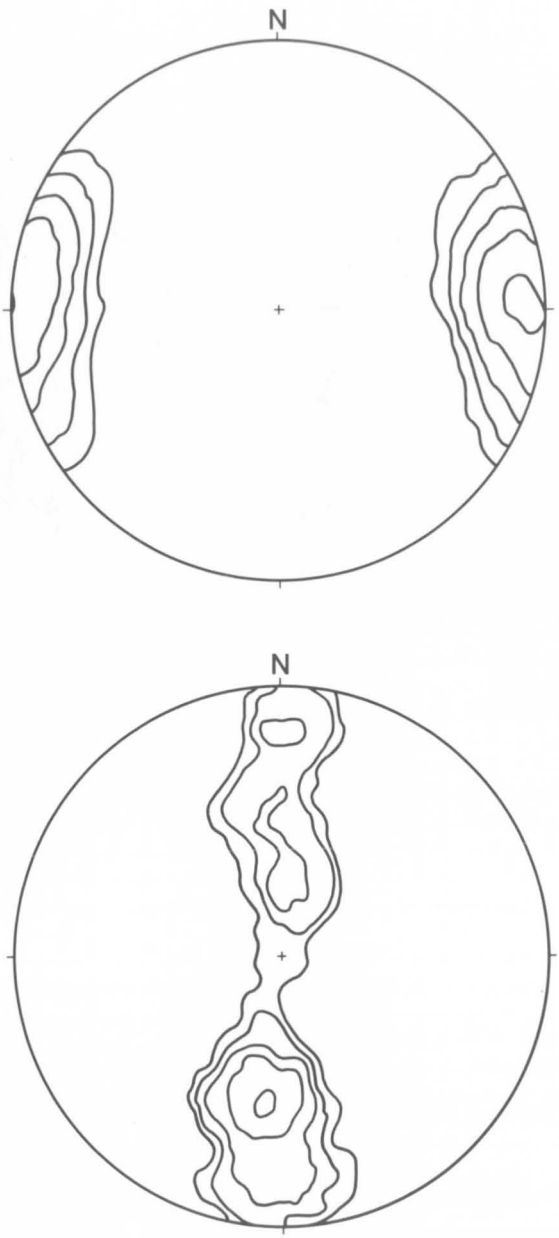


Fig. 13. (a) Orientation density diagram for S_0 poles. 978 readings. Contour intervals: 0.8/1.5/3.1/6.2/12.3%, maximum 13.3%. (b) Orientation density diagram for F^0_2 fold axes. 66 readings. Contour intervals: 1.1/2.1/4.2/8.4/16.8%, maximum 18.2%. (All orientation density diagrams are Schmidt equal area projections; contour levels per 1% area.)

extension. Accordingly, the maximum contractional, finite strain (lambda-3) was oriented east-west and horizontal, and the maximum extensional, finite strain (lambda-1) was oriented vertically. The considerable vertical stretching is particularly evident from the intense L^2_2.

Boudinage is common where beds of highly contrasting ductility are present, such as calc-silicate-



Fig. 14. Pervasive, subvertical S_2 schistosity in andalusite schist. View parallel to S_2.

feldspar-rich beds between calcitic ones, with calcite filling the extensional fractures. In metapelitic rocks, pinch-and-swell structures or boudins are developed where cordierite-quartz-rich or cordierite-aluminosilicate-rich layers are sandwiched between more micaceous rock (Fig. 16). Syn-D_2 pegmatite dykes are also boudinaged. On many subhorizontal rock faces, a horizontal component of stretching is evident, which is to be expected from the inhomogeneity of vertical extension.

Post-D_2 structures

Locally, post-D_2 deformation produced an S_3 spaced crenulation commonly striking west of north (Fig. 17) and rare kinks with east-striking axial planes. In most outcrops, however, and in most analysed samples, no modification of D_2 structures is apparent. Rocks containing F^2_3 crenulations and folds have no minerals aligned in the S_3 axial plane. No metamorphic D_3 imprint has been recognised.

The irregular distribution and the scarcity of D_3 structures can be explained by the very small angle between S_3 and S_2. D_3 shortening would commonly have caused reactivation of the pervasive S_2 rather than formation of a new foliation.

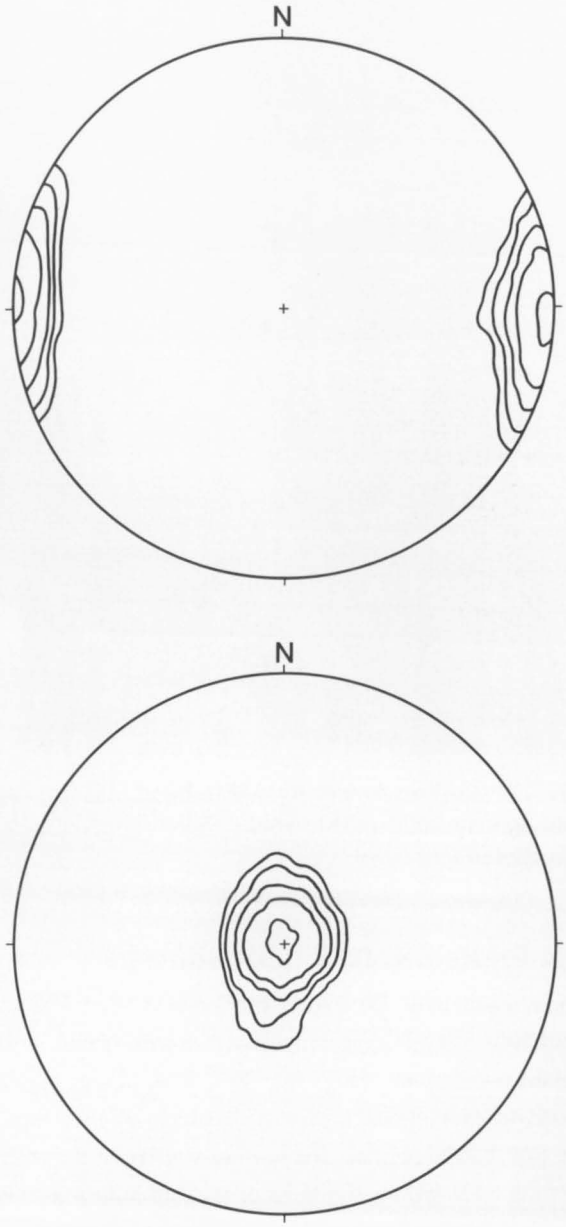


Fig. 15. (a) Orientation density diagram for S_2 poles. 341 readings. Contour intervals: 1.9/3.8/7.5/15.1/30.1, maximum 32.6%. (b) Orientation density diagram for L^2_2. 142 readings. Contour intervals: 2.3/4.5/9.0/18.1/36.2, maximum 39.1%.

Fractures and veins in calcareous rocks

The calcareous rocks of the Rosebud Syncline contain various sets of fractures or veins, cross-cutting each other. Certain vein sets can be dominant in one area, and subordinate or absent elsewhere.

The oldest identifiable vein set is well preserved in the pavements below Rosebud Dam. Closely spaced, mostly discontinuous remains of calcitic veins cross-cut the calc-silicate beds (Fig. 18; also seen in Fig. 3, right hand side).



Fig. 16. Boudinage in cordierite-andalusite-sillimanite schist. Competent mica-poor layers are fragmented.

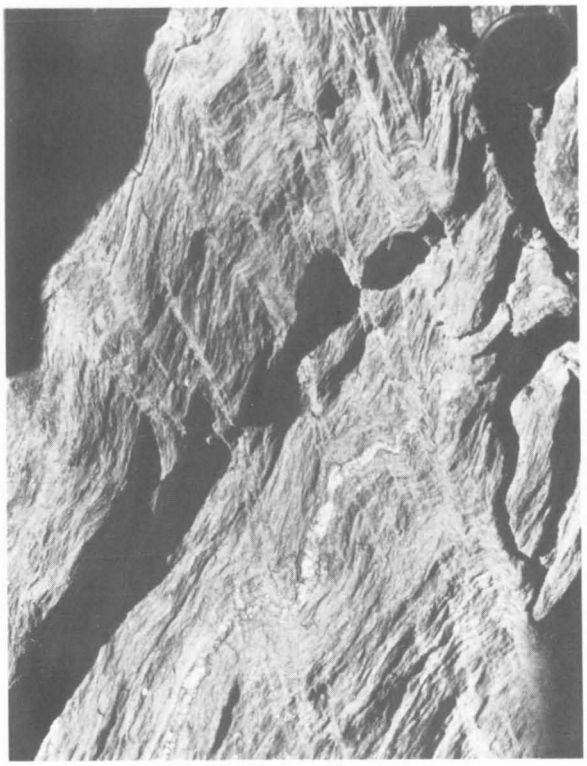


Fig. 17. Spaced S_3 crenulations in S_2 of a sillimanite schist.

The veins are strongly deformed and overprinted by D_2 and D_3. Some beds contain blotches of coarse calcite ± Ca-amphibole or clinopyroxene as the only indication of originally continuous veins, now partially obscured by metamorphic recrystallisation and reactions between wall rock minerals and original vein infill. The enveloping surface to these folded veins cuts S_0 at a high angle, and in many outcrops trends east-west. Its dip is moderately steep to near-vertical, and generally northward. The fractures may have formed pre-D_2 or early syn-D_2, although the intense overprinting by D_2 structures renders the first option more likely. These early fractures are cut by syn-D_2 'ac'-fractures which are oriented approximately orthogonal to the F^0_2 fold axes (Fig. 3).

Some localities, particularly in the northern syncline, show a different fracture set. In D_2 fold hinges, the fractures are parallel to the axial plane, with a spacing of 1 to 10 cm. On F^0_2 fold limbs, the cleavage refracts considerably from bed to bed and is deformed where its angle with the S_2 axial plane orientation is large (Fig. 19). This fracture set is considered as having formed early in D_2. Its strike is always parallel to S_2, and the geometric relationships with S_0 across F^0_2 fold hinges are consistent with an original D_2 axial plane cleavage (i.e., the F^0_2 folds are not transected). Such an axial planar structure could

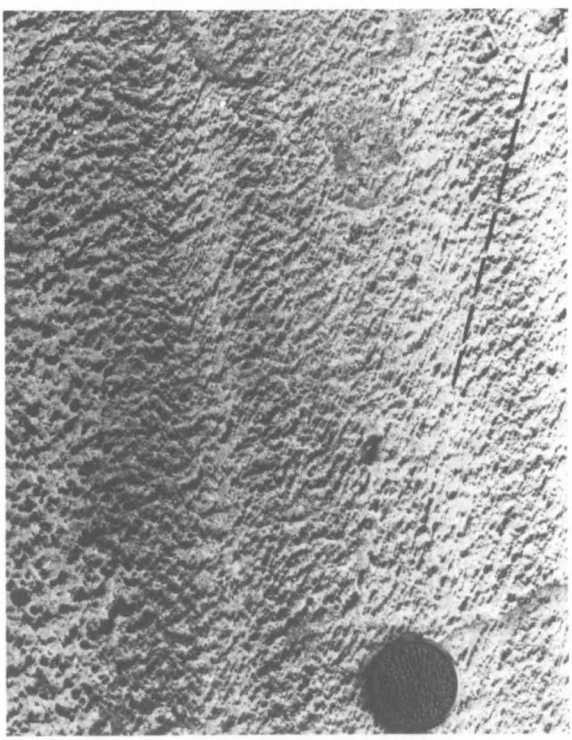


Fig. 18. Early-formed set of tightly spaced veins in calc-silicate rock, strongly overprinted by subsequent D_2 deformation and metamorphism. Thin S_2 seams (parallel to dashed line) cut across the discontinuous, patchy remains of the older veins. Plan view. Bedding parallel to long side of photograph.

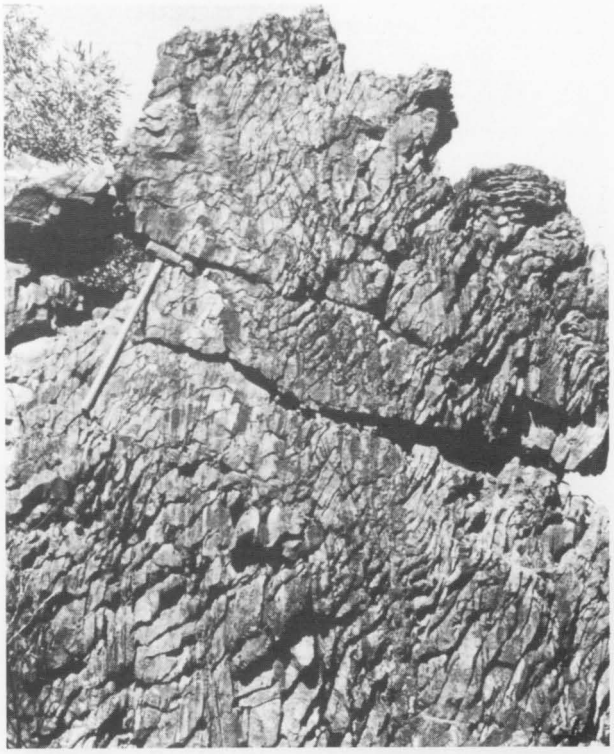


Fig. 19. Syn-D_2 fractures in calc-silicate rock. Bedding is near-vertical. Eastern limb of the Rosebud Syncline, view to south.

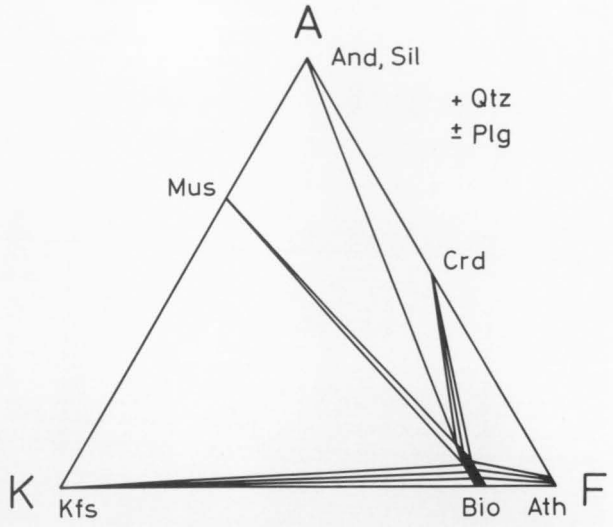


Fig. 20. AKF diagram with phase relationships in the metapelites of the Rosebud Syncline. All parageneses shown in this diagram are present in the field.

have originated as a fracture cleavage, or as a solution cleavage at low metamorphic grades. In some competent beds, the early-D_2 fractures rotated out of the axial plane orientation during progressive tightening of the folds.

Along major fracture zones which, with few exceptions, strike north, large amounts of calcite were introduced as both fracture infill and wholesale wallrock replacement. Some of the calcite pods have a weak S_2 mineral shape fabric, indicating a late-D_2 origin. This is further supported by calcite-dolomite thermometry on pods north of Mary Kathleen, with temperatures close to the D_2 thermal peak (Oliver & Wall, 1987). The calcite pods contain Cu sulphides and secondary Cu minerals, which have been mined in the past.

Undeformed veins with an S_3 orientation form the youngest set and crosscut all pre-D_2 and D_2 features. The various sets of fractures provided major fluid pathways during metamorphism. This is particularly evident where scapolitisation and feldspathisation occurred immediately adjacent to fractures.

Metamorphism

Aluminous schist

With the exception of garnet-bearing schist, the compatibility relationships for the Corella schists can be shown on an AKF projection (Fig. 20). Pelitic rock compositions range from microcline schist to andalusite-sillimanite schist, cordierite schist, and cordierite-anthophyllite rock. The cordierite-biotite tie lines separate aluminous and potassic compositions from anthophyllite- and talc-bearing assemblages discussed below in the section on 'Cordierite-orthoamphibole and associated rocks'. Cordierite was not found in stable coexistence with muscovite. Staurolite is present in a single sample as a retrograde mineral. Rare garnet is restricted to the most Fe-rich compositions and is invariably high in Mn.

Andalusite and sillimanite coexist over nearly the entire study area. The ratio of sillimanite to andalusite increases from southwest to east and northeast, where sillimanite dominates (Fig. 21). However, no isograd can be drawn, as the lowest-grade samples still contain tiny amounts of sillimanite. Hence, the present erosion surface exposes rocks that lie completely within the sillimanite-muscovite zone.

The andalusite-sillimanite reaction is divariant in this area, as significant amounts of Fe^{3+} have been detected (up to about 2 wt% Fe_2O_3 in andalusite). The $FeAlSiO_5$ component expands the andalusite stability field towards higher pressure and temperature (Grambling & Williams, 1985; Kerrick & Speer, 1988). However, the coexistence of two polymorphs in the Rosebud Syncline is not simply the result of this bivariance. Fe contents and reaction progress show nothing more than a crude correlation, and the degree of transformation varies even within single samples. This emphasises the importance of kinetic factors

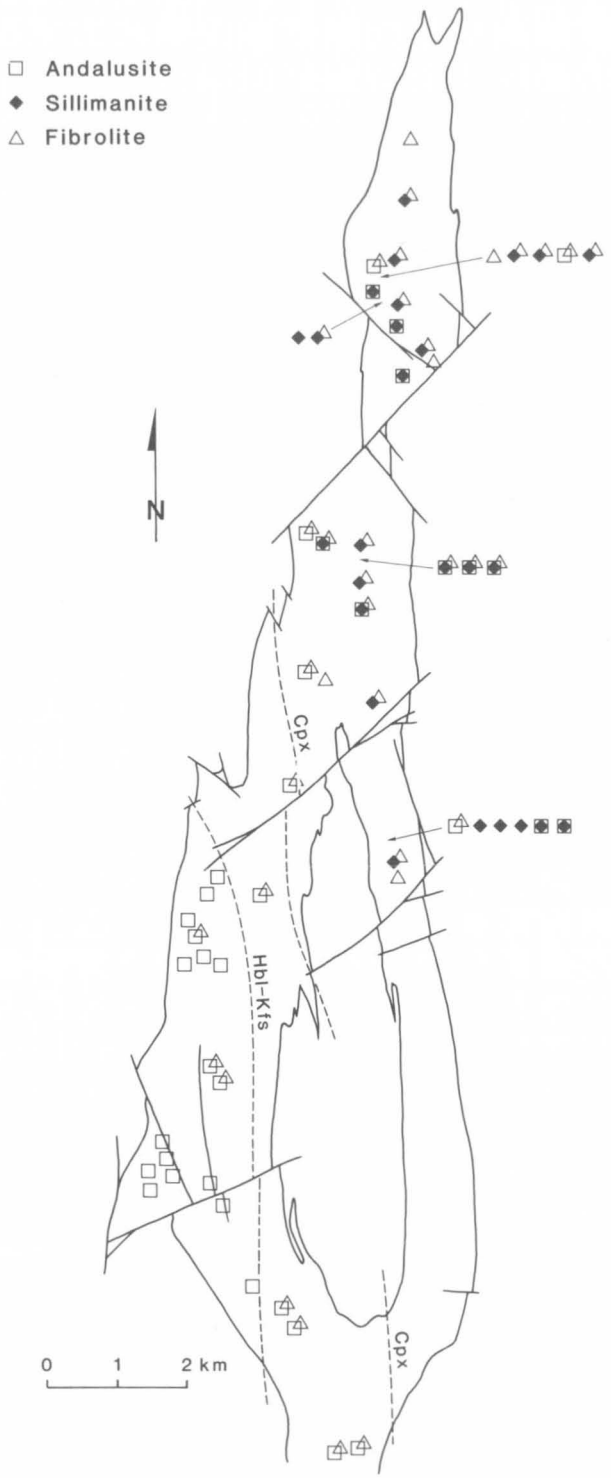


Fig. 21. Distribution of Al_2SiO_5 minerals across the study area, according to their proportion in the samples analysed. The symbols indicate the predominant species in each sample. Where proportions are roughly equal, two or three species are plotted together. Sillimanite occurs in all samples, but only in trace amounts in the lowest-grade area in the west. Coarse-grained sillimanite and fibrolite have been plotted separately. Also shown are two isograds in the calcareous rocks.

(such as fluids and deformation) for this notoriously sluggish reaction.

The metamorphic evolution of magnesian, alumino-potassic pelites can be appropriately shown in a P-T reaction grid for the system K_2O-FeO-MgO-Al_2O_3-SiO_2-H_2O (KFMASH), involving cordierite, chlorite, aluminosilicates (andalusite, sillimanite, kyanite), biotite, muscovite, K-feldspar, quartz, and H_2O. In the low-pressure amphibolite facies, Ca-Mn-poor, ferromagnesian garnet can form only in rocks with high Fe/Mg ratios (Spear & Cheney, 1989). As the metapelites are generally Fe-poor with MgO/(MgO+FeO) = 0.4, pyrope-almandine garnet can be excluded from the discussion of reaction sequences.

An internally consistent KFMASH reaction grid which includes staurolite is shown in Figure 22. Whether staurolite was ever present as an earlier prograde mineral in the Mg-poorer varieties of the Corella schist is not known because no relics are preserved. Biotite-rich pseudomorphs after presumably ferromagnesian minerals have been observed in some samples, but commonly the shape of the pseudomorphs indicates cordierite, and in some, cordierite relics are still present.

Reaction textures, overprinting relationships, and other microstructural criteria reveal growth sequences of metamorphic minerals, which correspond to a succession of prograde-retrograde reactions in a theoretical P-T reaction grid as in Figure 22, or in T-X projections (Reinhardt & Rubenach, 1989). For example, various generations of andalusite can be texturally distinguished: (1) early andalusite, most probably early-D_2, without biotite inclusions, rimmed by cordierite, (2) early-D_2 andalusite with inclusions of biotite, quartz, etc., that are not aligned parallel to S_2 and L^2_2, (3) late-D_2 andalusite with S_2 inclusion trails, in rocks in which cordierite has partly or completely reacted out, and (4) post-D_2 retrograde andalusite. Cordierite in anthophyllite-free rocks is generally early-D_2, with inclusion fabrics similar to andalusite under (2).

These features are consistent with a prograde P-T path crossing the bivariant reactions:

$$Chl + And + Qtz \leftrightarrow Crd + H_2O \quad (1)$$

$$Chl + Mus + Qtz \leftrightarrow Crd + Bio + H2O \quad (2)$$

$$Chl + Mus + Qtz \leftrightarrow Bio + And + H_2O \quad (3)$$

and the univariant reaction:

$$Chl + Mus + Qtz \leftrightarrow Crd + Bio + And + H_2O \quad (4)$$

and much of the large bivariant field of the reaction:

$$Crd + Mus \leftrightarrow Bio + And + Qtz + H_2O \quad (5)$$

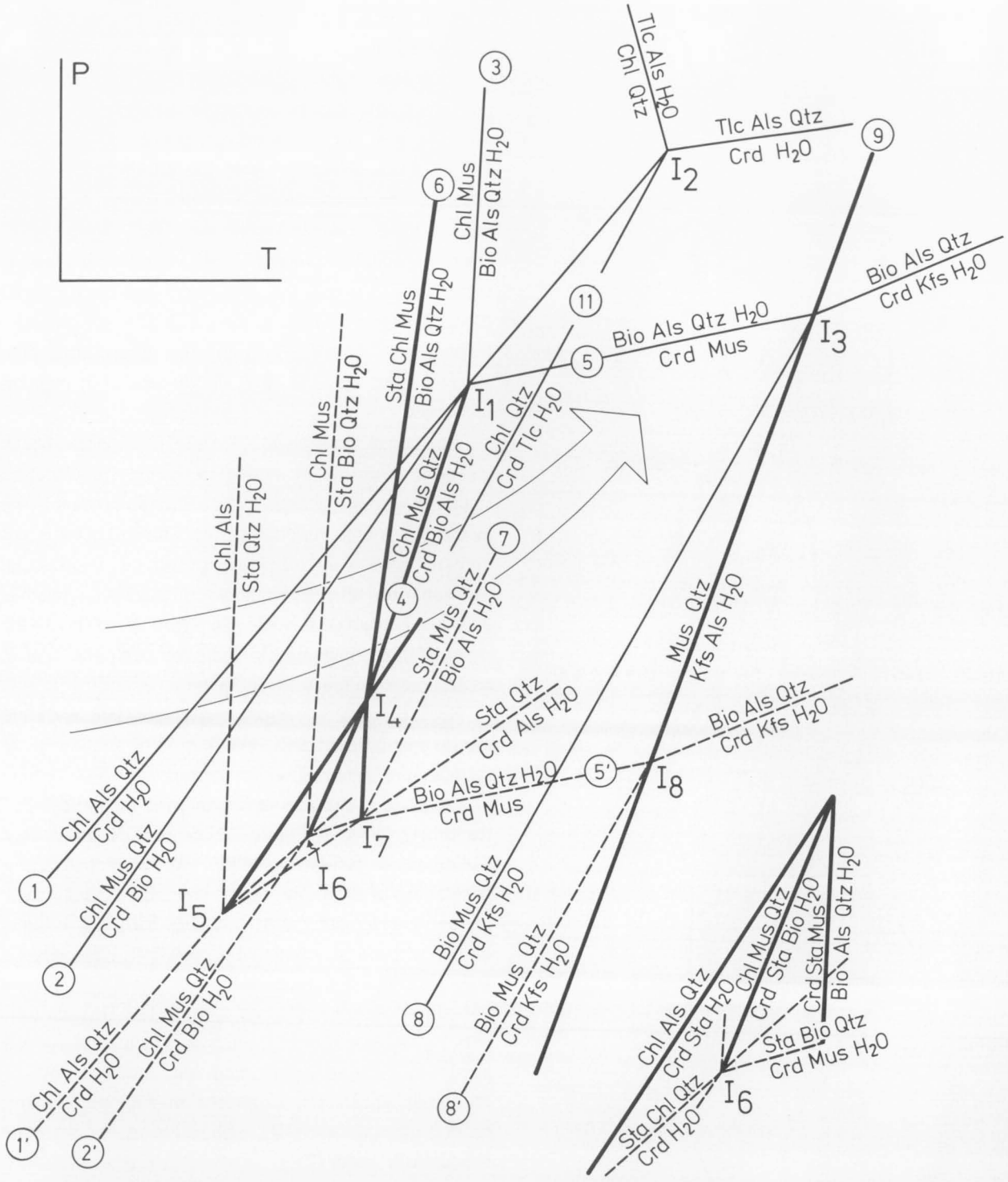


Fig. 22. Schematic reaction net for the system KFMASH in the low-pressure amphibolite facies (excess quartz, H_2O; no garnet or chloritoid). Thin solid lines: KMASH reactions. Dashed lines: KFASH reactions. Bold solid lines: univariant KFMASH reactions. Abbreviations: see Appendix. Reactions are numbered as in the text.

to its high pressure side (Fig. 22). The most magnesian cordierite analysed that had reacted to form andalusite and biotite has X_{Mg} = 0.8 (lower-grade area). If prograde staurolite were ever present, it would have disappeared through reactions 6 and 7 in Figure 22, forming biotite and an aluminosilicate at a relatively early stage of D_2. Reactions 8 and 9 have not been crossed as neither cordierite + K-feldspar nor sillimanite + K-feldspar are present.

Some of the cordierite-bearing schist shows a retrograde breakdown of cordierite to either andalusite + chlorite + quartz or kyanite + chlorite + quartz (reaction 1

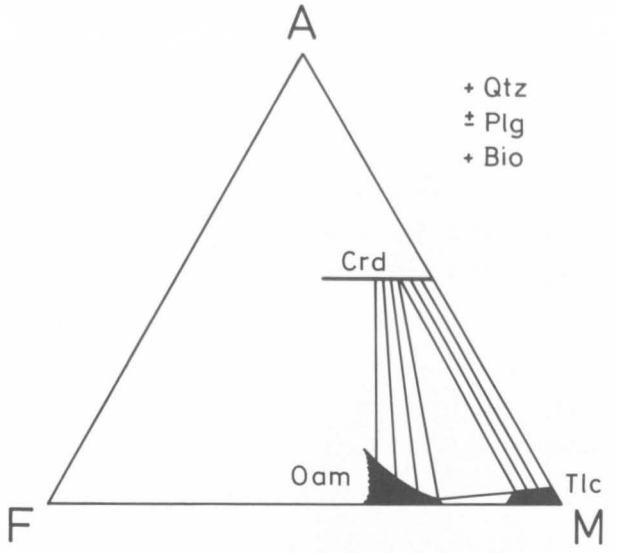


Fig. 23. (a) AFM phase relations in the Mg-rich metapelitic rocks.

above). The implications for the post-D_2 cooling path are discussed below in the section on 'Thermobarometry and P-T path'.

Minor Ca-rich layers in schist zones are typically rich in epidote. The assemblage plagioclase + calcite, which would indicate a CO_2-enriched fluid, was not found. Extrapolation of the data of Storre & others (1982) for the stability field of epidote with 'endmember' composition Ps_{33} at 400 MPa restricts the fluid composition to X_{CO2} values below 0.2. Hence, the high-grade metamorphic fluids in the schist zones were H_2O-rich. As the main dehydration reactions occurred well before the metamorphic peak, such fluid compositions were probably encountered already at lower amphibolite facies conditions.

Cordierite-orthoamphibole and associated rocks

The compatibility relations between cordierite, orthoamphibole, and talc, based on microprobe analyses of coexisting phases, are summarised in Figure 23a. The assemblages cordierite + anthophyllite, cordierite + anthophyllite + talc, and cordierite + talc correspond to an increase of MgO/(MgO+FeO) in the bulk rock. At the Fe-rich end of the compositional range, supersolvus amphiboles and gedrite-bearing assemblages appear. Silica-undersaturated rocks contain chlorite, coexisting with cordierite, anthophyllite, or talc, plus biotite and plagioclase (compare Reinhardt, 1987a).

Reaction grids can be constructed for a pure MASH system (Fig. 23b) or an FMASH system (Reinhardt, 1987b). With the addition of some Fe, all the univariant

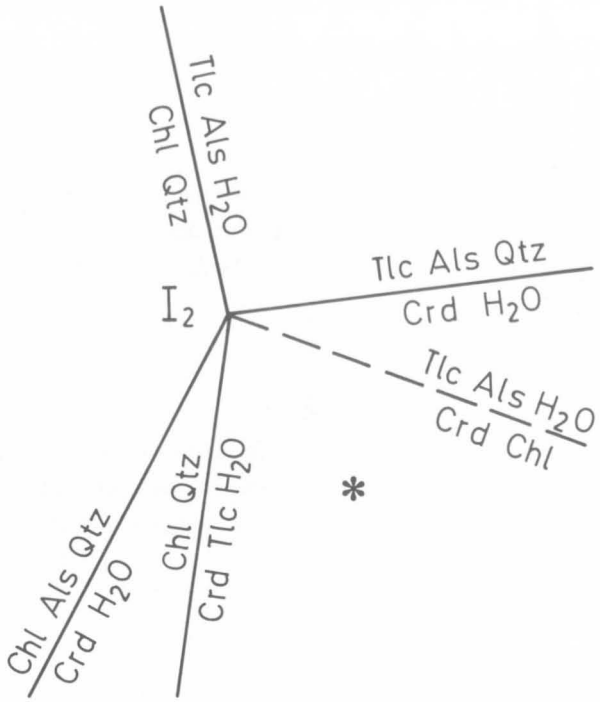


Fig. 23. (b) Schreinemakers bundle for reactions involving chlorite, talc, cordierite, Al_2SiO_5, quartz, H_2O in the system MgO-Al_2O_3-SiO_2-H_2O (MASH). *: P-T field in which the assemblages shown in (a) and the quartz-free assemblage cordierite + chlorite are stable. (From Reinhardt, 1987b).

MASH reactions in Figure 23b become bivariant, and anthophyllite enters the system. Of particular interest here are the main cordierite-, orthoamphibole-, and talc-producing reactions. If rock compositions have not changed significantly since low-grade conditions, the following reactions must have proceeded under lower amphibolite facies conditions:

$$Chl + Als + Qtz \leftrightarrow Crd + H_2O \quad (1)$$

$$Chl + Mus + Qtz \leftrightarrow Crd + Bio + H_2O \quad (2)$$

(see also Figure 22), and, at higher temperatures

$$Chl + Qtz \leftrightarrow Crd + Oam + H_2O, \quad (10)$$

or, if the rocks had very high MgO/(MgO+FeO),

$$Chl + Qtz \leftrightarrow Crd + Tlc + H_2O \quad (11)$$

Experimental investigations of reactions 10 and 11 do not give consistent results, but bracket their position between 550 and 600°C at 200 MPa, and around 620°C at 600 MPa (Fleming & Fawcett, 1976; Massonne, 1989).

The crest of the orthoamphibole solvus lies at about 600°C (Spear, 1980) which is very close to the orthamphibole-producing reaction in the KFMASH system. The presence of supersolvus orthoamphiboles is therefore indicative of high X_{H2O}. If X_{H2O} deviates

substantially from unity, the orthoamphibole-producing reaction shifts to lower temperature, into the two-amphibole field. At least part of the cordierite-orthoamphibole rock formed therefore at relatively high X_{H2O}.

Biotite from both aluminous schist and cordierite-orthoamphibole rock shows variable, and locally high, Cl contents (up to 0.29 wt% Cl). The Cl levels vary even within single outcrops indicating significant gradients in chlorine activity. As such Cl gradients cannot be maintained under conditions of high fluid/rock ratios, pervasive fluid infiltration during metamorphism is excluded (compare Wood & Walther, 1986). The saline fluids were most probably locally derived from original formation waters and chloride minerals in the sedimentary pile.

Calcschist and calc-silicate rock

Calcschist and calc-silicate rock with excess calcite contain the following assemblages:

Bio ± Mus + Cal ± Kfs + Scp + Qtz ± Tit ± FeOx ± Epi/All

in the west of the syncline, and farther east:

CaAm + Bio + Cal + Kfs + Plg and/or Scp + Qtz + Tit ± FeOx ± Epi/All, and:

Cpx + CaAm + Cal + Kfs + Plg and/or Scp + Qtz + Tit ± FeOx ± Epi/All.

Less common is:

Cpx + CaAm + Bio + Cal + Kfs + Plg and/or Scp + Qtz + Tit ± FeOx ± Epi/All.

The typical assemblage of para-amphibolite is:

CaAm + Bio + Kfs + Qtz + Scp ± Plg + Tit ± Epi.

Microcline- and scapolite-bearing schists form layers within the main calcareous units or at the contacts between the calcareous and pelitic units. Epidote in the above assemblages, particularly the higher-grade ones, is not generally part of the peak metamorphic assemblage. It may be present as a low-grade relict mineral, or as a retrograde mineral replacing amphibole. At a few localities, garnet is present in para-amphibolite.

The following isograds can be mapped in calcschist and calcsilicate rock (Fig. 21):

(1) the first appearance of Ca- amphibole + K-feldspar,

(2) the first appearance of clinopyroxene,

(3) the last appearance of the assemblage muscovite + calcite + quartz towards higher grade, which is just east of the clinopyroxene isograd.

Ca-amphibole can form at lower amphibolite facies conditions by the reaction:

$$Chl + Cal + Qtz \leftrightarrow CaAm + An + H_2O + CO_2 \quad (12)$$

(Ferry, 1976).

Ca-amphibole-K-feldspar assemblages enter at higher grades, where biotite + calcite + quartz become unstable:

$$Bio + Cal + Qtz \leftrightarrow CaAm + Kfs + H_2O + CO_2 \quad (13)$$

The assemblage muscovite + calcite + quartz reacts to produce feldspars:

$$Mus + Cal + Qtz \leftrightarrow Kfs + An + H_2O + CO_2 \quad (14)$$

The highest-grade index mineral present in the Rosebud Syncline is diopside, the lower stability limit of which is defined by the reaction:

$$Trm + Cal + Qtz \leftrightarrow Dio + H_2O + CO_2 \quad (15)$$

The Ca-amphibole compositions range from actinolitic to hastingsitic. Thus, FeO, Al_2O_3, Na_2O, and K_2O must be added to the simple CaO-MgO-SiO_2-H_2O-CO_2 system of reaction 15. The presence of alkalis in the amphiboles implies participation of plagioclase in reactions (13) and (15) thus:

$$Bio + Cal + Qtz + Ab \leftrightarrow CaAm + Kfs + An + H_2O + CO_2 \quad (16)$$

and

$$CaAm + Cal + Qtz \leftrightarrow Cpx + Plg + Kfs + H_2O + CO_2 \quad (17)$$

The Ca-amphibole-K-feldspar and clinopyroxene isograds in the Rosebud Syncline are based on reactions 13/16 and 15/17, respectively. As the temperatures of devolatilisation reactions in calcareous rocks are very much dependent on H_2O/CO_2 ratios, such isograds do not necessarily represent intersections of the erosion surface with simple P-T reaction surfaces, even if bulk rock compositions are uniform (compare Carmichael, 1970). Nonetheless, the isograd pattern in the calcareous rocks is in accordance with the general temperature trend of increasing metamorphic grade towards the east and north, as derived from the andalusite-sillimanite transformation. Consequently, systematic variations in fluid composition should have occurred only over smaller distances.

The first appearance of Ca-amphibole and clinopyroxene is to be expected in the most magnesian rocks, at the lowest X_{CO2} fluid compositions occurring (Fig. 24). Variations in fluid compositions are indicated by the persistence of Ca-amphibole + calcite, or even magnesian biotite + calcite, well beyond the clinopyroxene isograd. This suggests a larger degree of reaction buffering for the 'lower-grade' assemblages in the diopside zone.

The persistence of the assemblage muscovite + calcite

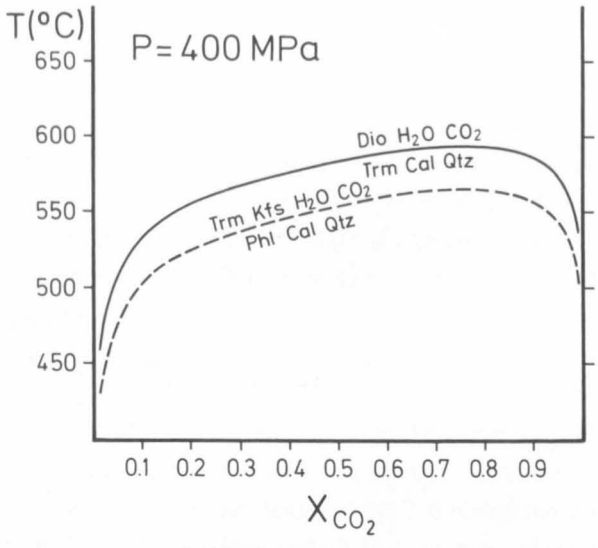


Fig. 24. Calculated T-X_{CO2} data for the reactions Phl + Cal + Qtz ↔ Trm + Kfs + H_2O + CO_2, and Trm + Cal + Qtz ↔ Dio + H_2O + CO_2. Activities for solid phases = 1. The presence of Fe shifts the reactions to higher temperatures. Note, however, that the rock-fluid systems of the calc-silicate rocks in the study area deviate considerably from such relatively simple systems. The reaction curves allow only minimum temperature estimates.

+ quartz to relatively high grades is possible only at X_{CO2} around 0.5, where the reaction temperatures reach a maximum. Still, the occurrence of this assemblage in the study area appears to be at variance with temperatures derived from other assemblages, if the experimentally determined maximum stability temperatures are considered (530°C at 400 MPa; Hewitt, 1973). A possible explanation is the relatively high Fe^{3+} content of muscovite, which shifts its stability limit to higher temperatures.

High fluid salinities are indicated by Cl-rich biotite, amphibole, and scapolite (maximum Cl contents: 0.60 wt%, 1.24wt%, 3.67 wt%, respectively). Actinolitic amphibole has generally low levels of Cl, whereas hastingsite can, but does not in general, have high Cl contents (Reinhardt, 1987b). Scapolite compositions range from 25% to 75.5% meionite (or 24% to 65.5% EqAn), with some SO_3 present in nearly all samples.

Scapolite is a sensitive monitor of fluid salinity and X_{CO2}. The compositional variation of scapolite in the study area, even on a layer-to-layer scale, excludes large-scale infiltration of externally derived fluids, but suggests variable proportions of evaporitic minerals in different layers and small-scale variations of fluid salinity during metamorphism. The formation of scapolite can be expressed by the endmember reactions:

$$An + CaCO_3 \leftrightarrow \text{meionite} \quad (18)$$

$$Ab + NaCl \leftrightarrow \text{marialite}, \quad (19)$$

$$An + CaSO_4 \leftrightarrow SO_3\text{-meionite}. \quad (20)$$

The presence of scapolite will affect any equilibrium which would otherwise involve plagioclase in the Cl-free system. These are essentially all the main reactions by which biotite, amphibole, and clinopyroxene form, plus the anorthite-forming reactions. For example, a possible low-grade reaction, which represents a combination of reactions 14, 18, and 19, is:

$$Mus + Cal + Ab + Qtz + NaCl \leftrightarrow Scp + Kfs + H_2O + CO_2 \quad (21)$$

Evidently, the calc-silicate rocks and calcschists of this area are chemically complex systems. Even if TiO_2, Fe_2O_3, MnO, and SO_3 are neglected, a ten-component system $CaO\text{-}Na_2O\text{-}K_2O\text{-}FeO\text{-}MgO\text{-}Al_2O_3\text{-}SiO_2\text{-}H_2O\text{-}CO_2\text{-}Cl$ remains, which is presently understood only in rather basic terms. A complication in modelling fluid-mineral equilibria is the presence of NaCl. In general, high NaCl contents increase the activity of CO_2 for H_2O-rich compositions and consequently increase the reaction temperatures of decarbonation reactions at low X_{CO2} (Jacobs & Kerrick, 1981). Considering the high salinities deduced from Cl contents of biotite, amphibole, and scapolite, it is likely that conditions of fluid immiscibility were reached during metamorphism, whereby a NaCl-rich hydrous fluid coexisted with a NaCl-poor CO_2-rich fluid (compare Skippen & Trommsdorff, 1986).

Metasomatic features are not uncommon in the calcareous rocks. Local changes of rock compositions (scapolitisation, albitisation) are particularly evident along major fluid conduits such as fractures. The rock volume visibly affected is commonly small, however, as the width of the metasomatic fringes is typically in the range of a few millimetres to centimetres.

The effects of more pervasive metasomatism are seen in some localities, where influx of alkalis and loss of Ca, Fe, and Mg has markedly changed the original rock composition on the scale of tens of metres. In general, however, metasomatism in the Rosebud Syncline is a small-scale phenomenon compared to the extent of mass transfer in some areas east of the Wonga Belt (compare Oliver & Wall, 1987). Because of its evaporitic character, the Corella Formation is the most likely source for the saline fluids responsible for infiltration-related secondary scapolite enrichment in calc-silicate rocks and metadolerite (Fig. 5).

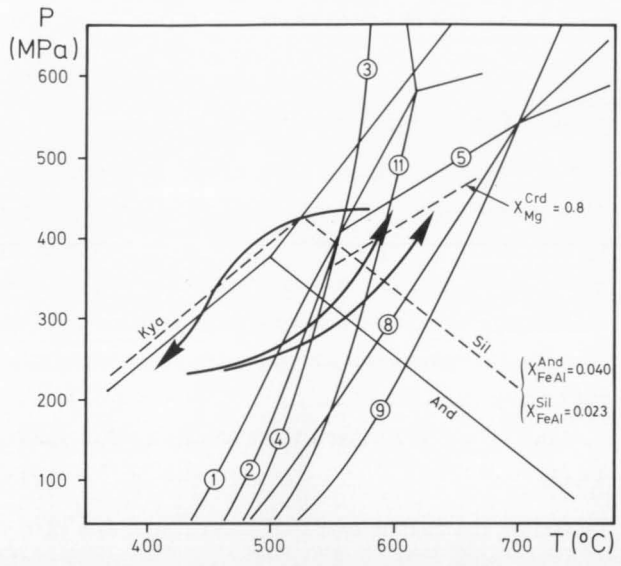


Fig. 25. Syn- and post-D_2 pressure-temperature paths. Prograde paths are shown for low- and high-grade areas. KMASH reaction curves have been calculated for a_{H2O} = 0.8, using the GE0/-CALC program of Berman & others (1987) and recent experimental data for reaction 5 (H.-J. Massonne, personal communication). The shift of the andalusite-sillimanite reaction due to Fe^{3+} incorporation is also shown. Reactions are numbered as in Figure 22 and in the text.

Thermobarometry and P-T path

The cordierite-bearing assemblages and the sequence andalusite --> sillimanite indicate a low-pressure, prograde metamorphic path. The metamorphic peak had been reached at temperatures between 580 and 640°C, and at pressures of 400-500 MPa. Pressures are constrained by reaction 5 (Figs. 22, 25) and by the Si content of muscovite in the assemblage Mus-Kfs-Bio-Qtz (Massonne & Schreyer, 1987), which reaches about 3.1 per formula unit. Relatively low peak pressures are also indicated by the persistence of andalusite in the higher-grade part of the syncline.

The lower temperature limit is set by the orthoamphibole solvus, which closes at temperatures of 600 ± 20°C (Spear, 1980). The reaction forming cordierite + orthoamphibole also takes place at around 600°C at P_{H2O} = 400-500 MPa (Fleming & Fawcett, 1976; Massonne, 1989). These temperatures are confirmed by the composition of the most CO_2-rich scapolites, which are close to EqAn = 67. The minimum temperature stability of such a scapolite is about 620°C (Aitken, 1983).

The deduced reaction sequences indicate a prograde P-T path with an early stage dominated by temperature rise and a later steepening towards the P axis (Fig. 22). This agrees with the relations found between increasing strain during D_2 compression and timing of mineral growth (Reinhardt & Rubenach, 1989). If the late-D_2 P-T path were steep, the actual temperature overstepping for the andalusite-sillimanite reaction would probably have been less than 20°C in the lowest-grade area.

The retrograde kyanite and andalusite in cordierite schist put important constraints on the cooling path. The P-T path must have crossed the respective stability fields between about 500-550°C (kyanite-sillimanite boundary) and 400°C (lower stability of Al_2SiO_5 + H_2O). The textural relations between the retrograde Al_2SiO_5 minerals imply that kyanite formed earlier than andalusite. Hence, the retrograde P-T path crossed from the sillimanite field into the kyanite field during a period of near-isobaric cooling, and then into the andalusite stability field (Reinhardt, 1989). The prograde-retrograde reaction sequences in the western Mary Kathleen Fold Belt document a complete anticlockwise pressure-temperature path (Fig. 25).

Conclusions

The Mid-Proterozoic Corella Formation in the Rosebud Syncline shows a rock association which is characteristic for a metamorphosed evaporite-bearing sequence (compare Moine & others, 1981). The main rock types were alumino-potassic mudstone with intermediate to high MgO/(MgO + FeO), less aluminous highly magnesian mudstone, limestone, dolostone, and a wide range of mixed carbonatic-pelitic rocks. Evaporitic chloride and sulphate minerals must have been present, but large amounts were probably lost by dissolution before metamorphism.

The volcano-sedimentary succession of the upper Tewinga Group and the Mary Kathleen Group is indicative of a former ensialic rift zone. The Corella Formation constitutes the sedimentary blanket of the final phase of thermal subsidence, preceeded by extensive bimodal volcanism and conglomeratic-psammitic sedimentation of the earlier rifting and subsidence stages.

The earliest deformation documented in the study area was south-directed D_1 thrusting characterised by interference of strike-slip shear zones (S_{1v}) with thrust planes (S_{1h}), resulting from differential lateral transport. D_1 thrusting can be traced from the Western Succession (Bell, 1983) and the West Leichhardt Klippe in the Kalkadoon-Leichhardt Block to the Mount Devine Thrust System (Loosveld & Schreurs, 1987), the Mary Kathleen

Fold Belt (this study), and the Tommy Creek Block east of the Wonga Belt (Hill & others, this volume).

The D_2 event was an east-west compressional, approximately bulk coaxial deformation with extensive vertical stretching. The minimum east-west horizontal shortening in the west-central Mary Kathleen Fold Belt was 50-60% (Reinhardt, 1992). This estimate agrees with those obtained from nearby areas (Holcombe & Fraser, 1979; Passchier, 1986). Folding on all scales was non-cylindrical, and caused the present-day pattern of doubly-plunging synforms. This structural pattern is particularly conspicuous immediately west of the Wonga Belt (Rosebud Syncline, Little Beauty Syncline, etc.).

D_3 was a minor shortening episode, with principal strain axes at low angles to those of D_2. The orientation of D_2 and D_3 structures correlates with that of D_2 and D_3 in the Leichhardt River Fault Trough to the west (Winsor, 1983, 1986; Page & Bell, 1986), suggesting a common deformational history (compare Table 2). Hence, the isotopic dates obtained for D_1 (1610 Ma), D_2 (1544 Ma), and D_3 (1500 Ma) in the Mount Isa area (Page & Bell, 1986) should also be valid for the Mary Kathleen Fold Belt.

Pre-D_2 mineral inclusions in porphyroblasts indicate low-grade metamorphic conditions during D_1. The metamorphic peak was reached during D_2, at 580-640°C and 400-500 MPa. The present erosion surface exposes rocks of the sillimanite-muscovite zone, wherein peak metamorphic temperatures were highest in the eastern and northern areas. The prograde metamorphism is characterised by reactions of the low-pressure facies series. Progressive deformation and increase of both pressure and temperature were synchronous, from the earliest to the latest stages of D_2. Hence, low-pressure metamorphism was contemporaneous with D_2 crustal shortening. From the metamorphic peak, the rocks cooled near-isobarically, before major decompression set in. The P-T-t path of the main metamorphic-deformational episode is anticlockwise.

Metamorphic fluid compositions were not uniform. Significant gradients existed in X_{CO2} and salinity, not only between metapelitic and calcareous rocks, but also within single units. Large parts of the metasedimentary sequence were essentially reaction-buffered rock-fluid systems, but locally, pervasive infiltration metasomatism is evident. The saline fluids were generally derived from within the Corella Formation. Fluid migration was controlled by permeability contrasts between different rock types and by the presence of major fluid pathways, such as the extensive fracture network in parts of the calc-silicate rocks.

Acknowledgements

I would like to thank Mike Rubenach and Tim Bell for many stimulating discussions during this project. During field work, I met numerous geologists, who contributed in one way or another to my understanding of Mount Isa geology. Thanks go in particular to Nick Oliver and Paul Pearson for being excellent company in the field. The hospitality of Bill and Di Perkins, Mount Isa, and the Campbells at Rosebud Homestead and at The Orchard was much appreciated. The Bureau of Mineral Resources, Canberra, provided generous logistic support during field work. The project was financed by a Willard C. Lacy Scholarship and various James Cook University Research Funds. The manuscript was improved through comments from Mike Rubenach, John Sheraton, and Alastair Stewart.

References

AITKEN, B.G., 1983 - T-X_{CO2} stability relations and phase equilibria of calcic carbonate scapolite. *Geochimica et Cosmochimica Acta* 47, 351-362.

BARLOW, S.D., 1969 - Geology of the Rosebud area, Mary Kathleen, north-western Queensland. B.Sc.(Hons.) thesis,University of Queensland (unpublished).

BAVINTON, O.A., 1969 - Aspects of the geology and mineralogy of the northern Green's Creek area, Mary Kathleen, north-west Queensland. B.Sc.(Hons.) thesis, University of Queensland (unpublished).

BEARDSMORE, T.J., NEWBERY, S.P., & LAING, W.P., 1988 - The Maronan Supergroup: an inferred early volcanosedimentary rift sequence in the Mount Isa Inlier, and its implications for ensialic rifting in the Middle Proterozoic of northwest Queensland. *Precambrian Research* 40/41, 487-507.

BEESON, R., 1988 - Identification of cordierite-anthophyllite rock types associated with sulphide deposits of copper, lead and zinc. *Transactions of the Institution of Mining and Metallurgy*, Section B, 97, 108-115.

BELL, T.H., 1983 - Thrusting and duplex formation at Mount Isa, Queensland, Australia. *Nature* 304, 493-497.

BELL, T.H., 1985. Deformation partitioning and porphyroblast rotation in metamorphic rocks: a radical reinterpretation. *Journal of Metamorphic Geology* 3, 109-118.

BELL, T.H., & DUNCAN, A.C., 1978 - A rationalised and unified shorthand terminology for lineations and fold axes in tectonites. *Tectonophysics* 47, T1-T5.

BELL, T.H., REINHARDT, J., & HAMMOND, R.L., 1992 - Multiple foliation development during thrusting and synchronous formation of vertical shear zones. *Journal of Structural Geology* 14 (in press).

BERMAN, R.G., BROWN, T.H., & PERKINS, E.H., 1987 - GE0-CALC: Software for calculation and display of P-T-X phase diagrams. *American Mineralogist* 72, 861-862.

BLAKE, D.H., 1980 - The early geological history of the Proterozoic Mount Isa Inlier, northwestern Queensland: an alternative interpretation. *BMR Journal of Australian Geology & Geophysics* 5, 243-256.

BLAKE, D.H., 1982 - A review of the Corella Formation, Mount Isa Inlier, Queensland. *BMR Journal of Australian Geology & Geophysics* 7, 113-118.

BLAKE, D.H., 1987 - Geology of the Mount Isa Inlier and environs, Queensland and Northern Territory. *BMR Bulletin* 225, 83 pp.

BULTITUDE, R.J., & WYBORN, L.A.I., 1982 - Distribution and geochemistry of volcanic rocks in the Duchess - Urandangi region, Queensland. *BMR Journal of Australian Geology & Geophysics* 7, 99-112.

BUTLER, R.W.H., 1982 - The terminology of structures in thrust belts. *Journal of Structural Geology* 4, 239-245.

CARMICHAEL, D.M., 1970 - Intersecting isograds in the Whetstone Lake area, Ontario. *Journal of Petrology* 11, 147- 181.

CARTER, E.K., BROOKS, J.H., & WALKER, K.R., 1961 - The Precambrian mineral belt of north-western Queensland. *BMR Bulletin* 51, 344 pp.

CHAMLEY, H., 1989. Clay Sedimentology. *Springer-Verlag, Berlin*, 623 pp.

CLIFFORD, N.J., 1969 - Structural analysis of the Corella Formation near Mary Kathleen, north-western Queensland. B.Sc.(Hons.) thesis, University of Queensland (unpublished).

DE ROSEN-SPENCE, A., 1969 - Genèse des roches à cordiérite-anthophyllite des gisements cupro-zincifères de la région de Rouyn-Noranda, Québec, Canada. *Canadian Journal of Earth Sciences* 6, 1339-1345.

DERRICK, G.M., 1982 - A Proterozoic rift zone at Mount Isa, Queensland, and implications for mineralization. *BMR Journal of Australian Geology & Geophysics* 7, 81-92.

DERRICK, G.M., & WILSON, I.H., 1981 - The early geological history of the Proterozoic Mount Isa Inlier, northwestern Queensland: An alternative interpretation: Discussion. *BMR Journal of Australian Geology & Geophysics* 6, 267-271.

DERRICK, G.M., WILSON, I.H., HILL, R.M., GLIKSON, A.Y., & MITCHELL, J.E., 1977. Geology of the Mary Kathleen 1:100 000 Sheet area, northwest Queensland. *BMR Bulletin* 193, 114 pp.

EDWARDS, A.B., & BAKER, G., 1954 - Scapolitisation in the Cloncurry district of north-western Queensland. *Journal of the Geological Society of Australia* 1, 1-33.

FERRY, J.M., 1976 - Metamorphism of calcareous sediments in the Waterville-Vassalboro area, south-central Maine: Mineral reactions and graphical analysis. *American Journal of Science* 276, 841-882.

FLEMING, P.D., & FAWCETT, J.J., 1976 - Upper stability of chlorite + quartz in the system MgO-FeO-Al_2O_3-SiO_2-H_2O at 2 kbar water pressure. *American Mineralogist* 61, 1175- 1193.

FROESE, E., 1969 - Metamorphic rocks from the Coronation mine and surrounding area. *Geological Survey of Canada Paper* 68-5, 55-77.

GLIKSON, A.Y., DERRICK, G.M., WILSON, I.H., & HILL, R.M., 1976 - Tectonic evolution and crustal setting of the Middle Proterozoic Leichhardt River fault trough, Mount Isa region, northwestern Queensland. *BMR Journal of Australian Geology & Geophysics* 1, 115-129.

GRAMBLING, J.A., & WILLIAMS, M.L., 1985 - The effect of Fe^{3+} and Mn^{3+} on aluminum silicate phase relations in north-central New Mexico, U.S.A. *Journal of Petrology* 26, 324- 354.

HEWITT, D.A., 1973 - Stability of the assemblage muscovite-calcite-quartz. *American Mineralogist* 58, 785-791.

HILL, E.J., LOOSVELD, R.J.H., & PAGE, R.W., this volume. Structure and geochronology of the Tommy Creek Block, Mount Isa Inlier. *In*: STEWART, A.J., & BLAKE, D.H. (Editors), Detailed Studies of the Mount Isa Inlier. *Bureau of Mineral Resources, Australia, Bulletin* 243.

HILL, R.M., 1968 - Geology of the Sunset area, Mary Kathleen, Queensland. B.Sc.(Hons.) thesis, University of Queensland (unpublished).

HOLCOMBE, R.J., & FRASER, S.J., 1979 - Structural and stratigraphic problems of the Argylla Formation near Mary Kathleen, Queensland. *Journal of the Geological Society of Australia* 26, 419-434.

JACKSON, M.J., SIMPSON, E.L., & ERIKSSON, K.A., 1990 - Facies and sequence stratigraphic analysis in an intracratonic, thermal-relaxation basin: the Early Proterozoic, Lower Quilalar Formation and Ballara Quartzite, Mount Isa Inlier, Australia. *Sedimentology* 37, 1053-1078.

JACOBS, G.K., & KERRICK, D.M., 1981 - Devolatilization equilibria in H_2O-CO_2 and H_2O-CO_2-NaCl fluids: an experimental and thermodynamic evaluation at elevated pressures and temperatures. *American Mineralogist* 66, 1135-1153.

KERRICK, D.M., & SPEER, J.A., 1988 - The role of

minor element solid solution on the andalusite-sillimanite equilibrium in metapelites and peraluminous granitoids. *American Journal of Science* 288, 152-192.

LOOSVELD, R.J.H., & SCHREURS, G., 1987 - Discovery of thrust klippen, northwest of Mary Kathleen, Mt. Isa Inlier, Australia. *Australian Journal of Earth Sciences* 34, 387-402.

LUCAS, J., 1962 - La transformation des minéraux argileux dans la sédimentation. Études sur les argiles du Trias. *Mémoires du Service de la Carte Géologique d'Alsace et de Lorraine* 23, 202 pp.

MASSONNE, H.-J., 1989 - The upper thermal stability of chlorite + quartz: an experimental study in the system MgO-Al_2O_3-SiO_2-H_2O. *Journal of Metamorphic Geology* 7, 567-581.

MASSONNE, H.-J., & SCHREYER, W., 1987 - Phengite geobarometry based on the limiting assemblage with K-feldspar, phlogopite, and quartz. *Contributions to Mineralogy and Petrology* 96, 212-224.

McKENZIE, D., 1978 - Some remarks on the development of sedimentary basins. *Earth and Planetary Science Letters* 40, 25-32.

MILLOT, G., 1970 - Geology of Clays. *Masson et Cie., Paris.*

MOINE, B., SAUVAN, P., & JAROUSSE J., 1981 - Geochemistry of evaporite-bearing series: A tentative guide for the identification of metaevaporites. *Contributions to Mineralogy and Petrology* 76, 401-412.

OLIVER, N., & WALL, V., 1987 - Metamorphic plumbing system in Proterozoic calc-silicates, Queensland, Australia. *Geology* 15, 793-796.

OLIVER, N., WALL, V., REINHARDT, J., PEARSON, P., HOLCOMBE, R., & RUBENACH, M., 1985. Metasomatism in polydeformed calc-silicates and related rocks of the Mary Kathleen Fold Belt, Queensland (Field guide). *Conference on Stable Isotopes and Fluid Processes in Mineralisation, Brisbane, 1985.*

PAGE, R.W., 1983a - Timing of superposed volcanism in the Proterozoic Mount Isa Inlier, Australia. *Precambrian Research* 21, 223-245.

PAGE, R.W., 1983b - Chronology of magmatism, skarn formation, and uranium mineralization, Mary Kathleen, Queensland, Australia. *Economic Geology* 78, 838-853.

PAGE, R.W., & BELL, T.H., 1986 - Isotopic and structural responses of granite to successive deformation and metamorphism. *Journal of Geology* 94, 365-379.

PASSCHIER, C.W., 1986 - Proterozoic deformation in the Duchess belt, Australia: A contribution to the BMR Mount Isa Regional Tectonic History Program. *Geologie en Mijnbouw* 65, 47- 56.

PEARSON, P.J., HOLCOMBE, R.J., & OLIVER, N.H.S., 1987 - The Mary Kathleen Fold Belt, northwest Queensland: D_1 - A product of crustal extension? *International Conference on Deformation of Crustal Rocks, Mt. Buffalo, Australia, 1987, Geological Society of Australia Abstracts* 19, 37-38.

RAMSAY, C.R., 1968. Petrology and geochemistry of the Green's Creek area, Mary Kathleen, north-western Queensland. B.Sc.(Hons.) thesis, University of Queensland (unpublished).

RAMSAY, C.R., & DAVIDSON, L.R., 1970 - The origin of scapolite in the regionally metamorphosed rocks of Mary Kathleen, Queensland, Australia. *Contributions to Mineralogy and Petrology* 25, 41-51.

RAMSAY, C.R., & DAVIDSON, L.R., 1974 - Cordierite-anthophyllite rocks formed by isochemical regional metamorphism at Mary Kathleen, northwestern Queensland, Australia. *Proceedings of the Royal Society of Queensland* 85, 43-55.

RAYNER, R.A., 1975 - Structural and stratigraphic relationships in the Lady Rose area, near Mary Kathleen, north-west Queensland. B.Sc.(Hons.) thesis, University of Queensland (unpublished).

REINHARDT, J., 1987a - Cordierite-anthophyllite rocks from north-west Queensland, Australia: metamorphosed magnesian pelites. *Journal of Metamorphic Geology* 5, 451-472.

REINHARDT, J., 1987b - Metamorphic and structural evolution of the Corella Formation in the Rosebud Syncline, north-west Queensland. Ph.D. thesis, James Cook University of North Queensland (unpublished).

REINHARDT, J., 1989 - Evidence for a complete anticlockwise P-T path in medium-grade schists of the central Mt. Isa Block, northeast Australia. *European Union of Geosciences, 5th Meeting, Strasbourg, Terra Abstracts* 1, 306.

REINHARDT, J., 1991 - Geology of the Rosebud Syncline (1:25 000 scale map), *Bureau of Mineral Resources, Canberra, Australia.* Available as a colour electrostatic plot on paper (AUD30), or in digital form on optical disc or Exabyte 8 mm tape (prices on application) both of which can be displayed on Intergraph Microstation software on computers that will run Unix. The digital data comprise a scanned raster image (.RLE format) of the black and white geological map, and an Intergraph vector design file containing the boundaries of coloured polygons. The coloured map and data are available from the Publication Sales Centre, Bureau of Mineral Resources, and an uncoloured Ozalar film or paper copy (AUD20) of the map is available from BMR Copy Service, both at GPO Box 378, Canberra, ACT, 2601, Australia. All orders to be prepaid to Collector of Public Monies.

REINHARDT, J., 1992 - Low-pressure, high-temperature metamorphism in a compressional tectonic setting:

Mary Kathleen Fold Belt, northeastern Australia. *Geological Magazine* 129, 41- 57.

REINHARDT, J., & RUBENACH, M.J., 1989 - Temperature-time relationships across metamorphic zones: evidence from porphyroblast-matrix relationships in progressively deformed metapelites. *Tectonophysics* 158, 141-161.

ROWLEY, M., 1969 - Amphibolites and associated rocks of the town area, Mary Kathleen, north-western Queensland. B.Sc.(Hons.) thesis, University of Queensland (unpublished).

SKIPPEN, G., & TROMMSDORF, V., 1986 - The influence of NaCl and KCl on phase relations in metamorphosed carbonate rocks. *American Journal of Science* 286, 81-104.

SPEAR, F.S., 1980 - The gedrite-anthophyllite solvus and the composition limits of orthoamphibole from the Post Pond Volcanics, Vermont. *American Mineralogist* 65, 1103-1118.

SPEAR, F.S., & CHENEY, J.T., 1989 - A petrogenetic grid for pelitic schists in the system SiO_2-Al_2O_3-FeO-MgO-K_2O-H_2O. *Contributions to Mineralogy and Petrology* 101, 149-164.

STORRE, B., JOHANNES, W., & NITSCH, K.-H., 1982 - The stability of zoisite in H_2O-CO_2 mixtures. *Neues Jahrbuch für Mineralalogie, Monatshefte* 1982, 395-406.

WATTS, A.B., KARNER, G.D., & STECKLER, M.S., 1982 - Lithospheric flexure and the evolution of sedimentary basins. *Philosophical Transactions of the Royal Society of London, Series A* 305, 249-281.

WHITE, N., & McKENZIE, D., 1988 - Formation of the 'steer's head' geometry of sedimentary basins by differential stretching of the crust and mantle. *Geology* 16, 250-253.

WILLIAMS, P.R., STEWART, A.J., & PEARSON, P.J., 1987 - Proterozoic continental extension in the Mount Isa Inlier, Queensland, Australia. *Symposium on Applied Extension Tectonics, Canberra, 1987, Extended Abstracts, Bureau of Mineral Resources, Australia, Record* 1987/51, 64-71.

WILSON, I.H., 1983 - Discussion: A review of the Corella Formation, Mount Isa Inlier, Queensland. *BMR Journal of Australian Geology & Geophysics* 8, 161-163.

WINSOR, C.N., 1983 - Syntectonic vein and fibre growth associated with multiple slaty cleavage development in the Lake Moondarra area, Mount Isa, Australia. *Tectonophysics* 92, 195-210.

WINSOR, C.N., 1986 - Intermittent folding and faulting in the Lake Moondarra area, Mount Isa, Queensland. *Australian Journal of Earth Sciences* 33, 27-42.

WOOD, B.J., & WALTHER, J.V., 1986 - Fluid flow during metamorphism and its implications for fluid-rock ratios. *In:* WALTHER, J.V., & WOOD, B.J. (Editors), Fluid-rock interactions during metamorphism. *Advances in Physical Chemistry* 5, 89-108.

WYBORN, L.A.I., & BLAKE, D.H., 1982 - Reassessment of the tectonic setting of the Mount Isa Inlier in the light of new field, petrographic, and geochemical data (Abstract). *BMR Journal of Australian Geology & Geophysics* 7, 143.

WYBORN, L.A.I., PAGE, R.W., & PARKER, A.J., 1987 - Geochemical and geochronological signatures in Australian Proterozoic igneous rocks. *In:* PHARAOH, T.C., BECKINSALE, R.D., & RICKARD, D. (Editors), Geochemistry and Mineralisation of Proterozoic Volcanic Suites. *Geological Society of London, Special Publication* 33, 377-394.

Appendix

Abbreviations used in text and figures:

D_1, D_2,...	Deformation events
S_0	Bedding
S_1, S_2, ...	Foliations formed during D_1, D_2, ...
F^0_1, F^0_2, ...	Folds and fold axes in S_0 formed during D_1, D_2, ...
L^1_1, L^2_2, ...	Mineral elongation lineations on S_1, S_2, formed during D_1, D_2 ...
L^0_2, L^1_2 ...	Intersection lineations (terminology according to Bell & Duncan, 1978)
EqAn	Equivalent anorthite

Minerals:

Ab	Albite
All	Allanite
Als	Aluminosilicate (And, Sil, Kya)
An	Anorthite
And	Andalusite
Ath	Anthophyllite
Bio	Biotite
CaAm	Calcic amphibole
Cal	Calcite
Chl	Chlorite
Cpx	Clinopyroxene
Crd	Cordierite
Dio	Diopside
Epi	Epidote
FeOx	Fe-oxide
Hbl	Hornblende
Kfs	K-feldspar
Kya	Kyanite
Mus	Muscovite
Oam	Orthoamphibole
Phl	Phlogopite
Plg	Plagioclase

Qtz	Quartz
Scp	Scapolite
Sil	Sillimanite
Sta	Staurolite
Tit	Titanite
Tlc	Talc
Trm	Tremolite

Page 256 is blank.

Structure of the Mary Kathleen Fold Belt

R. J. Holcombe [1], *P. J. Pearson* [1,2], *& N. H. S. Oliver* [3]

This paper is based on the following maps:

1. Holcombe, R.J., Pearson, P.J., & Sliwa, R., 1991 - Geology of the Mary Kathleen Area (1:25 000 scale map), Bureau of Mineral Resources, Canberra (two sheets).

2. Oliver, N.H.S, 1991 - Geology of the Mount Godkin Area (1:25 000 scale map), Bureau of Mineral Resources, Canberra.

3. Pearson, P.J., & Holcombe, R. J., 1991a - Geology of the Breakfast Creek Area (1:25 000 scale map), Bureau of Mineral Resources, Canberra.

4. Pearson, P.J., Horton, J.A., & Holcombe, R.J., 1991b - Geology of the East Limb, Little Beauty Syncline (1:15 000 scale map), Bureau of Mineral Resources, Canberra.

The Proterozoic Mary Kathleen Fold Belt in the Mount Isa Inlier consists of two distinct tectono-stratigraphic domains which are distinguished solely on the basis of the style and intensity of a pre-folding generation of structures (defined for this area as D^K_1). Intense shear-produced D^K_1 fabrics are exposed only in the core of a major D^K_2 anticlinorium (forming the Wonga Belt), and a smaller adjacent antiform, and diminish sharply upwards, above a zone of very high D^K_1 shear strain to form an overlying brittle-ductile slab now exposed as the 'flanking domains' along the limbs of the Wonga Anticlinorium. Abundant felsic and mafic magmas were intruded into shear-induced dilational sites during the shear process at about 1750-1730 Ma to form the gneissic Wonga Granite. Coeval magmatic bodies such as the Burstall and Mount Godkin Granites, the Lunch Creek Gabbro, and various sill-like mafic bodies were introduced into brittle dilation sites in the upper slab, and remained essentially undeformed until the D^K_2 folding at about 1550 Ma. (This folding was associated with a regional crustal contraction that elsewhere, and higher in the crust, began with thrusting probably around 1620 Ma). We interpret this geometry as being a mid-crustal (8-10 km) subhorizontal detachment surface formed during north-south crustal extension. Massive metasomatism accompanied the high thermal gradients associated with this shear zone and was a key factor in the primary transport and deposition of U-REE and other metals.

---

1 Department of Earth Sciences, University of Queensland, Qld, 4072.

[2] Present address: Carpentaria Exploration Pty Ltd, Star Gully Office, Mount Isa, Qld, 4825.

[3] Department of Earth Sciences, Monash University, Clayton, Vic, 3168.

Introduction

The Mary Kathleen Fold Belt is the zone of multiply-deformed Middle Proterozoic rocks that forms the central part of the Eastern Succession in the Mount Isa Inlier. It is centred on a major anticlinorium exposing in its core strongly deformed high-grade polymetamorphic rocks including sheared metagranite and amphibolite intrusives. These very strongly foliated rocks are flanked (overlain) by more variably deformed somewhat lower grade rocks intruded by mafic and felsic meta-igneous rocks, including relatively undeformed granite of the same age as the sheared gneissic granite (Fig. 1).

In a series of abstracts and papers (Holcombe & others, 1987; Pearson & others, 1987; Oliver & others, 1987; Pearson & others, 1990; Oliver & others, 1990a, b; Oliver & others, 1991; Holcombe & others, 1991), we outline our interpretation of the structural, metamorphic, and tectonic evolution of the Mary Kathleen Fold Belt. We suggest that the earliest pervasive deformation fabrics originated at a mid-crustal extensional detachment zone formed at about 1750-1730 Ma, and that this zone was subsequently folded in the Inlier-wide crustal shortening event at about 1550-1500 Ma. The subhorizontal detachment separates a lower plate of high grade strongly sheared rocks from an upper plate of lower grade more brittle rocks (Fig. 2). The detachment was a zone of very high heat flow and major metasomatic activity which was the likely precursor to copper, gold, and uranium-REE mineralisation localised during the later deformation.

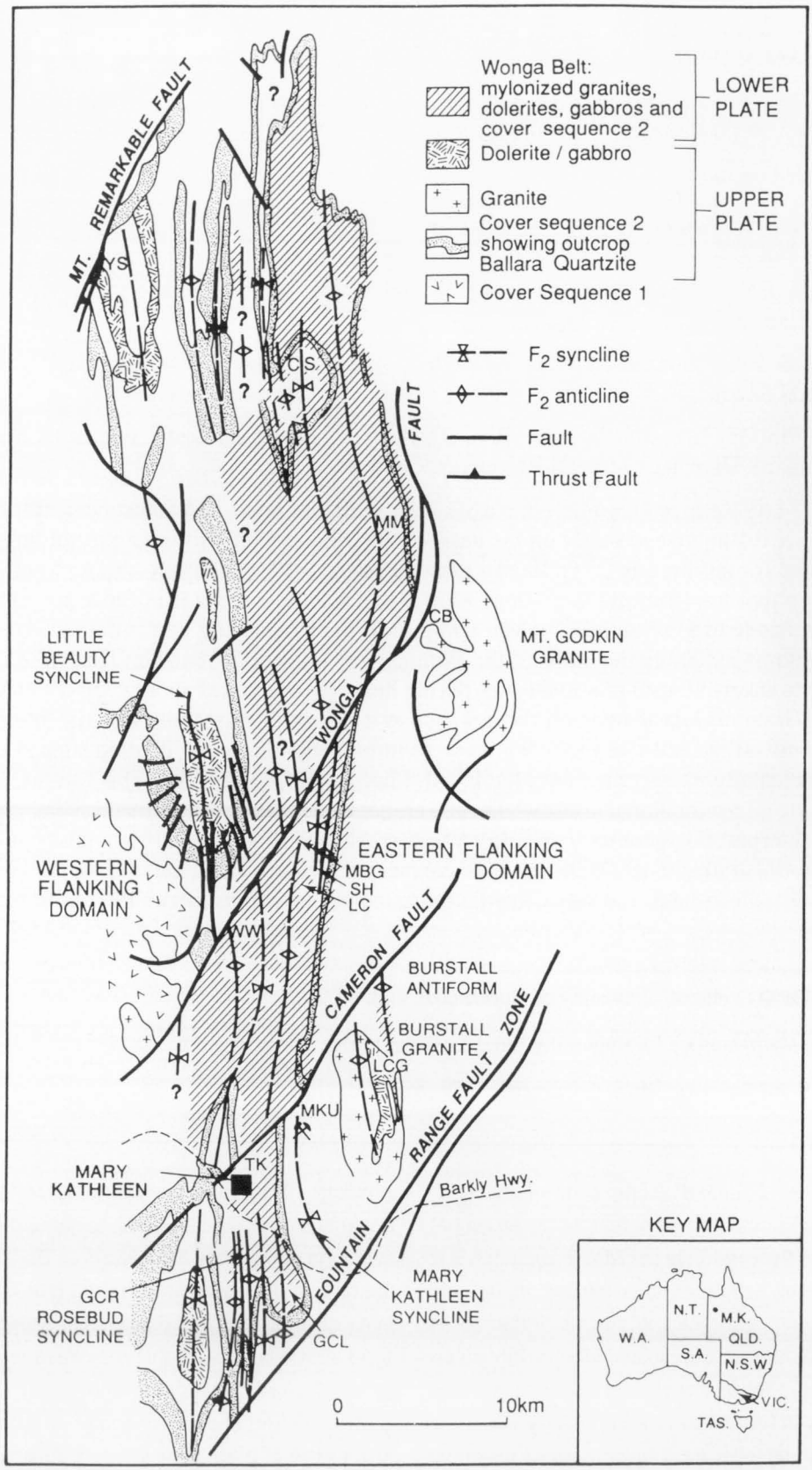


Fig. 1. General geology of the Mary Kathleen Fold Belt showing major structural elements and localities mentioned in the text. BG: Burstall Granite; CB: Copper Blonde mine; CS: 'Circular Structure'; GCL: Greens Creek, Lake Corella; GCR: Greens Creek, Rosebud; JS: Jubilee Springs; LBS: Little Beauty Syncline; LC: Lime Creek; LCG: Lunch Creek Gabbro; MBC: Middle Breakfast Creek; MGG: Mount Godkin Granite; MKS: Mary Kathleen Syncline; MKU: Mary Kathleen U-REE mine (abandoned); MM: Mount Maggie; RD: Rosebud Dam; RS: Rosebud Syncline; SH: 'Schist Hill'; TK: 'The Knob'; WC: Winston Churchill; WW: Wonga Waterhole; YS: Prospector 'Yamamilla' Syncline.

This paper will concentrate on the critical aspects of our interpretation of the structure, particularly the concept that the now dominantly vertical Wonga Belt foliation was originally a subhorizontal shear zone with north over south movement. The maps (Holcombe, 1991; Oliver, 1991; Pearson, 1991a, 1991b) are compilations of structural mapping by the authors (including the Ph.D. maps of Oliver, 1988, and Pearson, 1989) as well as a number of small areas mapped by University of Queensland Honours students since 1977 (Fraser, 1977; Lafferty, 1977; Maclean, 1977; Oliver, 1981; Pearson, 1982; Hamilton, 1985; Horton, 1985; Hill, 1986; Sliwa, 1986; and Jorgensen, 1986) under the supervision of R.J.Holcombe. The geological base has been the BMR Mary Kathleen, Marraba, Quamby, and Prospector 1:100 000 geological maps (Derrick & others, 1971, 1977b; Wilson & others, 1977, 1979).

Terminology

Deformation episodes in the Mary Kathleen Fold Belt are denoted by a superscript 'K'.

General geology

The Mary Kathleen Fold Belt (MKFB) is centred on the long (80+ km) narrow Wonga Belt, a zone of strongly deformed felsic metavolcanic and metasedimentary rocks intruded by gneissic Wonga Granite, metagabbro, and metadolerite (amphibolite). Pearson & others (this volume) discuss the igneous intrusive rocks in more detail.

The intense deformation that characterises the Wonga Belt is confined to the core of a doubly plunging anticlinorium (Wonga Anticline) and reappears to the east in the core of the adjacent 'Burstall Anticline'. The flanking limb areas are characterised by elongate doubly plunging synforms (Mary Kathleen Syncline, Rosebud Syncline, Little Beauty Syncline, Prospector ['Yamamilla'] Syncline) generally in much less deformed rocks with relatively coherent stratigraphic continuity. The major structural elements are thus the highly deformed 'Wonga Belt' and the less deformed 'flanking domains'. The boundary between the two types of domain is marked by a zone of very high strain.

Rocks exposed in the MKFB are dominantly those of cover Sequence 2 (Magna Lynn Metabasalt, Argylla Formation, Ballara Quartzite, and Corella Formation) of Blake (1987). Basement rocks (Leichhardt Volcanics) and the Magna Lynn Metabasalt are definitively recognised only to the west of the western flanking synforms. Within the Wonga Belt, primary lithologies intruded by the metagranite and metadolerite consist of felsic metavolcanics and thinly laminated graded commonly feldspathic pelitic units that we correlate with the *Argylla Formation.* Minor quartzite lenses on the western margin we consider to be infolded *Ballara Quartzite* (Holcombe & Fraser, 1979). Polyphase folding and the high deformation intensity within the Wonga Belt precludes detailed stratigraphic correlations, but it is likely that the metasedimentary rocks are stratigraphically high in the Argylla Formation, as observed outside the Wonga Belt in the Winston Churchill mine area. It is possible that basement units could be present within the Wonga Belt, but we have found no evidence of earlier deformation fabrics that would indicate this.

The high-strain transition between the Wonga Belt and the flanking domains occurs at somewhat lower stratigraphic levels on the western margin of the Wonga Belt, than on the east. On the western margin this transition occurs several hundred metres stratigraphically below the (disconformable) Ballara Quartzite/Argylla Formation contact. On the eastern margin of the Wonga Belt the transition occurs just below the Ballara Quartzite/Corella Formation boundary and the Ballara Quartzite is highly attenuated along this margin. Farther east in the core of the adjacent 'Burstall Anticline' the high-strain transition is within the lower part of the Corella Formation, the Ballara Quartzite apparently having been excised. In the northern part of the Wonga Belt (north of Dugald River), a median fold depression (a D^K_1/D^K_2 interference fold called the 'Circular Structure') exposes the transition, again within the lower part of the Corella Formation.

Figure 3 shows stratigraphic sequences from the Little Beauty and Mary Kathleen Synclines where layer-parallel discontinuities are minimal and well understood. The area proposed by Derrick & others (1977a) as a reference section for the Corella Formation across the eastern flanking domain is particularly difficult to interpret stratigraphically. In this section the Corella Formation/ Ballara Quartzite boundary is a high strain shear zone; the Lime Creek Metabasalt member is completely fault bounded (and unknown in any other section); and the internal structure of all calc-silicate units is dominated by pervasive isoclinal folding, bedding transposition, and multiple (D^K_1, D^K_2, and D^K_3) fold interference (Hill, 1986). The *Corella Formation* essentially comprises a lower pelite-dominated sequence, a thick calc-silicate-rich sequence in the middle, and quartzite- and conglomerate-bearing sequences near the top of the known

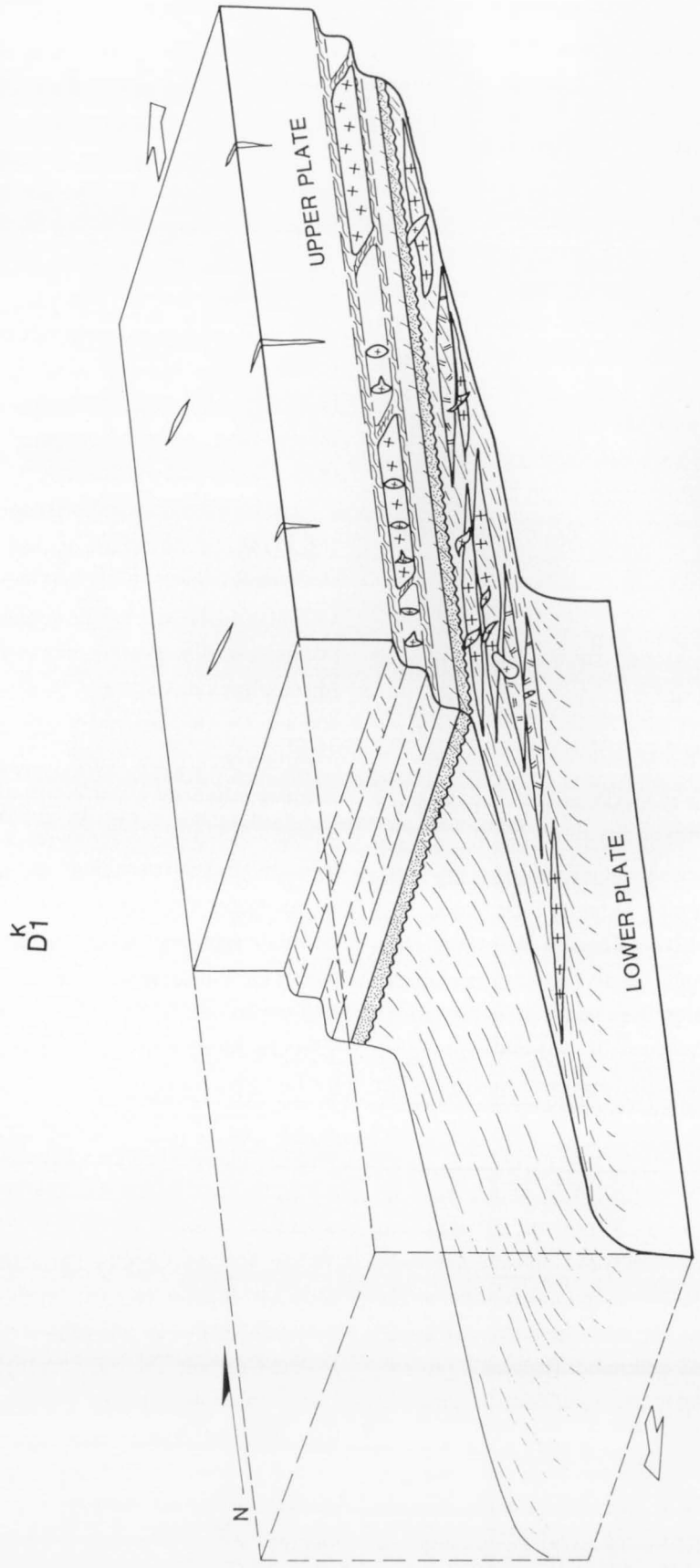
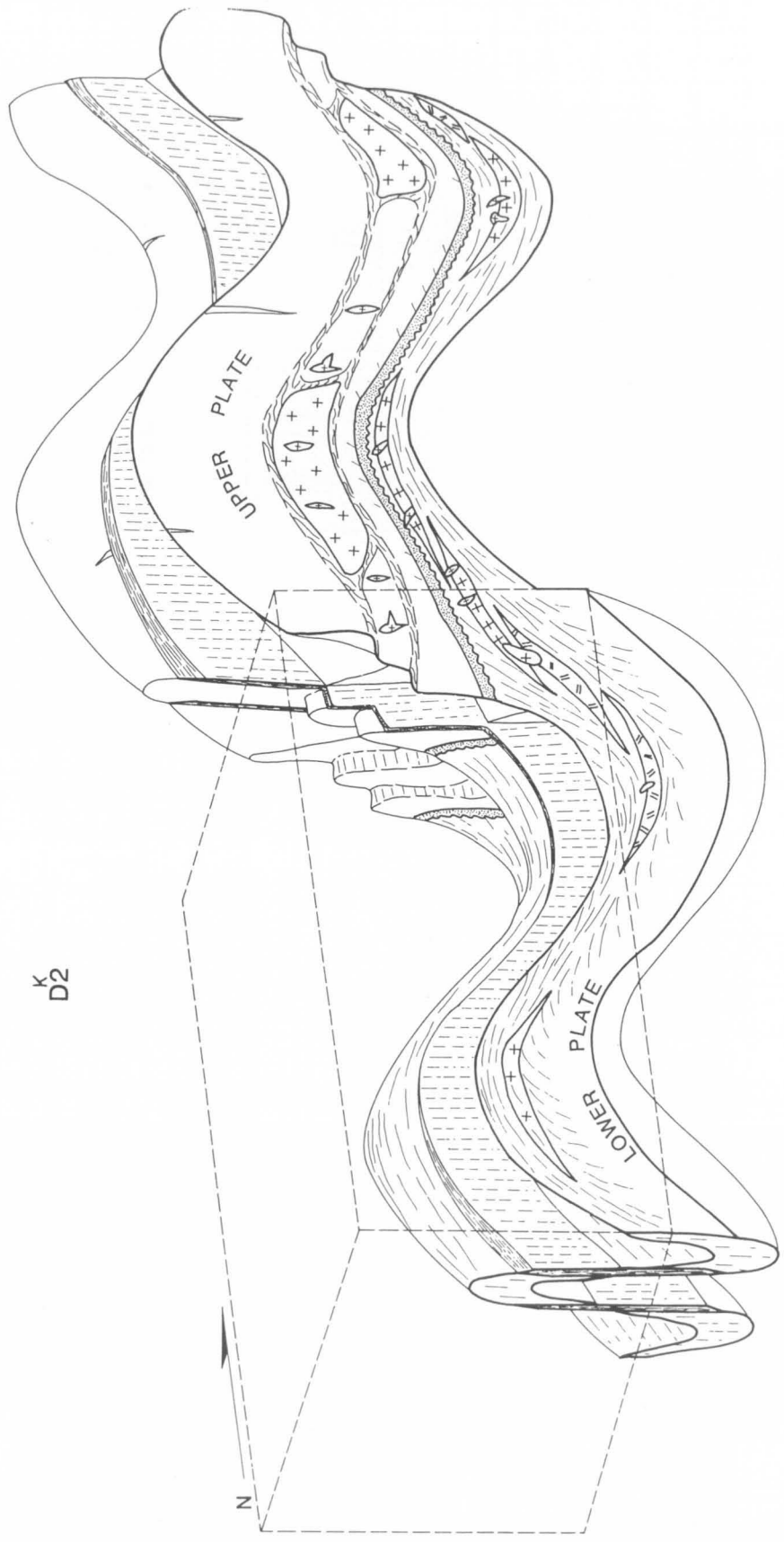


Fig. 2. Schematic model of the structural evolution of the Mary Kathleen Fold Belt during D^K_1 extension and D^K_2 folding. The Wonga Belt is modelled as a broad subhorizontal high-strain shear zone, mainly below the Ballara Quartzite (stippled). Sill-like mafic (= pattern) and felsic (+ pattern) intrusives occur in both the shear zone and the more brittly deforming upper plate.



Those within the shear zone are syntectonically deformed to gneissic metagranite; those in the upper plate remain internally undeformed. Extensional gashes (shown schematically at the upper surface) abound throughout the calc-silicate units in the upper plate.

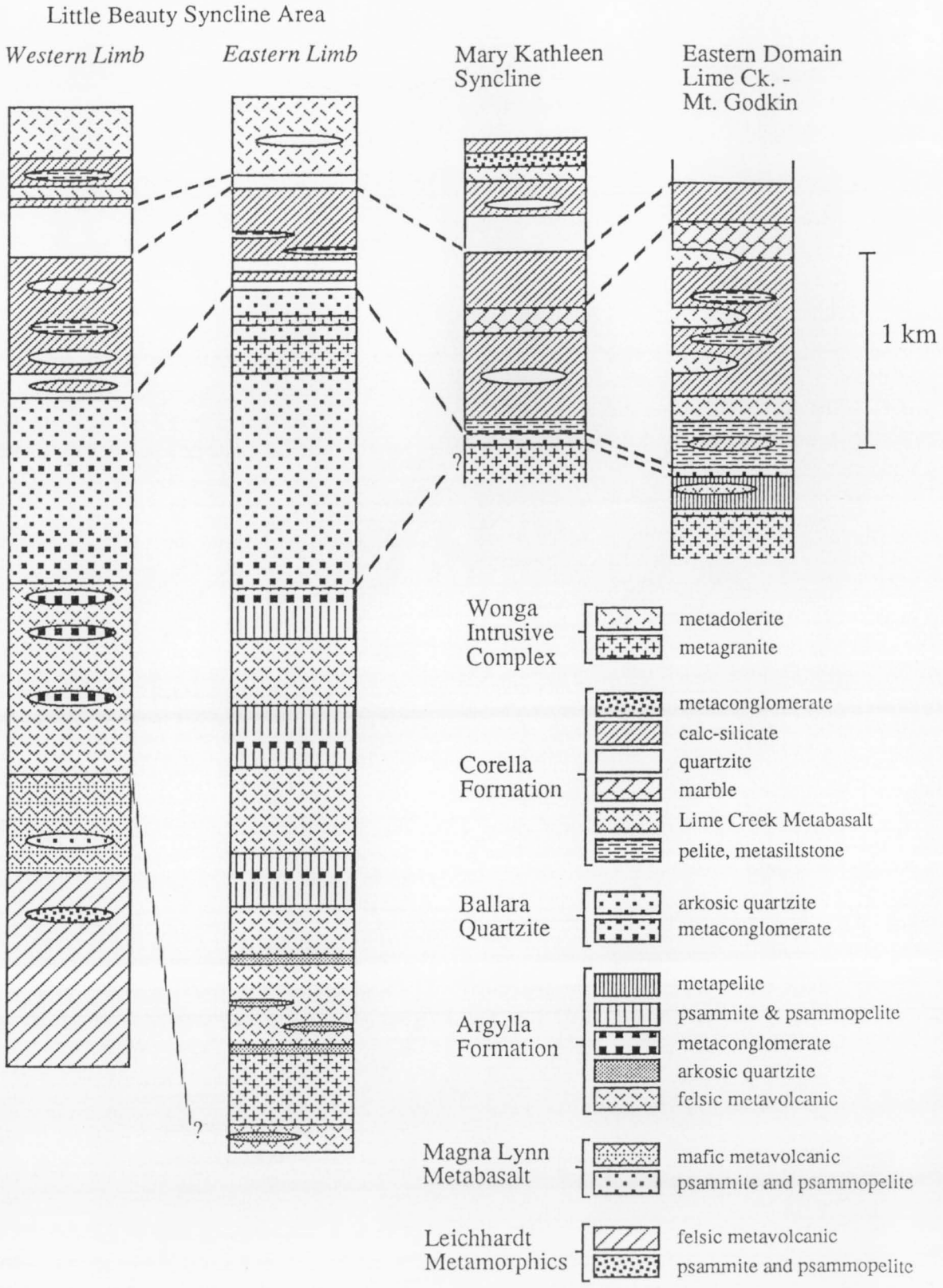


Fig. 3. Schematic stratigraphy of the the flanking 'domains' and correlations across the Wonga Belt between the Little Beauty and Mary Kathleen Synclines.

exposures, as suggested by Derrick & others (1977a, b). The lower parts of this stratigraphy can be recognised in both the eastern and western flanking domains, but the upper quartzite-rich sequences are confined to the core of the Mary Kathleen Syncline and around the Mount Godkin Granite.

Each of the major synforms in the western flanking domain commonly contains a large metadolerite sill within the Corella Formation. The intrusive nature of these is particularly well demonstrated by the locally discordant lower boundary of the metadolerite body in the Little Beauty Syncline.

The eastern flanking domain is characterised by the occurrence of relatively undeformed thick granitic sills (*Burstall* and *Mount Godkin granites*) and associated thick calc-silicate aureoles. The sill-like shape of the Burstall Granite in particular is well constrained. It is approximately 1 km thick, with the *Lunch Creek Gabbro* (showing mixed magma structures with the granite) at its base, the whole being roughly concordant with mapped stratigraphic units. A felsic dyke network (commonly with endoskarn alteration) intrudes the overlying calc-silicates from the upper surface of the sill (see cross-section in Holcombe, 1991).

The upper plate granites, together with their contact aureoles, appear to have behaved as mechanically resistant bodies during the folding event. The eastern flanking domain shows more variability of structural style than the western domain, probably as a result of geometrical heterogeneities (introduced by the granite bodies) which controlled the size and position of the major folds and faults.

The area is characterised by regional meridional upright folds including the Wonga anticlinorium and the various flanking synclines described above. This deformation is an Inlier-wide crustal shortening event that can be correlated with various 1550-1500 Ma isotopic dates (including part of the skarn mineralisation in the Mary Kathleen Syncline (Page, 1983), and that may have been preceded by thrust-dominated deformation perhaps as early as 1620 Ma (Bell, 1983; Loosveld & Schreurs, 1987; Loosveld, 1989). Throughout the Mary Kathleen Fold Belt, there is evidence of deformation that predated the major folding. This earliest deformation is defined for this area as D^K_1. The upright folding event is D^K_2, and later kink-dominated folding and conjugate strike-slip faulting is defined as D^K_3 (Table 1). (Note that the earliest deformation fabrics occurring in the MKFB, and defined for this area as D^K_1, do *not* appear to be related to the regional thrusting event which is commonly defined as D_1 in those areas where it occurs).

Wonga Belt

General features

The characteristic fabric of the Wonga Belt is a subvertical foliation parallel to compositional layering. Amphibolite and gneissic metagranitic intrusive bodies dominate, and these are intrusive into felsic metavolcanic and metasedimentary schist.

We infer that centimetre- to metre-scale compositional banding in the Wonga Granite is a combination of the following: extreme flattening of original compositional heterogeneities (xenoliths or different phases); textural and compositional changes associated with strongly heterogeneous shearing and mylonitisation; segregation of partly solidified melt by shear-enhanced 'filter pressing'; and transposition of the all these types of layering and earlier mylonitic foliations into the foliation orientation. Asymmetric shear fabrics, mylonitic zones, and refolded mylonitic zones are common, particularly in the central part of the Belt.

The margins of the Wonga Belt are more highly deformed than the central part. This is particularly noticeable along the eastern margin where there is a zone of very high strain several hundred metres wide. Relative to the core of the Wonga Belt the foliation in the marginal zones is very strong, the parallel compositional bands are narrower, planar, and more elongate, and planar mylonitic fabrics are more common.

Structural fabrics

Two sets of structures contribute almost equally to the Wonga Belt fabrics – early shear-dominated fabrics (D^K_1), and later fold and axial plane foliation fabrics (D^K_2). Fabric definitions and orientations are given in Table 1 and Figure 4.

The subvertical foliation is axial planar to mesoscopic upright D^K_2 folds (Fig. 5) associated with the regionally observed crustal shortening deformation. A down-dip mineral streaking lineation, generally defined by biotite and amphibole, is the stretching lineation associated with this folding, and both the axial plane foliation and the stretching lineation are remarkably constant in orientation throughout the whole of the Mary Kathleen Fold Belt (Fig. 4). Despite the very constant orientation of the imposed D^K_2 fabric elements, D^K_2 fold axes and the associated L_{21} intersection lineation vary considerably about the horizontal (Fig. 6), particularly in areas of high D^K_2 strain.

TABLE 1

Mary Kathleen Fold Belt FABRIC DEFINITIONS used in this study

D_1^K - the earliest recognizable generation of metamorphic fabrics in the MKFB;

- the earliest crustal deformation event affecting cover sequence two rocks (1750-1730Ma).

Imposed D_1^K fabrics

S_1 - the earliest metamorphic foliation observed in the MKFB. In areas of low D_1^K strain the S_1 fabric decomposes into anastomosing shears with variably developed s- and c- components. That is the fabric consists of either, or both, a shape fabric reflecting the local finite strain (s-surface) and surfaces of higher shear strain or discrete slip (c-surfaces).

L_1 - D_1 stretching lineation.

D_2^K - a generation of structures and fabrics associated with inlier-wide upright folds overprinting D_1^K structures; also includes related ductile shears and faults sharing the same subvertical maximum stretch.

- a crustal shortening event dated between 1620-1550Ma.
(Elsewhere thrust-related structures have been reported as forming the earliest generation of structures associated with this orogenic event. These have locally been referred to as D_1 (eg. Page and Bell, 1986) in those areas).

Imposed D_2^K fabrics

S_2 - D_2^K foliation; axial plane to D_2^K folds.

L_2 - D_2^K stretching lineation.

Composite D_2 fabrics

L_{20} - intersection lineation between S_2 and primary layering (S_0), and related fold axes.

L_{21} - intersection lineation between S_2 and S_1, and related fold axes.

D_3^K - a generation of brittle-ductile structures (conjugate kinks, faults) overprinting D_2 structures.

- fault-dominated crustal contraction (or perhaps shear) most likely associated with 1550-1500Ma isotopic dates. ("D_3^K" may simply represent the last generation of structures associated with the D_2^K crustal contraction.

The notation D_1, D_2, and D_3 to denote deformation events should be reserved for discrete major crustal events (orogenic events) each of which may have produced one or more generations of structures (defined on the basis of geometry). However the "D" notation is entrenched in Mount Isa Inlier literature to refer both to major crustal events and to the most prominent generation of structures associated with each event (commonly denoted by an "F" notation). To be consistent we have continued with this parochial use of the "D" notation in this paper.

TABLE 1. MARY KATHLEEN FOLD BELT FABRIC DEFINITIONS USED IN THIS STUDY.

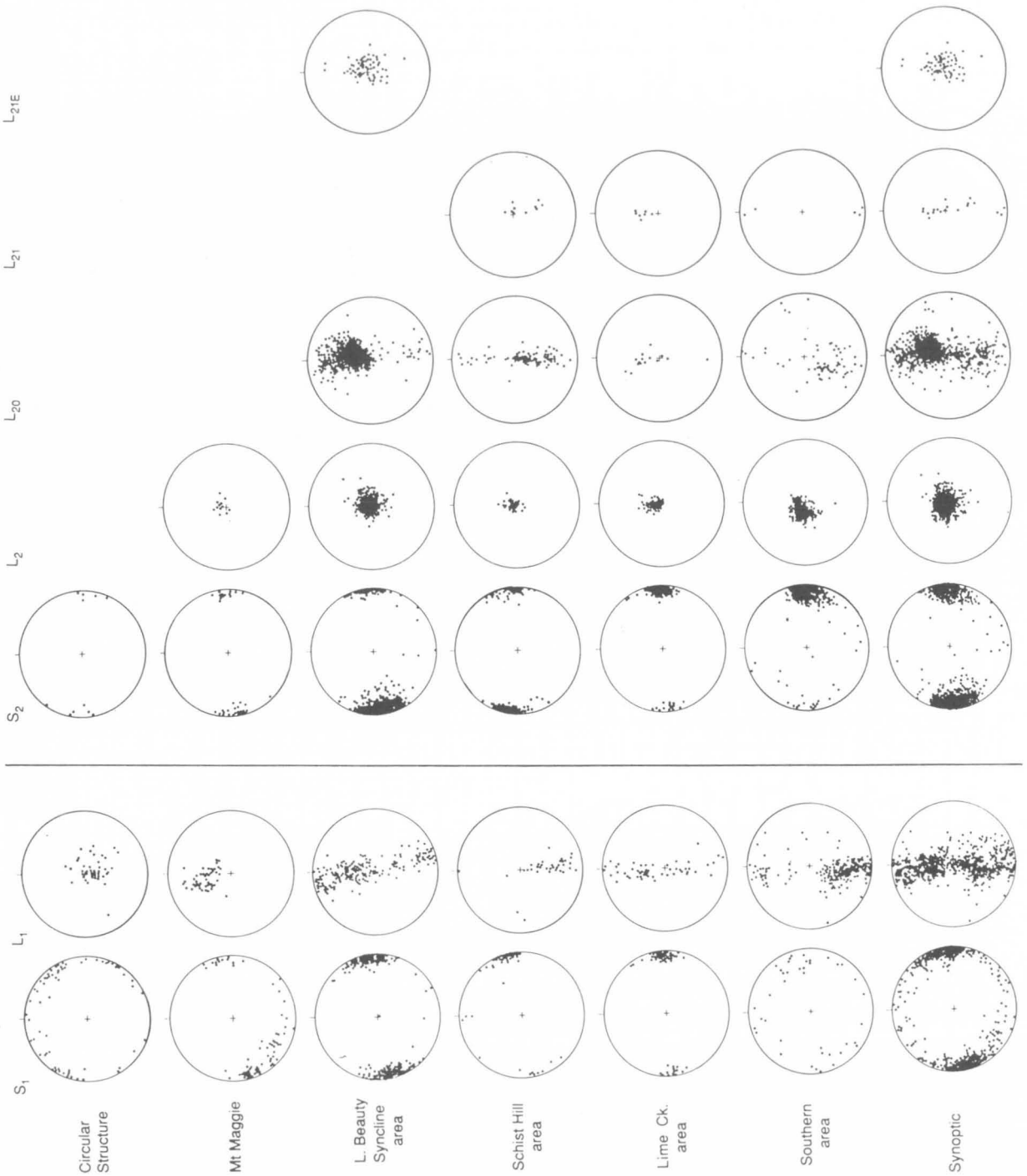


Fig. 4. Orientation distribution of D^K_1 and D^K_2 structural fabric elements in the Wonga Belt and environs. S_1 and L_1 are the early shear foliation and stretching lineation; S_2 and L_2 are the upright folding axial plane foliation and down-dip extension lineation; L_{21} is the intersection lineation parallel to D^K_2 fold axes in S_1; and L_{21E} is theold axis produced in early D^K_1 extensional veins by D^K_2 folding.

Although the initial fold axis variation can be attributed to D^K_1/D^K_2 overprinting geometry, the extreme nature of the L_{21} orientation dispersion is consistent with rotation of the axes towards the down-dip mineral extension lineation during the D^K_2 deformation. Locally, as in the area of very high D^K_2 strain around 'Schist Hill' (see Appendix), these doubly plunging folds approach sheath-like geometry around this prominent D^K_2 extension lineation. Rotation during high strain has been tested by comparing observed orientation distributions with theoretical distributions



Fig. 5. D^{K}_{2} fold in compositionally layered Wonga metagranite. Remnants of the D^{K}_{1} grain fabric can be traced parallel to layering around the fold. The pen is 15 cm long.



Fig. 6. Curved L_{21} intersection lineations on S_2 foliation surfaces in metapelite in the Lime Creek area. These lineations are parallel to D^{K}_{2} folds, and the axial plane foliation is quite planar. The pen is 15 cm long.

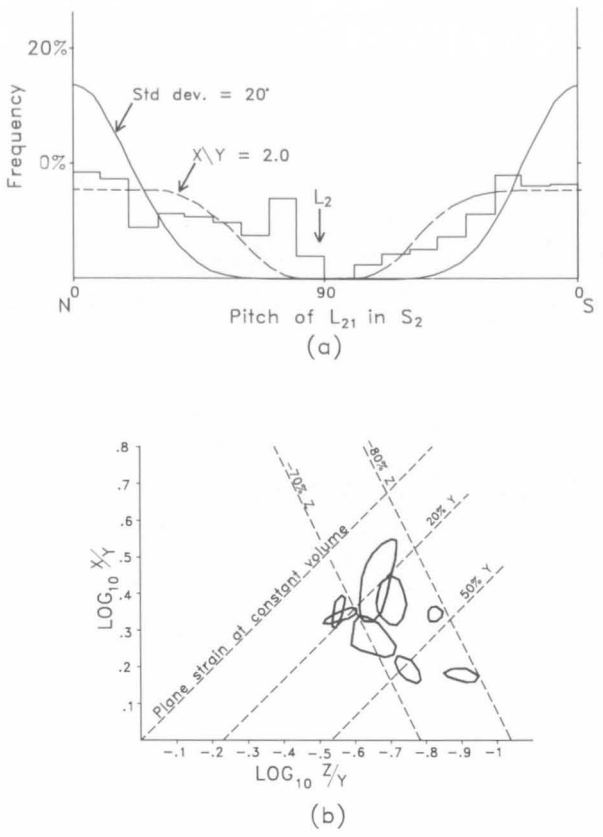


Fig. 7. (a) Orientation distribution of 360 L_{21} lineations in the southern part of the Wonga Belt (histogram); and curves (after Sanderson, 1973) showing the effect of passive rotation of lineation orientations due to deformation. The dashed curve shows the redistribution of an initial orientation distribution (solid line) after deformation (X/Y finite strain ratio of 2.0). The initial distribution, one of several similar solutions, has a standard deviation of 20° and a mean at 90° to the stretching lineation L_2. (b) Finite strain data from deformed metagranite at eight locations in the southern part of the Wonga Belt (south of the Wonga Fault). The strain analysis technique used (Talbot, 1970) is based on defining the surfaces of no finite longitudinal strain using thin folded and boudinaged pegmatite and quartzo- feldspathic veins as markers, and averages strain over large areas of outcrop. Strain orientation is determined independently of the fabric, and the maximum extension is consistently subvertical, indicating that the measured strain is dominantly D^K_2. This is consistent with the vein markers being late syn- to post-D^K_1. Location and orientation details are given in Holcombe & others (1991).

produced by dispersion in a given finite strain field (Sanderson, 1973). Analysis of 360 D^K_2 fold axes and intersection lineations in metasedimentary and metavolcanic schists in the southern part of the Wonga Belt shows that the present orientation distribution is consistent with dispersion of an original distribution with a mean perpendicular to the stretching lineation and a standard deviation of 20-30° (Fig. 7a) in a strain regime in which X/Y=2. This X/Y ratio is consistent with the average measured D^K_2 strain in this area (Fig. 7b).

Much of the dominantly vertical Wonga Belt foliation also shows strong shear characteristics, with a highly variable but essentially subhorizontal, north-south stretching lineation (Figs. 8, 9). Locally, at both mesoscopic and map scales, the shear fabric and shear-induced layering are overprinted by the upright D^K_2 folds (Fig. 10 a-b), and thus this early shear-related fabric is defined as D^K_1 in this study. In most outcrops the rocks have a composite fabric with a single planar foliation containing both sets of extension lineations (Fig. 11). It is important when analyzing Wonga Belt fabrics to realise the composite nature of the vertical planar fabric. Fabric development is strongly heterogeneous at all scales. Mesoscopic and map-scale remnants of lesser-strained rocks outlined by high-strain zones are scattered throughout the Wonga Belt. Some are remnants of low D^K_2 strain, but most are low D^K_1 strain as indicated by grain-shape fabric and intensity of shear zone development. It is only within these remnants (such as at 'Mount Maggie' or the 'Knob' dating site – see Appendix) that the two sets of fabrics can be clearly separated.

The D^K_1 deformation is shear-dominated. Shear fabrics are common in sections or faces parallel to the subhorizontal stretching lineation. These include local shear zones and mylonites (Figs. 12, 13), S-C shear fabrics (Fig. 13), sigmoidal strain fringes and shadows (Fig. 14), shear bands, and asymmetric quartz c-axis fabrics. Within areas of low D^K_1 strain, the rocks are cut by anastomosing networks of narrow shears and mylonites, commonly in conjugate arrays at relatively high angles to one another (Fig. 15) and with multiple generations of cross-cutting shears. D^K_1 folds that formed in original layering, or in earlier mylonitic foliation in higher-strain zones, are generally parallel to the stretching lineation. Sheath folds occur locally, particularly in the marginal high-strain zones. Thus the L_1 stretching lineation is generally enhanced by the L_{10} intersection lineation – a common phenomenon in high-strain shear zones. (In the Wonga Belt, this orientation generally coincides with the S_1/S_2 intersection lineation and D_2 folds, which further enhance this linear fabric – Fig. 16).

The crux of our structural interpretation of the Mary Kathleen Fold Belt, is that the original orientation of the D^K_1 shear fabric was subhorizontal. The reasoning for this is based on:

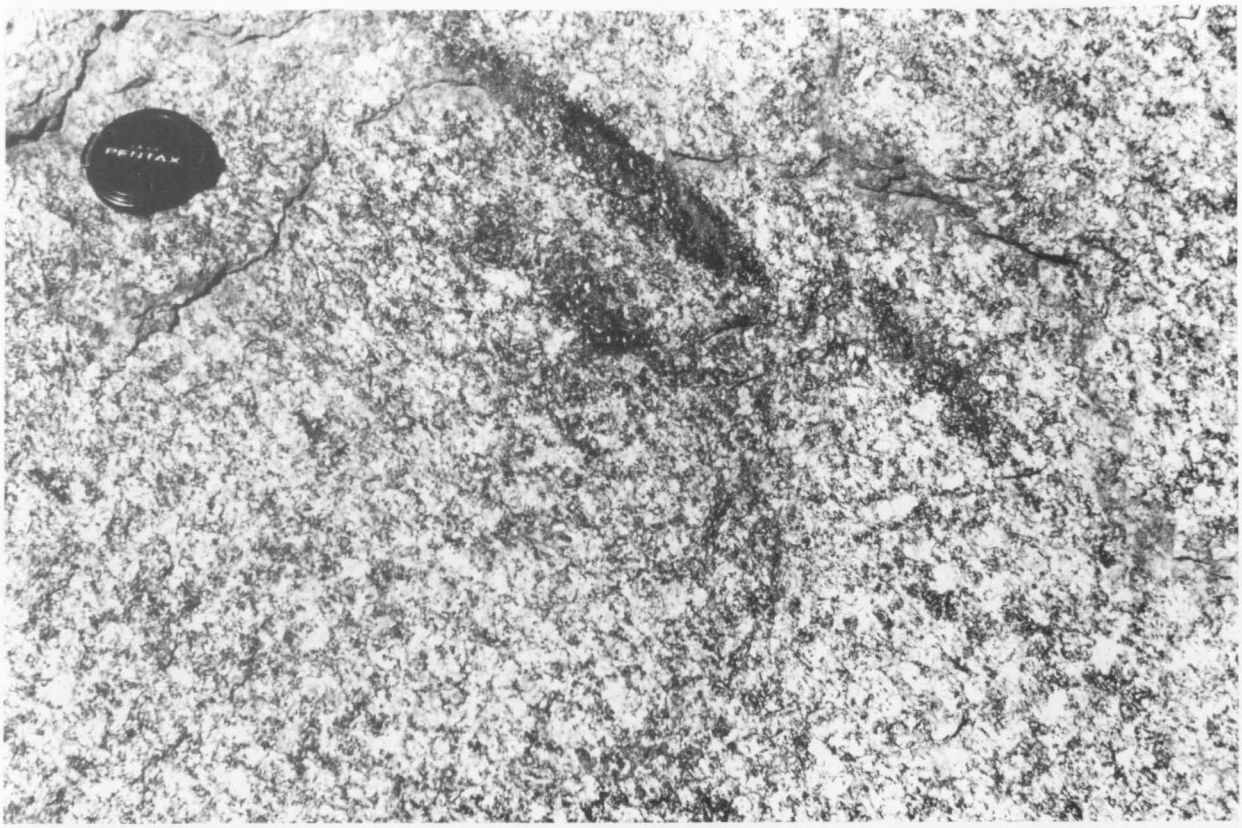


Fig. 8. Southerly-plunging L_1 extension lineation on an S_1 surface in Wonga metagranite near Greens Creek, Rosebud (see Appendix). A weak down-dip L_2 lineation (faintly observable within the mafic xenoliths) is defined by the alignment of individual biotite and amphibole grains. The lens cap is 6 cm across.

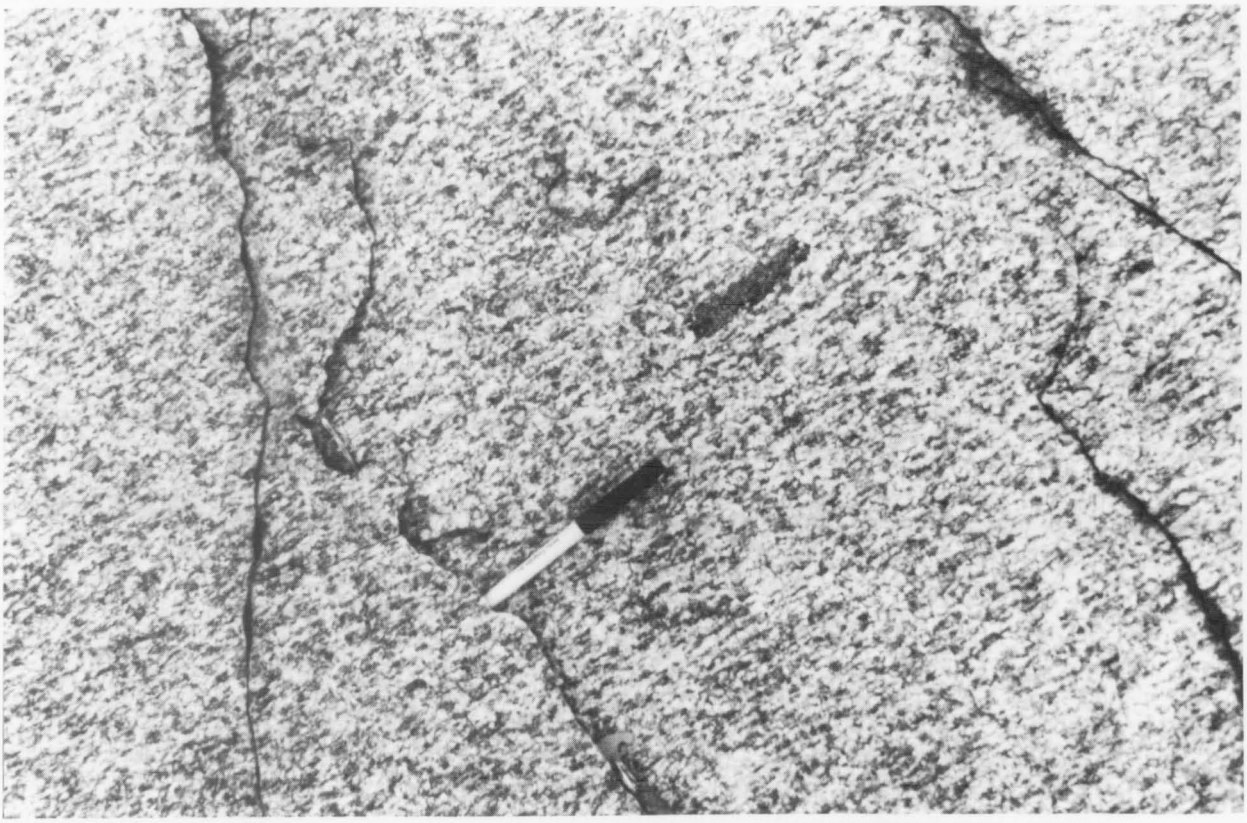


Fig. 9. Northerly-plunging L_1 extension lineation on an S_1 surface in metagranite in the core of the Burstall Antiform. Fabrics in this granite are identical to those in the main Wonga Belt. The pen is 15 cm long.

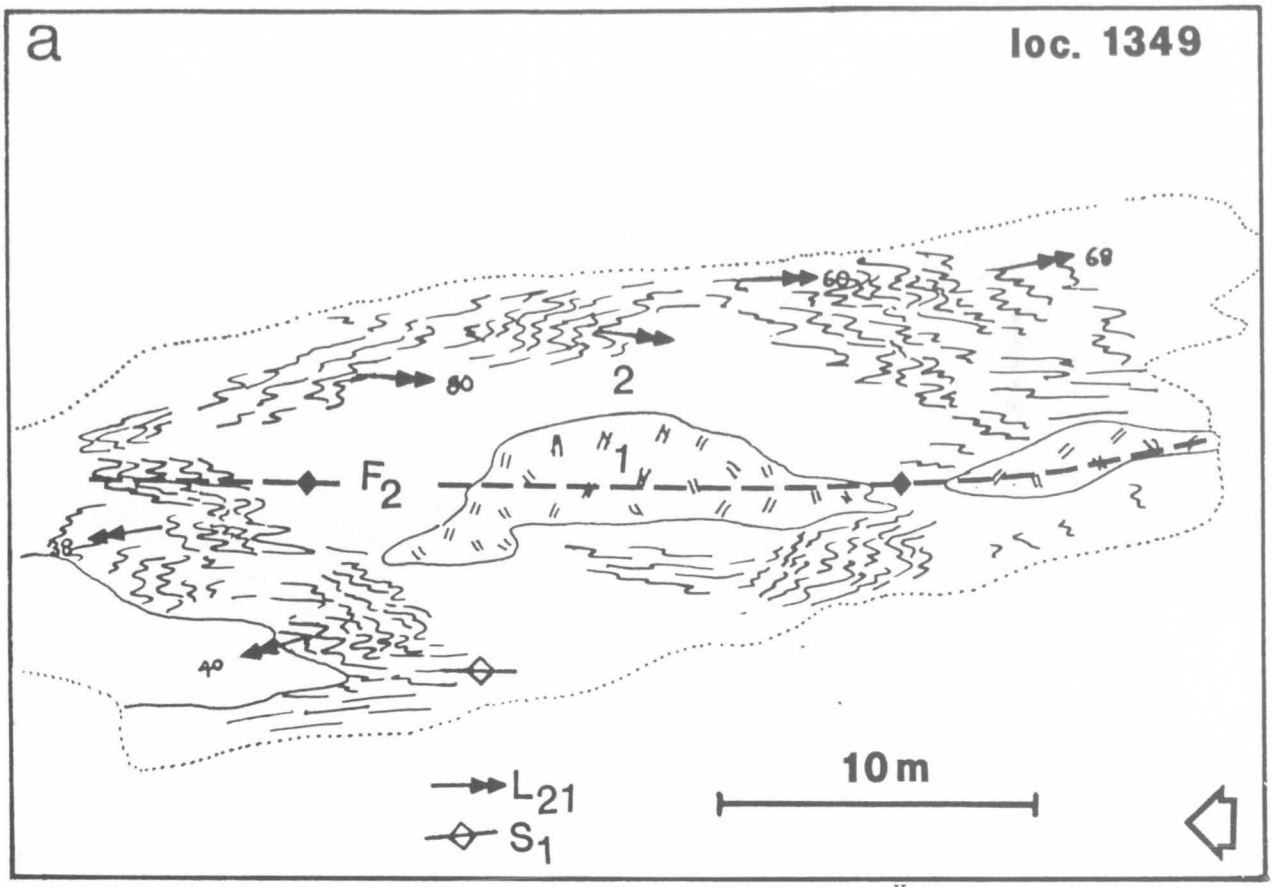
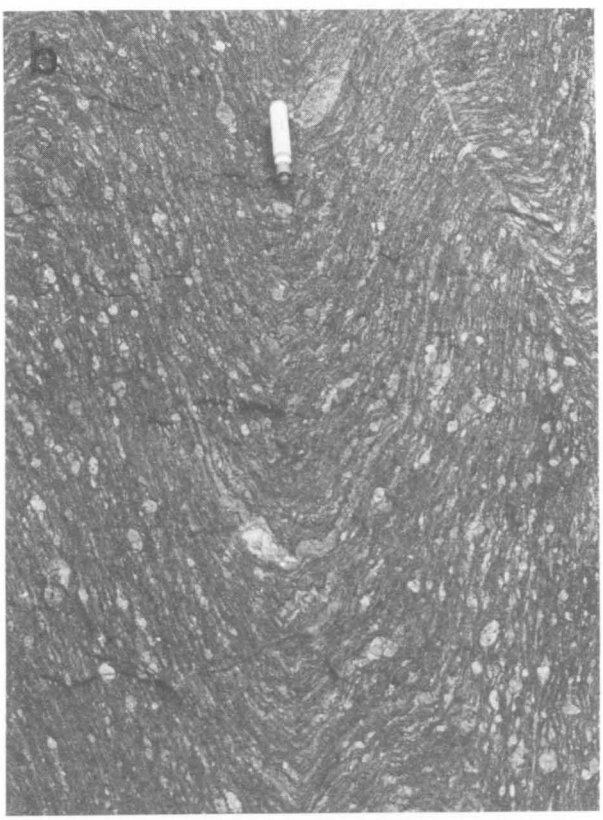


Fig. 10. S_1 foliation in Wonga blastoporphyritic metagranite overprinted by D^K_2 folds in the Middle Breakfast Creek area (see Appendix). (a) Outcrop map showing metadolerite (1) surrounded by metagranite (2) in the core of a doubly plunging D^K_2 antiform. (b) (below) Photograph of the folded D^K_1 fabric in hinge areas of D^K_2 folds. The pen in (b) is 15 cm long.

(1) Local and map-scale observations that the foliation was parallel to stratigraphic layering. In the southern closure of the Wonga Belt the early foliation is present in the bounding Ballara Quartzite, and can be mapped around part of the large D^K_2 closure. Early tight D^K_1 folds in Corella Formation calc-silicates with axial surfaces parallel to mapped stratigraphic boundaries are also common in this area.* In a large open D^K_2 hinge area in the 'Circular Structure' in the northern part of the belt, the early fabric is preserved in thin granitic sills, and is parallel to bedding and to a bedding-parallel foliation in the bounding Corella Formation metasediment.

*Blake (personal communication) has reported that an 'angular unconformity' exists below the Ballara Quartzite in this southern closure area. The persistence of identical structural elements on both sides of this boundary including layer-parallel D^K_1 fabrics suggests that the reported discordance is purely tectonic. Furthermore, since there is no angular discordance in D^K_2 fold axis orientations across this boundary, there are no grounds to suggest a pre-D^K_2 discordance (see discussion in Holcombe & Fraser, 1979).



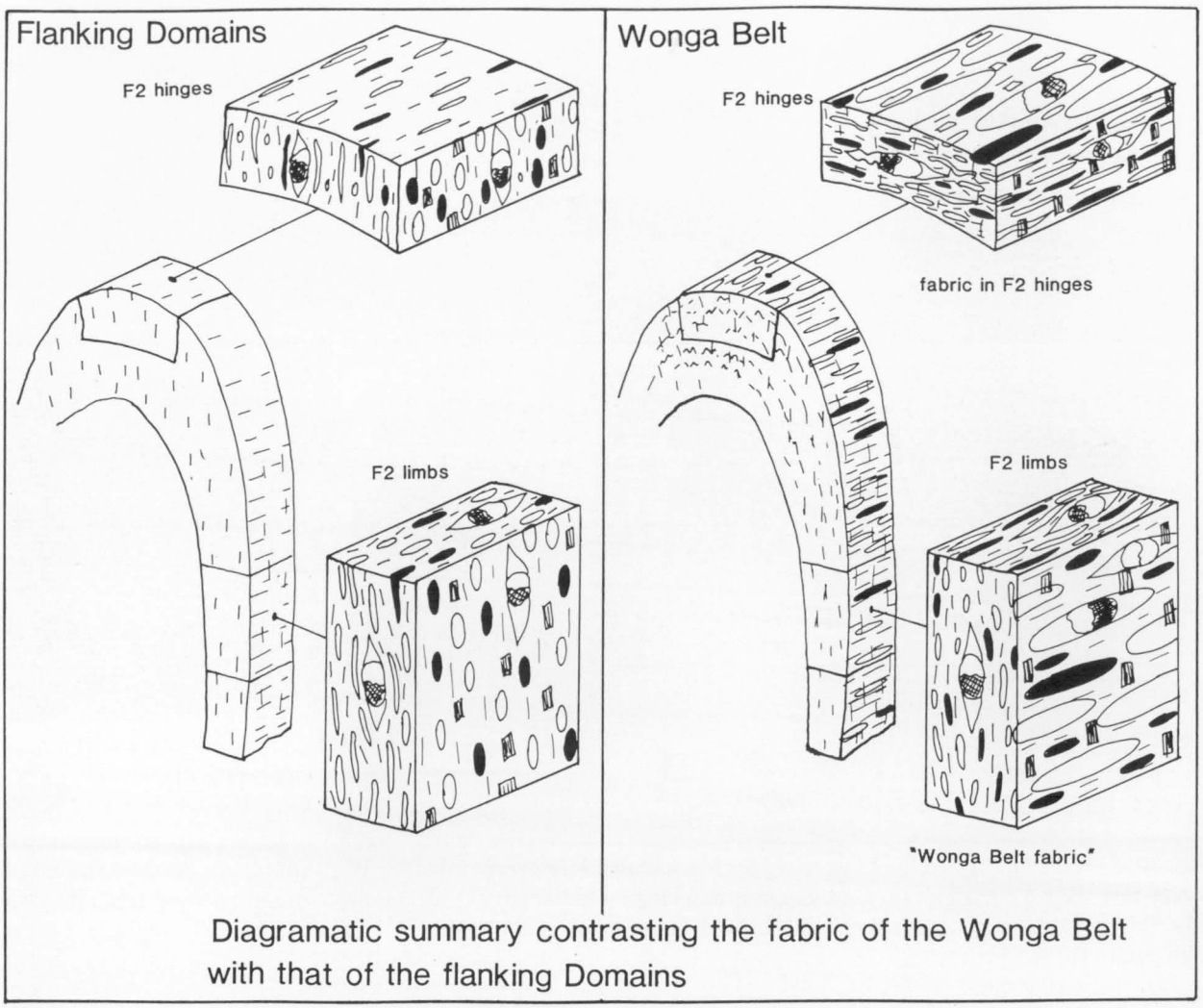


Fig. 11. Diagram showing the relationship between D^K_1 and D2 fabric elements in the Wonga Belt and flanking domains. Note the formation of a composite fabric on limb areas in the Wonga Belt in which a single foliation contains two stretching lineations.

(2) The observed abundance of D_2 folds in metagranite in the early fabric, in original compositional banding, and in the boundaries between phases. Thus the early metagranite fabric, layering, and phase boundaries were oriented at a high angle to the subvertical D^K_2 axial plane (within the shortening field of finite strain). Such an abundance of folds at all scales is not consistent with the early fabric and layering being subvertical. A good example of this occurs in the Cameron River near the Wonga Waterhole dating site (see Pearson & others, this volume), where large-scale granitic layering and the D^K_1 fabric are folded and have a subhorizontal enveloping surface.

(3) The orientation distribution of the S_1/S_2 intersection lineation. The pervasive S_1/S_2 intersection lineation is strongly doubly plunging throughout the Wonga Belt, but essentially the plunge variation is consistent with rotation of an originally *subhorizontal* lineation towards the vertical D^K_2 stretching lineation. Even in metagranitic rocks this lineation is parallel to D^K_2 fold axes in immediately adjacent metasediments irrespective of the actual orientation of the lineation. Hence the granite foliation fabric was either parallel to the layering in the adjacent metasediment, or it shared at least the same horizontal north-south strike as adjacent metasedimentary bedding orientations prior to the D^K_2 folding. This latter option is most unrealistic given that the early fabric appears in both metasedimentary and meta-igneous rocks, and that it is difficult to envisage any deformation process that would produce differently oriented fabrics of such intensity in intermingled rocks, given the locally observed parallelism. Local orientations of this intersection lineation are also parallel to known large-scale folds in bedding. For example, this lineation throughout the southern closure area of the Wonga Anticlinorium, including the metagranitic rocks, plunges

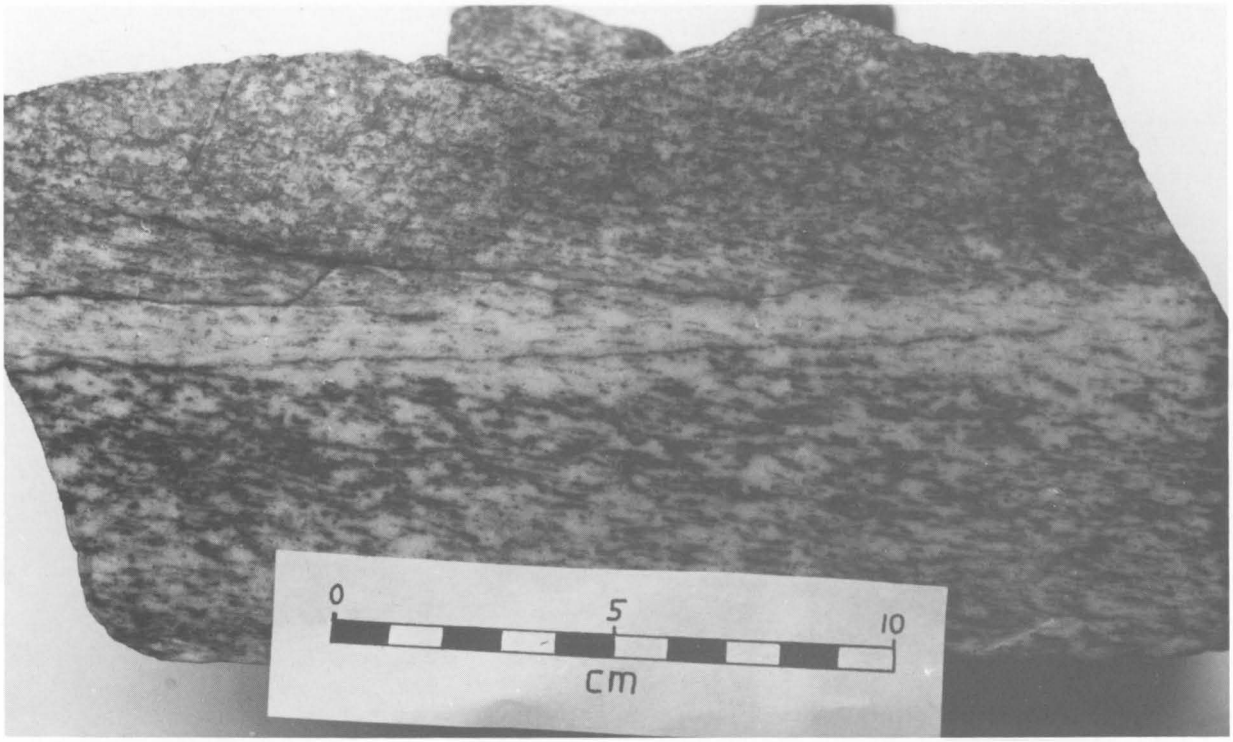


Fig. 12. Narrow shear zone from a system of anastomosing D^{K}_{1} shears in the Greens Creek-Lake Corella area. The shears in this area show constant shear sense and are foci for intense albitic metasomatic alteration. The pen is 15 cm long.

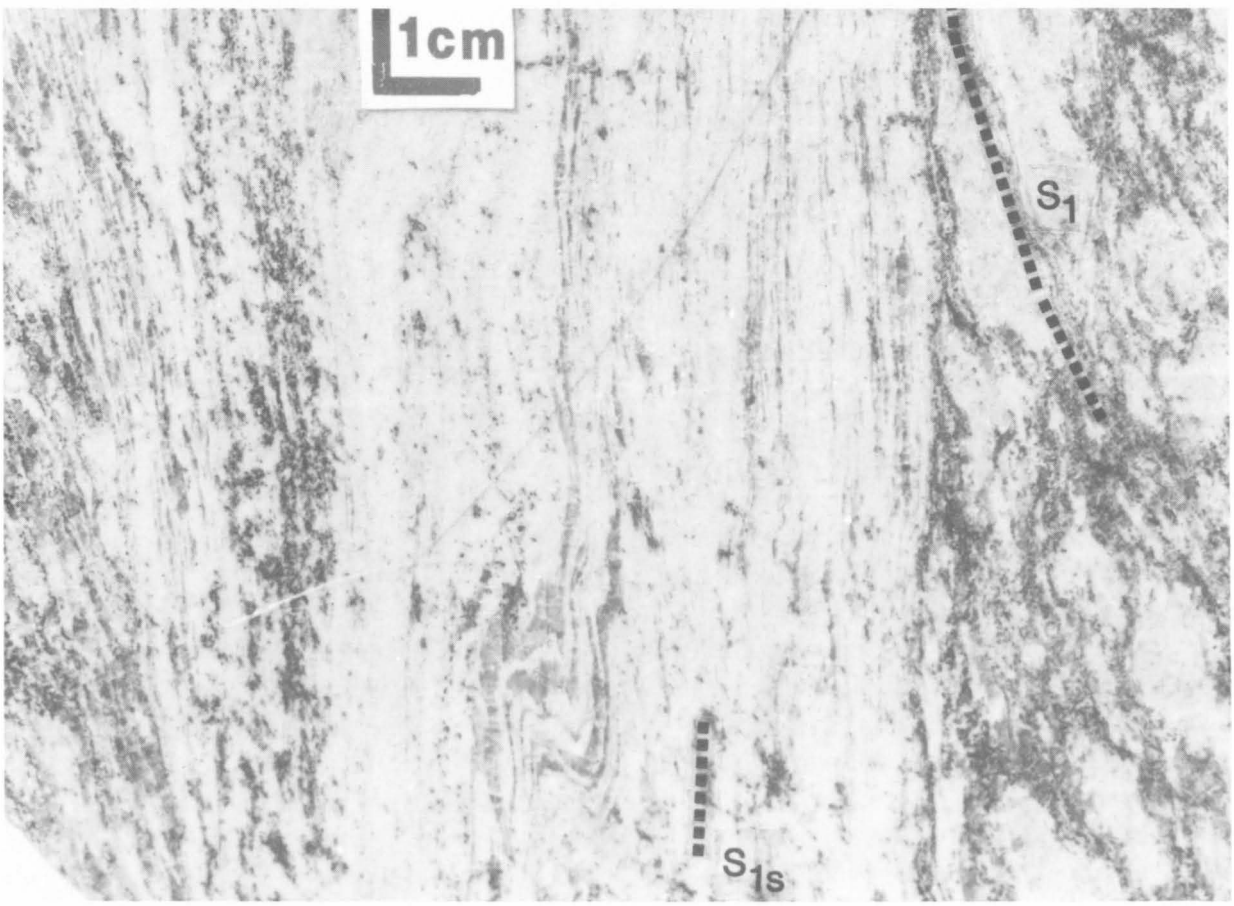


Fig. 13. Mylonite fabric (S_{1s}) in a D^{K}_{1} shear in coarse blastoporphyritic metagranite in the Mount Maggie area (see Appendix). The fold in the ribbon quartz lenticles may be either a refolding of the mylonitic fabric during D^{K}_{1}, or a later D^{K}_{2} fold. Note the strong albitic alteration confined to the shear zone itself.

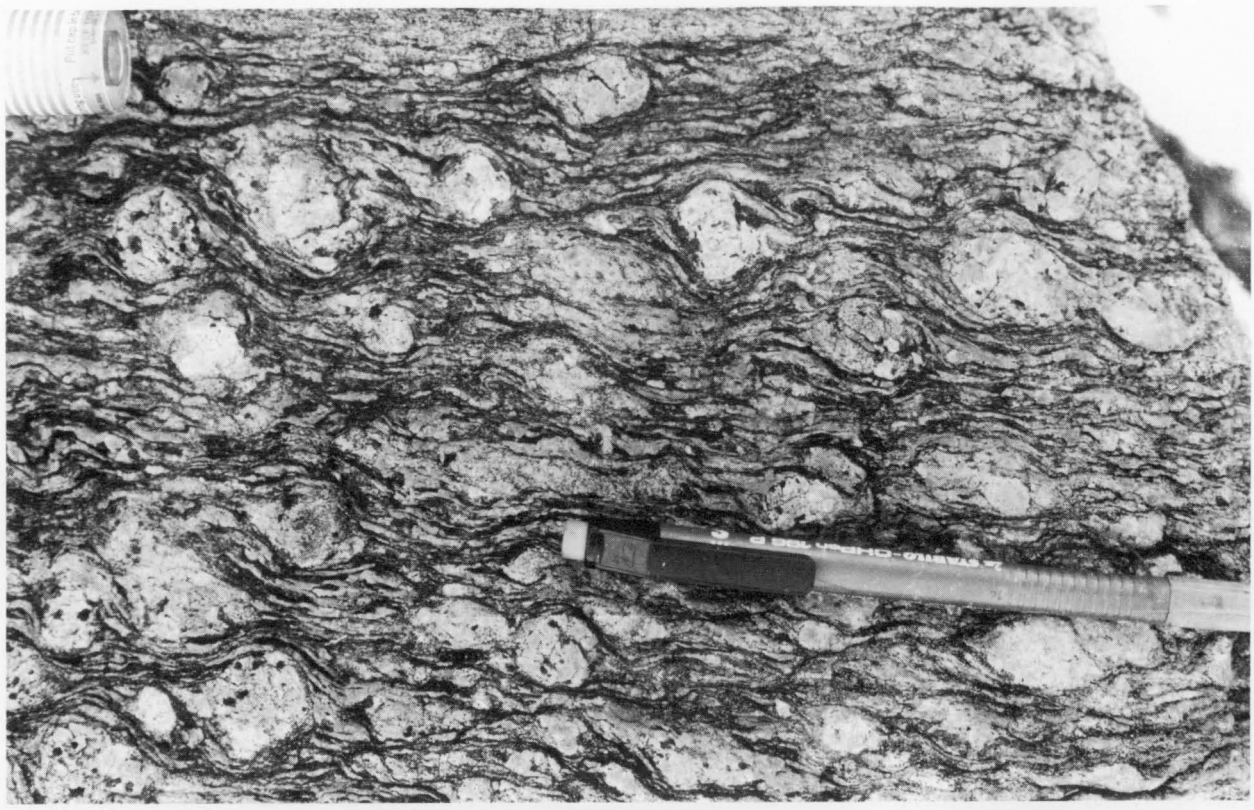


Fig. 14. Delta-type asymmetric augen shear structures in coarse blastoporphyritic metagranite from the Mount Maggie area. Sense of shear is sinistral. The pen is 15 cm long.

about 30° south – the southern plunge of the antiform. Thus the early fabrics in both metasedimentary and metagranitic rocks were most likely parallel, and this locally observed parallelism was pervasive throughout the Wonga Belt.

(4) The folding of the Wonga Belt strain transition boundary and the reappearance of Wonga Belt fabrics in the core of the next antiform to the east (the 'Burstall Anticline'). The strain transition is clearly folded around the southern closure of the Wonga Anticlinorium. Foliated metagranite with the characteristic Wonga Belt shallow stretching lineation reappears in the core of the adjacent 'Burstall Anticline' (see Fig. 9) indicating that the boundary between the Wonga Belt and the flanking domains is also essentially bedding-parallel. Taken together with the observation that the D^K_1 Wonga Belt fabric is shear-dominated, this is strong evidence that this was a major shear-related boundary, subparallel to stratigraphy, and therefore probably subhorizontal.

(5) The preservation of the early foliation consistently at a high angle to the D^K_2 foliation in the low-strain remnants throughout the area. This indicates that the common present coincidence of S_1 and S_2 was not the original relationship. Good examples of this occur in the Mount Maggie area, the 'Schist Hill' area, and the 'Knob' dating site area (see Appendix).

(6) The predominance of Ramsay (1967) Type 3 D^K_1/D^K_2 fold interference structures on both sides of the boundary with the flanking domains. The axial plane of D^K_1 folds in these interference structures is parallel to bedding (i.e., they were recumbent isoclinal structures), and the overprinting axial plane is at a high angle to the overprinted axial plane (further evidence of the high angle between the original S_1 and S_2).

(7) The reversal of apparent shear sense on opposite limbs of D^K_2 folds. The shear-sense reversals are consistent with the folding of a shear zone with a single sense of shear. Hence in order to be folded, the shear zone itself had to have been originally at a finite angle to the D^K_2 axial plane. (When unfolded to the horizontal this sense of shear is generally top-to-the-north).

(8) Bedding-parallel D^K_1 structures in the flanking domains. The Burstall Granite sill and an associated D^K_1 shear zone are roughly parallel to stratigraphic layering on one limb of the Mary Kathleen Syncline, and would have been horizontal before the D^K_2 folding (see discussion below). Thus what we see now in the Wonga Belt is the upper 1-1.5 km of a folded shear zone in which the shear intensity increased markedly in the upper few hundred metres. Although the shears were dominantly subhorizontal, it is possible that subvertical transfer faults

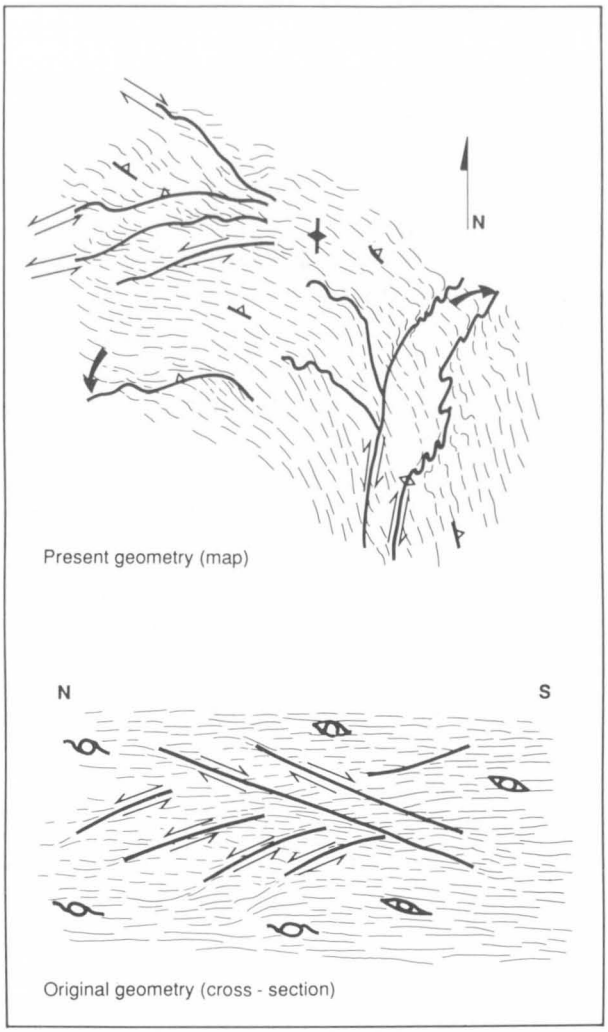


Fig. 15. Map of S_1 foliation and shear bands folded by D^K_2 in the Mount Maggie low-strain area, and their interpreted pre- folding configuration in a vertical north-south section. The shear zone shown in Figure 13 comes from one of these shear bands.

could also have existed. One candidate for such a structure would be along the western boundary of the Wonga Belt adjacent to the Little Beauty Syncline, where there is a possible reversal in shear sense. However, we stress that the Wonga Belt structures indicate not only that originally horizontal fabrics were dominant, but that the boundary was also subhorizontal and therefore the Wonga Belt as a whole cannot represent an originally *vertical* shear zone.

The L_1 stretching lineation in the Wonga Belt is in general indistinguishable in orientation from the S_1/S_2 intersection lineation and D^K_1 fold axes (Fig. 4), and it shows the same doubly plunging orientation distribution about the north-south horizontal as do D^K_2 folds. There is no evidence that the L_1 stretching lineation, and hence the D^K_1 shear movement direction, were ever oriented in any other direction except north-south. The stretching lineation does not fold over D^K_2 folds as would be

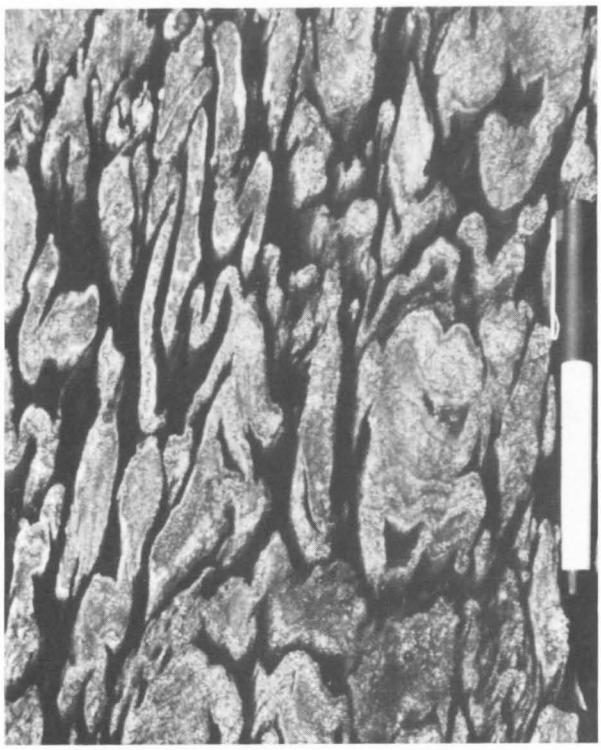


Fig. 16. D^K_1 folds refolded by D^K_2 in calc-silcate rocks. Type 3 interference folds dominate i.e., D^K_1 and D^K_2 fold axes are parallel. Local refolded sheath folds (e.g., just right of centre) attest to the intensity of the D^K_1 fabric and the fact that the D^K_1 folds are coincident with the D^K_1 stretching direction. The pen is 15 cm long.

expected if it had an original oblique orientation, and this is supported by the dominance of Ramsay Type 2 D^K_1/D^K_2 fold interference patterns throughout the Wonga Belt, including examples within the hinges of major D^K_2 folds. That is, D^K_1 shear folds are also parallel to this stretching lineation and they are also completely coaxial with the D^K_2 folds, with no suggestion of original obliquity. The D^K_1 stretching lineation in areas of low D^K_1 strain (e.g., Mount Maggie – see Appendix) shows some variation in orientation relative to the D^K_1/D^K_2 intersection lineation. However, D^K_1 shears in these areas are coarsely anastomosing (Fig. 15) and thus local shear directions may depart significantly from the bulk shear direction.

The upper boundary of the Wonga Belt high-strain shear zone had a slight westerly 'dip' relative to stratigraphy. Although this boundary is roughly stratigraphy-parallel in a north-south direction for about 80 km (i.e., parallel to the shear movement direction) it cuts slightly down section from east to west. Finite strain calculations on markers that record mainly the D^K_2 deformation component (e.g., Fig. 7b) vary from 30-80% maximum horizontal shortening with the average of the most reliable analyses indicating a likely bulk strain of

60-70% maximum shortening. Thus the Wonga Belt was at least double (and perhaps triple) its present width before D^K_2. Taking this D^K_2 shortening into account, the shear zone boundary had an original westward 'dip' of about 1-2° relative to the stratigraphy. Whether this represents the orientation of a westward-dipping sidewall ramp or whether it simply reflects an original stratigraphic gradient to the east is unknown. Such a gradient would support the eastward deepening stratigraphy proposed by Loosveld (1989).

The Wonga Belt is dominated by intrusive granitoid, metadolerite, and metagabbro bodies. The boundaries of the bodies are commonly parallel to primary layering in the country rock and to the early foliation, suggesting that they are mainly sill-like bodies with cross-connecting dykes. Net-veining and other mixed-magma structures between some felsic and mafic rocks (e.g., in the 'Circular Structure' in the northern part of the Wonga Belt, and along the Burstall Granite/Lunch Creek Gabbro contact – Blake, 1981), and their shared deformation history suggests that the intrusives are broadly coeval. There is abundant evidence that both the mafic and felsic bodies intruded synchronously with the D^K_1 deformation (see Pearson & others, this volume) over a period of time. All phases (except most pegmatites and a distinctive fine- to medium-grained leucocratic granite) contain the D^K_1 fabric. Where a relative time difference between two phases is indicated by cross-cutting relationships, the fabric is consistently stronger in the older phase. A large pavement in Greens Creek south of the Barkly Highway near Rosebud contains a good example of such a relationship (see Appendix).

Vein quartz, calcite, albite, metadolerite, and pegmatite are commonly spatially associated with D^K_1 shear zones. Holcombe & others (1991, Fig. 14) illustrate a small tabular metadolerite body that occupies a transtensional dilational site at a bend in a shear zone ('Middle Breakfast Creek' area – see Appendix). Syndeformational dilational sites are common in shear zones, and it is likely that the massive volume of intrusive material has been accommodated in similar, but larger, dilational sites throughout the major Wonga shear zone.

Zircon ages of all granitoids that contain evidence of the early fabric range from about 1760 Ma to 1730 Ma. Most ages are in the 1750 to 1730 Ma range and this also constrains the D^K_1 deformation. A lower age limit of 1671 Ma quoted in earlier papers has been discarded following re-examination of the granitoid in question (see Pearson & others, this volume).

Flanking domains

The most dominant structures in the flanking domains are the folds, axial plane foliation, and down-dip lineation of the crustal folding event (D^K_2). This deformation is itself very heterogeneous. Characteristically, folded layers form uniform wave trains in the hinges of folds (particularly synforms) but are strongly attenuated along the limbs. Steep shear zones with vertical movement, such as the Mary Kathleen Shear or the shear through the middle of the Burstall Granite, are common and have a sense of movement with the block closer to the Wonga Belt moving relatively upwards.

The major doubly plunging synforms adjacent to the Wonga Belt are D^K_2 folds. One of these, the Mary Kathleen Syncline, is tight, has a slightly curved axial trace, and is overturned along some of its outcrop length. The axial surface is cut by the subvertical Mary Kathleen Shear which truncates the Mary Kathleen uranium-REE ore body and has a west-side-up throw of about 1 km at that point (Pearson, 1982). The eastern limb of the Mary Kathleen Syncline containing the Burstall Granite and its aureole behaved as a single rigid unit, preserving the delicate reticulate geometry of dyke networks in the aureole. It is likely that the sudden change from rigid rotation behaviour to ductile folding is the underlying control on the location of the Mary Kathleen Shear. Similar geometric relationships occur in the Mount Godkin area between the Mount Godkin Granite, its aureole, the D^K_2 Cameronian and Mount Godkin faults, and the tightly folded calc-silicate rocks.

Ductile D^K_1 structures in the flanking domains are relatively pervasive adjacent to the high-strain transition to the Wonga Belt, but elsewhere D^K_1 fold occurrences are more scattered. Interference by D^K_2 folds causes complex outcrop patterns, particularly in the Corella Formation of the eastern flanking domain north of the Burstall Granite. In the area of high strain adjacent to the Wonga Belt, D^K_1 folds have subhorizontal axes, and interference by D^K_2 folds with subvertical axial planes produces exclusively Ramsay Type 3 interference patterns. The two sets of fold axes are coaxial and subhorizontal. Sheath folds are common in this zone, and the D^K_2 interference produces a pattern containing complex folded 'eyes'. A good example occurs in the Cameron River near Lime Creek. Local zones of high D^K_1 strain can be recognised at higher stratigraphic levels by the re-appearance of this refolded sheath interference pattern (Fig. 17). At most other localities in the flanking domains, D^K_1/D^K_2 fold interfence is of the Ramsay Type 1 or Type 2 pattern (Hill, 1986;

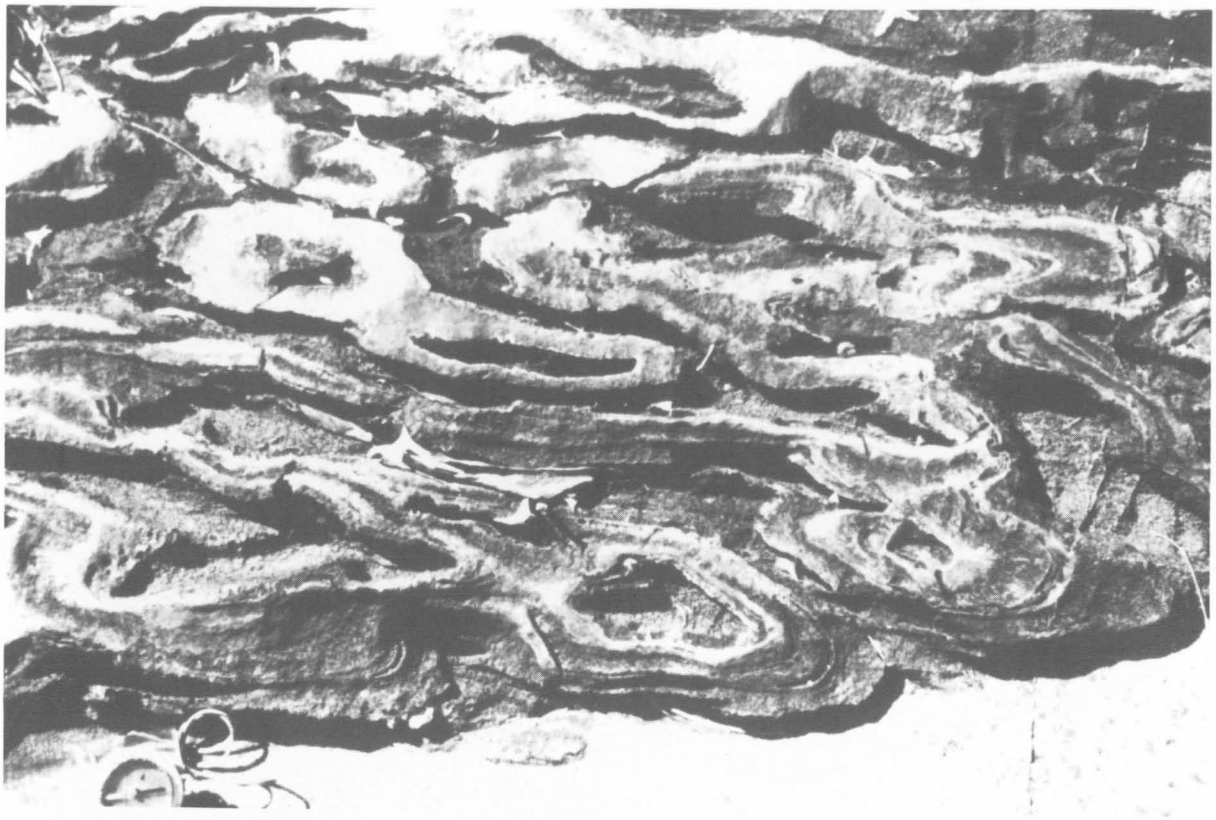


Fig. 17. Refolded D^{K}_{1} sheath folds in calc-silicates of the Corella Formation near Copper Blonde mine. The sheath folds indicate zones of high D^{K}_{1} strain. The compass is 7 cm across.

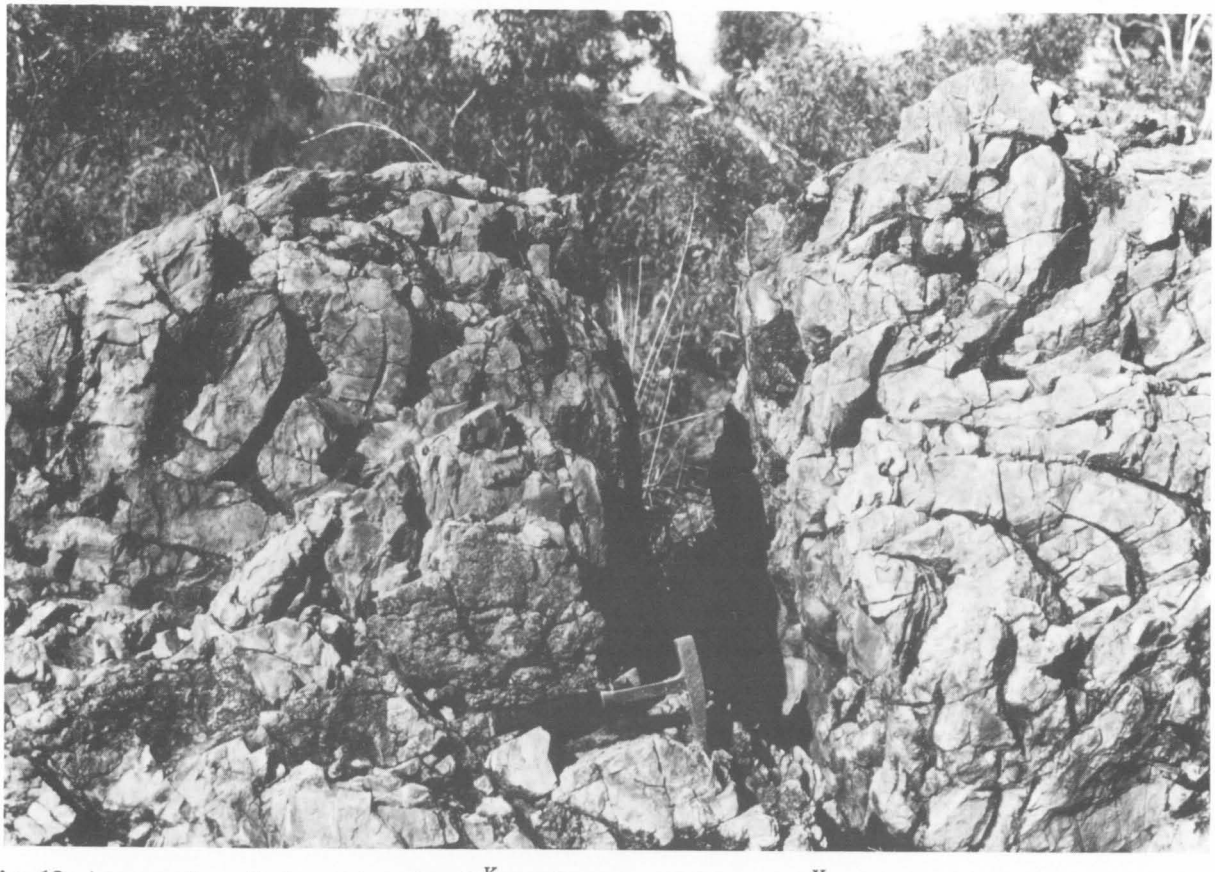


Fig. 18. Arrays of vertical east-trending D^{K}_{1} gash veins refolded by D^{K}_{2}. The veins contain deeply etched calcite-amphibolite and impart a 'bedded' appearance to the rock. The hammer is 40cm long.

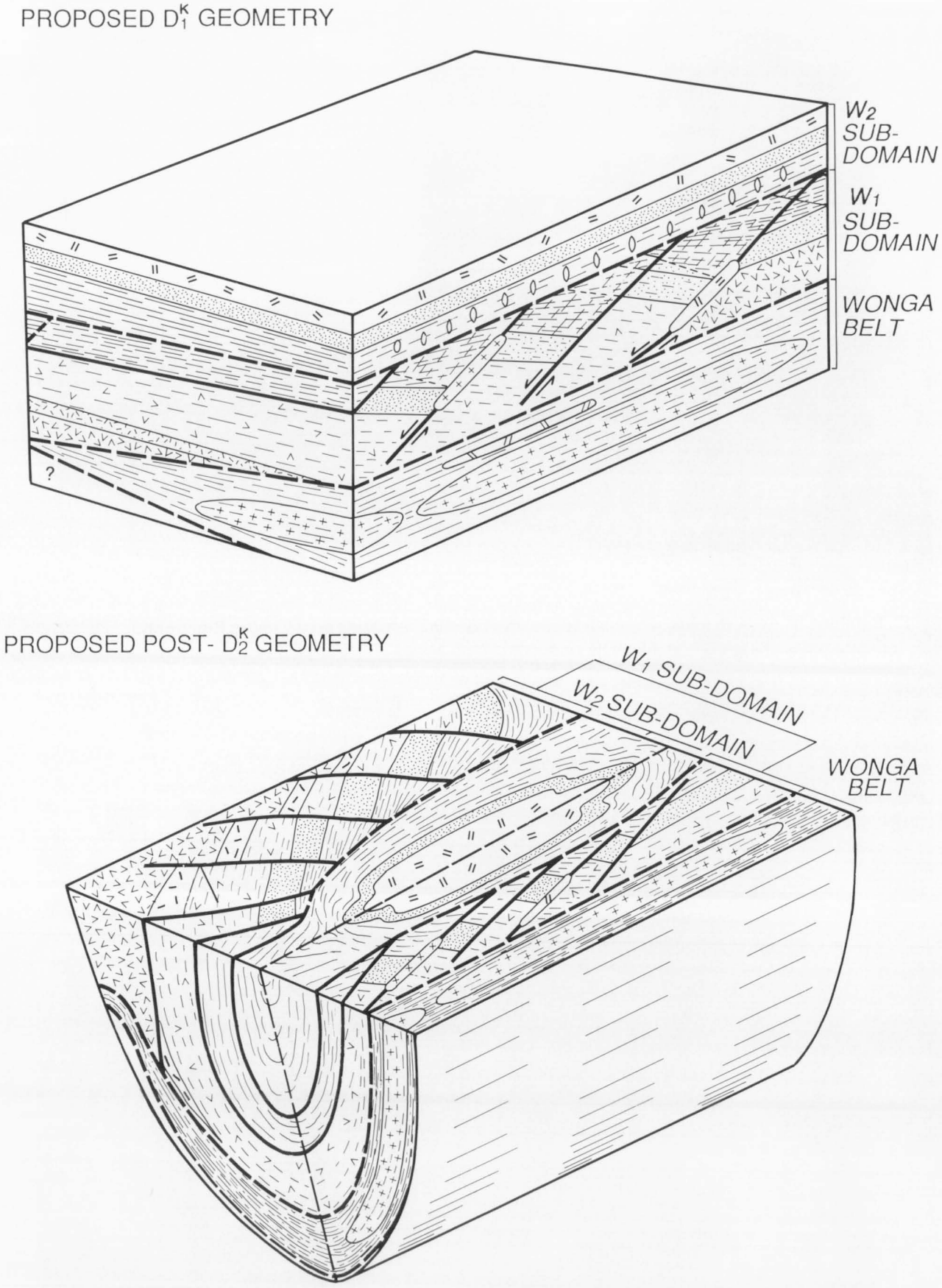
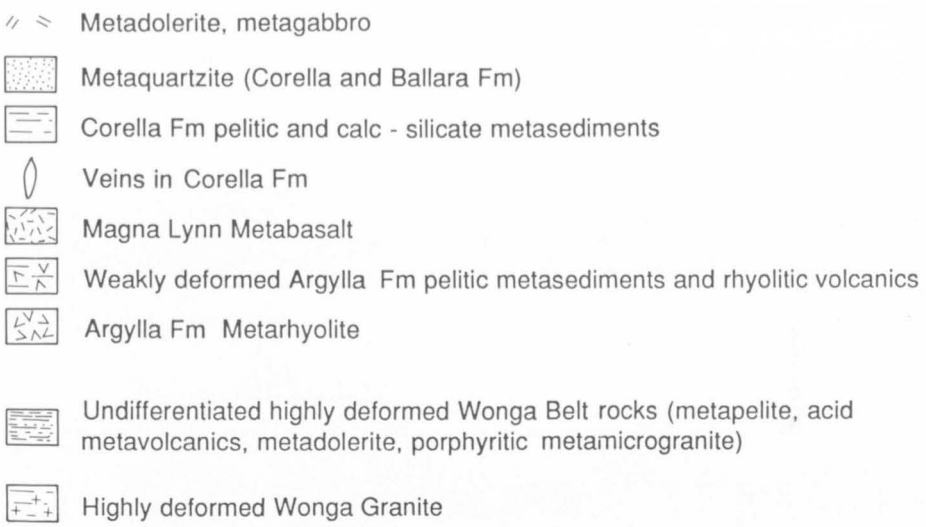


Fig. 19. Schematic diagrams showing the inferred relationship between fault arrays cutting the competent Ballara Quartzite unit along each limb of the Little Beauty Syncline. The W1 domains are inferred to represent a brittle extending slab between two more ductile layers.



Oliver & others, 1991). Hence the D^K_1 folds at these localities had variably oriented fold axes and axial planes. This variation of interference pattern is consistent with a decrease in the amount of shear in a thick stratigraphy-parallel shear zone (Holcombe & others, 1991).

Brittle effects attributed to D^K_1 are quite common in the flanking domains, particularly the widespread occurrence of extensional gash veins in the Corella Formation. These veins are typically rich in calcite, which, on surface exposures, is generally dissolved leaving open gashes. They commonly occur as widespread arrays of folded east-west trending subvertical veins (Fig. 18). Good examples occur in Breakfast Creek in the eastern domain, and at Rosebud dam in the western domain. (Note that we interpret these structures differently from Reinhardt & Rubenach [1989], who define these structures as a foliation).

Faults are more difficult to associate definitively with D^K_1. One such occurs in the Corella Formation at the northern margin of the Burstall Granite. It is now roughly strata-parallel (subvertical) and has been recognised on the basis of characteristic horizontal north-south shear-sense indicators and quartz c-axis fabrics, similar to those in the Wonga Belt (Sliwa, 1986). If unfolded to the horizontal, the sense of shear on this fault is the same as in the Wonga Belt (that is, top to the north). This fault divides into two shears that splay around the northern end of the pluton and are eventually overprinted by the granite. The Burstall Granite has the same general zircon age (1726 ± 8 and 1745 ± 17 Ma) as the Wonga Belt granites. The geometry, dextral sense of shear, and sense of curvature on these faults is consistent with the Burstall Granite occupying a transtensional dilational site on a curved fault with a movement of about 9 km. This fault would originally have been subhorizontal, and its counterpart on the western limb of the Mary Kathleen Syncline is likely to be a narrow belt of porphyroblastic schist within the Corella Formation with strong sinistral D^K_1 shear fabrics in adjacent non-porphyroblastic rocks (Jubilee Springs area).

The Burstall Granite is interpreted as having formed in brittle dilation sites produced in a slab undergoing brittle-ductile shear at the same time as the Wonga Belt granites were forming in a highly ductile shear environment immediately below this slab. Late stages of the granite have overridden parts of the bounding faults. The Mount Godkin Granite, the major metadolerite sills in the western synclines, and other igneous bodies are interpreted to have the same general origin. Their lack of internal D^K_1 fabrics is due to the generally brittle nature of the deformation of this high-level slab during D^K_1.

A complex array of brittle-ductile pre-D^K_2 shear zones cuts the relatively competent Ballara Quartzite along both limbs of the Little Beauty Syncline. On the eastern limb, the faults are bounded to the east (the original base) by the strong marginal shear of the Wonga Belt, and to the west by a prominent shear zone subparallel to stratigraphy. On the western limb, the faults are also bound to the east by a similar prominent stratigraphy-parallel shear zone and are 'blind' to the west. D^K_2 fold axes have anomalously steep plunges within the fault slices (compared to D^K_2 folds within the overlying Corella Formation calc-silicates) suggesting an original steep bedding dip. This area of normal faults and anomalous folds is shown as the 'W1 subdomain' in Pearson (1991a, 1991b). The overlying, more ductile zone is shown as the 'W2 subdomain'. This fault array is interpreted as a set of steep D^K_1 normal faults that have been folded during D^K_2 (Fig. 19). The fault blocks have undergone rotation during movement. There is some disagreement between the authors as to the overall sense of shear represented by this array of steep rotated

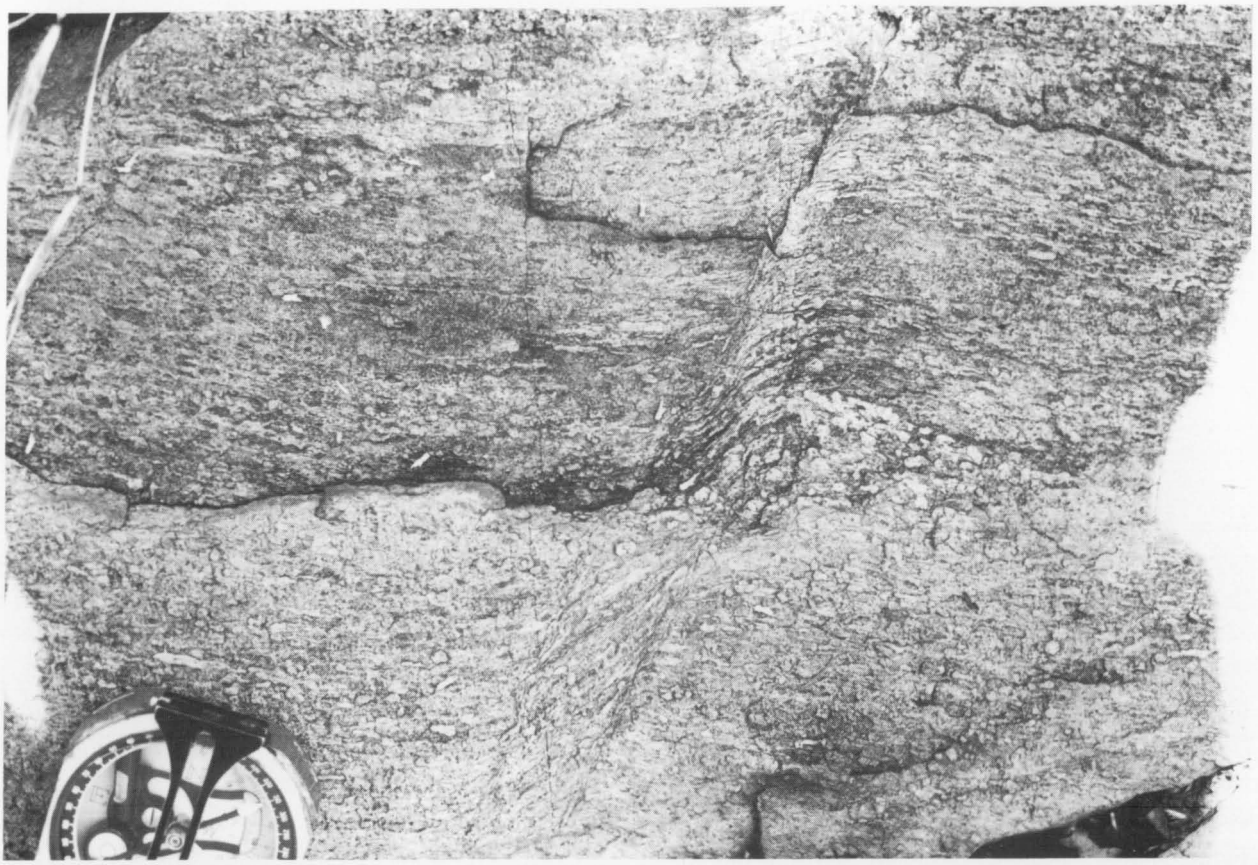


Fig. 20. North-dipping extensional shear cutting both D^{K}_{1} and D^{K}_{2} structures in the east of the Wonga Belt. These post-D^{K}_{2} shears, which are commonly associated with 'redrock' alteration, may represent a north-south extension component during D^{K}_{3}.

normal faults, but it is clear that they represent extension of a brittle horizontal slab between more ductile material.

Post-D^{K}_{2} deformation

Two sets of brittle-ductile structures overprint the earlier deformation fabrics. The earliest of these (D^{K}_{3}) is characterised by brittle-ductile deformation accompanying retrograde metamorphism, and consist of both macroscopic shears and faults, and localised zones of faulting, kinking, and fracturing (producing 'fold breccias'). The faults are steeply dipping, conjugate, and offset the major folds. One set strikes north-north east with dominantly dextral strike separation, the other strikes north-north west with sinistral offsets. The Mount Remarkable, Wonga, Cameron, and Trey Bit Faults are examples of the former. Mesoscopic D^{K}_{3} structures consist of angular monoclinal folds with steep north-northwest- or north-northeast-striking axial surfaces (rarely in conjugate sets); other D^{K}_{3} structures include fold breccias, faults, and shear zones. No axial plane mineral fabric is developed, and the structures are commonly spatially associated with 'redrock' alteration (local terminology), which makes the rock pink or red. This alteration commonly extends along the axial planes of D^{K}_{3} folds, and is more pervasive at outcrop scale in areas of strong D^{K}_{3} folding. Where abundant D^{K}_{3} folds overprint older intensively folded zones (D^{K}_{2} or D^{K}_{2}/D^{K}_{1} refolded folds), fold breccias are common. In these brecciated zones D^{K}_{3} fold breccias may overprint similar D^{K}_{2} breccias, and the distinction between the deformation phases becomes difficult. The common superposition of D^{K}_{3} fold breccias on areas of pre-existing fold hinges, refolded folds, or in strain shadow zones at the northern and southern ends of meta-intrusives, also suggests that the development of breccias is influenced by pre-existing strain anisotropies.

The kinematics of the macroscopic D^{K}_{3} fault zones are poorly understood, as mesoscopic indications of direction of shear and sense of shear are rare and generally ambiguous. However, the consistent offsetting of major D^{K}_{2} fold hinges, such as the Wonga Anticlinorium, and equivalent strike separation of limb areas, indicate a strong strike-slip component. Concurrent activity on the major conjugate fault sets is consistent with a net east-west shortening as suggested by Derrick (1978). Arrays of east-striking steeply northerly dipping post-D^{K}_{2} extensional shears are common in the pelites along the eastern margin

of the Wonga Belt (Fig. 20), and probably reflect the north-south extension component during this phase of moderate high level east-west pure shear shortening.

It is likely that D^K_3 represents the waning stages of the east-west crustal shortening event, and probably correlates with isotopic ages from the Mary Kathleen U-REE deposit ranging from about 1550 Ma to 1480 Ma (Page, 1978, 1983; Maas & others, 1988).

Isolated zones of folds, shear zones, and breccias are spatially related to the widely-spaced post-orogenic gabbro/dolerite dykes that transect the region. Fold development is extremely localised and clearly related to the emplacement of the 1122-1116 Ma dykes (Page, 1983).

Metamorphism

D^K_1 metamorphism

The effects of metamorphism during D^K_1 are partly obscured by overprinting during D^K_2 deformation and metamorphism. Despite this, it has been found possible to place broad constraints on the grades attained during D^K_1 by associating D1 tectonites with particular mineral assemblages.

In the Corella Formation of the upper plate, widespread contact metamorphism is manifest as exoskarn of clinopyroxene-rich hornfels adjacent to the Burstall and Mount Godkin Granites, which intruded at D^K_1 time. The contact aureoles are relatively large in comparison to the inferred size of the granites, and yet the granites contain small but significant proportions of marginal fine-grained phases, including chilled margins and felsic dykes. Together, these data suggest emplacement of granites and related contact metamorphism into the upper plate at approximately 5 km depth (Oliver & others, 1991).

In the upper plate away from the contact aureoles, D^K_1 metamorphic grade is low. S_1 foliation is rare, and where present is defined by biotite. As the Wonga Belt is approached, however, D^K_1 grade sharply increases. Clinopyroxene and amphibole are commonly aligned in S_1 in calc-silicate at the base of the Corella Formation, and S_1 sillimanite is present in both the lowermost Corella Formation at the base of the upper plate (near Jubilee Springs in the Mary Kathleen Syncline) and at the top of the lower plate in Argylla Formation metapelite.

Although schist in the Wonga Belt commonly bears sillimanite, at no point has true migmatite (partial melt) been observed, although its presence would not be unexpected. In areas of high shear strain, and particularly along the marginal zones of the Belt, a number of outcrops show features reminiscent of migmatite structures. Strongly contorted quartz veins and white, locally patchy, alteration zones (not leucosomes) are common. Metasomatic activity, particularly albitic or scapolitic alteration, generally is localised along shear zones, and in the high-strain marginal zone completely bleaches some outcrops. Extensional dilation within the shear zones most likely control both the transport of metasomatic fluids and the formation of extensional quartz veins, which subsequently became folded and refolded in the strongly heterogeneous non-coaxial strain field.

Relatively high metamorphic temperatures were reached in the lower plate Wonga Belt due to the association of D^K_1 deformation with abundant widespread intrusion of granitic and gabbroic rocks. As this occurred at relatively shallow levels in the crust (8-12 km (Holcombe & others, 1991; Oliver & others, 1991), metamorphic grade decreased rapidly upwards, accentuated by attenuation of the isograds due to subhorizontal shearing. High temperature contact metamorphism occurred around syn-D^K_1 upper plate granites emplaced in inferred dilational openings in synthetic D^K_1 fault splays.

D^K_2 metamorphism

During D^K_2 the peak of regional metamorphism varied across the belt (Oliver & others, 1991). Synchronism of D^K_2 with the metamorphic peak has been inferred from association of high-temperature mineral assemblages with D^K_2 tectonites, partial folding of isograds during D^K_2, and transection of isograds by late D^K_2 faults.

Peak grade ranged from greenschist facies in the western Little Beauty Syncline, to mid-amphibolite facies (530°C, 300-350 MPa) in the eastern Little Beauty Syncline (Oliver & others, 1991). The only suitable indicators in the Wonga Belt indicate uppermost amphibolite facies conditions in the eastern part of the belt, with sillimanite-K feldspar suggesting temperatures reached around 650°C at an inferred 400 MPa. In the eastern MKFB, peak metamorphic temperatures vary from 550°C to 630°C at an inferred pressure of 350-400 MPa (Oliver, 1988)

The overall distribution of D^K_2 grade is consistent with synchronism of D^K_2 deformation with peak metamorphism, such that the highest-grade rocks are exposed near the core of the D^K_2 Wonga Anticlinorium.

Retrograde post–D^K_2 metamorphism

Most retrograde metamorphic assemblages in metasediments are associated with late-D^K_2 breccias and/or D^K_3 structures. Commonly these structures are

locally superimposed, and it is difficult to relate particular structural elements to the various alteration assemblages. For example, the syn-D_2 assembage calcite-amphibole-clinopyroxene found as veins in albitic breccias is commonly overprinted by actinolitic amphibole-epidote, which in turn may be replaced by albite-hematite-chlorite ('redrock') associated with D^K_3. The syn-D^K_2 assemblage is constrained to 500°C by calcite-dolomite geothermometry. The later retrograde assemblages, in particular 'redrock' alteration, are characteristic of transitional greenschist-amphibolite facies metamorphism, and broad temperature conditions of around 300-450°C are inferred (see Oliver & others, 1991).

Metasomatism

Metasomatism is widespread and intense throughout the MKFB during both D^K_1 and D^K_2 deformation (Oliver & Wall, 1987; Oliver & others, 1990a, b). In all rock types of the Wonga Belt, and in the lowermost upper plate Corella Formation, polydeformed quartz veins and albitic, K-feldspar-rich, and scapolitic alteration zones (not leucosomes) are common. This alteration and veining is commonly localised along D^K_1 shear zones (Figs. 12, 13) suggesting syn-D^K_1 shear-related dilation was the primary mechanism for fluid transport. REE-depletion zones in Wonga albite-rich shears, as well as the pre-enrichment of U-REE in the Mary Kathleen Syncline skarns, indicate significant metal transport during D^K_1 times.

The most prominent forms of D^K_2 metasomatism are calcite-rich vein systems and related albitic haloes, and calcite-albite-rich shear zones. Syn-D^K_2 ages for U-REE mineralisation at Mary Kathleen (Maas & others, 1985, 1988) indicate significant U-REE transport and deposition at this time, as do local allanite-rich zones in association with albitic alteration of calcite veins. Cu-Fe sulphides are also common in syn-D^K_2 calcite vein systems. As in D^K_1, the primary cause of metasomatism during D^K_2 was the localisation of fluid pathways in regions of heterogeneous deformation, such as shear zones and large dilatant strain shadow regions (Oliver & others, 1990a).

Discussion and conclusions

The major structural conclusion of this study is that the pre- D^K_2 geometry of the area comprised:

- A subhorizontal high-strain high-temperature D^K_1 shear zone with top-to-the-north sense of shear, and synkinematic intrusion of mafic and felsic igneous rocks; this was overlain by:
- Lower-temperature less deformed stratigraphically higher rocks showing both brittle and ductile D^K_1 features with relatively undeformed granite and gabbroic bodies emplaced, at D^K_1 time, into discrete probably fault-related transtensional sites.

Intrusion of the gneissic Wonga Granite and metagabbro (amphibolite), the 'undeformed' Burstall and Mount Godkin Granites, Lunch Creek Gabbro, and other high-level mafic sill-like intrusives, plus primary skarn formation and other widespread metasomatic activity, were all broadly synchronous with this D^K_1 deformation between approximately 1750 to 1730 Ma (Page, 1983, 1985; Pearson & others, 1990) and preceded the regional crustal shortening and peak metamorphism by 150-200 million years.

Elsewhere (Pearson & others, 1987; Holcombe & others, 1991), we have argued that the D^K_1 shear geometry is most consistent with north-south crustal extension. The major lines of evidence include:

- Younger rocks in the upper plate consistently overlie older rocks in the lower plate;
- Lower D^K_1 metamorphic grade and brittle deformation characterise the upper plate, whereas higher D^K_1 grades and dominantly ductile structures characterise the lower plate;
- The existence of steep D^K_1 normal faults in the upper plate; and
- The large volume of mafic and felsic intrusives within the shear zone, and the relatively high level of emplacement are easier to explain in crustal extension than in crustal shortening and thrusting.

This hypothesis is supported by other detailed work in equivalent rocks to the south (Passchier, 1986; Passchier & Williams, 1989), and by Loosveld (1989) and Williams (1989) in rocks to the east, each suggesting north-south crustal extension at this (D^K_1) time. Pre-D^K_2 crustal extension has also been suggested for the Deighton 'klippe' area (Stewart & Williams, 1988; Stewart, 1989) although a thrust origin has also been proposed for this area (Loosveld & Schreurs, 1987). Williams & others (1987) invoke crustal extension to explain the geometry of rocks west of the Little Beauty Syncline, proposing an east-west movement direction. (However, this latter conclusion is not now supported by PJP, one of the authors of that paper).

D^K_2 folding was responsible for exhuming this D^K_1 shear zone and other D^K_1 structures in the MKFB. The localisation of dilational sites during heterogeneous D^K_2 deformation was the key factor involved in renewed fluid flow and metal transport at that time.

Deformation structures that predate the regional D_2 folding have been widely recognised in the Mount Isa Inlier since Bell's original postulation of pre-D_2 thrusts (Bell, 1983). Most of these structures and fabrics have been interpreted as thrust related (except see above) and generally are correlated with a 1620-1610 Ma event defined near Mount Isa (Page & Bell, 1986). The D^K_1 deformation described here (constrained by the syn-kinematic granitoid) occurs much earlier and at greater crustal depths than that described elsewhere. We have not observed any pre-D_2 folding structures that we would equate with such thrusting, although some of the refolded fold structures occurring high in the upper plate may reflect high-level thrusting (Hill, 1986) occurring at the later date. Reinhardt & Rubenach (1989) and Reinhardt (this volume) describe relatively minor thrusts within the Corella Formation in the Rosebud Syncline immediately adjacent to the Wonga Belt. These various thrust are not incompatible with the model presented here provided that D^K_1 defined here is not equated with the earliest deformation observed in those areas of thrusting (and therefore commonly defined as 'D_1'). It is to be expected that the D^K_1 structures and fabrics described here may not be seen outside the Mary Kathleen Fold Belt; some, however, are described in the Ballara-Mount Frosty area to the west (Stewart, this volume). The Wonga Belt exposes much deeper crustal levels than elsewhere, and D^K_1 strain drops off sharply in the upper plate. The slight westward 'dip' of the detachment surface relative to stratigraphy suggests that it may be exposed only to the east, but there structures of the MKFB are truncated by the somewhat enigmatic Pilgrim Fault.

D^K_1 deformation and metasomatism were clearly significant factors in the primary transport and deposition of U-REE and other metals. Thus, recognition and delineation of this now folded high-strain shear zone is important for regional metalliferous exploration in this area. Exploration targets will include both D^K_1 and D^K_2 dilation sites with appropriate wall-rock chemistry.

Although the Inlier-wide folding event is widely defined as D_2, there is considerable variation in the use and definition of D_1 to refer to earlier fabrics and structures (e.g., Page, 1985; Page & Bell, 1986). We recognise that applying such terminology to crustal extension events rather than orogenic contractional events will ultimately lead to Inlier-wide confusion. Clearly there must also have been earlier extension leading to the formation of the rift-fill and sag deposits of cover sequence 2. We recommend that the lucid terminology introduced by Loosveld (1989) be accepted for all deformation affecting cover sequence 2. In this terminology, extensional events are referred to as D_e starting with the original rift-basin formation as D_{e1} and our D^K_1 as D_{e2}. Contractional events and fabrics are then referred to as D_c. Within the regional context our upright folding event is D_{c2} (following the earlier D_{c1} thrusting that commenced the major contractional episode).

Acknowledgements

This work was conducted partly under the auspices of the Australian Bureau of Mineral Resources as part of the Mount Isa Regional Tectonic History Project. Their logistical support in this co-operative project is greatly appreciated. The research was carried out at the University of Queensland and Monash University while PJP and NHSO were recipients of Commonwealth Postgraduate Research awards. RJH acknowledges the early support of the Australian Reseach Grants Scheme, project #E76/15049. Final drafting was carried out by Draga Gelt (Monash University). Finally, ideas that have culminated in our interpretation of this area have arisen out of many years of discussion and arguments, not only between ourselves, but also with Tim Bell, Dave Blake, Mike Etheridge, Gordon Lister, Ramon Loosveld, Jürgen Reinhardt, Mike Rubenach, John Santul, Vic Wall, and the various Queensland University Honours students referred to in the text.

References

BELL, T.H., 1983 - Thrusting and duplex formation at Mount Isa, Queensland, Australia. *Nature* 304, 493-497.

BLAKE, D.H., 1981 - Intrusive felsic-mafic net-veined complexes in north Queensland. *BMR Journal of Australian Geology and Geophysics* 6, 95-99.

BLAKE, D.H., 1987 - Geology of the Mount Isa Inlier and environs, Queensland and Northern Territory. *Bureau of Mineral Resources, Australia, Bulletin* 225, 83 pp.

DERRICK, G.M., 1978 - Proterozoic igneous and sedimentary rocks and associated metamorphism and metasomatisn at Mary Kathleen, northwest Queensland. Ph.D. thesis, University of Queensland, Brisbane (unpublished).

DERRICK, G.M., WILSON, I.H., HILL, R.M., & MITCHELL, J.E., 1971 - Geology of the Marraba

1:100 000 sheet area, Queensland. *Bureau of Mineral Resources, Australia, Record* 1971/56, 192 pp.

DERRICK, G.M., WILSON, I.H., & HILL, R.M., 1977a - Revision of stratigraphic nomenclature in the Precambrian of northwestern Queensland, VI: Mary Kathleen Group. *Queensland Government Mining Journal* 78, 15-23.

DERRICK, G.M., WILSON, I.H., HILL, R.M., GLIKSON, A.Y., & MITCHELL, J.E., 1977b - Geology of the Mary Kathleen 1:100 000 sheet area, northwest Queensland. *Bureau of MineralResources, Australia, Bulletin* 193, 114 pp.

FRASER, S.J., 1977 - The structure and stratigraphy of the Cameron River Area, near Mary Kathleen, northwest Queensland. B.Sc.(Hons.) thesis, University of Queensland, Brisbane (unpublished).

HAMILTON, L.M., 1985 - Structure and metamorphism in high-grade shear zones and surrounding rocks, northwest of Mary Kathleen, northwest Queensland. B.Sc.(Hons.) thesis, University of Queensland, Brisbane (unpublished).

HILL, E.J., 1986 - Structural analysis and overprinting of early folds in the Corella Formation near Mary Kathleen, northwest Queensland. B.Sc.(Hons.) thesis, University of Queensland, Brisbane (unpublished).

HOLCOMBE, R.J., PEARSON, P.J., & SLIWA, R., 1991 - Geology of the Mary Kathleen Area (1:25 000 scale map). *Bureau of Mineral Resources, Canberra, Australia* (two sheets). Available as colour electrostatic plots on paper (AUD30), or in digital form on optical disc or Exabyte 8 mm tape (prices on application) both of which can be displayed on Intergraph Microstation software on computers that will run Unix. The digital data comprise a scanned raster image (.RLE format) of the black and white geological map, and an Intergraph vector design file containing the boundaries of coloured polygons. The coloured map and data are available from the Publication Sales Centre, Bureau of Mineral Resources, and an uncoloured Ozalar film or paper copy (AUD20) of the map is available from BMR Copy Service, both at GPO Box 378, Canberra, ACT, 2601, Australia. All orders to be prepaid to Collector of Public Monies.

HOLCOMBE, R.J., & FRASER, S.J., 1979 - Structural and stratigraphic problems of the Argylla Formation near Mary Kathleen, Queensland. *Journal of the Geological Society of Australia* 26, 419-434.

HOLCOMBE, R.J., PEARSON, P.J., & OLIVER, N.H.S., 1987 - The Mary Kathleen Fold Belt, northwest Queensland: geometry and timing of deformation. *In* International Conference on the Deformation of Crustal Rocks, Mount Buffalo, Australia. *Geological Society of Australia Abstracts*, 19, 35-36.

HOLCOMBE, R.J., PEARSON, P.J., & OLIVER, N.H.S., 1991 - Geometry of a Middle Proterozoic extensional decollement in northeastern Australia. *Tectonophysics* 191, 255-274.

HORTON, J.A., 1985 - The geology of the Bateman Hill-Little Beauty Syncline area, northwest Queensland. B.Sc.(Hons.) thesis, University of Queensland, Brisbane (unpublished).

JORGENSEN, G.C., 1986 - Geology of the Northern Burstall Granite area, Mary Kathleen, northwest Queensland. B.Sc.(Hons.) thesis, University of Queensland, Brisbane (unpublished).

LAFFERTY, S., 1977 - Geochemical and isotopic investigations of selected igneous and metamorphic rocks of the Mary Kathleen area, northwest Queensland. B.Sc.(Hons.) thesis, University of Queensland, Brisbane (unpublished).

LOOSVELD, R., 1989 - The intra-cratonic evolution of the central eastern Mount Isa Inlier, northwest Queensland, Australia. *Precambrian Research* 44, 243-276.

LOOSVELD, R., & SCHREURS, G., 1987 - Discovery of thrust klippen, northwest of Mary Kathleen, Mount Isa Inlier, Australia. *Australian Journal of Earth Sciences* 34, 387-402.

MAAS, R., McCULLOCH, M.T., PAGE, R.W., & CAMPBELL, I.H., 1985 - The Mary Kathleen U-REE deposit, Queensland: age and origin of mineralisation from Sm-Nd systematics. *In*: Tectonics and Geochemistry of Early to Middle Proterozoic Fold Belts, Darwin, August 1985, Abstracts. *Bureau of Mineral Resources, Australia, Record* 1985/28 (no page numbers).

MAAS, R., McCULLOCH, M.T., & CAMPBELL, I.H., 1988 - Sm-Nd isotope systematics in uranium rare-earth element mineralization at Mary Kathleen uranium mine, Queensland. *Economic Geology* 82, 1805-1826.

MACLEAN, K.H., 1977 - Structural and petrological controls of uranium mineralisation at Elaine Dorothy, Mary Kathleen, northwest Queensland. B.Sc.(Hons.) thesis, University of Queensland, Brisbane (unpublished).

OLIVER, N.H.S., 1981 - Structure, mineralogy and petrogenesis of skarn and related rocks near Mary Kathleen, northwestern Queensland. B.Sc.(Hons.) thesis, University of Queensland, Brisbane (unpublished).

OLIVER, N.H.S., 1988 - A metamorphic plumbing system: the Mary Kathleen Fold Belt, northwest Queensland. PhD thesis, Monash University, Victoria (unpublished).

OLIVER, N.H.S, 1991 - Geology of the Mount Godkin Area (1:25 000 scale map), *Bureau of Mineral Resources, Canberra, Australia.* Available as a colour electrostatic plot on paper (AUD30), or in digital form on optical disc or Exabyte 8 mm tape (prices on application) both of which can be displayed on

Intergraph Microstation software on computers that will run Unix. The digital data comprise a scanned raster image (.RLE format) of the black and white geological map, and an Intergraph vector design file containing the boundaries of coloured polygons. The coloured map and data are available from the Publication Sales Centre, Bureau of Mineral Resources, and an uncoloured Ozalar film or paper copy (AUD20) of the map is available from BMR Copy Service, both at GPO Box 378, Canberra, ACT, 2601, Australia. All orders to be prepaid to Collector of Public Monies.

OLIVER, N.H.S., HOLCOMBE, R.J., HILL, E.J., & PEARSON, P.J., 1991 - Tectono-metamorphic evolution of the eastern Mary Kathleen Fold Belt, northwest Queensland: A reflection of mantle plume processes? *Australian Journal of Earth Sciences* 38, 425-455.

OLIVER, N.H.S., PEARSON, P.J., WALL, V.J., GOLDING, S.D., & HOLCOMBE, R.J., 1987 - Structural controls on fluid infiltration and metasomatism in the Mary Kathleen Fold Belt - implications for large-scale fluid migration during deformation. *In*: International Conference on the Deformation of Crustal Rocks, Mount Buffalo, Australia. *Geological Society of Australia Abstracts* 19, 14-15.

OLIVER, N.H.S., VALENTA, R.K., & WALL, V.J., 1990a - The effect of heterogeneous stress and strain on metamorphic fluid flow, Mary Kathleen, Australia, and a model for large- scale fluid circulation. *Journal of Metamorphic Geology* 8, 311- 331.

OLIVER, N.H.S., & WALL, V.J., 1987 - Metamorphic plumbing system in Proterozoic calc-silicates, Queensland, Australia. *Geology* 15, 793-796.

OLIVER, N.H.S., WALL, V.J., PEARSON, P.J., & HOLCOMBE, R.J., 1990b - Unravelling more obscurities in the genesis of the Mary Kathleen U-REE orebody. *Monash University and Victorian Institute of Earth and Planetary Sciences, Mount Isa Inlier Geology Conference, November 1990,* 41-43.

PAGE, R.W., 1978 - Response of U-Pb zircon and Rb-Sr total rock and mineral systems to low-grade regional metamorphism in Proterozoic igneous rocks, Mount Isa, Australia. *Journal of the Geological Society of Australia* 25, 141-164.

PAGE, R.W., 1983 - Chronology of magmatism, skarn formation and uranium mineralization, Mary Kathleen, Queensland, Australia. *Economic Geology* 78, 838-853.

PAGE, R.W., 1985 - Isotopic record of crustal events in Northern Australia. *In*: Tectonics and Geochemistry of Early to Middle Proterozoic Fold Belts, Darwin, August 1985, Abstracts. *Bureau of Mineral Resources, Australia, Record* 1985/28 (no page numbers).

PAGE, R.W., & BELL, T.H., 1986 - Isotopic and structural responses of granite to successive deformation and metamorphism. *Journal of Geology* 94, 365-379.

PASSCHIER, C.W., 1986 - Evidence for early extensional tectonics in the Proterozoic Mount Isa inlier, Australia. *Geology* 14, 1008-1011.

PASSCHIER, C.W., & WILLIAMS, P.R., 1989 - Proterozoic extensional deformation in the Mount Isa Inlier, Queensland, Australia. *Geological Magazine* 126, 43-53.

PEARSON, P.J., 1982 - The structural and stratigraphic setting of the Mary Kathleen uranium orebody, northwest Queensland. B.Sc.(Hons.) thesis, University of Queensland, Brisbane, (unpublished).

PEARSON, P.J., 1989 - The structural and tectonic development of the Wonga Belt and surrounding Mary Kathleen Fold Belt, Mount Isa Inlier, northwest Queensland. Ph.D. thesis, University of Queensland, Brisbane (unpublished).

PEARSON, P.J., & HOLCOMBE, R.J., 1991a - Geology of the Breakfast Creek Area (1:25 000 scale map), *Bureau of Mineral Resources, Canberra, Australia.* Available as a colour electrostatic plot on paper (AUD30), or in digital form on optical disc or Exabyte 8 mm tape (prices on application) both of which can be displayed on Intergraph Microstation software on computers that will run Unix. The digital data comprise a scanned raster image (.RLE format) of the black and white geological map, and an Intergraph vector design file containing the boundaries of coloured polygons. The coloured map and data are available from the Publication Sales Centre, Bureau of Mineral Resources, and an uncoloured Ozalar film or paper copy (AUD20) of the map is available from BMR Copy Service, both at GPO Box 378, Canberra, ACT, 2601, Australia. All orders to be prepaid to Collector of Public Monies.

PEARSON, P.J., HORTON, J.A., & HOLCOMBE, R.J., 1991b - Geology of the East Limb, Little Beauty Syncline (1:15 000 scale map), *Bureau of Mineral Resources, Canberra, Australia.* Available as a colour electrostatic plot on paper (AUD30), or in digital form on optical disc or Exabyte 8 mm tape (prices on application) both of which can be displayed on Intergraph Microstation software on computers that will run Unix. The digital data comprise a scanned raster image (.RLE format) of the black and white geological map, and an Intergraph vector design file containing the boundaries of coloured polygons. The coloured map and data are available from the Publication Sales Centre, Bureau of Mineral Resources, and an uncoloured Ozalar film or paper copy (AUD20) of the map is available from BMR Copy Service, both at GPO Box 378, Canberra, ACT, 2601, Australia. All orders to be prepaid to Collector of Public Monies.

PEARSON, P.J., HOLCOMBE, R.J., & OLIVER, N.H.S., 1987 - The Mary Kathleen Fold Belt, northwest Queensland: D_1 - a product of crustal extension. *In:*

International Conference on the Deformation of Crustal Rocks, Mount Buffalo, Australia. *Geological Society of Australia, Abstracts* 19, 37-38.

PEARSON, P.J., PAGE, R.W., & HOLCOMBE, R.J., 1990 - Geology and geochronology of the Wonga Granite, northwest Queensland: implications for the timing of deformation of the Mary Kathleen fold belt. *Monash University and Victorian Institute of Earth and Planetary Sciences, Mount Isa Inlier Geology Conference, November 1990,* 13-15.

PEARSON, P.J., HOLCOMBE, R.J., & PAGE, R.W., this volume - The Middle Proterozoic Wonga Batholith, Mount Isa Inlier, Australia: contact, deformation, and age relationships. *In*: STEWART, A.J., & BLAKE, D.H. (Editors), Detailed Studies of the Mount Isa Inlier. *Bureau of Mineral Resources, Australia, Bulletin* 243.

RAMSAY, J.G., 1967 - Folding and Fracturing of rocks. *McGraw-Hill; New York.* 568 pp.

REINHARDT, J., this volume - The Corella Formation of the Rosebud Syncline (central Mount Isa Block): deposition, deformation, and metamorphism. *In*: STEWART, A.J., & BLAKE, D.H. (Editors), Detailed Studies of the Mount Isa Inlier. *Bureau of Mineral Resources, Australia, Bulletin* 243.

REINHARDT, J., & RUBENACH, M.J., 1989 - Temperature-time relationships across metamorphic zones: evidence from porphyroblast-matrix relationships in progressively deformed metapelites. *Tectonophysics* 158, 141-161.

SANDERSON, D., 1973 - The development of fold axes oblique to the regional trend. *Tectonophysics* 16, 55-70.

SLIWA, R., 1986 - Structural geology of the Wollondonga Mine area, Mary Kathleen, northwest Queensland. B.Sc.(Hons.) thesis, University of Queensland, Brisbane (unpublished).

STEWART, A.J., 1989 - Extensional faulting as the explanation for Mount Albert Group outliers, and a re-interpretation of the Deighton 'Klippe', Mount Isa Inlier, northwest Queensland. *Australian Journal of Earth Sciences* 36, 405-421.

STEWART, A.J., this volume - Stratigraphy, extension, and contraction in the Ballara-Mount Frosty area, Mount Isa Inlier, Queensland. *In*: STEWART, A.J., & BLAKE, D.H. (Editors), Detailed Studies of the Mount Isa Inlier. *Bureau of Mineral Resources, Australia, Bulletin* 243.

STEWART, A.J., & WILLIAMS, P.R., 1988 - Early extension in the Mount Isa Inlier, and a solution to the problem of the Deighton Quartzite Outliers. *Geological Society of Australia Abstracts* 21, 381-382.

TALBOT, C.J., 1970 - The minimum strain ellipsoid using deformed quartz veins. *Tectonophysics* 9, 47-76.

WILLIAMS, P.R., 1989 - Nature and timing of early extensional structures in the Mitakoodi Quartzite, Mount Isa Inlier, northwest Queensland. *Australian Journal of Earth Sciences* 36, 283-296.

WILLIAMS, P.R., STEWART, A.J., & PEARSON, P.J., 1987 - Proterozoic continental extension in the Mount Isa Inlier, Queensland, Australia. *In*: Extended Abstracts, Applied Extension Tectonics Symposium, Canberra, Australia. *Bureau of Mineral Resources, Australia, Record* 1987/51, 64-71.

WILSON, I.H., DERRICK, G.M., HILL, R.M., DUFF, B.A., NOON, T.A., & ELLIS, D.J., 1977 - Geology of the Prospector 1:100 000 sheet area, Queensland. *Bureau of Mineral Resources, Australia, Record* 1977/4, 197 pp.

WILSON, I.H., NOON, T.A., HILL, R.M., & DUFF, B.A., 1979 - Geology of the Quamby 1:100 000 sheet area, Queensland. *Bureau of Mineral Resources, Australia, Record* 1979/56, 123 pp.

Appendix

Listed below are short descriptions of key areas cited in the text.

(1) Greens Creek, Rosebud, Grid Reference 948975; large pavements in Greens Creek, several hundred metres west of the road to Rosebud Syncline, Ballara, and Fountain Range, illustrate the development of early D^K_1 mylonite fabrics and weaker D^K_1 fabrics in later Wonga Granite phases consistent with intrusion during ongoing deformation (Fig. 21). Coarse biotite-amphibole granite ('Highway phase') intrudes earlier layers including a mylonite of probable granitic parentage (Fig. 21a). The mylonite has intense D^K_1 fabrics including refolded mylonitic layering (quartz ribbon fabrics can be seen in thin section) and a very strong stretching lineation defined by relatively large quartz lenticles (and hence granite rather than felsic volcanic is the likely protolith). The intruding granite, however, also contains the D^K_1 stretching lineation, although considerably weaker (see Figs. 8, 21b). The coarse granite also intrudes an earlier amphibolite layer, but is itself cut by a later fine-grained granite showing only D^K_2 fabrics.

(2) 'Middle Breakfast Creek' dating site, Grid Reference 982234; low hills immediately north of Middle Breakfast Creek in the middle of the Wonga Belt. At the dating site (Pearson & others, this volume, fig. 23), one of the youngest Wonga Granite phases, showing no D^K_1 fabrics, contains xenoliths of already foliated coarse metagranite. The area around the dating site is a D^K_1 low-strain zone, and exhibits many examples of narrow cross-cutting D^K_1 shear zones (locally mylonitic) forming a coarse lozenge-shaped network. About 100 m north of



Fig. 21(a). Intrusive relationships at Greens Creek, Rosebud. (a) Coarse metagranite ('Highway phase') cuts amphibolite (black) and fine-grained previously mylonitised metagranite (fine lamination) layers. A later aplitic rock (near hammer) cuts all units. See text for details. Hammer is 30 cm long.

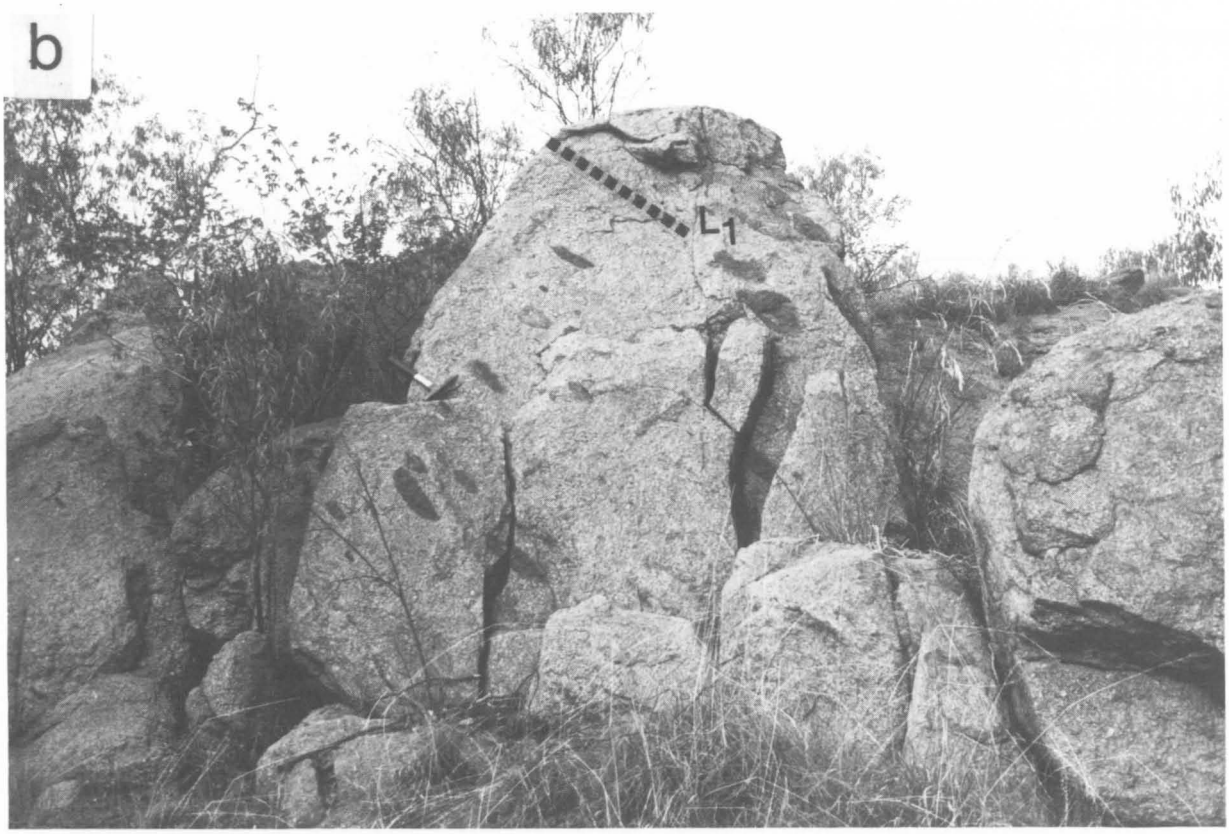


Fig. 21(b). The L_1 extension lineation in the cross-cutting 'Highway phase' metagranite defined by elongate mafic xenoliths (this is the same outcrop shown in Fig. 8).

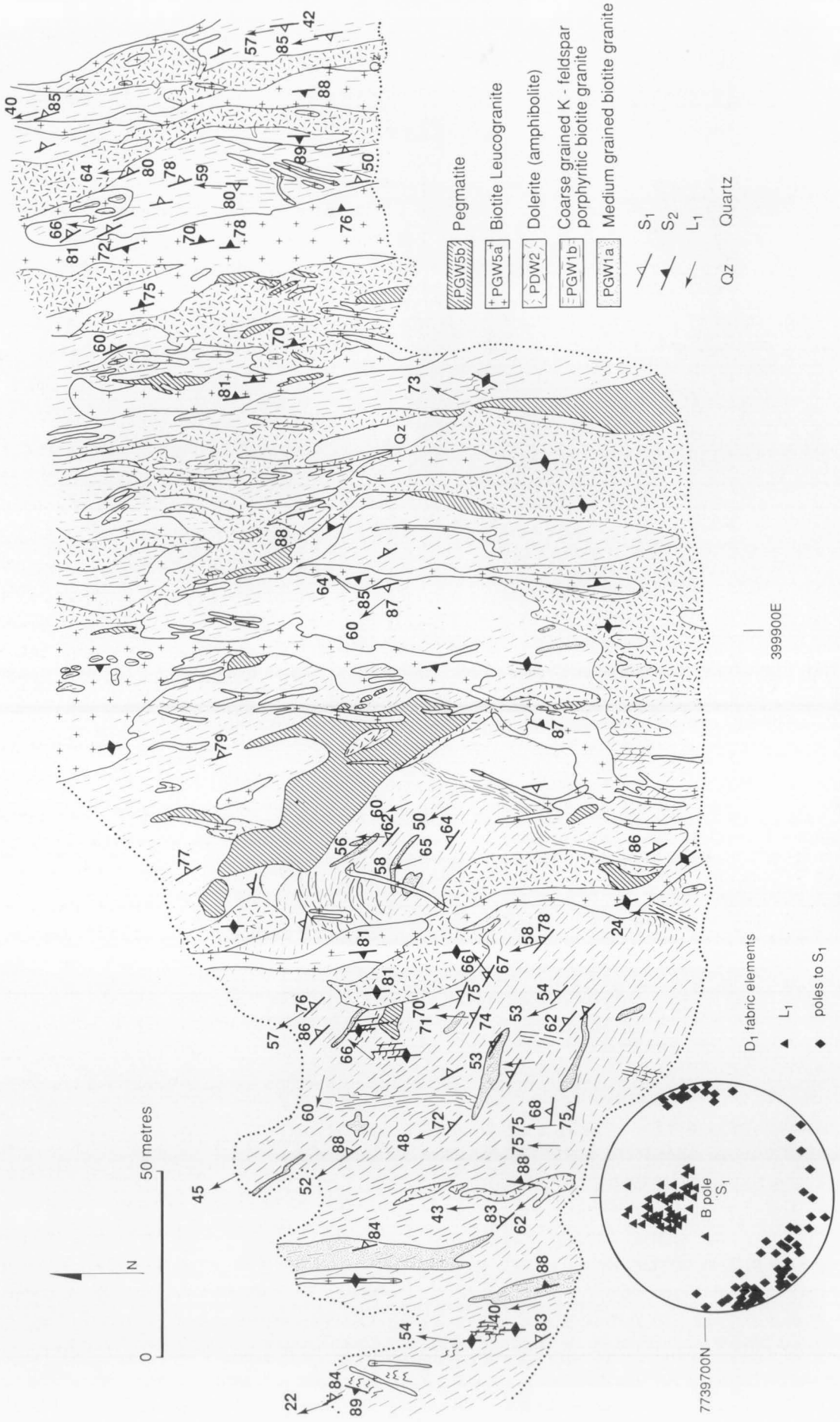


Fig. 22. Geologic and structural map of the Mount Maggie area.

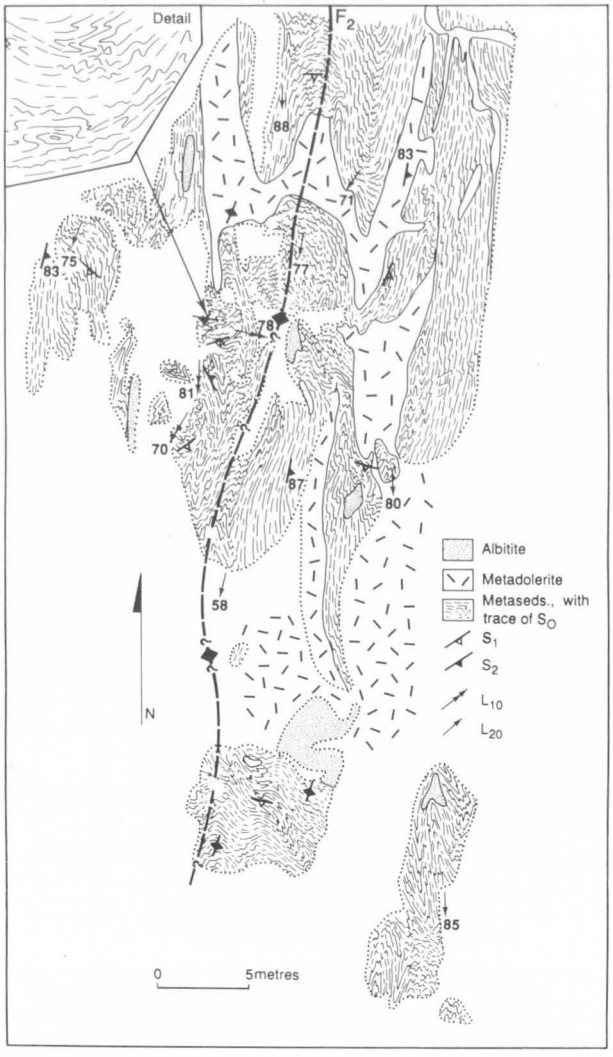


Fig. 23. Details of mapping in the 'Schist Hill' area showing the refolding of early D^{K}_{1} folds, metagranite, and metadolerite by D^{K}_{2}.

the dating site, a small dolerite body occupies a transtensional dilational site in a curved shear zone (Holcombe & others, 1991,Fig. 14).

(3) Mount Maggie, Grid Reference 999398, north of Dugald River; Mount Maggie is an area of low D^{K}_{1} and D^{K}_{2} strain (Fig. 22), showing folding of the D^{K}_{1} fabric and narrow shear zones by D^{K}_{2} (Fig. 15). A younger metagranite clearly truncates both the earlier D^{K}_{1} foliation and an older metagranite, but also contains the D^{K}_{1} fabric. The low D^{K}_{1} intensity is indicated by the orientation dispersion of the anastomosing shears, and the relative openness of both these and mesoscopic and macroscopic folds reflects the low D^{K}_{2} strain.

(4) The 'Knob' dating site, Grid Reference 950030, prominent small knolls immediately east of the old paved road between the old Mary Kathleen township and the MKU Mine; the dating site is on the northside of the lower, northernmost knoll. The 'Knob' (Pearson & others, this volume, fig. 20) is an area of low D^{K}_{1} strain in a D^{K}_{2} hinge area. The early D^{K}_{1} fabric is folded into angular symmetrical folds and is particularly well shown on the southern face of the smaller knoll. Immediately to the east of the 'Knob' is a D^{K}_{1} very high-strain zone. Metagranite bodies show a very strong moderately plunging D^{K}_{1} extension lineation defined by extremely elongate xenoliths.

(5) 'Schist Hill', Grid Reference 987216, north of Middle Breakfast Creek adjacent to the road going north from Lime Creek Mine is an area of very high D^{K}_{2} strains in sillimanite-bearing metapelite. D^{K}_{1} folds and D^{K}_{1}/D^{K}_{2} interference folds are common (Fig. 23). The most remarkable aspect of this area is the strong down-dip L_2 extension lineation bisecting the strongly curved (doubly plunging) L_{21} intersection lineation on very planar S_2 foliation surfaces. The area illustrates the parallelism of the L_1 extension lineation in metagranite and the L_{10} intersection lineation in adjacent metapelite, both of which are strongly curved. Small metagranite sills and their included early D^{K}_{1} fabric are folded around D^{K}_{2} hinges. The S_2 foliation crenulates early (pre-D^{K}_{2}) sillimanite, and syn-D^{K}_{2} sillimanite defines the down-dip D^{K}_{2} extension lineation. The area also contains late syn-D^{K}_{2} pegmatites.

(6) Greens Creek, west of Lake Corella, Grid Reference 963960, just above entrance of creek into Lake Corella - see inset map in Holcombe (1991); large bleached pavements in the high-strain marginal zone of the Wonga Belt, contain metasediment, amphibolite, and various metagranites, including early coarse augen granite and the Young Leucogranite (see Pearson & others, this volume). The outcrops are cut to multiple D^{K}_{1} shears, and it is the pervasive albitic alteration associated with these shears that gives the outcrop its bleached appearance (Fig. 12). There are numerous examples of albitic alteration associated with dilational gash veins formed in these shears. A dyke of the 'Late Leucogranite', which elsewhere shows little evidence of D^{K}_{1} deformation, here contains the D^{K}_{1} lineation fabric, and transgresses both early D^{K}_{1} shears and the associated albitic alteration (thus showing the synkinematic nature of this metasomatism). Areas of metasediment contain arrays of complexly folded quartz veins, superficially resembling migmatite structures.

Page 288 is blank.

Synkinematic emplacement of the Middle Proterozoic Wonga Batholith into a mid-crustal extensional shear zone, Mount Isa Inlier, Queensland, Australia

P. J. Pearson [1], *R. J. Holcombe* [2], *& R. W. Page* [3]

This paper is based on the following maps:

Holcombe, R.J., 1991 - Geology of the Mary Kathleen Area (1:25 000 scale map). Bureau of Mineral Resources, Canberra (two sheets).

Oliver, N.H.S., 1991 - Geology of the Mount Godkin Area (1:25 000 scale map). Bureau of Mineral Resources, Canberra.

Pearson, P.J., & Holcombe, R.J., 1991a - Geology of the Breakfast Creek Area (1:25 000 scale map). Bureau of Mineral Resources, Canberra.

Pearson, P.J., Horton, J.A., & Holcombe, R.J., 1991b - Geology of the East Limb, Little Beauty Syncline (1:15 000 scale map). Bureau of Mineral Resources, Canberra.

Regional east-west shortening at about 1550 Ma in the Mary Kathleen Fold Belt of the Mount Isa Inlier exposed different levels of an early extensional shear zone, which comprises an upper and lower plate separated by a mylonitic decollement. The extensional zone was intruded by voluminous bimodal igneous rocks of the Middle Proterozoic Wonga Batholith, consisting of A- and I- type felsic intrusions intimately associated with coeval tholeiitic mafic intrusions. Detailed field and fabric studies show that the intrusions were emplaced into the shear zone during extension, here designated D^W. Originally vertical variations in the style of extensional structures governed the shapes and deformational fabric of the intrusions. Emplacement into syn-D^W dilational sites occurred in both the upper and lower plates of the extensional system. Intrusive rocks in the pervasively sheared lower plate formed sills, which were progressively streaked out by ongoing D^W deformation. In contrast, sills, dykes, and apophyses in the heterogeneously sheared and stretched upper plate were much less modified by ongoing D^W deformation. Wonga Batholith intrusions display similar relative timing relationships to D^W in both the lower and upper plates of the system, and so demonstrate that D^W deformation was broadly synchronous in both. Three new ion-probe U-Pb zircon dates on the Wonga Batholith (1758 ± 8 Ma, 1742 ± 13 Ma and 1729 ± 5 Ma) date this regional (and probably continental-scale) deformation to between 1760 and 1720 Ma. Unlike the Phanerozoic low-angle mylonitic detachment terranes in the Basin and Range Province of the USA, the Wonga Batholith intrusions extensively intruded and contact metamorphosed both the lower and upper plates of the extensional system. We interpret this difference as a result of different large-scale extensional geometries, and invoke the delamination model (Lister & others, 1986) for this mid-Proterozoic intracratonic extension.

[1] Mount Isa Mines Exploration Pty. Ltd., Star Gully Office, Locked Bag Box 100, Mount Isa, Qld 4825.

[2] Department of Earth Sciences, University of Queensland, Qld 4072.

[3] Bureau of Mineral Resources, Geology and Geophysics, c/o Research School of Earth Sciences, Australian National University, GPO Box 4, Canberra, ACT 2601.

Introduction

Voluminous bimodal igneous rocks in many Australian Proterozoic provinces are geochemically distinct from their Archaean and Phanerozoic counterparts (Wyborn & others, 1987, 1988). U-Pb zircon dating indicates that Proterozoic magmatism occurred in distinct cycles or pulses (Wyborn & others, 1987, 1988). Magmatic cycles were separated by tens to hundreds of millions of years, and commonly are correlatable at continent scale. Magmatism occurred in intracratonic extensional settings, shown both by the bimodal compositional variation of the igneous rocks (Martin & Piwinskii, 1972) and by the broad association of the intrusive rocks, their coeval volcanic

rocks, and thick basin-fill sequences (Etheridge & others, 1987). However, except for the eastern Arunta Block of central Australia (Ding & James, 1985, 1987; James & Ding, 1987), little evidence has yet been documented that unequivocally relates emplacement of these major igneous suites to mid- to upper-crust extension.

In the Proterozoic Mount Isa Inlier of northwestern Queensland, major magmatic pulses occurred at approximately 1870 to 1840 Ma, 1800 to 1780 Ma, 1760 to 1720 Ma, 1670 to 1650 Ma, and 1500 Ma (Blake, 1987; Wyborn & others, 1987, 1989; Connors & Page, 1992). Bimodal intrusive rocks emplaced between about 1760 and 1720 Ma make up the extensive Wonga Batholith in the Mary Kathleen Fold Belt (Blake, 1987). Strong upright folding during crustal shortening at approximately 1550 Ma exposed different structural levels of an early extensional system into which the plutons making up the batholith were intruded, and thus affords an excellent opportunity to study the link between Proterozoic extensional structures and magmatism. This paper details recent structural work that demonstrates such a link, and presents new geochronological data that constrain this extensional deformation.

Deformation episodes in the area described in this paper are denoted by the superscript 'W' Grid references are located in the maps listed above (Holcombe, 1991; Oliver, 1991; Pearson, 1991a, 1991b) except where otherwise indicated.

Structural setting of Wonga Batholith intrusions

The Wonga Batholith (Blake, 1987) comprises numerous felsic and mafic igneous intrusions that cut Middle Proterozoic cover sequences in the Mary Kathleen Fold Belt of the Mount Isa Inlier (Fig. 1). The intrusions have been variously deformed, and range from ultramylonitic gneisses to weakly foliated igneous rocks. However, geochemical and isotopic dating results suggest that these variants are all parts of the same cogenetic suite. The intrusions crop out in a north-south elongate zone approximately 190 km long, and intrude cover sequences 1 and 2 defined by Blake (1987). Cover sequences 1, 2, and 3 encompass all exposed Lower and Middle Proterozoic sedimentary and volcanic rocks in the Inlier (Blake, 1987), and represent at least three distinct cycles of basin fill. The Mary Kathleen Fold Belt (Carter & others, 1961; Holcombe & Fraser, 1979; Holcombe & others, this volume) is the strongly deformed and regionally metamorphosed zone between the Kalkadoon-Leichhardt basement block to the west and the Pilgrim Fault Zone to the east (Fig. 1). In essence, the Fold Belt can be subdivided into three broad north-trending domains on the basis of deformational style. The central domain, known as the Wonga Belt, is a north-trending 5 to 10 km-wide belt of anomalously high ductile D^W_1 strain that forms the core of an upright north-trending anticlinorium (F2), which is characterised by two ductile deformations (D^W_1 and D^W_2). Within the Wonga Belt, generally north-trending plutons of polydeformed and gneissic metagranitoid (the Wonga Granite) and associated metadolerite and metagabbro intrude metavolcanic and metasedimentary rocks of cover sequence 2, including the Argylla Formation, Ballara Quartzite, and Corella Formation. Complex intertonguing and veining relationships are common between the felsic and mafic intrusions. In the Duchess area to the south (Fig. 1), the Wonga Belt narrows to about 2 km and is called the 'Shinfield Zone' (Passchier, 1986). Symmetrically flanking the Wonga Belt are the Eastern and Western Domains (Figs. 1, 2), characterised by only the second deformation (D^W_2). Holcombe & others (1987, 1991, this volume), Pearson & others (1987), and Pearson (1989) have interpreted the Wonga Belt as a kilometres-thick, originally subhorizontal zone of intense early ductile extensional deformation (D^W_1) that has been folded into its present shape by upright folding (D^W_2), which accompanied peak regional metamorphism.

The Eastern Domain comprises a thick, complexly folded and faulted sequence of largely metasedimentary rocks assigned to cover sequence 2 (Oliver, 1988; Oliver & others, 1991). Large plutons of inhomogeneously foliated metagranitoid of the Wonga Batholith (the Burstall and Mount Godkin Granites) and dykes and sills of metagabbro and metadolerite cut the metasedimentary sequence in the centre and north of the Mary Kathleen Fold Belt. In addition, numerous small fine-grained to pegmatitic felsic pods intrude the Corella Formation between the Mount Godkin and Burstall plutons, and are probably of similar age and affinity. To the south, flanking the Shinfield Zone, correlatives of these intrusive units include the Revenue and Overlander Granites, and the Mount Erle and Myubee Igneous Complexes (Blake, 1987; Passchier, this volume).

The Western Domain is a less complexly folded, but extensively faulted sequence of metasedimentary, metavolcanic, and meta-intrusive rocks of cover sequences 1, 2, and 3 (Derrick & others, 1977; Loosveld & Schreurs, 1987; Williams & others, 1987). Immediately west of the

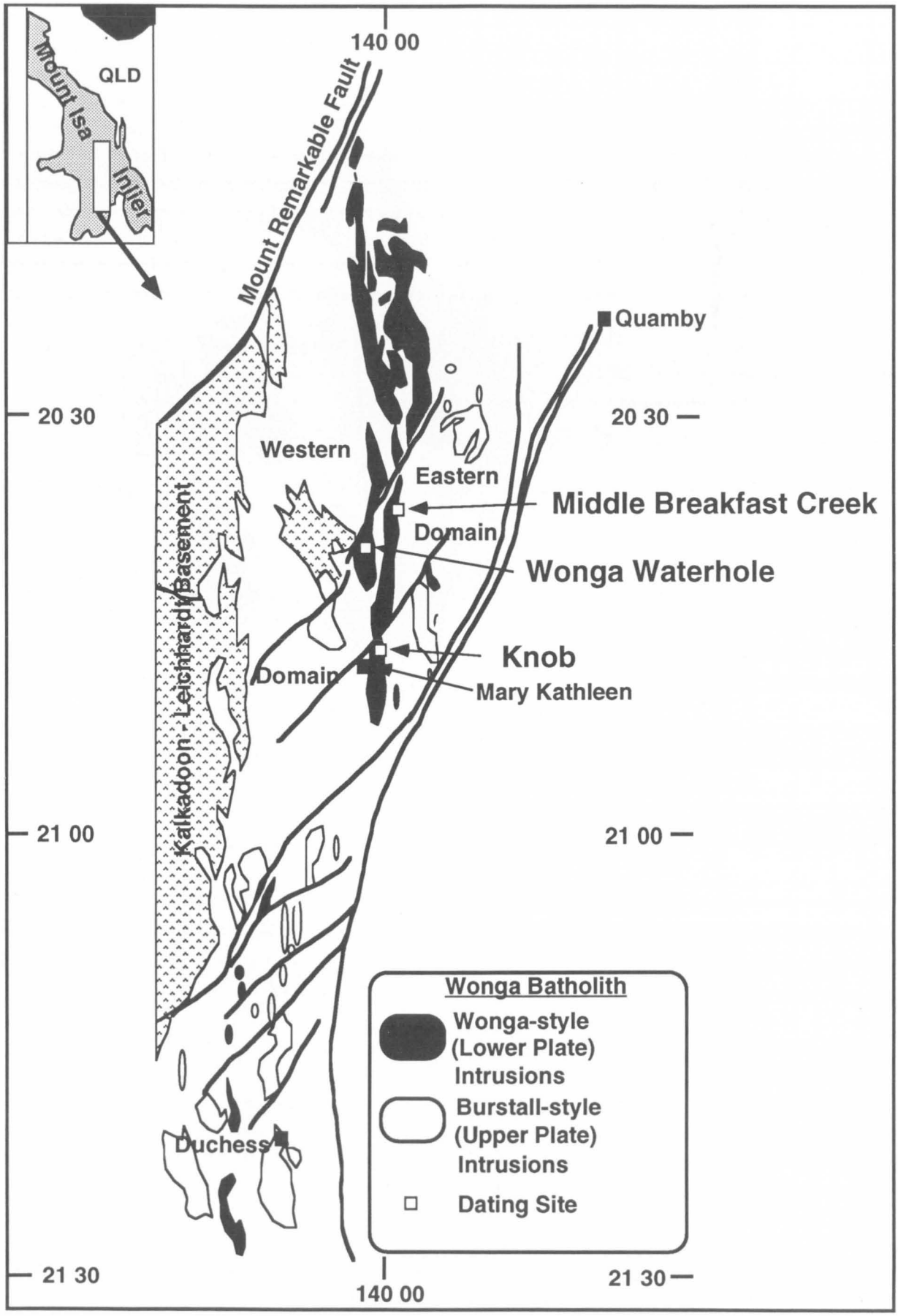


Fig.1. Locality map showing the Mount Isa Inlier, Mary Kathleen Fold Belt, and distribution of the Wonga Batholith.

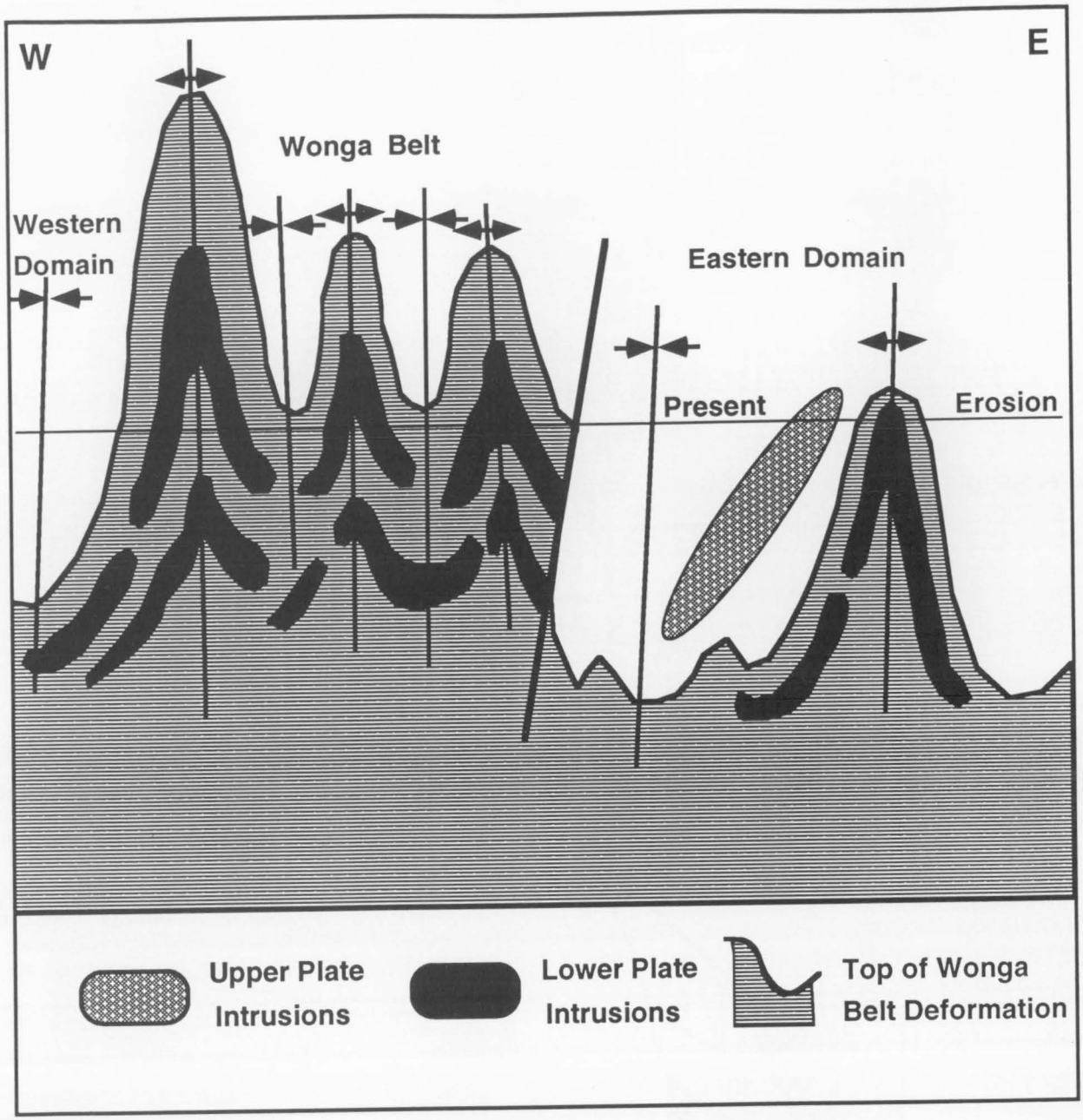


Fig. 2. Schematic cross-section through the Mary Kathleen Fold Belt, showing distribution of lower and upper plate intrusions.

Wonga Belt, Pearson (1989) mapped early high-angle normal brittle-ductile shear zones that are folded about a large F_2 syncline (Little Beauty Syncline). Early displacements on these shear zones caused large-scale block faulting and tilting of cover sequence 2, and resulted in regionally anomalous F_2 fold axis orientations. Similar high-angle structures have been mapped south and west of the Wonga Belt by Passchier (1986), Williams & others (1987), Passchier & Williams (1989), and Williams (1989). Cover sequences 1 and 2 in the Western Domain are also intruded by Wonga Batholith intrusions, represented by metagranitoid sills and dykes of the Hardway Granite, and by numerous metadolerite sills and dykes.

Detailed structural studies (Holcombe & others, 1987; Pearson & others, 1987; Oliver, 1988; Pearson, 1989) indicate that the Mary Kathleen Fold Belt underwent four deformational episodes of Middle to Late Proterozoic age. The deformations (designated D^W_1, D^W_2, D^W_3, and D^W_4) affected 1880 Ma to 1760 Ma-old volcano-sedimentary cover sequences and 1760 Ma to 1720 Ma-old felsic and mafic intrusive rocks.

D^W_4 involved localised brecciation, shearing, and folding in the hornfelsic contact aureoles of steeply

dipping post-orogenic dolerite/gabbro dykes (Pearson, 1989). The dykes are part of the Lakeview Dolerite Swarm dated by Page (1983b) at about 110 Ma.

Deformations D^W_2 and D^W_3 are part of a post-depositional orogeny (the Isan Orogeny of Blake & others, 1990) that terminated the Middle Proterozoic tectonic cycle proposed by Etheridge & others (1984, 1987). D^W_2 involved regional east-west crustal shortening that produced tight doubly plunging north-trending upright folds and an accompanying axial plane fabric at peak regional metamorphic grade. Variously oriented kink sets, attributed to late relaxation, overprint the earlier fabrics. D^W_3 involved conjugate strike-slip brittle-ductile shearing and kinking accompanied by retrogression. Based on the inferred similarity of their bulk kinematics, the D^W_3 deformation may be a late retrograde episode of progressive D^W_2 east-west shortening (Derrick & others, 1977; Oliver, 1988; Valenta, 1988).

Abundant evidence for pre-D^W_2 deformation (D^W_1) at 1760-1730 Ma occurs in cover sequence 2 and Wonga Batholith intrusions within and around the Wonga Belt. We argue below that the section exposed in the Wonga Belt and its flanking domains exposes an early extensional terrane floored by a mylonitic detachment zone.

Composition and texture of the intrusive rocks

The Wonga Batholith is a bimodal igneous suite (Blake, 1987; Wyborn & others, 1987, 1988) dominated by biotite- and/or amphibole-bearing metagranitoid (Pearson, 1989). Metagabbro and/or metadolerite are subordinate. In all felsic intrusions, abundant hornblende, biotite, and titanite, and the absence of cordierite, andalusite, and primary muscovite, suggest I-type or A-type, rather than S-type, affinities (Chappell & White, 1974; Collins & others, 1982; Wyborn & others, 1987, 1988). Mafic intrusions of the Wonga Batholith possess the geochemical signature of continental tholeiites (Ellis & Wyborn, 1984; Hamilton, 1985).

Fourteen mappable granitic types are distinguished by variations in the abundance and size of phenocrysts, the relative modal abundances of feldspars and quartz, the total ferromagnesian content, the relative modal abundances of biotite and amphibole, and the grainsize and accessory minerals of the groundmass (Table 1).

Figure 3 depicts the relative modal abundances of quartz, K-feldspar, plagioclase, and mafic minerals in representative samples of each type The felsic intrusions contain 20 to 50% quartz, and range from alkali granite to tonalite (Streckeisen, 1976), clustering in the field of true granite (syeno- to monzo-granite). This pattern is further strengthened by incorporation of modal data from Derrick & others (1977).

Significant compositional overlaps occur between the various igneous types (Fig. 3). However, individual intrusions generally occupy well defined fields with respect to the total modal abundances of mafic minerals, even though the total mafic mineral content ranges from 0 to 28% in the samples studied. Accessory minerals include titanite, apatite, zircon, fluorite, allanite, and tourmaline. Metasomatic alteration products include muscovite, scapolite, chlorite, and some opaques.

The original textures of the felsic intrusions are preserved in restricted zones of relatively low strain, and are transitional into mylonitic gneisses in zones of relatively high strain. Distinction here is based only on their modal composition.

Only a few granitic variants are recognised in the Eastern and Western Domains.

In the Eastern Domain, the Burstall Granite pluton comprises a coarse-grained porphyritic K-feldspar, biotite-amphibole granite and a finer leucocratic more even-grained marginal granite (Derrick, 1978; Jorgensen, 1986; Sliwa, 1986). These two granites may correlate respectively with Pgw_{1b} and Pgw_{5a} of the Wonga Belt. The Mount Godkin pluton consists largely of a medium-grained irregularly foliated metagranite, although abundant finer-grained and pegmatitic rocks occur on its margins (Oliver, 1988).

In the Western Domain, melanocratic, fine to medium-grained porphyritic K-feldspar and/or plagioclase, amphibole and/or biotite granite is correlated with Pgw_{2a} of the Wonga Belt; mesocratic to melanocratic fine-grained porphyritic quartz and K-feldspar, biotite and/or amphibole granite grading to alkali granite is correlated with Pgw_{2c}; and a leucocratic fine-grained variably porphyritic quartz and K-feldspar alkali granite is correlated with Pgw_{2d}. Dynamic recrystallisation of original minerals is ubiquitous.

Mafic intrusive rocks of the Wonga Belt and Eastern and Western Domains preserve their original gabbroic textures and minerals in zones of low ductile strain (Derrick, 1978; Pearson, 1982). Generally they grade into medium-grained amphibolite (amphibole + biotite + plagioclase + scapolite + titanite). In the Wonga Belt, many of the mafic rocks are represented by biotite schist.

Group	Description	Designation	Accessory Mineralogy Ap=Apatite Zr=Zircon Al = Allanite Sp=Sphene Fl=Fluorite Op=Opaques
Early medium- and coarse-grained granites	Leucocratic, medium-grained, biotite granite	1a	Ap-Zr-Fl-Al
	Mesocratic, coarse-grained, K-feldspar porphyritic, biotite and/or amphibole granite	1b	Ap-Sp-Zr-Fl-Al-Op
Granitoid porphyries	Melanocratic, fine to medium -grained, K-feldspar and/or plagioclase porphyritic, amphibole and/or biotite granite to tonalite	2a	Ap-Sp-Zr-Fl-Op
	Melanocratic, fine to medium-grained, K-feldspar, quartz, and plagioclase porphyritic, biotite and/or amphibole granite	2b	Ap-Sp-Zr-Fl-Op
	Mesocratic to melanocratic, fine-grained, quartz and K-feldspar porphyritic, biotite and/or amphibole granite to alkali feldspar granite	2c	Ap-Zr-Al-Op
	Leucocratic, fine-grained, variably quartz and K-feldspar porphyritic, alkali granite	2d	Zr-Al-Op
Medium- and coarse-grained granites	Melanocratic, medium- to coarse-grained, feldspar porphyritic, biotite-amphibole granite to granodiorite)	3a	Ap-Sp-Zr-Al-Op
	Mesocratic, medium-grained to slightly K-feldspar porphyritic, biotite and/or amphibole granite	3b	Ap-Zr-Al-Op
Circular Structure Granites	Melanocratic, medium- to coarse-grained K-feldspar porphyritic, biotite-amphibole granite	4a	No data
	Leucocratic to mesocratic, fine- to medium-grained, biotite leucogranite and aplite	4b	No data
Late leucogranites and pegmatites	Leucocratic to mesocratic, fine- to medium-grained, slightly K-feldspar porphyritic, biotite and/or amphibole granite	5a	Ap-Sp-Zr-Al-Op
	Leucocratic, coarse-grained, K-feldspar - quartz pegmatitic granite and pegmatite	5b	No data
	Leucocratic, coarse-grained, K-feldspar and plagioclase porphyritic, amphibole granite	5c	No data
Syn-D_2 pegmatites	Leucocratic, coarse-grained, K-feldspar - quartz-muscovite-tourmaline pegmatite	6	No data

TABLE 1. PETROGRAPHY OF FELSIC INTRUSIONS IN THE WONGA BATHOLITH.

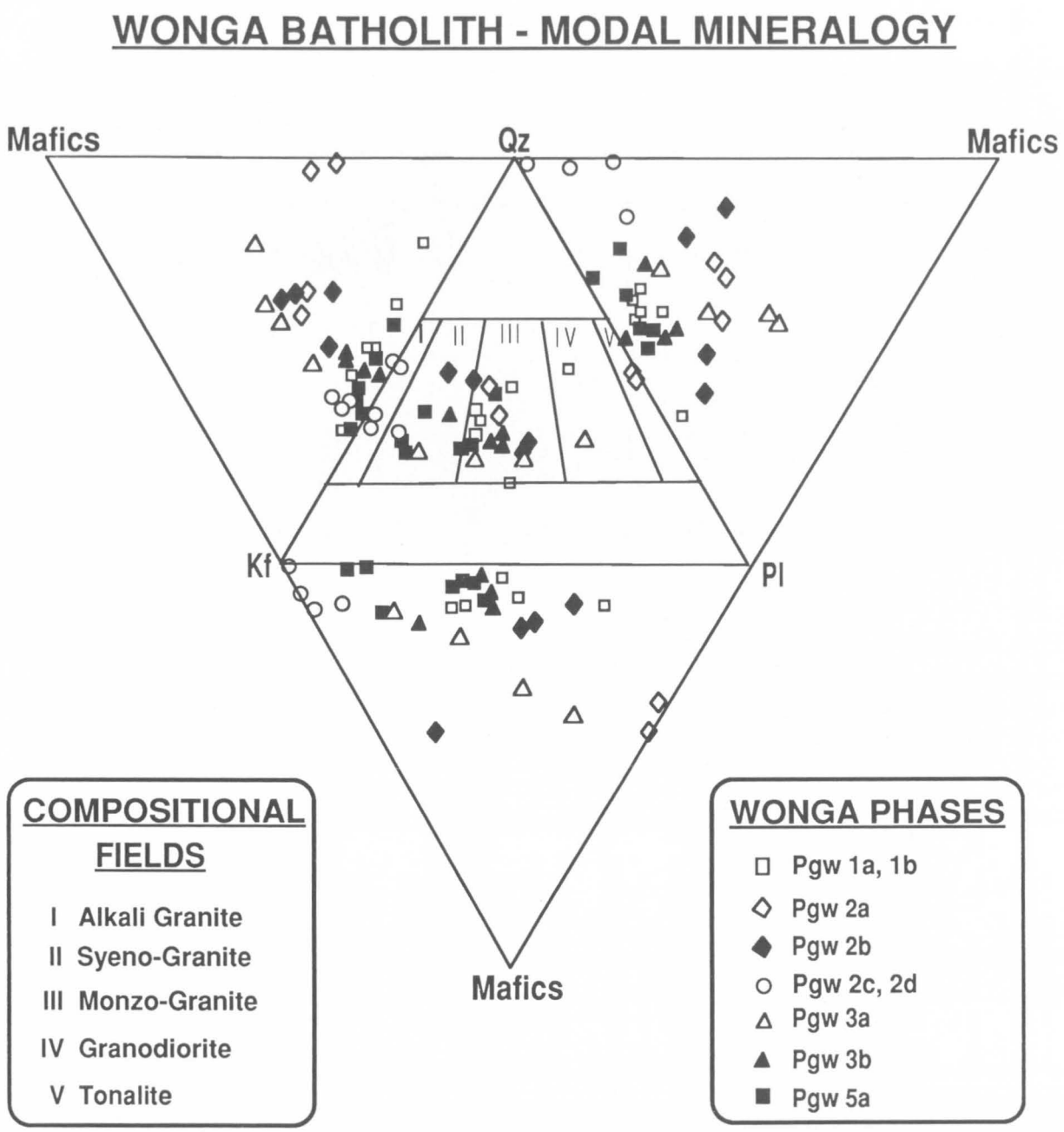


Fig. 3. Modal mineralogy ternary diagrams for felsic intrusions of the Wonga Batholith.

Geometry and contact relationships of intrusions

The Wonga Batholith intrusions range from simple concordant lenses, sills, or pods to complex networks of discordant veins or dykes. A few xenoliths from adjacent earlier intrusions or from the surrounding country rocks occur locally. Relatively passive emplacement, with only minor stoping and wallrock assimilation, is inferred.

Felsic rocks

Felsic intrusions occupy 20 to 40% of the Wonga Belt. The earlier intrusions crop out over tens of square kilometres and are injected by later discordant bodies. Many felsic intrusions originally formed concordant bodies or sills up to hundreds of metres thick, and were tightly folded by D^{w}_{2}. This is based on the following field observations:

- Intrusions trend north-south and occupy the cores of regional F_2 folds. Where tops and bottoms are exposed, the plutons are commonly at least 1 km thick;
- Intrusive contacts generally parallel primary layering and the S_1 foliation in the enclosing country rocks, particularly around F_2 fold closures (Fig. 4).

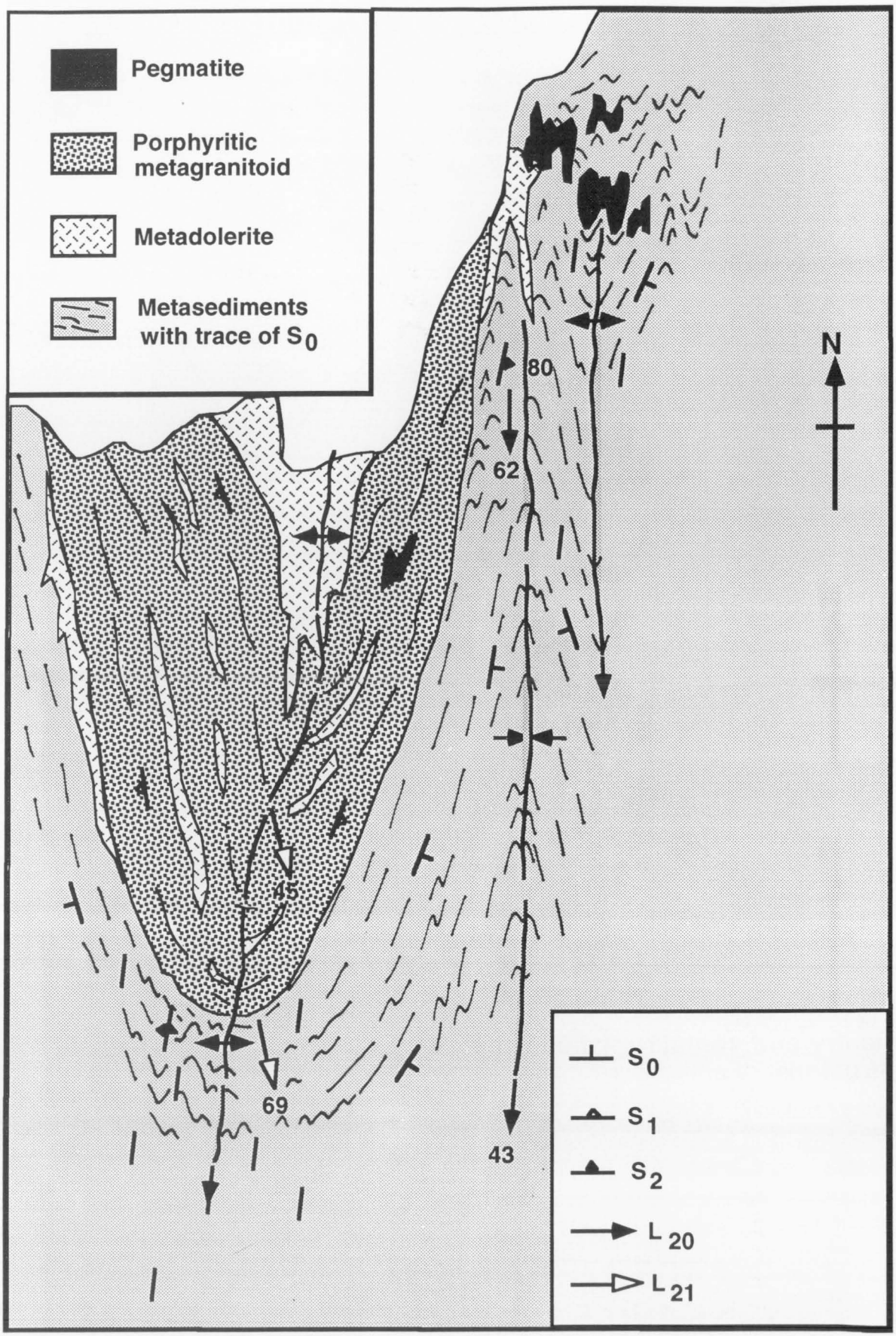


Fig. 4. Outcrop map showing a felsic porphyry sill (Pgw_{2a}) intrusive into pelitic metasedimentary rocks and folded by an F_2 fold in the Schist Hill area (grid reference 990223).

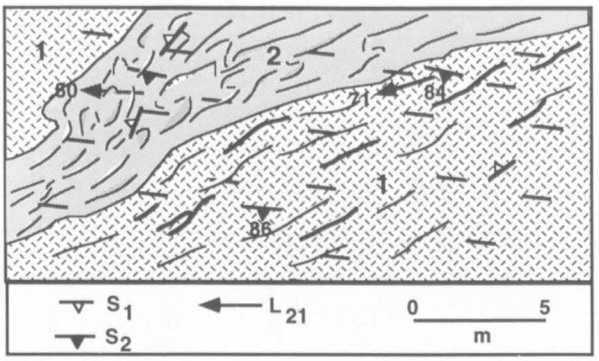


Fig. 5a. Outcrop map showing F_2 folds in a Pdw_1 dolerite sill (1) contact in the Lime Creek area (grid reference 972168). Note the broad parallelism between the intrusive contact, primary layering in the pelitic metasedimentary country rocks (2), and the S_1 foliation in both dolerite and country rocks.

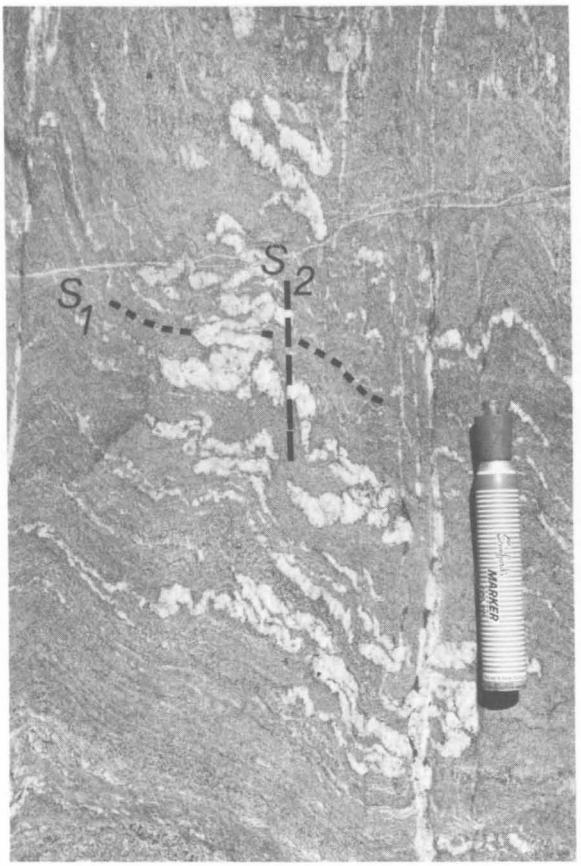


Fig. 5b. Field photograph showing how the axial planes of refolded originally recumbent F_1 folds in quartz-rich segregation veins in the country rocks parallel the dolerite contact at the above locality. The overprinting S_2 foliation is a high-grade schistosity/crenulation cleavage paralleling quartz-magnetite vein sets. The pen is 12 cm long.

Later felsic intrusions are more complex in outcrop, with discordant contacts. Relatively late granitic and pegmatitic dykes, veins, and apophyses form networks cutting both country rocks and earlier intrusions and their primary layering and D^W_1 foliation (see below and Fig. 21 of Holcombe & others, this volume).

Felsic intrusive rocks of the Eastern and Western Domains form thick sills, pod-like stocks, or complex dyke systems parallel to D^W_1 extension fractures or shear zones.

The Burstall Granite (Derrick & others, 1971; Derrick, 1977, 1978; Oliver, 1981; Jorgensen, 1986; Sliwa, 1986) and Mount Godkin Granite (Oliver, 1988) are thick folded granitic sheets. Detailed work by Sliwa (1986) indicates that the main Burstall pluton is an approximately 1 km-thick tabular body which broadly parallels the enclosing Corella Formation (Fig. 2). Both the Burstall and Mount Godkin Granites display complex net-veining relationships with associated tabular mafic intrusions (Derrick, 1978; Blake, 1981). Garnet and pyroxene exoskarns are extensive in their contact aureoles (Derrick, 1977; Cruikshank & others, 1980; Oliver, 1988).

On the eastern limb of the Mary Kathleen Syncline, numerous fine-grained felsic dykes emanating from the main Burstall pluton form a reticulate swarm within the enclosing country rocks. Dykes were commonly emplaced into steep east-west and north-south fractures. The low D^W_2 strains here suggest that the angular relationships between the dykes are probably preserved, and that they have been only passively rotated with the fold limb.

Sills and dykes of Wonga felsic rocks intrude both the eastern and western limbs of the Little Beauty Syncline in the Western Domain. There a thick Pgw_{2a} sill intrudes the Ballara Quartzite, and is cut by D^W_1 high-angle normal shear zones. Thin dykes of other Pgw_2 rock types have been emplaced along these shear zones.

Mafic rocks

Mafic intrusive rocks of the Wonga Batholith comprise 20 to 40% of the total outcrop area of the Wonga Belt, and continue into the structurally higher flanking domains. The earliest mafic intrusions are complex elongate dykes and sills linked by sheets, and range up to hundreds of metres thick. Like the earliest felsic intrusions, their contacts are broadly parallel to primary layering and the S_1 foliation around F_2 fold closures (Figs. 5a, b), indicating their original sill-like form. Later mafic intrusions form extremely complex anastomosing discordant dykes, which cut primary layering and the S_1 foliation in the country rocks and earlier mafic intrusions (Fig. 21 of Holcombe & others, this volume).

Some felsic and mafic intrusive types exhibit net-veining relationships, e.g., in the 'Circular Structure'

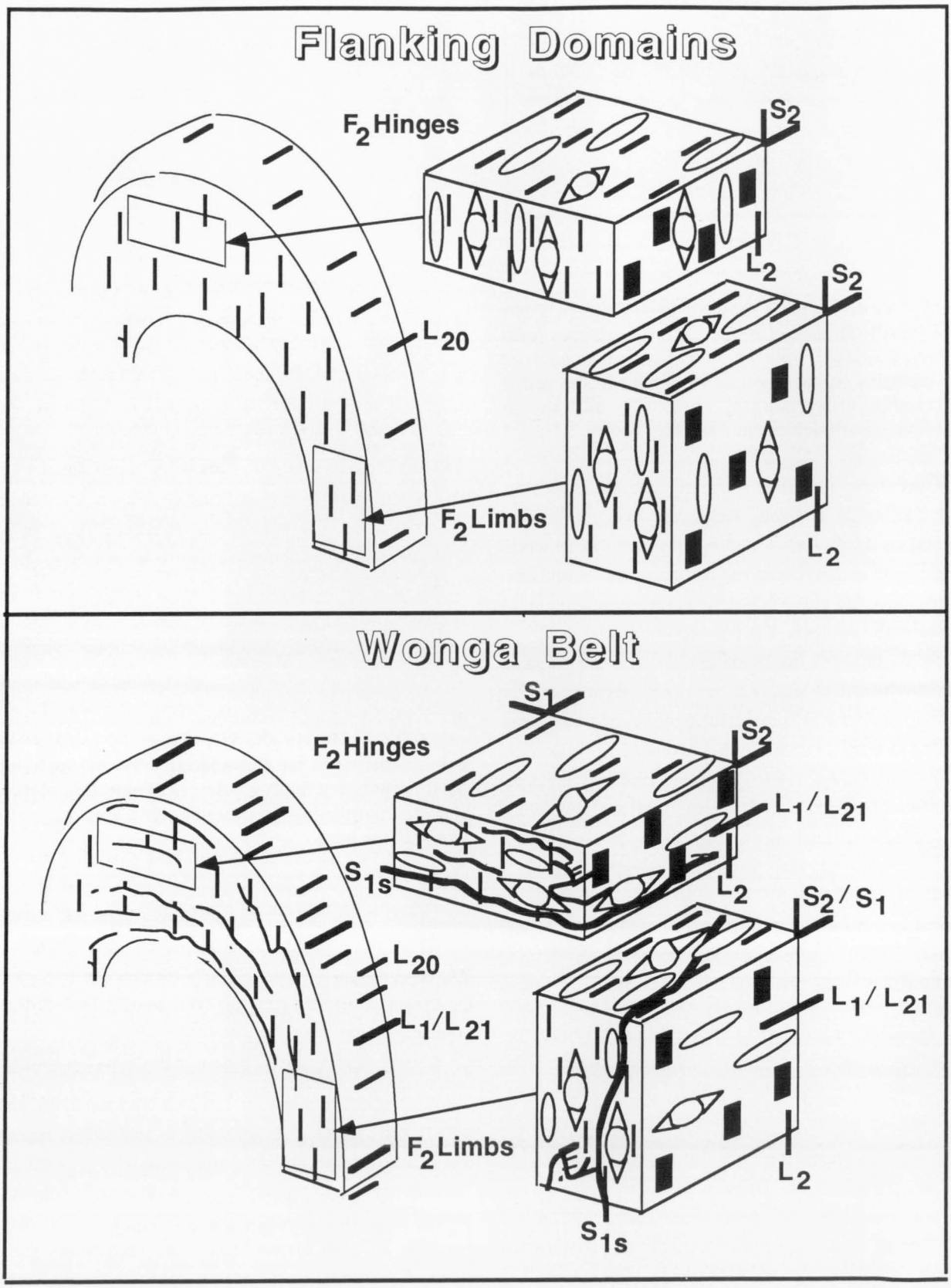


Fig. 6. Schematic diagram contrasting the D^{W}_{1} fabric of the Wonga Belt (a) with that in the flanking domains (b). Bold lines represent shear bands and recumbent folds.

centred on grid reference 953503 in Prospector 1:100 000 Sheet area in the north of the Wonga Belt, which indicate coeval felsic and mafic melts (Blake, 1981). Invariably, veining and xenolith relationships suggest that the mafic rock crystallised first.

Thick mafic sills are exposed in the cores of the Mary Kathleen, Little Beauty, and Rosebud Synclines. On the eastern limb of the Little Beauty Syncline, anastomosing Pdw_2 dykes form a continuous swarm between the Wonga Belt and the adjacent Western Domain. Within the Western Domain, the dykes cut across bedding within imbricates bounded by D^w_1 high-angle shear zones, or alternatively are intruded along the shear zones themselves. These relationships are identical to those described by Passchier (1986), Passchier & Williams (1989), and Williams (1989) from areas between 50 and 100 km to the south.

Fabric development in the intrusive rocks

Wonga Belt

A strong subvertical gneissic foliation bearing two extensional lineations dominates nearly all rock types within the Wonga Belt (Pearson, 1989; Holcombe & others, this volume). In felsic and mafic rocks, the foliation is defined by: flattened leaves of recrystallised quartz; flattened K-feldspar and plagioclase porphyroclasts and their recrystallised tails; flattened aggregates of recrystallised and aligned amphibole, biotite, and titanite; and by flattened mafic xenoliths. Some rocks have a vague millimetre- to centimetre-scale compositional banding, generally defined by variations in grainsize and/or ferromagnesian content.

The earliest most variably oriented extension lineation (L_1) is defined by the long axes of strongly elongated mineral aggregates or xenoliths within the foliation (Fig. 6). An overprinting fairly constantly oriented extension lineation (L_2) is defined by the down-dip alignment of the long axes of biotite or amphibole crystals within the foliation (Fig. 6).

The following evidence shows that the apparently simple gneissic fabric present throughout the Wonga Belt is a composite D^w_1/D^w_2 fabric resulting from overprinting of the D^w_1 structures by tight F_2 folds and crenulations attributed to D^w_2 (Pearson, 1989):

- the lateral transition of the Wonga Belt fabric (subvertical foliation with two extension lineations) dominating F_2 fold limbs into areas representing hinge zones, where abundant F_2 crenulations in S_1 foliation occur;
- syn-D^w_2 garnet porphyroblasts in biotite schist (metadolerite) contain relics of an S_1 foliation which is crenulated about F_2 axial planes. However, evidence for S_1 has been largely obliterated in the matrix;
- some dykes truncate an S_1 foliation in their host rocks, but the dykes themselves bear a strong S_2 schistosity at an angle to the truncated S_1 foliation. If the S_1 foliation lies in the shortening field of D^w_2 strain, S_2 in the discordant dykes parallels the axial planes of adjacent F_2 crenulations in S_1.

Table 2 lists the components of the overprinted D^w_1 fabric in the Wonga Belt and flanking domains. As shown in Figure 6, the D^w_1 fabric is a composite of an early penetrative foliation (S_1) and an extension lineation (L_1), early mesoscopic shear bands (S_{1s}) cutting S_1, and early recumbent folds (F_1).

Geometric, fabric, and kinematic arguments suggest that D^w_1 structures in the Wonga Belt developed in a zone of subhorizontal shear with the hanging wall block displaced to the north under amphibolite facies conditions (Pearson & others, 1987; Pearson, 1989; Holcombe & others, this volume). The result is that D^w_1 shear sense indicators, now rotated by D^w_2 folding, systematically switch apparent shear sense across F_2 fold axial planes. A possible reversal in D^w_1 shear sense occurred in the northwestern Wonga Belt (Little Beauty Syncline) across a postulated steep transfer zone; there, most kinematic indicators suggest an anomalous shear sense implying displacement of the hanging wall to the south when unfolded.

We conclude that deformation of this style occurred in the lower plate of a D^w_1 extensional system (Holcombe & others, this volume). This conclusion is based on:

- the style, and generally consistent shear sense of an early ductile subhorizontal shear fabric in the Wonga Belt (the lower plate);
- the general absence of early older-on-younger structures. In contrast, early younger-on-older high-angle normal shear zones are common in the structurally higher rocks (the upper plate) now exposed in the flanking Eastern and Western Domains;

	Western Domain			Wonga Belt			Eastern Domain		
Fabric Element	Distrib.	Units	Descript.	Distrib.	Units	Descript.	Distrib.	Units	Descript.
S_1	local.	all	mylonitic schistosity	pervasive	all, except Pgw5,6	mylonitic/ gneissic schistosity	local.	all	mylonitic schistosity
L_1	local.	all	mylonitic extension lineation	pervasive	all, except Pgw5,6	mylonitic/ gneissic extension lineation	local.	all	mylonitic extension lineation
L_{10} (BS^1S_0)	local.	all	axes of F_1 folds, intersection lineation	pervasive	all, except Pgw5,6	axes of F_1 folds, intersection lineation	local.	all	axes of F_1 folds, intersection lineation
S_{1s}	–	–	–	local.	all	mylonitic shear bands	–	–	–
L_{1s}	–	–	–	local.	all	mylonitic extension lineation	–	–	–
S_{1e}	local.	Ballara, Corella	extension fractures	–	–	–	local.	Ballara, Corella	extension fractures

TABLE 2. COMPONENTS OF THE DEFORMATIONAL FABRICS OF THE WONGA BELT AND FLANKING DOMAINS.

- the inferred original parallelism of early stretching lineations, reflecting bulk extension directions, in both the Wonga Belt and the flanking domains;
- the synchronous emplacement of bimodal Wonga Batholith intrusions into both the lower and upper plates during early ductile (lower plate) and brittle-ductile (upper plate) deformation.

Eastern and Western Domains

Table 2 lists the components of the D^W_1 fabric in the Eastern and Western Domains, and contrasts it with that in the Wonga Belt. Figure 6 shows the elements of the D^W_1 fabric. The D^W_2 fabric consists of a generally subvertical north-striking S_2 schistosity which is axial planar to F_2 folds and contains a down-dip L_2 mineral extension lineation (Fig. 6). Strain analysis (Holcombe, unpublished data; Pearson, 1989) shows that the S_2 foliation parallels the XY-plane, and L_2 parallels the X-axis of the D^W_2 finite strain ellipsoid.

The Burstall and Mount Godkin Granites of the Eastern Domain are more heterogeneously foliated than the felsic intrusions of the Wonga Belt. The bulk of this fabric is a simple D^W_2 fabric, although structural work by Sliwa (1986) suggests that pre-D^W_2 shear zones and folds developed around the northern margins of the Burstall pluton during granite emplacement.

Clearer evidence of inhomogeneous pre-D^W_2 fabric in the flanking domains occurs in the Little Beauty Syncline (Pearson, 1989). There, a mylonitic shear zone foliation (S_1) and stretching lineation (L_1) overprinted by the D^W_2 fabric occur in narrow zones up to several metres wide. These zones correspond to the traces of macroscopic high-angle normal pre-D^W_2 shear zones cutting up-section into the Argylla and Ballara formations. Metagranitoid and

metadolerite dykes emplaced into these zones possess a strong grain shape and mineralogically preferred composite D^W_1/D^W_2 fabric, whereas outside the shear zones they possess only the D^W_2 fabric.

Early brittle structures intimately associated with the pre-D^W_2 high-angle normal shear zones are common in the Little Beauty Syncline. These comprise zone-parallel veins, en-echelon veins, or saddle reefs overprinted by D^W_2 structures.

Spaced high-angle veins folded about F_2 axial planes are abundant in the Corella Formation. In some places, the frequency of these veins intensifies towards early high-angle shear zones with shallow stretching lineations, indicating that the veins accomodated subhorizontal stretching of layering during early shearing. Chaotic metasomatised breccias, with clasts now overprinted and aligned parallel to the D^W_2 fabric, are also common.

Geometric, fabric, and kinematic evidence suggest that D^W_1 structures in the flanking domains developed by north-south horizontal coaxial stretching and asymmetric boudinage of the beds by about 50% under greenschist to amphibolite facies conditions (Pearson & others, 1987; Pearson, 1989; Holcombe & others, this volume). We conclude that deformation of this style occurred in the upper plate of a D^W_1 extensional system.

Relative chronology of emplacement and fabric development of intrusions

Wonga Belt

Pre- to syn-D^W_1 intrusions

The earliest felsic and mafic rocks bear both a strong mylonitic D^W_1 fabric and the D^W_2 fabric, suggesting that their emplacement and crystallisation occurred pre- to syn-D^W_1. The microstructural character of the deformation fabrics clearly indicates that both the D^W_1 and the D^W_2 fabrics were imposed on igneous rocks that were already crystallised (Pearson, 1989). The strength of D^W_1 fabric suggests that emplacement and crystallisation were pre- to syn-D^W_1. These rocks tend to form concordant bodies, such as the Pgw_1 and Pgw_2 granitoids and the Pdw_1 dolerites, and are cut by later discordant intrusions.

Syn-D^W_1 intrusions

Felsic and mafic rocks assigned to this time range generally bear both a well developed D^W_1 fabric and the D^W_2 fabric, but also cut the D^W_1 fabric in earlier intrusions or in the country rocks. Their emplacement and crystallisation (as pulses) were clearly bracketed by D^W_1 deformation, suggesting a syn-D^W_1 age. These intrusions are themselves veined by later intrusions.

Included here are Pgw_3 granitoids (Fig. 20a of Holcombe & others, this volume) and Pgw_4 granitoids and their associated dolerites. Wispy equigranular pegmatitic patches and segregations generally truncate but do not possess the earlier fabric.

The Pgw_{4a} and Pgw_{4b} granitoids possibly correlate respectively with the widely distributed Pgw_{3a} and Pgw_{3b} granitoids, on the basis of similar composition, textures, and inferred timing with respect to D^W_1 deformation. Based on similar criteria, the dolerites with which the Pgw_4 granitoids are closely associated possibly correlate with the Pdw_2 metadolerites. Sills of both Pgw_4 granitoid and the associated dolerites bear a strong mylonitic S_1 foliation and L_1 stretching lineation, and isoclinal originally recumbent F_1 folds (Fig. 7a). However, only metres from such zones, interconnecting dykes of the same dolerite and granitoid (interpreted as a second magma pulse) cut the S_1 foliation in identical intrusive rocks (Fig. 7b) and cut the

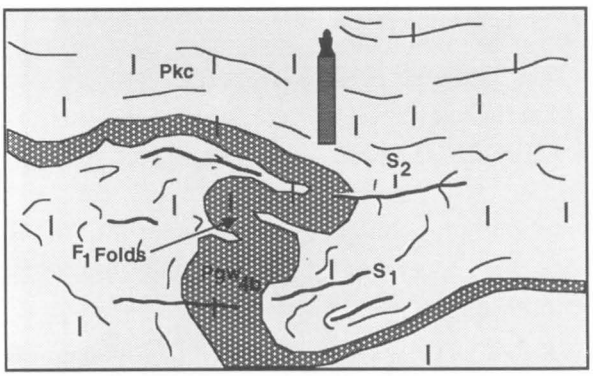


Fig. 7a. Drawing from a field photograph showing outcrop at grid reference 962522, where aplitic granite veins are folded into tight F_1 folds with the S_1 axial plane foliation. The overprinting S_2 schistosity parallels the pen (15 cm) and strikes north-south.

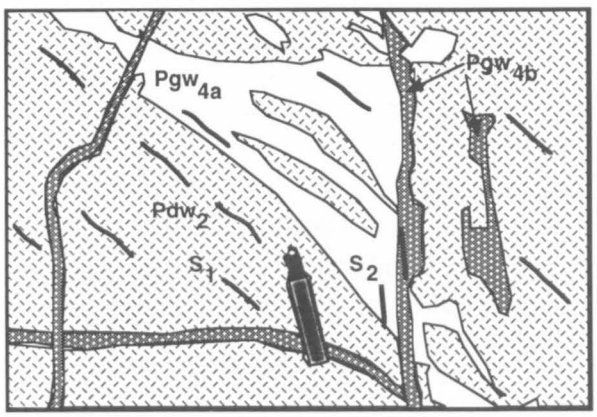


Fig. 7b. Drawing from a field photograph showing a dyke of aplitic granite (Pgw_{4b}) cutting undeflected across the enveloping surface of the S_1 foliation in granite with a mylonitic S_1 foliation. The pen parallels S_2. The outcrop is at grid reference 961523 in the Circular Structure area, Quamby 1:100 000 Sheet area. The pen is 15 cm long.

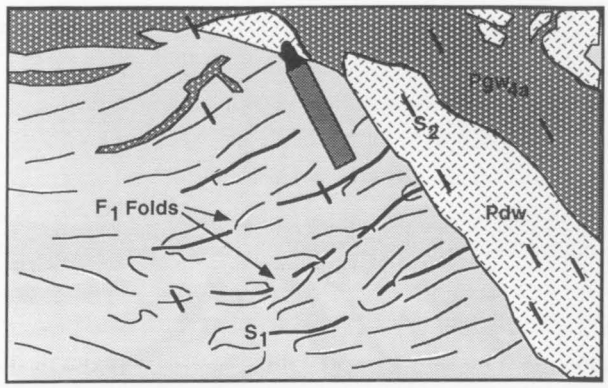


Fig. 7c. Drawing from a field photograph of dolerite and related blastoporphyritic granite (Pgw_{4a}) cutting the axial planes of tight F_1 folds in primary layering in calc-silicate rocks of the Corella Formation near Figure 7b. The pen (15 cm) parallels the orientation of the overprinting S_2 schistosity, which strikes north-south. The outcrop is at grid reference 961523 in the Circular Structure area.

axial planes of isoclinal F_1 folds in the country rocks (Fig. 7c). The S_1 foliation in the sills parallels the axial planes of the F_1 folds in the country rocks, both striking at a high angle to the overprinting S_2 schistosity.

In summary, the emplacement of some felsic and mafic intrusions was clearly bracketed by D^W_1 ductile deformation. The microstructural style of the D^W_1 fabric (Pearson, 1989) indicates that the rocks were largely crystallised when the remaining components of the D^W_1 fabric were superimposed. Their timing, therefore, is broadly syn-D^W_1.

Late syn- to post-D^W_1, pre-D^W_2 intrusions

Less voluminous felsic and mafic dykes cut the D^W_1 fabric in earlier intrusions or in the country rocks, and bear either an inhomogeneous D^W_1 fabric or, in most cases, no D^W_1 fabric at all. However, they generally possess a pervasive D^W_2 fabric. Direct control by systematically oriented dilational sites related to late D^W_1 shearing is evident at some localities. These relationships suggest a late syn- to post-D^W_1, pre-D^W_2 timing.

The Pgw_5 granitoids and Pdw_2 dolerites were intruded at this time, relatively late in D^W_1. Dykes of the Pgw_5 granitoids (Fig. 21 of Holcombe & others, this volume) cut the S_1 foliation form surfaces in earlier intrusions at macroscale. At mesoscale, the Pgw_5 dyke contacts sharply truncate both the S_1 foliation (Fig. 8a) and mylonitic S_{1s} shear bands (Fig. 8b), and the Pgw_5 dykes bear an S_2 schistosity and down-dip L_2 lineation. The S_2 schistosity parallels the axial planes of F_2 crenulations in the truncated D^W_1 planar fabric (Fig. 8a). The Pgw_5 dykes also bear direct and indirect evidence for localised D^W_1 deformation

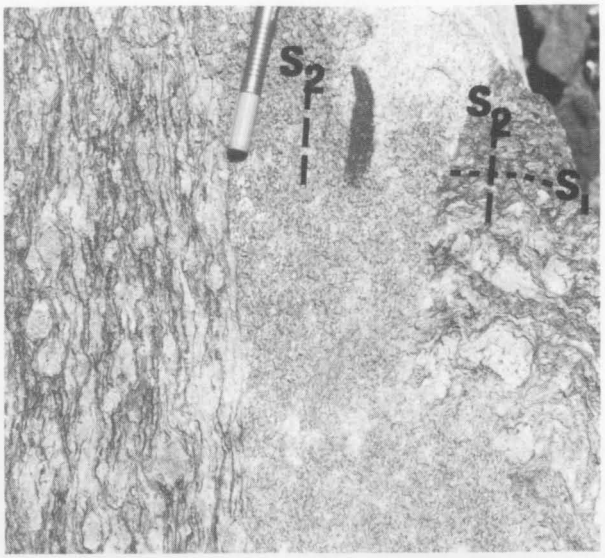


Fig. 8a. Field photograph showing a dyke of medium-grained Pgw_{5a} granite cutting across the gneissic S_1 foliation in earlier Pgw_{1b} coarse-grained granite at the Middle Breakfast Creek dating site (grid reference 983235). The later Pgw_{5a} granite bears only a strong S_2 schistosity parallel to the pen (15 cm), which is axial planar to F_2 crenulations in the S_1 foliation in the earlier gneissic granite.

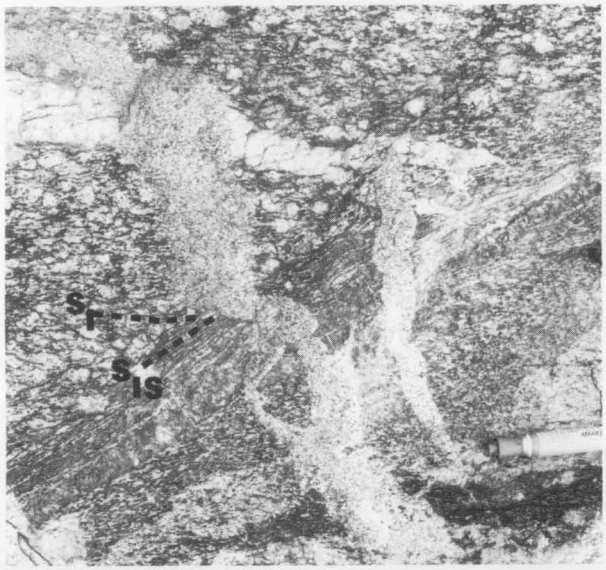


Fig. 8b. Field photograph showing dykes of medium-grained Pgw_{5a} granite cutting a mylonitic S_{1s} shear band in earlier coarse-grained Pgw_{1b} granite; grid reference 999398 in the Mount Maggie area, Quamby 1:100 000 Sheet area. The pen is 12 cm long.

in the form of: (a) zones a few metres wide of internal D^W_1 fabric; (b) discrete S_{1s} shear bands (Fig. 8c); (c) aureoles of strong D^W_1 fabric development around the transgressive veins in earlier rocks; (d) folded and boudinaged granitoid veins in D^W_1 shear zones.

Less commonly, the Pgw_5 granitoids show direct evidence for emplacement in syn-D^W_1 dilational sites, such

as tongues along S_{1s} shear bands (Fig. 8c), en-echelon extensional fractures in late D^W_1 shear zones (Fig. 8d), or zones of necking between D^W_1-boudinaged layering in the country rocks (Fig. 8e).

Similar, apparently conflicting, evidence exists in the relative timing of the Pdw_2 dolerites and the development of the D^W_1 fabric, for although they everywhere cut the D^W_1 fabric in the country rocks and earlier intrusions (Fig. 21 of Holcombe & others, this volume), they bear evidence for localised D^W_1 deformation (Figs. 9a, b). Less commonly, direct control of emplacement by dilation associated with shearing can be demonstrated where dolerite has been injected into transtensional gaps where the bounding shear zones change orientation (Figs. 10a, b). The anastomosing geometry of the Pdw_2 dolerite swarm possibly reflects large-scale control by zones of late D^W_1 shearing (S_{1s} shear bands).

In summary, the available evidence suggests that the bulk of penetrative D^W_1 fabric development occurred before emplacement of the Pgw_5 and Pdw_2 dykes, although late D^W_1 ductile deformation did affect some dykes. Emplacement into dilational sites associated with relatively late localised zones of D^W_1 shearing further suggests that emplacement postdated the bulk of D^W_1 deformation. This evidence and the D^W_2 fabric in the dykes suggest late syn- to post-D^W_1, pre-D^W_2 emplacement.

Syn-D^W_2 intrusions

Tourmaline-bearing granite pegmatites in the eastern Wonga Belt everywhere cut the D^W_1 fabric at various angles, but themselves nowhere bear the D^W_1 fabric, suggesting a post-D^W_1 age. The pegmatites are affected by tight F_2 folds, strong S_2 foliation, and L_2 lineation. Cross-cutting relationships at some outcrops, however, suggest that pegmatite emplacement postdated at least some D^W_2 deformation. For example, in the Circular Structure, pegmatite veins cut the axial planes of F_2 folds in primary layering (and in parallel S_1 foliation) in metasedimentary country rocks (Fig. 11). However, the veins themselves are also folded about parallel F_2 axial planes, suggesting that emplacement was bracketed by D^W_2 deformation. That is, their timing is broadly syn-D^W_2.

Eastern and Western Domains

There is only limited evidence to relate the emplacement of Wonga intrusions in the Eastern Domain with D^W_1 deformation. Sliwa (1986) noted that no D^W_1 fabric occurs within the Burstall Granite, although some late veins apparently cut mesoscopic F_1 folds in the Corella

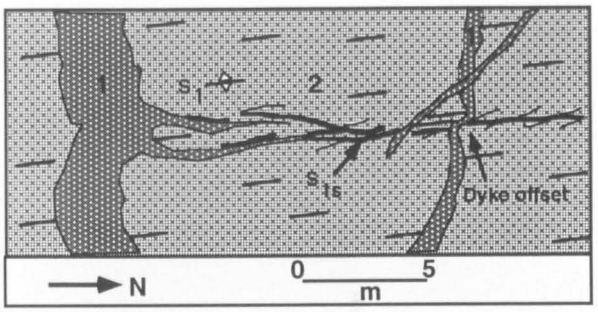


Fig. 8c. Outcrop map of grid reference 989280 in the North Breakfast Creek area, showing tongues of medium-grained Pgw_{5a} granite (1) intruded into dilational sites in S_{1s} shear bands in coarser-grained Pgw_{1b} granite (2). Note how earlier dykes of the same rock type are also displaced by the shear bands (arrowed).

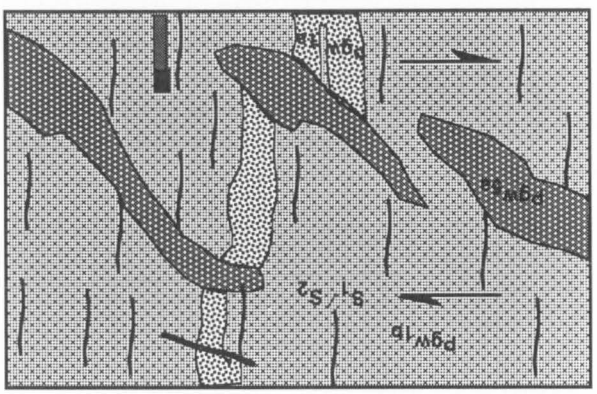


Fig. 8d. Drawing from a field photograph showing apophyses of Pgw_{5a} granite emplaced into arrays of en echelon D^W_1 extensional fractures at grid reference 989280 in the North Breakfast Creek area. The geometry of the array is consistent with a dextral component of subhorizontal shear, consistent with the bending of the earlier dyke through the incipient D^W_1 shear zone. The pen is 15 cm long.

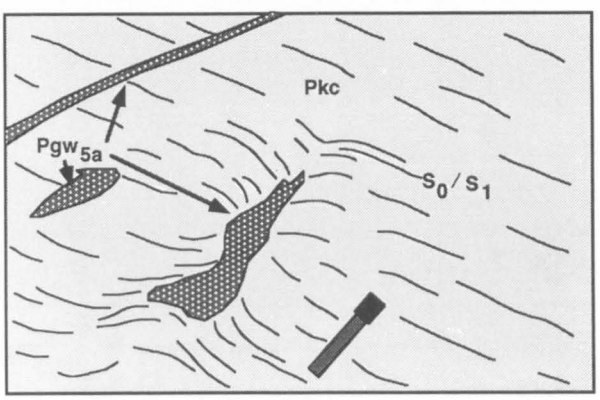


Fig. 8e. Field photograph of an apophysis of aplitic Pgw_{5a} granite emplaced into a dilational site between boudinaged skarn layers in calc-silicate rocks of the Corella Formation at grid reference 963494 in the Circular Structure area, Quamby 1:100 000 Sheet area. The pen is 15 cm long.

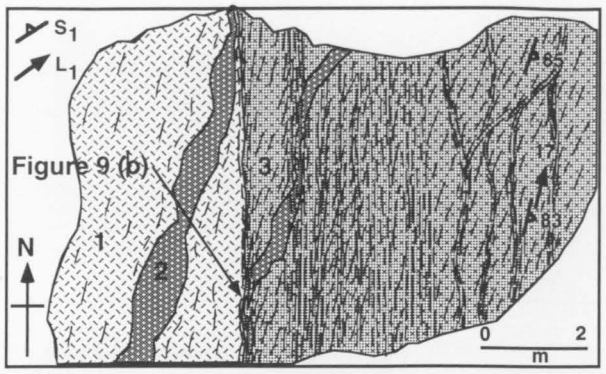


Fig. 9a. Outcrop map of an area on the eastern limb of the Little Beauty Syncline, showing inhomogeneous zones of D^{W}_{1} shear in coarse-grained Pgw_{1b} granite (3), subhorizontal shear and associated boudinage of transgressive pegmatite dykes (2), and subhorizontal shearing along the contact of cross-cutting Pdw_2 dolerite dyke (1); grid reference 944211.



Fig. 9b. Field photograph showing deflection and strong boudinage of pegmatite dyke by D^{W}_{1} shearing along the dolerite contact shown in Figure 9a. Note development of a dolerite/pegmatite hybrid rock, clearly resulting from strong shearing and attendant albitisation. The pen is 15 cm long.

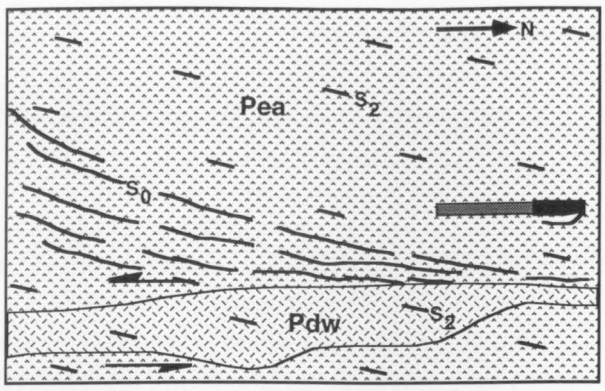


Fig. 10a. Drawing from a field photograph of an outcrop at grid reference 943212 on the eastern limb of the Little Beauty Syncline. A dyke of Pdw_2 dolerite has been emplaced into a dilational jog in a D^{W}_{1} shear zone cutting felsic metavolcanic rocks of the Argylla Formation. Both the wedge-shaped geometry of the dyke and the sense of deflection of earlier layering are consistent with a sinistral apparent shear sense. The pen is 15 cm long.

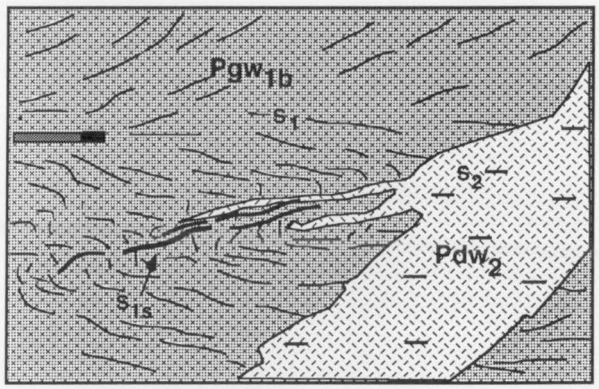


Fig. 10b. Drawing from a field photograph showing a dyke of Pdw_2 dolerite emplaced as tongues along dilational sites in S_{1s} shear bands cutting earlier Pgw_{1b} coarse-grained granite (grid reference 984242 in the Middle Breakfast Creek area). The pen is 15 cm long.

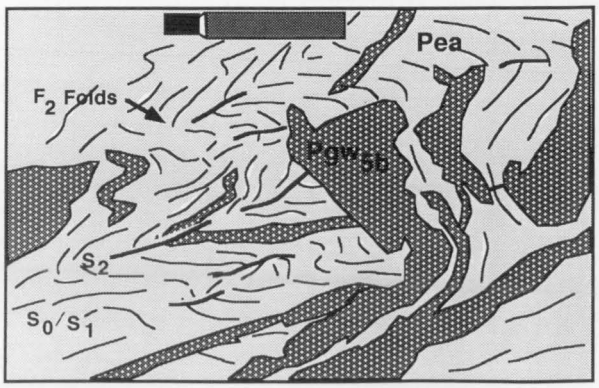


Fig. 11. Drawing from a field photograph showing a transgressive pegmatite dyke (Pgw_6) cutting the axial planes of mesoscopic F_2 crenulations in primary layering and the subparallel S_1 foliation in pelitic metasedimentary country rocks. The weakly foliated dyke itself is openly folded about F_2 axial planes. Grid reference 956540 in the Circular Structure area, Quamby 1:100 000 Sheet area. The pen is 12 cm long.

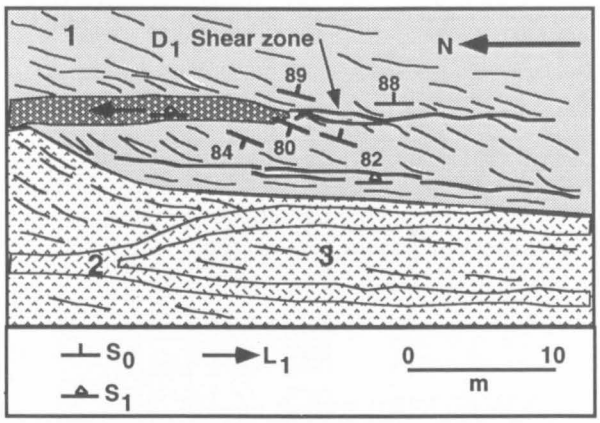


Fig. 12a. Outcrop map at grid reference 936231 on the eastern limb of the Little Beauty Syncline, showing high-angle normal D^W_1 shear zones cutting the Argylla Formation. A dyke of Pgw_{3c} granite porphyry has been emplaced along one of the shear zones. 1 = psammopelite, 2 = dolerite, 3 = felsic metavolcanics.

Formation in the northern part of the pluton. Combined with the fact that the felsic and mafic intrusions of the Eastern Domain bear an inhomogeneous D^W_2 fabric, the time of emplacement can be inferred only as earlier than D^W_2 and later than part of D^W_1.

Better timing criteria between the Wonga intrusions and ductile deformation is evident in the Western Domain on the eastern limb of the Little Beauty Syncline. There, sills of felsic porphyry (Pgw_{2a}) intruding the Ballara Quartzite are displaced by discrete D^W_1 high-angle normal shear zones, suggesting a pre- to syn-D^W_1 timing. However, later Wonga felsic porphyry dykes (Pgw_{2c} and Pgw_{2d}) have intruded along the same shear zones, suggesting that their emplacement was controlled by dilation synchronous with shearing (Fig. 12a). At mesoscale, these felsic dykes bear a mylonitic S_1 foliation and L_1 lineation which are overprinted by a strong D^W_2 fabric (Fig. 12b). This suggests that dyke emplacement and crystallisation were bracketed by ongoing D^W_1 shearing A broadly syn-D^W_1, pre-D^W_2 timing is therefore likely.

Similar evidence relates emplacement of the Pdw_2 dolerites to D^W_1 deformation in the Western Domain. The dolerite dykes cut the previously D^W_1-imbricated strata at various angles, although some dykes have intruded the high-angle normal D^W_1 shear zones, where they consistently cross-cut the syn-D^W_1 felsic dykes described above. However, the dolerites themselves bear an inhomogeneous D^W_1 shear fabric, characterised by planar zones of strong S_1 foliation parallel to high-angle D^W_1 shear zones in the wall rocks (Fig. 13). This suggests that emplacement of the Pdw_2 dolerite dykes was bracketed by

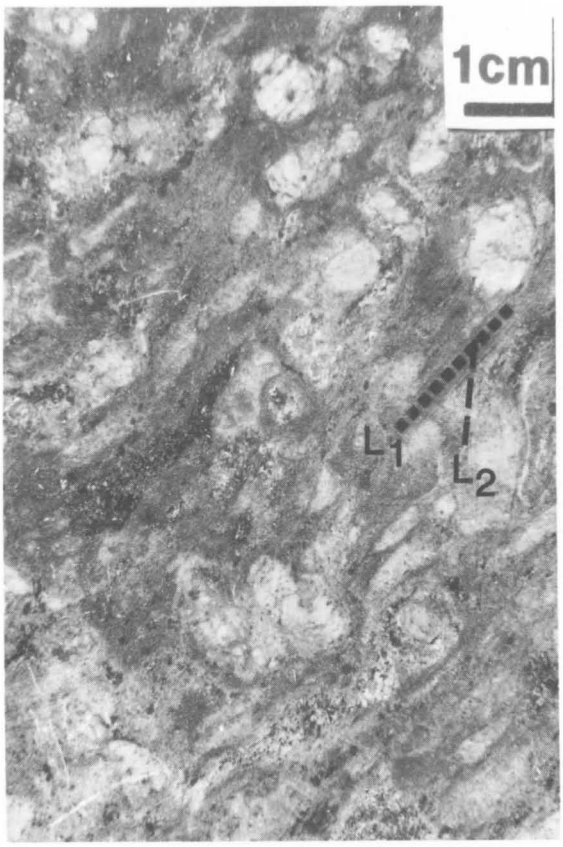


Fig. 12b. Field photograph showing the strong L_1 lineation in S_1 foliation faces in the granite porphyry dyke emplaced into the D^W_1 shear zone shown in (a). A steep down-dip lineation L_2 defined by biotite and amphibole overprints the L_1 lineation.

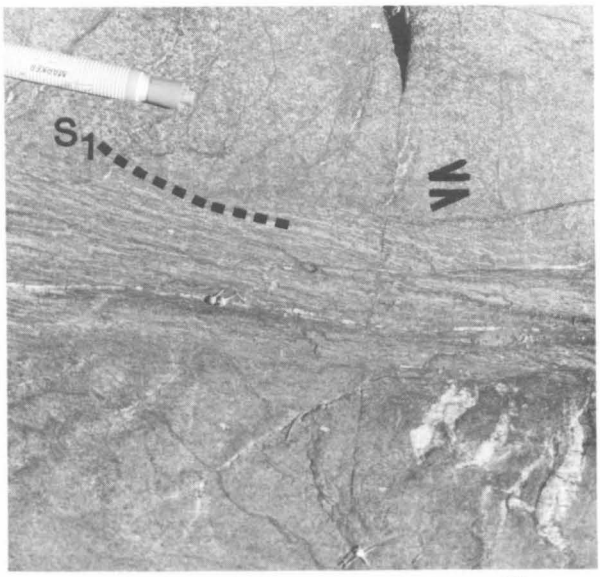


Fig. 13. Field photograph of a zone of strong D^W_1 fabric in Pdw_2 dolerite. The sense of deflection of the shear foliation (S_1) and the geometry of en echelon vein arrays indicates a sinistral apparent D^W_1 shear sense. The pen is 10 cm long.

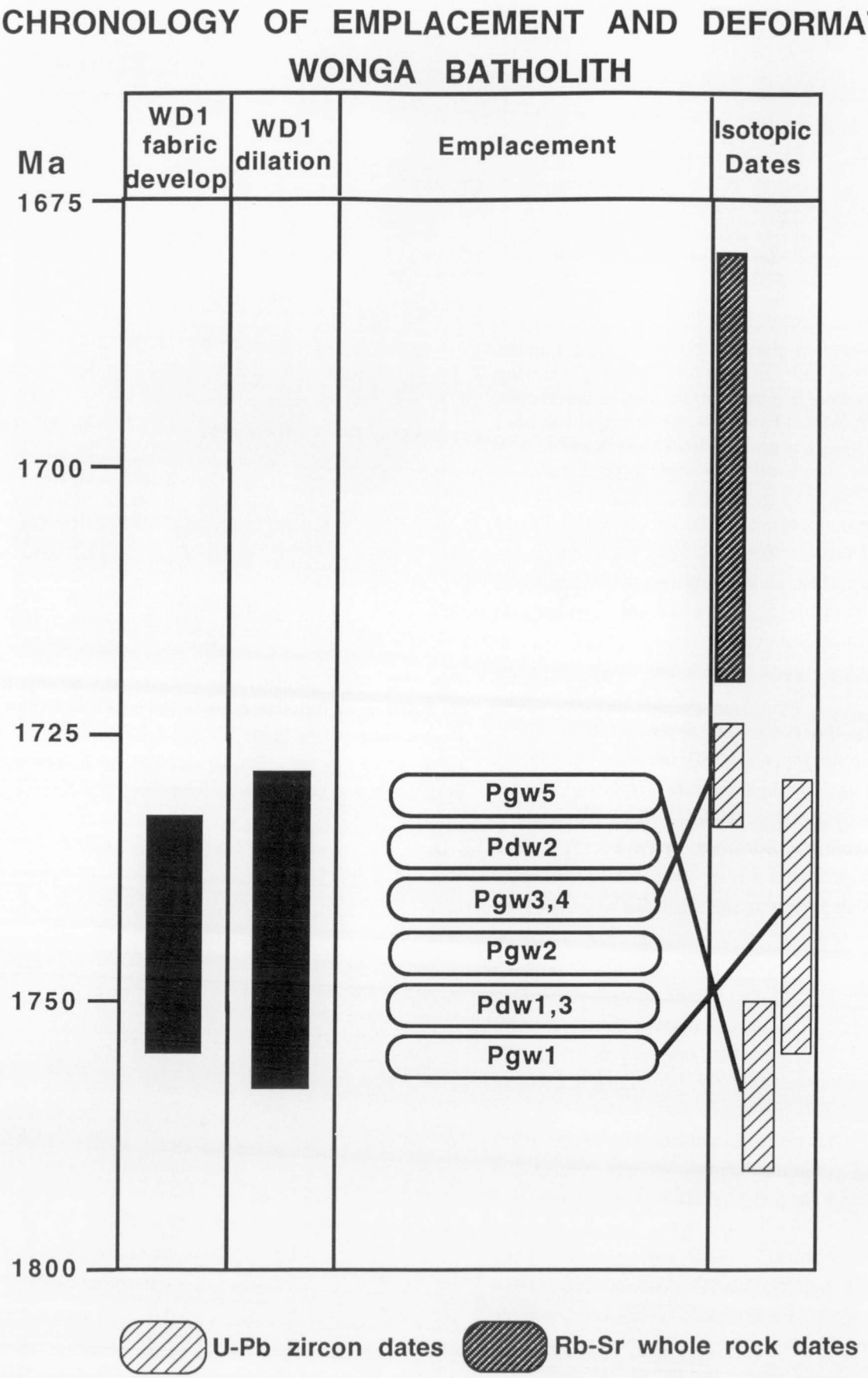


Fig. 14. Schematic summary of the relative and absolute chronologies of emplacement and deformation of the Wonga Batholith.

Unit	Mica K-Ar	Mica Rb-Sr	Whole rock Rb-Sr	Conv. Zircon U-Pb	Ion Probe Zircon U-Pb	Uraninite U-Pb	Whole rock Sm-Nd
Argylla Fm.	-	1490	1552±36 1567±30 1580±27	1766+23-19 1777±7 1783±5	-	-	-
Wonga Granite	1360-1530	-	1621±28 1629±25 1700±20	1671±8 1742±13* 1744±30* 1769±25*	1729±5* 1758±8*	-	-
Burstall Granite	-	-	1350-1600	1726±8 1745+17-15	-	-	-
Burstall rhyolite dykes	-	-	1315-1452	1737±15	-	-	-
Corella Fm. skarn	-	-	1160±120 1210±30 1350±24 1390±50	-	-	-	1580±50 1700±60
Uraninite in Corella Fm. skarn	-	-	-	-	-	1550±15	-
Lakeview Dolerite	-	1122 1121	1116±12	-	-	-	-

Units are Ma.
Data from Page (1978, 1983a, 1983b) and Maas & others, (1985).
New data documented in this study marked by "*"

TABLE 3. SUMMARY OF GEOCHRONOLOGICAL RESULTS RELEVANT TO THIS STUDY.

D^{W}_1 shearing deformation, and therefore occurred late syn-D^{W}_1, pre-D^{W}_2.

Summary

Figure 14 summarises the relative chronology of emplacement and deformation of the Wonga Batholith in the Wonga Belt. The continuous spectrum of timing relationships shown by the various intrusions indicates that at least four, and possibly five groups of A- and I-type intrusions forming the Wonga Batholith were synchronous with D^{W}_1 extensional deformation. Late tourmaline pegmatite (Pgw_6) appears to entirely postdate D^{W}_1 and so is not part of the Wonga Batholith. It was most likely emplaced during D^{W}_2 regional deformation and metamorphism. The general restriction of these pegmatites to the eastern part of the Wonga Belt, in the zone of highest D^{W}_2 metamorphic grade (sillimanite-K-feldspar zone), suggests that they are possibly S-type melts formed by syn-D^{W}_2 anatexis of structurally lower metapelite.

Geochronology and timing of deformations

Igneous rocks of the Mary Kathleen Fold Belt have previously been dated using U-Pb zircon and Rb-Sr mineral and whole rock isotopic methods (Page, 1978, 1983a, b). Table 3 lists the relevant geochronological results.

Until now, the best estimate for the emplacement age of the Wonga Batholith came from conventional U-Pb zircon results on a gneissic microgranite 2 km northeast of Mary Kathleen (site 72-253, BMR database #7220.5021, herein termed the Knob site in Fig. 1). Page (1978) interpreted a four-point discordia array (Fig. 15) as a simple cogenetic suite with a primary crystallisation age

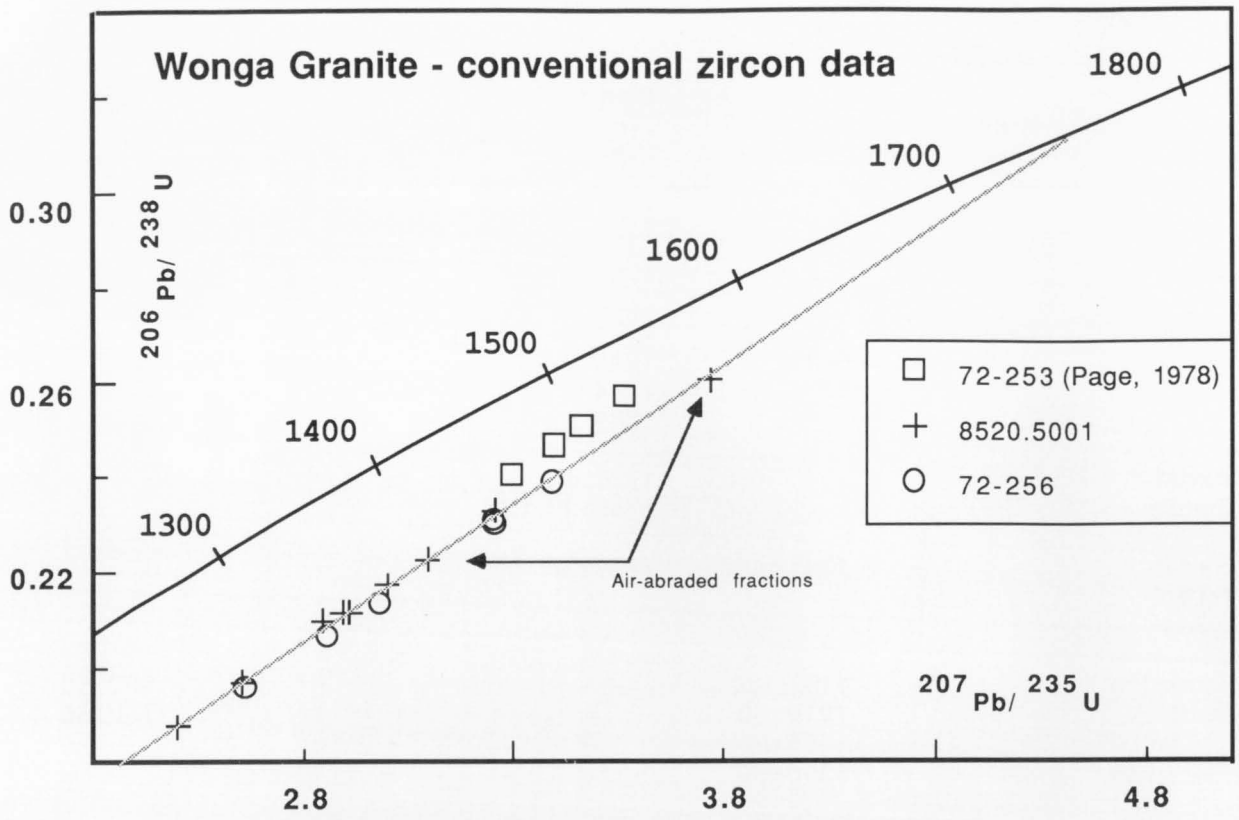


Fig. 15. Concordia plot of U-Pb data conventionally obtained on bulk multigrain fractions from sample 72-256 (Wonga Waterhole) and 8520.5001(Breakfast Creek area); 72-253 are data from Page (1978), Mary Kathleen area. The fitted discordia trajectory refers to sample 8520.5001, and has upper and lower intercepts at 1742 ±13 Ma and 365 ± 40 Ma.

of 1671 ± 8 Ma. This age was approximated by a regional Rb-Sr total rock isochron age of 1700 ± 20 Ma (initial ratio [I.R.] = 0.712 ± 0.004), and was then interpreted as reflecting the emplacement age of this syntectonic intrusion.

U-Pb (zircon) primary crystallisation ages for felsic metavolcanics of the intruded Argylla Formation (1777 ± 7 Ma and 1783 ± 5 Ma: Page, 1978) provide an older age limit for the Wonga Batholith. U-Pb zircon crystallisation ages for the Burstall Granite (1726 ± 8 Ma and 1745 +17-15 Ma), its comagmatic felsic dykes (1737 ± 15 Ma), and the Lunch Creek Gabbro (1740 +28-20 Ma) obtained by Page (1983a) constrain the younger age of the intruded Corella Formation. Accordingly, the older age limit of the Wonga Batholith (and D^{w}_{1} deformation) could have ranged between 1788 Ma and 1718 Ma, because the Batholith intrudes all of the above rock units.

Page (1978) also reported Rb-Sr total rock isochron ages of 1621 ± 28 Ma (I.R. = 0.739 ± 0.011) and 1629 ± 25 Ma (I.R. = 0.727 ± 0.006) for coarse-grained granitic gneisses near Wonga Waterhole (Fig. 1) and concluded from the combined U-Pb and Rb-Sr data that the deformational age for the Wonga Batholith was in the range 1670 to 1620 Ma.

New conventional and ion probe U-Pb zircon ages for these and other critical intrusions of the Wonga Batholith supersede the 1670 to 1620 Ma age estimate of igneous emplacement and hence D^{w}_{1} deformation. Critical to our arguments are the field relationships at each site (Pearson, 1989). Figure 1 shows the location of sampling sites, termed Wonga Waterhole, Knob, and Breakfast Creek dating sites.

Wonga Waterhole dating site (72-256)

Geochronology

Conventional U-Pb analysis (Table 4, Fig. 15) of six zircon fractions from one gneissic augen granite sample that defines the 1621 ± 28 Ma Rb-Sr isochron (Page, 1978) gives a sublinear discordant array (MSWD 4.1) with upper and lower intercepts on concordia at 1759 ± 22 Ma and 418 ± 59 Ma. Zircon U values (667-1141 ppm) are significantly lower than those at site 72-253 (7220.5021), and there is a direct correlation between the degree of discordance and U content. Deletion of the highest-U, most discordant fraction yields a model 1 age of 1742 ±13 Ma (lower

Size (μ), Mag. Suscb'y	Weight (mg)	Concentration U ppm	Pb ppm	$^{206}Pb/^{204}Pb$ meas.	Radiogenic Pb(ppm) 206	207	208	Atomic ratios $^{207}Pb/^{206}Pb$	$^{206}Pb/^{238}U$	$^{207}Pb/^{235}U$	$^{207}Pb/^{206}Pb$ age (Ma)
72-256 - Wonga Waterhole area (K6-22-23) - 72205025											
-400 NM1	1.39	817.8	205.0	1639	161.7	16.7	20.8	0.10252	0.23021	3.2542	1670
-150 NM1	4.15	666.6	174.0	1683	136.8	14.2	18.0	0.10301	0.23892	3.3934	1679
-150 M1	5.47	828.9	194.5	1417	152.0	15.5	20.4	0.10125	0.21351	2.9806	1647
-75 NM0	2.95	728.1	183.3	1611	144.4	14.8	18.6	0.10218	0.23087	3.2526	1664
-75 M0	3.19	877.4	199.2	1344	155.5	15.7	21.1	0.10040	0.20630	2.8559	1632
-60 M1	1.24	1140.7	246.8	1221	191.7	19.0	26.3	0.09867	0.19566	2.6620	1599
8520.5001 - Breakfast Creek area											
-150 NM2	1.16	702.6	158.8	2066	131.1	13.2	10.4	0.10006	0.21721	2.9967	1625
-150 M2	1.16	905.8	185.9	2023	153.3	15.0	12.6	0.09770	0.19697	2.6533	1581
-100 NM2	1.31	694.9	151.9	2207	126.3	12.6	9.2	0.09965	0.21160	2.9073	1618
-100 NM2*	0.28	601.8	139.6	2445	115.1	11.7	10.6	0.10081	0.22266	3.0947	1639
-100 M2	1.11	827.3	160.7	1845	133.4	12.9	9.7	0.09656	0.18765	2.4984	1559
-80 NM1	1.23	625.9	148.1	3705	125.3	12.7	8.0	0.10124	0.23307	3.2533	1647
-80 M1	1.68	733.8	158.8	2467	133.4	13.3	8.6	0.09914	0.21156	2.8919	1608
-80 M1*	0.41	429.3	114.8	4565	96.2	10.1	8.5	0.10483	0.26082	3.7698	1711
-45 NM3	0.41	951.5	202.0	2705	171.4	17.0	10.0	0.09839	0.20974	2.8454	1594

* Abraded in the presence of pyrite.

Pb blank corrections ~0.25 ng (206/204 = 17.97; 207/204 = 15.55; 208/204 = 37.7), and Broken Hill composition for initial Pb.

TABLE 4. CONVENTIONAL U-PB ZIRCON ANALYTICAL DATA FOR THE WONGA GRANITE.

intercept 365 ± 40 Ma). This is considered the best estimate for the magmatic age of this part of the Wonga Granite. As the data indicate that there are no substantial inheritance problems, we have virtually no reservations about the accuracy of this age, although ion microprobe work would be desirable to test the present interpretation properly.

Field relationships

Two distinct felsic intrusions form intermingled bands and lenses at the Wonga Waterhole dating site (Fig. 16). One intrusion is a coarse-grained porphyritic K-feldspar biotite granite (Pgw_{1b}, or 'Wonga Waterhole' type) The other is a leucocratic medium-grained biotite granite (Pgw_{1a}) that forms narrow centimetre to metre-wide lenses within the coarse-grained granite. Both granites bear a pervasive mylonitic S_1 foliation, an L_1 stretching lineation, and a strong overprinting L_2 lineation defined by the subvertical alignment of biotite crystals within S_1/S_2 foliation surfaces. A contact between the two intrusions passes through the centre of the blast hole locating the actual dating site. However, zircons culled from the Pgw_{1b} granite only were used to obtain the U-Pb zircon date.

A tight fold hinge in a vein of Pgw_{1a} granite is located close to the dating site, and many lenticular terminations of similar bands also appear to be fold closures. Some folds are F_1, as they possess a crenulated S_1 axial plane foliation. However, other folds are F_2, as the S_1 foliation wraps around the closure of intrusive vein contacts (Fig. 17). F_2 crenulation axes (L_{21}) parallel the local orientation of the gently to moderately south-plunging L_1 lineation.

The fabric in the dated rock indicates that it was emplaced and crystallised pre- to syn-D^w_1, pre-D^w_2 (consistent with Pgw_1 rock types throughout the Wonga Belt) and that the D^w_2 overprint was strong and involved penetrative dynamic recrystallisation (Pearson, 1989).

Knob dating site

Geochronology

Ion microprobe analyses of zircons from Knob samples (Table 5, Fig. 18) reveal intra- and inter-grain complexities that were masked in the four multigrain conventional analyses reported by Page (1978). The latter, plotted in Figure 18 with the ion microprobe analyses, are a discordant blend of magmatic grains, inherited grains, and high-U discordant grains, all of which are resolvable in the ion microprobe data. Hence the conventional 1671 ± 8 Ma age is the result of a fortuitous alignment that is now shown to be of no geological significance.

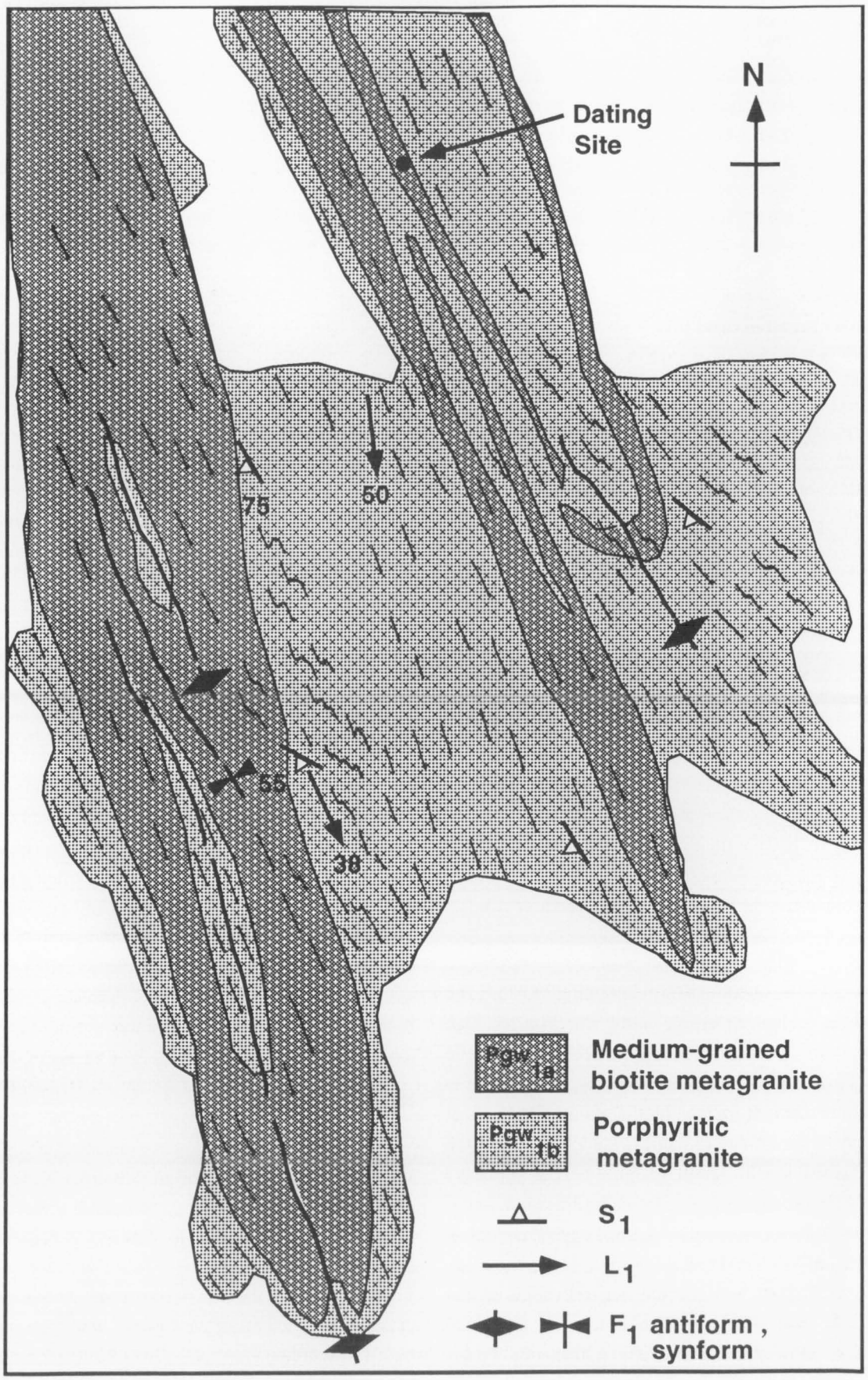


Fig. 16. Outcrop map showing field relationships at the Wonga Waterhole dating site.

Grain-spot	U ppm	Th/U	$^{206}Pb/^{204}Pb$	f206% a)	$^{208}Pb/^{206}Pb$	$^{206}Pb/^{238}U \pm 1\sigma$	$^{207}Pb/^{235}U \pm 1\sigma$	$^{207}Pb/^{206}Pb \pm 1\sigma$	.... Age (Ma)
1-1	944	0.16	6039	0.26	0.0579	0.2733±39	3.937±63	0.1045±6	1706
2-1	2810	0.56	2726	0.58	0.1693	0.1937±27	2.306±36	0.0864±4	1346
3-1	1905	0.71	5880	0.27	0.1899	0.2344±33	3.155±48	0.0976±4	1579
4-1	1138	0.30	113250	0.01	0.0934	0.3024±43	4.399±66	0.1055±4	1723
5-1	123	0.69	>100000	0.02	0.2126	0.2971±47	4.489±93	0.1096±12	1793
5-2	116	0.70	>100000	0.02	0.2104	0.2953±47	4.439±89	0.1090±11	1783
6-1	1486	0.79	20450	0.08	0.2412	0.3342±47	4.944±73	0.1073±3	1754
7-1	461	0.14	23987	0.07	0.0493	0.3214±47	4.819±78	0.1087±6	1778
8-1	151	1.08	>100000	0.02	0.3249	0.3003±46	4.453±83	0.1075±10	1758
9-1	1768	0.62	9282	0.17	0.1745	0.2916±41	4.254±63	0.1058±3	1729
10-1	1515	0.47	5764	0.27	0.1130	0.2319±33	3.239±50	0.1013±5	1648
11-1	1437	0.41	18308	0.09	0.1151	0.3162±45	4.590±68	0.1053±3	1719
12-1	1298	0.60	22134	0.07	0.1803	0.2543±36	3.638±55	0.1037±4	1692
13-1	1451	0.56	7485	0.21	0.1817	0.2947±42	4.316±65	0.1062±4	1735
14-1	2360	0.69	26589	0.06	0.1826	0.3722±52	5.646±82	0.1100±2	1800
15-1	1148	0.03	>100000	0.02	0.0094	0.2817±40	4.123±63	0.1062±5	1735
16-1	1342	0.55	25291	0.06	0.1483	0.2649±38	3.742±56	0.1025±4	1669
17-1	988	0.09	13355	0.12	0.0237	0.2930±42	4.256±64	0.1053±4	1720
18-1	1220	0.02	62775	0.03	0.0057	0.2460±35	3.219±48	0.0949±3	1526
19-1	1113	0.22	67204	0.02	0.0677	0.2965±42	4.319±64	0.1056±3	1725
20-1	1835	0.68	2726	0.57	0.2349	0.1809±26	2.307±37	0.0925±6	1477
21-1	939	0.27	29189	0.05	0.0753	0.2667±38	3.779±58	0.1028±4	1675
22-1	264	0.87	>100000	0.02	0.2570	0.3095±46	4.684±79	0.1097±7	1795
22-2	1840	0.52	4923	0.32	0.1548	0.2368±33	3.322±51	0.1018±4	1657
23-1	1280	0.31	6516	0.24	0.0892	0.2909±41	4.152±63	0.1035±4	1688
24-1	209	0.90	70922	0.02	0.2665	0.3161±47	4.696±83	0.1078±8	1762
25-1	1683	0.48	6234	0.25	0.1429	0.2930±41	4.117±62	0.1019±4	1659
26-1	1408	0.42	42373	0.04	0.1007	0.2670±38	3.747±56	0.1018±3	1657
27-1	2681	0.04	2513	0.62	0.0320	0.3068±43	4.206±64	0.0994±4	1613
28-1	1197	0.36	19940	0.08	0.0589	0.2593±37	3.639±56	0.1018±4	1657
29-1	1314	0.17	8197	0.19	0.0504	0.2660±38	3.650±56	0.0995±4	1615
30-1	2077	0.33	14896	0.10	0.1232	0.2752±39	3.825±57	0.1008±3	1639

a) Denotes the percentage of common ^{206}Pb in the total measured ^{206}Pb.

TABLE 5. ION MICROPROBE ANALYTICAL DATA FOR GNEISSIC MICROGRANITE, 72-253 (2 KM NORTHEAST OF MARY KATHLEEN).

The analysed zircons are generally zoned euhedral grains whose terminations are rounded and magmatically or more likely metamorphically resorbed, The high-U content of the bulk populations (1615-1735 ppm) is also shown in most of the individual grains (Table 5), but in addition there is also a clearly identifiable group of relatively low-U and generally high Th/U zircon analyses (5-1, 5-2, 7-1, 8-1, 22-1, 24-1). This low-U group forms a coherent cluster in $^{207}Pb/^{206}Pb$ age at 1778 ±15 Ma, clearly distinguishable from the remainder of the population. All these xenocrysts (except grain 7) comprise clear colourless cores and zoned darker rims typical of the main magmatic population. These xenocrysts are of the same age as, and were probably inherited from, felsic volcanics of the Argylla Formation, which the Wonga Batholith intrudes.

The magmatic zircons have much higher U (944-1768 ppm) than the xenocrystic zircons, and form a group that straddles and lies just below concordia, around a mean $^{207}Pb/^{206}Pb$ age of 1729 ± 5 Ma. Counting statistics enhanced by the higher U of the magmatic grains results in the clearly lower experimental errors of these analyses. We interpret the 1729 ± 5 Ma result as the age of magmatic crystallisation for this part of the Wonga Batholith. This is some 30 million years younger than the interpreted age (1758 ± 8 Ma) of the microgranite dated from the Middle Breakfast Creek site (see below). Statistically, there is a clear age difference between the two results, and the zircon populations have identifiably different geochemistry in terms of U and Th/U.

In sample 72-253, a third group of data forms a scattered array with a much lower $^{207}Pb/^{206}Pb$ ratio than the 1729 Ma magmatic zircons (Figs. 18, 19). This younger group includes mostly discordant grains with increasingly higher U up to 2810 ppm, and it would have dominated the four conventional bulk zircon analyses which plot in its

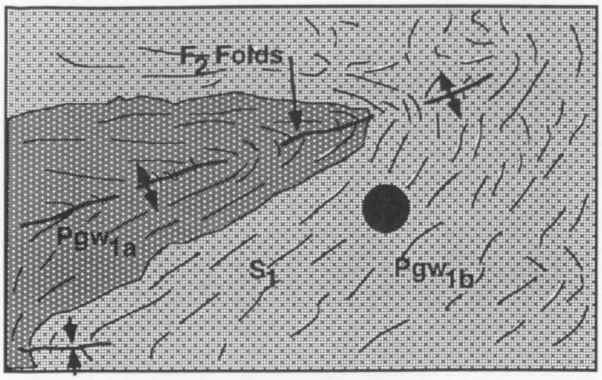


Fig. 17. Drawing from a field photograph showing the crenulated gneissic S_1 foliation in medium-grained (Pgw_{1a}) and coarse-grained (Pgw_{1b}) granites at the Wonga Waterhole dating site. Zones of crenulated S_1 are present throughout the site. The lenscap is 6 cm in diameter.

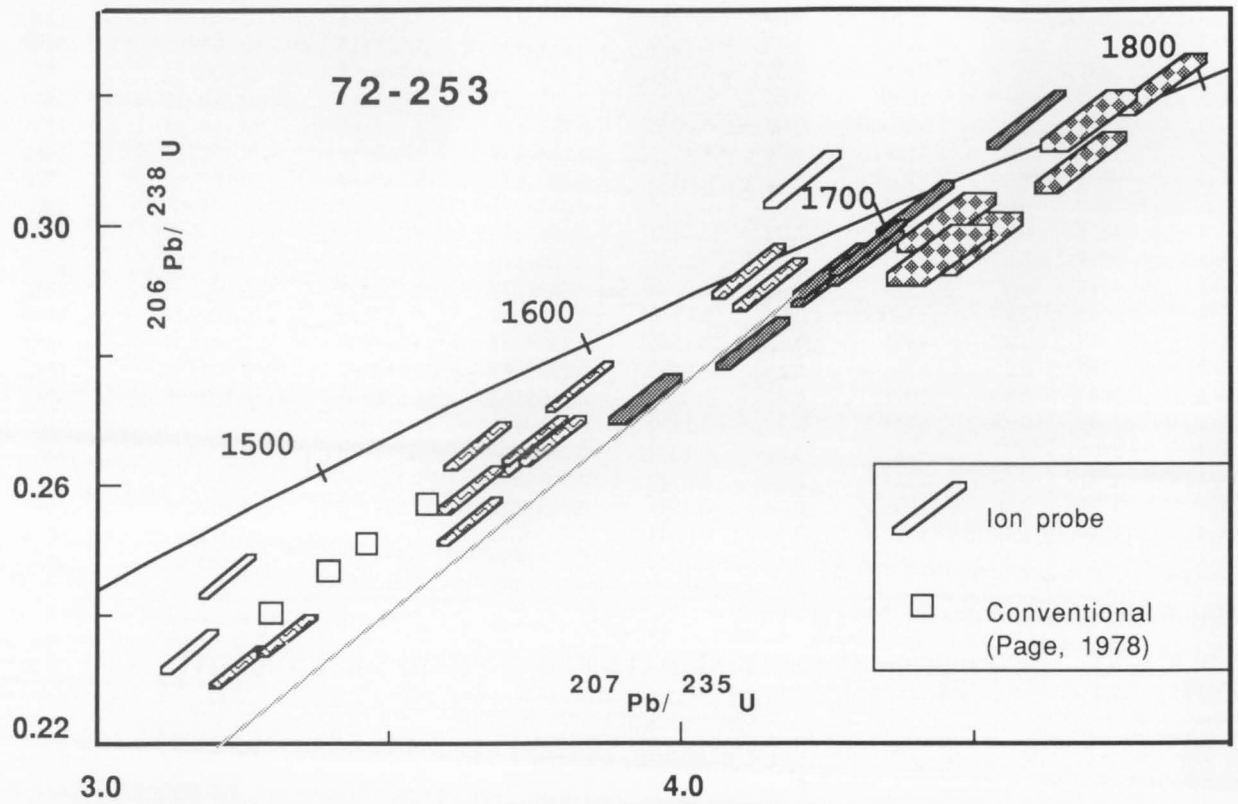


Fig. 18. Concordia plot of U-Pb zircon data for sample 72-253, determined by ion microprobe (showing 1-sigma errors) and conventional analysis (open squares). The low-U zircons (checkerboard pattern) are interpreted as xenocrysts, and have a pooled $^{207}Pb/^{206}Pb$ age of 1778 ± 15 Ma - this $^{207}Pb/^{206}Pb$ slope is shown. The group of magmatic high-U zircons (stipple pattern, grain 6-1 not shown) has a pooled $^{207}Pb/^{206}Pb$ age of 1729 ± 5 Ma. Three of the highest-U grains (2-1, 14-1, 20-1) are grossly discordant and are not shown. The unshaded and lightly shaded ion microprobe data form part of a third scattered array of high-U zircons that would have dominated the conventional analytical data.

midst. It is likely that this complex non-linear array is the result of either multiple Pb loss events, or zircon recrystallisation and resetting during metamorphism and deformation. No unambiguous age can be determined for this event(s) from these data alone. There are no morphological grounds such as zircon overgrowths to independantly distinguish this population, but the approximate $^{207}Pb/^{206}Pb$ grouping at 1660 ± 5 Ma for 11 of the analyses (including the subconcordant grains 23-1 and 25-1) suggests an important resetting event at that time.

Field relationships

Figure 20 shows the geological relationships around the Knob dating site, which lies between the northern boundary of a large pluton of the dated 'Knob' granite (Pgw_{3b}) and an area of interlayered lenses of other granitoids, dolerite, and quartzite. Cross-cutting and

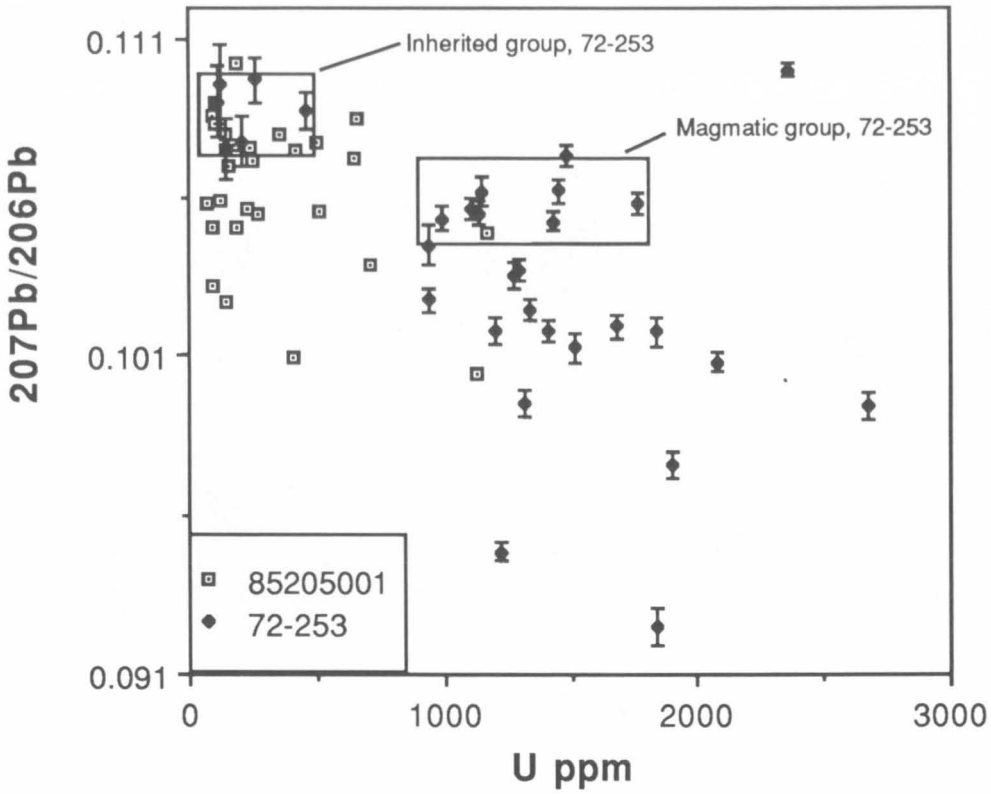


Fig. 19. Plot of U versus $^{207}Pb/^{206}Pb$ for ion microprobe zircon data from samples 8520.5001 and 72-253, showing the direct relationship between degree of discordance and U content. In general, zircons in 8520.5001 have much lower U contents. For sample 72-253, measured 1-sigma errors in $^{207}Pb/^{206}Pb$ are shown. There is a clear separation between the low-U 1778 Ma inherited population and the higher-U grains. Some of the latter belong to the 1729 Ma magmatic group, and others are generally very discordant and disturbed by a later event.

xenolith relationships clearly indicate the following relative timing sequence:

- (1) Quartzite (probably Argylla Formation);
- (2) Dolerite (Pdw_1);
- (3) Coarse-grained porphyritic K-feldspar amphibole-biotite granite to granodiorite (Pgw_{3a});
- (4) Medium-grained slightly porphyritic K-feldspar biotite granite (Pgw_{3b} or 'Knob' type) comprising the dated rock;
- (5) Aplite/pegmatite and pegmatite (Pgw_{5a} and Pgw_{5b}).

The relatively late Pgw_5 aplite and pegmatite that cut the dated rock bear only the D^W_2 fabric, in the form of a subvertical north-striking S_2 schistosity and L_2 down-dip lineation. All earlier rock types have both D^W_1 and D^W_2 fabrics. The quartzite possesses a strong L_1 grain-shape lineation that plunges moderately to steeply south and parallels the axes of mesoscopic F_2 folds in the primary layer-parallel S_1 foliation. A strong schistosity, interpreted as S_2, overprints the folded S_1 foliation in the quartzite. The generally steeply dipping foliation in the Pdw_1 dolerite and in the Pgw_{3a} and Pgw_{3b} granites has a southerly plunging lineation, subparallel to that in the quartzite. The lineation is either a vague compositional striping (L_{21} intersection lineation) or a modified L_1 stretching lineation defined by aligned xenoliths, quartz ribbons, and feldspar augen.

Within the dated Pgw_{3b} 'Knob' granite, less than 20 m from the dating site, the S_1 foliation commonly is overprinted by small angular chevron-like F_2 crenulations with wavelengths between 5 and 10 cm. The folded foliation is weak because of the overprinting D^W_2 recrystallisation, but remnants of the earlier S_1 alignment of quartz ribbons, K-feldspar augen, and aligned biotite crystals are preserved throughout. Zones of F_2 crenulations occur where S_2 axial plane foliation is weak.

Hence, a large component of the ductile foliation at the Knob dating site is a strong inhomogeneous overprinted S_1 foliation identical to that elsewhere in the Wonga Belt. Therefore, emplacement and crystallisation of the dated rock occurred pre- to syn-D^W_1 and pre-D^W_2. The presence of numerous vague patches of transgressive relatively

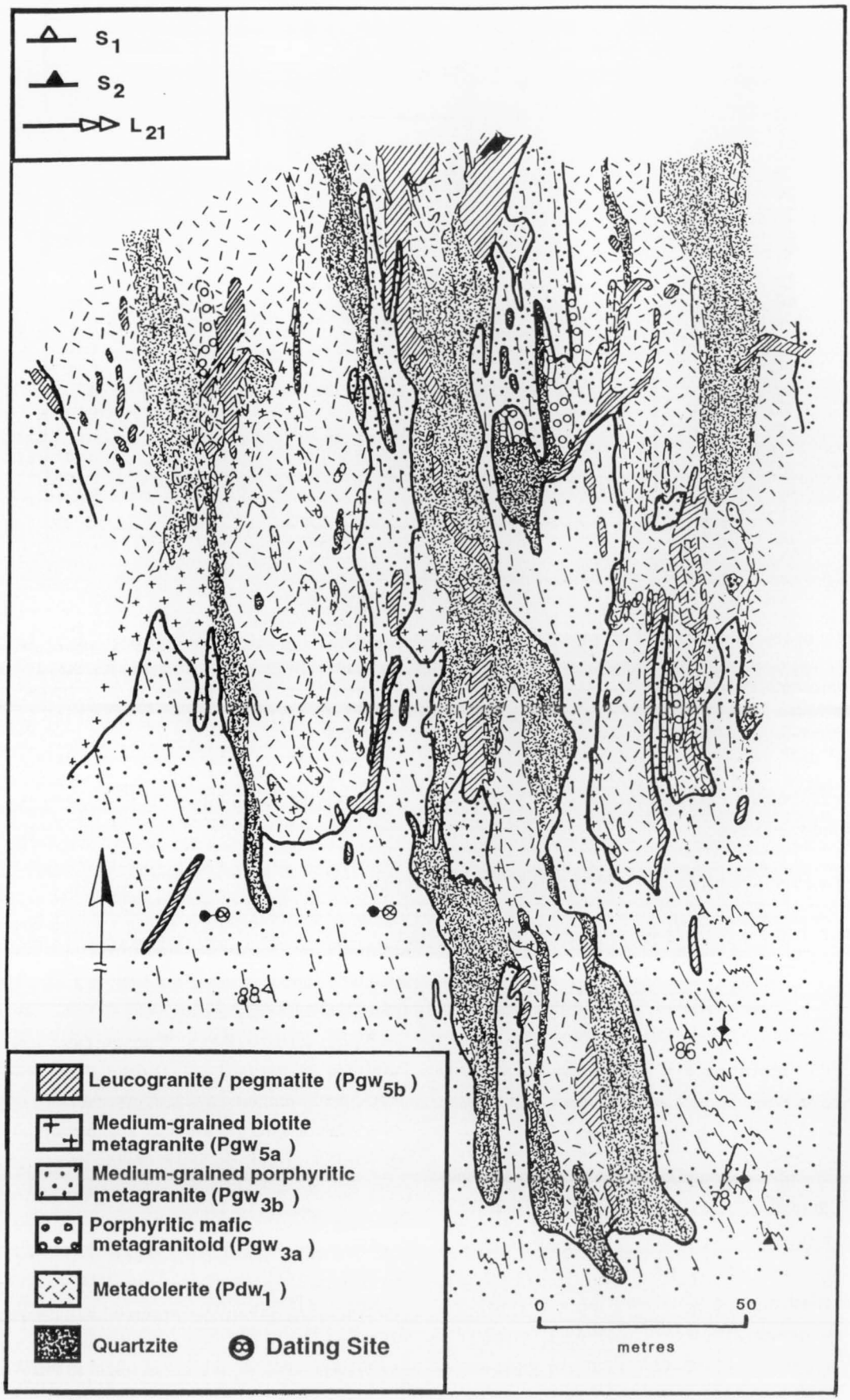


Fig. 20. Outcrop map showing field relationships at the Knob dating site.

Grain-spot	U ppm	Th/U	$^{206}Pb/^{204}Pb$	f206% a)	$^{208}Pb/^{206}Pb$	$^{206}Pb/^{238}U \pm 1\sigma$	$^{207}Pb/^{235}U \pm 1\sigma$	$^{207}Pb/^{206}Pb \pm 1\sigma$	.... Age (Ma)
1-1	146	0.85	631	2.48	0.2338	0.1654±24	2.342±87	0.1027±33	1674
1-2	410	0.25	1538	1.02	0.0588	0.2404±34	3.347±69	0.1010±13	1642
2-1	184	0.37	1947	0.8	0.1186	0.2919±42	4.439±90	0.1103±14	1804
3-1	146	0.8	3970	0.4	0.2314	0.3123±46	4.649±98	0.1080±14	1766
3-2	277	0.34	8718	0.18	0.1138	0.2709±39	3.939±70	0.1054±10	1722
4-1	354	0.28	6545	0.24	0.0614	0.3147±45	4.685±79	0.1080±8	1766
5-1	160	0.42	3893	0.4	0.1245	0.3211±46	4.735±93	0.1070±12	1748
6-1	176	0.56	1430	1.1	0.1564	0.3252±48	4.827±118	0.1076±19	1760
7-1	94	1.18	2347	0.67	0.3519	0.3223±49	4.825±122	0.1086±20	1776
7-2	94	0.55	1754	0.89	0.119	0.2975±45	4.311±119	0.1051±22	1716
8-1	71	0.99	1481	1.06	0.2793	0.305±47	4.449±136	0.1058±26	1728
9-1	2959	0.05	2343	0.69	0.0308	0.3001±42	3.741±56	0.0904±3	1434
9-2	419	0.94	10473	0.15	0.278	0.3138±45	4.649±76	0.1075±7	1757
10-1	252	0.57	1597	0.98	0.1803	0.3298±48	4.874±98	0.1072±13	1752
11-1	358	0.43	1964	0.78	0.0905	0.3388±48	5.396±97	0.1155±11	1888
12-1	238	0.57	6015	0.26	0.162	0.3198±46	4.743±88	0.1076±11	1759
12-2	504	0.37	16075	0.1	0.1077	0.3270±46	4.857±78	0.1077±6	1761
13-1	108	0.38	797	1.96	0.1365	0.2859±43	4.27±127	0.1083±26	1771
14-1	1133	0.2	8868	0.18	0.0563	0.3288±46	4.553±69	0.1004±4	1632
15-1	143	0.6	2753	0.57	0.1616	0.3289±48	4.875±108	0.1075±16	1757
16-1	2841	0.24	1408	1.11	0.0818	0.1307±18	1.420±24	0.0788±6	1166
17-1	643	0.8	3190	0.49	0.2215	0.3036±43	4.488±73	0.1072±7	1752
18-1	658	0.14	18639	0.08	0.0419	0.3148±45	4.710±75	0.1085±6	1775
19-1	127	0.76	2174	0.72	0.212	0.3289±49	4.803±113	0.1059±17	1730
20-1	235	0.46	2726	0.57	0.1304	0.3150±46	4.587±89	0.1056±12	1725
21-1	117	0.73	5718	0.24	0.2075	0.4950±74	12.341±221	0.1808±15	2660
21-2	1174	0.52	786	1.99	0.0514	0.2571±36	3.717±63	0.1048±8	1712
22-1	1263	0.38	7168	0.22	0.1123	0.1676±24	2.075±33	0.0898±5	1421
23-1	517	0.5	1425	1.1	0.1545	0.2592±37	3.771±69	0.1055±10	1723
24-1	90	0.55	2139	0.73	0.1513	0.3003±46	4.274±120	0.1032±22	1683
24-2	1725	0.03	3243	0.48	0.015	0.1881±26	2.339±38	0.0902±6	1429
24-3	183	0.98	2973	0.53	0.2747	0.3131±46	4.535±101	0.1051±16	1715
25-1	707	0.89	3246	0.48	0.2333	0.2778±39	3.979±65	0.1039±7	1694
26-1	108	0.52	4160	0.38	0.1496	0.3112±47	4.678±109	0.1090±18	1783

a) Denotes the percentage of common ^{206}Pb in the total measured ^{206}Pb.

TABLE 6. ION MICROPROBE ANALYTICAL DATA FOR GNEISSIC MICROGRANITE, 8520.5001 (BREAKFAST CREEK SITE).

unstrained granite pegmatite within the dated rock (possibly representing late differentiates of the latter) suggests that emplacement and crystallisation may have occurred very late in D^{w}_{1}. That is, a broadly syn-D^{w}_{1} age is consistent with regional observations on the timing of this widespread intrusion.

Middle Breakfast Creek dating site

Geochronology

Medium-grained biotite microgranite from the Middle Breakfast Creek dating site (Page's Site 8520.5001, Fig. 1) contains euhedral zircons, most of which are cracked and contain minute inclusions. A discordant array of nine conventionally measured U-Pb zircon fractions (Table 4, Fig. 15) is subparallel to, and generally slightly lower in 207Pb/206Pb ratio, than the Wonga Waterhole data and has apparent U-Pb intercept ages at 1769 ± 25 Ma and 509 ± 52 Ma (MSWD 7.9). Two of these fractions were abraded, including the least discordant analysis, a data point that is not co-linear with the other eight and strongly biases the regression towards a somewhat older age. Its deletion results in an age of 1744 ± 30 Ma (MSWD 5.7), and this is the preferred result, given the consistently younger $^{207}Pb/^{206}Pb$ ratio of eight analyses compared to the Wonga Waterhole data. However, neither interpretation can be accepted as a firm age for the microgranite, given the observed discordance and the likelihood of inheritance of some older zircon grains as indicated by the imperfect regression line fit.

To resolve these uncertainties, 34 ion microprobe measurements were made on 26 zircon grains from the microgranite (Table 6 and Fig. 21). Selective analyses of

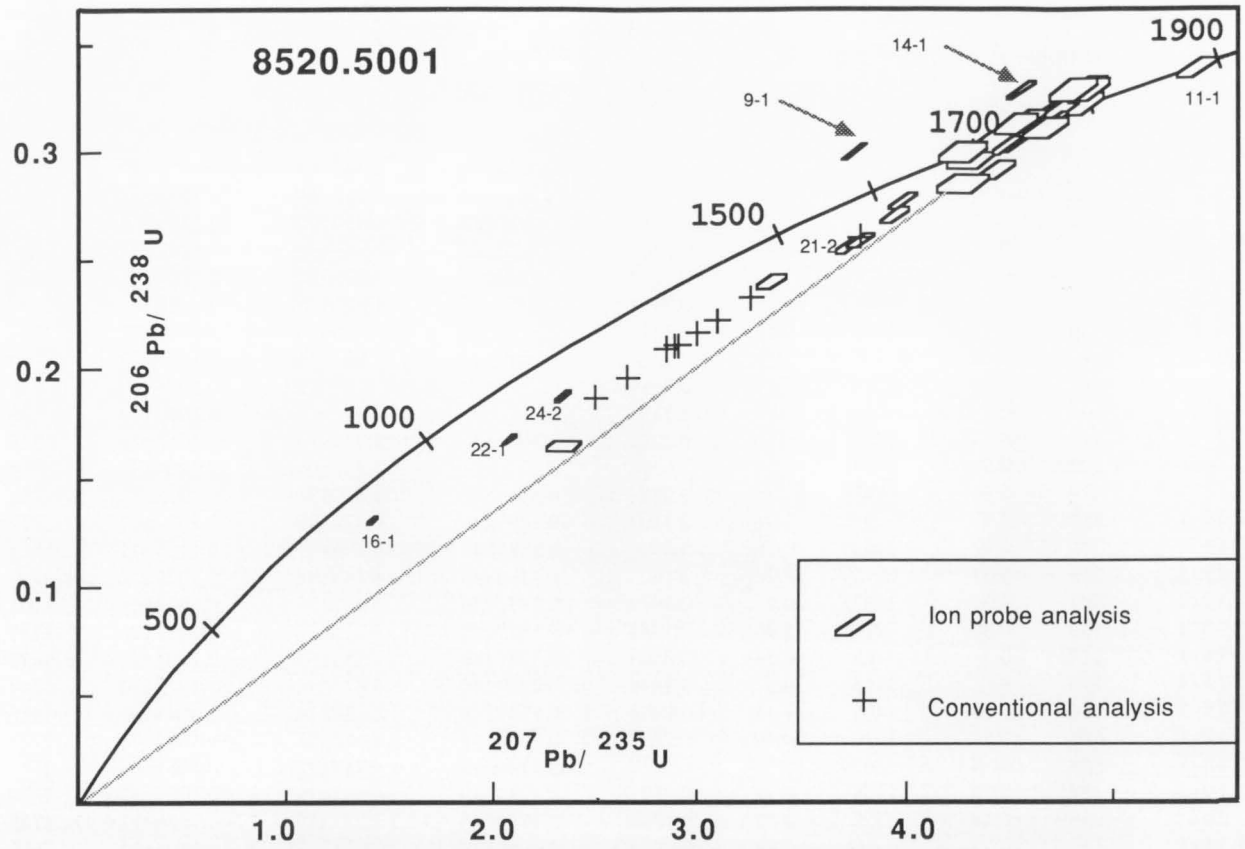


Fig. 21. Concordia plot of U-Pb zircon data for sample 8520.5001,determined by ion microprobe (showing 1-sigma errors) and conventional analyses (crosses). The ion microprobe results for magmatic zircons give an age of 1758 ± 8 Ma (this $^{207}Pb/^{206}Pb$ slope is shown), compared to extrapolation of the conventionally determined results, which indicates 1742 ± 13 Ma. Analysis 11-1 is of a xenocrystic grain approximately 1890 Ma old; analysis 21-1 (not shown) is a low-U (117 ppm) late Archean xenocryst approximately 2660 Ma old, rimmed by a high-U (1174 ppm) zoned selvedge (analysis 21-2) that, although discordant, is part of the magmatic population. Note that the different sized error ellipses are due to variable counting statistics, commonly related to relative U contents.

30-micron spots on individual zircon grains allows the analysis of regions free of cracks and inclusions, and avoidance of high-U grain margins. In these zircons, clear areas commonly correspond to zones of low U, between 90 and 500 ppm. Higher-U grains (up to 2960 ppm) and the nine bulk conventional analyses from Table 4 (430-950 ppm U) are much more discordant, a pattern that is clearly illustrated in the plot of U versus $^{206}Pb/^{238}U$ ratio (Fig. 22). The majority of the ion microprobe analyses are concordant, and 21 grains form a tight $^{207}Pb/^{206}Pb$ cluster within experimental error, indicating a primary magmatic age of 1758 ± 8 Ma. This result is much more precise than, but entirely consistent with, the age interpreted from the discordant conventionally measured zircon data.

The discordant conventional data, suggesting an average time of Pb loss at about 500 Ma, is mirrored by the few ion microprobe analyses of high-U grains, although in detail some very high-U areas (grain rim 9-1 and grain centre 14-1) plot curiously above concordia. Grain 9-1 has a $^{207}Pb/^{206}Pb$ age of 1434 Ma, close to that of the high-U, normally discordant grains 22-1 and 24-2, but the centre of grain 9 (analysis 9-2) is concordant, and has a $^{207}Pb/^{206}Pb$ age of 1757 Ma, in the middle of the magmatic population. A possible explanation is that the reversely discordant zones behaved as open systems and underwent strong early Pb loss followed by gain of U in the recent past. Alternatively, the aberrance of these two analyses may be of analytical origin. The general non-linearity of the high-U grains may be explained if the U/Pb measurements for these damaged and altered zircons are in error; i.e., that the U/Pb calibration derived from the standard SL3 is inappropriate for these damaged zircons.

Zircon inheritance, partly evident from the conventional zircon measurements, is more clearly demonstrated in the ion microprobe data. Grain 11-1, identical in appearance to many of the 1758 Ma magmatic population, is concordant with a $^{207}Pb/^{206}Pb$ age of 1888 Ma, clearly a relic of the Kalkadoon-Leichhardt basement terrane of this age. A brown low-U core (analysis 21-1, 117 ppm U) is a late Archean xenocryst ($^{207}Pb/^{206}Pb$ age

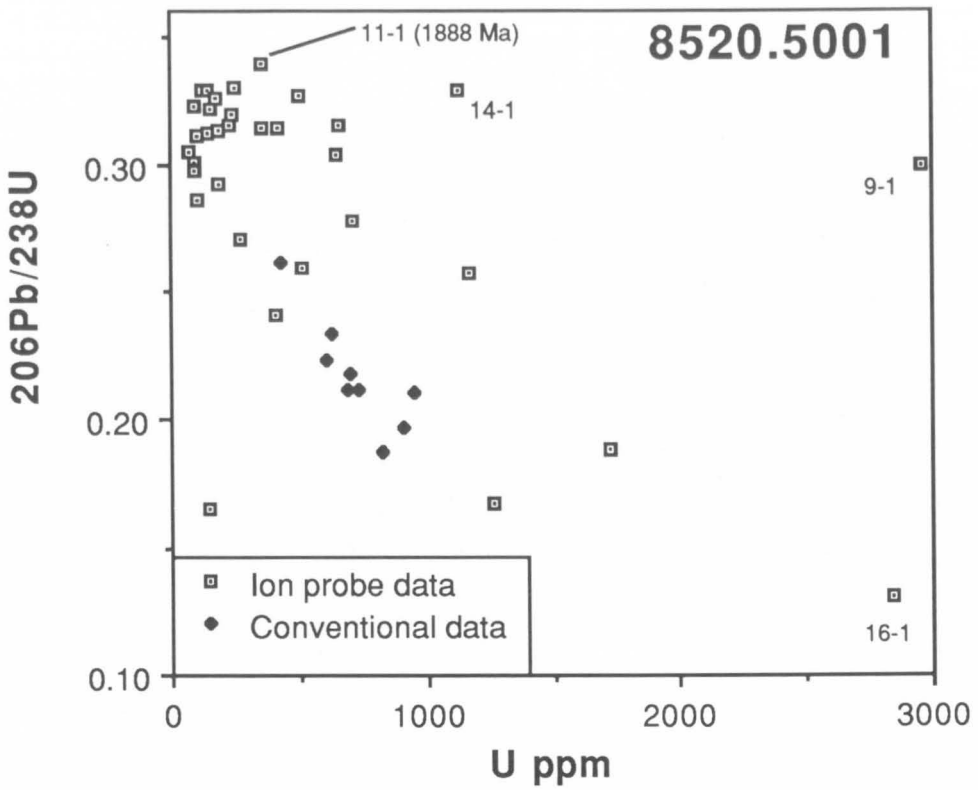


Fig. 22. Plot of U versus $^{206}Pb/^{238}U$ for ion microprobe and conventional zircon data from sample 8520.5001, showing the direct relationship between the degree of discordance and the U content. The approximately 2660 Ma analysis (21-1) is not shown.

2660 Ma – not plotted in Fig. 21) surrounded by a discordant magmatic rim with 1174 ppm U. Evidence of minor zircon inheritance of Archaean age is now found in a number of the early to middle Proterozoic terranes of northern Australia (Page, 1988).

However, the resolution of a 1778 Ma inherited zircon component from the 1729 Ma magmatic zircons in sample 72-253 (Knob site) prompts the question as to whether any such inheritance is unrecognised in the data for sample 8520.5001 from Middle Breakfast Creek. Unfortunately, lower U in sample 8250.5001 and shorter experimental counting times (10 seconds, compared to 40 seconds for sample 72-253), might have precluded the finding of inherited zircons only a few tens of millions of years older than the magmatic group. If this were the case, it would mean that 1758 ± 8 Ma is a maximum age for magmatic crystallisation of the Middle Breakfast Creek microgranite.

Field relationships

Figure 23 shows the geological relationships around the Middle Breakfast Creek dating site. Cross-cutting and xenolith relationships indicate the following emplacement sequence:

- (1) Coarse-grained porphyritic K-feldspar biotite granite and medium-grained biotite granite. The two granites correlate respectively with Pgw_{1b} and Pgw_{1a} of the Wonga Waterhole dating site. Pgw_{1b} is the major 'matrix' rock in the area shown;
- (2) Dolerite (Pdw_1);
- (3) Fine- to medium-grained porphyritic K-feldspar biotite-amphibole granite (Pgw_{2a});
- (4) Leucocratic fine- to medium-grained biotite granite (Pgw_{5a} or 'Middle Breakfast Creek' microgranite). This is the dated rock;
- (5) Quartz-K-feldspar pegmatite (Pgw_{5b}).

Rock types 1 to 3 bear a strong D^W_1 fabric, consisting of a subvertical S_1/S_2 gneissic/mylonitic foliation containing a moderately south-plunging L_1 stretching lineation. They also bear a strong D^W_2 fabric, characterised by a down-dip alignment of biotite grains within the S_1/S_2 foliation. In contrast, rock types 4 and 5 bear only a variably developed D^W_2 fabric; dykes are folded into open F_2 folds, and a moderately developed axial plane S_2 schistosity and L_2 down-dip lineation are defined by a grain shape and mineral fabric. Dolerite xenoliths in the

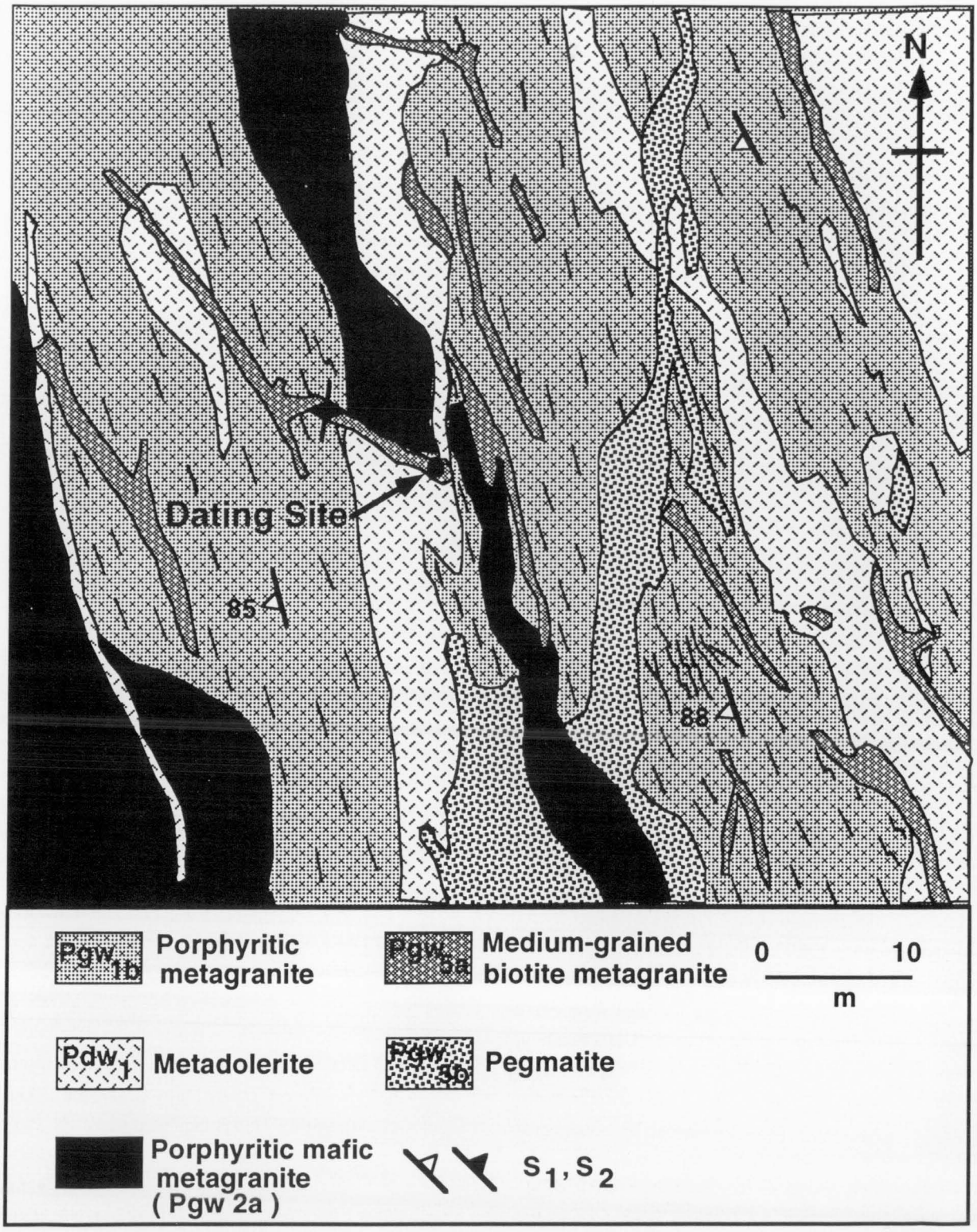


Fig. 23. Outcrop map showing field relationships at the Breakfast Creek dating site.

dated 'Middle Breakfast Creek' microgranite (Pgw_{5a}) are flattened in the S_2 schistosity and are elongate parallel to the L_2 down-dip lineation. As elsewhere in the Wonga Belt, veins of the Pgw_{5a} microgranite cross-cut and thus postdate the D^w_1 fabric at all scales.

The most definitive timing relationships occur where xenoliths of the coarse-grained granite (Pgw_{1b}) are included within the dated rock. The S_1 foliation in the xenoliths is variably oriented with respect to the S_2 schistosity, and is sharply truncated against the contact with the dated rock (Fig. 8a). In the xenoliths shown, the S_1 foliation lies within the D^w_2 shortening field, and is folded about steeply dipping north-striking F_2 axial planes. This orientation parallels the S_2 schistosity in the enclosing

dated rock. In those orientations lying within the D^W_2 extension field, the S_1 foliation is planar and somewhat attenuated. The folded foliation in the xenoliths clearly represents an inherited S_1 foliation that predates emplacement of the dated rock.

The relationships indicate that, in this area, emplacement of the dated Pgw_{5a} granite was bracketed by D^W_1 and D^W_2 fabric development, and thus occurred post-D^W_1 and pre-D^W_2.

Use of the U-Pb zircon dates to date the D^W_1 deformation

The three U-Pb ion probe zircon dates (1758 ± 8 Ma, 1742 ± 13 Ma, and 1729 ± 5 Ma) for critical parts of the Wonga Granite show that the Wonga Batholith intruded between 1766 and 1724 Ma. These dates are broadly coincident with the U-Pb zircon dates of the structurally higher Burstall Granite (1726 +8-7 Ma and 1745 +17-15 Ma: Page, 1983b), its late felsic dykes (1737 ± 15 Ma: Page, 1983b) and the Lunch Creek Gabbro (1740 +28-20 Ma: Page, 1983b).

Field relationships suggest that the emplacement of the various intrusions of the Wonga Batholith spanned the duration of the D^W_1 extensional deformation around the Wonga Belt. Therefore, these U-Pb dates collectively mark a major regional intrusive, thermal, and D^W_1 deformational event in the Mary Kathleen Fold Belt which occurred between about 1760 and 1720 Ma. They also demonstrate that original igneous zircons and their U and Pb contents can survive intact through two overprinting amphibolite facies thermal episodes (D^W_1 and D^W_2). Figure 14 shows the inferred time framework for the emplacement and deformation of the Wonga Batholith.

There are problems with the internal consistency of the ion probe dates. The youngest rock in the relative timing sequence (the post-D^W_1, pre-D^W_2 Pgw_{5a} microgranite from Middle Breakfast Creek) gives the oldest ion probe U-Pb date (1758 ± 8 Ma). However, as mentioned above, this is a maximum age, and we attribute this apparent conflict to inheritance of undetected 1778 Ma zircons in this granite. If the field correlations are correct, a slightly younger real age (ideally younger than the 1729 ± 5 Ma Knob age) is likely.

Previously published isotopic dates and their use in dating deformations

Rb-Sr whole rock systems in metamorphosed igneous rocks generally record metamorphic rather than igneous crystallisation ages, as the system is prone to resetting (Page & Bell, 1986). Widespread resetting is likely in the Wonga Belt, where the imprints of at least two major tectono-metamorphic episodes are shown by pervasive dynamic recrystallisation and high-grade fabric development. Pearson (1989) showed that in some zones of very strong D^W_1 shearing deformation and attendant high fluid/rock ratios, a gross disturbance of the Rb-Sr system occurred in the granitoids such that 'normal' Rb/Sr ratios between about 1 and 4 commonly were reduced to less than 0.5.

It is possible that the 1700 ± 20 Ma Rb-Sr whole rock result determined for the 'Knob' granite in the Mary Kathleen area (Page, 1978) may record the age of the D^W_1 deformation, as it is broadly consistent with the U-Pb zircon ages constraining D^W_1. The Rb-Sr whole rock work preferentially sampled large tors of 'Knob' granite. They probably represent resistant regions of low D^W_2 strain surrounded by more easily eroded zones of high D^W_2 strain, because S_1-parallel grain elongations in the tors are commonly preserved around the hinges of F_2 crenulations in S_1, with little evidence for S_2 axial plane foliation (Pearson, 1989). Therefore, it is conceivable that such areas could preserve the Rb-Sr isotopic signature of the earliest deformation (D^W_1).

The 1621 ± 28 Ma and 1629 ± 25 Ma Rb-Sr whole rock dates obtained from the 'Wonga Waterhole' granite by Page (1978) probably represent isotopic resetting during the 1610 ± 13 Ma D_1 deformation of the Western Fold Belt (Page & Bell, 1986) and inferred in the Eastern Fold Belt by Loosveld (1987, 1989) and Hill (1990). Around the Wonga Belt, limited evidence for shortening of this age includes the existence of an early schistosity of variable orientation within syn-D^W_2 porphyroblasts in the Rosebud Syncline west of the Wonga Belt (Reinhardt & Rubenach, 1989), the existence of some pre-D^W_2 folds just east of the Wonga Belt (Hill, 1986), and the existence of apparently anomalous pre-D^W_2 shear senses within the Wonga Belt itself (Fig. 25; Pearson, 1989). If thrusting in a north-south direction did occur around 1610 Ma, the older subhorizontal extensional shear zone may have been reactivated in zones, even though largely indistinguishable from the earlier fabrics because of the broadly parallel kinematic axes and perhaps similar metamorphic grade.

K-Ar mica ages for various Wonga Batholith intrusions lie within the range of most mica ages in the Mount Isa Inlier, namely 1460 to 1360 Ma (Richards & others, 1963). A total-fusion $^{40}Ar/^{39}Ar$ age measured by Green (1975) is somewhat older (1530 Ma), but all these ages reflect post-deformation cooling of the terrane.

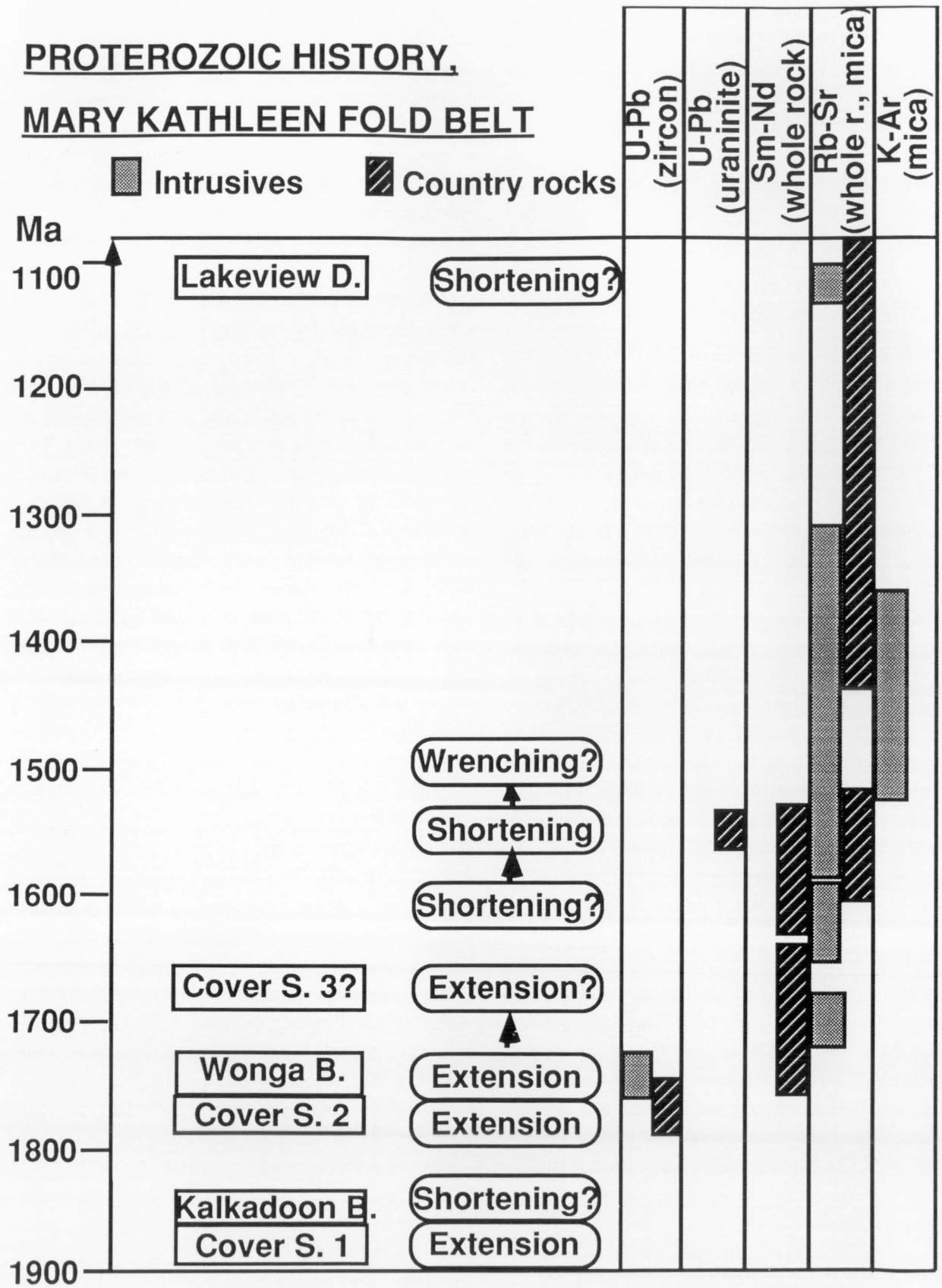


Fig. 24. Summary of Proterozoic history, Mary Kathleen Fold Belt.

EASTERN SUCCESSION				WESTERN SUCCESSION			
This study	Loosveld (1989)	Passchier & Williams (1989)	Loosveld & Schreurs (1987)	Valenta (1988)	Rickard (1987)	Page & Bell (1986)	Winsor (1986)
D^{w}_4	-	-	-	-	-	-	-
-	-	-	-	D_4,D_5	-	-	-
D^{w}_3	D_{c3+}	Fountain Range Phase	D_3	-	-	D_4	-
-	-	-	-	D_3	-	D_3	D_3
D^{w}_2	D_{c2}	Duchess Phase	D_2	D_2	D_4	D_2	D_2
?	D_{c1}	Malbon Phase	D_1	D_1	D_3	D_1	D_1
D^{w}_1	D_{e2}	Alligator Phase	-	-	-	-	-
-	D_{e1}	-	-	-	-	-	-
-	Rifting?	-	-	-	-	-	-
-	Barramundi Orogeny	-	-	-	D_1,D_2	-	-

TABLE 7. TERMINOLOGY AND CORRELATION OF DEFORMATIONS IN THE MOUNT ISA INLIER.

Figure 24 and Table 7 show the inferred correlations and ages of deformational episodes that affected the Mount Isa Inlier.

Discussion

Wyborn & others (1987) proposed that the general absence of S-type granitoids in the Australian Proterozoic precludes significant regional overthrusting or subduction of supracrustal source rocks to depths where substantial partial melting might have occurred. Instead, melt generation during extensional thinning of previously underplated crust appears to be more likely (Wyborn & others, 1987).

We have confirmed this conclusion by demonstrating that early extensional deformation accompanied a major pulse of bimodal igneous intrusion in the eastern Mount Isa Inlier. Bimodal magmatism is generally considered to be diagnostic of crustal extension (Lipman & others, 1972; Martin & Piwinskii, 1972), and accords with the tectonic model proposed for D^{w}_1. The dominantly I- and A-type felsic rocks and tholeiitic mafic rocks of the Wonga Batholith were probably derived from melting of deep crustal and upper mantle sources (White & Chappell, 1983; Wyborn & others, 1987).

Figure 25 shows a scheme for passive emplacement of the Wonga Batholith intrusions that explains why their internal deformational style was so dependent on their vertical position in the extensional system. Wonga Belt (lower plate) intrusions were emplaced synkinematically into a subhorizontal region of bulk D^{w}_1 shearing, while flanking domain (upper plate) intrusions were synkinematically emplaced into a region of D^{w}_1 bulk north-south stretching.

In both the upper and lower plates, emplacement commonly occurred into dilational sites controlled by bends in developing low-angle and high-angle shear zones, or by en echelon fracturing initiated at some angle to the bulk shear planes (Fig. 25). In the upper plate, such as in the Mary Kathleen Syncline, felsic dykes were emplaced into steep east-striking extensional fractures inferred to have formed normal to the D^{w}_1 regional minimum principal compressive stress orientation, which was most likely to have been north-south and subhorizontal.

The different relative abundances of intrusive rocks in

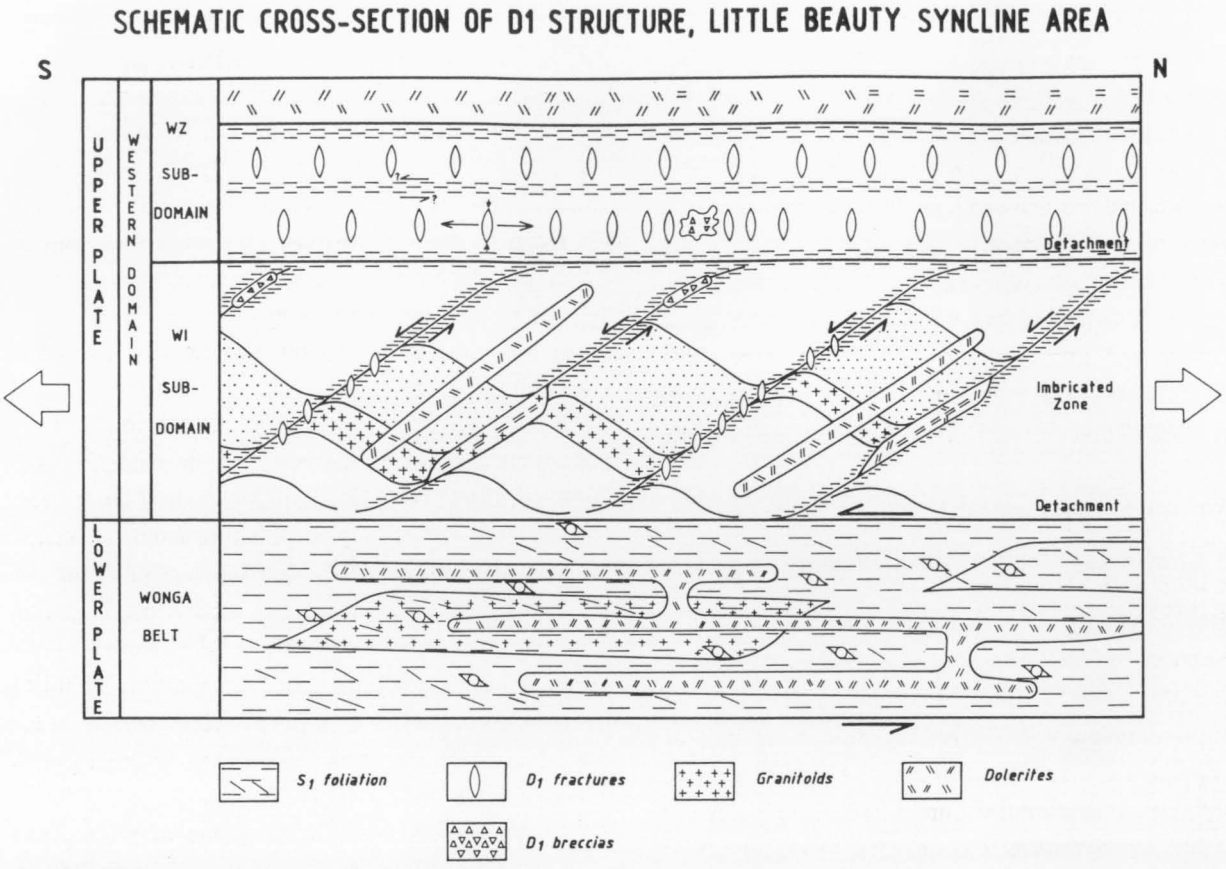


Fig. 25. Schematic diagram showing emplacement mode of Wonga Batholith intrusions into different structural levels of the D^W_1 extensional system, typified by the section exposed on the eastern limb, Little BeautySyncline. The geometric relationships shown here apply to the whole Wonga Belt, but the anomalous D^W_1 shear sense (i.e., hanging wall block to the south) is specific to the northwestern Wonga Belt only (see text); hence, 'N' and 'S' in top corners should be transposed for the Wonga Belt as a whole.

the two plates clearly reflect the control exerted on their emplacement by the style of D^W_1 deformation. The pervasively sheared lower plate provided abundant dilational sites during ongoing deformation, concentrating the largest volume of intrusive material. The less homogeneously deformed upper plate concentrated a smaller proportion of intrusive material in dilational sites.

We infer near-lithostatic conditions during each intrusive pulse, such that elevated fluid pressure due to both igneous crystallisation and devolatilisation of the intruded country rocks aided the initiation of both systematically and non-systematically oriented hydrofractures into which intrusive rocks were emplaced. Subsequent to each pulse of igneous emplacement into the lower plate, pervasive ongoing D^W_1 shearing imposed a mylonitic fabric upon the already emplaced intrusive rocks. Cyclic transitions between ductile deformation and brittle hydrofracturing (with emplacement) are therefore implied.

Extensional deformation in D^W_1 was marked by a steep thermal gradient between the upper and lower plates, controlled to a large extent by igneous emplacement. In the lower plate, the style of quartz, K-feldspar, and plagioclase deformation, the presence of S_1-parallel sillimanite, and the formation of early pyroxene-bearing skarns, imply amphibolite facies conditions during D^W_1 (Pearson, 1989; Oliver & others, 1991). In the cooler, yet still considerably metamorphosed upper plate, local greenschist to amphibolite facies conditions during D^W_1 are inferred from broad garnet-pyroxene skarns and hornfelsic aureoles around the upper plate granites (Oliver, 1988; Oliver & others, 1991) and from early foliation relics preserved in andalusite porphyroblasts (Pearson, 1989).

In contrast to the Cordilleran metamorphic core complexes of the western USA (Anderson & Rowley, 1981; Davis & others, 1986; Reynolds & others, 1986), where the upper limits of the intrusions are generally truncated against a sharp detachment fault which separates them from an essentially intrusion-free upper plate (Crittenden & others, 1980; Anderson & Rowley, 1981), the Wonga Belt represents a bedding-parallel flat which extends for at least 100 km parallel to the

(north-south) bulk tectonic transport direction in a regional extensional decollement. The amount of shear translation on this surface was insufficient to bring up lower crustal rocks against the upper plate rocks. Instead, structural continuity appears to have been preserved at the macroscale, and this allowed igneous rocks emplaced into the lower plate shear zone to 'leak' into the upper plate, rather than being truncated at a discrete detachment fault. Heat from the emplaced igneous material metamorphosed the lower and upper plates, and drove large-scale hydrothermal systems (e.g., Derrick, 1977; Cruikshank & others, 1980; Oliver, 1988; Oliver & others, 1986, 1987, 1991).

We interpret the flat in the extensional decollement as paralleling the Proterozoic brittle-ductile transition, akin to the delamination model for crustal extension proposed by Lister & others (1986). Therefore, estimates of 6 to 10 km proposed by Holcombe & others (1991) and Oliver & others (1991) for the depth of emplacement of Wonga Batholith intrusions approximate the original depth to the Proterozoic brittle-ductile transition. In detail, because of the thermal and fluid pressure pulses accompanying continuing synkinematic intrusion, the precise depth of this transition was probably dynamic in space and time.

We infer some pure shear stretching of the lower crust below the extensional decollement exposed in the Wonga Belt, even though the consistency of D^{W}_{1} shear-sense indicators suggest uniform simple shear at the presently exposed crustal levels. The possibility of deep pure shear stretching is suggested by the north-south distance (over 100 kilometres) over which the Wonga Batholith intruded the flat in the decollement; voluminous melt migration up and along a flat in a discrete simple shear system from a displaced melt generation region in itself appears difficult. Instead, deep melt generation over such large distances parallel to the tectonic transport direction might have been achieved more efficiently by a component of pure shear stretching of the lower crust.

The Wonga Belt extension took place over about 30 Ma, similar to that in the Basin and Range Province of the USA (Reynolds, 1987). We correlate it with magmatism and extension documented in the eastern Arunta Inlier of central Australia by Ding & James (1985, 1987) and James & Ding (1987).

Conclusions

(1) The synkinematic Wonga Batholith is a voluminous suite of multiple felsic and mafic intrusions emplaced at different times into different structural levels of a subhorizontal D^{W}_{1} regional extensional system that formed after deposition of cover sequence 2 in the Mary Kathleen Fold Belt of the Mount Isa Inlier. Later folding (D^{W}_{2}) and erosion exposed the D^{W}_{1} extensional zone in the core of a regional anticline, the Wonga Belt.

(2) The felsic rocks range widely in composition, include both I- and A- types, and are intimately associated with tholeiitic mafic intrusions. This implies melting of infrastructural source rocks in an intracratonic setting triggered by lithospheric thinning.

(3) Most intrusions in the pervasively deformed Wonga Belt (lower plate) form streaked-out sheets with a mylonitic D^{W}_{1} foliation and lineation, and an overprinting D^{W}_{2} shortening fabric. In contrast, intrusions in the heterogeneously deformed flanking domains (upper plate) were less modified by D^{W}_{1} deformation, and their internal fabric is dominated by D^{W}_{2}. Emplacement into both the upper and lower plates of the extensional system commonly occurred into sites of syn-D^{W}_{1} dilation.

(4) U-Pb zircon dating of the Wonga Batholith intrusions in both the lower and upper plates constrains the time of the D^{W}_{1} regional extensional deformation to between 1760 and 1720 Ma.

(5) 1760 to 1720 Ma was a time of widespread extension in the Australian Proterozoic, characterised by voluminous bimodal igneous rocks intruded into the middle and upper crust.

(6) D^{W}_{1} extension in the Mary Kathleen Fold Belt differed from the classic low-angle mylonitic detachment terranes described from the Basin and Range Province of the USA, in that the upper plate in the Mary Kathleen area was also intruded by synkinematic igneous rocks and extensively contact metamorphosed. We interpret this difference as a consequence of differing large-scale extensional geometries and mechanisms.

Acknowledgements

The authors wish to thank the Bureau of Mineral Resources, Geology and Geophysics for logistic support during the course of this work. We thank in particular Mike Etheridge, Gordon Lister, David Blake, and Lesley Wyborn for thought-provoking discussion. Nick Oliver, Tim Bell, Jurgen Reinhardt, Cees Passchier, Ramon Loosveld, and June Hill also contributed much in the way of ideas and discussion, as did many of the postgraduate students from the University of Queensland under the supervision of Rod Holcombe. Alastair Stewart, Jurgen Reinhardt, and Cees Passchier reviewed the manuscript. Paul Pearson gratefully acknowledges the support of a Commonwealth Postgraduate Research Award.

References

ANDERSON, J.L., & ROWLEY, M.C., 1981 - Synkinematic intrusion of two-mica and associated metaluminous granitoids, Whipple Mountains, California. *Canadian Mineralogist* 19, 83-101.

BLAKE, D.H., 1981 - Intrusive felsic-mafic net-veined complexes in north Queensland. *BMR Journal of Australian Geology & Geophysics* 6, 95-99.

BLAKE, D.H., 1987 - Geology of the Mount Isa Inlier and environs, Queensland and Northern Territory. *Bureau of Mineral Resources, Australia, Bulletin* 225, 83 pp.

BLAKE, D.H., ETHERIDGE, M.A., PAGE, R.W., STEWART, A.J., WILLIAMS, P.R., & WYBORN, L.A.I., 1990 - Mount Isa Inlier - regional geology and mineralisation. *In* HUGHES, F.E. (Editor), Geology of the Mineral Deposits of Australia and Papua New Guinea. *Australasian Institute of Mining and Metallurgy, Monograph* 14, 915-925.

CARTER, E.K., BROOKS, J.H., & WALKER, K.R., 1961 - The Precambrian mineral belt of northwestern Queensland. *Bureau of Mineral Resources, Australia, Bulletin* 51, 344 pp.

CHAPPELL, B.W., & WHITE, A.J.R., 1974 - Two contrasting granite types. *Pacific Geology 8, 173-174.*

COLLINS, W.J., BEAMS, S.D., WHITE, A.J.R., & CHAPPELL, B.W., 1982 - Nature and origin of A-type granites with particular reference to southeastern Australia. *Contributions to Mineralogy and Petrology* 80, 189-200.

COMPSTON, W., WILLIAMS, I.S., & MEYER, C., 1984 - U-Pb geochronology of zircons from Lunar breccia 73217 using a sensitive high mass-resolution ion microprobe. *Proceedings of the 14th Lunar and Planetary Sciences Conference, Part 2, Journal of Geophysical Research* 89, Supplement, B525-B534.

COMPSTON, W., KINNY, P.D., WILLIAMS, I.S., & FOSTER, J.J., 1986 - The age and Pb loss behaviour of zircons from the Isua supracrustal belt as determined by ion microprobe. *Earth and Planetary Science Letters 80, 71-81.*

CONNORS, K.A., & PAGE, R.W., 1992 - Age relationships between granite intrusion, metamorphism, and deformation in the Mount Isa Inlier. *In:* 11th Australian Geological Convention, Ballarat, Victoria. *Geological Society of Australia, Abstracts* 32, 229-230.

CRITTENDEN, M.D., CONEY, P.J., & DAVIS, G.H. (Editors), 1980 - Cordilleran metamorphic core complexes. *Geological Society of America, Memoirs* 153.

CRUIKSHANK, B.I., FERGUSON, J., & DERRICK, G.M., 1980 - The association of uranium and skarn development in the Mary Kathleen area, Queensland. Proceedings of the International Symposium on the Pine Creek Geosyncline, Sydney, 1979. *International Atomic Energy Agency, Vienna,* 693-706.

CUMMING, G.L., & RICHARDS J.R., 1975 - Ore lead isotopes in a continuously changing earth. *Earth and Planetary Science Letters* 28, 155-171.

DAVIS, G.A., LISTER, G.S., & REYNOLDS, S.J., 1986 - Structural evolution of the Whipple and South Mountains shear zones, southern United States. *Geology* 14, 7-10.

DERRICK, G.M., 1977 - Metasomatic history and origin of uranium mineralization at Mary Kathleen, northwest Queensland. *BMR Journal of Australian Geology & Geophysics 123-130.*

DERRICK, G.M., 1978 - Proterozoic igneous and sedimentary rocks and associated metamorphism and metasomation at Mary Kathleen, northwest Queensland. PhD Thesis, University of Queensland, Brisbane (unpublished).

DERRICK, G.M., WILSON, I.H., HILL, R.M., GLIKSON, A.Y., & MITCHELL, J.E., 1971 - Geology of the Marraba 1:100 000 sheet area, Queensland. *Bureau of Mineral Resources, Australia, Record* 1971/56, 193 pp.

DERRICK, G.M., WILSON, I.H., HILL, R.M., GLIKSON, A.Y., & MITCHELL, J.E., 1977 - Geology of the Mary Kathleen 1:100,000 sheet area, northwest Queensland. *Bureau of Mineral Resources, Australia, Bulletin* 193, 114 pp.

DING, P., & JAMES, P.R., 1985 - Structural evolution of the Harts Range and its implication for the development of the Arunta Block, central Australia. *Precambrian Research* 27, 251-276.

DING, P., & JAMES, P.R., 1987 - The Harts Range Mobile Belt: A short-lived intraplate orogen from the eastern Arunta Inlier of central Australia. International Conference on the Deformation of Crustal Rocks, Mt. Buffalo, Australia. *Geological Society of Australia, Abstracts* 19, 53-54.

ELLIS, D.J., & WYBORN, L.A.I., 1984 - Petrology and geochemistry of Proterozoic dolerites from the Mount Isa Inlier. *BMR Journal of Australian Geology & Geophysics* 9, 19-32.

ETHERIDGE, M.A., WYBORN, L.A.I., RUTLAND, R.W.R., PAGE, R.W., BLAKE, D.H., & DRUMMOND, B.J., 1984 - The BMR Model - a discussion paper. *In:* Workshop on Early to Middle Proterozoic of Northern Australia. *Bureau of Mineral Resources, Australia, Record* 1984/31, 8 pp.

ETHERIDGE, M.A., RUTLAND, R.W.R., & WYBORN, L.A.I., 1987 - Orogenesis and tectonic process in the Early to Middle Proterozoic of Northern Australia. *In:* KRONER, A. (Editor), Proterozoic Lithosphere Evolution. *American Geophysical Union, Geodynamics Series* 17, 131-147.

GREEN, D.C., 1975 - Geochronology of the Cloncurry

Complex, northwest Queensland, with particular emphasis on the later Carpentarian events. *In:* Mount Isa Field Conference guidebook, *Geological Society of Australia (Queensland Division)*, June 1975, 29-33.

HAMILTON, L.M., 1985 - Structure and metamorphism in high-grade shear zones and surrounding rocks, northwest of Mary Kathleen, northwest Queensland. B.Sc. Honours Thesis, University of Queensland, Brisbane (unpublished).

HILL, E.J., 1986 - Structural geology of the Knobby Mine area, north of Mary Kathleen, Queensland. B.Sc. Honours Thesis, University of Queensland, Brisbane (unpublished).

HILL, E.J., 1990 - The Tommy Creek Block, eastern Mount Isa Inlier. *In:* Mount Isa Inlier Geology Conference, *Monash University and Victorian Institute of Earth and Planetary Sciences, Melbourne, Australia, Abstracts* 16-18.

HOLCOMBE, R.J., 1991 - Geology of the Mary Kathleen Area (1:25 000 scale map). *Bureau of Mineral Resources, Canberra, Australia* (two sheets). Available as colour electrostatic plots on paper (AUD30), or in digital form on optical disc or Exabyte 8 mm tape (prices on application) both of which can be displayed on Intergraph Microstation software on computers that will run Unix. The digital data comprise a scanned raster image (.RLE format) of the black and white geological map, and an Intergraph vector design file containing the boundaries of coloured polygons. The coloured map and data are available from the Publication Sales Centre, Bureau of Mineral Resources, and an uncoloured Ozalar film or paper copy (AUD20) of the map is available from BMR Copy Service, both at GPO Box 378, Canberra, ACT, 2601, Australia. All orders to be prepaid to Collector of Public Monies.

HOLCOMBE, R.J., & FRASER, S.J., 1979 - Structural and stratigraphic problems of the Argylla Formation near Mary Kathleen, Queensland. *Journal of the Geological Society of Australia* 26, 419-434.

HOLCOMBE, R.J., PEARSON, P.J., & OLIVER, N.H.S., 1987 - The Mary Kathleen Fold Belt, northwest Queensland: geometry and timing of deformation. *In:* International Conference on the Deformation of Crustal Rocks, Mt. Buffalo, Australia. *Geological Society of Australia, Abstracts* 19, 35-36.

HOLCOMBE, R.J., PEARSON, P.J., & OLIVER, N.H.S., 1991 - Geometry of a Middle Proterozoic extensional detachment surface in northeastern Australia. *Tectonophysics* 191, 255-274.

HOLCOMBE, R.J., PEARSON, P.J., & OLIVER, N.H.S. (this volume) - Structure of the Mary Kathleen Fold Belt. *In:* STEWART, A.J. & BLAKE, D.H. (Editors), Detailed Studies of the Mount Isa Inlier. *Bureau of Mineral Resources, Australia, Bulletin* 243.

JAMES, P.R., & DING, P., 1987 - An Early-Middle Proterozoic short-lived extension-collision intraplate orogeny: the Strangways Orogeny of the eastern Arunta Inlier, central Australia. *In:* International Conference on the Deformation of Crustal Rocks, Mt. Buffalo, Australia. *Geological Society of Australia, Abstracts* 19, 55.

JORGENSEN, G.C., 1986 - Geology of the northern Burstall Granite area, Mary Kathleen, northwest Queensland. B.Sc. Honours Thesis, University of Queensland, Brisbane (unpublished).

KROGH, T.E., 1973 - A low-contamination method for hydrothermal decomposition of zircon and extraction of U and Pb for isotopic age determination. *Geochimica et Cosmochimica Acta* 37, 490-494.

LIPMAN, P.W., PROSTKA, H.J., & CHRISTIANSEN, R.L., 1972 - Cenozoic volcanism and plate-tectonic evolution of the western United States. 1. Early and Middle Cenozoic. *Philosophical Transactions of the Royal Society of London, Series A* 271, 217-248.

LISTER, G.S., ETHERIDGE, M.A., & SYMONDS, P.A., 1986 - Detachment faulting and the evolution of passive continental margins. *Geology* 14, 246-250.

LOOSVELD, R., 1987 - A complex fold nappe within the Soldiers Cap Group, Mount Isa Inlier, Queensland, Australia. *In:* International Conference on the Deformation of Crustal Rocks, Mt. Buffalo, Australia. *Geological Society of Australia, Abstracts* 19, 45-46.

LOOSVELD, R., 1989 - The intracratonic evolution of the central eastern Mount Isa Inlier, northwest Queensland, Australia. *Precambrian Research* 44, 243-276.

LOOSVELD, R., & SCHREURS, G., 1987 - Discovery of thrust klippen, northwest of Mary Kathleen, Mount Isa Inlier, Australia. *Australian Journal of Earth Sciences* 34, 387-402.

MARTIN, R.F., & PIWINSKII, A.J., 1972 - Magmatism and tectonic settings. *Journal of Geophysical Research* 77, 4966-4975.

OLIVER, N.H.S., 1981 - Structure, mineralogy and petrogenesis of skarn and related rocks near Mary Kathleen, northwestern Queensland. B.Sc. Honours Thesis, University of Queensland, Brisbane (unpublished).

OLIVER, N.H.S., 1988 - A metamorphic plumbing system - the Mary Kathleen Fold Belt, northwest Queensland. PhD Thesis, Monash University, Melbourne (unpublished).

OLIVER, N.H.S., 1991 - Geology of the Mount Godkin Area (1:25 000 scale map). *Bureau of Mineral Resources, Canberra.* Available as a colour electrostatic plot on paper (AUD30), or in digital form on optical disc or Exabyte 8 mm tape (prices on application) both of which can be displayed on Intergraph Microstation software on computers that will run Unix. The digital data comprise a scanned raster image (.RLE format) of the black and white geological map, and an Intergraph vector design file

containing the boundaries of coloured polygons. The coloured map and data are available from the Publication Sales Centre, Bureau of Mineral Resources, and an uncoloured Ozalar film or paper copy (AUD20) of the map is available from BMR Copy Service, both at GPO Box 378, Canberra, ACT, 2601, Australia. All orders to be prepaid to Collector of Public Monies.

OLIVER, N.H.S., WALL, V.J., & PEARSON, P.J., 1986 - The Mary Kathleen uranium-REE deposit: a product of regional metamorphism. *In*: 8th Australian Geological Convention, Adelaide, Australia. *Geological Society of Australia, Abstracts* 15, 149-150.

OLIVER, N.H.S., PEARSON, P.J., WALL, V.J., GOLDING, S.D., & HOLCOMBE, R.J., 1987 - Structural controls on fluid infiltration and metasomatism in the Mary Kathleen Fold Belt - implications for large-scale fluid migration during deformation. *In:* International Conference on the Deformation of Crustal Rocks, Mt. Buffalo, Australia. *Geological Society of Australia, Abstracts* 19, 14-15.

OLIVER, N.H.S., HOLCOMBE, R.J., HILL, E.J., & PEARSON, P.J., 1991 - Tectono-metamorphic evolution of the Mary Kathleen Fold Belt, northwest Queensland: A reflection of mantle-plume processes? *Australian Journal of Earth Sciences* 38, 425-455.

PAGE, R.W., 1978 - Response of U-Pb zircon and Rb-Sr total-rock and mineral systems to low grade regional metamorphism in Proterozoic igneous rocks, Mount Isa, Australia. *Journal of the Geological Society of Australia 25, 141-164.*

PAGE, R.W., 1983a - Timing of superposed volcanism in the Proterozoic Mount Isa Inlier, Australia. *Precambrian Research* 21, 223-245.

PAGE, R.W., 1983b - Chronology of magmatism, skarn formation and uranium mineralization, Mary Kathleen, Queensland, Australia. *Economic Geology* 78, 838-853.

PAGE, R.W., 1988; Geochronology of Early to Middle Proterozoic fold belts in northern Australia: a review. *Precambrian Research* 40/41, 1-19.

PAGE, R.W., & BELL, T.H., 1986 - Isotopic and structural responses of granite to successive deformation and metamorphism. *Journal of Geology* 94, 365-379.

PASSCHIER, C.W., 1986 - Evidence for early extensional tectonics in the Proterozoic Mount Isa inlier, Australia. *Geology* 14, 1008-1011.

PASSCHIER, C.W. (this volume) - Geology of the Myubee area, Mount Isa Inlier, Queensland. *In:* STEWART, A.J., & BLAKE, D.H. (Editors), Detailed Studies of the Mount Isa Inlier. *Bureau of Mineral Resources, Australia, Bulletin,* 243.

PASSCHIER, C.W., & WILLIAMS, P.R., 1989 - Proterozoic extensional deformation in the Mount Isa Inlier, Queensland, Australia. *Geological Magazine* 126, 43-53.

PEARSON, P.J., 1982 - The structural and stratigraphic setting of the Mary Kathleen uranium orebody, northwest Queensland. B.Sc. Honours Thesis, University of Queensland, Brisbane (unpublished).

PEARSON, P.J., 1989 - The structural and tectonic development of the Wonga Belt and surrounding Mary Kathleen Fold Belt, Mount Isa Inlier, northwestern Queensland. PhD Thesis, University of Queensland, Brisbane (unpublished).

PEARSON, P.J., & HOLCOMBE, R.J., 1991a - Geology of the Breakfast Creek Area (1:25 000 scale map). *Bureau of Mineral Resources, Canberra.* Available as a colour electrostatic plot on paper (AUD30), or in digital form on optical disc or Exabyte 8 mm tape (prices on application) both of which can be displayed on Intergraph Microstation software on computers that will run Unix. The digital data comprise a scanned raster image (.RLE format) of the black and white geological map, and an Intergraph vector design file containing the boundaries of coloured polygons. The coloured map and data are available from the Publication Sales Centre, Bureau of Mineral Resources, and an uncoloured Ozalar film or paper copy (AUD20) of the map is available from BMR Copy Service, both at GPO Box 378, Canberra, ACT, 2601, Australia. All orders to be prepaid to Collector of Public Monies.

PEARSON, P.J., HORTON, J.A., & HOLCOMBE, R.J.,1991b - Geology of the East Limb, Little Beauty Syncline (1:15 000 scale map). *Bureau of Mineral Resources, Canberra.* Available as a colour electrostatic plot on paper (AUD30), or in digital form on optical disc or Exabyte 8 mm tape (prices on application) both of which can be displayed on Intergraph Microstation software on computers that will run Unix. The digital data comprise a scanned raster image (.RLE format) of the black and white geological map, and an Intergraph vector design file containing the boundaries of coloured polygons. The coloured map and data are available from the Publication Sales Centre, Bureau of Mineral Resources, and an uncoloured Ozalar film or paper copy (AUD20) of the map is available from BMR Copy Service, both at GPO Box 378, Canberra, ACT, 2601, Australia. All orders to be prepaid to Collector of Public Monies.

PEARSON, P.J., HOLCOMBE, R.J., & OLIVER, N.H.S., 1987 - The Mary Kathleen Fold Belt, northwest Queensland: D_1 - a product of crustal extension? *In:* International Conference on the Deformation of Crustal Rocks, Mt. Buffalo, Australia. *Geological Society of Australia, Abstracts* 19, 37-38.

REINHARDT, J., & RUBENACH, M.J., 1989 - Temperature-time relationships across metamorphic zones: evidence from porphyroblast-matrix

relationships in progressively deformed metapelites. *Tectonophysics* 158, 141-161.

REYNOLDS, S.J., 1987 - Continental extension and related igneous history in the Basin and Range Province, USA. *In:* Extended Abstracts, Applied Extension Tectonics, 16th BMR Research Symposium, Canberra. *Bureau of Mineral Resources, Australia, Record* 1987/51, 10-15.

REYNOLDS, S.J., SHAFIQULLAH, P.D., & DEWITT, E., 1986 - Early Miocene mylonitization and detachment faulting, South Mountains, Central Arizona. *Geology* 14, 283-286.

RICHARDS, J.R., COOPER, J.A., & WEBB, A.W., 1963 - Potassium-argon ages on micas from the Precambrian region of northwestern Queensland. *Journal of the Geological Society of Australia* 10, 299-312.

SLIWA, R., 1986 - Structural geology of the Wollondonga Mine area, Mary Kathleen, northwest Queensland. B.Sc. Honours Thesis, University of Queensland, Brisbane (unpublished)

STEIGER, R.H., & JÄGER, E., 1977 - Subcommission on geochronology: Convention on the use of decay constants in geo- and cosmochronology. *Earth and Planetary Science Letters* 36, 359-362.

STRECKEISEN, A.L., 1976 - To each plutonic rock its proper name. *Earth Science Reviews* 12, 1-33.

VALENTA, R.K., 1988 - Deformation, fluid flow and mineralisation in the Hilton area, Mount Isa, Australia. PhD Thesis, Monash University, Melbourne (unpublished).

WHITE, A.J.R., & CHAPPELL, B.W., 1983 - Granitoid types and their distribution in the Lachlan Fold Belt, southeastern Australia. *In:* RODDICK, J.C. (Editor), Circum-Pacific plutonic terranes. *Geological Society of America, Memoirs* 159, 21-34.

WILLIAMS, P.R., 1989 - Nature and timing of early extensional structures in the Mitakoodi Quartzite, Mount Isa Inlier, northwest Queensland. *Australian Journal of Earth Sciences* 36, 283-296.

WILLIAMS, P.R., STEWART, A.J., & PEARSON, P.J., 1987 - Proterozoic continental extension in the Mount Isa Inlier, Queensland, Australia. *In*: Extended Abstracts, Applied Extension Tectonics Symposium, Canberra, Australia. *Bureau of Mineral Resources, Australia, Record* 1987/51, 64-71.

WYBORN, L.A.I., PAGE, R.W., & PARKER, A.J., 1987 - Geochemical and geochronological signatures in Proterozoic igneous rocks. *In:* PHARAOH, T.C., BECKINSALE, R.D., & RICKARD, D. (Editors), Geochemistry and Mineralisation of Proterozoic Volcanic Suites. *Geological Society of London, Special Publication* 33, 377-394.

WYBORN, L.A.I., PAGE, R.W., & McCULLOCH, M.T., 1988 - Petrology, geochronology and isotope geochemistry of the post-1820 Ma granites of the Mount Isa Inlier: mechanisms for the generation of Proterozoic anorogenic granites. *Precambrian Research* 40-41, 509-541.

YORK, D., 1969 - Least-squares fitting of a straight line with correlated errors. *Earth and Planetary Science Letters* 5, 320-324.

Appendix: General analytical techniques

Zircon was separated from approximately 25 kg samples collected from each of the sites shown in Figure 1, using a Wilfley table and normal heavy liquid and isodynamic magnetic methods. The isotope dilution analyses used ^{208}Pb and ^{235}U spikes and conventional U-Pb anion exchange and mass spectrometric techniques (Krogh, 1973). The laboratory Pb blank for multigrain dissolutions and chemistry averaged about 0.25 ng. Regression of the U-Pb discordia line employed a modified York (1969) program, and assigned 1-sigma errors of 0.5% (U-Pb) and 0.1% ($^{207}Pb/^{206}Pb$), and a sample coefficient of 0.98.

Sample numbers referred to in the text and map (5001, 5025 etc.) are abbreviated from catalogued BMR sample numbers (85205001, 72205025, etc.) fully listed in tables and U-Pb concordia plots, and accessible in BMR's OZCHRON and PETCHEM databases. Note the equivalent laboratory numbers used in Page (1978): 72-253 = 72205021; 72-256 = 72205025.

Ion microprobe analytical techniques

Detailed descriptions of the techniques for zircon U-Th-Pb analysis using the 'SHRIMP' ion microprobe are given by Compston & others (1984, 1986). In brief, zircons were mounted in epoxy, polished to expose their centres, and carbon coated. They were analysed using a 10 kV primary beam of negative oxygen ions focussed to an area on the zircon crystal 25 to 40 micrometres in diameter. Positive sputtered secondary ions were extracted normally to the surface, accelerated to 11 kV, and transferred to a double focussing mass spectrometer operated at a mass resolution of 6500.

Isotopic ratios were measured directly using an electron multiplier in ion counting mode, and no correction was made for the small amount of mass dependent mass fractionation (approximately 2.5 per mil per mass unit) that may be induced by the sputtering process and ion extraction system. Corrections were made for initial Pb in the zircons, using values from Cumming & Richards (1975), based upon the measured $^{204}Pb/^{206}Pb$. Although this method suffers from poor ^{204}Pb counting statistics, it was used because Th/U or $^{208}Pb/^{206}Pb$ in many analysed

zircons had been disturbed other than by radioactive decay or by the addition of common Pb.

Pb/U was determined by reference to a standard zircon (SL3, 572 Ma old and having $^{206}Pb/^{238}U$ ratio of 0.0928) using an empirical quadratic relationship between UO+/U+ and Pb+/U+ established from accumulated analyses of the standard, and monitored frequently during each analytical session. Pb/Th was calculated from Th/U determined directly from ThO+/UO+ using a constant multiplier of 1.11.

Data were collected in a set of seven scans through the ionic species of interest. Analytical uncertainties for isotopic ratios were governed predominantly by counting statistics, and differed according to the concentrations of Pb, U, Th, and common Pb in each area analysed. The sensitivity of the ion microprobe ranged from 3 to 29 counts per second per ppm for each Pb isotope, as a function of primary beam intensity and spot size. The uncertainty in Th/U was governed largely by a 1% uncertainty in the 1.11 multiplier. Uncertainties in Pb/U and Pb/Th included an additional component derived from uncertainty in the quadratic calibration curve for the standard for each session. This component dominated the uncertainty of 1.4% (1-sigma) in these ratios. Uncertainties in absolute elemental concentrations were much larger (20%) due to a 20% variation in Pb, U, and Th concentrations in SL3.

Decay constants used in this paper are those recommended by the IUGS Subcommission on Geochronology (Steiger & Jäger, 1977). Unless otherwise stated, uncertainties in calculated ages are quoted as 95% confidence limits.

Structure and geochronology of the Tommy Creek Block, Mount Isa Inlier

E. J. Hill [1,2], *R. J. H. Loosveld* [3,4], *& R.W. Page* [1]

This paper is based on the following map:

Hill, E.J., 1991 - Geology of the Tommy Creek Block (1:25 000 scale map). Bureau of Mineral Resources, Canberra (two sheets).

The Tommy Creek Block (TCB) in the eastern Mount Isa Inlier is an anomalously high-grade sequence of metamorphic rock, adjacent to and overlying older, lower-grade greenschist facies rocks to the south and east. New U-Pb zircon data indicate that the time of igneous crystallisation of felsic metavolcanics (formerly the 'Tommy Creek microgranite') in the sequence was around 1626 ± 4 Ma. The TCB is bounded by faults and shear zones and is multiply deformed. Deformation was intense, and produced mylonitic textures, transposition layering, and in some areas extreme flattening of grains. Three major generations of folds have been documented, D^{T}_{1a}, D^{T}_{1b}, and D^{T}_{2}. The shear boundaries of the TCB are related to deformation during D^{T}_{1a}. Amphibolite-grade metamorphism accompanied both the D^{T}_{1} and D^{T}_{2} phases of deformation. Hence, the emplacement of the TCB adjacent to the surrounding greenschist facies rocks postdates the D^{T}_{2} deformation, but the movement zones are coincident with the D^{T}_{1a} shear zones. The contrasting ages, deformation styles, and metamorphism between the TCB and surrounding areas suggest that the TCB may be allochthonous.

---

[1] Bureau of Mineral Resources, Geology & Geophysics, GPO Box 378, Canberra, 2601, Australia.

[2] Present address: Department of Earth Sciences, Monash University, Clayton, Victoria, 3168, Australia.

[3] Department of Geology, Australian National University, G.P.O. Box 4, Canberra, 2601, Australia.

[4] Present address: Koninklijke/Shell Exploration and Production Laboratories, P.O. Box 60, 2280 AB Rijswijk, The Netherlands.

Introduction

The Tommy Creek Block (TCB; Hill, 1991) is an unusual tectonostratigraphic domain in the central eastern Mount Isa Inlier (Fig. 1). It is included in the Marraba 1:100 000 Sheet area, described by Derrick & others (1971) and Derrick (1980). These authors assigned most rock types in the block to the Corella Formation, Mary Kathleen Group. Blake (1982) reviewed the Corella Formation, and suggested that the Tommy Creek meta-rhyolite does not belong to the ~1760 Ma-old Mary Kathleen Group, but is a much younger unit. The only other published work carried out in the area is a conventional U-Pb zircon geochronological study by Page (1983a) and a structural study by Hill (1987). In this paper, we describe some aspects of the geology of the Tommy Creek area, and discuss their implications. The study of the Tommy Creek block has provided more questions than answers, and further detailed work – particularly on the metamorphic conditions during deformation and on the direction of shearing - is needed.

Geological setting

The TCB is fault and shear-bounded, which results in a roughly triangular shape. The southern boundary is marked by shearing and brecciation, and there is an abrupt metamorphic transition from amphibolite facies in the TCB to lower greenschist facies in the Mitakoodi area to the south (Derrick & others, 1971). The eastern boundary is marked by a shear zone, and there is a metamorphic transition across this boundary from amphibolite facies in the TCB to upper greenschist facies in the rocks of the Fox Mountain area to the east. The western boundary is part of the Pilgrim Fault System, believed to have moved during the Proterozoic and Phanerozoic, and appears to truncate all structures of the TCB. The TCB is poorly

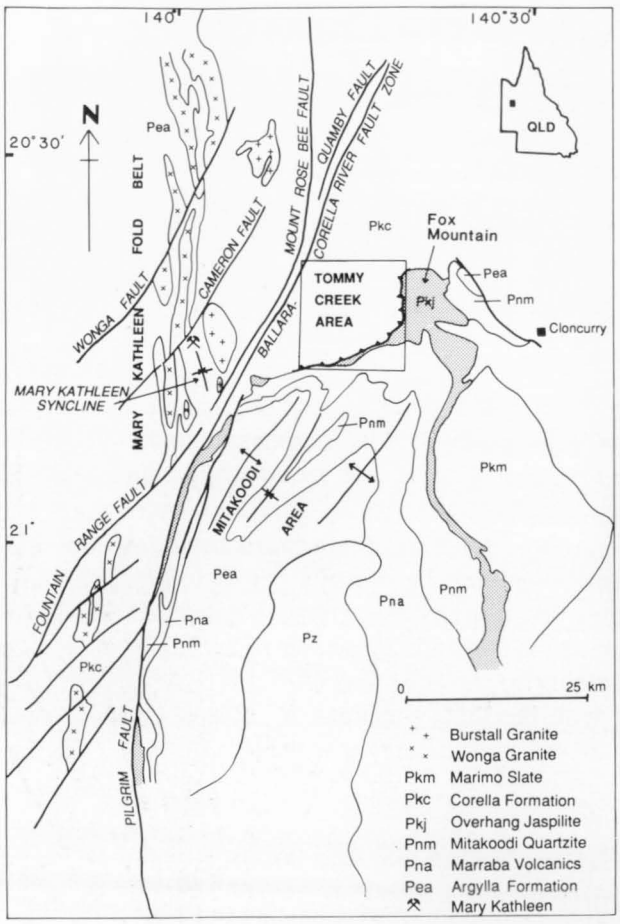


Fig. 1. Generalised geology of the central-eastern part of the Mount Isa Inlier, showing the location of the Tommy Creek Block, the Mitakoodi area to the south, and the Fox Mountain area to the east.

exposed in the north, where it is overlain by Cainozoic sediments. The northern area is not included in this study, but given the orientation of the eastern and western boundaries, it should be bounded by the Pilgrim Fault System and the eastern shear boundary, the former truncating the latter. Despite its relatively high metamorphic grade, the TCB occupies high levels, both stratigraphically and structurally. The kinematic history of the boundaries of the TCB is, however, enigmatic. Only the southern and eastern boundaries have been studied in this current work (Fig. 2).

To the west of the TCB lies the Mary Kathleen Fold Belt, a north-trending zone of intensely deformed rocks (Holcombe & others, 1987; Pearson & others, 1987). The TCB is separated from the Mary Kathleen Fold Belt by an extensive north to north-northeast-striking fault system which includes the Fountain Range Fault, the Pilgrim Fault, and the Ballara-Corella River Fault System. It has been suggested that this fault system (here referred to as the Pilgrim Fault System) is a terrane boundary (BMR, 1988b).

To the south lies the Mitakoodi Anticlinorium, a large north-northeast-plunging structure comprising rocks of the Argylla Formation, the Malbon Group (Marraba Volcanics and Mitakoodi Quartzite), and the Overhang Jaspilite. Rocks of the TCB are faulted against the Mitakoodi Quartzite and Overhang Jaspilite. The boundary between these two areas not only marks an abrupt change in metamorphic grade, but also a change in structural style from rocks dominated by east-west structures and a few north-south structures to the north, to less deformed rocks with northeast-trending structures to the south of the boundary. The boundary is marked by shearing and brecciation, by low-angle truncation or thinning of some lithological units, and by late breccias (Fig. 2).

The boundary between the TCB and the Overhang Jaspilite of the Fox Mountain area to the east is a lithological and structural discontinuity. A strongly deformed shear zone lies between the two areas and is continuous with the shear zone along the southern boundary. There is an abrupt change in style of deformation across the boundary. The rocks of the TCB west of the boundary are multiply folded with well-developed foliations and lineations. Transposition and shearing has commonly destroyed original sedimentary stuctures and volcanic textures. To the east, the rocks, although complexly folded, appear less deformed, e.g., sedimentary structures such as halite casts and small-scale cross bedding are perfectly preserved, and cleavage is poorly developed or non-existent.

The original aims of this study were to understand the structure of the TCB, especially the nature and timing of east-west folding, and to relate the structural history to the differences in metamorphic grade found in adjacent areas by previous workers. However, the story became more complicated. Hill (1987) proposed that the 'Tommy Creek microgranite' was volcanic in origin and assumed that the 1600 Ma dates determined by Page (1983a) were metamorphic ages rather than intrusive ages. Recent work by Page (this paper) has shown that these are in fact igneous crystallisation ages, and that the TCB must therefore be significantly younger than surrrounding areas. Some relevant geochronology for the TCB is summarised in Figure 3.

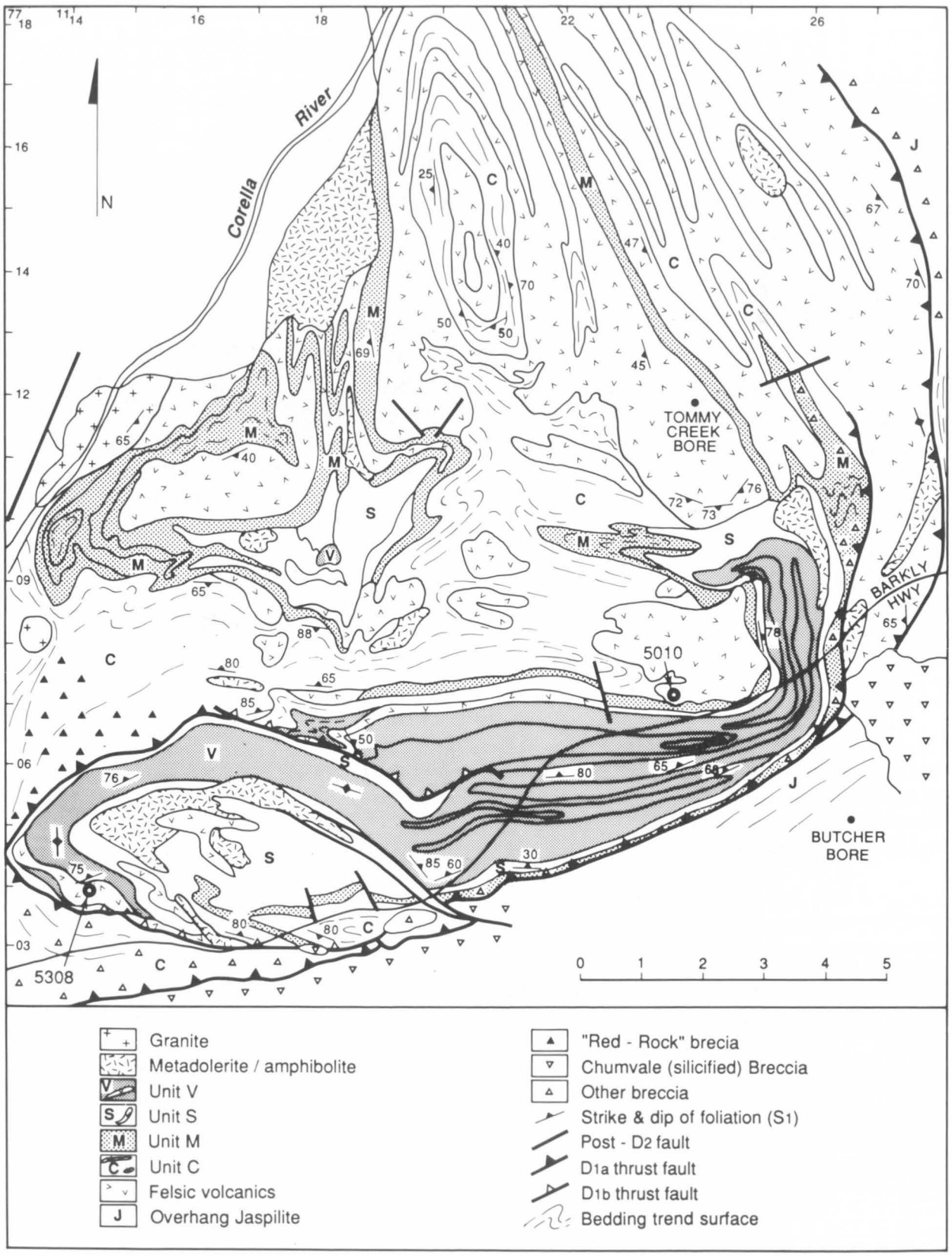


Fig. 2. Simplified geological map of the TCB, with the locations of the two sampling sites for ion microprobe analyses (5308 & 5110). Map boundaries are outlined in Figure 1.

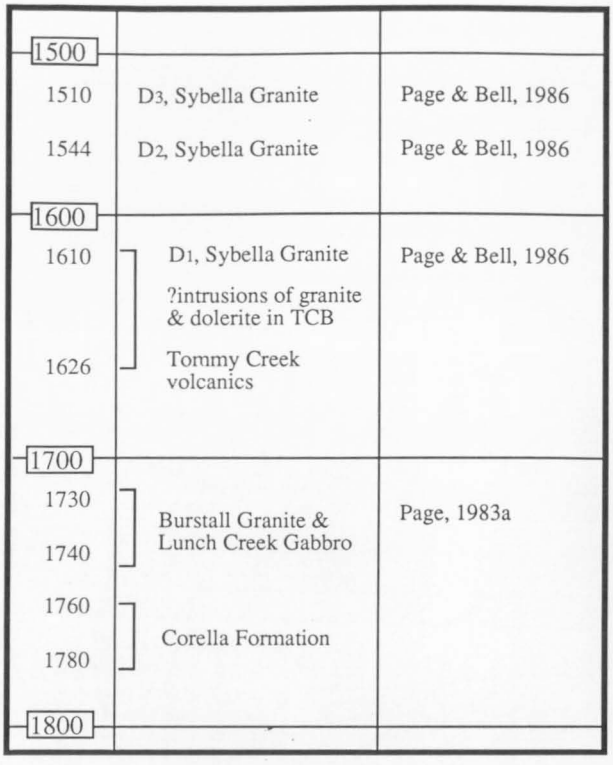


Fig. 3. Selected geochronology for the TCB and Mount Isa Inlier to show relative timing of events in the TCB.

Structural terminology

Deformation episodes in the Tommy Creek Block are denoted by a superscript 'T'.

Stratigraphy

The rocks of the TCB were originally assigned to the Corella Formation, a sequence of calcareous and evaporitic shallow-water sediments (Derrick & others, 1971) of the Mary Kathleen Group (Derrick & others, 1977). The TCB sequence is now informally called the *Tommy Creek beds,* and can be divided into a lower and an upper part (Fig. 4a,b). Both are interlayered with porphyritic igneous rocks, originally mapped as the Tommy Creek microgranite (Derrick & others, 1971). The lower part consists of calcareous granofels (unit C on the map; Hill, 1991) interbedded with massive bodies of porphyritic felsic rock (unit FV1). The upper part consists of calcareous granofels, quartzite, marble, and volcanic sandstone (unit M), schist and pelitic sediments (unit S), and intermediate to mafic metavolcanics (unit V). Massive porphyritic igneous bodies (unit FV2) are smaller than those of the lower unit and show gradational changes in composition and texture.

Unit C, the lowest unit, consists mainly of well-bedded, medium to fine-grained calc-silicate granofels and minor layers of massive felsic volcanic rock, and layered, commonly fragmentary, mafic volcanic rock. The calc-silicate rocks are reminiscent of unit Pkc_2 of Derrick & others (1971), and commonly have diopside and/or garnet porphyroblasts. Ripples, small-scale cross-beds, halite casts, and graded beds are preserved. A stable shallow-water depositional environment is inferred. Unit C contains layers of massive porphyritic felsic rock (subunit FV1). The layers are thick but laterally discontinuous; near the edges, the felsic bodies are interlayered with metasediments and mafic metavolcanics. Extensive recrystallisation of phenocrysts and groundmass has occurred in many areas (including both the geochronological sites) producing an equidimensional polygonal texture.

Unit M consists dominantly of marble, quartzite, and calc-silicate rock. Sedimentary structures are abundant in the northwest and include graded bedding, ripple marks, mud cracks, and small-scale cross-bedding; in this area, the lowermost part of the unit is a quartz-pebble conglomerate, overlain by minor graded laminae of siltstone, and marl (subunit Mq). Subunit Mm is largely marble, with subordinate quartzite, sandstone, siltstone and marl. Subunit Mc consists of thinly layered fine-grained calc-silicate rocks (with alternating feldspar-rich and diopside-rich layers), and minor amounts of quarztite, sandstone, siltstone, and conglomerate. Unit M resembles units Pkc, Pkc_{2l} , and part of Pkc_{2s} of Derrick & others (1971). Unit M marks a small and temporary but abrupt increase in the energy of the depositional environment , resulting in a change from a largely evaporitic/carbonate sequence to one with significant coarse clastic material.

Unit S is made up of schist, slate, phyllite, and minor quartz-pebbble sandstone. It is divided into two subunits. Dark bluish-grey to black graphitic schist and slate with minor chert and rare tuff form subunit Sg, whereas reddish to pinkish-brown micaceous schist and phyllite with minor volcanoclastics form subunit Sm. Unit S resembles parts of units Pkc_{2s} and Pkc_{2t} of Derrick & others (1971).

Unit V comprises mafic to intermediate volcanics with minor sediments, and resembles most of unit Pkc_{2t} of Derrick & others (1971). Subunit Vm comprises fragmentary lavas and pyroclastic rocks of mafic to felsic composition with ubiquitous abundant garnet porphyroblasts (commonly up to 5 cm in diameter). Dark fine-grained plagiophyric basalt and minor sediments are also present. Subunit Vi comprises pods of massive intermediate lava with abundant inclusions of mafic (biotite-rich) material, and subunit Vt consists of

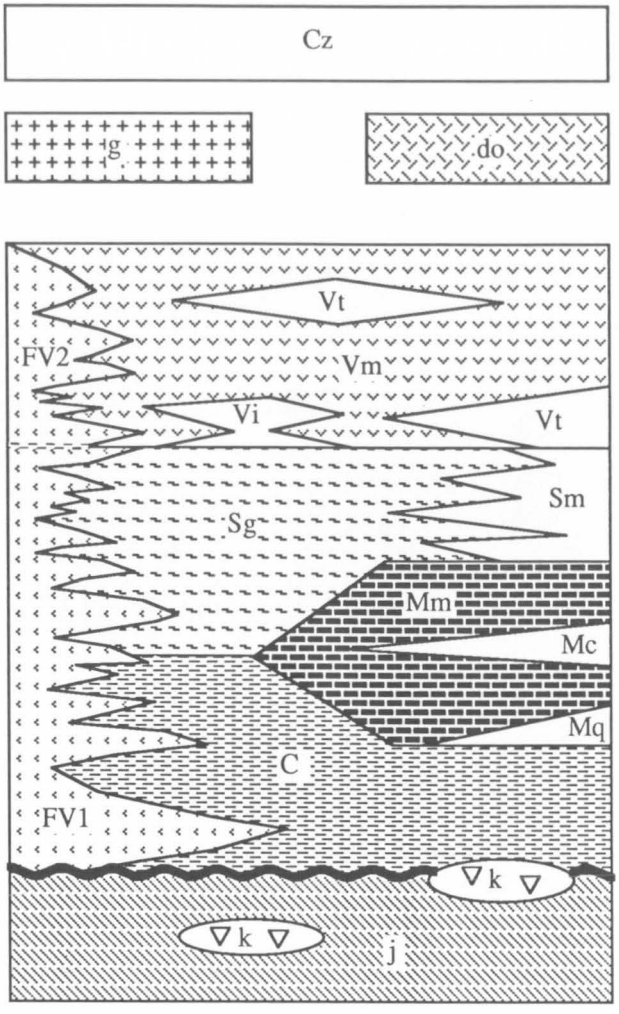


Fig. 4. (a) Schematic representation of the stratigraphic relations within the TCB. FV1 and FV2 interdigitate with the sedimentary units.

FORMATION		UNIT	SUB-UNIT	ROCK TYPES
		Cz		alluvium;
TOMMY CREEK SEQUENCE	UPPER	FV	FV2	porphyritic felsic volcanics, generally micaceous;
		V	Vm	porphyritic mafic lavas, fragmentary mafic and intermediate lavas, minor sediments;
			Vt	finely banded tuff;
			Vi	massive intermediate lavas;
		S	Sg	graphitic schist, minor chert;
			Sm	muscovite-garnet schist;
		M	Mm	marble, minor siltstone, sandstone & calcareous granofels;
			Mc	calcareous granofels, minor quartzite, marble, siltstone & sandstone;
			Mq	quartzite conglomerate, sandstone, marble, quarzite;
	LOWER	FV	FV1	porphyritic felsic volcanics;
		C		calcareous granofels, minor mafic & felsic volcanics;
CHUMVALE BRECCIA		k		silicified breccia;
OVERHANG JASPILITE		j		jaspilite, limestone, shale & marl;
		g		granite;
		do		metadolerite, amphibolite.

Fig. 4 (b) Summary of rock types found in the map area.

yellowish-grey finely banded schist, probably originally tuff.

In the upper part of the sequence (units M, S, & V), felsic igneous bodies are abundant. They are grouped together here for convenience as subunit FV2. These bodies are very similar to those of subunit FV1, except that they generally have more muscovite, fewer phenocrysts, and in places show compositional layering and a schistosity (because of the greater muscovite content). On the map scale, the FV2 bodies are thinner and more elongate than the FV1 bodies.

The origin of subunits FV1 and FV2

Subunits FV1 and FV2 consist of large discontinuous masses of strongly recrystallised porphyritic felsic igneous rock which are concordant with their host rocks. They show no flow banding, but the upper units of subunit FV1 commonly have internal layering, defined by the abundance of muscovite, on the centimetre to metre scale. Some finer-scale layering was previously interpreted as flow banding in rhyolite (e.g., dating site 5308 in Fig. 2). However, it is locally developed in an area of high strain, and in thin section is clearly a mylonitic layering (described below in the section on 'Structure'). Composition and textures of the subunits indicate that they represent either rhyolitic lava, or pyroclastic, or volcaniclastic rock, or granitic sills. However, relationships to surrounding rocks, as discussed below, indicate that they are unlikely to be intrusive in origin.

Recrystallisation has destroyed the groundmass, so it is not possible to estimate the original grain size of these igneous rocks. The present grain size is that of a microgranite, but thin sections show that the texture is a polygonal (or 'foam') texture typical of recrystallised metamorphic rock, not an igneous texture. Composition, size, and texture of the bodies change gradually upwards in the stratigraphic sequence, which is consistent with a volcanic origin where composition of the erupted products changed with time. Small (1 to 2 cm in width and 2 to 10 cm in length) elongate or flattened lenses of muscovite-rich rock occur in the otherwise massive units of FV1 in the northern half of the Tommy Creek Block.

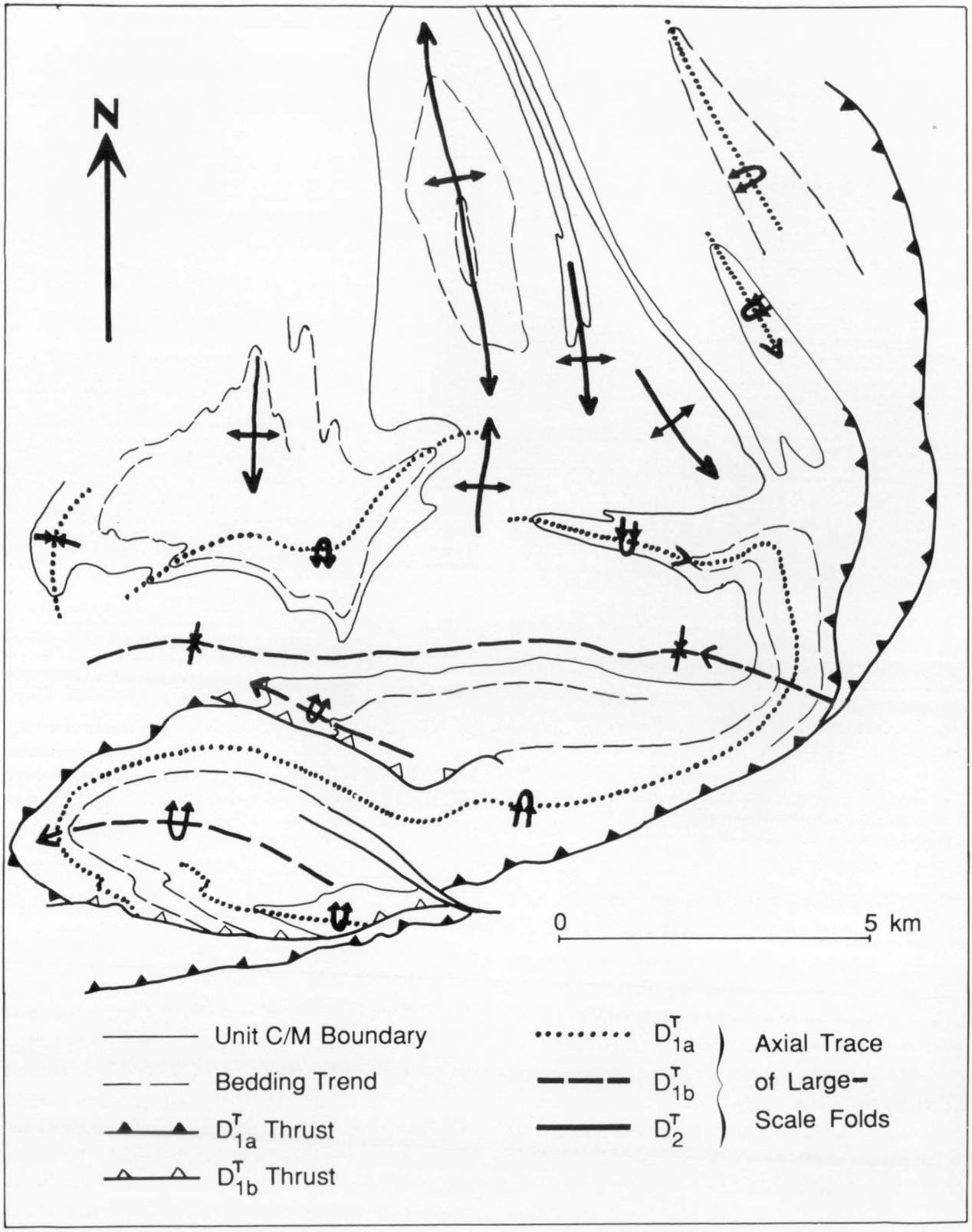


Fig. 5. Map showing the main structural elements of the TCB.

They do not resemble xenoliths found elsewhere in these igneous bodies, but may be fiamme (flattened pumice) indicating a pyroclastic origin for these units. Further compelling evidence that these bodies are volcanic and not intrusive is the centimetre-scale interfingering of layers of sedimentary strata with the felsic rock on the edges of the bodies. The felsic bodies do not truncate the sediments. However, one must be careful to distinguish between the

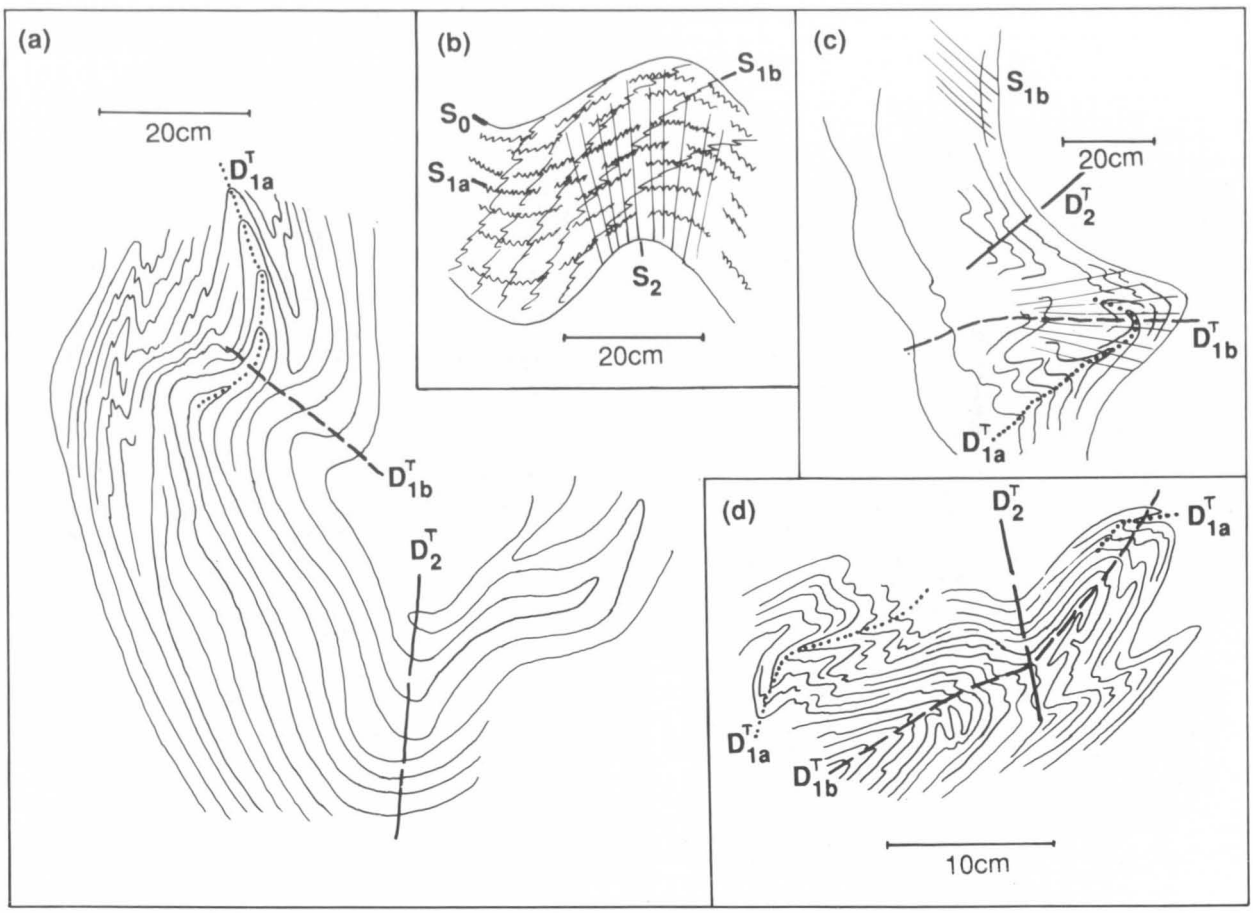


Fig. 6. Field sketches of fold overprinting patterns. (a) Refolded folds in calcareous granofels showing relationships between D^T_{1a}, D^T_{1b}, and D^T_2 folds. (b) Crenulations in graphitic schist. Schistosity S_{1a} is folded and crenulated by crenulaton cleavage S_{1b}, which is in turn broadly folded and crenulated around S_2. (c) Overprinting realationships in graphitic schist. Folds are D^T_{1a} and D^T_{1b} ; S_{1b} is a crenulation cleavage and is gently folded around S_2. (d) Refolded folds in graphitic schist showing overprinting of D^T_{1a} and D^T_{1b} folds by D^T_2 folds.

FV subunits and the abundant granitic veins which are superficially very similar in appearance. Thus, it is concluded that these bodies are of volcanic origin and have since undergone substantial recrystallisation. They may be ignimbrites, which would explain their massive appearance and the presence of possible fiamme.

Igneous Intrusives

Small *granitic bodies* (100 m to 3 km in plan view) intrude the western and central parts of the TCB. They are weakly foliated and may be related to the Naraku Granite, which crops out to the east of the TCB. Granitic veins and pegmatites are also common. Pegmatites and granitic veins in the felsic volcanics are coarse-grained and consist dominantly of quartz + K-feldspar, whereas those in metapelites are relatively fine-grained and muscovite-rich. Early, small (generally less than 1 km diameter) *amphibolite* bodies (metadolerite) are strongly foliated and lineated. Later undeformed *dolerite dykes* cross-cut all structures.

Structure

Field evidence indicates at least three major generations of deformation: D^T_{1a}, D^T_{1b}, and D^T_2. (Note: Figure 2 does not show all measured structural elements; for a complete dataset see Hill, 1987, 1991). Figure 5 outlines the distribution of the main structural elements. D^T_{1a} and D^T_{1b} are two discrete phases of thrust-related deformation, but, considering the similarities in styles of folding and associated faulting, orientation of structures, and coincidence of location, they probably reflect one ongoing tectonic regime. D^T_{1b} clearly overprints D^T_{1a} (Figs. 6, 7) often in the form of crenulation of the D^T_{1b} foliation. D^T_2 is characterised by north-trending upright folds. Figure 8 schematically shows the three-dimensional geometry of the TCB after D^T_2. Post-D^T_2 structures are faults and local crenulations with various orientations.



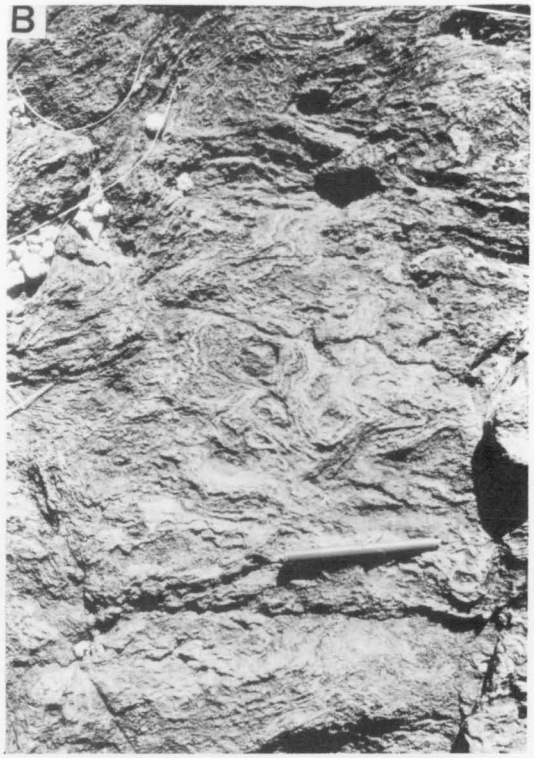
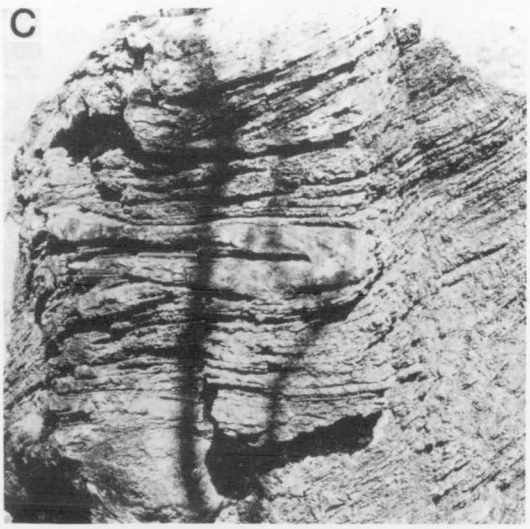


Fig. 7. Field photographs of structures. (a) Upright D^T_2 fold refolding D^T_{1a} fold in hinge, calcareous granofels. (b) Non-cylindrical D^T_{1a} folds, calcareous granofels.



(c) Recumbent D^T_{1a} fold, calcareous granofels.

Correlation of deformational episodes in the TCB with those of Page & Bell (1986) are as follows:

Tommy Creek Block	Page & Bell (1986)	Date (Ma)
D^T1	D_1	1610
D^T2	D_2	1544

Early thrusting, D^T1a and D^T1b

In the south and centre of the area, D^T_{1a} folds are recumbent to inclined, isoclinal, and strongly non-cylindrical, with roughly east-striking axial planes. Fold interference patterns, and orientations of relatively undisturbed folds (i.e., not refolded) suggest that all folds were probably originally recumbent or gently inclined northward, and were steepened by subsequent deformation. In the north, D^T_{1a} folds are generally gently plunging with inclined to horizontal axial planes; some folds, however, have variable orientations due to the later D^T_2 folding. The S_{1a} foliation is well developed in all rock types as a schistosity, cleavage, or transposition layering. D^T_{1a} faults are marked by zones of brecciation, mylonitisation, and shearing. These faults are folded by D^T_{1b} folds (Fig. 5). Small zones (generally less than 2 m wide) of mylonite are found throughout the felsic volcanics, quartzite, and chert.

The mylonitic felsic volcanic rocks contain stretched phenocrysts in a fine-grained groundmass. The groundmass shows typical mylonitic textures including extremely flattened grains with undulose extinction and development of subgrains with serrate boundaries. Where mylonites formed in quartzite, they commonly have a second foliation in the subgrains at high angles to the main

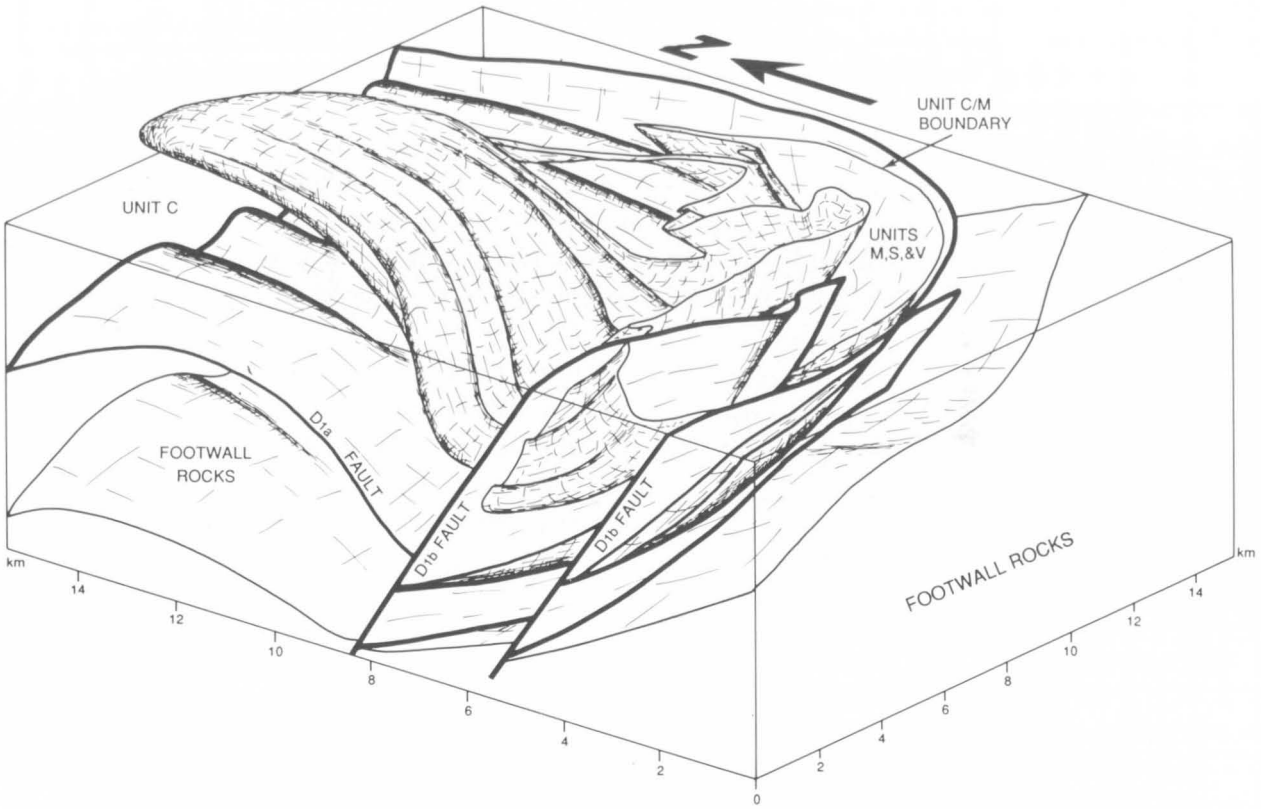


Fig. 8. Schematic block diagram showing the structure of the TCB after D^T_2 folding. Contacts between units C and M are used to illustrate the geometry. The main D^T_{1a} fault, which separates the TCB from the footwall rocks, and the later D^T_{1b} faults are also shown. The C/M contact illustrates a large doubly-refolded sheath fold.

foliation (45-60°). These can be interpreted as S-C structures indicating that the mylonites formed during simple shear (i.e., non-coaxial deformation). Alternatively this new foliation may be a result of recrystallisation and deformation during D^T_2. Asymmetric microshear zones apparently related to S_{1a} are developed in some of the deformed FV1 subunits, further indicating non-coaxial deformation. The mylonites and shear zones have a strong mineral lineation, which is weak to moderate outside these zones. The lineation varies in orientation due to later deformation. Similarly, there has been widespread rodding in quartzite, elongation of phenocrysts, and elongation and boudinage of breccia fragments and pebbles.

D^T_{1b} structures are commonly localised in zones related to steeply dipping faults; folds are tight to isoclinal adjacent to the faults and become open away from the faults. The folds have inclined to upright, approximately east-striking axial planes, and verge southward; they refold D^T_{1a} folds and steepen D^T_{1a} structures in the south. The S_{1b} foliation is commonly a crenulation cleavage in schist, and decreases in intensity away from the steeply dipping D^T_{1b} faults.

The intensity of D^T_1 deformation increases towards the south and southeast. However, D^T_1 structures do not cross the sheared boundary between the TCB and the Mitakoodi structural area. Rare isoclinal pre-D_2 sheath folds are found in the Overhang Jaspilite near the Tommy Creek/Mitakoodi boundary to the south and southeast of the TCB (R.J. Holcombe, personal communication), but otherwise no pre-D_2 structures have been recorded farther south in the Mitakoodi rocks.

Macroscopic D^T_1 structures

The structure of the TCB is dominated by a map scale, strongly non-cylindrical, tongue-shaped D^T_{1a} fold which has been refolded twice (by D^T_{1b} and D^T_2) resulting in a complex fold interference pattern (Fig. 5) and unusual cross-sections (see Hill, 1991). Large-scale D^T_{1a} and D^T_{1b} folds are generally non-cylindrical, but commonly verge southward and flank northward-dipping D^T_{1a} and D^T_{1b} faults (respectively) indicating thrusting on these faults. The emplacement of the higher-grade TCB over the lower-grade surrounding rocks to the south and east supports the interpretation of these faults as thrusts (Hill, 1987). The largest D^T_{1a} thrust fault is a shear zone between the TCB and the underlying Overhang Jaspilite to the south (Fig. 8).

It appears that two episodes of deformation accompanied thrusting. The second episode (D^T_{1b}) resulted in higher-angle structures which steepened D^T_{1a} structures. The effects of D^T_{1a} were more widespread and much stronger in the southern area than those of D^T_{1b}, the latter being localised near small reverse faults in the south of the TCB. The shear zone on the eastern side of the TCB may represent a lateral ramp on the thrust sheet, or a part of the thrust which has been folded by later deformation.

The granitic bodies, granitic veins, pegmatites, and metadolerites contain D^T_{1a} fabrics; veins and pegmatites are commonly folded by D^T_{1a}. Thus, the intrusion of granite and metadolerite bodies must be synchronous with, or pre-date, this deformation.

Upright folding, D^T_2

D^T_2 has resulted in abundant tight to isoclinal, kilometre-scale folds in the northwest, which become more open towards the east, and quite broad towards the south, where D^T_2 deformation is almost entirely accommodated by crenulation of earlier fabrics. The D^T_2 axial-plane foliation (S_2) strikes north-northwest in the northern area and north in the southern area. It is a weakly to moderately developed foliation or crenulation cleavage. Most D^T_2 folds are slightly non-cylindrical due to overprinting on to earlier folds. Map-scale folds have axial planes which are dominantly upright, and generally plunge gently northward or southward. In sharp contrast to the north or north-northwest-trending D^T_2 structures in the TCB, D_2 structures in the Mitakoodi area directly south of the TCB trend north or northeast. It is likely that either post- D^T_2 rotation has occurred between the two areas, or D^T_2 in the TCB does not correlate with D_2 in the Mitakoodi area.

Breccias and alteration, post-D^T_2

Breccias are widespread in metasediments and metavolcanics. They are commonly near faults, but some breccias are distributed over large areas in calcareous granofels and have undergone widespread metasomatic alteration ('red-rock' alteration; Edwards & Baker, 1954; Oliver & others , 1990); these are apparently unrelated to faulting and postdate D^T_2. 'Red-rock' alteration includes the formation of albite, epidote, and fine-grained hematite. Alteration is also present adjacent to the large felsic volcanic bodies, where the development of coarse specular hematite veins is common. Other breccias are also extensive in the calcareous rocks, but their origin is not well understood; Glikson (1972), Ryburn & others (1988) and Tunks (1987) discuss similar breccias in the Cloncurry area.

Fragments in fault breccias are commonly flattened and elongate, and are aligned parallel to D^T_1 fabrics. However, the matrix is rarely foliated (except in breccias of felsic volcanics) suggesting that the matrices generally formed later or were altered or reactivated subsequent to D^T_1 deformation. Many of the fault-related breccias, especially those in calcareous rocks, appear to have been reactivated at some later stage causing local disruptions to the alignment of breccia fragments.

Silicification and Fe and Mn staining of the breccias are common and appear to be post-deformational, as they also affect undeformed breccias.

Metamorphism

The TCB is a polymetamorphic domain, with peak metamorphic conditions higher than those of the surrounding areas. Its metamorphic grade is of the amphibolite facies, whereas areas to the west and east are upper greenschist facies, and the Mitakoodi block to the south is lower greenschist facies (Derrick, 1980). No metamorphic pressure or temperature estimates were included in this study, but foliation development and porphyroblast relationships allow some generalisations concerning the timing of metamorphism in the TCB. There appear to be two episodes of amphibolite-grade metamorphism: an early growth of garnet and staurolite in schist, and diopside and amphibole in calc-silicate rock, and later growth of sillimanite (as fibrolite) in metapelite, indicating higher temperatures. Typical metamorphic assemblages are summarised in Table 1.

Most of the assemblages involve minerals which define the S_{1a} foliation. However, many rocks appear to have been recrystallised post-D^T_1. These new assemblages probably represent metamorphism around the time of D^T_2 deformation. Porphyroblast relationships are shown in Figure 9. Figure 9a shows boudinaged inclusion-rich staurolite parallel to the D^T_{1a} extension direction, with growth of new inclusion-poor staurolite in the boudin gap. Inclusion trails of graphite show a foliation at a steep angle to S_{1a}, indicating either that there is a pre-D^T_{1a} foliation or that the porphyroblast has rotated. Figure 9b shows two stages of growth in garnet: an inclusion-rich stage overgrowing the D^T_{1a} schistosity, and a second inclusion-poor stage overgrowing the beginnings of crenulation of the schistosity (S_{1b}). Figure 9c shows staurolite (inclusion-rich and inclusion-poor), biotite, and quartz growing in the pressure shadow developed around

TABLE 1. TYPICAL METAMORPHIC ASSEMBLAGES FOR METAMORPHIC ROCKS OF THE TCB.

Rock Type	Mineral Assemblage	Relative Age
calc-silicate	mcl + diop + amph + cc + scap	defines S_{1a} foliation
	plag + diop + qz amph	recrystallised, S_2
	plag + cc + amph	recrystallised, S_2
amphibolite (metadolerite)	plag + hbl	defines S_{1a} foliation
	wo + act	postdates S_2
schist	qz + musc + bt gn	garnet growth during D^T_{1a} and D^T_{1b}
	qz + musc + bt + sill	sillimanite growth late- or post-D^T_2
	qz + stt + fdp + gn + graphite	staurolite growth pre- or syn-D^T_1
metavolcanics	qz + mcl + bt gn cal	garnet growth late-D^T_1
	plag + hb gn	defines S_{1a} foliation
	plag + bt + gn	defines S_{1a} foliation

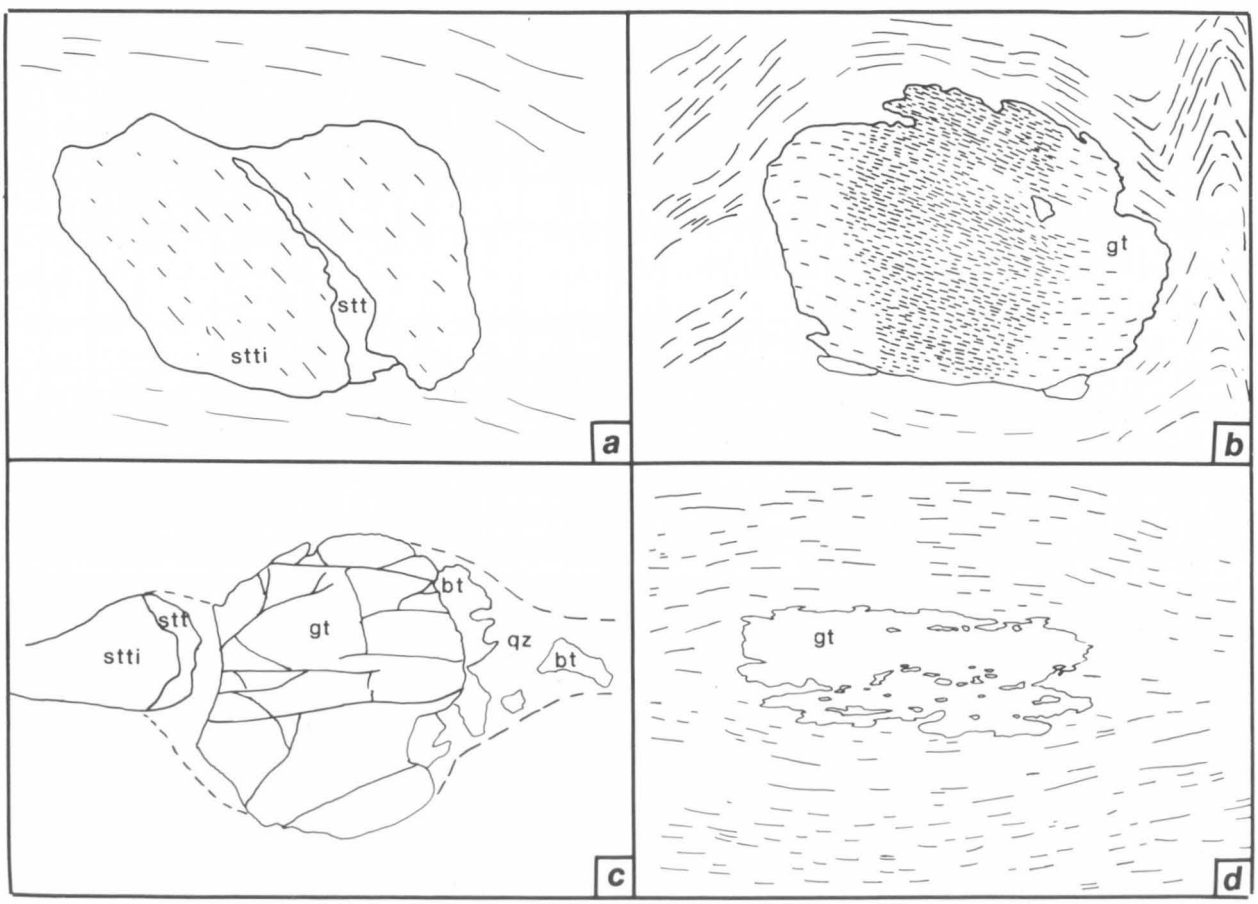


Fig. 9. Sketches of thin section relationships. (a) Boudinaged inclusion-rich staurolite (stti) parallels the D^T_{1a} extension direction. New inclusion-poor staurolite (stt) has grown in the boudin gap. Inclusion trails of graphite in the staurolite grain show a foliation at a steep angle to S_{1a}. (b) Two stages of growth in garnet (gt), one inclusion-rich overgrowing the D^T_{1a} schistosity and a second inclusion-poor overgrowing the beginnings of crenulation of the schistosity (S_{1b}). (c) Staurolite (inclusion-rich, stti, and inclusion-poor, stt), biotite (bt) and quartz (qtz) growing in pressure shadow around garnet during D^T_{1a}. (d) Garnet (gt) overgrowing S_{1b} foliation with some flattening of the foliation around the porphyroblast indicating growth late in S_{1b}.

Table 2. Zircon ion microprobe analytical data for Tommy Creek Beds, felsic volcanic sample 7720.5010.

Grain-spot	U ppm	Th/U	$^{206}Pb/^{204}Pb$	f206% a)	$^{208}Pb/^{206}Pb$	$^{206}Pb/^{238}U \pm 1\sigma$	$^{207}Pb/^{235}U \pm 1\sigma$	$^{207}Pb/^{206}Pb$ .... $\pm 1\sigma$	Age (Ma)
1-1	468	0.70	7704	0.21	0.1536	0.2638±44	3.645±69	0.10018±68	1627
2-1	432	0.68	10111	0.16	0.1990	0.2857±48	3.953±74	0.10036±62	1631
3-1	843	0.15	27755	0.06	0.0380	0.2739±46	3.684±65	0.09755±38	1578
4-1	263	0.55	6376	0.25	0.1599	0.2717±46	3.705±77	0.09889±131	1603
4-2	433	0.59	24456	0.07	0.1803	0.2724±46	3.744±68	0.09971±53	1619
4-3	301	0.70	4115	0.39	0.2030	0.2746±46	3.751±76	0.09906±91	1607
5-1	1165	1.02	41511	0.04	0.3054	0.2897±48	3.997±69	0.10007±31	1625
6-1	681	0.72	17790	0.09	0.2180	0.2799±47	3.870±69	0.10028±43	1629
7-1	1218	1.13	30404	0.05	0.3375	0.2964±49	4.086±70	0.09997±29	1623
8-1	502	0.66	13879	0.11	0.1988	0.2881±48	3.981±72	0.10022±52	1628
8-2	693	0.62	19298	0.08	0.1864	0.2895±48	4.000±71	0.10022±44	1628
9-1	310	0.63	6131	0.26	0.1839	0.2743±46	3.781±75	0.09996±84	1623
10-1	950	0.84	38595	0.04	0.2504	0.2851±47	3.930±68	0.09996±35	1623
10-2	591	0.68	36284	0.04	0.2073	0.2766±46	3.823±68	0.10025±45	1629

a) Denotes the percentage of common ^{206}Pb in the total measured ^{206}Pb.

TABLE 2. ION MICROPROBE ANALYTICAL DATA FOR FELSIC VOLCANIC SAMPLE 7720.5010.

garnet during D^T_{1a}. Figure 9d shows garnet overgrowing S_{1b} foliation with some flattening of the foliation around the porphyroblast, indicating growth late in S_{1b}.

To summarise, these relationships indicate that inclusion-rich staurolite grew syn-D^T_{1a} or pre-D^T_{1a} and inclusion-poor staurolite grew early during D^T_{1a}. Garnet formed during D^T_{1a} and D^T_{1b}.

Sillimanite was found in one area in the centre of the TCB as small clots of fibrolite, which overgrow D^T_2 crenulations. Therefore, sillimanite-grade of metamorphism was reached late D^T_2 or post-D^T_2. The metamorphism associated with the growth of sillimanite was probably also responsible for the widespread recrystallisation of D^T_1 fabrics. Metamorphism associated with similar north-south folds is well documented elsewhere in the Mount Isa Inlier, e.g., west of the Pilgrim Fault (Wilson, 1973; Passchier, 1986b); in the Mary Kathleen area, adjacent to the TCB (Derrick & others, 1977, Oliver & others, 1990); and to the east of the TCB in the Cloncurry/Selwyn area (Loosveld, 1989a, this volume; local D_1 of Jaques & others, 1982). In these areas, metamorphism is interpreted as a low-pressure facies. It is possible that the D^T_2 metamorphic event in the Tommy Creek area correlates with the D_2 metamorphic event elsewhere, if the D^T_2 structures in the Tommy Creek area can be correlated with those elsewhere.

Previous geochronological work

U-Pb zircon analyses on a 'rhyolitic lava' (sample 7920.5308; Marraba 1:100 000 Sheet Grid Reference 143041) and a 'leucocratic microgranite sill' (sample 7720.5010; Marraba 1:100 000 Sheet Grid Reference 234075; localities in Fig. 2) in the TCB were undertaken by Page (1983a) as part of a regional dating study of Mount Isa stratigraphic sequences, in this case, volcanic components in what was believed to be part of the Corella Formation. At that time, existing geochronological constraints on the minimum age of the Corella Formation came from the Mary Kathleen Fold Belt, 15 km west of Tommy Creek, where the unit is intruded by several granitic bodies, including the Burstall Granite, dated at 1740-1720 Ma (Page, 1983b). Conventional multi-grain U-Pb zircon analyses yielded good age agreement, 1603 ± 6 Ma and 1600 ± 13 Ma, for the two TCB rock type from sites 10 km apart. The belief at that time that one of these (sample 5010) was a high-level intrusive is not supported by current mapping and petrography as presented here. Both of the rock types dated are recrystallised felsic volcanic material, and at site 5308 a strong mylonitic fabric is developed. Recognition of the intensity of this deformation, together with later documentation of an early D_1 deformation at 1610 ± 13 Ma in the western part of the

Mount Isa Inlier (Page & Bell, 1986), cast doubt on Page's (1983a) interpretation that 1600 Ma was the age of igneous crystallisation, and hence that this part of the Corella Formation was so young. The possibility that the rocks of the Corella Formation east of the Mary Kathleen Fold Belt (namely, in the Tommy Creek area) were not the same as those within the fold belt had also been suggested by Blake (1980, 1982).

In situ ion microprobe U-Pb analyses have now been carried out on the same zircon fractions that were previously analysed by conventional bomb dissolution and mass spectrometry. The purpose was to check the 1600 Ma ages, and to see if any complexities resulting from inheritance or metamorphic overgrowths had influenced the conventionally determined 1600 Ma ages. Of particular interest are the U-Pb zircon systematics in the mylonitised felsic volcanic sample (5308), since the literature contains opposing views as to whether dynamic metamorphism affects zircon ages. For example, zircons in mylonites in the Brevard Fault Zone, North Carolina, appear to have been substantially modified through U gain (Sinha & Glover, 1978), whereas the U-Pb zircon system in mylonitic lithologies in the Pan-African mobile belt, western Africa, remained unaffected, even where the grains were broken and rolled in the ductile matrix (Lancelot & others, 1983).

New U-Pb zircon data

Detailed description of ion microprobe techniques used for analysing the U-Th-Pb isotopes in a ~30μ m diameter area of a zircon grain are given by Compston & others (1984, 1986). In the present study, corrections for common Pb are based on the small measured ^{204}Pb signals, using compositions from Cumming & Richards (1975). Absolute values for Pb/U and Pb/Th are referenced to ^{206}Pb*/^{238}U in zircon standard SL3, taken as 0.0928 equivalent to an age of 572 Ma.

Sample 7720.5010

The less-deformed Tommy Creek felsic volcanic rock (sample 7720.5010, previously termed 'microgranite') contains abundant concentrically zoned euhedral zircons up to 350μ m across. Predictably, the geochemistry of the ion microprobe analyses mimics the conventional zircon data, revealing moderately high U and virtually zero common Pb, but there are small differences resulting from the very different volumes of zircon sampled by the analytical procedures.

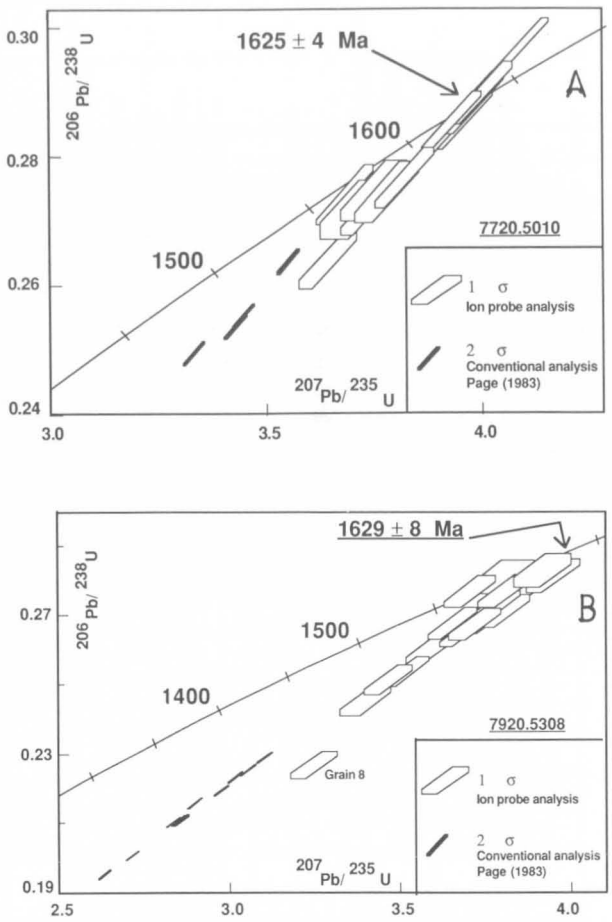


Fig. 10. U-Pb concordia diagrams of ion microprobe zircon data (open error boxes) and conventional zircon data (black error boxes) from Tommy Creek felsic volcanic rocks 7720.5010 (A) and 7920.5308 (B). Indicated igneous crystallisation ages and 2 sigma errors from the ion microprobe data are 1625 4 Ma (13 analytical points) and 1629 8 Ma (19 analytical points) respectively.

The 14 U-Pb data points (Table 2) from 10 zircon grains form a coherent array that straddles the concordia curve (Fig. 10a). The data are well clustered in ^{207}Pb/^{206}Pb and degree of concordance, despite a wide range of U contents (Fig. 11a). The 14 analyses form a ^{207}Pb/^{206}Pb age population at 1620 ± 8 Ma (2 sigma error of the mean). Grain 3 has a much younger ^{207}Pb/^{206}Pb age (1578 Ma) which significantly enlarges the observed standard error, and also has anomalously low Th/U (0.15) compared to the rest of the group (average 0.73 ± 0.17). Its deletion results in a pooled error for the remaining 13 analyses which is within analytical uncertainties, and the pooled ^{207}Pb/^{206}Pb age becomes 1625 ± 4 Ma. This close grouping can be unambiguously interpreted as the crystallisation age of the zircon population.

Because of a degree of scatter within four conventional multi-grain analyses (replotted in Fig. 10a), Page (1983a)

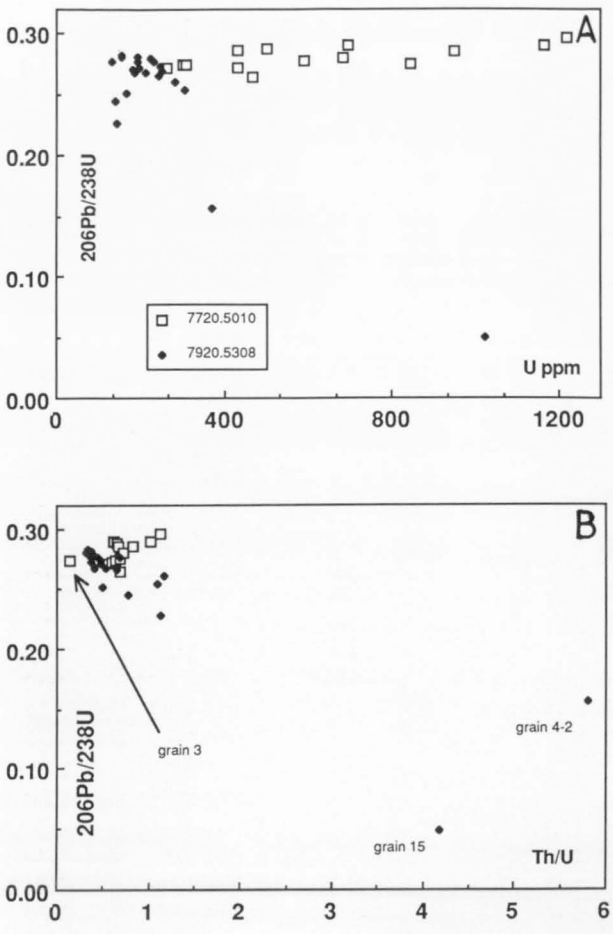


Fig. 11. Plots of U versus $^{206}Pb/^{238}U$ (A) and Th/U versus $^{206}Pb/^{238}U$ (B) for ion microprobe zircon data from Tommy Creek felsic volcanic rocks.

had considered that some inheritance was present in the two coarser fractions ($^{207}Pb/^{206}Pb$ ages 1587 and 1590 Ma), and had extrapolated a U-Pb age based on only the two finer fractions ($^{207}Pb/^{206}Pb$ ages 1566 and 1582 Ma) of $1600\ ^{+15}_{-11}$ Ma. The ion-probe data do not reveal any such inheritance and hence do not justify the $1600\ ^{+15}_{-11}$ Ma age from the conventional data, nor the supposition that inheritance was important. In fact, multiple analyses on grains 4 and 8, which appeared to have discrete cores, show no discernible age difference between cores and edges of the grains, all of which are part of the 1625 ± 4 Ma population. Non-linearity of the four conventional data is probably due to one or more episodes of non-zero Pb loss that have led to imbalanced Pb/U in different size fractions of the population. The four conventional data points are several percent discordant with respect to the ion probe data and have lower $^{207}Pb/^{206}Pb$ ratios, presumably because the Pb loss takes place mainly from cracked areas of the grains, which could be deliberately avoided in the ion-probe analyses.

In summary, the zoning in these zircons together with the coherent U-Pb age pattern of the ion-probe analyses indicate that the zircons are igneous, and crystallised at 1625 ± 4 Ma.

Sample 7920.5308

Zircons in the mylonitised porphyritic rhyolite are equally abundant, but somewhat smaller than those in sample 5010, 10 km away. The unbroken grains are euhedral, but the grain edges are almost everywhere embayed and corroded, presumably as a result of fluid reaction during deformation. Twenty of the 22 analytical points (Table 3) have a narrow range of U and Th/U, but the dark interior of grain 15 and a dark selvedge of grain 4 (analysis 4-2) have significantly higher U and Th/U (Fig. 11a, b) and have lost major proportions of radiogenic Pb. In the rim of grain 4, this occurred during the Palaeozoic, whereas grain 15 shows only recent Pb loss. It will be seen that these differences affected both the earlier interpretation and the resultant date based on the multi-grain conventional zircon data (Page, 1983a).

The remaining 20 zircon data points lie on or a few percent below the concordia curve (Fig. 10b) broadly in accord with their U and Th/U values, despite having much lower U than the generally concordant zircons from sample 7720.5010 (Fig. 11a, b). The coherence in $^{207}Pb/^{206}Pb$ for all except grain 8, gives an age of 1629 ±8 Ma (2 sigma error of the mean). Grain 8 has no morphological features that would distinguish it from the main group, but its higher $^{207}Pb/^{206}Pb$ indicates a component of inherited Pb. With respect to the ion-probe data, the multi-grain conventional data from Page (1983a) are discordant in a manner similar to sample 5010. The previously determined U-Pb discordia intersection of 1603 ± 6 Ma is younger than the ion-probe result. Lower $^{207}Pb/^{206}Pb$ and greater discordance together reflect the fact that most of the whole zircon grains are imperfect closed systems, the cracks and inclusions being areas of enhanced Pb loss, which affected those segments both in the Palaeozoic and recent time. In contrast, the 30 μm-diameter ion probe analyses represent samples of relatively pristine grain segments isolated from what may be other cracked areas of the grain.

Both the individual data points and the age determined for this sample of mylonitised porphyritic rhyolite are indistinguishable from those of the less-deformed sample 5010. The $^{207}Pb/^{206}Pb$ age derived from pooling 22 near-concordant analyses from the two samples is 1626 ± 4 Ma. As the two suites are geologically coeval and the observed standard error lies within experimental

Table 3. Zircon ion microprobe analytical data for Tommy Creek Beds, felsic volcanic sample 7920.5308.

Grain-spot	U ppm	Th/U	$^{206}Pb/^{204}Pb$	f206% a)	$^{208}Pb/^{206}Pb$	$^{206}Pb/^{238}U \pm 1\sigma$	$^{207}Pb/^{235}U \pm 1\sigma$	$^{207}Pb/^{206}Pb$ .... $\pm 1\sigma$	Age (Ma)
1-1	247	0.48	15586	0.10	0.1419	0.2734±46	3.777±75	0.1002±83	1628
2-1	225	0.38	32362	0.05	0.1164	0.2793±48	3.857±77	0.10016±87	1627
3-1	280	1.17	11925	0.13	0.1197	0.2600±44	3.587±70	0.10004±105	1625
4-1	231	0.37	9348	0.17	0.1109	0.2775±47	3.842±77	0.1004±88	1631
4-2	372	5.81	1594	1.00	0.0623	0.1558±26	1.975±50	0.09194±231	1466
5-1	130	0.70	11569	0.14	0.1235	0.2768±48	3.839±93	0.10059±148	1635
6-1	305	1.10	6692	0.24	0.1373	0.2538±43	3.518±69	0.10053±81	1634
7-1	242	0.65	39620	0.04	0.1248	0.2654±45	3.688±72	0.10079±75	1639
8-1	141	1.12	140056	0.01	0.1189	0.2268±39	3.248±68	0.10384±103	1694
9-1	137	0.77	7059	0.23	0.1036	0.2451±42	3.399±76	0.10058±122	1635
10-1	156	0.32	4170	0.38	0.0900	0.2810±48	3.806±88	0.09825±187	1591
11-1	251	0.41	24777	0.06	0.1142	0.2691±46	3.760±72	0.10135±70	1649
12-1	180	0.48	7353	0.22	0.1456	0.2711±47	3.795±85	0.10154±122	1652
13-1	197	0.36	29586	0.05	0.1100	0.2724±46	3.775±77	0.10051±93	1634
14-1	194	0.37	41152	0.04	0.1152	0.2812±48	3.948±79	0.10182±87	1657
14-2	191	0.37	21848	0.07	0.1068	0.2769±48	3.808±78	0.09974±93	1619
15-1	1023	4.18	5063	0.31	0.0819	0.0494±8	0.672±14	0.09855±99	1597
16-1	153	0.34	7746	0.21	0.1007	0.2827±49	3.919±85	0.10053±153	1634
17-1	186	0.53	13699	0.12	0.1162	0.2674±46	3.719±76	0.10086±95	1640
18-1	166	0.50	15674	0.10	0.0662	0.2514±43	3.467±71	0.10001±94	1624
19-1	214	0.40	43365	0.04	0.0943	0.2675±46	3.654±71	0.09906±76	1606
20-1	232	0.44	4995	0.32	0.1296	0.2768±47	3.704±77	0.09706±96	1568

a) Denotes the percentage of common ^{206}Pb in the total measured ^{206}Pb.

TABLE 3. ION MICROPROBE ANALYTICAL DATA FOR FELSIC VOLCANIC SAMPLE 7920.5308.

uncertainties, this pooled age is regarded as the best determination for their igneous crystallisation and hence the stratigraphic age of the Tommy Creek sequence.

It could be argued that the 1626 ± 4 Ma age is a result of the principal D^T_1 deformational event in the TCB, but if so we would expect to see further vestiges of some earlier primary age, either as cores or discrete grains. Instead, all grains analysed from both the more and less-deformed sites, apart from one in sample 5308 and those with anomalous Th/U, are concordant or near-concordant and have the same age to within experimental error. In addition, the prominent compositional zoning, especially evident in the very coarse zircons from site 5010, is almost certainly of igneous origin, and apart from grain-edge corrosion embayments in sample 5308, the zircons are unmodified by any post-igneous deformation. Thus the agreement of the ion-microprobe zircon U-Pb ages from these two differently deformed rock types in the TCB substantiates the general arguments and the ~1600 Ma ages derived from the previously published conventional zircon results. The present work confirms the interpretation that the Tommy Creek beds are substantially younger than parts of the Corella Formation in the Mary Kathleen Fold Belt known to be at least 1740 Ma old.

Discussion

Field evidence suggests two episodes of thrusting which emplaced higher-grade polydeformed rocks over lower-grade undeformed rocks. This was followed by east-west compression which refolded the sequence. However, a number of problems arise with this model; these are:

- Both the previously reported and present U-Pb zircon data indicate that felsic volcanism in the TCB occurred at 1626 ± 4 Ma. This is considerably younger than even the youngest

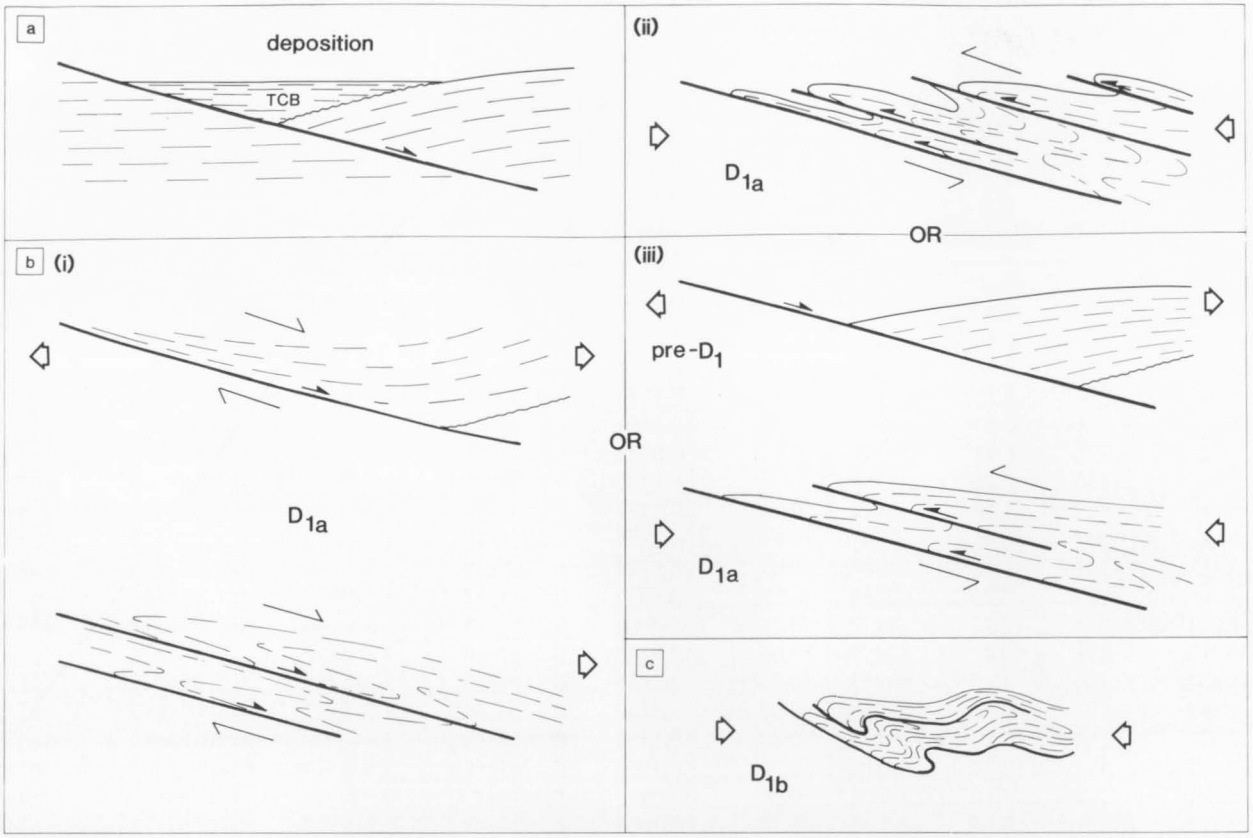


Fig. 12. Formation and early deformation of the TCB: (a) Local deposition of the Tommy Creek beds around 1626 4 Ma. (b) Alternative models for the early deformation history: (i) extensional deformation during D^T_{1a} accompanied by shearing and folding, resulting in burial and metamorphism of the TCB; or (ii) burial and metamorphism of the TCB by overthrusting of other units over the TCB during D^T_{1a}, these units having been subsequently eroded; or (iii) early pre-D^T_1 extensional deformation resulting in burial and metamorphism of the TCB; followed by uplift during D^T_{1a} thrusting. (c) Thrusting (not shown) and folding in D^T_{1b}.

volcano-sedimentary package elsewhere in the Inlier (Mount Isa Group, 1670^{+20}_{-17} Ma; Page, 1981). Hence, thrusting apparently resulted in emplacement of younger rocks over older rocks, the opposite of that normally expected in thrust terranes.

- Thrusting (D^T_1) pre-dates peak metamorphism (sillimanite grade) and therefore cannot account for the jump in metamorphic grade across the boundaries of the TCB. D_2 structures in the Mitakoodi area to the south of the TCB do not have the same orientation as those in the TCB.
- Younger, stratigraphically and structurally higher rocks have reached higher grades of metamorphism than the adjacent older, stratigraphically and structurally lower rocks.

Pre-D^T_1 deformation

The relatively young age of the Tommy Creek beds indicates that they are neither correlative with the Corella Formation, nor with any other known volcano-sedimentary sequence in the Mount Isa Inlier. The Tommy Creek block probably developed as a small localised sedimentary basin (Fig. 12a) which may have resulted from a pre-D_1 extensional event documented by Passchier (1986a), Williams & others (1987), BMR (1988a), Passchier & Williams (1989), Stewart (1989), Williams (1989), and Loosveld (1988; 1989b) at various localities in the inlier. Holcombe & others (1987; this volume), Pearson & others (1987; this volume), Pearson (1988), and Oliver & others (1991) argue for a major extensional event in the Mary Kathleen Fold Belt between 1760 and 1730 Ma. The extent and nature of such a basin cannot be estimated without knowing more about the effects of the extension around the Tommy Creek area. In this case, the boundary between the Tommy Creek beds and the Corella Formation, where not faulted, must be an unconformity.

Apparent thrusting of younger rocks of the TCB (that have undergone anomalously high-grade metamorphism)

over older rocks of the Mitakoodi block led Hill (1987) to propose that the Tommy Creek beds were originally placed at greater depths by an extensional event before thrusting emplaced them in their current position (Fig. 12d).

Evidence for pre-D^T_1 structures in the TCB is sparse, but even so any pre-D^T_1 deformation that may have occurred in the TCB would be masked by the intensity of the D^T_1 deformation. Some staurolite porphyroblasts overgrow a foliation oblique to the D^T_{1a} foliation. This is possibly an earlier fabric (pre-D^T_{1a}), but this angular discordance can also be interpreted as due to rotation of the porphyroblasts during D^T_{1a}. Thinning, and locally even complete excision, of the Overhang Jaspilite along the TCB/Mitakoodi structure contact (except for one small fault bounded block in the far west) may have been caused by early normal faulting. Truncation of units on almost the same structural level to the southwest of the TCB is explained by Williams (1989) as being the result of extensional faulting.

Microstructures indicate that metamorphism took place during D^T_1 and again late or post-D^T_2. If the TCB had been buried beneath older rocks early in its history, it should have been metamorphosed then, but no pre-D^T_1 metamorphic event is preserved in the TCB.

Peak metamorphism (sillimanite grade) postdates thrusting

As peak metamorphism of the TCB post-dates shearing, the high-grade metamorphism in the TCB relative to surrounding areas no longer supports the earlier proposal of Hill (1987) that the shears were thrusts. It is possible that the sense of movement on the 'thrusts' (i.e., the shears) has been misinterpreted, and that they actually represent normal faults. Normal faulting generally results in younger rocks being emplaced over older rocks, as is found in the TCB. Unfortunately, evidence is lacking for orientation of movement along D^T_1 shear zones. A study of the kinematics of the D^T_1 shears would be a major contribution towards solving the problems of deformation in the TCB. Furthermore, the calculation of the pressure conditions that existed during deformation may provide clues to the nature of the deformation, whether extensional or compressional. If the D^T_1 shear zones were normal faults, they could have resulted in the relative downward movement of young rocks accompanied by metamorphism (Fig. 12b). Subsequent post-D^T_2 uplift could emplace these rocks of the TCB adjacent to older, lower metamorphic grade rocks (i.e., the Mitakoodi rocks)

It is also possible that the faults were originally dipping in the opposite direction and have been tipped back due to later folding. This is unlikely, as the later folding event (D^T_2) resulted in north-south folds and should not have significantly affected the dip direction of east-west oriented structures.

Final emplacement post-dates peak metamorphism

Change in metamorphic grade across the boundaries of the TCB indicates that final emplacement of the TCB must post-date peak metamorphism, i.e., emplacement must post-date D^T_2. Late breccias and faults along and near the southern boundary indicate that late reactivation may have occurred along the old steepened D^T_{1a} shears. Such evidence for late movement on the eastern boundary has not been found, but outcrop along this boundary is not good and so reactivation cannot be discounted. The extent and sense of movement along late faults is not known, but they must be sufficient to juxtapose the amphibolite-grade TCB against the greenschist facies rocks of the Mitakoodi area. This late fault movement may be related to the D_3 structures of Loosveld (1989b) which resulted from north-south contraction. Furthermore, late movement along the boundary between the TCB and the Mitakoodi area explains discrepancies between the orientation of D_2 structures in these two areas. The thinning and local excision of the Overhang Jaspilite along the TCB/ Mitakoodi contact may be due to this late fault movement rather than early normal faulting, as discussed above.

The western boundary provides no clues to the solution of the origin of the TCB as the boundary is the Ballara-Corella River Fault Zone, a northerly extension of the Pilgrim Fault. It has been suggested that the Pilgrim Fault System is a terrrane boundary on the basis of indications of large amounts of movement on the fault, and on differences in stratigraphy and structural grain on either side of the fault (BMR, 1988b), and that movement on the Pilgrim Fault post-dates extension and thrusting in the Mount Isa Inlier. If this is true, then the TCB cannot be correlated with the rocks and structural history of the area west of the fault.

Higher grades of metamorphism reached in stratigraphically and structurally higher rocks

The rocks of the TCB were metamorphosed to higher grades than the greenschist facies of the adjacent Mitakoodi and Fox Mountain areas before final emplacement. These high-grade conditions must have

been in existence during D^T1 and D^T_2. We can see two possible solutions to this problem:

(1) The rocks of the TCB were subject to some pre-D^T_{1a} or syn-D^T_{1a} deformation which resulted in their burial; either by downfaulting of the TCB along a normal fault as suggested by Hill (1987), or by overthrusting on to the TCB of other rocks, which have subsequently been removed by erosion (Fig. 12c, d).

(2) The TCB is allochthonous, possibly a separate terrane, that formed separately from areas it now adjoins. It must be noted, however, that the combination of east-trending D_1 structures and north-trending D_2 structures are characteristic of many parts of the Mount Isa Inlier (Bell, 1983; Loosveld & Schreurs, 1987; Loosveld, 1988, this volume). This suggests that although the TCB may be allochthonous, it appears to have undergone a very similar deformation history to the rest of the Mount Isa Inlier. Large amounts of movement of the TCB to its present position could be accommodated by large-scale movements along the northern part of the Pilgrim Fault System, and by reactivation along the old D^T_1 thrusts.

Unfortunately, the lack of evidence at present does not allow more than speculations on the early origins of the TCB.

Synthesis of present knowledge

- (1) Carbonate, evaporites, fine-grained clastics, and bimodal pyroclastics (units C, M, S, and F) were deposited in generally calm, shallow water, briefly interrupted by conglomerate deposition (base of unit M).
- (2) The Tommy Creek beds contain significant amounts of volcanic material, including that previously mapped by Derrick & others (1971) as Tommy Creek 'microgranite'. The volcanic interpretation is based on field relationships, as original textures have been largely destroyed.
- (3) The age of igneous crystallisation of the felsic volcanic units is 1626 ± 4 Ma and hence is regarded as the stratigraphic age of the Tommy Creek sequence.
- (4) Limited evidence has been found for a pre-D^T_1 deformation in the TCB. These oldest structures may correlate with extensional structures documented elsewhere in the Mount Isa Inlier.
- (5) The major deformation event (D^T_1) involved shearing of the boundaries of the TCB accompanied by intense foliation development and folding on all scales. The shear zone is preserved on the eastern and southern sides of the TCB. The latter boundary, however, appears to have been reactivated by later movement. The sense of shear on the boundaries of the TCB is presently unknown.
- (6) D^T_1 occurred in two separate events: D^T_{1a} and D^T_{1b}. East-west folds are recumbent or inclined northward due to refolding. The geometry of the TCB is dominated by a very large non-cylindrical D^T_{1a} fold, which has been refolded during D^T_{1b} and D^T_2, giving it a tongue-like shape.
- (7) Amphibolite-grade fabrics developed during D^T_{1a}, including the growth of garnet and staurolite.
- (9) All D^T_{1a} and D^T_{1b} fabrics and structures have been folded by a later pervasive deformational event, D^T_2. Structures of D^T_2 are upright and trend north-south in the southern part of the TCB and north-northwest-south-southeast in the northern part.
- (10) Amphibolite-grade metamorphism also accompanied D^T_2, and produced sillimanite. Thus, the juxtaposition of the high-grade TCB and the lower-grade Mitakoodi structure must post-date D^T_2.
- (11) The boundaries of the TCB are marked by a change in metamorphic grade, and are coincident with D^T_1 shear zones.
- (12) Emplacement of the TCB against the adjacent areas, particularly the Mitakoodi area to the south and the Fox Mountain area to the east, must postdate metamorphism, i.e. postdate D^T_1 and D^T_2.
- (13) Therefore, considering points 11 and 12, emplacement must have occurred post-D^T_2 by reactivation along the old D^T_1 structures.

Acknowledgements

This work was largely carried out while EJH was employed by the Bureau of Mineral Resources, and RJHL held a Ph.D. Scholarship at the Australian National

University. The isotopic study was carried out on the SHRIMP instrument, A.N.U., and we are grateful to Ian Williams and John Foster for their assistance. The paper benefited from reviews by Gordon Lister, Alastair Stewart, Karl Wolf, and two anonymous referees, and from advice from Dave Blake, Mike Etheridge, Nick Oliver, and Rick Valenta. Draga Gelt assisted with the illustrations.

References

BELL, T.H., 1983 - Thrusting and duplex formation at Mount Isa, Queensland, Australia. *Nature* 304, 493-497.

BLAKE, D.H., 1980 - The early geological history of the Proterozoic Mount Isa Inlier, northwestern Queensland: an alternative interpretation. *BMR Journal of Australian Geology and Geophysics* 5, 243-256.

BLAKE, D.H., 1982 - A review of the Corella Formation, Mount Isa Inlier, Queensland. *BMR Journal of Australian Geology and Geophysics* 7, 113-118.

BMR, 1988a - Extension tectonics extended: new results from the Mount Isa Inlier. *BMR Research Newsletter* 8, 2-4.

BMR, 1988b - Block and possible terrane boundaries in the Mount Isa Inlier. *BMR Research Newsletter* 9, 2-3.

COMPSTON, W., WILLIAMS, I.S., & MEYER, C., 1984 - U-Pb geochronology of zircons from lunar breccia 73217 using a sensitive high mass-resolution ion microprobe. *Proceedings of the 14th Lunar & Planetary Science Conference, Part 2. Journal of Geophysical Research* 89, Supp., B525-B534.

COMPSTON, W., KINNY, P.D., WILLIAMS, I.S., & FOSTER, J.J., 1986. The age and Pb loss behaviour of zircons from the Isua supracrustal belt as determined by ion microprobe. *Earth & Planetary Science Letters* 80, 71-81.

CUMMING, G.L., & RICHARDS, J.R., 1975 - Ore lead isotopes in a continuously changing earth. *Earth & Planetary Science Letters* 28, 155-171.

DERRICK, G.M., 1980 - Marraba, Queensland. 1:100 000 *Bureau of Mineral Resources, Australia Geological Map Commentary* 33 pp.

DERRICK, G.M., WILSON, I.H., HILL, R.M., GLIKSON, A.Y., & MITCHELL, J.E., 1977 - Geology of the Mary Kathleen 1:100 000 Sheet area, northwest Queensland. *Bureau of Mineral Resources, Geology and Geophysics, Australia, Bulletin* 193, 114 pp.

DERRICK, G.M., WILSON, I.H., HILL, R.M., & MITCHELL, J.E., 1971 - Geology of the Marraba 1:100 000 Sheet area, Queensland. *Bureau of Mineral Resources, Australia, Record* 1971/56, 192 pp.

EDWARDS, A.B. & BAKER, G., 1954 - Scapolitization in the Cloncurry district of north-western Queensland. *Journal of the Geological Society of Australia* 1, 1-33.

GLIKSON, A.Y., 1972 - Structural setting and origin of Proterozoic calc-silicate megabreccias, Cloncurry region, northwestern Queensland. *Journal of the Geological Society of Australia* 19, 53-63.

HILL, E.J., 1987 - Structural geology of the Tommy Creek area, Mount Isa Inlier, NW Queensland. *Bureau of Mineral Resources, Australia, Record* 1987/20, 51 pp.

HILL, E.J., 1991 - Geology of the Tommy Creek Block (1:25 000 scale map). Bureau of Mineral Resources, Canberra, Australia (two sheets). Available as colour electrostatic plots on paper (AUD30), or in digital form on optical disc or Exabyte 8 mm tape (prices on application) both of which can be displayed on Intergraph Microstation software on computers that will run Unix. The digital data comprise a scanned raster image (.RLE format) of the black and white geological map, and an Intergraph vector design file containing the boundaries of coloured polygons. The coloured map and data are available from the Publication Sales Centre, Bureau of Mineral Resources, and an uncoloured Ozalar film or paper copy (AUD20) of the map is available from BMR Copy Service, both at GPO Box 378, Canberra, ACT, 2601, Australia. All orders to be prepaid to Collector of Public Monies.

HOLCOMBE, R.J., PEARSON, P.J., & OLIVER, N.H.S., 1987. The Mary Kathleen Fold Belt, northwest Queensland: geometry and timing of deformation. *Geological Society of Australia, Abstracts* 19, 35-36.

HOLCOMBE, R.J., PEARSON, P.J., & OLIVER, N.H.S., this volume. Structure of the Mary Kathleen Fold Belt. *In* STEWART, A.J. & BLAKE, D.H. (Editors), Detailed Studies of the Mount Isa Inlier. *Bureau of Mineral Resources, Australia, Bulletin* 243.

JAQUES, A.L., BLAKE, D.H., & DONCHAK, P.J.T., 1982 - Regional metamorphism in the Selwyn area, northwest Queensland. *BMR Journal of Australian Geology and Geophysics* 7, 181-196.

LANCELOT, J.R., BOULLIER, A.M., MALUSKI, H., & DUCROT, J., 1983 - Deformation and related radiochronology in a late Pan-African mylonitic shear zone, Adrar des Iforas (Mali). *Contributions to Mineralogy & Petrology* 82, 312-326.

LOOSVELD, R.J.H., 1988 - Structure and tectono-thermal history of the eastern Mount Isa Inlier, Australia. Ph.D. Thesis, Australian National University, 216 pp. (unpublished).

LOOSVELD, R.J.H., 1989a - The synchronism of crustal thickening and high T/low P metamorphism in the Mount Isa Inlier, Australia. Part I: an example, the central Soldiers Cap belt. *Tectonophysics* 158, 173-190.

LOOSVELD, R.J.H., 1989b. The ensialic tectonic evolution of the central eastern Mount Isa Inlier, NW

Queensland, Australia. *Precambrian Research* 44, 243-276.

LOOSVELD, R.J.H., this volume - Structural geology of the central Soldiers Cap Belt, Mount Isa Inlier, Australia. *In*: STEWART, A.J. & BLAKE, D.H. (Editors), Detailed Studies of the Mount Isa Inlier. *Bureau of Mineral Resources, Australia, Bulletin* 243.

LOOSVELD, R.J.H., & SCHREURS, G.M.M.F., 1987 - Discovery of thrust klippen, northwest of Mary Kathleen, Mount Isa Inlier, Australia. *Australian Journal of Earth Sciences* 34, 387-402.

OLIVER, N.H.S., VALENTA, R.K., & WALL, V.J., 1990 - The effect of heterogeneous stress and strain on metamorphic fluid flow, Mary Kathleen, and a model for large-scale fluid migration. *Journal of Metamorphic Geology* 8, 311-331.

OLIVER, N.H.S., HOLCOMBE, R.J., HILL, E.J., & PEARSON, P.J., 1991 - Tectono-metamorphic evolution of the Mary Kathleen Fold Belt, northwest Queensland: A reflection of mantle plume processes? *Australian Journal of Earth Sciences* 38, 425- 455.

PAGE, R.W., 1981 - Depositional ages of the stratiform base metal deposits at Mount Isa and McArthur River, Australia, based on U-Pb zircon dating of concordant tuff horizons. *Economic Geology* 76, 648-658.

PAGE, R.W., 1983a - Timing of superposed volcanism in the Proterozoic Mount Isa Inlier, Australia. *Precambrian Research* 21, 223-245.

PAGE, R.W., 1983b - Chronology of magmatism, skarn formation and uranium mineralization, Mary Kathleen, Queensland, Australia. *Economic Geology* 78, 838-853.

PAGE, R.W., & BELL, T.H., 1986 - Isotopic and structural responses of granite to successive deformation and metamorphism. *Journal of Geology* 94, 365-379.

PASSCHIER, C.W., 1986a - Evidence for extensional tectonics in the Proterozoic Mount Isa inlier. *Geology* 14, 1008-1011.

PASSCHIER, C.W., 1986b - Proterozoic deformation in the Duchess belt, Australia: a contribution to the Mount Isa Regional Tectonic History program. *Geology en Mijnbouw* 65, 47-56.

PASSCHIER, C.W. & WILLIAMS, P.R., 1989 - Proterozoic extensional deformation in the Mount Isa Inlier, Queensland, Australia. *Geological Magazine* 126, 43-53.

PEARSON, P.J., 1988 - The structural and tectonic development of the Wonga Belt and surrounding Mary Kathleen Fold belt, Mt. Isa Inlier, northwestern Queensland. Ph.D. Thesis, University of Queensland (unpublished).

PEARSON, P.J., HOLCOMBE, R.J. & OLIVER, N.H.S., 1987 - The Mary Kathleen Fold Belt: D1 - a product of crustal extension? *Geological Society of Australia, Abstracts* 19, 37-38.

PEARSON, P.J., HOLCOMBE, R.J. & OLIVER, N.H.S., this volume - Synkinematic emplacement of the Middle Proterozoic Wonga Batholith into a mid-crustal extensional shear zone, Mount Isa Inlier, Queensland, Australia. *In*: STEWART, A.J., & BLAKE, D.H., (Editors). Detailed Studies of the Mount Isa Inlier. *Bureau of Mineral Resources, Australia, Bulletin* 243.

RYBURN, R.J., WILSON, I.H., GRIMES, K.G., & HILL, R.M., 1988 - Cloncurry, Queensland. *Bureau of Mineral Resources, Australia, 1:100 000 Geological Map Commentary* 30 pp.

SINHA, A.K., & GLOVER, L., III, 1978 - U/Pb systematics of zircons during dynamic metamorphism: a study from the Brevard Fault Zone. *Contributions to Mineralogy & Petrology* 66, 305-310.

STEWART, A.J., 1989 - Extensional faulting as the explanation for the Deighton 'Klippe' and other Mount Albert Group outliers, Mount Isa Inlier, northwestern Queensland. *Australian Journal of Earth Sciences* 36, 405-421.

TUNKS, A., 1987 - Breccias and metasomatism in the Corella Formation, Cloncurry, Queensland. B.Sc. (Hons.) Thesis, Monash University, 127 pp. (unpublished).

WILLIAMS, P.R., STEWART, A.J., & PEARSON, P.J., 1987 - Proterozoic continental extension in the Mount Isa Inlier. *Bureau of Mineral Resources Symposium on Extension Tectonics, Extended Abstracts,* 64-71.

WILLIAMS, P.R., 1989 - Nature and timing of early extensional structures in the Mitakoodi Quartzite, Mount Isa Inlier, northwest Queensland. *Australian Journal of Earth Sciences* 36, 283-296.

WILSON, C.J.L., 1973 - The prograde microfabric in a deformed quartzite sequence, Mount Isa, Australia. *Tectonophysics* 19, 39-81.

Structural geology of the central Soldiers Cap Belt, Mount Isa Inlier, Australia

Ramon J. H. Loosveld [1,2]

This paper is based on the following map:

Loosveld, R.J.H., 1991 - Structural Geology of the Central Soldiers Cap Group (1:100 000 scale map). Bureau of Mineral Resources, Canberra.

The main structural elements of the central Soldiers Cap Belt in the eastern part of the Mount Isa Inlier are D^S_1 fold and thrust nappes and related folds, upright north to northeast-trending D^S_2 folds, and west or northwest-trending D^S_3 folds and faults. Low-P amphibolite facies metamorphism accompanied D^S_2 in the lower Soldiers Cap Group (SCG; 1780-1750 Ma) making up the belt, and indicate a geothermal gradient of at least 41°C/km. The Soldiers Cap Belt is separated from the greenschist-facies Marimo-Staveley Block by the post-D^S_2 steeply east-northeast-dipping Cloncurry Overthrust.

[1]Department of Geology, Australian National University, G.P.O. Box 4, Canberra, A.C.T. 2601, Australia.

[2] Present address: Koninklijke/Shell Exploration and Production Laboratories, P.O. Box 60, 2280 AB Rijswijk, The Netherlands.

Introduction

The Soldiers Cap Group (SCG; Derrick & others, 1976) in the east of the Mount Isa Inlier crops out in a narrow northern belt north of Quamby, and the wider Soldiers Cap Belt south of Cloncurry (Blake, 1987; Beardsmore & others, 1988). The central Soldiers Cap Belt described here (see Loosveld, 1991) is located between the Marimo-Staveley Block to the west and sediments of the Mesozoic Eromanga Basin to the east. The area is located between latitudes 20° 36' and 21° 07'S and longitudes 14° 032' and 14° 055'E, and lies within the Cloncurry (BMR, 1988) and Kuridala (BMR, 1983) 1:100 000 sheet areas. In this study, the emphasis is on the structural deformation of the SCG, and only brief stratigraphic descriptions are given. Detailed litho-stratigraphic desciptions have been published by Glikson & Derrick (1970), Derrick & others (1976), Donchak & others (1983), Beardsmore & others (1988), and Ryburn & others (1988).

Structural terminology

Deformation episodes in the central Soldiers Cap Belt are denoted by the superscript 'S'.

General geology

Carter & others (1961) recognised three subdivisions within the SCG. Derrick & others (1976) formally defined these, from base to top, as: the Llewellyn Creek Formation (Pol); the Mount Norna Quartzite (Pon); and the Toole Creek Volcanics (Pot). Boundaries between the three formations are gradational. Beardsmore & others (1988) defined two more formations underlying the Llewellyn Creek Formation in the southern Soldiers Cap Belt and Kuridala Belt (Selwyn Region 1:100 000 Sheet area BMR, 1988), but these are not exposed in the central Soldiers Cap Belt.

The SCG overlies banded and brecciated calc-silicate rocks of the Mary Kathleen Group, but the contact, where exposed, is invariably tectonic; faults parallel or subparallel to bedding separate the SCG from the underlying Mary Kathleen Group metasediments in the north, and the Cloncurry Overthrust, a late high-angle reverse fault, separates the two groups in the southwest (Fig. 1). Within the upper Mary Kathleen Group in the Marimo-Staveley Block are eight masses of fine to medium-grained well-bedded *Roxmere Quartzite* (Loosveld, 1989c). One of these lies in the map area around grid reference 550990. All three formations of the SCG are intruded by dolerite sills and dykes up to 700 m thick. Some of the dykes occupy the approximate axial surface of kilometre-scale folds.

The *Llewellyn Creek* Formation consists of a series of well-bedded (2 cm-2 m thick) metaturbidite. Complete Bouma-profiles are common. The basal units only rarely contain pebbles. Reverse grading due to porphyroblastesis (mainly andalusite, garnet, staurolite, sillimanite, biotite) in the pelitic tops of the metaturbidites is also common. The *Mount Norna Quartzite* conformably overlies the

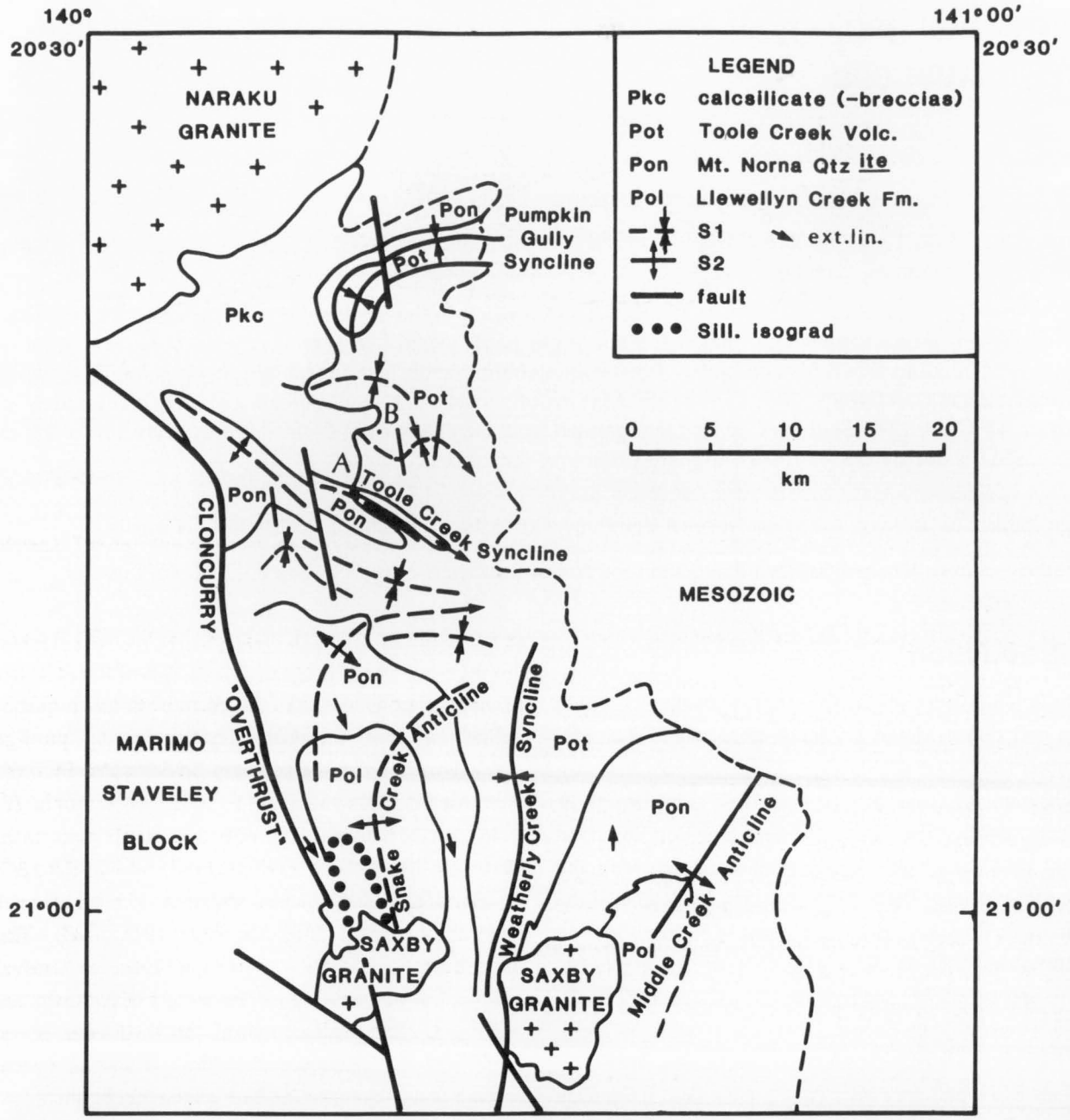


Fig. 1. Schematic map of the main structural elements of the central Soldiers Cap Belt. At locality A, a vertical east-striking crenulation cleavage is developed; at B, a steeply south-southwest-dipping differentiated crenulation cleavage. After Loosveld (1989a).

Llewellyn Creek Formation. It comprises a massive clean quartzite up to 150 m thick (Pon_q), overlain by metaturbidite which is mostly incomplete (base-missing), and by mature medium-grained quartzite; metasiltstone, phyllite, banded iron formation, and basalt increase in amount towards the top of the member. Conformably overlying the Mount Norna Quartzite are the poorly exposed *Toole Creek Volcanics*, mostly basalt with lesser phyllite, metasiltstone, and chert. In the Weatherly Creek Syncline (Fig. 1), limestone and carbonaceous slate also occur.

The Mount Norna Quartzite and Toole Creek Volcanics are unconformably overlain by calc-silicate breccia, previously attributed to the Corella Formation (Mary Kathleen Group), but now regarded as a much younger unit, the *Gilded Rose Breccia* (P_{br}; Ryburn & others, 1988). This has been studied by Glikson (1972), Tunks (1987), and Ryburn & others (1988). The breccia obscures post-metamorphic D^S_3 faults (e.g., at grid reference 607822, where it overlies the Cloncurry Overthrust), indicating that its deposition (or remobilisation) postdated D^S_3.

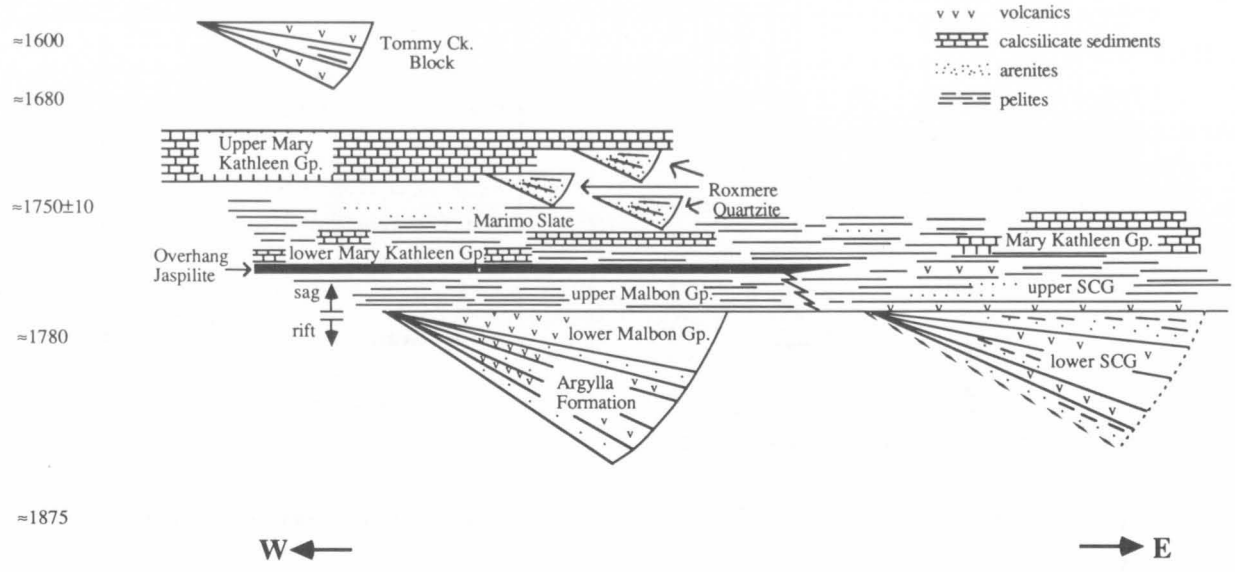


Fig. 2. Proposed tectono-stratigraphic correlation of the Soldiers Cap Group with units to the west (after Loosveld, 1989c). The architecture of the infra-rift basins is unknown.

Litho-stratigraphic correlation

The age of the SCG and its litho-stratigraphic correlation with other units are still problematical (Blake & others, 1983, 1984; Beardsmore & others, 1988; Ryburn & others, 1988). No isotopic dates have as yet been obtained on the SCG. The only geochronological constraint is defined by the young post-tectonic plutons of the approximately 1500 Ma old Williams and Naraku Batholiths (Nisbet & others, 1983; R.W. Page, personal communication, 1986; Wyborn & others, 1988), namely the Saxby Granite (belonging to the Williams Batholith) in the south and the Naraku Granite in the north (Fig. 1), both of which intrude the SCG.

The SCG contains the only turbiditic sequence in the Mount Isa Inlier, which, among other evidence, has led to suggestions that the SCG represents the eastern margin of a Proterozoic continent (a 'mobilist's' viewpoint, e.g., Wilson, 1978). Wyborn & Blake (1982) and Blake (1986), however, contested the 'mobilists' ' arguments and refuted the theory of a Proterozoic continental margin in the eastern Mount Isa Inlier. Subsequently, the evolution of the Mount Isa Inlier has been interpreted as entirely ensialic (Ellis & Wyborn, 1984; Blake, 1986, 1987; Etheridge & others, 1987; Wyborn & others, 1988).

Blake & others (1983), Laing & Beardsmore (1986), and Beardsmore & others (1988) correlated the SCG with the lithologically similar Kuridala Formation (in the southern Kuridala and Selwyn Region 1:100 000 Sheet areas). Correlation of the SCG with other units can be only speculative at this stage, as: (1) there is no useful age control on the SCG; (2) lithologically, the SCG is unique in the Mount Isa Inlier; and (3) contacts of the SCG (and Kuridala Formation) with possible correlative sequences are invariably tectonic or obscured by younger calc-silicate breccias. The contact of the central SCG with the Marimo-Staveley Block is either tectonic (the Cloncurry Overthrust) or obscured under calc-silicate breccias. Beardsmore & others (1988) correlated the SCG with Blake's (1987) cover sequence 1, the Leichhardt Volcanics (1875 to 1865 Ma; Page, 1978, 1983). Their arguments have, however, been questioned by Loosveld (1988, 1989c), who argued for an age of approximately 1780-1750 Ma, and correlated the SCG with Blake's (1987) cover sequence 2. The correlation scheme proposed by Loosveld (1989c) is shown in Figure 2.

Structure

Structural domains

Unlike the constant longitudinal grain of tectono-stratigraphic units west of the Pilgrim Fault, the central SCG area may be subdivided into five domains, which are characterised by different structural styles and orientations: the Snake Creek Anticline trends north-northwest, the Weatherly Creek Syncline trends north, the Middle Creek Anticline trends northeast, the Toole Creek Syncline fold system trends east-southeast, and most of the Pumpkin Gully Syncline trends east-northeast. The continuity of the penetrative slaty foliation, S_1, enables these five domains to be correlated. Loosveld (1988, 1989a) reviewed the different interpretations of the

structural framework of the central SCG area by Glikson & Derrick (1970) and Ryburn & others (1988), who all regarded the Toole Creek and Weatherly Creek Synclines as part of the same fold generation, and offered a third interpretation, which was based on the overall geometry of S_1. Stereographic representation of the main structural elements is given in Loosveld (1988, 1989a).

The Snake Creek Anticline (Fig. 1) is a north-northwest-trending, tight to isoclinal, inclined to reclined, synformal anticline in the Llewellyn Creek Formation and Mount Norna Quartzite. Axial-plane foliation dips steeply east-northeast and is a well-developed slaty cleavage in pelitic units and a precipitation/solution cleavage in psammitic units. Related fold axes are moderately to steeply south-southeast-plunging in the south of the anticline, but progressively steepen to vertical in the north. In the hinge zone within the Mount Norna Quartzite they plunge steeply northeast, and tracing the hinge zone even further, east-southeast in the Toole Creek Syncline area; in the intervening area, the axes are vertical. As the axial plane foliation (S_1) is the oldest recognisable structural element in the area, the Snake Creek Anticline is a D^S_1 fold. The axial-plane foliation can be traced into the Toole Creek Syncline area (see below), where it is also axial-planar. In the high-grade core of the Snake Creek Anticline (see below), an extension lineation is well developed in both limbs of the structure, and plunges approximately southeast. On the western limb, boudinage and transposition occur in a zone of high ductile shear strain which passes gradationally into the Cloncurry Overthrust, a late high-angle reverse fault system (Fig. 1).

The Weatherly Creek Syncline (Fig. 1) is an upright, tight to isoclinal, north-plunging, upward-facing syncline. Its axial plane surface is exposed in the Toole Creek Volcanics. Metamorphic grade is approximately lower to middle greenschist facies. Minor fold axes plunge gently to moderately north. Axial plane foliations are weak, and are mostly of precipitation/solution character. As the slaty cleavage, S_1, is weak and rare, crenulation cleavages are also not common. A Type 2 fold overprint pattern (Ramsay, 1967) can be observed on the eastern limb of the syncline (Cloncurry 1:100 000 Sheet grid reference 744878), where a 10 cm-scale tight north-plunging fold and its associated weak slaty cleavage obliquely transect isoclinal steeply southwest-plunging folds. Another argument for a post-D^S_1 origin of the Weatherly Creek Syncline is the fact that the L^1_1 extension lineation is folded around the syncline: L^1_1, steeply south- or

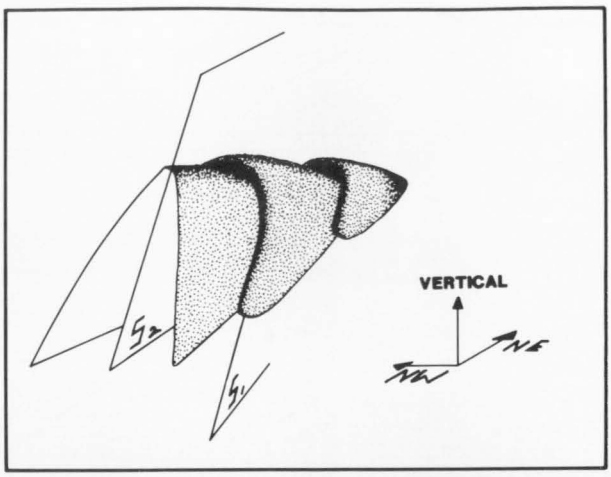


Fig. 3. Diagrammatic structure of the Middle Creek Anticline, a Type 2 (Ramsay, 1967) fold overprinting pattern. This type of overprint is scale-independent in the Middle Creek Anticline area.

southeast-plunging in the Snake Creek Anticline area, is moderately north-plunging in the eastern limb of the Weatherly Creek Syncline (in the Llewellyn Creek Formation and upper Mount Norna Quartzite). By analogy with style and orientation of D^S_2 folds in other parts of the inlier, the Weatherly Creek Syncline is probably a D^S_2 structure.

The Middle Creek Anticline (Fig. 1), the easternmost exposed structure in the Mount Isa Inlier, is a moderately northeast-plunging, upward-facing, tight anticline. A strong, moderately to steeply northwest-dipping crenulation cleavage is axial planar to it, and overprints an equally well-developed slaty cleavage. The angular relationship between bedding, slaty cleavage (S_1), and crenulation cleavage (S_2) define a Type 2 fold overprint pattern (Ramsay, 1967) with the Middle Creek Anticline overprinting west-northwest-verging D^S_1 folds. Extension lineations plunge northward in the western limb of the anticline and southward in the eastern limb. Overprinting relationships are visible around a D^S1 fold with a half-wavelength of 300 m in the eastern limb of the anticline (Kuridala 1:100 000 Sheet grid reference 890813). Figure 3 schematically shows the structure of the Middle Creek Anticline.

The Toole Creek Syncline (Fig. 1) is a system of tight, gently to steeply east-southeast-plunging folds with upright to steeply south-southwest-inclined axial planes. These folds are mainly exposed in the Toole Creek Volcanics; the upper Mount Norna Quartzite crops out in the cores of two antiforms. A pervasive slaty cleavage is present in the axial planar region of these folds, and can be traced into the axial plane of the Snake Creek Anticline.

The Toole Creek Syncline is therefore a D^S_1 structure. In two localities where a crenulation cleavage, crenulating an earlier slaty cleavage, is axial planar to the fold system (localities A and B, Fig. 1), Loosveld (1989a) suggested the two foliations may have formed progressively during one deformational event; either the slaty cleavage developed and subsequently rotated in the compressional field, or the compressional field rotated.

The Pumpkin Gully Syncline (Fig. 1) is a refolded, tight, mainly east-northeast-trending, upward-facing syncline, in which the Toole Creek Volcanics are exposed, with a thin rim of Mount Norna Quartzite in the north and a remnant of Mount Norna Quartzite in the southern limb. The syncline structurally overlies brecciated and banded calc-silicate rocks. If the calc-silicate rocks are part of the Mary Kathleen Group, they are younger than the SCG, and so the contact is interpreted as a thrust. The fold hinge on the Toole Creek Volcanics/Mount Norna Quartzite contact is well exposed, and shows a strong bedding-parallel foliation (S_1) which is crenulated around the vertical, locally northeast-trending axial plane of the Pumpkin Gully Syncline (D^S_2). The bedding-parallel foliation is associated with rootless isoclinal folds in banded iron formation. The syncline itself is clearly refolded around an approximately northwest trend (D^S_3), and its northern limb is transected by a sinistral north-striking fault. The time relationship between the fault and the D^S_3 fold is not clear.

D^S_1 thrusting

At least three deformational events can be recognised in the central Soldiers Cap Belt. An early event formed the Snake Creek Anticline and Toole Creek Syncline fold system, west- to northwest-verging asymmetric folds in the Middle Creek Anticline area, and a bedding-parallel foliation in the Pumpkin Gully Syncline area. The asymmetry of the Snake Creek Anticline, its original flat-lying orientation, and the ductile shear zone below the lower limb indicates it may be a fold nappe. Various brittle thrust contacts in the Oonoomurra and Pumpkin Gully Syncline areas indicate a more widespread thrusting event.

Determination of the D^S_1 movement vector in the central Soldiers Cap Belt is difficult, because of the overprinting of D^S_1 sense-of-shear indicators by later structural or metamorphic fabric elements, and by rotation during later folding. As the mechanisms of later folding (D^S_2, D^S_3) are unclear, backrotation of D^S_1 structures to their original position is speculative. The variable rotation of S_1 with respect to S_0 during D^S_2 and D^S_3, and the rotation of L^0_1 towards L^1_1 and L^2_2 respectively during D^S_1 and D^S_2 further hamper backrotation of D^S_1 fabric elements. In D^S_2 hinges of the southern Weatherly Creek Syncline, where, assuming plane strain during D^S_2, the orientation of L^1_1 is unaltered by D^S_2, L^1_1 is oriented in a (sub-)horizontal northwest direction, indicating a northwest-southeast *direction* of shear (e.g., Kuridala 1:100 000 Sheet grid reference 802662).

Three arguments can be used to determine the approximate *sense* of shear in the Snake Creek Anticline-Weatherly Creek Syncline area. First, the closure of the Snake Creek Anticline towards the north indicates a northward movement component. Second, a similar component is implied by the downward incision in the stratigraphic sequence by the ductile strain zone towards the south-southeast (thrusts tend to climb through the sequence in the direction of movement). Finally, asymmetric folds in the western (lower) limb show, despite their strong non-cylindricity, an overall north-northwest-vergence. A possible explanation for the development of similarly verging second-order folds on both limbs of a first order fold may be that bedding has rotated (almost) into the shear plane, after which a perturbation in the flow field can result in unusually vergent folds. Such a perturbation is more likely to occur in a well-layered medium, as bedding-parallel slip may occur in the lower limb of a fold nappe when a local simple shear system, slightly deviating from the overall simple shear, reactivates the bedding-anisotropy (Fig. 4). It is unlikely that early-D^S_1 parasitic folds have rolled passively from the upper limb through the fold nappe hinge, as no west-verging folds were observed in the hinge of the Snake Creek Anticline.

Determination of the D^S_1 movement vector in the Middle Creek Anticline area yields a slightly more westward orientation. Here, only the upper D^S_1 limb is exposed, folded around the northeast-plunging D^S_2 Middle Creek Anticline. The D^S_1-vergence is variable, but, after backrotation of D_2, has a westward component.

The backrotation technique consists of two steps: first a passive rotation of L^2_0 through a vertical plane back to horizontal; L^1_0 and L^1_1 are rotated along the same horizontal rotation axis. Then, L^1_0 and L^1_1 are rotated along the new L^2_0 rotation axis until they are horizontal. This way of backrotation is probably valid as the two clusters of L^1_1 converge to only one remaining cluster. This L^1_1 cluster indicates an east-southeast/west-northwest to east-west direction of shear. This, combined with the generally westward D^S_1 vergences, gives a west

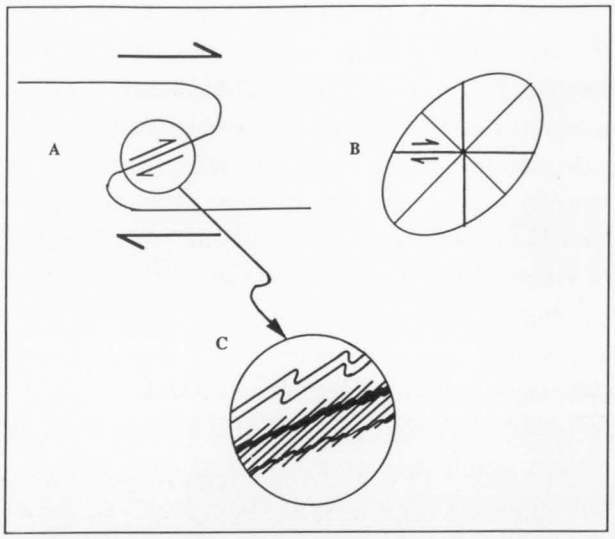


Fig. 4. Schematic development of asymmetric parasitic folds (1-10 cm scale) of equal vergence in both the upper and the lower limbs of a fold nappe. A: late stage in the development of a fold nappe. B: the associated incremental strain ellipsoid. C: Enlargement from the short limb of the fold in A. See text for explanation.

to northwest sense of shear (the L^1_0) cluster remains, as expected with the non-cylindrical D^S_1 folds, very wide after the backrotation). No sense-of-shear indicators have been found in the north of the study area.

It is not clear how the west- to northwest-directed sense of shear of the Snake Creek fold nappe relates to the more northern west-northwest-trending D^S_1 folds in the Toole Creek, Oonoomurra, and Pumpkin Gully Syncline areas.

D^S_2 folding

During the second deformation (D^S_2), the original D^S_1 Snake Creek inclined fold structure was rotated (west-side-up) and subsequently flattened. The Weatherly Creek and Pumpkin Gully Synclines and the Middle Creek Anticline formed during D^S_2, as did the approximately north-trending second generation folds overprinting the Toole Creek Syncline system. The style of D^S_2 in the central SCG area is similar to that of D^S_2 in other parts of the Mount Isa Inlier: north-trending, close to isoclinal, non-cylindrical and crudely symmetrical folds are associated with a vertical to steeply south-plunging extension lineation. As in other areas of the inlier, the trend of D^S_2 folds is dominantly north-south (if unaffected by later folding), except in the Middle Creek Anticline area where S_2 dips to the northwest.

Post-D^S_2 structures

A variety of non-correlative (discontinuous) post-D^S_2 structures are present in the central Soldiers Cap Belt. These include the northwest-trending fold deforming the Pumpkin Gully Syncline, the Cloncurry Overthrust, a west-northwest-trending fold affecting the western limb of the Snake Creek Anticline, two west-northwest-trending lineaments in the Middle Creek Anticline area (the northern one dextral with north-block-up-movement), and various crenulations, kinks, small-scale faults, and joints. The relationships between these structures and their relative timing to each other are unknown.

Metamorphism

Jaques & others (1982) made a detailed metamorphic study of the southern Soldiers Cap Belt. Except for a slightly higher-grade first metamorphic event (sillimanite/K-feldspar), their observations and conclusions appear to be equally valid in the central Soldiers Cap Belt. Pelites of the Llewellyn Creek Formation and the Mount Norna Quartzite have undergone two distinct metamorphic events: 1) An early low-pressure (high T/P ratios), prograde regional metamorphism with diagnostic minerals such as garnet, andalusite, staurolite, chloritoid, and sillimanite (but no K-feldspar; Table 1). 2) A second, retrograde metamorphism, its highest grade defined by biotite.

Just west of the axial plane of the Snake Creek Anticline and north of the Saxby Granite (at Cloncurry 1:100 000 Sheet grid reference 650791), up to 2 cm long sillimanite pseudomorphs (or partial pseudomorphs) after chiastolitic (sub-)prismatic andalusite are present. Andalusite persists in this area (and also in the sillimanite-grade core of the Middle Creek Anticline). Jaques & others (1982) reported the coexistence of anthophyllite + cordierite ± garnet in metamorphosed dolomitic(?) marls. These prograde metamorphic assemblages are associated with D^S_2; they define S_2 and L^2_2 or, in the Snake Creek Anticline, commonly a reactivated S_1 and L^1_1.

The co-existence of staurolite and andalusite constrains the metamorphic gradient to a minimum of 41°C/km (using equilibrium conditions after Richardson, 1968; Hoschek, 1969; and Holdaway, 1971, and assuming a specific density of the crust of 2700 kg/m^3; Fig. 5). The maximum metamorphic temperature is defined by the intersection of the water-saturated granite melting curve (Merrill & others, 1970) and the 'muscovite + quartz + K-feldspar + sillimanite + H_2O' phase boundary (Helgeson & others, 1978) at 665°C. No detailed geothermometry and geobarometry studies have been undertaken, but the similarity of mineral assemblages

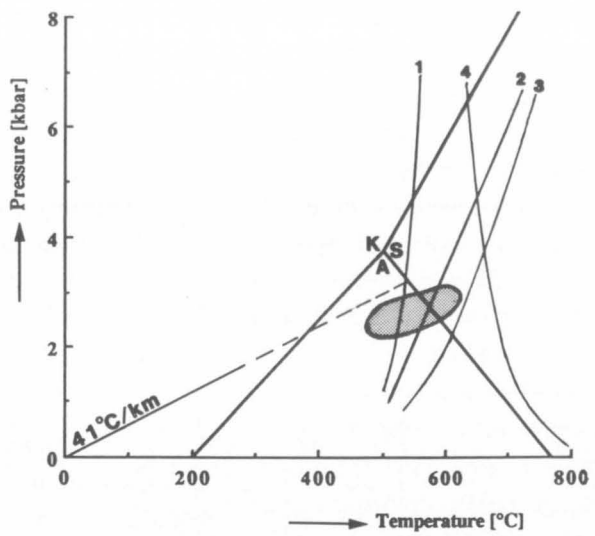


Fig. 5. P-T diagram showing the approximate equilibrium conditions (stippled area) for the prograde metamorphism of the lower SCG in the central Soldiers Cap Belt. Reaction (1) lower staurolite limit (after Richardson, 1968); (2) staurolite + muscovite + quartz ↣ Al_2SiO_5 + biotite + H_2O (Hoschek, 1969); (3) muscovite + quartz ↣ K-feldspar + Al_2SiO_5 + H_2O (Helgeson & others, 1978); and (4) water-saturated granite melting curve (Merrill & others, 1970). If peak-metamorphic conditions are succeeded by isobaric cooling, an anti-clockwise P-T-t path similar to that deduced for the Little Beauty area (J. Reinhardt & L. Hamilton, personal communication), will result. These equilibrium conditions coincide with those of Jaques & others' (1982) metamorphic zones 'A' and 'B' of the Selwyn Region and Kuridala 1:100 000 Geological Sheet areas (compare with Jaques & others' figure 9). Choice of reactions is after Jaques & others (1982).

(Table 1) in the central Soldiers Cap Belt with those of the southern Soldiers Cap Belt (Jaques & others, 1982) indicate similar P/T ratios for the prograde sequence. The shaded area in Figure 5 represents the approximate peak-metamorphic pressure and temperature conditions of the SCG. Jaques & others (1982) calculated metamorphic pressures of 300-400 MPa and temperatures of 450-680°C for the prograde metamorphism in the southern area.

The steeply east-northeast-dipping Cloncurry Overthrust (first defined by Honman & others, 1939) forms a metamorphic discontinuity. Amphibolite-grade rocks of the Soldiers Cap belt to the east are juxtaposed against greenschist-grade rocks of the Marimo-Staveley Block to the west. The Cloncurry Overthrust in the area is therefore interpreted as a post-metamorphic reverse fault.

To date, no P-T-t paths have been constructed for any particular rockmass within the Soldiers Cap Belt. The metamorphism and structural character of the Soldiers Cap Belt resemble those of the Little Beauty area (Mary Kathleen Fold Belt), where J. Reinhardt & L. Hamilton (personal communication) interpreted an anti-clockwise P-T-t path and also the Rosebud Syncline (Reinhardt, this volume). These paths approximated those of Loosveld (1989b) and Loosveld & Etheridge (1990), who modelled crustal thickening associated with (convective) thinning of the mantle lithosphere.

The sillimanite isograd in the Snake Creek Anticline

In the Snake Creek Anticline, isograds appear to be (sub-)parallel to bedding, and folded around the D^S_1 fold nappe. Sillimanite is found only in the Llewellyn Creek Formation, whereas andalusite-staurolite-garnet schist generally occurs from the sillimanite isograd upward for about 1 km into the Mount Norna Quartzite. Biotite, muscovite, and chlorite are diagnostic minerals for the upper Mount Norna Quartzite and the Toole Creek Volcanics. In the Middle Creek Anticline area (Fig. 1), the isograd pattern is more complex, as sillimanite occurs both in the core and in isolated occurrences away from the core (S. Walters, personal communication, 1987). Isograds have not been accurately mapped here because of the poor exposure.

In detail, however, the sillimanite isograd lies just west of the axial plane of the Snake Creek Anticline, but mimics the D^S_1 fold nappe (Fig. 1; see Loosveld, 1991). Small deviations from perfect parallelism with D^S_1 structures, like this 'shifted' sillimanite isograd may reflect the shape of the isotherms during, or just after, the formation of the fold nappe during the sillimanite blastesis, when the isotherms had not yet completely readjusted to horizontal planes. In other words, the folded sillimanite 'isotherm' had sunk below the now exposed axial zone of the D^S_1 Snake Creek fold nappe, but had not yet equilibrated into a horizontal plane (Loosveld's fig. 8, 1989a) at the onset of D^S_2. Generally, however, isotherms with shapes reflecting D_x structures, but whose minerals have grown synchronously with (early-)D_{x+1}, indicate a very brief time-interval between D_x and D_{x+1}, as relaxation of 1-10 km-scale thermal structures is rapid (Carslaw & Jaeger, 1959). Indeed, the semi-analogous saw-tooth thermal perturbations of thrust nappes with a periodicity of L_t (thickness of the thrust) decay with a time constant of $L_t^2/\pi^2 k$ (k is thermal diffusivity), so if for example $L_t = 5$ km and $k = 10^{-6}$ m^2/s, the time constant is only about 80,000 years (Carslaw & Jaeger, 1959). The time-gap

between D^S_1 and D^S_2, then, must have been very narrow, and in fact, for all reasonable strain rates and strains, D^S_1 and D^S_2 would have been indistinguishable, i.e. would have been part of one progressive deformation event rather then of two discrete pulses of deformation. This interpretation is at odds with the interpreted 66 ± 25 Ma time-gap between D_1 and D_2 in the Sybella Granite area to the west (Page & Bell, 1986).

Alternatively, as the curved sillimanite isograd implies, growth of the sillimanite during or before the 'curving', and because the sillimanite porphyroblasts are syn-D^S_2, the sillimanite isograd in the Snake Creek Anticline area could reflect an as yet unrecognised large D^S_2 structure. The anomalously weak development of S_2 (crenulations) in the Snake Creek Anticline area may indicate reactivation during D^S_2 of a preferentially orientated S_1 (S_1 in D^S_2 compressional regime). Thus, the D^S_2 anticline would have steepened and flattened the D^S_1 structure.

Structural correlation

The structural trends of the central Soldiers Cap Belt are more diverse than in many other parts of the Mount Isa Inlier. This is due mainly to the fact that D^S_1 is more strongly developed than elsewhere, and a greater variety of pre-D^S_2 orientations existed. The early deformational history (D^S_1 and D^S_2) shows similarities with other parts of the inlier. D^S_1 thrusts have now been documented in the West Leichhardt Klippe (Loosveld & Schreurs, 1987; Blake, this volume) and the Tommy Creek Block (Hill, this volume), and proposed for the thrust complex north of Mount Isa (Bell, 1983), . A west/northwest movement vector was also deduced for the Deighton Klippe (Loosveld & Schreurs, 1987). The second deformational event is not as dominant in the central Soldiers Cap Belt as it is in most other parts of the inlier. As elsewhere, though, it is characterised by north-trending non-cylindrical folds, steep to vertical extension lineations, and well-developed axial-plane foliations.

Conclusion

The Snake Creek Anticline results from D^S_2 refolding, steepening, and flattening of an approximately northwest-verging D^S_1 fold nappe. The geometrical effect of D^S_2 in the Snake Creek Anticline area is not yet fully understood. D^S_1 axial planes can be traced from the Snake Creek Anticline into the axial planes of the Toole Creek Syncline fold system. The Weatherly Creek Syncline and the Middle and Pumpkin Gully Anticlines are all D^S_2 structures. D^S_2 was accompanied by low-pressure metamorphism.

Acknowledgements

During this study (1986-1988), I was in receipt of an Australian National University Ph.D. Scholarship. Additional financial and logistic support was given by the Bureau of Mineral Resources (BMR) and the Broken Hill Proprietary Co. Ltd, Brisbane. I thank Dave Blake, Alastair Stewart, Mike Etheridge, Bob Skrzeczynski, Steve Walters, and Ineke de Bruyn for discussions and reviews, and all members of the BMR Mount Isa field parties of 1984-1987 for their cooperation. Ms Diana Pillinger (BMR) drafted the map and cross-sections. Drs R. Blewett, A. J. Stewart, and P. Stuart-Smith reviewed a previous version of this manuscript.

References

BEARDSMORE, T.J., NEWBERY, S.P., & LAING, W.P., 1988 - The Maronan Supergroup: an inferred early volcanosedimentary rift sequence in the Mount Isa Inlier, and its implications for ensialic rifting in the Middle Proterozoic of northwest Queensland. *Precambrian Research* 40/41, 487-507.

BELL, T.H., 1983 - Thrusting and duplex formation at Mount Isa, Queensland, Australia. *Nature* 304, 493-497.

BLAKE, D.H., 1986 - Middle Proterozoic evolution of the Mount Isa Inlier, north-western Queensland, Australia: a synthesis. *Transactions of the Geological Society of South Africa* 89, 253-262.

BLAKE, D.H., 1987 - Geology of the Mount Isa Inlier and environs, Queensland and Northern Territory. *Bureau of Mineral Resources, Australia, Bulletin* 225, 83 pp.

BLAKE, D.H., this volume - Stratigraphy, folding, and faulting within the Quilalar Fault System Mount Isa Inlier. *In:* STEWART, A.J., & BLAKE, D.H. (Editors), Detailed Studies of the Mount Isa Inlier. *Bureau of Mineral Resources, Australia, Bulletin* 243.

BLAKE, D.H., BULTITUDE, R.J., DONCHAK, P.J.T., WYBORN, L.A.I., & HONE, I.G., 1984 - Geology of the Duchess-Urandangi region, Mount Isa Inlier, Queensland. *Bureau of Mineral Resources, Australia, Bulletin* 219, 96 pp.

BLAKE, D.H., JAQUES, A.L., & DONCHAK, P.J.T., 1983 - Selwyn region, Queensland. *Bureau of Mineral Resources, Australia, 1:100 000 Geological Map Commentary,* 29 pp.

CARSLAW, H.S., & JAEGER, J.C., 1959 - Conduction of heat in solids (2nd edition). *Oxford, Clarendon Press* , 510 pp.

CARTER, E.K., BROOKS, J.H., & WALKER, K.R., 1961 - The Precambrian Mineral Belt of northwestern

Queensland. *Bureau of Mineral Resources, Australia, Bulletin* 51, 344 pp.

DERRICK, G.M., WILSON, I.H., & HILL, R.M., 1976 - Revision of the stratigraphic nomenclature in the Precambrian of northwestern Queensland. V: Soldiers Cap Group. *Queensland Government Mining Journal* 77, 601-604.

DONCHAK, P.J.T., BLAKE, D.H., JAQUES, A.L., & NOON, T.A., 1983 - Kuridala region, Queensland. *Bureau of Mineral Resources, Australia, 1:100 000 Geological Map Commentary*, 32 pp.

ELLIS, D.J., & WYBORN, L.A.I., 1984 - Petrology and geochemistry of Proterozoic dolerites from the Mount Isa Inlier. *BMR Journal of Australian Geology and Geophysics* 9, 19-32.

ETHERIDGE, M.A., RUTLAND, R.W.R., & WYBORN, L.A.I., 1987 - Orogenesis and tectonic process in the Early to Middle Proterozoic of northern Australia. *American Geophysical Union, Geodynamics Series* 17, 131-147.

GLIKSON, A.Y., 1972 - Structural setting and origin of Proterozoic calc-silicate megabreccias, Cloncurry region, northwestern Queensland. *Journal of the Geological Society of Australia* 19, 53-63.

GLIKSON, A.Y., & DERRICK, G.M., 1970 - The Proterozoic metamorphic rocks of the Cloncurry 1:100 000 Sheet area (Soldiers Cap Belt), northwestern Queensland. *Bureau of Mineral Resources, Australia, Record* 1970/24, 108 pp.

HELGESON, H.C., DELANY, J.M., NESBITT, H.W., & BIRD, D.K., 1978 - Summary and critique of the thermo-dynamic properties of the rock-forming minerals. *American Journal of Science* 271, 97-131.

HILL, E.J., LOOSVELD, R.J.H., & PAGE, R.W., this volume - Structure and geochronology of the Tommy Creek Block, Mount Isa Inlier, Australia. *In:* STEWART, A.J., & BLAKE, D.H. (Editors), Detailed Studies of the Mount Isa Inlier. *Bureau of Mineral Resources, Australia, Bulletin* 243.

HOLDAWAY, M.J., 1971 - Stability of andalusite and the aluminum silicate phase diagram. *American Journal of Science* 271, 97-131.

HONMAN, C.S., CLAPPISON, R.J.S., RAYNER, E.O., & BOOTH, A.C., 1939 - The Soldiers Cap area, Cloncurry district. *Aerial Geological and Geophysical Survey of Northern Australia, Queensland Report* 18, 39 pp.

HOSCHEK, G., 1969 - The stability of staurolite and chloritoid and their significance in metamorphism of pelitic rocks. *Contributions to Mineralogy and Petrology* 22, 208-232.

JAQUES, A.L., BLAKE, D.H., & DONCHAK, P.J.T., 1982 - Regional metamorphism in the Selwyn area, northwest Queensland. *BMR Journal of Australian Geology and Geophysics* 7, 181-196.

LAING, W.P., & BEARDSMORE, T.J., 1986 - Stratigraphic rationalisation of the eastern Mount Isa block, recognition of key correlations with Georgetown and Broken Hill blocks in an eastern Australian Proterozoic terrain, and their metallogenic implications. *Eighth Australian Geological Convention, Geological Society of Australia, Adelaide, Abstracts* 15, 163-164.

LOOSVELD, R.J.H., 1988 - Structure and tectono-thermal history of the eastern Mount Isa Inlier, Australia. Ph.D. thesis, Australian National University, 216 pp. (unpublished).

LOOSVELD, R.J.H., 1989a - The synchronism of crustal thickening and high T/low P metamorphism in the Mount Isa Inlier, Australia. Part I: an example, the central Soldiers Cap belt. *Tectonophysics* 158, 173-190.

LOOSVELD, R.J.H., 1989b - The synchronism of crustal thickening and low P facies metamorphism in the Mount Isa Inlier, Australia. Part II: fast convective thinning of the mantle lithosphere during crustal thickening. *Tectonophysics* 165, 191-218.

LOOSVELD, R.J.H., 1989c - The ensialic tectonic evolution of the central eastern Mount Isa Inlier, NW Queensland, Australia. *Precambrian Research* 44, 243-276.

LOOSVELD, R.J.H., 1991 - Structural Geology of the Central Soldiers Cap Group (1:100 000 scale map). *Bureau of Mineral Resources, Canberra, Australia.* Available as a colour electrostatic plot on paper (AUD30), or in digital form on optical disc or Exabyte 8 mm tape (prices on application) both of which can be displayed on Intergraph Microstation software on computers that will run Unix. The digital data comprise a scanned raster image (.RLE format) of the black and white geological map, and an Intergraph vector design file containing the boundaries of coloured polygons. The coloured map and data are available from the Publication Sales Centre, Bureau of Mineral Resources, and an uncoloured Ozalar film or paper copy (AUD20) of the map is available from BMR Copy Service, both at GPO Box 378, Canberra, ACT, 2601, Australia. All orders to be prepaid to Collector of Public Monies.

LOOSVELD, R.J.H., & ETHERIDGE, M.A., 1990 - A model for low-pressure facies metamorphism during crustal thickening. *Journal of Metamorphic Geology* 8, 257-267.

LOOSVELD, R.J.H., & SCHREURS, G.M.M.F., 1987 - Discovery of thrust klippen, northwest of Mary Kathleen, Mount Isa Inlier, Australia. *Australian Journal of Earth Sciences* 34, 387-402.

MERRILL, R.B., ROBERTSON, J.K., & WYLLIE, P.J.,

1970 - Melting reactions in the systems $NaAlSi_3O_8$-SiO_2-H_2O to 20 kilobars compared with results for other feldspar-quartz-H_2O and rock-H_2O systems. *Journal of Geology* 78, 558-569.

NISBET, B.W., DEVLIN, S.P., & JOYCE, P.J., 1983 - Geology and suggested genesis of cobalt-tungsten mineralisation at Mount Cobalt, northwestern Queensland. *Proceedings of the Australasian Institute of Mining and Metallurgy* 287, 9-17.

PAGE, R.W., 1978 - Response of U-Pb zircon and Rb-Sr total-rock mineral systems to low-grade regional metamorphism in Proterozoic igneous rocks, Mount Isa, Australia. *Journal of the Geological Society of Australia* 25, 141-164.

PAGE, R.W., 1983 - Timing of superposed volcanism in the Proterozoic Mount Isa Inlier, Australia. *Precambrian Research* 21, 223-245.

PAGE, R.W., & BELL, T.H., 1986 - Isotopic and structural responses of granite to successive deformation and metamorphism. *Journal of Geology* 94, 365-379.

RAMSAY, J.G., 1967 - Folding and fracturing of rocks. *McGraw-Hill, New-York,* 568 pp.

REINHARDT, J., this volume - The Corella Formation of the Rosebud Syncline (central Mount Isa Inlier): deposition, deformation, and metamorphism. *In* STEWART, A.J., & BLAKE, D.H. (editors). Detailed Studies of the Mount Isa Inlier. *Bureau of Mineral Resources, Australia, Bulletin* 243.

RICHARDSON, S.W., 1968 - Staurolite stability in a part of the system Fe-Al-Si-O-H. *Journal of Petrology* 9, 467-488.

RYBURN, R., WILSON, I.H., GRIMES, K.G., & HILL, R.M., 1988 - Cloncurry, Queensland. *Bureau of Mineral Resources, Australia, 1:100 000 Geological Map Commentary,* 30 pp.

TUNKS, A., 1987 - Breccias and metasomatism of the Corella Formation, Cloncurry area, Queensland. B.Sc. (Hons.) thesis, Monash University, Melbourne, 127 pp. (unpublished).

WILSON, I.H., 1978 - Volcanism on a Proterozoic continental margin in northwestern Queensland. *Precambrian Research* 7, 205-235.

WYBORN, L.A.I., & BLAKE, D.H., 1982 - Reassessment of the tectonic setting of the Mount Isa Inlier in the light of new field, petrographic, and geochemical data. *Abstract, 11th BMR Symposium, Canberra, 4-5 May, 1982.* Reprinted in *BMR Journal of Australian Geology and Geophysics* 7, 143.

WYBORN, L.A.I., PAGE, R.W., & MCCULLOCH, M.T., 1988 - Petrology, geochronology, and isotope geochemistry of the post-1820 Ma granites of the Mount Isa Inlier: mechanisms for the generation of Proterozoic anorogenic granites. *Precambrian Research* 40/41, 509-541.

Appendix: notes concerning map and cross-sections (Loosveld, 1991)

Map: Structural geology of the central Soldiers Cap Group

The map is a revised version of Loosveld's (1988) unpublished thesis map. D_{c1}, D_{c2} and D_{c3} on the map correspond with, respectively, D^S_1, D^S_2 and D^S_3 in the text (Loosveld, 1988, used D_{e1}, D_{e2}, and D_{e3} for the three extensional events that affected the Mount Isa Inlier before D_{c1}). As the Mary Kathleen Group (Pkc) and the Gilded Rose Breccia (P_{br}) are commonly closely spatially related, and the latter is probably derived from the former, the distinction between the two is generally not made on the map and on the cross-sections. Exposures of Gilded Rose Breccia, however, normally have capricious boundaries, and unconformably overlie other volcano-sedimentary units, major granitoids, and D^S_3 faults. See Cloncurry 1:100 000 Geological Map (BMR, 1988) for precise localities of the Gilded Rose Breccia.

Notes on map profiles (Loosveld, 1991)

The extreme non-cylindricity of folds in the area inhibits construction of profiles (sections perpendicular to fold axes). As structures are generally steep in the Snake Creek area, the map here almost coincides with the profile. The three cross-sections on the map (Loosveld, 1991) are all vertical, except for ABC which dips 45° towards 200°. Information was projected on to the section parallel to the locally dominant fold-axis. Kinks in the profile have been avoided as these lead to compatibility problems at depth.

SECTION ABCD was chosen in a east-southeast/ west-northwest direction, as this is perpendicular to the overall trend of the southern central Soldiers Cap Belt, and because this direction is probably close to the D^S_1 movement direction.

SECTION ABC: To avoid parallelism with the axis of the northern part of the Snake Creek Anticline, the section was constructed on a moderately south-southwest-dipping plane (200°/45°): this has the advantage that the Snake Creek Anticline does not project as a synform.

SECTION CD: As L^1_0 is vertical and lies in the section plane, the D^S_1 fold vergence is not clear in the section, and may give steep S- as well as steep Z-vergences.

SECTION BF: The influence of D^S_2 on the geometry is not clear in this section, because the axial surface of the D^S_2 overprinting fold in the Oonoomurra Syncline area is subparallel to the section.

SECTION CE: In this vertical section, the intersection of the Snake Creek Anticline is synformal, in contrast to the antiform in section ABC.

TABLE 1. MINERAL ASSEMBLAGES OF THE CENTRAL SOLDIERS CAP BELT:

ab, albite; act, actinolite; and, andalusite; anth, anthophyllite; bi, biotite; cc, calcite; chl, chlorite; cpx, clinopyroxene; epi, epidote; fs, feldspar; ga, garnet; hbl, hornblende; ilm, ilmenite; mu, muscovite; pl, plagioclase (An, anorthite-percentage); qtz, quartz; sill, sillimanite; st, staurolite.

Pelitic	Psammitic	Mafic
qtz + bi + mu + si + ga	qtz + fs + ga ± mu	pl (An 25-55) + hbl ± cpx ± ga ± ilm
qtz + bi + mu + ga ± fs	qtz + fs ± bi mu	pl + hbl + epi + ilm + qtz ± act
qtz + bi + mu + st + ga	qtz + mu + bi ga fs	qtz + ab + epi + chl ± hbl
qtz + bi + mu ± fs	qtz + mu + bi ± fs ± anth ± cc	
qtz + bi + mu + st ± and	qtz + fs + mu + chl	
qtz + bi + mu + ga + and		
qtz + bi + mu + and + fs		
qtz + bi + mu ± fs		
qtz + mu + chl		

Page 360 is blank.

The BMR 1983 – 1990 Mount Isa Project: results, some remaining problems, and bibliography

D. H. Blake [1] *& A. J. Stewart* [1]

This paper is accompanied by the following map:

Blake, D.H., & Stewart, A.J., 1992 - Geology of the Mount Isa - Cloncurry Transect (1:250 000 scale map). Bureau of Mineral Resources, Canberra.

Significant results of the BMR 1983-1990 Mount Isa Project, together with some of the important problems yet to be solved, are summarised in this contribution according to: stratigraphy and sedimentology; igneous intrusions; structure and metamorphism; alteration, metasomatism, and metallogenesis; geophysics; the Lawn Hill circular structure; and databases. An accompanying bibliography lists maps, databases, refereed papers, and other articles resulting from the project. The results of detailed mapping by geologists involved with the project in the Mount Isa, Mary Kathleen, Marraba, and Cloncurry 1:100 000 Sheet areas are shown in generalised form on the 1:250 000 scale geological map accompanying this volume.

[1] Bureau of Mineral Resources, GPO Box 378, Canberra, ACT, 2601, Australia.

Stratigraphy and sedimentology

The early and middle Proterozoic sedimentary and volcanic rocks of the Mount Isa Inlier are assigned to four major sequences (Blake, 1987): basement, which was folded and regionally metamorphosed during the Barramundi Orogeny of Etheridge & others (1987) around 1870 Ma ago (Page, 1988), and overlying cover sequences 1, 2, and 3, which predate the 1620-1520 Ma Isan Orogeny of Blake & others (1990).

Basement (pre-1870 Ma)

Turbiditic protoliths of the basement Yaringa Metamorphics west of Mount Isa were deposited between 2200 Ma, the age of detrital zircon, and 1890 ± 8 Ma, the age of metamorphic zircon formed during the Barramundi Orogeny (Page & Williams, 1988).

A likely correlative of the Yaringa Metamorphics, the Kurbayia Migmatite, crops out on the east side of the Leichhardt River Fault Trough (LRFT) and in the Kalkadoon-Leichhardt Belt to the east (Blake, 1987 and in press a; Blake & Page, 1988). The protoliths were metamorphosed to migmatite, probably during the Barramundi Orogeny, before being intruded at around 1860 Ma by Kalkadoon Granite (Blake & Page, 1988).

Cover sequence 1 (1870-1850 Ma)

Cover sequence 1 consists mainly of Leichhardt Volcanics, dated at 1870-1850 Ma (e.g., Page, 1988), but is also taken to include a newly recognised unit of metasediments and minor possible volcanics, named the Orient beds, which is confined to the Orient Block in the western part of the Kalkadoon-Leichhardt Belt (Blake, this volume a).

An unsolved problem is the age of the Orient beds relative to the Leichhardt Volcanics and also to the possibly correlative Candover Metamorphics.

Cover sequence 2 (1790-1720? Ma)

Structural evidence (Connors & others, this volume) supports the view that the May Downs Gneiss west of Mount Isa correlates with the lower Mount Guide Quartzite of the Haslingden Group (e.g., Hill & others, 1975), rather than with the basement Yaringa Metamorphics (e.g., Blake, 1987).

Sedimentological studies of cover sequence 2 in the LRFT and Kalkadoon-Leichhardt Belt suggest a two-stage model of rift/sag basin formation, with an upper crustal extension factor of at least 2 (Eriksson & others, 1992a, b). The first stage, confined to the LRFT, consists of rift-type bimodal volcanics and coarse clastics of the Bottletree Formation and lower Mount Guide Quartzite overlain by sag (thermal relaxation) phase quartz sandstone of the upper Mount Guide Quartzite; the quartz sandstone represents possibly 20 Ma of tidal sedimentation (Eriksson & Simpson, 1990; Simpson & Eriksson, 1991). The second stage extends eastwards across the Kalkadoon-Leichhardt Belt to the Pilgrim Fault; rift-fill volcanics and clastic sediments are represented by the Eastern Creek

Volcanics and Myally Subgroup in the west and probably by Magna Lynn Metabasalt and Argylla Formation to the east; and the sag phase consists of Quilalar Formation and correlative Ballara Quartzite and Corella Formation. The Quilalar Formation and correlatives were deposited in a basin at least 100 km wide centred within the Kalkadoon-Leichhardt Belt (Jackson & others, 1990), where they lie unconformably on Kurbayia Migmatite (e.g., in the Wonga Belt – Blake, in press a) and Kalkadoon Granite (e.g., at Black Mountain - Williams & Blake, this volume), as well as conformably on second-stage rift-phase Myally Subgroup.

Horsts and graben (flower structures) resulting from transpressional faulting were formed during deposition of the Myally Subgroup in the LRFT north of Mount Isa (Nijman & others, this volume a and b); the Myally sediments here were derived from the west and deposited as deltas.

The Quilalar Formation includes the sedimentary rocks previously mapped as Surprise Creek beds in the western part of the Kalkadoon-Leichhardt Belt – in the West Leichhardt Klippe (Blake, this volume a) and at Black Mountain (Williams & Blake, this volume).

The upper part of the Argylla Formation near Ballara, in the Kalkadoon-Leichhardt Belt, has been distinguished as the Mount Frosty Member (Stewart, this volume b). Consisting mainly of feldspathic sandstone, but also including felsic volcanics and calcareous sediments, it passes conformably up into Ballara Quartzite and Corella Formation. This lends support to the view of Blake (1987) that the Argylla Formation is probably an eastern stratigraphic correlative of the Myally Subgroup underlying the Quilalar Formation (a correlative of the Ballara Quartzite), rather than of the Bottletree Formation underlying the Haslingden Group, as favoured by Derrick (1991).

Outcrops of Mount Albert Group units – Deighton Quartzite and White Blow Formation – in the central part of the Kalkadoon-Leichhardt Belt have been interpreted by Loosveld & Schreurs (1987) as thrust klippen formed of Ballara Quartzite and Corella Formation correlatives transported tectonically from the east. However, this interpretation has been challenged by Stewart (1989, and this volume b), who has found that in places the Deighton Quartzite passes conformably down into, and hence overlies and is younger than, the Corella Formation. In either case, both units of the Mount Albert Group clearly belong to cover sequence 2 rather than cover sequence 3, as tentatively suggested by Blake (1987).

In the Kalkadoon-Leichhardt Belt, along the east side of the Wonga Belt, rocks underlying Ballara Quartzite and previously mapped as Argylla Formation are assigned to the basement Kurbayia Migmatite by Blake (in press a).

The sequence of impure metacarbonates, meta-evaporites, and brecciated equivalents in the Cloncurry 1:100 000 Sheet area of the Eastern Fold Belt has been mapped as Corella beds, rather than Corella Formation, by Ryburn & others (1988), because of uncertainty in correlation with the Corella Formation mapped west of the Pilgrim Fault.

Major stratigraphic problems yet to be resolved include the following:

- The correlation of cover sequence 2 units across the Pilgrim Fault Zone, from the Eastern Fold Belt to the Kalkadoon- Leichhardt Belt and Western Fold Belt.
- The age of the Soldiers Cap Group in the Eastern Fold Belt: does this group correlate with units of cover sequence 2 to the west, as suggested, for example, by Blake (1987), or with cover sequence 1 (see Beardsmore & others, 1988, discussion in Loosveld, 1989a), or even with the Tommy Creek beds of cover sequence 3 (e.g., Derrick, 1991)?
- The relationship of the Overhang Jaspilite in the Eastern Fold Belt to the Marimo Slate and other 'overlying' units.
- Whether or not the Argylla Formation in the Eastern Fold Belt is the same age as that in the Kalkadoon-Leichhardt belt;
- The age of felsic volcanics in the Corella Formation of the Mary Kathleen Zone;
- The age of the Mount Albert Group formations in the Dugald River area, west of Quamby; do they belong to cover sequence 2, like other formations of the group, or to cover sequence 3 (compare Blake, 1987)?

Cover sequence 3 (1680-1625 Ma)

Felsic porphyry previously mapped as part of the Yaringa Metamorphics west of Mount Isa, at grid reference Mount Isa 115035, belongs to the Carters Bore Rhyolite (Rickard, 1987, 1990). Here a basal conglomerate containing basement and granite clasts passes up into the felsic porphyry, a possible composite extrusion (it is

characterised by abundant small mafic inclusions) dated at 1680 Ma (R.W.Page, BMR, unpublished data).

In the LRFT north of Mount Isa, the Surprise Creek Formation is, at least in part, the stratigraphic correlative of the Warrina Park Quartzite and Moondarra Siltstone of the Mount Isa Group. A newly named unit here, the Hero Formation, which correlates with part of the Warrina Park Quartzite, was deposited as a fan delta along a sinistral strike-slip proto-Hero Fault (Nijman & others, this volume b). Faulting accompanying deposition of both cover sequence 3 and the underlying Myally Subgroup of cover sequence 2 in this area is attributed to overall north-south tension.

The fault-bounded Tommy Creek Block, on the west side of the Eastern Fold Belt, consists of a newly named unit, the Tommy Creek beds (Hill & others, this volume), which contains felsic metavolcanics dated at 1624 ± 4 Ma, indicating that this unit postdates the Mount Isa Group. The Tommy Creek beds also contain metasediments, including carbonates and evaporites, and metabasalt, and were previously mapped as Tommy Creek Microgranite and Corella Formation.

Questions yet to be resolved include:

- The depositional age of the McNamara Group west of Mount Isa, and of the correlative Mount Isa Group to the east, relative to the emplacement of the 1670 Ma-old Sybella Batholith; and
- The age of the Fiery Creek Volcanics.

Post – cover sequence 3

Much of the calc-silicate breccia in the Eastern Fold Belt was deformed during the Isan Orogeny, but some post-dates the main folding and metamorphism of this orogeny. This younger breccia, named the Gilded Rose Breccia by Ryburn & others (1988), is related to granite emplacement (Wyborn & others, 1988).

The age and tectonic significance of the unmetamorphosed Quamby Conglomerate have yet to be determined.

Igneous intrusions

According to geochemical and geochronological studies by Wyborn (1988) and Wyborn & others (1987, 1988) the granitic rocks of the Mount Isa Inlier are mainly I-types, derived from Proterozoic rather than Archaean precursors. They have higher K_2O, Rb, Zr, La, Ce, Th, and U contents and lower MgO and CaO contents than typical Archaean and Phanerozoic I-type granites. Relatively rare S-types also appear to have Proterozoic sources, and could be derived from feldspathic metasediments. Granite emplacement took place at around 1860-1840 Ma (Kalkadoon and Ewen Batholiths), 1820 Ma (Yeldham Granite), 1800 (Big Toby Granite), 1740-1720 Ma (Wonga Batholith; also 1760-1730 Ma - Pearson & others, this volume), 1700 Ma (Weberra Granite), 1670 Ma (Sybella Batholith), and 1550-1480 Ma (Williams and Naraku Batholiths). The I-type granites and related felsic volcanics may be derived from mantle-derived material accreted to the base of the crust during crustal extension.

Many of the granite intrusions that predate the Isan Orogeny were probably emplaced as sills or sheet-like bodies e.g., Big Toby Granite intruding Yaringa Metamorphics (Rickard, 1987, 1990); Wonga Granite and Burstall Granite of the Wonga Batholith intruding cover sequence 2 (Holcombe & others, this volume; Pearson & others, this volume); and Sybella Granite intruding cover sequence 2 (Connors & others, this volume).

At least twelve separate ages of mafic intrusions can be inferred for the Mount Isa Inlier (Blake, 1987), ranging from older than 1870 (pre-Barramundi Orogeny) to about 1120 Ma (post-Isan Orogeny).

Additional geochronology on granitic rocks is needed to answer questions such as:

- The ranges in age of the Kalkadoon, Williams, and Naraku Batholiths;
- The age of the Maramungee Granite and other foliated and recrystallised granites which intrude the Soldiers Cap Group and are associated spatially with banded iron formation-type base metal deposits in the Eastern Fold Belt.

Structure and metamorphism

Barramundi Orogeny, ~1880 Ma

The Yaringa Metamorphics west of Mount Isa were tightly to isoclinally folded and regionally metamorphosed to upper amphibolite facies during this orogeny (e.g., Rickard, 1987, 1990; Wyborn & others, 1988).

The deformation and metamorphism causing partial melting in the Kurbayia Migmatite to the east is probably of similar age (Blake & Page, 1988); the migmatitic foliation in this unit trends roughly north-south and is subvertical, like the main foliation developed during the much younger Isan Orogeny (Blake, in press b).

Extensional deformation before 1620 Ma

Extensional faulting accompanied deposition of cover sequences 2 and 3 in the LRFT of the Western Fold Belt north of Mount Isa (Nijman & others, this volume a and b).

Several examples of extensional deformation affecting cover sequence 2, but predating the Isan Orogeny, have been reported in the Kalkadoon-Leichhardt Belt: in the Wonga Belt north of the Fountain Range Fault (Holcombe & others, 1991 and this volume; Oliver & others, 1991; Pearson & others, this volume); to the south in the 'Shinfield Zone', Alligator Syncline, and Mary Kathleen Fold Belt (Passchier, 1986a, 1986b, 1991, and this volume; Passchier & Williams, 1989); and in the area of Mount Albert Group outcrops west of the Wonga Belt (Stewart, 1989, and this volume b).

How much, if any, of the described extension is related to basin formation and cover sequence 3 deposition has yet to be determined.

The highly deformed Wonga Belt is considered by Holcombe and coworkers (Holcombe & others, 1991 and this volume; Oliver & others, 1991; Pearson & others, this volume) to represent a zone where major north-south extension took place between 1760 and 1720 Ma, during emplacement of granite (Wonga Batholith); an upper plate, characterised by brittle deformation, moved north relative to a lower plate along an originally subhorizontal detachment zone of very high strain, and later tight folding during the Isan Orogeny resulted in originally flat-lying structures becoming subvertical. This interpretation is questioned by Blake (in press b) because it does not take into account the abrupt change in stratigraphy across, rather than along, the Wonga Belt, or the problem of distinguishing extensional features from both earlier and later (Barramundi and Isan) compressional structures.

Passchier (1986a, 1991, this volume; Passchier & Williams, 1989) have recognised pre-Isan extensional structures affecting cover sequence 2 south of the area studied by Holcombe and co-workers. The extensional deformation is overprinted and largely obscured by subsequent intense ductile compressional deformation (Isan Orogeny) in the Shinfield Zone (= southerly continuation of the Wonga Belt), but is well displayed in the Alligator Syncline to the west, where brittle fractures are occupied by mafic intrusions, and in the Mary Kathleen Fold Belt to the east, where extension was accompanied by granite emplacement.

Partly fault-bounded outcrops of Mount Albert Group west of the Wonga Belt are interpreted by Stewart (1989) as resulting from southwesterly-directed extension along low-angle normal faults that predate the main deformation of the Isan Orogeny.

Brittle extensional structures of probably similar age have been described from the western limb of the Bulonga Anticline, on the west side of the Eastern Fold Belt (Williams, 1989; Passchier & Williams, 1989). Extension is also evident farther east, on the east limb of the Duck Creek Anticline, where a swarm of east-trending mafic dykes cuts Mitakoodi Quartzite (Loosveld, 1989a); these dykes appear to postdate tight folding, and hence may be related to local extension during the Isan Orogeny.

Isan Orogeny, 1620-1550 Ma

The dominant deformation and metamorphism in all the areas mapped are attributed to the Isan Orogeny. Rickard (1987, 1990) has suggested that west of Mount Isa there may have been a precursor to this orogeny during deposition of cover sequence 3, i.e., an additional deformation between 1680 Ma - the age of the Carters Bore Rhyolite - and 1670 Ma, when the overlying McNamara Group was deposited. This seems unlikely, however, as no evidence of an intervening deformation has been found at exposed contacts between the two units, and there are no indications of a deformation at this time elsewhere in the Mount Isa Inlier.

The Isan Orogeny consisted of two main phases, which correspond to D_1 and D_2 of Bell (1983; 1991). D_1, related to north-south compression, is not evident in all of the areas recently mapped. D_2, which is generally the dominant phase, involved east-west compression and regional metamorphism up to upper amphibolite facies, and resulted in the north-south structural grain characteristic of most of the Mount Isa Inlier.

Examples of D_1 include north-south thrusting in the West Leichhardt Klippe and Rifle Creek Block (Blake, this volume a), in the Ballara-Mount Frosty area (Stewart, this volume), and possibly southeast of Lake Moondarra (Bain & others, this volume b); an east-west trending fold at Black Mountain (Williams & Blake, this volume); and fold nappes in the Eastern Fold Belt – in the Soldiers Cap area (Loosveld, 1989a and this volume), the Tommy Creek Block (Hill & others, this volume), and the Marimo area (Loosveld, 1989a).

The existence of a major D_1 thrust duplex involving north-south shortening exceeding 200 km in the LRFT north of Mount Isa, as postulated by Bell (1983, 1991), has not been confirmed. However, the hypothesis, although

disputed by Lister (1990) and Stewart (this volume a 1992), cannot be completely disproved on currently available evidence. A major problem with the hypothesis is that faults considered by Bell to be essential parts of the duplex appear to be younger than the D_2 event of the Isan Orogeny.

Typical D_2 folds are upright and open to tight, with trends between north-northeast and north-northwest, and have a pronounced axial planar cleavage (see papers in this volume).

Irregularities in the pattern of D_2 folds west of the Sybella Batholith may be due to reactivation of structures in the basement and deposition of cover sequences 2 and 3 on an uneven surface (Prihardjo, 1987), and also to the presence of large pre-deformation granite bodies.

Detailed studies in the Mount Novit area by Connors & others (this volume) have revealed a complex succession of fold and cleavage generations, ductile faults, and shear zones affecting cover sequences 2 and 3 and Sybella Granite. Overall, the deformation reflects east-west to northeast-southwest shortening with west-over-east movement, suggesting a general correlation with the regional D_2 phase of the Isan Orogeny. In contrast to Page & Bell (1986), who dated the D_1 deformation phase from this area, no evidence of an earlier north-south thrusting event, equivalent to Bell's D_1, has been found in this area by Connors & others.

Thus, the time of D1 deformation in the Mount Isa Inlier is yet to be determined.

East-over-west thrusting near Lake Mary Kathleen, in the Kalkadoon-Leichhardt Belt, is attributed to the D_2 phase by Blake (this volume b).

D_2 folds in the Eastern Fold Belt include the north to northeast-trending Duck Creek Anticline, Wakeful Syncline, and Bulonga Anticline in the west, and smaller, tight to isoclinal northerly-trending folds in the Marimo area to the east (Loosveld, 1989a). The Snake Creek Anticline in the Soldiers Cap area farther east is interpreted by Loosveld (1989a and this volume) as a northwest-verging major D_1 fold nappe which was refolded and flattened during D_2, when the Weatherly Creek Syncline was formed. Loosveld suggests that in this area D_1 and D_2 are closely comparable in age – part of the same progressive deformational event.

The regional metamorphism accompaning D_2 was of low pressure/high temperature type characterised by an anti-clockwise P-T-t path, with a geothermal gradient in the range 40-50°C/km (Etheridge & others, 1984, 1987; Reinhardt & Rubenach, 1989; Loosveld, 1989b; Loosveld & Etheridge, 1990; Oliver & Wall, 1987; Oliver & others, 1991; Reinhardt, 1992; and papers in this volume).

In the Mary Kathleen Fold Belt near Mary Kathleen, regional amphibolite facies metamorphism during tight to isoclinal D_2 folding was accompanied by heterogeneous fluid/rock interaction in calc-silicate rocks of the Corella Formation and pretectonic mafic and felsic intrusions (Oliver & Wall, 1987; Oliver & others, 1991). Peak metamorphism ranged from 550 to 650°C at 300 to 400 MPa, and resulted in the development of scapolitised and albitised rocks, calcite vein systems, and localised fracturing and brecciation. Oliver & others (1991) suggest an intracratonic mantle plume model to explain the D_2 crustal shortening and preceding 1780-1720 Ma extension; the extension took place during mantle-plume ascent, and the shortening resulted from thermal decay as the plume subsided.

Faulting and related deformation post-dating the Isan Orogeny

Most of the major faults mapped in the Mount Isa Inlier cut, and therefore postdate, D_2 folds, although some of these faults may have been initiated before or during the Isan Orogeny. Fault displacements appear to be largely horizontal, probably exceeding ten kilometres in many cases, and the associated deformation is of mainly brittle, rather than ductile, type. Examples include the Mount Isa, Quilalar, and Pilgrim Faults.

The Mount Isa Fault is one of several closely spaced subparallel faults that make up the Mount Isa Fault Zone, considered by Blake & Stewart (this volume a and in BMR, 1988a) to represent one of the major block boundaries in the Mount Isa Inlier. In the Mount Novit area south of Mount Isa, the Mount Isa Fault is described by Connors & others (this volume) as steeply dipping and showing both ductile and brittle features, with the ductile features indicating west-over-east, rather than strike-slip, movement during the Isan Orogeny. A displacement of many kilometres is implied for this fault, because of problems in correlating stratigraphic units across the fault and the fact that the fault here coincides with a marked change in metamorphic grade. On regional grounds a large strike-slip component (involving brittle deformation at the present level of exposure?) is favoured for the Mount Isa Fault Zone as a whole, with movement continuing into the Palaeozoic (Blake, 1987).

The Quilalar Fault Zone, a group of anastomosing faults marking the boundary between the Western Fold Belt and the Kalkadoon-Leichhardt Belt to the east, is

considered to represent dextral strike-slip displacement exceeding 60 km (Blake, this volume a). Faulting may have commenced during deposition of cover sequence 2, as the fault zone corresponds closely to the eastern margin of the depositional LRFT during early Haslingden Group time, but most of the visible strike-slip displacement postdates D_2 structures of the Isan Orogeny. Offshoots from the zone include faults along the east sides of the Rifle Creek and Orient Blocks, and faults with associated pop-up structures near Lake Julius (Lister, in BMR, 1986a) and a pull-apart graben at Black Mountain (Williams & Blake, this volume).

The group of conjugate strike-slip faults and arcuate east-west faults cutting the Haslingden Group in the LRFT southeast of Lake Moondarra (Bain & others, this volume; Henderson & Bain, 1991) may also be related to movement along the Quilalar Fault Zone. The faults postdate D_2 folds and are cut off to the east by, or emanate from, the fault zone. Reactivation of some of the faults, mainly those striking north-south, resulted in the formation of late shatter zones with alteration haloes.

The Pilgrim Fault, separating the Eastern Fold Belt from the Kalkadoon-Leichhardt Belt, is marked by a zone of brecciated rocks, in places more than a kilometre wide, which postdates Isan folds. Probable splays include the southwest-striking Mount Remarkable and Fountain Range Faults, both of which in places have dextral displacements of more than 20 km, and numerous smaller subparallel faults (e.g., the Wonga Fault). Differences in stratigraphy, structure, and plutonism indicate displacement sufficient for the Pilgrim Fault to be regarded as a terrane boundary (Blake & Stewart, in BMR, 1988b).

The Cloncurry 'Overthrust' is a major fault postdating D_2 of the Isan Orogeny in the Eastern Fold Belt (Loosveld, 1989a and this volume). It dips moderately to steeply east, separating the Soldiers Cap Group of the Snake Creek Anticline area to the east from the Mary Kathleen Group to the west.

Another major fault of possibly similar age in the Eastern Fold Belt may be represented by a narrow band of breccia which separates the Overhang Jaspilite of the Duck Creek Anticline area to the west from units of the Marimo area to the east.

Alteration, metasomatism and metallogenesis

Four main types of alteration have been documented in the Eastern Creek Volcanics of the Western Fold Belt (Wyborn, 1987), each involving a different fluid. The earliest type, albite + actinolite alteration, predates the main Isan deformation event, and may be related to diagenesis of the Mount Isa Group and formation of the lead-zinc deposits at Mount Isa and Hilton mines. Epidote + sphene and calcite + magnetite alteration types are associated with the main regional metamorphism and the formation of some small uranium deposits. The youngest and most profound type, characterised by albite + chlorite + rutile, involved depletion of Cu, Fe_2O_3, Ni, MnO, and Ba and enrichment in MgO and SiO_2. This last type may be linked to the formation of the Mount Isa copper orebody towards the end of the Isan Orogeny.

A more detailed study of the Eastern Creek Volcanics southeast of Lake Moondarra by Bain & others (this volume) shows that uranium mineralisation here is related to calcite + chlorite alteration associated with shatter zones along reactivated faults cutting the D_2 foliation and epidote alteration. The late alteration may be attributed to downward infiltration of oxidised fluids rich in NaCl and/or CO2, like those involved in the main stage of copper mineralisation at Mount Isa mine (Heinrich & others, 1989).

Sulphur isotope systematics of the copper orebodies at Mount Isa mine (Andrew & others, 1989) indicate that most of the sulphur in the ore came from the host, highly pyritic Urquhart Shale of the Mount Isa Group, but some was introduced, together with copper, by hydrothermal brine. Important controls on the mineralisation are association with a major lithological contact and a metasedimentary host which is both dolomitic and pyritic (Heinrich & others, 1990).

'Red rock' alteration, characteristic of large parts of the Mount Isa Inlier, represents retrograde metamorphism post-dating D_2 near Mary Kathleen (Oliver & others, 1991), and possibly developed at 300-450°C around 1400 Ma ago. To the east, in the eastern Fold Belt, the red rock alteration is probably related to the emplacement of the Williams and Naraku Batholiths at around 1500 Ma (e.g., Wyborn & others, 1988; Laing, 1990).

There is no convincing evidence to show that any of the major mineral deposits in the Mount Isa Inlier are directly related to igneous processes, although igneous rocks may have been a source of metals in some mineral deposits related to deformation and metamorphism. The mafic igneous rocks are probable sources for Cu, Co, and Au deposits, and felsic igneous rocks, especially those younger than 1800 Ma, are locally associated with deposits of U and Be (Wyborn, 1990a).

No economically important mines are located in

granite. However, Wyborn (in BMR, 1992) has pointed out that some granites of the Williams and Naraku Batholiths are similar in many respects – such as isotopic age, chemical composition, oxidation state, and association with breccia – to granite hosting Au-Cu-U mineralisation at Roxby Downs, South Australia. Also, Solomon & Heinrich (1992) have suggested that the development of giant sedimentary-hosted lead-zinc deposits of Mount Isa type may be dependent on the presence of underlying fractionated high-heat-producing granite.

Geophysics

Most of the Mount Isa Inlier lies within the Mount Isa Geophysical Domain of Wellman (this volume). This domain extends for 200 km north and 250 km south of the exposed inlier, and is characterised by north-trending features. It is inferred from truncation relationships of both gravity and magnetic trends to be younger than crust to the east and west and older than crust to the north and south. Boundaries of geophysical zones within the domain are broadly consistent with the boundaries of the main tectonic units of Blake & Stewart (this volume a). The most westerly part of the Mount Isa Inlier is characterised by northwesterly-trending geophysical anomalies of the Arunta Block; these are truncated by, and hence predate, the Mount Isa Domain anomalies.

Magnetic anomalies indicate two main faulting sets in the Mount Isa Domain and surrounding crust (Wellman, this volume): northwest-striking normal faults in the north and northeast-striking dextral faults in the central part.

Lawn Hill circular structure

The Lawn Hill circular structure, 250 km north-northwest of Mount Isa, is a ring of low hills formed of Cambrian limestone which reflects a late Proterozoic impact structure (Stewart & Mitchell, 1987); shatter cones and other shock features are developed in cover sequence 3 rocks, but not in unconformably overlying Cambrian strata.

Databases

Mineral deposit data have been entered into MINLOC and MINDEP databases. Data for the main deposits (about 240) are also available as a separate Mount Isa mineral deposit EXCEL database (Raymond & Fortowski, in press 1992). BMR is currently (1992) preparing a metallogenic analysis and Geographic Information System of the Mount Isa Inlier in ARC/INFO format (Wyborn & Gallagher, in preparation), which will incorporate the following digital datasets: the 1:500 000 scale geological map of Blake (1987); geochemical data; regional geophysical data; metallogenic data (Raymond & Fortowski, in press); and Landsat TM imagery. Chemical analyses of about 2650 igneous and other rocks from the Mount Isa Inlier have been entered into the BMR ROCKCHEM database (Wyborn & Ryburn, 1991). These databases are available for purchase from BMR.

Summary

The Mount Isa Inlier is a region of Proterozoic sedimentation, igneous activity, deformation, metamorphism, and mineralisation typical of an intraplate ensialic setting. Sedimentation was predominatly of shallow-water type, and took place in response to crustal extension. Three main cycles of rift-sag deposition have been identified: the first two are represented by cover sequence 2 (1790-1720? Ma) and the third by cover sequence 3 (1680-1625 Ma). The rift phases were dominated by volcanics (felsic or mafic or both) and coarse clastics, and the sag phases by finer clastics and carbonates. Stretching of the crust was accompanied by periodic emplacement of granite bodies and mafic dyke swarms.

At around 1600 Ma, extension tectonics was succeeded by crustal shortening associated with the Isan Orogeny. The earliest Isan contractional structures are east-trending thrusts and folds, including some kilometre-scale nappes and thrust sheets in the east. A thrust nappe with more than 200 km of southward translation, postulated by Bell (1983, 1991) in the Leichhardt River Fault Trough of the Western Fold Belt, however, is not supported by detailed mapping by Stewart (this volume a and 1992) and Connors & others (this volume).

The main contractional phase of the Isan Orogeny, at around 1550 Ma, formed the prominent north-trending upright folds of the inlier, and was accompanied or followed shortly after by the peak of regional metamorphism, which shows the anticlockwise P-T-t path typical of ensialic settings.

After the Isan folding, major strike-slip faulting took place along north-south faults such as the Pilgrim, Quilalar, and possibly the Mount Isa Faults. Brittle deformation perhaps related to this faulting caused shattering of dolomitic siltstone in the Mount Isa Group (Urquhart Shale), allowing ingress of alkali-rich fluid derived from metamorphism of evaporites and containing

copper leached from mafic volcanics to form the copper orebodies at Mount Isa.

A final episode of felsic magmatism occurred at around 1500 Ma in the east of the inlier, shortly after the Isan Orogeny. Some of the resulting granites are similar to that spatially associated with the major Au-Cu-U deposit at Roxby Downs, South Australia.

Acknowledgements

We thank J.H.C.Bain, C.A.Heinrich, and L.A.I.Wyborn for reviewing this paper.

References not in following bibliography

BEARDSMORE, T.J., NEWBERRY, S.P., & LAING, W.P., 1988 - The Maronan Supergroup - an inferred early volcanosedimentary rift sequence in the Mount Isa Inlier, and its implications for ensialic rifting in the Middle Proterozoic of northwest Queensland. *Precambrian Research* 40/41, 487-507.

BELL, T.H., 1983 - Thrusting and duplex formation at Mount Isa, Queensland, Australia. *Nature* 304, 493-497.

BELL, T.H., 1991 - The role of thrusting in the structural development of the Mount Isa mine and its relevance to exploration in the surrounding region. *Economic Geology* 86, 1602-1625.

HEINRICH, C.A., ANDREW, A.S., WILKINS, R.W.T., & PATTERSON, D.J., 1989 - A fluid inclusion and stable isotope study of synmetamorphic copper ore formation at Mount Isa, Australia. *Economic Geology* 84, 529-550.

HILL, R.M., WILSON, I.H., & DERRICK, G.M., 1975 - Geology of the Mount Isa 1:100 000 Sheet area, northwest Queensland. *Bureau of Mineral Resources, Australia, Record* 1975/175, 112pp.

LAING, W.P., 1990 - The Cloncurry terrane: an allochthon of the Diamantina Orogen rafted on to the Mount Isa Orogen, with its own distinctive metallogenic signature. *Mount Isa Inlier Geology Conference, Monash University*, 19-22.

Bibliography for the BMR Mount Isa Project

Maps (Bureau of Mineral Resources, Australia)

BLAKE, D.H., 1987 - Geology of the Mount Isa Inlier and environs, Queensland and Northern Territory - 1:500 000 scale.

BLAKE, D.H., 1991a - Geology of Black Mountain, Duchess - 1:5000 scale.

BLAKE, D.H., 1991b - Geology of the Lake Mary Kathleen Zone - 1:50 000 scale.

BLAKE, D.H., 1991c - Geology of the Rifle Creek Region - 1:50 000 scale (two sheets).

BLAKE, D.H., 1991d - Geology of the West Leichhardt Klippe and the Gorge Creek sector of the Quilalar Fault Zone - 1:50 000 scale.

BLAKE, D.H., & STEWART, A.J., 1992 - Geology of the Mount Isa - Cloncurry transect - 1:250 000 scale.

BMR, 1988 - Cloncurry, Queensland - 1:100 000 Geological Series, Sheet 7056.

CONNORS, K.A., PROFFETT, J.M., LISTER, G.S., SCOTT, R.J., OLIVER, N.H.S., & YOUNG, D.J., 1991 - Geology of the Mount Novit area - 1:25 000 scale (two sheets).

HENDERSON, G.A.M., & BAIN, J.H.C., 1991 - Geology of the Haslingden Group, east Moondarra area - 1:35 000 scale.

HILL, E.J., 1991 - Geology of the Tommy Creek Block - 1:25 000 scale (two sheets).

HOLCOMBE, R.J., 1991 - Geology of the Mary Kathleen area - 1:25 000 scale map (two sheets).

LOOSVELD, R.J.H., 1991 - Structural geology of the central Soldiers Cap Group - 1:100 000 scale.

NIJMAN, W., 1991 - Geology of the Paroo Range-Hero/Western Fault Zone - 1:20 000 scale (2 sheets).

OLIVER, N.H.S, 1991 - Geology of the Mount Godkin area - 1:25 000 scale.

PASSCHIER, C.W., 1991 - Geology of the Myubee area - 1:25 000 scale.

PEARSON, P.J., 1991a - Geology of the East Limb, Little Beauty Syncline - 1:15 000 scale.

PEARSON, P.J., 1991b - Geology of the Breakfast Creek area - 1:25 000 scale.

REINHARDT, J., 1991 - Geology of the Rosebud Syncline - 1:25 000 scale.

STEWART, A.J., 1991 - Geology of the Ballara-Mount Frosty Region - 1:25 000 scale (two sheets)

BMR Bulletin

BLAKE, D.H.,1987 - Geology of the Mount Isa Inlier and environs, Queensland and Northern Territory. *Bureau of Mineral Resources, Australia, Bulletin* 225, 83pp.

BMR Map Commentary

RYBURN, R.J., WILSON, I.H., GRIMES, K.G., & HILL, R.M., 1988 - Cloncurry, Queensland. *Bureau of Mineral Resources, Australia, 1:100 000 Geological Map Commentary.*

BMR Data sets

RAYMOND, O., & FORTOWSKI, D., in press 1992 - Mount Isa Inlier mineral deposit database, with explanatory notes. *Bureau of Mineral Resources, Australia, Record and Database.*

WYBORN, L.A.I., & GALLAGHER, R., in preparation - Mount Isa Inlier Geographic Information System. *Bureau of Mineral Resources, Australia.*

WYBORN, L.A.I., & RYBURN, R.J., 1991 - Mount Isa ROCKCHEM data set documentation. *Bureau of Mineral Resources, Australia, Record* 1991/37, 35pp.

Refereed papers

ANDREW, A.S., HEINRICH, C.A., WILKINS, R.W.T., & PATTERSON, D.J., 1989 - Sulfur isotope systematics of copper ore formation at Mount Isa, Australia. *Economic Geology* 84, 1614-1626.

BAIN, J.H.C., HEINRICH, C.A., & HENDERSON, G.A.M., this volume - Stratigraphy, structure, and metasomatism of the Haslingden Group, east Moondarra area, Mount Isa: a deformed and mineralised Proterozoic multistage rift-sag sequence. *In:* STEWART, A.J., & BLAKE, D.H. (Editors), Detailed Studies of the Mount Isa Inlier. *Bureau of Mineral Resources, Australia, Bulletin* 243.

BLAKE, D.H., 1986 - Middle Proterozoic evolution of the Mount Isa Inlier, northwestern Queensland, Australia: a synthesis. *Transactions of the Geological Society of South Africa* 89, 253-262.

BLAKE, D.H., in press a - Documentation and significance of a major unconformity in the Wonga Belt of the Mount Isa Inlier, northwest Queensland. *Australian Journal of Earth Sciences.*

BLAKE, D.H., in press b - Discussion: Tectono-metamorphic evolution of the Mary Kathleen Fold Belt, northwest Queensland: A reflection of mantle plume processes? *Australian Journal of Earth Sciences.*

BLAKE, D.H., this volume a - The compressional Lake Mary Kathleen Fold and Thrust Zone, Mount Isa Inlier. *In* STEWART, A.J., & BLAKE, D.H. (Editors), Detailed Studies of the Mount Isa Inlier. *Bureau of Mineral Resources, Australia, Bulletin* 243.

BLAKE, D.H., this volume b - Stratigraphy, folding, and faulting within the Quilalar Fault System, Mount Isa Inlier. *In:* STEWART, A.J., & BLAKE, D.H. (Editors), Detailed Studies of the Mount Isa Inlier. *Bureau of Mineral Resources, Australia, Bulletin* 243.

BLAKE, D.H., ETHERIDGE, M.A, PAGE, R.W., STEWART, A.J., WILLIAMS, P.R., & WYBORN, L.A.I., 1990 - Mount Isa Inlier - regional geology and mineralisation. *Australasian Institute of Mining and Metallurgy, Monograph* 14, 1, 915-925.

BLAKE, D.H., & PAGE, R.W., 1988 - Early Proterozoic migmatitic basement in the Kalkadoon-Leichhardt Belt of the Mount Isa Inlier, northwest Queensland. *BMR Journal of Australian Geology & Geophysics,* 10, 323-328.

BLAKE, D.H., & STEWART, A.J., this volume a - Stratigraphic and tectonic framework, Mount Isa Inlier. *In:* STEWART, A.J., & BLAKE, D.H. (Editors), Detailed Studies of the Mount Isa Inlier. *Bureau of Mineral Resources, Australia, Bulletin* 243.

BLAKE, D.H., & STEWART, A.J., this volume b - The BMR 1983-1990 Mount Isa project: results, some remaining problems, and bibliography. *In:* STEWART, A.J., & BLAKE, D.H. (Editors), Detailed Studies of the Mount Isa Inlier. *Bureau of Mineral Resources, Australia, Bulletin* 243.

CONNORS, K.A., PROFFETT, J.M., LISTER, G.S., SCOTT, R.J., OLIVER, N.H.S., & YOUNG, D.J., this volume - Geology of the Mount Novit Ranges, southwest of Mount Isa mine. *In:* STEWART, A.J., & BLAKE, D.H. (Editors), Detailed Studies of the Mount Isa Inlier. *Bureau of Mineral Resources, Australia, Bulletin* 243.

ERIKSSON, K.A., & SIMPSON, E.L., 1990 - Recognition of high- frequency sea-level fluctuations in Proterozoic siliciclastic tidal deposits, Mount Isa, Australia. *Geology* 18, 474- 477.

ERIKSSON, K.A., & SIMPSON, E.L., 1992a - Siliciclastic braided-alluvial sediments intercalated within continental flood basalts in the Early to Middle Proterozoic Mount Isa Inlier, Australia. *In:* PUIGDEFABREGAS, C. (Editor), Fluvial Sedimentology. *International Association of Sedimentologists, Special Publication.*

ERIKSSON, K.A., SIMPSON, E.L., & JACKSON, M.J., 1992b - Stratigraphic evolution of a Proterozoic synrift to post-rift basin: constraints on nature of lithospheric extension in the Mount Isa Inlier, Australia. *In* STEEL, R., & FROSTIAK, L. (Editors), Tectonics and Sedimentation. *International Association of Sedimentologists, Special Publication.*

ERIKSSON, K.A., TAYLOR, S.R., & KORSCH, R.J., 1992 - Geochemistry of 1.8-1.67 Ga mudstones and siltstones from the Mount Isa Inlier, Queensland, Australia: Provenance and tectonic implications. *Geochimica et Cosmochimica Acta* 56, 899-909.

ETHERIDGE, M.A., RUTLAND, R.W., & WYBORN, L.A.I., 1987 - Orogenesis and tectonic process in the Early to Middle Proterozoic of northern Australia. *American Geophysical Union, Geodynamic Series* 17, 131-147.

HILL, E.J., LOOSVELD, R.J.H., & OLIVER, N.H.S., this volume - Structure and geochronology of the Tommy Creek Block, Mount Isa Inlier. *In:* STEWART, A.J., & BLAKE, D.H. (Editors), Detailed Studies of the Mount Isa Inlier. *Bureau of Mineral Resources, Australia, Bulletin* 243.

HOLCOMBE, R.J., PEARSON, P.J., & OLIVER, N.H.S., 1991 - Geometry of a Middle Proterozoic extensional decollement in northeastern Australia. *Tectonophysics* 191, 255-274.

HOLCOMBE, R.J., PEARSON, P.J., & OLIVER, N.H.S., this volume - Structure of the Mary Kathleen Fold Belt. *In:* STEWART, A.J., & BLAKE, D.H. (Editors),

Detailed Studies of the Mount Isa Inlier. *Bureau of Mineral Resources, Australia, Bulletin* 243.

JACKSON, M.J., SIMPSON, E.L., & ERIKSSON, K.A., 1990 - Facies and sequence stratigraphic analysis in an intracratonic thermal-relaxation basin: the Early Proterozoic, Lower Quilalar Formation and Ballara Quartzite, Mount Isa Inlier, Australia. *Sedimentology* 37, 1053-1078.

LOOSVELD, R.J.H., 1989a - The intra-cratonic evolution of the central eastern Mount Isa Inlier, northwest Queensland, Australia. *Precambrian Research* 44, 243-276.

LOOSVELD, R.J.H., 1989b - The synchronism of crustal thickening and high T/low P metamorphism in the central Mount Isa Inlier, Australia. Part I: an example, the central Soldiers Cap belt. *Tectonophysics* 158, 173-190.

LOOSVELD, R.J.H., 1989c - The synchronism of crustal thinning and low pressure facies metamorphism in the Mount Isa Inlier, Australia. II: fast convective thinning of the mantle lithosphere during crustal thickening. *Tectonophysics* 165, 191-218.

LOOSVELD, R.J.H., 1989d - Reply to discussion: Discovery of thrust klippen, northwest of Mary Kathleen, Mount Isa Inlier, Australia. *Australian Journal of Earth Sciences* 36, 147-148.

LOOSVELD, R.J.H., this volume - Structural geology of the central Soldiers Cap Belt, Mount Isa Inlier, Australia. *In:* STEWART, A.J., & BLAKE, D.H. (Editors), Detailed Studies of the Mount Isa Inlier. *Bureau of Mineral Resources, Australia, Bulletin* 243.

LOOSVELD, R.J.H., & ETHERIDGE, M.A., 1990 - A model for low-pressure facies metamorphism during crustal thickening. *Journal of Metamorphic Geology* 8, 257-267.

LOOSVELD, R., & SCHREURS, G., 1987 - Discovery of thrust klippen, northwest of Mary Kathleen, Australia. *Australian Journal of Earth Sciences* 34, 387-402.

NIJMAN, W., LOCHEM, J.H.VAN, SPLIETHOFF, H.M., & FEIJTH, J., this volume a - Deformation model and sedimentation patterns of the Proterozoic of the Paroo Range, Mount Isa Inlier, Queensland, Australia. *In:* STEWART, A.J., & BLAKE, D.H. (Editors), Detailed Studies of the Mount Isa Inlier. *Bureau of Mineral Resources, Australia, Bulletin* 243.

NIJMAN, W., MIJNLIEF, H.M., & SCHALKWIJK, G., this volume b - The Hero Fan Delta (Lower Mount Isa Group) and its structural control: deformation in the Hero/Western Fault Zone and Paroo Range compared, Proterozoic, Mount Isa Inlier, Queensland, Australia. *In:* STEWART, A.J., & BLAKE, D.H. (Editors), Detailed Studies of the Mount Isa Inlier. *Bureau of Mineral Resources, Australia, Bulletin* 243.

OLIVER, N.H.S., HOLCOMBE, R.J., HILL, E.J., & PEARSON, P.J., 1991 - Tectono-metamorphic evolution of the Mary Kathleen Fold Belt, northwest Queensland: A reflection of mantle plume processes? *Australian Journal of Earth Sciences* 38, 425-455.

OLIVER, N.H.S., & WALL, V.J., 1987 - Metamorphic plumbing systems in Proterozoic calc-silicates, Queensland, Australia. *Geology* 15, 793-796.

PAGE, R.W., 1988. Geochronology of Early to Middle Proterozoic fold belts in northern Australia: a review. *Precambrian Research* 40/41, 1-19.

PAGE, R.W., & BELL, T.H., 1986 - Isotopic and structural responses of granite to successive deformation and metamorphism. *Journal of Geology* 94, 365-379.

PAGE, R.W., & WILLIAMS, I.S., 1988 - Age of the Barramundi Orogeny in northern Australia by means of ion microprobe and conventional U-Pb zircon studies. *Precambrian Research* 40/41, 21-36.

PASSCHIER, C.W., 1986a - Evidence for early extensional tectonics in the Proterozoic Mount Isa inlier, Australia. *Geology* 14, 1008-1011.

PASSCHIER, C.W., 1986b - Proterozoic deformation in the Duchess belt, Australia: a contribution to the BMR Mount Isa regional tectonic history program. *Geologie en Mijnbouw* 65, 47-56.

PASSCHIER, C.W., 1991 - Deformation in the Revenue granite pluton, Mount Isa Inlier, Australia. *Geologie en Mijnbouw,* 70, 275- 285.

PASSCHIER, C.W., this volume - Geology of the Myubee area, Mount Isa Inlier, Queensland. *In:* STEWART, A.J., & BLAKE, D.H. (Editors), Detailed Studies of the Mount Isa Inlier. *Bureau of Mineral Resources, Australia, Bulletin* 243.

PASSCHIER, C.W., & WILLIAMS, P.W., 1989 - Proterozoic extensional deformation in the Mount Isa Inlier, Queensland, Australia. *Geological Magazine* 126, 43-53.

PEARSON, P.J., HOLCOMBE, R.J., & PAGE, R.W., this volume - Synkinematic emplacement of the Middle Proterozoic Wonga Batholith into a mid-crustal extensional shear zone, Mount Isa Inlier, Queensland, Australia. *In:* STEWART, A.J., & BLAKE, D.H. (Editors), Detailed Studies of the Mount Isa Inlier. *Bureau of Mineral Resources, Australia, Bulletin* 243.

REINHARDT, J., 1987 - Cordierite-anthophyllite rocks from north-west Queensland, Australia: metamorphosed magnesian pelites. *Journal of Metamorphic Geology* 5, 451-472.

REINHARDT, J., 1992 - Low-pressure, high-temperature metamorphism in a compressional tectonic setting: Mary Kathleen Fold Belt, northeastern Australia. *Geological Magazine* 129, 41-57.

REINHARDT, J., this volume - The Corella Formation of the Rosebud Syncline (central Mount Isa Inlier): deposition, deformation, and metamorphism. *In:* STEWART, A.J., & BLAKE, D.H. (Editors), Detailed Studies of the Mount Isa Inlier. *Bureau of Mineral Resources, Australia, Bulletin* 243.

REINHARDT, J., & RUBENACH, M.J., 1989 - Temperature-time relationships across metamorphic zones: evidence from porphyroblast-matrix relationships in progressively deformed metapelites. *Tectonophysics* 158, 141-161.

SIMPSON, E.L., & ERIKSSON, K.A., 1991 - Depositional facies and controls on parasequence development in siliciclastic tidal deposits from the Lower Proterozoic, upper Mount Guide Quartzite, Mount Isa Inlier, Australia. *Canadian Society of Petroleum Geologists, Memoir* 16, 371-387.

SIMPSON, E.L., & ERIKSSON, K.A., in revision - Thin-bedded eolianites: Early Proterozoic Whitworth Formation, Mount Isa Inlier, Australia. *Sedimentary Geology*.

SOLOMON, M., & HEINRICH, C.A., 1992 - Are high-heat-producing granites essential to the origin of giant lead-zinc deposits at Mount Isa and McArthur River, Australia? *Exploration and Mining Geology* 1, 85-91.

STEWART, A.J., 1989 - Extensional faulting as the explanation for the Deighton 'Klippe' and other Mount Albert Group outliers, Mount Isa Inlier, northwestern Queensland. *Australian Journal of Earth Sciences* 36, 405-421.

STEWART, A.J., this volume a - Geology of the Horse's Head structure, north of Mount Isa, and its bearing on the 'roof thrust + imbricate stack' hypothesis, Mount Isa Inlier, Queensland. *In:* STEWART, A.J., & BLAKE, D.H. (Editors), Detailed Studies of the Mount Isa Inlier. *Bureau of Mineral Resources, Australia, Bulletin* 243.

STEWART, A.J., this volume b - Stratigraphy, extension, and contraction in the Ballara-Mount Frosty area, Mount Isa Inlier, Queensland. *In:* STEWART, A.J., & BLAKE, D.H. (Editors), Detailed Studies of the Mount Isa Inlier. *Bureau of Mineral Resources, Australia, Bulletin* 243.

STEWART, A.J., 1992 - The role of thrusting in the structural development of the Mount Isa mine and its relevance to exploration in the surrounding region: a discussion. *Economic Geology* 87.

STEWART, A., & MITCHELL, K., 1987 - Shatter cones at the Lawn Hill circular structure, northwestern Queensland: presumed astrobleme. *Australian Journal of Earth Sciences* 34, 477-485.

STEWART, A.J., & PASSCHIER, C.W., 1987 - Comment and Reply on 'Evidence for early extensional tectonics in the Proterozoic Mount Isa inlier, Australia'. *Geology* 15, 976-978.

WELLMAN, P., 1988 - Development of the Australian Proterozoic crust as inferred from gravity and magnetic anomalies. *Precambrian Research* 40/41, 89-100.

WELLMAN, P., this volume - Structure of the Mount Isa region inferred from gravity and magnetic anomalies. *In:* STEWART, A.J., & BLAKE, D.H. (Editors), Detailed Studies of the Mount Isa Inlier. *Bureau of Mineral Resources, Australia, Bulletin* 243.

WILLIAMS, P.R., 1989 - Nature and timing of early extensional structures in the Mitakoodi Quartzite, Mount Isa Inlier, northwest Queensland. *Australian Journal of Earth Sciences* 36, 283-296.

WILLIAMS, P.R., 1992 - Reply to discussion: Nature and timing of early extensional structures in the Mitakoodi Quartzite, Mt Isa Inlier, northwest Queensland. *Australian Journal of Earth Sciences* 39, 125-126.

WILLIAMS, P.R., & BLAKE, D.H., this volume - Black Mountain - a strike-slip pull-apart structure in the Quilalar Fault System, Mount Isa Inlier. *In:* STEWART, A.J., & BLAKE, D.H. (Editors), Detailed Studies of the Mount Isa Inlier. *Bureau of Mineral Resources, Australia, Bulletin* 243.

WYBORN, L.A.I., 1987 - The petrology and geochemistry of alteration assemblages in the Eastern Creek Volcanics, as a guide to copper and uranium mobility associated with regional metamorphism and deformation, Mount Isa, Queensland. *Geological Society Special Publication* 33, 425-434

WYBORN, L.A.I., 1988 - Petrology, geochemistry and origin of a major Australian 1880-1840 Ma felsic volcano-plutonic suite: a model for intracontinental felsic magma generation. *Precambrian Research* 40/41, 37-60.

WYBORN, L.A.I., PAGE, R.W., & PARKER, A.J., 1987 - Geochemical and geochronological signatures in Australian Proterozoic igneous rocks. *Geological Society Special Publication* 33, 377- 394.

WYBORN, L.A.I., PAGE, R.W., & McMCULLOCH, M.T., 1988 - Petrology, geochronology and isotope geochemistry of the post-1830 Ma granites of the Mount Isa Inlier: mechanisms for the generation of Proterozoic anorogenic granites. *Precambrian Research* 40/41, 509-541.

Other articles

BAIN, J.H.C., HENDERSON, G.A.M., & HEINRICH, C.A., 1989 - Structural and metasomatic history of the Eastern Creek Volcanics, east Moondarra area, Mount Isa. *Geological Society of Australia, Abstracts* 24, 3-4.

BATSON, R., 1990 - A stratigraphic and structural reinterpretation of the Lake Julius area (southern Myally Shelf). *Mount Isa Inlier Geology Conference, Monash University, Abstracts* 26-27.

BETTESS, D.E., 1987 - The structural evolution of the Deighton thrust nappe complex, Mount Isa, Queensland. *Geological Society of Australia, Abstracts* 19, 41-42.

BLAKE, D.H., 1984 - Middle Proterozoic evolution of the Mount Isa Inlier, northwestern Queensland, Australia: a synthesis. Conference on Middle to Late Proterozoic lithosphere evolution. *Precambrian Research Unit, University of Cape Town, Abstracts*, 23-25.

BLAKE, D.H., 1985 - Tectonic development of the Proterozoic Mount Isa Inlier, northwest Queensland (abstract). *Bureau of Mineral Resources, Australia, Record* 1985/28 (no page numbers).

BLAKE, D.H., 1990 - A terrane analysis of the Mount Isa Inlier. *Mount Isa Inlier Geology Conference, Monash University, Abstracts,* 8.

BLAKE, D.H., LISTER, G.S., WYBORN, L.A.I., & PERKINS, W.G., 1985 - Mount Isa field excursion guide, 14-22 August 1985. *Bureau of Mineral Resources, Australia, Record* 1985/24, 69pp.

CONNORS, K.A., 1989 - Implications of an early fold-thrust event in the western Mount Isa Inlier. *Geological Society of Australia, Abstracts* 24, 25-26.

CONNORS, K.A., 1990a - D2 fault and shear zone development in the Mount Isa area. *Geological Society of Australia, Abstracts* 25, 175-176.

CONNORS, K.A., 1990b - Metasomatism and structurally controlled fluid pathways, southwest of Mount Isa mine. *Mount Isa Inlier Geology Conference, Monash University, Abstracts* 53-55.

CONNORS, K.A., & PAGE, R.W., 1992 - Age relationships between granite intrusion, metamorphism, and deformation in the Mount Isa Inlier. *Geological Society of Australia, Abstracts* 32, 229-230.

DERRICK, G.M., 1991 - 1991 field conference Mount Isa Inlier. *Geological Society of Australia, Queensland Division.*

ETHERIDGE, M.A., 1990 - The Early to Middle Proterozoic tectonic evolution of the Australian craton: where does the Mt Isa Inlier fit? Mount Isa Inlier Geology Conference, Monash University, Abstracts, 1-3.

ETHERIDGE, M.A., WYBORN, L.A.I., RUTLAND, R.W.R., PAGE, R.W., BLAKE, D.H., & DRUMMOND, B.J., 1984 - Workshop on Early to Middle Proterozoic of northern Australia, 5-6 November, 1984: the BMR model - a discussion paper. *Bureau of Mineral Resources, Australia, Record* 1984/31, 8pp.

HEINRICH, C.A., WARING, C.L., & WALL, V.J., 1990 - Essential chemical ingredients for Mount Isa-style copper mineralisation. *Mount Isa Inlier Geology Conference, Monash University, Abstracts,* 72-73.

HILL, E.J., 1987a - Structural geology of the Tommy Creek area, Mount Isa Inlier, NW Queensland. *Bureau of Mineral Resources, Australia, Record* 1987/20, 51pp.

HILL, E.J., 1987b - The Tommy Creek area, NW Queensland. *Geological Society of Australia, Abstracts* 19, 26.

HILL, E.J., 1990 - The Tommy Creek Block, eastern Mount Isa Inlier. *Mount Isa Inlier Geology Conference, Monash University, Abstracts,* 16-18.

HOLCOMBE, R.J., PEARSON, P.J., & OLIVER, N.H.S., 1987 - The Mary Kathleen Fold Belt, northwest Queensland: geometry and timing of deformation. *Geological Society of Australia, Abstracts* 19, 35-36.

LISTER, G.S., 1990 - The interaction of brittle and ductile processes in the mid-crust during Proterozoic wrenching in the Mount Isa Inlier. *Mount Isa Inlier Geology Conference, Monash University, Abstracts,* 23-25.

LISTER, G.S., ETHERIDGE, M.A., & STEWART, A.J., 1985a - Structure and tectonics of the Precambrian Mount Isa Inlier, northwest Queensland. *Bureau of Mineral Resources, Australia, Record* 1985/33, 37.

LISTER, G.S., THOMAS, A., & DUNN, J., 1985b - The significance of transpressional strike-slip faulting in the Lake Julius area, Mount Isa Inlier. *Bureau of Mineral Resources, Australia, Record* 1985/33, 43.

LISTER, G.S., THOMAS, A., & DUNN, J., 1986 - Tectonic processes in the Mount Isa Inlier: the significance of transpressional strike-slip faulting. *Geological Society of Australia, Abstracts* 15, 127-128.

LISTER, G.S., THOMAS, A.D., & DUNN, J., 1987 - The significance of transpressional strike-slip faulting in the Lake Julius area, Mount Isa Inlier. *Geological Society of Australia, Abstracts* 19, 39-40.

LOOSVELD, R.J.H., 1987 - A complex fold nappe within the Soldiers Cap Group, Mount Isa Inlier, Queensland, Australia. *Geological Society of Australia, Abstracts* 19, 45-46.

LOOSVELD, R.J.H., 1988a - Numerical simulations of high-T metamorphism and coeval crustal thickening, with reference to the Mount Isa Inlier. *Geological Society of Australia, Abstracts* 21, 256-257.

LOOSVELD, R.J.H., 1988b - Structure and tecton-thermal history of the eastern Mount Isa Inlier, Australia. Ph.D. thesis, Australian National University.

OLIVER, N.H.S., 1988 - A metamorphic plumbing system - the Mary Kathleen Fold Belt, northwest Queensland. Ph.D. thesis, Monash University.

OLIVER, N.H.S., & WALL, V.J., 1986 - Scapolite paragenesis in calc-silicates at Mary Kathleen, NW Queensland: implications for metamorphic fluid evolution. *Geological Society of Australia, Abstracts* 15, 147-148.

OLIVER, N.H.S., WALL, V.J., & PEARSON, P.J., 1986 - The Mary Kathleen uranium-REE deposit; a product of regional metamorphism. *Geological Society of Australia, Abstracts* 15, 149-150.

OLIVER, N.H.S, PEARSON, P.J., WALL, V.J., GOLDING, S.D., & HOLCOMBE, R.J., 1987 - Structural controls on fluid infiltration and metasomatism in the Mary Kathleen Fold Belt: implications for large-scale fluid migration during

deformation. *Geological Society of Australia, Abstracts* 19, 14-15.

OLIVER, N.H.S., WALL, V.J., PEARSON, P.J., & HOLCOMBE, R.J., 1990 - Unravelling more obscurities in the genesis of the Mary Kathleen U-REE orebody. *Mount Isa Inlier Geology Conference, Monash University, Abstracts,* 41-43.

PAGE, R.W., 1990 - Developments in U-Pb zircon geochronology in the Mount Isa Inlier. *Mount Isa Inlier Geology Conference, Monash University, Abstracts,* 4-5.

PEARSON, P.J., 1989 - The structural and tectonic development of the Wonga Belt and surrounding Mary Kathleen Fold Belt, Mount Isa Inlier, northwestern Queensland. Ph.D. thesis, University of Queensland.

PEARSON, P.J., HOLCOMBE, R.J., & OLIVER, N.H.S., 1987 - The Mary Kathleen Fold Belt, northwest Queensland: D1 - a product of crustal extension? *Geological Society of Australia, Abstracts* 19, 37-38.

PEARSON, P.J., PAGE, R.W., & HOLCOMBE, R.J., 1990 - Geochronology of the Wonga Granite, northwest Queensland: implications for the timing of deformation in the Mary Kathleen Fold Belt. *Mount Isa Inlier Geology Conference, Monash University, Abstracts*, 13-15.

PRIHARDJO, S., 1987 - Structural setting of the McNamara Group in the Yaringa Creek-Big Toby Creek area, Mount Isa, Queensland, Australia. *Bureau of Mineral Resources, Australia, Record* 1987/33, 13pp.

REINHARDT, J., 1986 - Alumino-magnesian clays as precursors of cordierite-anthophyllite rocks in the Rosebud Syncline (Mt. Isa Inlier): geochemical evidence and field relations. *Geological Society of Australia, Abstracts* 15, 163-164.

REINHARDT, J., 1987 - Metamorphic and structural evolution of the Corella Formation in the Rosebud Syncline, north-west Queensland. Ph.D. thesis, James Cook University of North Queensland.

REINHARDT, J., 1989 - Evidence for a complete anticlockwise P-T path in medium-grade schist of the central Mt Isa block, northeast Australia. *Terra Abstracts* 1, 306.

REINHARDT, J., 1990 - Low-pressure/high temperature metamorphism, crustal shortening and isobaric cooling in the Mary Kathleen Fold Belt, northeast Australia. *Terra Abstracts* 2, 31.

REINHARDT, J, & BELL, T.H., 1987 - Microstructural evidence for early thrusting and contemporaneous strike-slip shears in a subsequently folded and metamorphosed terrain (Rosebud Syncline, north-east Australia). *Terra Cognita* 7, 65-66.

REINHARDT, J., & RUBENACH, M.J., 1987 - Growth of porphyroblasts relative to progressive deformation, temperature increase and time during prograde metamorphism. *Geological Society of Australia, Abstracts* 19, 100-101.

RICKARD, M.J., 1987 - Structure of the Yaringa Metamorphics - western basement to the Mt. Isa basin. *Geological Society of Australia, Abstracts* 19, 23-24.

RICKARD, M.J., 1990 - The western edge of the Mt Isa Inlier and the May Downs Fault system. *Mount Isa Inlier Geology Conference, Monash University, Abstracts* 9.

SOLOMON, M., HEINRICH, C.A., & SWIFT, M., 1991 - Are hot granites essential for the formation of giant sedex-type lead-zinc deposits? *Bureau of Mineral Resources, Australia, Record* 1990/95, 78-79.

STEWART, A.J., 1989 - Extensional orogeny at Mount Isa,Australia. *28th International Geological Congress, Washington, D.C. Abstracts* 3, 180.

STEWART, A.J., 1990 - Extension and contraction in the Ballara-Mount Frosty area, Mount Isa Inlier. *Mount Isa Inlier Geology Conference, Monash University, Abstracts,* 11-12.

STEWART, A.J., & WILLIAMS, P.R., 1988 - Early extension in the Mount Isa Inlier, and a solution to the problem of the Deighton Quartzite outliers. *Geological Society of Australia, Abstracts* 21, 381-382.

TUNKS, A.J., 1987 - Breccias and metasomatism of the Corella Formation, Cloncurry area, Queensland. B.Sc. (Hons) thesis, Monash University.

WELLMAN, P., 1986 - Mount Isa block as a 700 km-long zone of reworking of Proterozoic crust: an interpretation based on gravity and magnetic anomalies. *Bureau of Mineral Resources, Australia, Record* 1986/31, 25-28.

WILLIAMS, P.R., STEWART, A.J., & PEARSON, P.J., 1987 - Proterozoic continental extension in the Mount Isa Inlier, Queensland, Australia. *Bureau of Mineral Resources, Australia, Record* 1987/51, 64-67.

WYBORN, L.A.I., 1990a - Geochemical evolution of the felsic igneous rocks of the Mount Isa Inlier and their significance for mineralisation. *Mount Isa Inlier Geology Conference, Monash University, Abstracts,* 6-7.

WYBORN, L.A.I., 1990b - Putting Mount Isa in the metallogenic context of the Proterozoic of northern Australia. *Mount Isa Inlier Geology Conference, Monash University, Abstracts,* 50-51.

YOUNG, D.J., 1990 - Aspects of structure and metamorphism in the 'vortex', southwest of Mount Isa. *Mount Isa Inlier Geology Conference, Monash University, Abstracts,* 32-34.

BMR Research Newsletter

BMR, 1985a - Nappe tectonics in the Mount Isa Inlier. 2, 11.

BMR, 1985b - ?Lower Proterozoic migmatites in the Mount Isa Inlier. 2, 14.
BMR, 1986a - Transpressional strike-slip faulting in the Mount Isa Inlier. 4, 1-2.
BMR, 1986b - Proof of explosive origin for the Lawn Hill circular structure. 4, 10-11.
BMR, 1986c - US/Australian joint scanner project. 4, 14-15.
BMR, 1987a - Changes in Proterozoic granitoid compositions with time. 6, 3-4.
BMR, 1987b - Alteration styles in the Eastern Creek Volcanics. 6, 4-5.
BMR, 1987c - Extensional structures in the Mount Isa Inlier. 6, 10-11.
BMR, 1987d - Stratigraphy and structure in theTommy Creek, area, Mount Isa Inlier. 6, 13-14.
BMR, 1988a - Extensional tectonics extended: new results from the Mount Isa Inlier. 8, 2-4.
BMR, 1988B - Block and possible terrane boundaries in the Mount Isa Inlier. 9, 2-3.
BMR, 1989 - Sequence-stratigraphy, rifts, and tides at Mount Isa. 10, 8-10.
BMR, 1990 - New results from the Mount Isa geotratraverse. 12, 6-8
BMR, 1992 - Granites, breccias and large-scale regional alteration of Williams and Naraku Batholiths, eastern Mount Isa Inlier: an analogue for the Olympic Dam granites? 16, 13-16.

BMR Yearbook

Project 2B.02: Mount Isa base-metal province. BMR 83, 50.
Project 2B.02: Mount Isa base-metal province. BMR 84, 74-75.
Project 2B.02: Mount Isa base-metal province. BMR 85, 83-84.
Project 2B.02: Metallogeny and crustal evolution in the Mount Isa province. BMR 86, 69-70.
Project 2B.02: Integrated studies of the tectonic history of the Mount Isa base-metal province, Queensland. BMR 87, 100-102.
Project 9170.01: Integrated geological and geophysical analysis of the Mount Isa Base Metal Province, Queensland. BMR 88, 83- 85.
Project 170.01: Integrated geological and geophysical analysis of the Mount Isa Base Metal Province, Queensland. BMR 89, 92- 93.
Mount Isa project draws to a close. BMR 90, 15-16.

GEOLOGY OF THE

MOUNT ISA – CLONCURRY TRANSECT

by D.H. Blake and A.J. Stewart, 1992

AUSTRALIA 1 : 250 000 GEOLOGICAL MAP

QUEENSLAND

SCALE 1 : 250 000

5 0 5 10 15 20 25 Kilometres

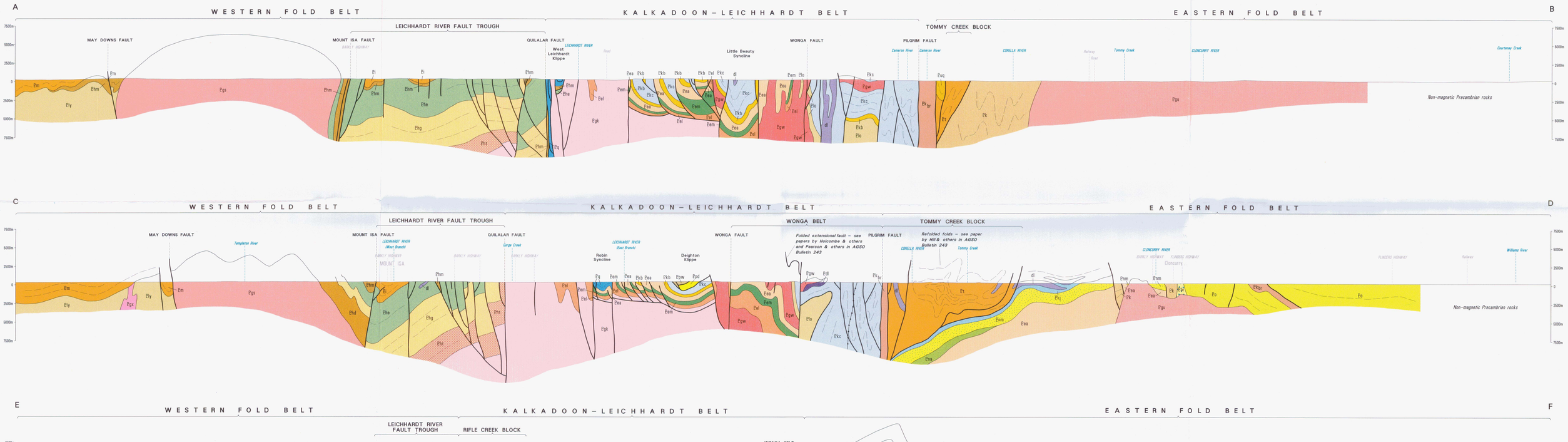
UNIVERSAL TRANSVERSE MERCATOR PROJECTION

LATITUDE OF ORIGIN : 0°, LONGITUDE OF ORIGIN : 141° E

SCHEMATIC SECTIONS

Phanerozoic sediments omitted

Scale: V/H = 1



WESTERN FOLD BELT | KALKADOON – LEICHHARDT BELT | EASTERN FOLD BELT

LEICHHARDT RIVER FAULT TROUGH | WONGA BELT | RIFLE CREEK BLOCK | TOMMY CREEK BLOCK

MOUNT ISA FAULT | QUILALAR FAULT | WONGA BELT FAULT | PILGRIM FAULT

CAINOZOIC — Cz — Unconsolidated sediments

CAMBRIAN — Є — Sedimentary rocks

Quamby Conglomerate — Pvq — Conglomerate, sandstone

Lakeview Dolerite ~ 1116 Ma

Gilded Rose Breccia — Pbr — Breccia

Mount Philp Breccia — Pdb — Intrusive breccia

Naraku Granite and Williams Granite — Pgu ~ 1500 Ma, Pgi — Granite, generally non-foliated

ISAN OROGENY 1520 – 1620 Ma

REGIONAL METAMORPHISM
Greenschist to amphibolite facies

dl — Metadolerite of various ages

Tommy Creek beds ~ 1635 Ma — Pt — Calcareous and pelitic sedimentary rocks, mafic and felsic volcanics

Sybella Granite — Pgs ~ 1670 Ma

MOUNT ISA GROUP

McNAMARA GROUP — Pm — ~ 1670 Ma

Surprise Creek Formation — Pr

Carters Bore Rhyolite — Pfc ~ 1680 Ma

Bigie Formation — Pbt

MARY KATHLEEN GROUP

Roxmere Quartzite — Pqr

Staveley Fm — Pks

Marimo Slate — Pkm

Corella beds — Pk

Wonga Granite — Pgw — 1720 – 1759 Ma

Lunch Creek Gabbro — Pdl ~ 1740 Ma

MOUNT ALBERT GROUP

Quilalar Formation — Pq

White Blow Fm — Ppw

Deighton Quartzite — Ppd

Corella Formation — Pkc

Ballara Quartzite — Pkb

Argylla Formation — Pea — ~ 1760 Ma

Pem — Mount Frosty Member

Magna Lynn Metabasalt

Corella Formation — Pkc

Ballara Quartzite — Pkb

Overhang Jaspilite — Pkj

Mitakoodi Quartzite — Pqm

Marraba Volcanics — Pma

Argylla Formation — Pea

MALBON GROUP

SOLDIERS CAP GROUP — Pep ?

HASLINGDEN GROUP

MYALLY SUBGROUP — Phm

Eastern Creek Volcanics — Phe

Mount Guide Quartzite — Phg

May Downs Gneiss — Phd

Bottletree Formation — Pbt ~ 1780 Ma

Pgx ~ 1800 Ma — Big Toby Granite

Kalkadoon Granite — Pgk ~ 1850 Ma

Leichhardt Volcanics — Pel ~ 1865 Ma

Peo — Orient beds

BARRAMUNDI OROGENY 1870 – 1890 Ma

Yaringa Metamorphics — Ply

Kurbayia Migmatite — Plo

REGIONAL METAMORPHISM
Amphibolite facies

PROTEROZOIC — COVER SEQUENCE 3 / COVER SEQUENCE 2 / COVER SEQUENCE 1 / BASEMENT

Geological boundary

Fault

Thrust fault, triangle on upper plate

Dyke or vein: (Lakeview Dolerite)

Anticline showing plunge

Syncline showing plunge

Overturned anticline

Overturned syncline

Strike and dip of strata

Vertical strata

Horizontal strata

Strike and dip of inverted strata

Strike and dip of strata, facing not known

Trend–line, airphoto interpretation

Strike and dip of foliation

Vertical foliation

Strike and dip of cleavage

Vertical cleavage

Major mine

Abandoned mine or prospect

Highway

Railway

Aerodrome

Built–up area

Corella Park Homestead

+507 Elevation in metres

Trigonometrical station

Pbt Biotite granite, commonly foliated and porphyritic; minor leucogranite

Peo Sandstone, siltstone, conglomerate, calcareous rocks, ?volcanics

Pgk Biotite granite, commonly foliated and porphyritic; minor leucogranite

Pel Porphyritic felsic volcanics

Ply Schist, gneiss, migmatite

Plo Migmatite, gneiss, schist

Pgx, Ply

Pgs

Ehm

Ehe

Ehg

Ehd

Pbt

Pfc

Pr

Pi

Ehm

Pgk

Pel

Pem

Pea

Pkb

Pkc

Pkj

Pdb

Pgw

Pdl

Pqm

Pma

Pep

Pk

Pkm

Pks

Pgi

Pgu

Pt

Pbr

Pvq

Eq

Pq

Ppw

Ppd

Pkc

Pkb

Pea

Pem

Pqr

Pks

Pk

Pkm

Pdl

Pgw

Pdb

Pkc

Pkj

Pma

Pqm

Pep

Eq

Pea

Pem

Pel

Pgk

Phm

Phe

Phg

Phd

Pbt

Pfc

Pr

Pi

Ply

Pgx

Pgs

Pm

Cz

Є

Pvq

Pbr

Pgu

Pgi

Pt

Pk

Pkm

Pks

Pkj

Pkc

Pkb

Pdb

Pgw

Pdl

Pea

Pem

Pel

Pgk

Phm

Phe

Phg

Phd

Pbt

Pfc

Pr

Pi

Ply

Pgx

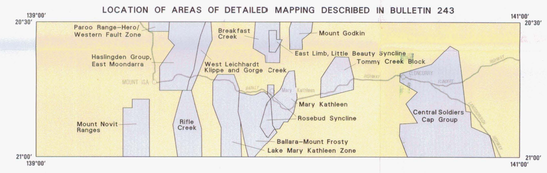
Pgs

Pm

Cz

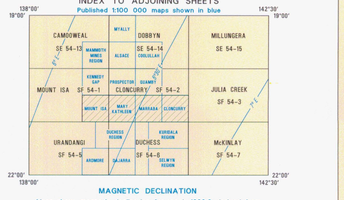
Є

LOCATION OF AREAS OF DETAILED MAPPING DESCRIBED IN BULLETIN 243



INDEX TO ADJOINING SHEETS

Published 1:100 000 maps shown in blue



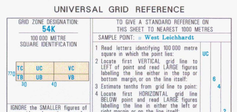
MAGNETIC DECLINATION

Lines show magnetic declination for epoch 1992.0 derived from 1990 AGRF model. Annual change is 12.6' per year easterly at the centre of the map. Information is current to 1995

MINERAL DEPOSITS

No	Name	Commodity
1	Big Beryl	Be
2	Copalert	Pb,Zn,Ag
3	Mount Novit	Pb,Zn,Ag
4	Hilton	Pb,Zn,Ag
5	Cresent	Cu
6	Mount Isa	Pb,Zn,Ag,Cu
7	Native Bee	Cu
8	Bemborough	Pb,Zn,Ag
9	Counter (Anderson's Lode)	U
10	Barbara	Cu
11	Angel	Cu
12	King Solomon	Cu
13	Mount Devine	Cu
14	Edna May (Willoughby)	Cu
15	Blockade (Argylla)	Cu
16	Rocky Home	Cu
17	OL	Cu
18	Trey (Bit	Cu,Au
19	Non Parrel	Cu
20	Megaphone (The Belfast)	Cu
21	Gosp (Blue Moon)	Cu
22	Iron Duke	Cu
23	Blue Star (Double F)	Cu
24	Kings (Cross)	Cu
25	Melba	Cu
26	Mount Frosty	Cu
27	Inkerman	Cu
28	Mount Philp	Fe
29	Wee MacGregor	Cu,Au
30	Great Central (Grand Central)	Cu
31	Wallaroo	Cu,Au
32	Prince of Wales	Cu
33	Lady Eileen	Cu
34	Little Beauty (McMillans)	Cu
35	Lady Jenny	Cu
36	Rosebud Extented	Cu
37	Rosebud	Cu
38	Winston Churchill	Cu
39	Lady Rose, Jola Rose	Cu,Au
40	Sunset	Cu
41	Amy (Lady Amy)	Cu
42	Warrenhole	Cu
43	Pup	Cu
44	Mount Debbie	Cu
45	Secret	Cu
46	Trafalgar	Cu,Au
47	Springs	Cu
48	Jubilee	Cu
49	Mary Kathleen	U,REE
50	Even Steven	Cu
51	Apple Pie	Cu
52	Tom Cat	Cu
53	Lakeview	Cu
54	Pearl	Cu
55	Bobby Rod	Cu
56	Mount Colin	Cu
57	Woolaroonga	Cu
58	Mount Lindsay	Cu
59	Lady Vera	Cu
60	Pommers	Cu
61	Wonder Valley	Cu
62	Mona (Joy)	Cu,Cu
63	Federal	Cu,Au,Ag
64	Milo	U
65	Dolphin	Cu
66	Pioneer	Cu,Au
67	Celestial (Telegraph)	Cu
68	Dairy	Cu
69	Chineman	Cu
70	Success	Cu
71	(Varie's Success)	Cu,Cu,Au
72	Mount Minda	Cu
73	Longara	Cu
74	Timberoo	Cu
75	Fairfield	Cu
76	Double Oxide	Cu
77	Chum	Cu
78	Overhang	Mn
79	Mount McNamara	Cu,Au
80	Magpie	Cu
80	Dolomite	Cu
81	Jessie	Cu
82	Great Australia	Cu,Au
83	Australian Margaret	Cu
84	Surprise (Cloncurry Surprise)	Au
85	Rohur	Cu
86	Gilded Rose Group	Au
87	Brilliant	Cu,Au
88	King Edward	Cu
89	Uncle Tom	Au
90	Monakoff (Tinbolt)	Cu,U
91	Maria Dell (UL)	Cu,Au
92	Mount Norna (Mountain Home)	Cu,Ag
93	The Joker (Old Joker)	Cu
94	Comstock	Au
95	Mount Freda (Garaanascal	Au
96	Evening Star (Mount Wheeler)	Cu,Au
97	Falcon (Rose & Thistle)	Au
98	Kangaroo Rat (Wallaby)	Cu,Au
99	Flagship	Cu

UNIVERSAL GRID REFERENCE



Blue numbered lines are 10 000 metre intervals of the Australian Map Grid, Zone 54. Grid values are shown in full only at the southwest corner of the map

MAP LOCALITY



Geology compiled 1991–1992 by D.H. Blake and A.J. Stewart, AGSO from maps produced during the 1983–1990 AGSO Mount Isa Project and from 1969–1977 mapping by the AGSO and the Geological Survey of Queensland

Cartography by N. Jeffery, R.A. Swoboda, AGSO

Compiled and produced by Cartographic Services Unit, AGSO using Intergraph graphics applications

Printed by Mercury–Walch, Hobart, Australia

© Commonwealth of Australia 1992

Published by the Australian Geological Survey Organisation, Department of Primary Industries and Energy, Canberra
Issued under the authority of the Minister for Primary Industries and Energy

Base map compiled by the Australian Geological Survey Organisation from 1:250 000 scale topographic maps supplied by the Australian Surveying and Land Information Group, Department of Administrative Services

This map is accompanied by a text publication:
Stewart, A.J., Blake, D.H., & others, 1992– Detailed studies of the Mount Isa Inlier, Queensland. Australian Geological Survey Organisation, Canberra, *Bulletin* 243

It is recommended that this map be referred to as:
Blake, D.H., & Stewart, A.J., 1992– *Geology of the Mount Isa – Cloncurry Transect*, (1:250 000 scale map). Australian Geological Survey Organisation, Canberra

Digital data:
The digital geological data for this map were compiled on the AGSO Intergraph System and, in some circumstances, may be suitable for transfer to other digital systems. Further information on data release conditions, formats, and costs can be obtained by writing to:
Chief,
Minerals and Land Use Program,
Australian Geological Survey Organisation,
GPO Box 378,
Canberra ACT 2601
(Ph 06 2499111 Fax 06 2499983)

AGSO AUSTRALIAN GEOLOGICAL SURVEY ORGANISATION

BUREAU OF MINERAL RESOURCES LIBRARY 8 FEB 1993 CANBERRA, A.C.T.

GEOLOGY OF THE
MOUNT ISA – CLONCURRY TRANSECT
FIRST EDITION 1992

BMR PUBLICATIONS COMPACTUS (LENDING SECTION)
BMR 555(94) Bul. 45